Spatial and Temporal Variations in Hydroclimatic Variables Affecting Streamflow across Western Canada

by

Hayley Christina Linton
B.Sc., University of Victoria, 2010

A Thesis Submitted in Partial Fulfillment
of the Requirements for the Degree of

MASTER OF SCIENCE

in the Department of Geography

Supervisory Committee

Spatial and Temporal Variations in Hydroclimatic Variables Affecting Streamflow across Western Canada

by

Hayley Christina Linton
B.Sc., University of Victoria, 2010

Supervisory Committee

Dr. Terry Prowse (Department of Geography)
Supervisor

Dr. Yonas Dibike (Department of Geography)
Departmental Member

Dr. Barrie Bonsal (Department of Geography)
Departmental Member

Abstract

Supervisory Committee
Dr. Terry Prowse (Department of Geography)
Supervisor
Dr. Yonas Dibike (Department of Geography)
Departmental Member
Dr. Barrie Bonsal (Department of Geography)
Departmental Member

A large portion of the freshwater in western Canada originates as snowpack from the northern Rocky Mountains. The temperature and precipitation in these areas controls the amount of snow accumulated and stored throughout the winter, and the amount and timing of melt that occurs during the spring freshet. Therefore, a better understanding of past and future changes to the extent of snowpack and timing of melt can modify the timing of peak river flow on a continental scale. Trends in temperature, precipitation, snow accumulation, and snowmelt are examined using the Mann-Kendall non-parametric test on a high resolution gridded climate dataset over western Canada for the period 1950-2010. In addition, projected changes in temperature, precipitation, snow water equivalent, and snowmelt are examined through comparison of the current (1971-2000) and future (2041-2070) time periods incorporating several regional climate models. The temporal and spatial analyses of these key hydroclimatic variables indicate that changes vary greatly over space and time. Results reveal that while both maximum and minimum temperature have increased in the past 60 years, minimum temperature has increased more than maximum temperature and is likely to continue doing so in the future. This trend is particularly evident during the colder months of the year, and at higher elevations, contributing to earlier spring melt. Between 1950 and 2010, precipitation has

decreased throughout the colder months of the year and increased in the warmer months, particularly in the northern half of the study area. Future projections show increased precipitation, specifically in the north. Throughout the historical period snow accumulation has experienced decreases across the study area and through all months of the year, except for increases at high elevations. In the coldest months of the year snow accumulation is projected to increase in high elevation and northern areas while decreasing across the rest of study area in the future. Snowmelt results indicate slight increases in mid-winter melt events and an earlier onset of the spring freshet; this change is expected to continue into the future period. This study provides a summary of detected trends and potential future changes in key hydroclimatic variables across western Canada with regard to the effects these changes can have on the spring freshet and streamflow, and thus water resources, throughout the study area.

Table of Contents

Supervisory Committee ..... **ii**

Abstract ..... **iii**

Table of Contents ..... **v**

List of Tables ..... **viii**

List of Figures ..... **ix**

Acknowledgements ..... **xiv**

1. Chapter 1: Introduction **1**

1.1 Introduction 1

1.2 The CROCWR Project 4

1.3 Objectives 5

1.4 Thesis Structure 6

Presentations and Publications 6

References 8

2. Chapter 2: Literature Review **11**

2.1 Introduction 11

2.2 Historical Trends in Climatic and Hydrologic Variables 12

2.3 Future Projections in Climatic and Hydrologic Variables 17

2.4 Study Area 21

2.5 Hydroclimatic Data Sources 23

2.5.1 Historical Climate Data 23

2.5.2 Future Climate Projections 25

2.6 Methodology 28

2.6.1 Watershed Delineation 28

2.6.2 Modelling Snowpack Data 29
2.6.3 Trend Detection 32
2.6.4 Spatial Analysis and Interpolation 35
2.7 Conclusions 39
References 41
3. Chapter 3: Spatial and temporal analysis of hydroclimatic variables affecting streamflow in western Canada from 1950-2010 51
Abstract 51
3.1 Introduction 52
3.2 Study Area 56
3.3 Data and methods 58
3.4 Results and Discussion 63
3.4.1 Maximum and Minimum Temperature 63
3.4.1.1 Hydrologic Relevance of Temperature Trends 70
3.4.2 Precipitation 71
3.4.2.1 Hydrologic Relevance of Precipitation Trends 76
3.4.3 Snow Accumulation 76
3.4.4 Snowmelt 80
3.4.4.1 Hydrologic Relevance of Snow Accumulation and Melt Trends 83
3.4.5 Hydrologic Relevance of Calculated Trends in Climate 84
3.5 Conclusion 86
References 88
4. Chapter 4: Spatial and temporal analysis of projected changes in hydroclimatic variables affecting streamflow in western Canada 110
Abstract 110

4.1 Introduction 111
4.2 Study Area 114
4.3 Data and Methods 116
4.4 Results and Discussion 120
4.4.1 Maximum and Minimum Temperature 120
4.4.1.1 Hydrologic Relevance of Temperature Changes 123
4.4.2 Precipitation 124
4.4.2.1 Hydrologic Relevance of Precipitation Changes 126
4.4.3 Snow Water Equivalent (SWE) 127
4.4.4 Snowmelt 130
4.4.4.1 Hydrologic Relevance of SWE and Snowmelt Changes 133
4.4.5 Hydrologic Relevance of Predicted Changes in Climate 134
4.5 Conclusion 135
References 138
5. Chapter 5: Conclusion 172
APPENDICES 176
APPENDIX A – Supplementary material for Chapter 3 177
APPENDIX B – Supplementary material for Chapter 4 269

List of Tables

Table 3.1. Regional averages of Tmax and Tmin, from 1950-2010 ……64

Table 3.2. Tmax and Tmin rate of change averaged over each study region. Averages include all calculated trend values for the time period 1950-2010 ……...65

Table 3.3. Mean annual precipitation and precipitation trend averaged across each study region for the time period 1950-2010 ……72

Table 3.4. Total annual snow accumulation and snow accumulation trend values spatially averaged across each study region for the time period 1950-2010. Spatial averages include all calculated trend values ……77

Table 3.5. Total annual snowmelt and snowmelt trend values spatially averaged across each study region for the time period 1950-2010. Spatial averages include all calculated trend values ……..81

List of Figures

Figure 2.1. CROCWR study area with watersheds labeled by name and study regions identified by colour ……..50

Figure 2.2. Hypsometric curves of each study region identified in Figure 2.1 ……50

Figure 3.1. Map of study area, gray outlines indicate study watersheds, while coloured polygons show study regions used in analysis ……93

Figure 3.2. Hypsometric curves of each study region identified in Figure 3.1 ……93

Figure 3.3. Annual means and trends in daily maximum (Tmax) and minimum (Tmin) temperatures during 1950-2010 (a) mean annual Tmax in ^{o}C (b) mean annual Tmin in ^{o}C (c) mean annual Tmax trend in ^{o}C/decade, and (d) mean annual Tmin trend in ^{o}C/decade. Only trend results statistically significant at 10% or better are shown …….. 94

Figure 3.4. Daily average Tmax and Tmin for each month spatially averaged for each study region. Tmax shown with solid symbols and lines, Tmin shown with unfilled symbols and dashed lines ……... 95

Figure 3.5. Spatially averaged regional rate of change monthly mean Tmax and Tmin. Results include all calculated trend values. Tmax shown with solid symbols, Tmin shown with unfilled symbols …….. 96

Figure 3.6. Daily Tmax trends in ^{o}C/decade, 1950-2010, for (a) January, (b) April, (c) July, and (d) December. Only trend results statistically significant at 10% or better are shown …….. 97

Figure 3.7. Daily Tmin trends in ^{o}C/decade, 1950-2010, for (a) January, (b) April, (c) July, and (d) December. Only trend results statistically significant at 10% or better are shown …….. 98

Figure 3.8. Trend persistence maps where colour corresponds to number of months with increasing trend through the cold season (November to April) or the warm season (May to October). (a) Tmax increasing trend persistence through the cold season. (b) Tmax increasing trend persistence through the warm season. (c) Tmin increasing trend persistence through the cold season. (d) Tmin increasing trend persistence through the warm season ……. 99

Figure 3.9. Precipitation average annual total and annual trends for 1950-2010. (a) Precipitation average annual total in millimeters, (b) precipitation annual trend in mm/decade. Only trend results statistically significant at 10% or better are shown …… 100

Figure 3.10. Spatially averaged regional precipitation totals for each month ……100

Figure 3.11. Spatially averaged rate of change of monthly total precipitation in mm/decade, from 1950-2010. Results include all calculated trend values ……101

Figure 3.12. Precipitation trends in mm/decade, 1950-2010, for (a) March, (b) May, and (c) July, and (d) November. Only trend results statistically significant at 10% or better are shown …… 102

Figure 3.13. Trend persistence maps where colour corresponds to number of months with increasing or decreasing trend through the cold season (November to April) or the warm season (May to October) (a) decreasing precipitation trend persistence through the cold season, (b) increasing precipitation trend persistence through the warm season ……. 103

Figure 3.14. Mean annual snow accumulation and trends for 1950-2010. (a) mean annual snow accumulation in mm SWE, (b) annual trend of snow accumulation in mm SWE/decade. Only trend results statistically significant at 10% or better are shown ……103

Figure 3.15. Spatially averaged snow accumulation totals for each month …….. 104

Figure 3.16. Monthly snow accumulation trends in mm SWE/decade spatially averaged for each study region, from 1950-2010. Results include all calculated trend values ……...105

Figure 3.17. Snow accumulation trends in mm SWE/decade, 1950-2010, for (a) November, (b) December, (c) January, (d) February, (e) March, and (f) April. Only trend results statistically significant at 10% or better are shown ……. 106

Figure 3.18. Snow accumulation trend persistence through the cold season (November to April). Colour corresponds to number of months with increasing or decreasing trend. (a) decreasing trend persistence, (b) increasing trend persistence …… 107

Figure 3.19. Mean annual snowmelt and trends for 1950-2010. (a) Mean annual snowmelt in mm SWE, (b) annual snowmelt trends in mm SWE/decade. Only trend results statistically significant at 10% or better are shown……...107

Figure 3.20. Spatially averaged snowmelt totals for each month ……..108

Figure 3.21. Spatially averaged rate of change of monthly total snowmelt in mm/decade, from 1950-2010. Results include all calculated trend values ……108

Figure 3.22. Snowmelt trends in mm/decade, 1950-2010, for (a) January, (b) February, (c) March, (d) April, (e) May, and (f) June. Only trend results statistically significant at 10% or better are shown ……. 109

Figure 4.1. CROCWR study area with watersheds labeled by name and study regions identified by colour ……142

Figure 4.2. Hypsometric curves of each study region ……142

Figure 4.3. Multi-model mean of mean annual maximum temperature for the current and future time periods, and the expected difference. (a) Current, (b) future, (c) difference ……..143

Figure 4.4. Multi-model mean of mean annual minimum temperature for the current and future time periods, and the expected difference. (a) Current, (b) future, (c) difference ……144

Figure 4.5. Daily average Tmax for each month during the current and future periods spatially averaged for each study region. Current period shown with unfilled symbols and dashed lines, future period shown with solid symbols and lines ……145

Figure 4.6. Daily average Tmin for each month during the current and future periods spatially averaged for each study region. Current period shown with unfilled symbols and dashed lines, future period shown with solid symbols and lines ……146

Figure 4.7. Spatially averaged regional change in monthly mean Tmax and Tmin between the current and future periods. Tmax shown with solid symbols, Tmin shown with unfilled symbols ……147

Figure 4.8. Multi-model mean difference between Tmax values between the current and future periods during (a) January, (b) April, (c) July, and (d) November …….148

Figure 4.9. Multi-model mean difference between Tmin values between the current and future periods during (a) January, (b) April, (c) July, and (d) November …….149

Figure 4.10. Number of models showing increasing or decreasing rates of change in Tmax during the current and future time periods during January …….150

Figure 4.11. Number of models showing increasing or decreasing rates of change in Tmin during the current and future time periods during January ……..150

Figure 4.12. Number of models showing increasing or decreasing rates of change in Tmax during the current and future time periods during April ……151

Figure 4.13. Number of models showing increasing or decreasing rates of change in Tmin during the current and future time periods during April ……..151

Figure 4.14. Number of models showing increasing or decreasing rates of change in Tmax during the current and future time periods during July ……...152

Figure 4.15. Number of models showing increasing or decreasing rates of change in Tmin during the current and future time periods during July ……..152

Figure 4.16. Number of models showing increasing or decreasing rates of change in Tmax during the current and future time periods during November ……...153

Figure 4.17. Number of models showing increasing or decreasing rates of change in Tmin during the current and future time periods during November ……...153

Figure 4.18. Multi-model mean of mean annual precipitation for the current and future time periods, and the expected difference. (a) Current, (b) future, (c) difference ……...154

Figure 4.19. Precipitation during each month in the current and future periods spatially averaged for each study region. Current period shown with unfilled symbols and dashed lines, future period shown with solid symbols and lines ……...155

Figure 4.20. Spatially averaged regional change in monthly precipitation between the current and future periods ……..156

Figure 4.21. Multi-model mean difference between monthly precipitation between the current and future periods during (a) January, (b) May, (c) August, and (d) November ……..157

Figure 4.22. Number of models showing increasing or decreasing rates of change in precipitation during the current and future time periods during January ……..158

Figure 4.23. Number of models showing increasing or decreasing rates of change in precipitation during the current and future time periods during May ……...158

Figure 4.24. Number of models showing increasing or decreasing rates of change in precipitation during the current and future time periods during August ……..159

Figure 4.25. Number of models showing increasing or decreasing rates of change in precipitation during the current and future time periods during November ……..159

Figure 4.26. Multi-model mean of April 1st SWE for the current and future time periods, and the expected difference. (a) Current, (b) future, (c) difference ……..160

Figure 4.27. SWE at the end of each month in the current and future periods spatially averaged for each study region. Current period shown with unfilled symbols and dashed lines, future period shown with solid symbols and lines ……...161

Figure 4.28. Spatially averaged regional change in monthly SWE between the current and future periods …… 162

Figure 4.29. Multi-model mean difference between monthly SWE between the current and future periods during (a) January, (b) April, (c) September, and (d) November ……163

Figure 4.30. Number of models showing increasing or decreasing rates of change in SWE during the current and future time periods during January ……164

Figure 4.31. Number of models showing increasing or decreasing rates of change in SWE during the current and future time periods during April ……164

Figure 4.32. Number of models showing increasing or decreasing rates of change in SWE during the current and future time periods during November ……165

Figure 4.33. Multimodel mean of annual snowmelt for the current and future time periods, and the expected difference. (a) Current, (b) future, (c) difference ……166

Figure 4.34. Monthly snowmelt in the current and future periods spatially averaged for each study region. Current period shown with unfilled symbols and dashed lines, future period shown with solid symbols and lines ……167

Figure 4.35. Spatially averaged regional change in monthly snowmelt between the current and future periods ……..168

Figure 4.36. Multimodel mean difference between monthly snowmelt between the current and future periods during (a) January, (b) February, (c) March, (d) April, (e) May, and (f) June ……169

Figure 4.37. Number of models showing increasing or decreasing rates of change in snowmelt during the current and future time periods during January ……..170

Figure 4.38. Number of models showing increasing or decreasing rates of change in snowmelt during the current and future time periods during April ……...170

Figure 4.39. Number of models showing increasing or decreasing rates of change in snowmelt during the current and future time periods during May ……...171

Acknowledgements

First and foremost, I would like to thank my supervisor, Dr. Terry Prowse, and committee members, Dr. Yonas Dibike and Dr. Barrie Bonsal, for all the guidance, support, and feedback they provided on this work. Your knowledge and experience taught me a great deal during the course of this research. I also want to thank the other members of the CROCWR team, Dr. Don Burn and Dr. Tom Edwards, in addition to Dr. Prowse, Dr. Dibike, and Dr. Bonsal, for contributing to the idea of a multi-disciplinary hydroclimatic research project, and for providing ideas and expertise. I am also grateful for the ideas, discussions, support, and friendship of the CROCWR students Roxy Ahmed, Allison Bawden, and Brandi Newton. It was a privilege to work with all of you. Thank you to my parents, Patricia and Larry Linton, and my brother Brett Linton, for love and support throughout my education. Thank you for always being there for me. A special thank you as well to my grandparents, Beecher and Evelyn Linton, for wanting to provide all their grandchildren with the opportunity to get an education, this would have been much more difficult without your generosity. Last, but certainly not least, thank you to my amazing and loving fiancé, Lucas O'Neil, for the unconditional support in everything I do and inspiring me to be my best.

1. Chapter 1: Introduction

1.1 Introduction

The world's freshwater reserves fluctuate widely by season and region due to variations in climate. Climate is a major controlling factor of the hydrological cycle; and the availability of water resources on a regional scale is one of the most important aspects of climate change related to the modification of the hydrological cycle (Xu & Singh 2004). Numerous changes have already been linked to rising air temperatures, including increasing atmospheric water vapour content and the resulting changes in precipitation patterns, snow cover reductions, melting of ice, and fluctuations in runoff and soil moisture (Bates et al. 2008). Therefore, examining the linkages between hydrologic and climatic variables, such as temperature, precipitation, snow depth, and snowmelt, can also supply additional insight into the causes of observed trends in river flow. Study of spatial and temporal variations in trends of hydrologic and climatic variables will provide a better understanding of what changes have occurred, and through the use of global and regional climate models, what changes may occur in the future. Water is tremendously important for both society and nature, and understanding how a change in global climate could affect regional water supplies is essential for future water resources planning (Xu & Singh 2004; Kienzle et al. 2012).

Much of the river flow in western Canada originates as mountain snowpack, particularly from the northern Rocky Mountains, so any change in climate of this region will result in substantial shifts to runoff patterns (Payne et al. 2004). The northern Rocky Mountains form the headwaters of some of North America's largest river systems: the Mackenzie

River, the Saskatchewan River and the Columbia River (Stewart et al. 2004; Déry 2005). Mountain watersheds are a key source of water for downstream users; the spring freshet provides a significant contribution to annual streamflow of rivers originating in the Rocky Mountains, and is comprised of snowmelt from accumulation of snow during the cold season (Prowse et al. 2010; Kienzle et al. 2012). Mountain snowpack and snowmelt runoff are important sources of water throughout the study area for water resource management, agriculture, hydro-electric power generation, management of fisheries, and plant and animal communities (Cohen 1991; Fleming et al. 2007).

The major drainage basins of western Canada drain in different directions to various bodies of water, and across the border into the United States. The Mackenzie River is the main North American river that transports freshwater to the Arctic Ocean (Woo & Thorne 2003). The freshwater inflow to the Arctic is an important factor in determining ocean convection in the sub-Arctic seas. Any alteration to the Arctic or sub-Arctic hydrological cycle can lead to changes in the amount of freshwater reaching the Arctic Ocean, which may have implications for global thermohaline circulation and ultimately global climate (Holland et al. 2007; Min et al. 2008). Flow from rivers such as the Saskatchewan and Columbia is critical to water-resource use, particularly in the dry, prairie interior of the mid-west. Given that these are primarily nival river regimes, any climate-induced changes that affect the magnitude of their alpine snow accumulations, or the timing and volume of their subsequent melt, can have widespread downstream implications. For example, if snowmelt occurs earlier, it will likely decrease summer-autumn flows, extend summer drought in downstream dry regions and, because of lower flows and higher water temperatures, stress aquatic ecosystems (e.g., Stewart 2009). The

boundaries between these major watersheds are in close proximity, so the spatial distribution of snowfall and snowmelt can determine whether snowmelt contributes to the Mackenzie, Saskatchewan or Columbia rivers. Any north-south or east-west shifts in temperature and precipitation can have major effects on where the snowfall and snowmelt occur, and thus what water resources are available in each region.

A large portion of previous research has focused on the above-mentioned topics in the Mackenzie Basin, which includes the Peace River, Athabasca River, Liard River, Great Slave Lake and Mackenzie River (Moore & McKendry 1996; Woo & Thorne 2003; Burn 2008; Burn et al. 2005). These studies have generally focused on researching river flow, trends in temperature and precipitation, influences of climate on river flow, trends in hydrological variables, trends in snow accumulation and snowmelt, and comparing trends between watersheds. Further understanding of how climate affects hydrologic regimes would be beneficial for water-resources planning. Improving scientific knowledge of continental-scale as well as regional climatic and hydrologic processes will also help to determine how long-term variations in snow cover affect discharge in large, high-latitude watersheds (Dyer 2008). Studying the linkages between climate change and observed hydrologic trends are a common recommendation in previous research (Abdul Aziz & Burn 2006; Burn & Hag Elnur 2002).

The scope of many previous studies provides valuable information on individual river systems and watersheds or very large continental-scale regions, but this approach does not provide insight into hydroclimatic changes that modify the spatial distribution of rainfall and snowfall between the drainage basins of western Canada, and thus regional

water availability in these major river systems. This research includes analysis of temporal trends as well as spatial distribution of trend values within multiple major drainage basins, which has not been previously done at this scale; the combination of a very large study area in addition to a high spatial resolution dataset is rare in previous studies. The inclusion of trend persistence analysis is also uncommon in previous research, since many studies focus on seasonal or annual trends rather than monthly results. The results of this study provide information on annual as well as intra-annual trends and spatial variation in climate variables that are most likely to affect streamflow, including maximum and minimum air temperature, precipitation, snow accumulation, and snowmelt. These variables affect streamflow in both small regional scale watersheds as well as large drainage basins on a continental scale.

1.2 The CROCWR Project

Hydroclimatic changes have been previously documented for western Canada, though research has primarily focused on small regions or at coarser scales. Given the heterogeneous changes to surface climate regimes in western Canada, it is necessary to evaluate hydroclimatic trends and variability within sub-basins of large watersheds to determine ‘water rich’ and ‘water poor’ regions as well as north-south or east-west shifts to precipitation and snowfall patterns that can modify drainage patterns affecting freshwater input to the Hudson Bay as well as the Arctic and Pacific Oceans. The Climatic Redistribution of western Canadian Water Resources (CROCWR) project was designed to quantify past, current, and potential future changes to water distribution in Canada. The analysis includes several individual studies that focus on evaluation of a series of hydroclimatic variables including atmospheric circulation patterns,

hydroclimatic variables affecting streamflow, and streamflow (Prowse et al. 2013). Water resources are essential for hydroelectricity generation, agricultural production, municipal and industrial use, and ecological integrity. Therefore, results from the CROCWR study will be invaluable to water resource managers and policy makers, as well as an integral component to evaluating the freshwater budget of the Arctic Ocean.

1.3 Objectives

This research investigates the temporal and spatial variations in hydroclimatic conditions across western Canada, including analysis of historical trends and projected future conditions, with emphasis on assessing the spatial redistribution of western Canadian water resources. This involves meeting three primary objectives: (1) the first objective is to assess historical trends in hydroclimatic variables affecting river flows in western Canada using interpolated, gridded data (temperature, precipitation, snow depth, snowmelt) for the time period 1950-2010, (2) the second objective is to assess possible future scenarios in the same hydroclimatic variables using regional climate model outputs for the time period 2041-2070, and (3) the third objective is to assess spatial variation in historical trends and possible future changes of the above hydroclimatic variables across western Canada. The variables chosen for study were selected for their strong influence on streamflow, particularly the spring freshet. There are many other climatic variables that also affect streamflow, but the scope of the research was not large enough to include all possible variables.

1.4 Thesis Structure

This thesis contains five chapters. Chapter 1 includes a general background to the research, gaps in the literature, and the main purpose and objectives of the study. Chapter 2 reviews the literature relevant to this research including background knowledge regarding the techniques employed in the various analyses. Chapter 3 addresses objectives 1 and 3 in a journal-style manuscript. Chapter 4 addresses objectives 2 and 3, also written as a journal-style manuscript. The summary and conclusions are located in Chapter 5. Due to Chapters 3 and 4 being written as scientific journal-style manuscripts, some material presented in Chapter 1 and 2 will be repeated in Chapter 3 and 4 where necessary.

Presentations and Publications

The section below provides a comprehensive list of conference presentations and published proceedings that contain results from research, or components thereof, appearing in Chapters 3 and 4.

Linton, H.C., Prowse, T.D., Dibike, Y.B. & Bonsal, B.R. (2012). Spatial and temporal variation in the hydroclimatology of western Canada: Methodology and preliminary results (poster). Presented at annual meeting of the Canadian Geophysical Union and Canadian Water Resources Association, Banff, AB, Canada.

Linton, H.C., Prowse, T.D., Dibike, Y.B. & Bonsal, B.R. (2012). Climatic Redistribution of Western Canadian Water Resources (CROCWR): Spatial and temporal variation in the hydroclimatology of western Canada (poster). Presented at the annual meeting of the American Geophysical Union, San Francisco, CA, USA.

Linton, H.C., Prowse, T.D., Dibike, Y.B. & Bonsal, B.R. (2012). Spatila and temporal trends in hydroclimatic variables across the Mackenzie River basin (poster). Presented at the ArcticNet annual scientific meeting, Vancouver, BC, Canada.

Linton, H.C., Prowse, T.D., Dibike, Y.B. & Bonsal, B.R. (2013). Temporal and spatial variations in hydroclimatic variables affecting streamflow across western Canada: a CROCWR component (oral presentation). Presented at the annual meeting of the Canadian Geophysical Union, the Canadian Water Resources Association, and Canadian Meteorological and Oceanographic Society, Saskatoon, SK, Canada.

Linton, H.C., Prowse, T.D., Dibike, Y.B. & Bonsal, B.R. (2013). Spatiotemporal trends in climatic variables affecting streamflow across western Canada from 1950-2010: a CROCWR component. Proceedings of the 19th Northern Research Basins Symposium, ed. Stuefer, S.L. and Bolton, W.R., Southcentral Alaska, pp. 167S177.

Linton, H.C., Prowse, T.D., Dibike, Y.B. & Bonsal, B.R. (2013). Spatiotemporal trends in climatic variables affecting streamflow across western Canada from 1950-2010: a CROCWR component (oral presentation). Presented at the 19th Northern Research Basins Symposium, Southcentral Alaska, AK, USA.

References

Abdul Aziz, O. & Burn, D. 2006. Trends and variability in the hydrological regime of the Mackenzie River Basin. *Journal of Hydrology, 319*, 282-294.

Bates, B.C., Kundzewicz, Z.W., Wu S. & Palutikof, J.P. Eds. 2008. *Climate Change and Water: IPCC Technical Paper VI*, Geneva: IPCC Secretariat.

Bhangu, I. & Whitfield, P.H. 1997. Seasonal and long-term variations in water quality of the Skeena River at Usk, British Columbia. *Water Resources, 31*(9), 2187-2194.

Burn, D.H. 2008. Climatic influences on streamflow timing in the headwaters of the Mackenzie River Basin. *Journal of Hydrology, 352,* 225- 238.

Burn, D.H., Abdul Aziz, O.I. & Pietroniro, A. 2005. A Comparison of Trends in Hydrological Variables for Two Watersheds in the Mackenzie River Basin. *Canadian Water Resources Journal, 29*(4), 283-298.

Burn, D.H. & Hag Elnur, M.A. 2002. Detection of hydrologic trends and variability. *Journal of Hydrology, 255*.

Cohen, S.J. 1991. Possible impacts of climatic warming scenarios on water resources in the Saskatchewan River sub-basin, Canada. *Climatic Change, 19,* 291-317.

Dyer, J. 2008. Snow depth and streamflow relationships in large North American watersheds. *Journal of Geophysical Research, 113*(D18), 1-12.

Fleming, S.W., Whitfield, P.H., Moore, R.D. & Quilty, E.J. 2007. Regime-dependent streamflow sensitivities to Pacific climate modes cross the Georgia-Puget transboundary ecoregion. *Hydrological Processes, 21*, 3264-3287.

Holland, M.M., Finnis, J., Barrett, A.P. & Serreze, M.C. 2007. Projected changes in Arctic Ocean freshwater budgets. *Journal of Geophysical Research, 112,* doi:10.1029/2006JG000354.

Kienzle, S.W., Nemeth, M.W., Byrne, J.M. & MacDonald, R.J. 2012. Simulating the hydrological impacts of climate change in the upper North Saskatchewan River basin, Alberta, Canada. *Journal of Hydrology, 412,* 76-89

Leconte, R., Peters, D., Pietroniro, A. & Prowse, T. 2006. Modelling climate change impacts in the Peace and Athabasca catchment and delta: II - variations in flow

and water levels with varying winter severity. *Hydrological Processes*, *20*, 4215-4230.

McCuaig, S.J. & Roberts, M.C. 2002. Topographically-independent ice flow in northwestern British Columbia: implications for Cordilleran Ice Sheet reconstruction. *Journal of Quaternary Science*, *17*(4), 341-348.

Min, S.K., Zhang, X. & Zwiers, F. 2008. Human-induced Arctic moistening. *Science*, *320*, 518-520.

Moore, R. & McKendry, I. 1996. Spring snowpack anomaly patterns and winter climatic variability. *Water Resources Research*, *32*(3), 623-632.

Payne, J.T., Wood, A.W., Hamlet, A.F., Palmer, R.N. & Lettenmaier, D.P. 2004. Mitigating the effects of climate change on the water resources of the Columbia River Basin. *Climate Change*, *62*, 233-256.

Pederson, G.T., Gray, S.T., Woodhouse, C.A., Betancourt, J.L., Fagre, D.B., Littell, J.S., Watson, E., Luckman, B.H. & Graumlich, L.J. 2011a. The unusual nature of recent snowpack declines in the North American cordillera. *Science*, *333*, 332-335.

Pederson, G.T., Gray, S.T., Ault, T., Marsh, W., Fagre, D.B., Bunn, A.G., Woodhouse, C.A. & Graumlich, L.J. 2011b. Climatic controls on the snowmelt hydrology of the Northern Rocky Mountains. *Journal of Climate*, *24*(6), 1666-1687.

Prowse, T., Shrestha, R., Bonsal, B. & Dibike, Y. 2010. Changing spring air-temperature gradients along large northern rivers: Implications for severity of river-ice floods. *Geophysical Research Letters*, *37*, doi:10.1029/2010GL044878

Prowse, T.D., Bonsal, B.R., Burn, D.H., Dibike, Y.B., Edwards, T., Ahmed, R., Bawden, A.J., Linton, H.C., Newton, B.W. & Walker, G.S. 2013. Climatic Redistribution of Canada's Western Water Resources (CROCWR). Proceedings of the 19th International Northern Research Basins Symposium and Workshop, Southcentral Alaska, USA, August 11-17th, 2013.

Stewart, I.T. 2009. Changes in snowpack and snowmelt runoff for key mountain regions. *Hydrological Processes*, *23*, 78-94.

Thorne, R. & Woo, M. 2011. Streamflow response to climatic variability in a complex mountainous environment: Fraser River Basin, British Columbia, Canada. *Hydrological Processes*, *25*, 3076-3085.

Woo, M.-ko & Thorne, R. 2003. Streamflow in the Mackenzie Basin, Canada. *Arctic Institute of North America, 56*(4), 328-340.

Xu, C.Y. & Singh, V.P. 2004. Review on regional water resources assessment models under stationary and changing climate. *Water Resources Management, 18*, 591-612.

2. Chapter 2: Literature Review

2.1 Introduction

Freshwater reserves throughout the world fluctuate widely by season and region due to climate change and variability. Changes to regional water availability will affect many aspects of human society, from agricultural productivity and energy use to flood control, municipal and industrial water supply, and fisheries and wildlife management (Xu & Singh 2004). Examining the linkages between hydrologic and climatic variables, such as temperature, precipitation, snow depth, and snowmelt, can also supply more information on observed trends in river flow. Numerous changes have been linked to increasing air temperatures, including increasing atmospheric water vapour content and the resulting changes in precipitation patterns, snow cover reductions, melting of ice, and changes to runoff and soil moisture (Bates et al. 2008). Understanding how such changes in climate affect hydro-climatic conditions in critical water-supply regions is essential for effective water-resource planning (Xu & Singh 2004).

A large portion of the river flow to the Canadian Arctic originates in the mid-latitudes, particularly from alpine snowpacks of the Northern Rocky Mountains, which serves as the headwaters of some of the largest river systems in North America, including the Mackenzie, Saskatchewan and Columbia rivers (Stewart et al. 2004; Déry 2005). These rivers are primarily nival river regimes, therefore any climate-induced changes that affect the magnitude of their alpine snow accumulations, or the timing and volume of their subsequent melt, can thus have widespread downstream implications (Bates et al. 2008).

This chapter provides a summary of previous research which covers detected trends in historical and projected hydroclimatic variables; these are discussed on a global/continental basis, followed by national and regional trends within the study area of western Canada. Then research gaps are identified for both the historical and future periods. Background information about the study region of western Canada follows, which includes the Mackenzie River, Saskatchewan River, the Fraser and Columbia Rivers, and several smaller rivers which drain northern BC to the Pacific Ocean. Sources of data are then identified for the historical and future time periods followed by methods of spatial and temporal analysis. As this thesis is presented in manuscript format, some material from this chapter may be repeated in Chapters 3 and 4 where necessary.

2.2 Historical Trends in Climatic and Hydrologic Variables

Previous studies have detected trends in many climatic and hydrologic variables. Between 1901 and 2005, the global temperature has increased by 0.74^{o}C, but with warming occurring at a greater rate since the 1970s (Bates et al. 2008). However, temperature increases are not spatially or temporally uniform, and many areas of the world have experienced temperature changes that differ from the global mean. For example, temperatures in northern latitudes have warmed more than the global mean, with an increase of 1.2^{o}C in the annual mean temperature over Canada between 1953 and 2005 (Vincent et al. 2007). Diurnal temperature range is another important aspect of climate variability, and daily minimum temperatures have been shown to be rising twice to three times as much as the daily maximum temperatures, thus decreasing the diurnal temperature range (Akinremi et al. 1999; Karl et al. 1993). Although there is evidence that the rate of decrease to the diurnal temperature range has slowed or perhaps stopped

in some parts of the northern hemisphere, including western Canada (Vose et al. 2005). Zhang et al. (2000) detected an average temperature increase of 0.9^{o}C between 1900 and 1999 throughout southern Canada with the largest seasonal increases occurring during winter and spring. The Prairies show a range of seasonal warming of 1-3^{o}C for the same time period (Zhang et al. 2000). Temperature increases also occurred throughout BC and the Yukon between 1976 and 1995, with the greatest increases during winter and spring (Whitfield 2001).

Precipitation has also changed over many regions of the world. However, unlike temperature, it tends to show a greater degree of spatial, and in some cases, inter-decadal variability. Bates et al. (2008) detected increased precipitation over northern latitudes (30-85^{o}N). Heavy precipitation events throughout Canada have increased between 1945 and 1995, but this is attributed mostly to winter precipitation increases in northern Canada, with little change throughout the remainder of the country (Zhang et al. 2001b). In southern Canada, precipitation has increased by 12-13% since the early 1900s (Groisman & Easterling 1994; Zhang et al. 2000). Vincent & Mekis (2006) show that the number of days with precipitation has increased over much of southwestern Canada from 1950-2003, though the number of days with rainfall each year has increased, the snow to total precipitation ratio has decreased. This trend has also been detected over the past 75 years, with rainfall increasing while snowfall decreases, likely due to increased temperatures (Akinremi et al. 1999). Precipitation in coastal BC increased 7.2% during the instrumental record of 1920-2001 (Groisman et al. 2005). Throughout non-coastal BC, precipitation during winter increased between 1986 and 1995 compared to the previous ten years, while precipitation decreased during fall (Whitfield 2001).

Snow is considered to be an important climate change indicator because of its sensitivity to temperature changes, and also because climate change is predicted to have the greatest warming effects in northern snow-covered areas (Brown & Braaten 1998). Snow cover across North America is generally decreasing in depth as well as extent. Temperature increases can modify the proportion of rainfall to snowfall, this has been particularly evident at northern latitudes (Davis et al. 1999). As temperatures fluctuate across the freezing point of water, snowpack in mountainous regions are directly affected by changes to the percentage of precipitation falling as rain or snow and melt anomalies (Kapnick & Hall 2011). Widespread warming has occurred across North America between 1916 and 2003, which has resulted in an overall decrease in snow water equivalent (Hamlet et al. 2005). Western North America is particularly sensitive to this, since many mountainous areas near the Pacific coast have average winter and spring temperatures only slightly below 0^{o}C (Adam et al. 2009). Between 1949 and 2004, the fraction of precipitation that fell as snow declined in the western United States while the fraction that fell as rain increased, this change was particularly evident during the November-March cold season and at low to moderate elevations (Knowles et al. 2006). Throughout Canada, snow and ice cover are disappearing earlier in the year and monthly snow depth measurements show decreasing patterns in nearly all months of the year (Brown & Braaten 1998). In southern Canada, snowfall decreased 10-20% between 1950 and 2003 (Vincent & Mekis 2006). Declines to the maximum snowpack as well as the annual number of days with snowpack have also occurred throughout the Prairies since the 1950s (Schindler & Donahue 2006). Northwestern Canada has shown a statistically significant decreasing trend in snow depth of -0.25cm per year between 1960 and 2000

(Dyer & Mote 2006). Mote et al. (2005) estimated April 1st snow depths in the northern Rockies to have decreased 15-30% between the time periods 1945-1955 and 1990-1997.

Contrary to most detected trends, some areas located at higher elevations and higher latitudes have shown an upward trend in snow water equivalent (Hamlet et al. 2005). Zhang et al. (2001b) detected increases in snowfall in northern Canada between 1900 and 1998, particularly during autumn and winter. Arctic regions of Canada also experienced snowfall increases between 1950 and 2003, with values up to 50mm SWE total increase (Vincent & Mekis 2006). Moore & McKendry (1996) detected a heavier than average snowpack over many regions within British Columbia beginning in the late 1970s. The study also detected a variable pattern of low and high snowpacks, with either a greater than average snowpack in the northern areas and less than average snowpacks in the southern regions, or a less than average snowpack over most of the study area (Moore & McKendry 1996).

There are many ways in which climate affects hydrology. However, a few of the currently known and detected changes in climate can have varied effects on hydrologic regimes. For example, an increase in precipitation can cause an increase in streamflow, but the relationship will not necessarily be a direct, linear relationship (Zhang et al. 2000). The spatial and temporal distributions of snow cover can have impacts on local snowmelt release, global and regional atmospheric circulation, and global and local climate and hydrological cycles (Farmer et al. 2009). Research has shown that winter snow storage and melt are strongly related to both the peak magnitude and total discharge of high-latitude rivers, particularly in the late winter and early spring as a result of spring

runoff (Dyer 2008). An increase in average temperature can also lead to increased evaporation, potentially decreasing streamflow, increasing spring temperatures may cause an earlier ice break-up, and warmer winter temperatures may cause a decrease in the snowpack which can lead to a decreased spring freshet (Zhang et al. 2000; Burn & Elnur 2002).

Burn & Elnur (2002) detected that spring freshet was occurring earlier, ice conditions were ending earlier, winter flows were increasing and annual mean flow was decreasing across Canada for the period of 1960-1997. Annual mean flow is mostly decreasing throughout western Canada, but flow increases have been detected in BC during March and April, which are likely related to earlier snowmelt (Burn & Elnur 2002). The winter increases to streamflow throughout western Canada, particularly in the south and at lower elevations, are likely related to a greater frequency of mid-winter snowmelt (Moore & McKendry 1996). The spring freshet date is occurring earlier in the Mackenzie Basin (Burn 2008; de Rham et al. 2008), as well as throughout western Canada (Zhang et al. 2001a; Bonsal & Prowse 2003; Stewart et al. 2005; Schindler & Donahue 2006). The southern Prairies also show decreasing annual streamflow (St. Jacques et al. 2010), with decreases of 20-84% to summer flow since the early 20th century (Schindler & Donahue 2006).

Many aspects of historical climate have been studied in Canada, with a great deal of research focusing on temperature and precipitation either annually or seasonally on either very small areas (watersheds) or very large areas (Canada or Mackenzie River basin). Another common research focus is snow depth and snowmelt, often focusing on snow

cover extent or SWE measurements and snowmelt timing. However, research at a high spatial resolution has not previously been completed on temperature, precipitation, snow depth, and snowmelt over a large geographic area such as western Canada. Generally, high spatial resolution data are used over small areas and coarser resolution data are used over large areas as they are more readily available over large, spatially continuous regions.

2.3 Future Projections in Climatic and Hydrologic Variables

Global temperature has been increasing over the past century and the warming is expected to accelerate in the future due to anthropogenic forcing (Meehl et al. 2007). Between the 1971-2000 and 2041-2070 time periods, surface air temperatures in the Northern Hemisphere are projected to increase 0.5-3°C, with the greatest warming occurring in Arctic regions (Adam et al. 2009). Reduced snow cover and decreased albedo are likely to create a positive feedback loop in Arctic regions, and thus increase temperature in northern latitudes by as much as 10^{o}C by 2099, while projected increases across North America range from 3-5^{o}C during the summer months (Christensen et al. 2007). Warming is expected across North America at a rate greater than the global mean, with the higher latitudes and colder months of the year likely to experience the most warming (Christensen et al. 2007; Šeparović et al. 2013). Increases in annual mean temperature of 2-3^{o}C are forecast across Western North America for the same time period (Stewart et al. 2004). The projected temperature changes during winter include a strong north-south warming gradient in many RCMs, though summer warming does not show a clear pattern (de Elía et al. 2013). Annually, mean temperature throughout the Prairies is predicted to increase 4.8-8.4^{o}C at specific study sites by 2100, as estimated by the CGCM

model when driven by the A2 emissions scenario (Schindler & Donahue 2006). Bonsal et al. (2012) stated that annual temperature in the southern Prairies is likely to increase 4.0-5.6^{o}C by the late twenty-first century, according to several GCM runs forced with the A2 emissions scenario. Climate projections also show increases to annual mean temperature throughout BC, agreed upon by multiple models driven by multiple global climate models (GCMs) and emission scenarios (Schnorbus et al. 2014).

Precipitation is projected to increase in many areas as well. Precipitation is expected to increase over much of the global land surface, particularly over the mid- to high-latitudes in the Northern Hemisphere (Adam et al. 2009). The majority of GCMs project increases in high-latitude precipitation (Min et al. 2008). However, multi-model means sometimes tend to significantly underestimate observed trends (Zhang et al. 2007), which implies that projections of future precipitation may also be underestimated (Min et al. 2008). Annual mean precipitation in northern regions is predicted to increase by at least 20% by 2099, with increases of up to 30% in the winter months, but decreases of -20% during the summer months (Christensen et al. 2007). Increases in annual precipitation of 5-15% in western Canada are expected by GCMs when CO_2 in the future is anticipated to double by 2040-2060 (Groisman et al. 2005). RCM analysis indicates possible precipitation increases during winter of 10-40%, mostly in areas of low elevation, and summer decreases of -10 to -40% in coastal areas and the Prairies by 2100 when compared to 1981-2000 (Šeparović et al. 2013). Schnorbus et al. (2014) stated that precipitation in the Columbia River basin is projected to increase mostly in the fall and winter by the 2050s, with decreases during the summer.

Increases in extreme precipitation are also expected across much of North America. One potential cause for increasing precipitation is that a warmer atmosphere will allow for a higher water vapour content, thus precipitation–producing systems will have increased availability of atmospheric moisture (Kunkel 2003; Davis et al. 1999). The Northern Hemisphere is projected to receive increased instances of heavy and extreme precipitation, especially when models include human-induced increases to greenhouse gases in the atmosphere (Min et al. 2011). Heavy precipitation is expected in the form of snowfall events in northern Canada throughout the fall and winter (Zhang et al. 2001b). RCMs predict extreme precipitation events will increase 5-12% in the Pacific and Prairie regions, 13-19% in the Yukon and Mackenzie Basin, and 11-13% in the Western Cordillera and Rocky Mountain regions by the 2041-2070 time period when compared to a current period covering 1961-1990 (Mladjic et al. 2011). However, RCMs also predict an increase in dry days and dry spells in southern regions of Canada (Sushama et al. 2010). Droughts in the southern Canadian Prairies are likely to be longer and more frequent in the twenty-first century than those that occurred throughout the current twentieth century (Bonsal et al. 2012).

Snowpacks in western North America have also declined in recent decades, and are likely to continue declining throughout the twenty-first century (Pederson et al. 2011a). Projected trends in snowfall indicate the possibility of positive trends at higher latitudes and higher elevations, with negative trends in the midlatitudes (Krasting et al. 2013). In northern Canada, SWE is predicted to increase due to projected increases in precipitation, but in southern Canada early spring SWE is likely to decline due to increased surface air temperature and decreases to the number of snowfall events (Zhang et al. 2001b; Adam et

al. 2009). SWE is projected to decline throughout the Peace and at lower elevations in the Columbia, while SWE at higher elevations in the Columbia is expected to increase (Schnorbus et al. 2014).

The increases in temperature and precipitation cause many changes to the other aspects of climate and hydrology of a region. Increasing spring temperatures lead to an earlier ice break-up and warmer winter temperatures contribute to decreased snowpack which can lead to a decreased spring freshet and a decline in the amplitude of the snowmelt flood wave (Burn & Elnur 2002; Kerkhoven & Gan 2011). In western Canada, the spring freshet is expected to occur anywhere from 5-35 days earlier by 2099, with the largest changes expected to occur in the Pacific Northwest and Rocky Mountains (Stewart et al. 2004). Reduced summer streamflow is also anticipated throughout the Rocky Mountains, with declines in low flows during low flow months (Kerkhoven & Gan 2011). Streamflow in the Peace and Upper Columbia Rivers is predicted to decrease during the summer and fall, while flow in the winter and spring may increase (Schnorbus et al. 2014).

Previous research utilizing GCMs and RCMs are mostly focused on either very large areas (Northern Hemisphere, North America) or very small areas (watersheds). Some analysis has been done on a national scale, showing expected changes to temperature and precipitation over Canada on an annual, or sometimes seasonal, basis. Many previous studies have used GCMs, either at their original resolution or at a higher resolution using statistical downscaling methods, but RCMs have not been extensively analysed over the region of western Canada or on a monthly basis.

2.4 Study Area

The study area for this project covers western Canada, from the west coast of British Columbia to western Manitoba and from the Canada-United States border to the Mackenzie River Delta in the northernmost reaches of continental Canada (Figure 2.1). This includes the Saskatchewan, Mackenzie, Fraser, and Columbia River Basins, as well as several small basins that drain British Columbia to the Pacific. A companion study (Bawden et al. 2013) has identified a series of hydrometric stations that correspond to distinct hydro-climatic regions contained within the study area. The identified region in Figure 2.1 is based on drainage areas of 37 hydrometric stations, but these are amalgamated into eight regions for analysis.

The study area includes a variety of climatic regions, including prairie, mountain and northern permafrost areas. Much of this area exists within the alpine region, with the remainder at lower elevations in the boreal plains or prairies (Figure 2.2). The Mackenzie River basin is one of the largest river systems in the world, with a drainage area of 1,800,000km^2 (Burn 2008). The basin covers several climatic regions, including cold temperate, mountain, sub-Arctic, and Arctic zones (Woo & Thorne 2003). Several main tributaries contribute to the Mackenzie River. Both the Athabasca and Peace Rivers have their headwaters in the Rocky Mountains and then flow across prairie landscapes to the Peace-Athabasca Delta (Burn 2008). The Athabasca and Peace Rivers both contribute flow to the Peace-Athabasca Delta, which drains into Lake Athabasca. Lake Athabasca is drained by the Slave River, which flows north into Great Slave Lake (Leconte et al. 2006). The primary outlet of Great Slave Lake is the Mackenzie River, which flows north to the Arctic Ocean. The Liard River joins the Mackenzie River near

Great Slave Lake, contributing flows from headwater locations in the Yukon, Northwest Territories, British Columbia, and Alberta (Burn 2008).

The Saskatchewan River Basin has a drainage area of approximately 364,000km^2, and includes the North and South Saskatchewan Rivers which are fed by the Red Deer and Bow Rivers (Cohen 1991). Headwaters originate as glacier and snow melt in the Rocky Mountains and flow east through the prairie grasslands, where very little runoff is contributed to the streamflow.

The Fraser River Basin covers a drainage area of approximately 217,000km^2 (Thorne & Woo 2011). The watershed boundaries consist of the Rocky Mountains in the east and the Coast Mountains in the west, with the Interior Plateau in the center. The flow of the Fraser River originates from a variety of sources, including snowmelt in spring, glacier melt in summer, and some rainfall throughout the year (Thorne & Woo 2011). The Columbia River Basin covers a portion of seven western states in the US and part of British Columbia, and has a total drainage area of approximately 696,000km^2 (Payne et al. 2004). A large portion of the flow for the Columbia River Basin is obtained from the Northern Rocky Mountains (Pederson et al. 2011b).

The basins contained in the Pacific Region consist of several rivers with small watershed areas that drain the Coast Mountains of British Columbia to the Pacific, including the Taku, Stikine, Iskut, Nass, Skeena, Kitimat, Atnarko, Bella Coola, Wannock, and Homathko Rivers. The Skeena River, for example, is one of the larger coastal basins and has a drainage area of approximately 54,000km^2 from the Central Coast of British Columbia (Bhangu & Whitfield 1997). The landscape consists of steep-sided fjords and

valleys with mountain peaks up to 2265m above sea level and alpine ice fields and glaciers occurring at the high elevations (McCuaig & Roberts 2002).

2.5 Hydroclimatic Data Sources

2.5.1 Historical Climate Data

Historical climate data can be difficult to work with in a spatial capacity due to the lack of spatial and temporal uniformity in the data; models of daily weather variables that are spatially continuous are in increasingly high demand (Hutchinson et al. 2009). Meteorological stations are generally clustered around urban and agricultural areas, but there is often a need for estimates far away from existing meteorological stations (McKenney et al. 2011). Some of the areas of greatest concern regarding climate change are the boreal forest and tundra climatic regions of central and northern Canada, but these areas have sparse coverage of meteorological stations and long term records are often incomplete (Price et al. 2000). This data requirement is met by spatial climate models which provide estimates in the form of uniform grids (McKenney et al. 2011). Few daily weather datasets exist due to various challenges in addition to those encountered when producing monthly climate datasets. These challenges include the tracking of spatial patterns related to weather fronts, vegetation, elevation, and location in relation to water bodies, as well as requiring tremendous computing power to produce and store the datasets (Hutchinson et al. 2009).

There are several datasets available for the historical period that contain data for a variety of time periods at different temporal and spatial resolutions. One of the available datasets is the North American Regional Reanalysis (NARR) dataset. NARR has a 32km x 32km

spatial resolution at 3-hourly time steps for the time period from 1979-2012 (Mesinger et al. 2006). Climate Forecast System Reanalysis (CFSR), NCEP, and ERA40 are also examples of commonly used historical reanalysis datasets. Most historical reanalysis datasets have spatial resolutions of 0.5^{o} x 0.5^{o} or 2.5^{o} x 2.5^{o} and cover the time period 1979-2012, with the exception of NCEP which covers 1948-2012 (Dee et al. 2014). The coarse spatial resolution of the reanalysis products does not capture the spatial variation throughout small, topographically complex areas within a study region.

Another option for historical analysis is gridded, interpolated climate station data. A new dataset produced by Natural Resources Canada using ANUSPLIN interpolation software has a spatial resolution of 10km x 10km, with daily timesteps, and temporal coverage from 1950-2010 (Hutchinson et al. 2009; McKenney et al. 2011). As this dataset has yet to be officially named, it is referred to in this thesis as the NRCan 2012 dataset. Hutchinson et al. (2009) describes the use of thin-plate smoothing splines used to model the complex spatial patterns that occur daily across Canada as spatially continuous functions of latitude, longitude, and elevation. Thin-plate trivariate splines are considered superior to other common interpolation methods since they tend to produce the most accurate results (Price et al. 2000; Xia et al. 2001). Since its inception, the ANUSPLIN software that utilizes thin-plate smoothing splines has grown in popularity to become one of the leading technologies in the development of climate models and has been applied in many locations around the world (McKenney et al. 2011). This climate data interpolation method is considered very effective; however it does have some limitations. ANUSPLIN-generated data incorporates the effects of elevation in the calculation of point values, since elevation is an important controlling factor in many

aspects of climate. When compared with satellite data, it appears that the method predicts values quite well over the majority of land cover types except over very high elevations (>1500m) and large bodies of water where climate stations are sparse (Bussieres and Milewska 2010). It is also possible that precipitation is underestimated due to the variability of precipitation patterns in time and space; precipitation events may have occurred that were not recorded by any climate stations and therefore cannot be accounted for in the dataset (Hutchinson et al. 2009). Despite a few potential estimation issues over some land cover types, the ANUSPLIN interpolation method is generally quite accurate at interpolating data from climate stations. The NRCan 2012 dataset was tested using a generalized cross-validation method; this is a commonly used validation measure and is considered a reliable estimate of predictive error. A second method of withholding data at spatially representative locations during the surface fitting procedure was also used and the predictive error statistics were similar, and reasonably small, for both validations tests though errors at northern latitudes were somewhat higher than those in more southern areas (McKenney et al. 2011).

The NRCan 2012 dataset was chosen for this research over the reanalysis datasets because of its high spatial resolution and temporal coverage, its daily temporal resolution, and its inclusion of maximum and minimum temperature and precipitation (Hutchinson et al. 2009; McKenney et al. 2011).

2.5.2 Future Climate Projections

Potential future climate scenarios are incredibly useful for understanding climate change and planning for resource use. However, the amount of projected change is dependent on

a variety of factors, including greenhouse gas emissions. Hence, the future climate is modelled using a variety of emission scenarios as a driving force. The IPCC has identified many possible future scenarios, but there are four main emissions scenarios used to drive most climate models: A1, A2, B1, B2 (Nakicenovic & Swart 2000). The four scenarios are characterized by emphasis on either economic and environmental values or increasing globalization and regionalization and the range of greenhouse gas emissions associated with each; the most optimistic scenarios are the A1 and B1 while the A2 and B2 are more pessimistic in terms of increased emissions in the future (Nakicenovic & Swart 2000). A newer set of emissions scenarios has also been produced that incorporate climate change mitigation into the multiple scenarios, named RCP2.6, RCP4.5, RCP6.0, and RCP8.5 for their projected radiative forcing levels in 2100 (Moss et al. 2010). Climate models produced in the past few years may use these new emissions scenarios, but many still use the previous scenarios.

Projected climate data can be obtained from multiple sources or modelled individually for research studies using various time periods and emission scenarios. Climate models are computer-based simulations of geophysical processes, and offer researchers a way to study what may occur in the near future; however, there are many uncertainties in these simulations and they all contain biases which skew the results to some extent; (Sain & Furrer 2010). One way to attempt to compensate for some of the model bias, is to complete a multi-model mean, or weighted average of available models (Sain & Furrer 2010).

Global climate models are useful for determining possible change around the globe or for studies of the northern or southern hemisphere with a resolution that allows some regional variations to be visible. Some examples of GCM research are done at the original 2.5^{o} x 2.5^{o} spatial resolution (e.g., Bonsal & Kochtubajda 2009; Mote & Salathe 2010). However, the spatial resolution of GCMs is very coarse, therefore many other researchers opt to downscale the data to improve spatial resolution through statistical downscaling (e.g., Salathe 2005; Gachon & Dibike 2007; Bonsal et al. 2012; Schnorbus et al. 2014).

Regional climate models can provide information on local and regional scale processes that are important for understanding impacts of climate variability and change (Arritt & Rummukainen 2011). One available source for modelled data in North America is NARCCAP (North American Regional Climate Change Assessment Program). NARCCAP is an international research program that provides climate scenario data for the United States, Canada and Mexico. It uses RCMs driven by a set of GCMs. The regional climate models produced by NARCCAP provide high spatial resolution (50km x 50km) climate change simulations for generation of future climate change scenarios that can be used in impacts research and cover the time periods 1971-2000 and 2041-2070 (Mearns et al. 2009). All RCMs provided by NARCCAP are based on the A2 SRES emissions scenario (Nakicenovic & Swart 2000).

This research utilized a series of models provided by NARCCAP and used an ensemble approach to view potential changes on a monthly and annual basis. The GCMs used to drive the RCMs include: Geophysical Fluid Dynamics Laboratory (GFDL) by the

National Oceanic and Atmospheric Administration, Canadian Global Climate Model 3 (CGCM3) by Environment Canada, and Community Climate System Model (CCSM) by University Corporation for Atmospheric Research. The regional climate models included are: Canadian Regional Climate Model (CRCM), Regional Climate Model 3 (RCM3) by University Corporation for Atmospheric Research, and Weather Research and Forecasting (WRFG) by Pacific Northwest National Lab. The combinations of GCMs with RCMs that are considered in the present study are as follows: CRCM-CGCM3, CRCM-CCSM, RCM3-GFDL, RCM3-CGCM3, WRFG-CGCM3, and WRFG-CCSM. The six models utilized in the analysis of possible future scenarios were chosen because they provided the appropriate spatial and temporal coverage, as well as the required variables. There were also many other regional climate models available, but those listed previously were the only ones that contained the required variables.

2.6 Methodology

2.6.1 Watershed Delineation

Watershed delineations can be created based on a series of latitude-longitude points which correspond to a selection of points located within watershed basins, hydrometric stations from Environment Canada's HYDAT database are one example. The hydrometric network is operated by the Water Survey of Canada, a branch of Environment Canada, and has 2500 active and 5500 inactive stations across the country (Environment Canada 2011). Tools in ArcGIS are capable of delineating watersheds based on a stream network consisting of connected line features, a digital elevation model (or DEM), and a series of points to distinguish each watershed outlet (Fürst & Hörhan

2009). The ArcGIS tools package ArcHydro can delineate the contributing areas for each chosen point or hydrometric station. ArcHydro is an object-oriented model capable of establishing a topological network that includes flow direction, connectivity and upstream/downstream relationships of stream segments (Fürst & Hörhan 2009). The ArcHydro package was created by ESRI (the creators of ArcGIS) along with several other researchers in order to better manage and process watershed information and improve watershed delineation methods (Hollenhorst et al. 2007).

Watershed delineations were created for the study area based on a series of latitude-longitude points which correspond to hydrometric stations from Environment Canada's HYDAT database. ArcHydro was used to delineate the contributing areas for each hydrometric station using a digital elevation model, a stream network, and points to distinguish watershed outlets (Fürst & Hörhan 2009).

2.6.2 Modelling Snowpack Data

Seasonal accumulation and melt of snow are controlling factors in the annual patterns of streamflow all around the world (Jost et al. 2012). Snowpack and snowmelt can be modeled in a variety of ways; the two primary methods include energy-balance methods and temperature-index methods. Energy-balance models provide a potentially more accurate physical basis for estimating amounts of snowmelt, but the data required to solve the energy equations are very extensive and temperature-index, or degree-day, methods can provide snowmelt estimates that are comparable to those determined by energy-balance methods (Gray & Prowse 1993). The primary advantages of temperature-index models are the wide availability of both daily temperature and daily precipitation data and

generally accurate model performance despite computational simplicity (Hock 2003; Jost et al. 2012).

Temperature-index models are based on the proportional relationship between snowmelt and air temperature (Hock 1999). Many previous studies have revealed a strong relationship between air temperature and snowmelt, including correlation coefficients as high as 0.96 between ice ablation and positive air temperature (Hock 2003). Air temperature can be a reasonable index of the energy available for snowmelt in maritime and forest climates, though it is slightly less reliable in open, exposed areas (Gray & Prowse 1993). Degree-day factors are generally considered constant across space when few temperature data points are available, which can decrease model accuracy particularly in regions with varying topography (Hock 1999). However, the use of spatially interpolated temperature and snow depth data may decrease uncertainty of temperature-index methods since data are continuous across the study area.

The most common, and simplest, snowmelt equation is

$$M = M_f(T_i - T_b)$$

where M is the meltwater depth produced over a selected interval of time, M_f is the melt factor, T_i is the air temperature, and T_b is the base temperature (Gray & Prowse 1993). T_i and T_b represent the daily mean air temperature and 0^{o}C, respectively.

As Gray & Prowse (1993) explained, there are no universal temperature-index snowmelt equations available. Atmospheric conditions, topography, geographical location, properties of the snow cover, and sometimes, time of year all modify the snowmelt

properties and so many variations on the snowmelt equation exist. The text includes multiple snowmelt equations specific to differing regions in North America, including the following equation for the mountainous region of Western Canada:

$$M = 3.0\left(T_m + \beta\left\{\left[\frac{(T_{max} - T_{min})}{8}\right] + T_{min}\right\}\right)$$

$$\beta = 0 \ when\ T_{min} \leq 0$$

$$\beta = T_{min}/4.4 \ when\ T_{min} < 0$$

And the following equations for boreal forest regions:

Midseason snowmelt equation for boreal forest:

$$M = 0.58T_m$$

Period of major melt equation for boreal forest:

$$M = 1.83(T_m - 3.5)$$

The following equation is for prairie regions:

$$M = 1.8(T_m)$$

Where M is the meltwater depth in millimeters, T_m is the daily mean air temperature in ^{o}C, T_{max} is the daily maximum air temperature in ^{o}C, T_{min} is the daily minimum air temperature in ^{o}C (Gray & Prowse 1993). The equations utilize maximum and minimum temperature to calculate potential melt in millimeters, and then calculated values were

compared to precipitation amounts and temperature to determine whether precipitation fell as rain or snow.

From the NRCan 2012 dataset, snow accumulation and snowmelt were modelled using the previously described temperature-index method. Due to varying topography and climatic regions in the study area, the equations for mountainous regions, boreal forests, and prairie regions were employed in the snowmelt model. More details on the temperature-index model are located in Chapter 3.3.

2.6.3 Trend Detection

Climate change is likely to cause variation in many climatic and hydrologic variables. Change can occur in numerous ways, such as by gradual or rapid steady trends or abruptly as a step-change. Such changes are reflected in the mean, median, and variance of the data (Kundzewicz & Robson 2004). There are many different statistical tests that can be used to analyze trend.

The Mann-Kendall non-parametric test (MK) is one of the most widely used non-parametric tests to detect significant trends in hydrological and meteorological time series (Mann 1945; Kendall 1975). It is a rank-based procedure that can be useful for assessing spatial and temporal differences in trend (Partal & Kahya 2006). It is a function of the ranks of the observations, rather than actual values, and so it is not affected by the actual data distribution, and is also less sensitive to outliers (Hamed 2008). The Seasonal Kendall test is another option related to the Mann-Kendall test. The Seasonal Kendall test is a version of the Mann-Kendall test that allows for seasonality in the data (Kundzewicz & Robson 2004). Parametric trend tests are generally more powerful, but

are more sensitive to outliers and also require that the data be normally distributed, the Mann-Kendall non-parametric test, along with other non-parametric trend tests, are more suited to trend detection in hydrological time series since the data are usually not normally distributed and generally contain outliers (Hamed 2008). To complete the statistical test, the null hypothesis must be defined to determine the significance of the trend. Significance level (or p-value) and slope magnitude are the two main parameters produced by the Mann-Kendall test. The significance level is related to the strength of the trend, and slope magnitude indicates the direction and magnitude of the trend (Burn & Elnur 2002). To determine significance of the calculated trends, the test is applied to a large number of random permutations of the dataset to then obtain a test statistic distribution; the original test statistic is then compared to the distribution to determine significance (Burn & Elnur 2002).

Kundzewicz & Robson (2004) describe the resampling techniques used for estimating the significance level of a test statistic. Either a permutation or bootstrap approach can be used. The permutation approach involves re-ordering the dataset multiple times and calculating the test statistic for each permutation to see if a trend exists. If the original data set is very different from the various permutations, then a trend exists; if the original data are very similar to the permutations, then there is no trend. The bootstrap method is slightly different than the permutation method. In the bootstrap method, the original dataset is sampled and re-ordered with randomly generated values that provide the same distribution as the original data. The bootstrap is generally more flexible than permutation methods and can be used in a wider variety of circumstances, but the permutation approach is more powerful. (Kundzewicz & Robson 2004)

Burn and Hag Elnur (2002) used the Mann-Kendall non-parametric test to determine trends for 18 hydrologic variables, including annual mean flow, maximum daily flow, minimum daily flow, dates of start and end of ice conditions, number of ice days, and monthly mean flow. The Mann-Kendall non-parametric test is often utilized in hydrologic trend studies for a variety of variables, and also for temperature and precipitation trend analyses. Some examples include Burn (1994), Zhang et al. (2000), Zhang et al. (2001a), Yue et al. (2002), Abdul Aziz & Burn (2006), and Hamed (2008). The Mann-Kendall test is also often paired with the Sen's slope estimator (Sen 1968), to calculate an estimate of the slope of the linear trend line (e.g., Zhang et al. 2000; Zhang et al. 2001b; Vincent et al. 2007; de Rham et al. 2008; Goulding et al. 2009).

Spearman's rho is another trend test that can be used. It is more commonly used for testing the correlation between variables, or between time and the data series (Kundzewicz & Robson 2004). Correlations can be useful for determining linkages between meteorological variables and hydrologic variables. Burn (2008) used correlation analysis to attempt to determine linkages between meteorological variables, like temperature and precipitation, with climate indices. Then the correlations were used to help determine whether river freezeup and breakup dates were moving earlier or later in the year due to climate change or climate variability (Burn 2008). Ge & Gong (2009) also used correlation to determine linkages between climate indices, snow depth, and snow extent. They established linkages between both the Pacific Decadal Oscillation as well as the Pacific North America teleconnection and snow depth and snow extent during the winter and spring months (Ge & Gong 2009). Coulibaly (2006) also used correlation

analysis to determine if precipitation was correlated with any of the major climatic indices, including ENSO, PDO, and PNA.

Linear regression is an option as well; it is one of the most common tests for trend, though it assumes that the data are normally distributed (Kundzewicz & Robson 2004). Akinremi et al. (1999) used regression analysis to determine linear trends in amount of precipitation, number of precipitation events and precipitation variance at a number of stations across the Canadian prairies. Dyer (2008) also used regression analysis to determine the strength of the relationship between streamflow and snow cover of study basins in North America. Separate regression analyses were completed using discharge and snow volume during both the accumulation and ablation phases of all snow seasons (Dyer 2008). Linear regression analysis can also be used to examine changes in monthly snow depth and seasonal snow cover duration for a specified time period (Brown & Braaten 1998).

The Mann-Kendall non-parametric test was selected for analysis of the NRCan 2012 data for trend, then the results were used to determine rate of change per decade using Sen's slope method (Kendall 1975; Mann 1945; Sen 1968). The trend slope provides the direction and magnitude of the trend in ^{o}C per decade or millimeters per decade. More details on how the Mann-Kendall test was used to assess trend in the historical and future periods are in Chapters 3.3 and 4.3.

2.6.4 Spatial Analysis and Interpolation

Trend analysis can be completed in a variety of ways, and digital change detection can be used to quantify temporal phenomena from multi-date imagery (Coppin et al. 2004).

Pixel trajectory analysis involves tracking temporal changes of each pixel through time, and mapping the results over the study area. Spatial analysis of trends can be completed using pixel trajectory analysis using a combination of ArcGIS and MATLAB. Pixel trajectory analysis is a form of digital change detection, and is used for a variety of research topics, some of the more common applications include forest fire pattern analysis (e.g., Gralewicz et al. 2012) and land and forest cover change (e.g., Masek et al. 2008).

Temporal analysis associated with pixel trajectory analysis can include calculation of mean, standard deviation, coefficient of variation, and rate of change and p-value of the data. This method is used to determine regional changes in temperature, precipitation, snow depth, and snowmelt. Each data point receives a unique spatial identifier, and each point is then analyzed individually for temporal trends (Farmer et al. 2009).

After pixel trajectory analysis is complete, measures of spatial autocorrelation can be determined, and are useful in identifying clusters of statistically significant change. Autocorrelation can occur in several different ways: positive autocorrelation, negative autocorrelation and zero autocorrelation. Positive autocorrelation is the most common type of spatial autocorrelation and occurs when nearby observations are likely to be similar to other nearby observations (O'Sullivan & Unwin 2010). Positive autocorrelation is likely to occur in climatic and hydrologic data, due to the nature of the data; areas of high precipitation will likely be near other areas of high precipitation. Negative autocorrelation is less common than positive autocorrelation and occurs when observations that are close together are more likely to be different from one another, and

zero autocorrelation (or noncorrelation) occurs when the dataset appears to occur randomly throughout space, this is usually the null hypothesis of complete spatial randomness (O'Sullivan & Unwin 2010). Surfaces showing temporal changes in data can be tested for spatial autocorrelation to determine hotspots of change, to allow better understanding of change patterns. Testing for positive autocorrelation can provide indications of clustering that deviates from the mean (Boots 2002).

Spatial autocorrelation can be measured locally or globally. Spatial autocorrelation can be measured using Local or Global Moran's *I* (Moran 1950; Anselin 1995). Local Moran's *I* is a commonly used measure of spatial autocorrelation. It is considered a local indicator of spatial association (LISA) statistic. A LISA statistic must fulfill the following two requirements: the local measure for any data site should provide an indication of the extent of significant spatial clustering of similar data values around the data site, and the sum of the local measures should be proportional to a global measure defined over all data sites (Boots 2002). The values calculated for Local and Global Moran's *I* range from -1 to +1, and if the value is close to zero, there is less spatial autocorrelation (Mitchell 2005). If the value is close to +1, it indicates that clustering of similar values (positive autocorrelation), and if the value is close to -1, it indicates that similar values are dispersed, or not clustered (negative autocorrelation) (Balling & Goodrich 2010). These tests are useful for determining regions of similar change or overall spatial autocorrelation, but not all areas that are significantly clustered contain statistically significant trend values and not all significant trends occur within statistically significant clusters of similar values.

Following the statistical analysis on each data point, the point files may be converted to raster format using Inverse Distance Weighting (IDW). The IDW algorithm can interpolate data points on a grid into a continuous surface which can then be projected onto a two-dimensional Cartesian plane, or base map (Dyer & Mote 2006). When converting data from point to raster, there are many characteristics of the data and interpolation methods to be taken into account. Interpolators can be either exact or inexact, with the limitation of exact interpolation methods being that they are incapable of estimating values higher than maximum or lower than minimum data values; to create an accurate surface, the dataset must contain both the highest and lowest values in the study area, as well as peaks and lows that occur throughout (O'Sullivan & Unwin 2010). Exact interpolation honours all data points so that the surface passes through all points of known value after interpolation is complete (Babish 2006). IDW is an exact interpolator used to create a surface where interpolated values are most influenced by the closest points, and less influenced by points farther away (O'Sullivan & Unwin 2010). Interpolation methods, particularly simple methods like IDW, tend to work best and have the least error when used with datasets with even, dense sample distributions (Babish 2006).

The methods described above were all employed to spatially analyse the trend results for the period 1950-2010. After calculating snow accumulation and snowmelt using the NRCan 2012 dataset and temperature-index snowpack model, pixel trajectory analysis was used to track temporal changes of each pixel through time, using the Mann-Kendall non-parametric test. Point surfaces of trend data were then tested for spatial autocorrelation to provide better understanding of change patterns. Spatial

autocorrelation was measured using both Local and Global Moran's *I*. For visual analysis, the point surfaces containing rate of change data were interpolated using IDW with parameters chosen to minimize interaction between points. The calculated trend values were also averaged by study region to obtain zonal means of rate of change for each month and each variable. Further description of the spatial analysis methods used can be found in Chapter 3.3.

Analysis of the future time period included a series of RCMs, which were analysed and mapped monthly and annually. Pixel trajectory analysis was used to track temporal changes of each pixel through time, and then map the results over the study area. Each data point (50km x 50km pixel) received a unique spatial identifier, and each point was analyzed individually for temporal changes. Each model contains a future and current time period, so the potential future change was determined using a delta method (Future - Current = Change) for the study area. The change in annual average values between time periods was combined to create a multi-model mean. The change in average values for both annual and monthly results was mapped for visual interpretation. Further description of the methods used can be found in Chapter 4.3.

2.7 Conclusions

This chapter included a summary of the literature relating to hydroclimatic trends in western Canada, a description of the study area selected for this research, potential datasets, and temporal and spatial analysis techniques. It has become apparent that warming trends exist throughout the past and further warming is expected in the future with north-south and seasonal shifts in precipitation and snow. Assessment of spatial

variation in these hydroclimatic variables across large, topographically complex areas requires gridded data, in the form of interpolated climate station data or regional climate models. Various techniques have been applied to test for trend, but the Mann-Kendall non-parametric test is the most commonly used. The combination of pixel trajectory analysis and trend or change analysis provides the ability to complete various types of spatial analysis and also provides visual output for additional qualitative analysis. Previous studies have focused primarily on small regions (individual watersheds) or on much larger scales (Canada or North America). The following chapters will analyse key hydroclimatic variables for temporal changes and spatial variability on a historical (Chapter 3) and future projection (Chapter 4) basis.

References

Abdul Aziz, O. & Burn, D. 2006. Trends and variability in the hydrological regime of the Mackenzie River Basin. *Journal of Hydrology, 319*, 282-294.

Adam, J., Hamlet, A. & Lettenmaier, D. 2009. Implications of global climate change for snowmelt hydrology in the twenty-first century. *Hydrological Processes, 23*, 962-972.

Akinremi, O.O., McGinn, S.M. & Cutforth, H.W. 1999. Precipitation Trends on the Canadian Prairies. *Journal of Climate, 12*(10), 2996–3003.

Anselin, L. 1995. Local indicators of spatial association - LISA. *Geographical Analysis, 27*(2), 92-115.

Arritt, R.W. & Rummukainen, M. 2011. Challenges in Regional-Scale Climate Modeling. *Bulletin of the American Meteorological Society*, *92*(3), 365–368.

Babish, G. 2006. *Geostatistics without tears: A practical guide to surface interpolation, geostatistics, variograms, and kriging*. Edition 2006.03. Regina, SK, Canada: Environment Canada.

Balling, R.C. & Goodrich, G.B. 2010. Interannual variations in the local spatial autocorrelation of tropospheric temperatures. *Theoretical and Applied Climatology, 103*(3-4), 451-457.

Bates, B.C., Kundzewicz, Z.W. & Palutikof J.P. (Eds.) 2008. *Climate Change and Water: IPCC Technical Paper VI*, Geneva, Switzerland: IPCC Secretariat.

Bawden, A.J., Burn, D.H. & Prowse, T.D. 2013. An analysis of spatial and temporal trends and patterns in western Canadian runoff: A CROCWR component. *Conference Proceedings of the 19th International Northern Research Basins Symposium, Southcentral Alaska, USA, August 2013.*

Bonsal, B.R., Aider, R., Gachon, P. & Lapp, S. 2012. An assessment of Canadian prairie drought: past, present, and future. *Climate Dynamics*. DOI:10.1007/s00382-012-1422-0

Bonsal, B.R. & Kochtubajda, B. 2009. An assessment of present and future climate in the Mackenzie Delta and the near-shore Beaufort Sea region of Canada. *International Journal of Climatology, 29*, 1780-1795.

Boots, B. 2002. Local measures of spatial autocorrelation. *Ecoscience*, *9*(2), 168–176.

Brown & Braaten. 1998. Spatial and Temporal Variability of Canadian Monthly Snow Depths , 1946-1995. *Atmosphere-Ocean, 36*(1), 37–54.

Burn, D.H. 2008. Climatic influences on streamflow timing in the headwaters of the Mackenzie River Basin. *Journal of Hydrology, 352*, 225– 238.

Burn, D.H. & Hag Elnur, M.A. 2002. Detection of hydrologic trends and variability. *Journal of Hydrology, 255*.

Christensen, J.H. Hewitson, B. , Busuioc, A., Chen, A., Gao, X., Held, I., Jones, R., Kolli, R.K., Kwon, W.-T., Laprise, R., Magaña Rueda, V., Mearns, L., Menéndez, C.G., Räisänen, J., Rinke, A., Sarr, A.& Whetton, P. 2007. Regional Climate Projections. In *Climate Change 2007: The Physical Science Basis. Contribution of Working Group I to the Fourth Assessment Report of the Intergovernmental Panel on Climate Change*. Cambridge, United Kingdom: Cambridge University Press.

Cohen, S.J. 1991. Possible impacts of climatic warming scenarios on water resources in the Saskatchewan River sub-basin, Canada. *Climatic Change*, *19*, 291-317.

Coulibaly, P. 2006. Spatial and temporal variability of Canadian seasonal precipitation (1900-2000). *Advances in Water Resources, 29*(12), 1846-1965.

Davis, R.E., Lowit, M.B., Knappenberger, P.C. & Legates, D.R. 1999. A climatology of snowfall-temperature relationships in Canada. Journal of Geophysical Research, *104*(10), 11,985–11,994.

de Elía, R., Biner, S. & Frigon, A. 2013. Interannual variability and expected regional climate change over North America. *Climate Dynamics, 41*(5-6), 1245-1267.

de Rham, L.P., Prowse, T.D. & Bonsal, B.R. 2008. Temporal variations in river-ice break-up over the Mackenzie River Basin, Canada. *Journal of Hydrology, 349*, 441-454.

Dee, D., Fasullo, J., Shea, D., Walsh, J. & National Center for Atmospheric Research (NCAR) Staff (Eds). Last modified 03 Jan 2014. "The Climate Data Guide: Atmospheric Reanalysis: Overview & Comparison Tables." Retrieved from https://climatedataguide.ucar.edu/ climate-data/atmospheric-reanalysis-overview-comparison-tables

Déry, S.J. 2005. Decreasing river discharge in northern Canada. *Geophysical Research Letters, 32*(10), L10401,

Dyer, J. 2008. Snow depth and streamflow relationships in large North American watersheds. *Journal of Geophysical Research, 113*(D18), 1-12.

Dyer, J. & Mote, T.L. 2006. Spatial variability and trends in observed snow depth over North America. *Geophysical Research Letters, 33*(16), L16503.

Farmer, C.J.Q., Nelson, T.A., Wulder, M.A. & Derksen, C. 2009. Spatial-temporal patterns of snow cover in western Canada. *Canadian Geographer, 4*, 473-487.

Fürst, J. & Hörhan, T. 2009. Coding of watershed and river hierarchy to support GIS-based hydrological analyses at different scales. *Computers & Geosciences, 35*(3), 688–696.

Gachon, P. & Dibike, Y. 2007. Temperature change signals in northern Canada: convergence of statistical downscaling results using two driving GCMs. *International Journal of Climatology, 27*, 1623-1641.

Ge, Y. & Gong, G. 2009. North American Snow Depth and Climate Teleconnection Patterns. *Journal of Climate, 22*(2), 217–233.

Gralewicz, N., Nelson, T. & Wulder, M. 2012. Spatial and temporal patterns of wildfire ignitions in Canada from 1980 to 2006. *International Journal of Wildland Fire, 21*(3), 230-242.

Groisman. P.Y. & Easterling, D.R. 1994. Variability and trends of total precipitation and snowfall over the United States and Canada. *Journal of Climate, 7*, 184-205.

Groisman, P.Y., Knight, R.W., Easterling, D.R., Karl, T.R., Hegerl, G.C. & Razuvaev, V.N. 2005. Trends in intense precipitation in the climate record. *Journal of Climate, 18*, 1326-1350.

Goulding, H.L., Prowse, T.D. & Bonsal, B.R. 2009. Hydroclimatic controls on the occurrence of break-up and ice-jam flooding in the Mackenzie Delta, NWT, Canada. *Journal of Hydrology, 379*, 251-267.

Hamed, K. 2008. Trend detection in hydrologic data: The Mann–Kendall trend test under the scaling hypothesis. *Journal of Hydrology, 349*(3-4), 350–363.

Hamlet, A.F., Mote, P.W., Clark, M.P. & Lettenmaier, D.P. 2005. Effects of Temperature and Precipitation Variability on Snowpack Trends in the Western United States*. *Journal of Climate*, *18*(21), 4545–4561.

Hock, R. 1999. A distributed temperature-index ice- and snowmelt model including potential direct solar radiation. *Journal of Glaciology*, *45*(149), 101–111.

Hock, R. 2003. Temperature index melt modelling in mountain areas. *Journal of Hydrology*, *282*(1-4), 104–115.

Hutchinson, MF, McKenney, DW, Lawrence, K, Pedlar, JH, Hopkinson, RF, Milewska, E, & Papadopol, P. 2009. Development and Testing of Canada-Wide Interpolated Spatial Models of Daily Minimum–Maximum Temperature and Precipitation for 1961–2003. *Journal of Applied Meteorology and Climatology*, *48*(4), 725–741.

Jost, G., Moore, R.D., Smith, R. & Gluns, D.R. 2012. Distributed temperature-index snowmelt modelling for forested catchments. *Journal of Hydrology*, 420-421, pp.87–101.

Kapnick, S. & Hall, A. 2011. Causes of recent changes in western North American snowpack. *Climate Dynamics, 38*(9-10), 1885-1899.

Karl, T., Jones, P.D., Knight, R.W., Kukla, N.P., Razuvayev, V., Gallo, K.P., Lindseay, J., Charlson, R.J. & Peterson, T.C. 1993. A new perspective on recent global warming: Asymmetric trends of daily maximum and minimum temperature. *Bulletin of the American Meteorological Society*, *74*(6), 1007-1023.

Kendall, M.D. 1975. *Rank correlation measures*, Charles Griffin, London, UK.

Kerkhoven, E. & Gan, T. 2011. Differences and sensitivities in potential hydrologic impact of climate change to regional-scale Athabasca and Fraser River basins of the leeward and windward sides of the Canadian Rocky Mountains respectively. *Climatic Change*, *106*(4), 583-607.

Knowles, N., Dettinger, M. & Cayan, D. 2006. Trends in snowfall versus rainfall in the western United States. *Journal of Climate, 19*, 4545-4559.

Krasting, J., Broccoli, A., Dixon, K.W. & Lanzante, J.R. 2013. Future changes in Northern Hemisphere snowfall. *Journal of Climate, 26*, 7813-7828.

Kundzewicz, Z.W. & Robson, A.J. 2004. Change detection in hydrological records — a review of the methodology. *Hydrological Sciences, 49*(1), 7–19.

Kunkel, K.E. 2003. North American trends in extreme precipitation. *Natural Hazards*, 29, 291–305.

Leconte, R., Peters, D., Pietroniro, A. & Prowse, T. 2006. Modelling climate change impacts in the Peace and Athabasca catchment and delta: II - variations in flow and water levels with varying winter severity. Hydrological Processes, 20, 4215-4230.

Maidment, D.R. 1993. *Handbook of Hydrology*, McGraw-Hill, New York, USA.

Mann, H.B. 1945. Non-parametric tests against trend. *Econometrica*, 13, 245-259.

Masek, J.G., Huang, C., Wolfe, R., Cohen, W., Hall, F., Kutler, J. & Nelson, P. 2008. North American forest disturbance mapped from a decadal Landsat record. *Remote Sensing of the Environment, 112*(6), 2914-2926.

McCuaig, S.J. & Roberts, M.C. 2002. Topographically-independent ice flow in northwestern British Columbia: implications for Cordilleran Ice Sheet reconstruction. Journal of Quaternary Science, 17(4), 341-348.

McKenney, D., Hutchinson, M.F., Papadopol, P., Lawrence, K., Pedlar, J., Campbell, K., Milewska, E., Hopkinson, R.F., Price, D. & Owen, T. 2011. Customized spatial climate models for North America. *Bulletin of the American Meteorological Society*, 1611–1622.

Meehl, G.A., Stocker, T.F., Collins, W.D., Friedlingstein, P., Gaye, A.T., Gregory, J.M., Kitoh, A., Knutti, R., Murphy, J.M., Noda, A., Raper, S.C.B., Watterson, I.G., Weaver, A.J. & Zhao, Z.-C. 2007. Global Climate Projections. In *Climate Change 2007: The Physical Science Basis. Contribution of Working Group I to the Fourth Assessment Report of the Intergovernmental Panel on Climate Change*. Cambridge, United Kingdom: Cambridge University Press.

Mesinger, F., DiMego, G., Kalnay, E., Shafran, P., Ebisuzaki, W., Jovic, D., Woollen, J., Mitchell, K., Rogers, E., Ek, M., Fan, y., Grumbine, R., Higgins, W., Li, H., Lin, Y., Manikin, G., Parrish, D. & Shi, W. 2006. North American Regional Reanalysis. Bulletin of the American Meteorological Society, *87*, 343-360.

Min, S.K., Zhang, X. & Zwiers, F. 2008. Human-induced Arctic moistening. Science, *320*, 518-520.

Min, S.K., Zhang, X., Zwiers, F. & Hegerl, G.C. 2011. Human contribution to more-intense precipitatino extremes. *Nature, 470*(7334), 378-381.

Mitchell, A. 2005. *The ESRI Guide to GIS Analysis, Volume 2: Spatial Measurements & Statistics*, ESRI Press, Redlands, USA.

Mladjic, B., Sushama, L., Khaliq, M.N., Laprise, R., Caya, D. & Roy, R. 2011. Canadian RCM Projected Changes to Extreme Precipitation Characteristics over Canada. *Journal of Climate*, 24(10), pp.2565–2584.

Moore, R. & McKendry, I. 1996. Spring snowpack anomaly patterns and winter climatic variability. *Water Resources Research, 32*(3), 623–632.

Moran, P.A.P. 1950. Notes on continuous stochastic phenomena. *Biometrika, 37*(1/2), 17-23.

Moss, RH, Edmonds, JA, Hibbard, KA, Manning, MR, Rose, SK, van Vuuren, DP, Carter, TR, Emori, S, Kainuma, M, Kram, T, Meehl, GA, Mitchell, JFB, Nakicenovic, N, Riahi, K, Smith, SJ, Stouffer, RJ, Thomson, AM, Weyant, JP & Wilbanks, TJ. 2010. The next generation of scenarios for climate change research and assessment. *Nature, 463*, 747-756.

Mote, P.W., Hamlet, A.F., Clark, M.P. & Lettenmaier, D.P. 2005. Declining Mountain Snowpack in Western North America. Bulletin of the American Meteorological Society, *86*(1), 39-49.

Mote, P.W. & Salathé. 2010 . Future climate in the Pacific Northwest. *Climatic Change, 102*(1-2), 29-50.

Nakicenovic, N. & Swart, R. (Eds.). 2000. *Special Report on Emissions Scenarios*. Geneva, Switzerland: IPCC Secretariat.

O'Sullivan, D., & Unwin, D.J. 2010. *Geographic Information Analysis*. 2nd ed. Hoboken, NJ, USA: Wiley & Sons, Inc.

Payne, J.T., Wood, A.W., Hamlet, A.F., Palmer, R.N. & Lettenmaier, D.P. 2004. Mitigating the effects of climate change on the water resources of the Columbia River Basin. Climate Change, *62*, 233-256.

Pederson, G.T., Gray, S.T., Woodhouse, C.A., Betancourt, J.L., Fagre, D.B., Littell, J.S., Watson, E., Luckman, B.H. & Graumlich, L.J. 2011a. The unusual nature of recent snowpack declines in the North American cordillera. *Science, 333*, 332-335.

Pederson, G.T., Gray, S.T., Ault, T., Marsh, W., Fagre, D.B., Bunn, A.G., Woodhouse, C.A. & Graumlich, L.J. 2011b. Climatic controls on the snowmelt hydrology of the Northern Rocky Mountains. *Journal of Climate*, *24*(6), 1666-1687.

Price, D.T., McKenney, D.W., Nalder, I.A., Hutchinson, M.F. & Kesteven, J.L. 2000. A comparison of two statistical methods for spatial interpolation of Canadian monthly mean climate data. *Agricultural and Forest Meteorology*, *101*(2-3), 81–94.

Sain, S.R. & Furrer, R. 2010. Combining climate model output via model correlations. *Stochastic Environmental Research and Risk Assessment*, *24*(6), 821–829.

Salathé, E. 2005. Downscaling simulations of future global climate with application to hydrologic modelling. *International Journal of Climatology*, *25*(4), 419-436.

Schindler, D. & Donahue, W. 2006. An impending water crisis in Canada's western prairie provinces. Proceedings of the National Academy of Sciences, *103*(19), 7210-7216.

Schnorbus, M., Werner, A. & Bennett, K. 2014. Impacts of climate change in three hydrologic regimes in British Columbia, Canada. *Hydrological Processes*, *28*(3), 1170-1189.

Sen, P.K. 1968. Estimates of the regression coefficient based on Kendall's Tau. *Journal of the American Statistical Association*, *63*(324), 1379-1389.

Šeparović, L., Alexandru, A., Laprise, R., Martynov, A., Sushama, L., Winger, K., Tete, K. & Valin, M. 2013. Present climate and climate change over North America as simulated by the fifth-generation Canadian regional climate model. Climate Dynamics, *41*(11-12), 3167-3201.

St. Jacques, J., Sauchyn, D.J. & Zhao, Y. 2010. Northern Rocky Mountain streamflow records: Global warming trends, human impacts or natural variability? *Geophysical Research Letters*, *37*(6), L06407.

Stewart, I.T., Cayan, D. & Dettinger, M. 2004. Changes in snowmelt runoff timing in western North America under a 'business as usual' climate change scenario. *Climate Change*, *62*, 217-232.

Stewart, I.T., Cayan, D. & Dettinger, M. 2005. Changes toward earlier streamflow timing across western North America. *Journal of Climate*, *18*(8), 1136-1155.

Stewart, I.T. 2009. Changes in snowpack and snowmelt runoff for key mountain regions. *Hydrological Processes, 23*, 78-94.

Thorne, R. & Woo, M. 2011. Streamflow response to climatic variability in a complex mountainous environment: Fraser River Basin, British Columbia, Canada. *Hydrological Processes, 25*, 3076-3085.

Vincent, L., van Wijngaarden, W. & Hopkinson, R. 2007. Surface temperature and humidity trends in Canada for 1953-2005. *Journal of Climate, 20*(20), 5100-5113.

Vose, R., Easterling, D. & Gleason, B. 2005. Maximum and minimum temperature trends for the globe: An update through 2004. *Geophysical Research Letters, 32*(23), L23822.

Whitfield, P.H. 2001. Linked hydrologic and climate variations in British Columbia and Yukon. *Environmental Monitoring and Assessment, 67*(1-2), 217-238.

Woo, M. & Thorne, R. 2003. Streamflow in the Mackenzie Basin , Canada. *Arctic Institute of North America, 56*(4), 328–340.

Xia, Y., Fabian, P., Winterhalter, M. & Zhao, M. 2001. Forest climatology: estimation and use of daily climatological data for Bavaria, Germany. *Agricultural and Forest Meteorology, 106*(2), 87–103.

Xu, C. & Singh, V.P. 2004. Review on Regional Water Resources Assessment Models under Stationary and Changing Climate. *Water Resources Management, 18*, 591–612.

Yue, S., Pilon, P. & Cavadias, G. 2002. Power of the Mann-Kendall and Spearman's rho tests for detecting monotonic trends in hydrological series. *Journal of Hydrology, 259*, 254-271.

Zhang, X., Vincent, L., Hogg, W. & Niitsoo, A. 2000. Temperature and precipitation trends in Canada during the 20th century. *Atmosphere-Ocean*, 38(3), 395-429.

Zhang, X., Harvey, K.D, Hogg, W.D. & Yuzyk, T.R. 2001a. Trends in Canadian streamflow. *Water Resources Research*, 37(4), 987-998.

Zhang, X., Hogg, W.D. & Mekis, E. 2001b. Spatial and temporal characteristics of heavy precipitation events over Canada. *Journal of Climate, 14*, 1923-1936.

Zhang. X., Zwiers, F.W., Hegerl, G.C., Lambert, F.H., Gillett, N.P., Solomon, S., Stott, P.A. & Nozawa, T. 2007. Detection of human influence on twentieth-century precipitation trends. *Nature*, 448, 461-465.

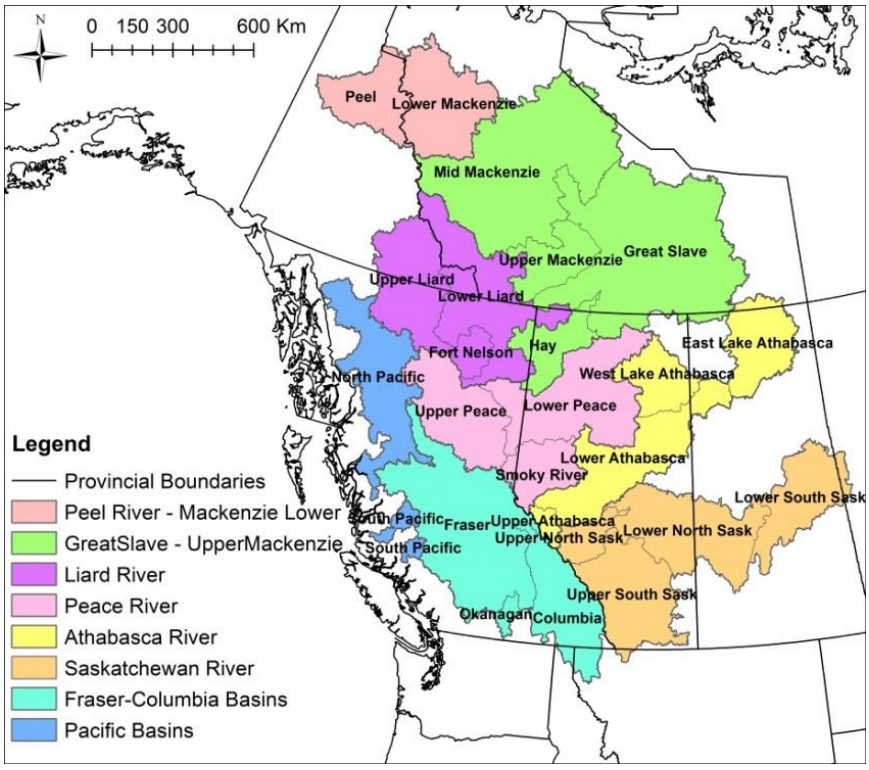

Figure 2.1. CROCWR study area with watersheds labeled by name and study regions identified by colour.

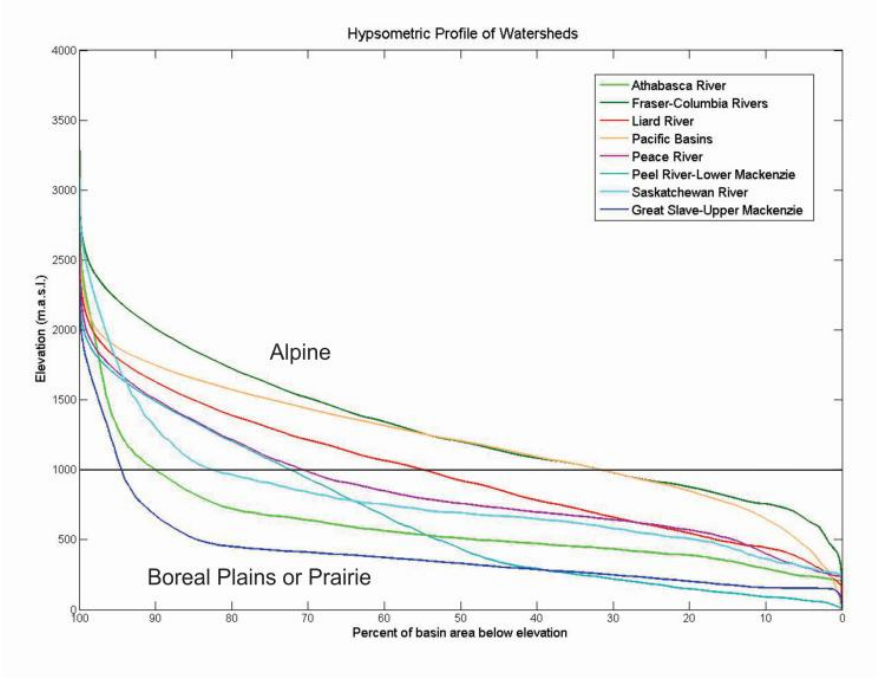

Figure 2.2. Hypsometric curves of each study region identified in Figure 2.1.

3. Chapter 3: Spatial and temporal analysis of hydroclimatic variables affecting streamflow in western Canada from 1950-2010

Abstract

A large portion of the freshwater in western Canada originates as snowpack from the northern Rocky Mountains. The temperature and precipitation in these areas control the amount of snow accumulated and stored throughout the winter, and the amount and timing of melt that occurs during the spring freshet. Changes in the extent and timing of snowpack and melt modify the timing of peak river flow on a continental scale. Trends in temperature, precipitation, snow accumulation, and snowmelt are examined using the Mann-Kendall non-parametric test on a high resolution gridded climate dataset over western Canada for the period 1950-2010. The temporal and spatial analyses of these key hydroclimatic variables indicate that changes vary greatly over space and time. Results reveal that minimum temperature has increased more than maximum temperature, particularly during the colder months of the year, and at higher elevations, contributing to earlier spring melt. Precipitation has decreased throughout the colder months of the year and increased in the warmer months, particularly in the northern half of the study area. Snow accumulation has experienced decreases across the study area and through all months of the year. Snowmelt results indicate slight increases in mid-winter melt events and an earlier onset of the spring freshet. This study provides a summary of detected trends in key hydroclimatic variables across western Canada with regard to the effects these changes can have on the spring freshet and streamflow throughout the study area.

3.1 Introduction

Changes to regional water availability will affect many aspects of human society, from agricultural productivity and energy use to flood control, municipal and industrial water supply, and fisheries and wildlife management (Xu & Singh 2004). Climate change and variability are associated with a variety of impacts on the hydrologic regime of a watershed. Examining the linkages between hydrologic and climatic variables, such as air temperature, precipitation, snow depth, and snowmelt, will also supply more information about observed trends in river flow. Many changes have already been linked to warmer air temperatures, including increasing atmospheric water-vapour content and the resulting changes in precipitation patterns, snow cover reductions, melting of ice, and changes to runoff and soil moisture (Bates et al. 2008). Understanding how such changes in climate affect hydroclimatic conditions in critical water-supply regions is essential for effective water-resource planning (Xu & Singh 2004).

A large portion of the river flow to the Canadian Arctic originates in the mid-latitudes, particularly from alpine snowpacks of the Northern Rocky Mountains, which includes the headwaters of some of the largest river systems in North America, including the Mackenzie, Saskatchewan and Columbia rivers (Stewart et al. 2004; Déry 2005). The boundaries between these major watersheds are in close proximity, and as a result, the spatial distribution of snowfall and snowmelt determines whether snowmelt contributes to the Mackenzie, Saskatchewan or Columbia rivers. Any north-south or east-west shifts in regional climate including temperature and precipitation can have major effects on the location of snowfall and snowmelt, and thus the amount of water resources available in each region. Flow from the Mackenzie River to the Arctic Ocean is of importance to

ocean convection, thermohaline circulation, and ultimately to global climate (Min et al. 2008; Holland et al. 2007). Flow from rivers such as the Saskatchewan and Columbia is critical to water-resource use, particularly in the dry, prairie interior of the mid-west. Given that these are primarily nival river regimes and mountain snowpack serves as a natural precipitation reservoir in the cold season, any climate-induced changes that affect the magnitude of their alpine snow accumulations, or the timing and volume of their subsequent melt, can thus have widespread downstream implications (Stewart 2009).

A number of changes in the hydroclimatic regime of western Canada have already been identified. Temperatures in northern latitudes show greater increases than in southern areas, with an increase of 1.2^{o}C in the annual mean temperature throughout Canada between 1953 and 2005 (Vincent et al. 2007). Hamlet et al. (2005) detected large scale warming across North America between 1916 and 2003, which has been linked to an overall decrease in snow water equivalent; though higher elevations have experienced an upward trend because of the corresponding increase in winter precipitation. Through the 20th century, Zhang et al. (2000) detected an increase of 0.9^{o}C in average air temperature across southern Canada with the largest seasonal increases during winter and spring. In addition to focusing on average temperature, some studies have also examined both maximum and minimum daily temperature, with results showing that minimum temperatures have been rising twice to three times more quickly than maximum temperatures across western Canada (Karl et al. 1993; Akinremi et al. 1999).

Precipitation has also changed in many areas but unlike temperature, it has been characterized by significant spatial and inter-decadal variability. Increases in

precipitation have been detected over northern latitudes (30-85^{o}N) (Bates et al. 2008). In southern Canada, precipitation has increased by 12-13% since the early 1900s (Groisman & Easterling 1994; Zhang et al. 2000). Increases in northern latitude temperatures have also alter the proportion of rainfall to snowfall. Higher temperatures lead to total snowfall increasing since warmer air temperatures can hold more moisture, or a higher proportion of the total precipitation falling as rain if the air temperature increases enough to remain above 0^{o}C (Davis et al. 1999). Western North America is particularly sensitive to this, since many mountainous areas near the Pacific coast have average winter and spring temperatures only slightly below 0^{o}C (Adam et al. 2009). An increase in average temperature can also lead to increased evaporation, which can cause decreased streamflow (Zhang et al. 2000).

Snow cover is considered an important climate change indicator because of its sensitivity to temperature changes, and also because climate change is predicted to have the greatest warming effects in northern snow-covered areas (Brown & Braaten 1998). The spatial and temporal distributions of snow can have impacts on local snowmelt release, global and regional atmospheric circulation, and global and local climate and hydrological cycles (Farmer et al. 2009). Northwestern Canada has shown a statistically significant decreasing trend in snow depth of -0.25cm per year between 1960 and 2000 (Dyer & Mote 2006). In southern Canada, snowfall precipitation decreased 10-20% between 1950 and 2003 (Vincent & Mekis 2006). Declines to the annual number of days with snowpack as well as the maximum snowpack have also occurred throughout the Prairies since the 1950s (Schindler & Donahue 2006). High latitude rivers are closely tied to

winter snow storage and melt, therefore any changes to quantities of snowfall and the timing of snowmelt can change the response of the hydrograph (Dyer 2008).

Burn & Hag Elnur (2002) detected that spring freshet was occurring earlier, winter flows were increasing, ice conditions were ending earlier, and annual mean flow was decreasing for the period of 1960-1997 throughout Canada. Annual mean flow is mostly decreasing throughout western Canada, but some flow increases have been detected in BC during March and April (Burn & Hag Elnur 2002). The spring freshet date has also been shown to be occurring earlier in the Mackenzie Basin (e.g., Burn 2008), as well as throughout western Canada (e.g., Zhang et al. 2001; Stewart et al. 2005).

Many previous studies focused on either individual watersheds or drainage basins or the focus is on very large areas of a national to continental scale. This provides valuable information on individual river systems and watersheds as well as large scale trends, but does not provide information on the hydroclimatic changes that modify the spatial distribution of rainfall and snowfall between the drainage basins of western Canada, and thus regional water availability in these major river systems. The research presented in this paper is part of a larger assessment of Canadian water resources; see Prowse et al. (2013). The project assesses a range of factors, including atmospheric synoptic patterns, key hydroclimatic variables, and the corresponding streamflows. This research includes analysis of temporal trends as well as spatial distribution of trend values within multiple major drainage basins, which has not been previously done at this scale; the combination of a very large study area in addition to a high spatial resolution dataset is rare in previous studies. The results of this study provide information on annual as well as intra-annual

trends and spatial variation in climate variables that are most likely to affect streamflow, including maximum and minimum air temperature, precipitation, snow accumulation, and snowmelt. This includes analysis of climatic variables affecting streamflow using interpolated, gridded data (maximum and minimum temperature, precipitation, snow depth, and snowmelt) for the time period 1950-2010, and analysis of spatial variation in the above hydroclimatic variables across western Canada.

3.2 Study Area

The study area covers western Canada, from the west coast of British Columbia to western Manitoba and from the Canada-United States border to the Mackenzie River Delta in the northernmost reaches of continental Canada (Figure 3.1). This includes the Saskatchewan, Mackenzie, Fraser, and Columbia River Basins, as well as several small basins that drain British Columbia to the Pacific. A companion study (Bawden et al. 2013) has identified a series of hydrometric stations that correspond to distinct hydro-climatic regions contained within the study area. The study area is based on drainage areas of 37 hydrometric stations in western Canada; however, these are amalgamated into eight study regions for analysis. These study regions include the Athabasca River, Peace River, Liard River, Saskatchewan River, Fraser and Columbia Rivers, the Great Slave-Upper Mackenzie region, the Peel River-Lower Mackenzie region, and the Pacific region which contains several small basins that drain the northern coast of British Columbia to the Pacific Ocean.

The identified region incorporates a variety of climatic regions; much of the study area exists within the alpine region, and the remainder is at lower elevations in the boreal

plains or prairies (Figure 3.2). The Mackenzie River basin covers several climatic regions, including cold temperate, mountain, sub-Arctic, and Arctic zones (Woo & Thorne 2003). The Athabasca and Peace Rivers have their headwaters in the Rocky Mountains and then flow across prairie landscapes to the Peace-Athabasca Delta, which drains into Lake Athabasca and then flows north into Great Slave Lake (Burn 2008). The primary outlet of Great Slave Lake is the Mackenzie River, which flows north to the Arctic Ocean. The Slave River, Great Slave Lake, and most of the Mackenzie River are contained within the Great Slave-Upper Mackenzie region, which consists primarily of low elevation boreal forest and Shield catchments characterized by plateaus and lowlands without much topography (Gibson et al. 2006). The Liard River joins the Mackenzie River basin near Great Slave Lake, contributing flows from headwater locations in the Yukon, Northwest Territories, British Columbia, and Alberta (Burn 2008). The Peel River converges with the Mackenzie River basin near the delta.

The Saskatchewan River Basin includes the North and South Saskatchewan Rivers, which are fed by the Red Deer and Bow Rivers. Headwaters originate as glacier and snowmelt in the Rocky Mountains and flow east through the prairie grasslands, where very little runoff is contributed to the streamflow (Cohen 1991). The Fraser River receives flow from snowmelt in spring, glacier melt in summer, and some rainfall throughout the year (Thorne & Woo 2011). The Columbia River Basin covers parts of seven western states and part of British Columbia, and a large portion of the flow is obtained from the Northern Rocky Mountains (Pederson et al. 2011b). The smaller basins draining to the Pacific consist of several rivers with small watershed areas that drain the Coast Mountains of British Columbia. The landscape consists of steep-sided

fjords and valleys with mountain peaks up to 2265m above sea level and alpine ice fields and glaciers occurring at the high elevations (McCuaig & Roberts 2002).

3.3 Data and methods

Analysis was completed on a monthly basis to identify month to month variation in the selected hydroclimatic variables and to determine trend persistence through multiple months. Though data was analyzed monthly, results were discussed and spatially analyzed on a cold/warm season as well as seasonal basis. The cold season was determined to include November through April with the warm season covering May to October. The cold season covers most of the snow accumulation through to the spring breakup across most of the study area, with the warm season including the end of breakup in the north through the dry summer months to the beginning of freezeup. The seasonal analysis includes four seasons: January through March characterized the snow accumulation period, April through June covers the spring breakup across most of the study area, July through September covers the majority of the hot, dry period, and October through December includes the fall freezeup and beginning of the snow accumulation season. The seasons vary across the study area due to variations in elevation as well as the large range of latitudes; however, the seasonal definitions were chosen to represent the cold and warm halves of the year as well as the hydrologic seasons as they exist throughout the majority of the study area. Monthly examples from each season are included in each results section, the full suite of results can be seen in Appendix A.

Watershed delineations for the eight study regions stated above were created based on a series of latitude-longitude points that correspond to the selected hydrometric stations from Environment Canada's HYDAT database. ArcHydro was used to delineate the contributing areas for each hydrometric station. ArcHydro is an object-oriented model that is capable of establishing a topological network that includes flow direction, connectivity and upstream/downstream relationships of stream segments using a digital elevation model, a stream network, and points to distinguish watershed outlets (Fürst & Hörhan 2009).

Daily temperature and precipitation values were obtained from an ANUSPLIN-generated dataset that covers Canada for the period 1950-2010 and has a spatial resolution of 10km x 10km (Hutchinson et al. 2009; McKenney et al. 2011). McKenney et al. (2011) produced this dataset in conjunction with Natural Resources Canada and is herein referred to as the NRCan 2012 dataset. ANUSPLIN-generated data incorporates the effects of elevation in its calculation of point values, since elevation is an important controlling factor of climate, an important consideration in the study area of western Canada. The NRCan 2012 dataset was chosen for its high spatial resolution and temporal coverage, its daily resolution, and its inclusion of maximum and minimum temperature and precipitation. However, as with all modelled or interpolated datasets, there are some limitations. When compared with satellite data it appears that the method predicts values quite well over the majority of land cover types except over very high elevations (>1500m) and large bodies of water where climate stations are sparse (Bussieres and Milewska 2010). It is also possible that precipitation is underestimated due to the variability of precipitation patterns in time and space; precipitation events may have

occurred that were not recorded by any climate stations, therefore these very small scale precipitation events cannot be accounted for in the dataset (Hutchinson et al. 2009). Despite a few potential estimation issues over some land cover types, the ANUSPLIN method is generally quite accurate at interpolating data from climate stations. The dataset was tested using a generalized cross-validation method and by withholding data at spatially representative locations during the surface fitting procedure and the predictive error statistics were similar, and reasonably small, for both validations tests (McKenney et al. 2011).

The NRCan 2012 dataset included daily maximum and minimum temperature and precipitation; therefore snow accumulation and snowmelt were modelled using a temperature-index method. A temperature-index method was chosen due to data availability and generally accurate model performance despite computational simplicity (Jost et al. 2012). The temperature-index model assumed precipitation occurring at temperatures below 0^{o}C to be snow and added the amount to the snowpack, while temperatures above 0^{o}C were considered to cause snowmelt. Due to varying topography and climatic regions in the study area, multiple snowmelt equations were employed in the snowmelt model. The equations used were taken from Gray & Prowse (1993), and vary based on atmospheric conditions, topography, geographical location, properties of the snow cover, and occasionally time of year. The melt equations are specific to differing regions and time periods (including mountains of western Canada, midseason boreal snowmelt, period of major melt for boreal forest, and prairie snowmelt); the equations used are listed in Chapter 2.4.2 (Gray & Prowse 1993). The equations utilized maximum and minimum temperature to calculate potential melt in millimeters, and then calculated

values were compared to snow accumulation and temperature to determine whether or not the snowmelt was deducted from the snow pack. Both snow accumulation and snowmelt were reported in millimeters of snow water equivalent as a total amount per month.

After calculating snow accumulation and snowmelt, pixel trajectory analysis was used to track temporal changes of each pixel through time, and then map the results over the study area. Each data point (10km x 10km pixel) received a unique spatial identifier, and each point was analyzed individually for temporal trends. The Mann Kendall (MK) test was used to calculate a trend value for each pixel, then the MK results were used to determine rate of change per decade using Sen's slope method (Kendall 1975; Mann 1945; Sen 1968). The trend slope provides the direction and magnitude of the trend in ^{o}C per decade or millimeters per decade.

Point surfaces of rate of change data were tested for spatial autocorrelation to determine hotspots of change, and thus a better understanding of change patterns. Spatial autocorrelation was measured using both Local and Global Moran's *I* which indicate amount of significant clustering in the dataset and whether values are negatively or positively autocorrelated (values range from -1 to +1, respectively) (Mitchell 2005). These tests are useful for determining regions of similar change, but not all areas that are significantly clustered contain statistically significant trend values and not all significant trends occur within statistically significant clusters of similar values. Autocorrelation values lower than the mean do not necessarily indicate decreasing trends; rather they are indicative of values lower than the mean of the trend results for a particular month. All

Local Moran's *I* calculations were completed using a fixed distance band of 2 decimal degrees of latitude and longitude that includes the 7 nearest neighbours in the autocorrelation calculation.

For visual analysis, the point surfaces containing rate of change data were interpolated using Inverse Distance Weighting (IDW). IDW was chosen because it honours all data points so that the surface passes through all points of known value and because simple interpolation methods like IDW tend to work best and have the least error when used on datasets with even, dense sample distributions (Babish 2006). To test efficacy of this method, cross-validation tests were employed to determine error in the raster surfaces. Five raster surfaces were tested, and all had an RMS error of less than 0.05, indicating that this method of converting point data to pixel data incorporates very little error into the data. IDW parameters were chosen to minimize interaction between points, so that each pixel value would not be greatly affected by neighbouring values. This involved selecting input cell size and distance band to 0.08333 decimal degrees, the same size as the point spacing. The calculated trend values were then averaged by study region to obtain zonal means of rate of change for each month and each variable. Trend maps only display values with a statistical significance of 10% or better.

Trend persistence was also tested through the reclassification of each monthly interpolated trend map into increasing/decreasing values. This was accomplished by changing all statistically significant trend values greater than 0.1 ^{o}C/decade or mm/decade to the value of 1 and all other values to 0 or changing all values less than -0.1 ^{o}C/decade or mm/decade to the value of 1 and all other values to 0 then adding multiple

month layers together to view increasing/decreasing trend persistence through multiple months. The values 0.1 and -0.1 were chosen for the reclassification because it allows inclusion of most moderate to strong positive or negative rates of change, without including the weak changes close to zero. This was done on both a cold season/warm season basis as well as a seasonal basis, to view the trend persistence through a longer time period as well as on a seasonal basis more reflective of the hydrologic seasons. Only the cold season/warm season trend persistence maps are included in the results for each variable since the seasonal analysis did not add any significantly different information to the analysis. The seasonal trend persistence results can be viewed in Appendix A.

3.4 Results and Discussion

3.4.1 Maximum and Minimum Temperature

Annual temperatures range from -15^{o}C to 15^{o}C across western Canada; for the time period 1950-2010, daily maximum temperature (Tmax) ranges from -5^{o}C in the north to 15^{o}C in the south (Figure 3.3a), and daily minimum temperatures (Tmin) range from -15^{o}C in the north to 5^{o}C in the south (Figure 3.3b). Tmax and Tmin spatially averaged by study region are shown in Table 3.1.

Table 3.1. Regional averages of Tmax and Tmin, from 1950-2010.

Study Region	Maximum Temperature (^{o}C)	Minimum Temperature (^{o}C)
Peel River-Lower Mackenzie	-2.7	-12.4
Great Slave-Upper Mackenzie	-1.1	-10.7
Liard River	2.0	-9.0
Peace River	5.5	-5.6
Athabasca River	4.5	-6.6
Saskatchewan River	8.1	-4.1
Fraser-Columbia Basins	8.1	-3.5
Pacific Basins	4.5	-5.2

The trend analysis results indicate Tmax and Tmin have changed at the rate of -0.5^{o}C to 1.4^{o}C per decade when averaged over the time period 1950-2010. The greatest Tmax trends are located in the northern and eastern portions of the study area, including the Peel River-Lower Mackenzie, Great Slave-Upper Mackenzie, Liard, Peace, Athabasca, and Saskatchewan regions, with slightly lower rates of change in the Fraser and Pacific Regions (Figure 3.3c). Tmin shows the largest trends in the mountainous regions which occupy the western half of the study area, particularly in the Fraser-Columbia Basins, the Upper Peace River, Pacific Basins, Upper Liard and Fort Nelson basins, the western portion of the Great Slave-Upper Mackenzie, and the Peel River basin (Figure 3.3d). These areas have experienced Tmax increases from 0.5 to 0.8^{o}C/decade and Tmin increases from 0.7 to 1.2^{o}C/decade. The Tmin increases are statistically significant in the interior regions as well, but with values slightly lower overall. Nearly all statistically

significant trend results are positive, indicating widespread warming throughout the study area.

The regional trend averages for both Tmax and Tmin are summarized in Table 3.2. The regional trends appear to be similar across the study area, but there are many small variations across each study region that are not captured by viewing only regional averages.

Table 3.2. Annual Tmax and Tmin rates of change averaged over each study region. Averages include all calculated trend values for the time period 1950-2010.

Study Region	**Maximum Temperature (^{o}C/decade)**	**Minimum Temperature (^{o}C/decade)**
Peel River-Lower Mackenzie	0.5	0.6
Great Slave-Upper Mackenzie	0.4	0.4
Liard River	0.4	0.4
Peace River	0.4	0.4
Athabasca River	0.4	0.4
Saskatchewan River	0.3	0.4
Fraser-Columbia Basins	0.2	0.4
Pacific Basins	0.2	0.5

Trend results in Figures 3.3c and 3.3d indicate that warming is occurring at greater rates in areas of high elevation. Increases to Tmax are located more at northern latitudes, while increases to Tmin occur more at high elevations in the western half of the study area. The Tmin trends are also slightly higher than the Tmax changes, indicating a decrease in the overall temperature range across most of the study area.

Monthly trend results provide a more in depth view of what changes have occurred to Tmax and Tmin throughout the year between 1950 and 2010. Tmax and Tmin were averaged across each of the 8 study regions, with Tmax values from -23.4°C to -5.6°C in January and 16.7°C to 23.4°C in July, and Tmin values from -31.8°C to -14.4°C in January and 5.3°C to 9.9°C in July (Figure 3.4). The coolest temperatures occur in the northern regions during winter with the warmest temperatures in inland basins during the summer where the moderating influence of the ocean on temperature is less than in study regions in close proximity to coastal areas. Regional trend averages are highest during the cold season (particularly January and February), with spatially averaged results ranging from 0.8 to 1.5°C/decade, and lowest during the warm season with the spatially averaged trend results ranging from 0.2 to 0.4°C/decade (Figure 3.5).

The greatest Tmax and Tmin trends are during the colder months of the year, particularly during winter (Figures 3.6a and 3.7a). Tmax trends range from 0.3 to 1.2°C/decade in the Fraser-Columbia region and Tmin trends throughout the study area mostly range from 1.0 to 1.5°C/decade. The highest Tmax values of 2.1°C/decade and Tmin values of 1.6 to 2.5°C/decade are located at high elevations in the Liard and Peace Rivers and some portions of the Peel River-Lower Mackenzie regions. Statistically significant spatial autocorrelation of Tmax and Tmin trend values higher than the mean are located throughout all study regions during winter, with the exception of the Fraser-Columbia region which contains no significant spatial autocorrelation. Significant clustering occurs in most study regions, generally in the areas with the greatest trend values. These clusters of trend values indicate regions of similar change.

Spring has experienced slightly lower trend values throughout the study area, with Tmax trend values of 0.3 to 1.0°C/decade in the early spring (Figure 3.6b) and 0.2 to 0.5°C/decade later in the season. Tmax trends of -0.2 to -0.3°C/decade also occur in the late spring in the Pacific region and some parts of the Rocky Mountains. Tmin trends during spring also show lower values throughout the study area than in winter, with trend values of 0.2 to 0.9°C/decade over most of the study area throughout the season, but Tmin trends in early spring reach values of 1.0 to 1.3°C/decade in the far north of the study area (Figure 3.7b). Local spatial autocorrelation indicates clustering of Tmax and Tmin trend values higher than the mean mostly throughout the northern half of the study area in all spring months, and clustering of Tmin values in British Columbia. The cluster patterns indicate a region of similar change and correspond to the areas with the greatest trend values.

Temperature trends during summer are less spatially continuous than in the earlier months of the year. Increasing Tmax trends of 0.2 to 0.6°C/decade were detected mostly in the northern half of the study area (Figure 3.6c), though some decreasing trends of -0.3 to -0.4°C/decade were also detected in the Pacific region in late summer. Tmin trends range from 0.2 to 0.8°C/decade over mostly the western half of the study area, with less spatial continuity in the east and north (Figure 3.7c). Clustering of values higher and lower than the mean mostly correspond with the increasing and decreasing Tmax trend patterns, though most cluster patterns extend beyond the significant trend values indicating increasing or decreasing tendencies that are not significant trends. Tmin spatial autocorrelation patterns are similar throughout most of the summer, with values higher than the mean throughout the western half of the study area. These clusters

correspond to the areas of significant trends, indicating that this is a region of similar change throughout most of the summer.

Fall Tmax trends range from 0.3 to 0.9^{o}C/decade while Tmin trends range from 0.2 to 1.3^{o}C/decade early in the season (Figure 3.6d and 3.7d). Later in the fall Tmax trends range from 0.5 to 1.7^{o}C/decade and Tmin trends reach a maximum of 1.8^{o}C/decade. The northern latitudes and higher elevations experienced the greatest temperature increases, with the largest trends occurring in December. Decreasing trends of -0.2 to -0.7^{o}C/decade were also detected in the southwest of the study area at high elevations in the southern Rocky Mountains. Significant clustering of Tmax and Tmin values higher than the mean occurs in the northern half of the study area, and to a lesser degree, the western half. These cluster patterns mostly correspond to the locations of significant trends during this season.

Global Moran's *I* values for Tmax exceed 0.95 in all months of the year, and the Global Moran's *I* values for Tmin exceed 0.91 in all months of the year, indicating strong positive spatial autocorrelation and a high degree of trend clustering throughout all months of the temperature data. Many of the trend values for Tmin are greater than those for Tmax, and the greatest warming occurs during the cold season, with lower trend magnitudes during the warmer months. Trends for summer and fall are generally lower than the remainder of the year. The majority of the trends in Tmax calculated for the summer and fall months are not statistically significant. Tmax during spring and summer has experienced lower rates of change throughout most study regions, including some decreasing temperature trends over large bodies of water. While some aspect of these

detected negative trends may be real, it is possible that they are part of the dataset limitations. The ANUSPLIN approach to dataset interpolation works well over most land cover types, except very high elevations and large water bodies, where climate stations are few and sparsely located (McKenney et al. 2011). Some slight decreasing temperature trends in the Fraser-Columbia and Pacific regions occur in high elevation areas during the warmer months of the year, as well as November and December. Previous studies have mentioned the possibility of warming at the lower and mid-elevations with some slight cooling at very high elevations, though due to the complex topography, general inaccessibility, and lack of monitoring in these areas it is difficult to determine if these trends are real (McGuire et al. 2012). It is also possible that the high elevation trends may be related to the same dataset limitation mentioned previously.

Trend persistence also varies spatially and temporally throughout the year. Tmax trends during the cold season, defined as November through April, occur over the entire study area. Increasing trends in maximum temperature during the cold season are concentrated in the Upper Peace and Liard River regions, as well as the Peel River-Lower Mackenzie region (Figure 3.8a). These areas contain increasing Tmax trends for 4-6 months of the cold season while the remainder of the study area contains increasing trends from 1-4 months during the cold season. When compared to cold season Tmax trends, Tmin trends are generally more persistent. Increasing Tmin trends throughout the cold season are most concentrated at higher elevations in the western half of the study area, from southern British Columbia in the Fraser-Columbia region to the Peel River-Lower Mackenzie region (Figure 3.8c). These high elevation areas experienced increasing trends through 5-6 months of the cold season. The remainder of the study area

shows persistence of increasing trends to be mostly 3-4 months with some small areas showing trend persistence of only 1-2 months. There were very few decreasing cold season Tmax and Tmin trends that persisted throughout multiple months, so they are not shown.

The warm season (May to October) shows fewer Tmax trends that persist through multiple months. Increasing trends are located in part of the Fraser-Columbia, the eastern part of the Athabasca River, and parts of the Peel River-Lower Mackenzie and Liard River regions through multiple months of the warm season (Figure 3.8b). The majority of persistent increasing trends in Tmin occur in the western half of the study area in the Fraser-Columbia, Pacific, Upper Peace, and Liard River regions (Figure 3.8d). Most of British Columbia experienced increasing Tmin trends throughout all 6 months of the warm season, with scattered patches of persistent trends through the rest of the study area. There were very few decreasing warm season trends in Tmax and Tmin, so they are not shown.

3.4.1.1 Hydrologic Relevance of Temperature Trends

Air temperature is an important factor in local and downstream water availability through its influence on evaporation and evapotranspiration in a watershed. Temperature is also a primary controlling factor of whether or not precipitation occurs as rain or snow, and influences the rate and timing of snowmelt. Therefore, the increasing trends in temperature presented in the previous section modify the proportion of rainfall to snowfall in the study area and also result in a shorter cold season and earlier start to the spring melt season. Shifts in precipitation type from snow to rain have already been

documented in previous research (Davis et al. 1999; Burn et al. 2004; Knowles et al. 2006), and earlier spring melt has also been detected in several previous studies (Brown & Braaten 1998; Burn & Hag Elnur 2002; Burn 2008).

Temperature increases during the summer also contribute to less water being available for streamflow. Though the trend magnitudes are lower in the warmer months of the year than the colder months, the increasing minimum temperature trends that persist throughout the headwaters of the Saskatchewan River basin may be a contributing factor to the decreased summer streamflow in this area detected by Rood et al. (2008) and Bawden et al. (2013). The increasing temperature trends during the colder months of the year also contribute to more frequent mid-winter melt events in areas of lower elevation throughout the study area. Further analysis of maximum and minimum daily air temperature into the future period can be seen in Chapter 4.4.1.

3.4.2 Precipitation

Mean annual precipitation varies across western Canada ranging from 1200 to 1800mm/year in the west to 100 to 300mm/year in the north, and 300 to 700mm/year in the interior portions of the study area (Figure 3.9a & Table 3.3).

Table 3.3. Mean annual precipitation and precipitation trend averaged across each study region for the time period 1950-2010.

Study Region	Annual Precipitation Total (mm)	Precipitation Trend (mm/decade)
Peel River-Lower Mackenzie	309.7	-0.2
Great Slave-Upper Mackenzie	309.1	-0.6
Liard River	486.7	13.1
Peace River	497.9	-9.7
Athabasca River	455.8	0.6
Saskatchewan River	448.3	0.4
Fraser-Columbia Rivers	721.5	12.6
Pacific Basins	819.3	16.3

The trend analysis results indicate that total annual precipitation trends range from -46 to 100mm/decade over the time period 1950-2010. Decreasing trends occur primarily at lower elevations, particularly east of the Rocky Mountains, where precipitation has decreased at a rate of -30mm/decade. Increasing precipitation rates occur in higher elevation areas, with values reaching 100mm/decade in the southern Rocky Mountains though most values fall between 20 to 60mm/decade (Figure 3.9b). The average rates of change across each study region are also shown in Table 3. The regional averages provide a reasonable indication of the conditions in each study region, though there are many small variations that occur within each region that are not captured by the averages. Each study region contains both increasing and decreasing significant trends, so the average trend in some regions is close to zero, even though not all trend results in the region are close to that value.

Precipitation is extremely variable over the course of the year, so analysis of monthly trends in precipitation patterns can provide insight to why the annual trends are so heterogeneous. Monthly total precipitation ranges from 13 to 97mm per month across each of the 8 study regions (Figure 3.10). The highest trend values occur during the summer months, with values of 31-65mm per month in all study regions, with the exception of the more coastally influenced Pacific basins, where the greatest precipitation amounts fall during the cooler months of the year, with values of 55 to 97mm per month. Monthly precipitation trends show decreases during the colder months in most regions, and increases during the warmer months (Figure 3.11).

Precipitation patterns have experienced a combination of increasing and decreasing trends between 1950 and 2010, which appear to vary greatly depending on time of year and location. Winter precipitation has decreased -1 to -4mm/decade in lower elevation areas east of the Rocky Mountains (Figure 3.12a). Increasing trends up to 10mm/decade have also occurred, primarily at high elevation areas within the Rocky Mountains, this may be related to increased temperature leading to increased atmospheric moisture (Davis et al. 1999). The largest precipitation increases are located at high elevations with smaller increases at lower elevations. The positive trends in the Fraser-Columbia region are associated with statistically significant clustering of values higher than the mean and the decreases east of the Rocky Mountains fall within clusters of values lower than the mean, indicating that these regions are spatially autocorrelated and are regions of similar change.

Precipitation has increased 1.5 to 5mm/decade throughout the spring, with increases in

the west and north of the study area. The greatest increases reach 8mm/decade, mostly within the Liard River region (Figure 3.12b). Decreases of -0.5 to -5mm/decade occur in parts of the northern half of the study area as well as the Prairies. The increasing precipitation trends in the west of the study area correspond to statistically significant clusters of values higher than the mean, though the clusters extent beyond the extent of significant trend values. The decreasing trends in parts of the northern half of the study area and in the Prairies are mostly within larger clusters of values lower than the mean.

During the summer months precipitation has experienced increases of 2 to 10mm/decade with the largest trend values in the Liard River and Pacific regions (Figure 3.12c). Decreasing trends of -3 to -6mm/decade also occur in small pockets throughout the Fraser-Columbia, Athabasca, and Saskatchewan River regions in the late summer. The increasing trends in the Liard and Pacific regions are located within large clusters of values higher than the mean, indicating a region of similar change.

Trends in the fall are almost entirely negative, with values of -2 to -5mm/decade over most of the study area and decreases as low as -10mm/decade in coastal areas (Figure 3.12d). The western half of the study area contains clusters of values lower than the mean while the negative trends in the north and east of the study area do not correspond to any significant clustering of values.

Global Moran's *I* values range from 0.77 in January to 0.97 in July and August, indicating greater positive autocorrelation and a greater degree of significant clustering in the summer than the winter. December, January, and February have also experienced precipitation decreases across much of the study area, mostly in non-coastal regions. In

mountainous regions, particularly the Liard River basin, trend analysis shows that winter precipitation is decreasing while summer precipitation is increasing. The decreases in lower-latitude winter precipitation along with the increases in higher-latitude summer precipitation indicate a shift toward precipitation occurring more at northern latitudes (Bates et al. 2008; Zhang et al. 2007). Screen and Simmonds (2012) also detected increases in northern latitude precipitation, as well as an increase in rainfall compared to snowfall. Precipitation is also shifting to the summer months in some areas, and toward higher elevations.

Throughout the cold season, November to April, decreasing trends occur in most months throughout a large portion of the study area (Figure 3.13a). The Athabasca, Peace, Liard, and Saskatchewan regions experience persistent decreases in precipitation throughout 4-5 months of the cold season, while the remainder of the study area contains decreasing trends throughout 1-3 months of the cold season. There are very few increasing trends during the cold season, with only the Pacific, a small part of the Fraser-Columbia and the easternmost portion of the Athabasca experiencing increasing trends throughout 2-3 months of the cold season.

The warm season, May to October, experienced very few decreasing trends, with a persistence of only 1-2 of the 6 months covering very little of the study area. Increasing trends during the warm season are much more persistent, with the Liard River region experiencing increasing trends during 4-6 months of the warm season (Figure 3.13b). Persistent trends are also located in the eastern Athabasca, Pacific, and southern Fraser-Columbia, with increases during 2-4 months of the warm season.

3.4.2.1 Hydrologic Relevance of Precipitation Trends

Precipitation is one of the primary contributing factors to streamflow. Any changes to amount and timing of precipitation can modify streamflow. The increased summer precipitation in the Liard River region and surrounding areas may have led to increased summer streamflow in the northern half of the study area. Conversely, the persistent trends in decreasing cold season precipitation that occur throughout most of the study area likely contribute to decreased snow accumulation. If the detected trends in fall and winter precipitation continue, the decreased precipitation during winter throughout the study area along with the decreases to lower latitude precipitation during spring and summer may make water management more difficult for dry areas of Canada, particularly the Prairies. The detected precipitation trends have contributed to decreased streamflow and drier conditions across the Prairies in summer (Bawden et al. 2013). Analysis of potential future scenarios in precipitation can be seen in Chapter 4.4.2.

3.4.3 Snow Accumulation

Annual snow accumulation ranges from 0mm up to 700mm SWE across western Canada. The highest values of 500 to 700mm SWE per year occur in the coastal and Rocky mountain ranges, with values of 150 to 300mm SWE per year at the middle elevations, and lower values of 70 to 140mm SWE per year at lower elevations and in the Prairies (Figure 3.14a). The spatially averaged snow accumulation totals for each study region are shown in Table 3.4.

Table 3.4. Total annual snow accumulation and snow accumulation trend values spatially averaged across each study region for the time period 1950-2010. Spatial averages include all calculated trend values.

Study Region	Annual Snow Accumulation Total (mm SWE)	Snow Accumulation Trend (mm SWE/decade)
Peel River-Lower Mackenzie	155.9	-2
Great Slave-Upper Mackenzie	134.4	-4
Liard River	200.7	-9
Peace River	182.5	-9
Athabasca River	141.8	-7
Saskatchewan River	119.4	-6
Fraser-Columbia Rivers	320.9	-6
Pacific Basins	387.0	-10

The trend analysis results indicate rates of change for annual total snow accumulation that range from -70 to 65mm SWE/decade over the time period 1950-2010 (Figure 3.14b). Snow accumulation has decreased across most of the study area annually, though there are some small areas of increased snow accumulation. The coastal mountains of British Columbia have experienced decreases from -70mm SWE/decade to -35mm SWE/decade, while most of the study area contains more moderate decreases between -3mm SWE/decade and -15mm SWE/decade. The increases in snow accumulation occur in both the Rocky Mountains and the coastal mountains in the northern Pacific study region, with rates of 10-30mm SWE/decade with some values as high as 60mm SWE/decade.

Snow accumulation is greatest through the cold season in all study regions, with most snow accumulation taking place during the late fall and winter months (Figure 3.15).

Snow accumulation trends show statistically significant decreases across most of the study area in most months of the year. November through April, snow accumulation has decreased by -1 to -3mm SWE/decade, particularly in the Liard, Peace, Athabasca, and Saskatchewan River basins (Figure 3.16). There were very few significant trends from June through September, as most areas have no snow cover during these months of the year.

Winter snow accumulation has declined -2 to -5mm/decade across most of the study area with some larger decreases in coastal areas (Figures 3.17a and 3.17b). Some increases of 5 to 10mm/decade also occurred at high elevations in coastal areas and the Rocky Mountains (Figure 3.17c). The decreasing trends in snow accumulation all correspond to significant clusters of values lower than the mean, while the increases are within statistically significant clusters of values higher than the mean though the clusters extend beyond the boundaries of the significant trends, so these regions likely contain increasing tendencies that are not statistically significant.

Snow accumulation during spring has also decreased -1 to -5mm/decade, with the largest decreases located in coastal British Columbia and near the Saskatchewan River headwaters (Figure 3.17d). Later in the spring, most of the study area does not contain statistically significant trends, but those that exist range from -1 to -2mm/decade. The larger snow accumulation decreases early in the spring correspond to significant clusters of values lower than the mean, indicating similar change throughout these regions; the clusters follow the higher elevation areas from south to north within the dataset.

Summer has experienced very few statistically significant trends. However, September does show some small patches of decreasing trends of -0.5 to -1mm SWE/decade in mountainous areas in the southwest of the study area that are likely related to the statistically significant increases in minimum temperature in these areas, causing precipitation to fall as rain rather than snow.

Widespread decreases of -1 to -7mm/decade occurred throughout the fall, particularly in November (Figure 3.17e) and December (Figure 3.17f) while October did not experience many significant trends. However, snow accumulation did increase 2-10mm/decade at high elevations in the Pacific and southern Fraser-Columbia regions. These increasing trends were located within a cluster of values higher than the mean while the northern half of the study area and Prairies contained large clusters of values lower than the mean indicating that these areas are regions of similar change.

The months of October through May show Global Moran's *I* values of 0.82-0.91, indicating strong spatial autocorrelation and clustering among calculated trends in these months. Brown & Braaten (1998) detected decreasing snowpack and shorter snow cover duration across most of Canada in nearly all months of the year. Small pockets of increasing trends have also been identified in the Fraser/Columbia region during November, January, and March, despite most significant trends during these months being negative. Statistically significant precipitation increases in these areas during January and March, as well as increasing tendencies (not statistically significant) in November and February, combined with increases in minimum temperature during these months indicates a greater capacity for water vapour storage, thus increasing moisture

content in the air, potentially leading to an increase in the accumulation of snow at these higher elevations (Hamlet et al. 2005; Moore & McKendry 1996).

Decreasing trends were quite persistent throughout the cold season across the study area. All study regions contain some areas with decreasing trends in snow accumulation through multiple months (Figure 3.18a). The most persistent trends occur in the Athabasca, with decreasing trends through all 6 months of the cold season. The Liard and Saskatchewan also contain persistent trends with decreasing trends through 4-5 months of the cold season. The southern Fraser-Columbia has experienced increasing trends during 3 months of the cold season, indicating an overall increase in snow accumulation in this high elevation area, while the remainder of the study area shows very few persistent trends (Figure 3.18b).

3.4.4 Snowmelt

Annual snowmelt shows a wide range of values across western Canada, with average values of 250 to 960mm/year in the west at high elevations and 80 to 120mm/year in the north and the interior portions of the study area (Figure 3.19a). The annual totals averaged across each study region are shown in Table 3.5.

Table 3.5. Total annual snowmelt and snowmelt trend values spatially averaged across each study region for the time period 1950-2010. Spatial averages include all calculated trend values.

Study Region	Annual Snowmelt Total (mm)	Snowmelt Trend (mm/decade)
Peel River-Lower Mackenzie	156.8	-4
Great Slave-Upper Mackenzie	133.9	-4
Liard River	198.9	-10
Peace River	181.2	-10
Athabasca River	141.0	-8
Saskatchewan River	118.3	-7
Fraser-Columbia Rivers	316.9	-5
Pacific Basins	387.7	-12

The trend analysis results indicate rates of change for annual total snowmelt from -70 to 70mm/decade over the time period 1950-2010. Decreasing trends occur across the majority of the study area, particularly at lower or mid-elevation areas in interior regions; these areas have experienced decreasing snowmelt of -2 to -15mm/decade while the increases are mostly in higher elevation areas, with values of 25 to 65mm/decade in the southern Rocky Mountains and northern Pacific region (Figure 3.19b). The average rates of change across each study region are also shown in Table 3.5. The regional averages provide a reasonable indication of the conditions in each study region, though there are spatial variations in trend values within the study regions that are not captured by only looking at the averages. Most study regions contain both increasing and decreasing

significant trends, so some region averages are slightly negative even though parts of the study region may show strongly positive trend results.

Snowmelt peaks in most regions during April or May, with monthly totals of 50 to 170mm; this melt is a major contributing factor of spring and summer streamflow throughout the study region (Figure 3.20). Values through the remainder of the year are very low. Trends throughout the study area indicate increased snowmelt during January through April, and decreased snowmelt through May and June (Figure 3.21). The increases in January and February are small, with much larger increases in April. May and June have experienced snowmelt decreases in all study regions.

Snowmelt in the early winter has increased 0.2 to 4mm/decade at lower elevations in the western half of the study area (Figure 3.22a and 3.22b). These are indicative of increased instances of mid-winter melt caused by rising temperatures. Later in the winter the largest statistically significant snowmelt increases are located in the lower elevations of the Fraser-Columbia and Pacific regions, with snowmelt increases of 1.5 to 7mm/decade, and maximum increases up to 10mm/decade (Figure 3.22c). Snowmelt increases east of the Rocky Mountains are smaller, with values from 0.1 to 2mm/decade, or negative with values of -2 to -4mm/decade that may be related to the decreased snow accumulation in the Prairies during the winter months.

Early spring contains some of the largest snowmelt increases, with values up to 10mm/decade, particularly in the Liard and Pacific regions (Figure 3.22d). In the southern half of the study area, lower elevation areas contain decreasing snowmelt trends, likely due to the increased snowmelt in the winter as well as the decreased snow

accumulation. Snowmelt trends are mostly negative later in the spring with values of -5 to -15mm/decade (Figure 3.22e and 3.22f). The greatest decreases occurred at higher latitudes and in non-coastal areas. In late spring, the decreasing trends are generally located in areas where that snowmelt increased during previous months. The areas of higher elevation throughout the study area are also significantly clustered, indicating similar changes throughout this region.

3.4.4.1 Hydrologic Relevance of Snow Accumulation and Melt Trends

A large portion of the streamflow in western Canada originates in the Rocky Mountains and is dependent upon winter snow accumulation and spring melt. The Rocky Mountains store water in the form of snow and ice all winter, then as the snow melts during the spring it provides flow to the Fraser and Columbia Rivers which flow to the Pacific, the Saskatchewan River which flows across the Prairies and eventually to Hudson Bay, and to the Peace, Athabasca, and Liard Rivers which feed the Mackenzie River and eventually the Arctic Ocean. The spring freshet volume is largely dependent upon winter snow accumulation, thus the widespread decreases to winter snow accumulation have likely contributed to decreases in spring freshet volume as well as decreased summer streamflow throughout western Canada. The trend results show some increases to mid-winter snowmelt at lower elevations in the southwest of the study area, contributing to increases in winter streamflow, particularly in the Fraser-Columbia, Pacific, and Peace River regions (Moore & McKendry 1996; Rood et al. 2008). The timing of the spring freshet is important as well, since it generally peaks in the spring and then the snowmelt continues slowly throughout the summer, providing flow to much of western Canada during the driest times of year. Increased winter streamflow may lead to decreased spring

freshet volume in some parts of the study area if the snow already melted earlier in the year.

Trends also indicate peak snowmelt has been shifting earlier in the year, from April and May toward March. Areas that experienced significant increases in snowmelt during March and April also experienced significant decreases during May and June. Earlier snowmelt has been detected by many previous studies. This trend corresponds to increased temperatures during these months, resulting in an earlier onset of the spring freshet (Burn 2008; Zhang et al. 2001; Stewart et al. 2005; Schindler & Donahue 2006; Whitfield 2001). Further analysis of snow depth and snowmelt in the future period can be seen in Chapter 4.4.3 and 4.4.4.

3.4.5 Hydrologic Relevance of Calculated Trends in Climate

The variables analysed in this research are all individually important factors in hydroclimate of a watershed and all have their own impacts on streamflow, but they also interact in numerous ways to produce changes at both regional and continental scales. The increasing trends in both maximum and minimum temperature have contributed to a shortened cold season, so while snow accumulation has decreased throughout the cold season, it also accumulates for a shorter period of time. In addition to being dependent upon precipitation, snow accumulation and snowmelt are also dependent upon temperature, since it determines whether precipitation accumulates as snow or becomes streamflow.

Throughout the cold season, precipitation has mostly decreased; this corresponds to the detected decreases to snow accumulation over much of the study area. These results are

consistent with increased frequencies of mid-tropospheric synoptic climate types associated with high air temperatures and low precipitation throughout the cold season (Newton et al. 2013). In contrast to the general decrease in precipitation over most of the study area, areas of very high elevation are somewhat of an exception to this trend, since the increased temperatures in these areas cause increased water vapour storage in the air and thus more precipitation occurs, but temperatures are still below zero so snow accumulation has increased slightly. During the warm season precipitation increased in some areas, particularly in the Liard River region, and to a lesser extent, the Peace River and Pacific regions. This has likely resulted in the increased spring and summer streamflow detected in the Lower Liard region between 1976 and 2000 (Bawden et al. 2013). Streamflow increases were also detected as far downstream as the Lower Mackenzie region.

The shortening of the cold season associated with the detected increases in temperature also means that snowmelt begins earlier in the year, with increased snowmelt values in March and April and then decreases during May and June. Snowmelt has also increased during the winter at lower elevations, which is related to the increased temperatures detected during January and February in particular; this increase in mid-winter melt has contributed to increased winter streamflow in some parts of the study area, primarily the Fraser-Columbia and Pacific regions (Bawden et al. 2013).

The interactions between trends in hydroclimatic variables within the study area combine to point out several major trends. The cold season has decreased in length, with the snowmelt and spring freshet occurring earlier in the year. The decreased cold season

length along with decreases in precipitation has led to a less snow accumulation and less snowmelt, and likely a decreased spring freshet volume. Precipitation has also shifted more toward warm season months and more northern latitudes, with less precipitation falling in the driest parts of the study area, so summer streamflow is expected to be greater in the northern watersheds of the study area while the southern watersheds show less streamflow during the warm season.

3.5 Conclusion

Climate variables related to streamflow were assessed for trend over the period 1950-2010 using the Mann-Kendall non-parametric test and various spatial analysis techniques. Maximum and minimum temperatures have increased, both on an annual basis as well as through most months of the year. Minimum temperatures have generally increased more than maximum temperature, decreasing the overall temperature range. The greatest increases to both maximum and minimum temperature appear to occur during the winter months. The temperature also seems to increase more at northern latitudes, as well as at higher elevations in the mountain ranges located within the study area. The results also indicate a redistribution of precipitation toward summer months and northern latitudes. This is shown in the precipitation trend results that indicate a concentration of increasing precipitation during the summer months in the Liard River region as well as some of the surrounding areas while the cold season contains results that are almost entirely negative. Snow accumulation during the cold season has decreased as a result of the decreased precipitation, and snowmelt has increased throughout most winter and spring months, indicating greater mid-winter melt and an earlier spring freshet.

To further this research, it would be helpful to complete trend analysis on a seasonal and cold season/warm season basis as an addition to the monthly analysis to provide more insight into seasonal shifts in these hydroclimatic variables. Analysis of future scenarios would also be useful to determine if trends detected in the current time period are likely to continue into the future; this is further explored in Chapter 4.

References

Adam, J., Hamlet, A. & Lettenmaier, D. 2009. Implications of global climate change for snowmelt hydrology in the twenty-first century. Hydrological Processes, 23, 962-972.

Akinremi, O.O., McGinn, S.M. & Cutforth, H.W. 1999. Precipitation Trends on the Canadian Prairies. *Journal of Climate*, 12(10), 2996-3003.

Babish, G. 2006. *Geostatistics without tears: A practical guide to surface interpolation, geostatistics, variograms, and kriging*. Edition 2006.03. Regina, SK, Canada: Environment Canada.

Bates, B.C., Kundzewicz, Z.W. & Palutikof J.P. (Eds.) 2008. *Climate Change and Water: IPCC Technical Paper VI*, Geneva, Switzerland: IPCC Secretariat.

Bawden, A.J., Burn, D.H. & Prowse, T.D. 2013. *Recent changes in patterns of western Canadian river flow and association with climatic drivers: A CROCWR component*. M.A.Sc Thesis. University of Waterloo, Ontario, Canada.

Brown & Braaten. 1998. Spatial and Temporal Variability of Canadian Monthly Snow Depths , 1946-1995. *Atmosphere-Ocean*, 36(1), 37-54.

Burn D.H., Abdul Aziz, O.I., Pietroniro, A. 2004. A comparison of trends in hydrological variables for two watersheds in the Mackenzie River Basin. *Canadian Water Resources Journal*, 29(4), 283-298.

Burn, D.H. 2008. Climatic influences on streamflow timing in the headwaters of the Mackenzie River Basin. *Journal of Hydrology*, 352, 225- 238.

Burn, D.H. & Hag Elnur, M.A. 2002. Detection of hydrologic trends and variability. *Journal of Hydrology*, 255.

Bussieres, N. & Milewska, E. 2010. Potential limitations of using satellite data to evaluate the spatial detail in climatological air temperature maps. *Atmosphere-Ocean*, 48(8), 294-307.

Cohen, S.J. 1991. Possible impacts of climatic warming scenarios on water resources in the Saskatchewan River sub-basin, Canada. *Climatic Change*, 19, 291-317.

Davis, Lowit, Knappenberger, & Legates. 1999. A climatology of snowfall-temperature relationships in Canada. Journal of Geophysical Research, 104(10), 11,985–11,994.

Déry, S.J. 2005. Decreasing river discharge in northern Canada. *Geophysical Research Letters, 32*(10), L10401

Dyer, J. 2008. Snow depth and streamflow relationships in large North American watersheds. *Journal of Geophysical Research*, 113(D18), 1-12.

Dyer & Mote 2006. Spatial variability and trends in observed snow depth over North America. *Geophysical Research Letters*, 33(16), 1-6.

Farmer, C.J.Q., Nelson, T.A., Wulder, M.A. & Derksen, C. 2009. Spatial-temporal patterns of snow cover in western Canada. *Canadian Geographer, 4*, 473-487.

Fürst, J. & Hörhan, T. 2009. Coding of watershed and river hierarchy to support GIS-based hydrological analyses at different scales. *Computers & Geosciences*, 35(3), 688–696.

Gibson, J., Prowse, T., & Peters, D. 2006. Hydroclimatic controls on water balance and water level variability in Great Slave Lake. *Hydrological Processes*, 20, 4155-4172.

Gray, D.M. & Prowse, T.D. 1993. "Chapter 7: Snow and Floating Ice". In *Handbook of Hydrology*, McGraw-Hill, New York, USA.

Groisman. P.Y. & Easterling, D.R. 1994. Variability and trends of total precipitation and snowfall over the United States and Canada. *Journal of Climate, 7*, 184-205.

Hamlet, A.F., Mote, P.W., Clark, M.P. & Lettenmaier, D.P. 2005. Effects of Temperature and Precipitation Variability on Snowpack Trends in the Western United States*. *Journal of Climate*, *18*(21), 4545–4561.

Holland, M., Finnis, J., Barrett, A., & Serreze, M. 2007. Projected changes in Arctic Ocean freshwater budgets. *Journal of Geophysical Research*, 112.

Hutchinson, MF, McKenney, DW, Lawrence, K, Pedlar, JH, Hopkinson, RF, Milewska, E, & Papadopol, P. 2009. Development and Testing of Canada-Wide Interpolated Spatial Models of Daily Minimum–Maximum Temperature and Precipitation for 1961–2003. *Journal of Applied Meteorology and Climatology*, *48*(4), 725–741.

Jost, G., Moore, R.D., Smith, R., & Gluns, D., 2012. Distributed temperature-index snowmelt modelling for forested catchments. *Journal of Hydrology*, 420-421, 87–101.

Karl, T., Jones, P.D., Knight, R.W., Kukla, N.P., Razuvayev, V., Gallo, K.P., Lindseay, J., Charlson, R.J. & Peterson, T.C. 1993. A new perspective on recent global warming: Asymmetric trends of daily maximum and minimum temperature. *Bulletin of the American Meteorological Society, 74*(6), 1007-1023.

Kendall, M.D. 1975. *Rank correlation measures*, Charles Griffin, London, UK.

Knowles, N., Dettinger, M. & Cayan, D. 2006. Trends in snowfall versus rainfall in the western United States. *Journal of Climate, 19*, 4545-4559.

Mann, H.B. 1945. Non-parametric tests against trend. *Econometrica*, 13, 245-259.

McGuire, C.R., Nufio, C.R., Bower, M.D., & Guralnik, R.P. 2012. Elevation-dependent temperature trends in the Rocky Mountain Front Range: changes over a 56- and 20-year record. *PLoS one*, 7(9), e44370.

McKenney, D., Hutchinson, M.F., Papadopol, P., Lawrence, K., Pedlar, J., Campbell, K., Milewska, E., Hopkinson, R.F., Price, D. & Owen, T. 2011. Customized spatial climate models for North America. *Bulletin of the American Meteorological Society*, 1611–1622.

Min, S.-K., Zhang, X. & Zwiers, F. 2008. Human-induced Arctic moistening. *Science*, 320(5875), 518–20.

Mitchell, A. 2005. *The ESRI Guide to GIS Analysis, Volume 2: Spatial Measurements & Statistics*, ESRI Press, Redlands, USA.

Moore, RD & McKendry, I. 1996. Spring snowpack anomaly patterns and winter climatic variability. *Water Resources Research*, 32(3), 623-632.

Pederson, G.T., Gray, S.T., Ault, T., Marsh, W., Fagre, D.B., Bunn, A.G., Woodhouse, C.A. & Graumlich, L.J. 2011. Climatic controls on the snowmelt hydrology of the Northern Rocky Mountains. *Journal of Climate*, 24(6): 1666-1687.

Prowse, T.D., Bonsal, B.R., Burn, D.H., Dibike, Y.B., Edwards, T., Ahmed, R., Bawden, A.J., Linton, H.C., Newton, B.W. & Walker, G.S. 2013. Climatic Redistribution of Canada's Western Water Resources (CROCWR). Proceedings of the 19th International Northern Research Basins Symposium and Workshop, Southcentral Alaska, USA, August 11-17th, 2013.

Rood, S.B., Pan, J., Gill, K.M., Franks, C.G., Samuelson, G.M., Shepherd, A. 2008. Declining summer flows of Rocky Mountain rivers: Changing seasonal hydrology and probable impacts on floodplain forests. *Journal of Hydrology*, 349, 397-410.

Schindler, D. & Donahue, W. 2006. An impending water crisis in Canada's western prairie provinces. *Proceedings of the National Academy of Sciences*, 103(19), 7210-7216.

Screen, J. & Simmonds, I. 2012. Declining summer snowfall in the Arctic: causes, impacts and feedbacks. *Climate Dynamics*, 38(11-12), 2243-2256.

Sen, P.K. 1968. Estimates of the regression coefficient based on Kendall's Tau. *Journal of the American Statistical Association*, 63(324), 1379-1389.

Stewart, I.T., Cayan, D. & Dettinger, M. 2004. Changes in snowmelt runoff timing in western North America under a 'business as usual' climate change scenario. *Climate Change, 62,* 217-232.

Stewart, I.T., Cayan, D., & Dettinger, M. 2005. Changes toward earlier streamflow timing across western North America. *Journal of Climate*, 18(8), 1136-1155.

Stewart, I.T. 2009. Changes in snowpack and snowmelt runoff for key mountain regions. *Hydrological Processes*, 23, 78-94.

Thorne, R. & Woo, M. 2011. Streamflow response to climatic variability in a complex mountainous environment: Fraser River Basin, British Columbia, Canada. *Hydrological Processes*, *25,* 3076-3085.

Vincent, L.A. & Mekis, É. 2006. Changes in daily and extreme temperature and precipitation indices for Canada over the twentieth century. *Atmosphere-Ocean, 44*(2), 177-193.

Vincent, L., van Wijngaarden, W. & Hopkinson, R. 2007. Surface temperature and humidity trends in Canada for 1953-2005. *Journal of Climate*, *20*(20), 5100-5113.

Whitfield, P. 2001. Linked hydrologic and climate variations in British Columbia and Yukon. *Environmental Monitoring and Assessment*, 67(1-2), 217-238.

Woo, M. & Thorne, R. 2003. Streamflow in the Mackenzie Basin , Canada. *Arctic Institute of North America*, *56*(4), 328–340.

Xu, C.Y. & Singh, V.P., 2004. Review on regional water resources assessment models under stationary and changing climate. *Water Resources Management*, 18, 591-612.

Zhang, X., Vincent, L., Hogg, W., & Niitsoo, A. 2000. Temperature and precipitation trends in Canada during the 20th century. *Atmosphere-Ocean*, 38(3), 395-429.

Zhang, X., Harvey, K.D, Hogg, W.D., Yuzyk, T.R. 2001. Trends in Canadian streamflow. *Water Resources Research*, 37(4), 987-998.

Zhang. X., Zwiers, F.W., Hegerl, G.C., Lambert, F.H., Gillett, N.P., Solomon, S., Stott, P.A. & Nozawa, T. 2007. Detection of human influence on twentieth-century precipitation trends. *Nature*, 448, 461-465.

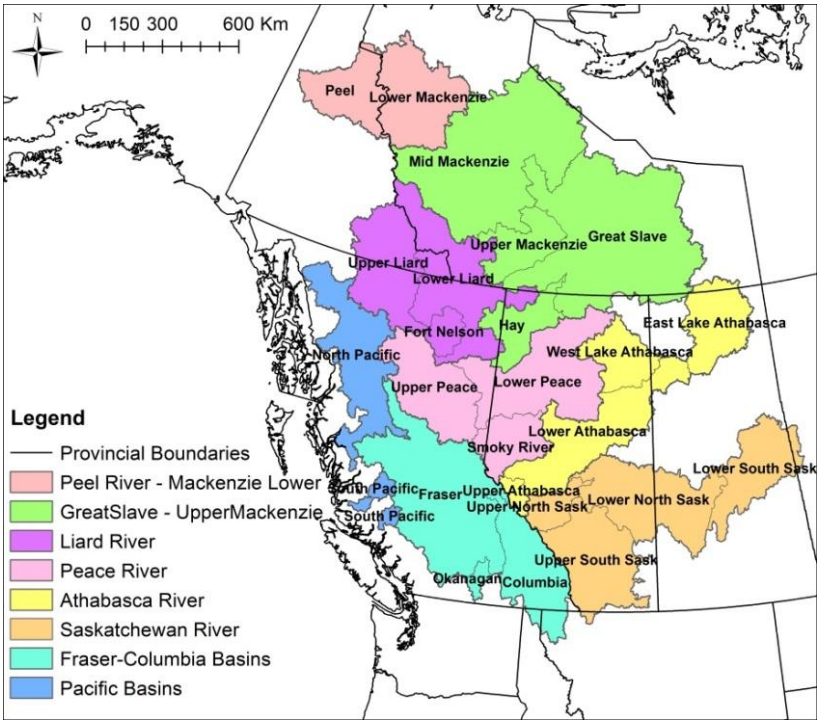

Figure 3.1. Map of study area, gray outlines indicate study watersheds, while coloured polygons show study regions used in analysis.

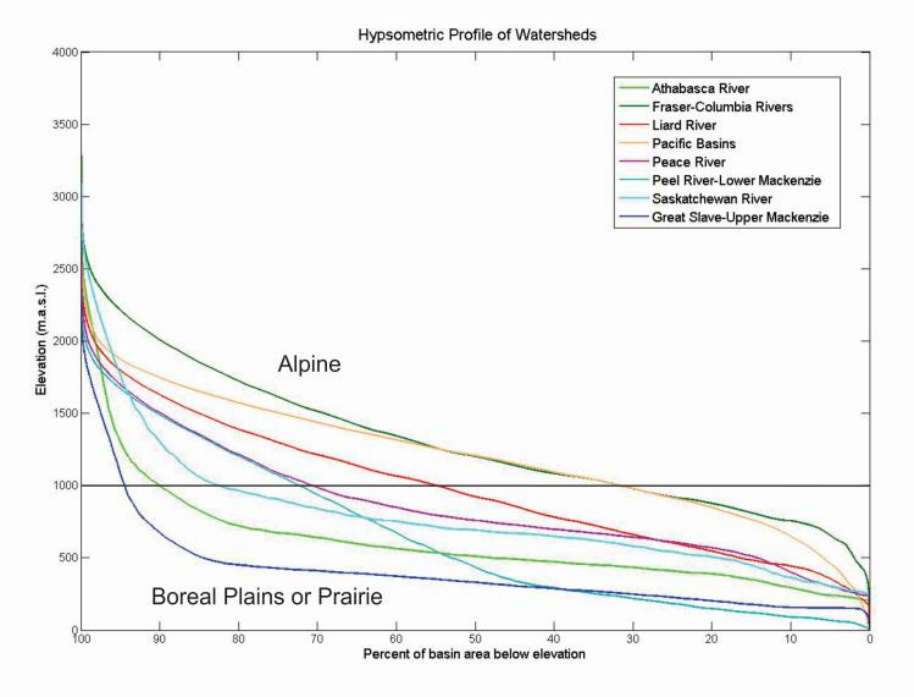

Figure 3.2. Hypsometric curves of each study region identified in Figure 3.1.

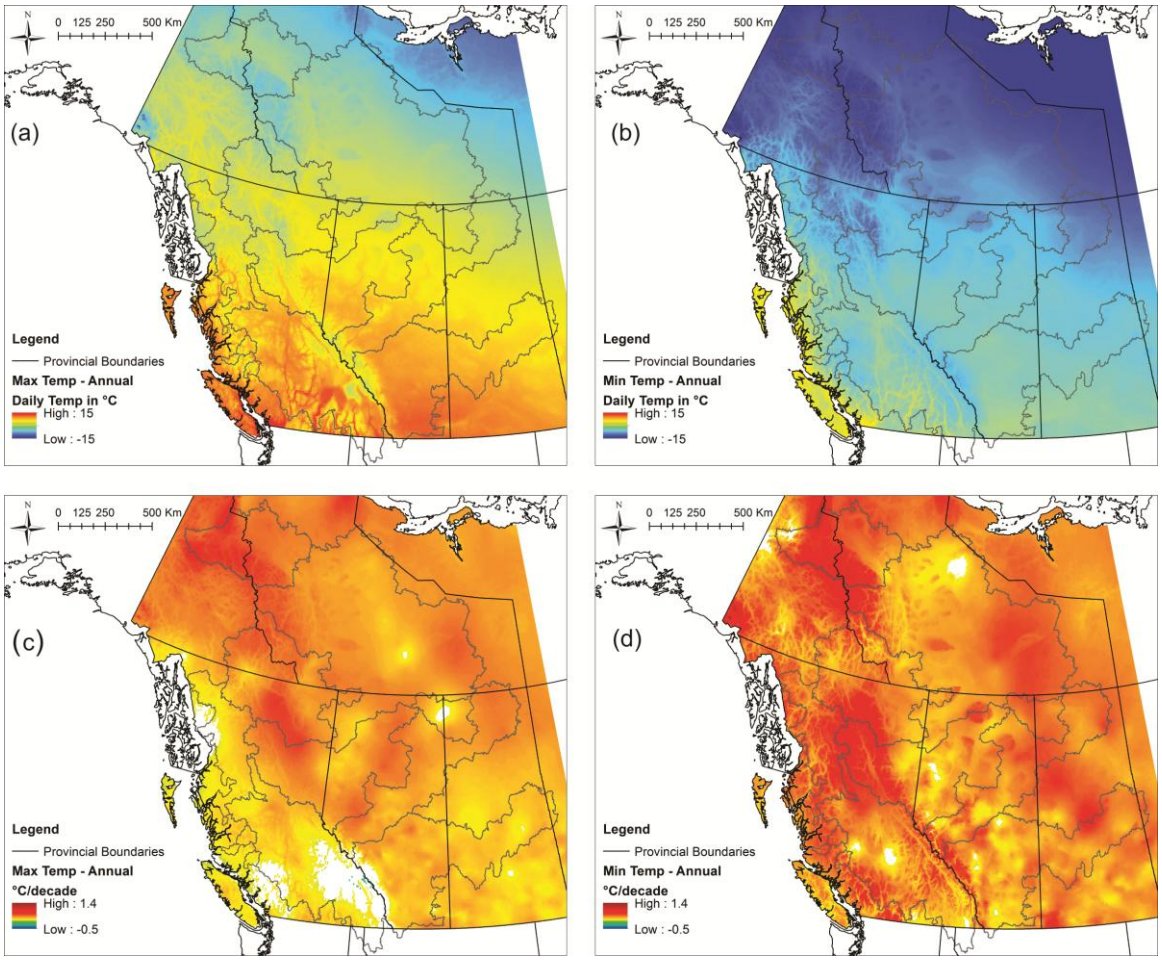

Figure 3.3. Annual means and trends in daily maximum (Tmax) and minimum (Tmin) temperatures during 1950-2010 (a) mean annual Tmax in ^{o}C (b) mean annual Tmin in ^{o}C (c) mean annual Tmax trend in ^{o}C/decade, and (d) mean annual Tmin trend in ^{o}C/decade. Only trend results statistically significant at 10% or better are shown.

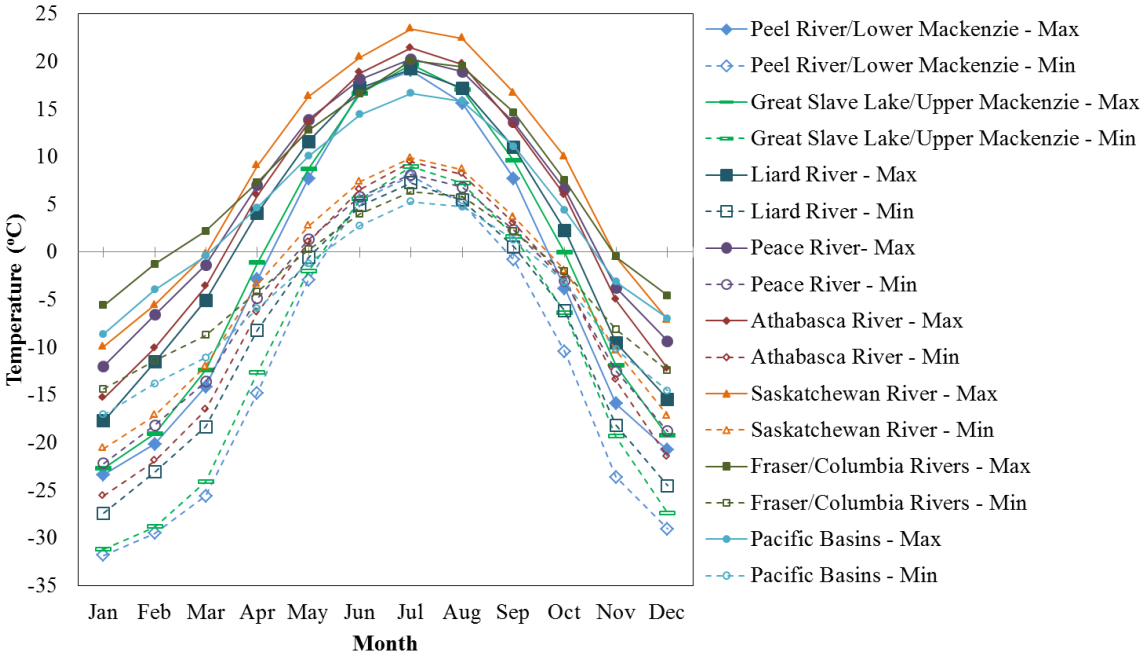

Figure 3.4. Daily average Tmax and Tmin for each month spatially averaged for each study region. Tmax shown with solid symbols and lines, Tmin shown with unfilled symbols and dashed lines.

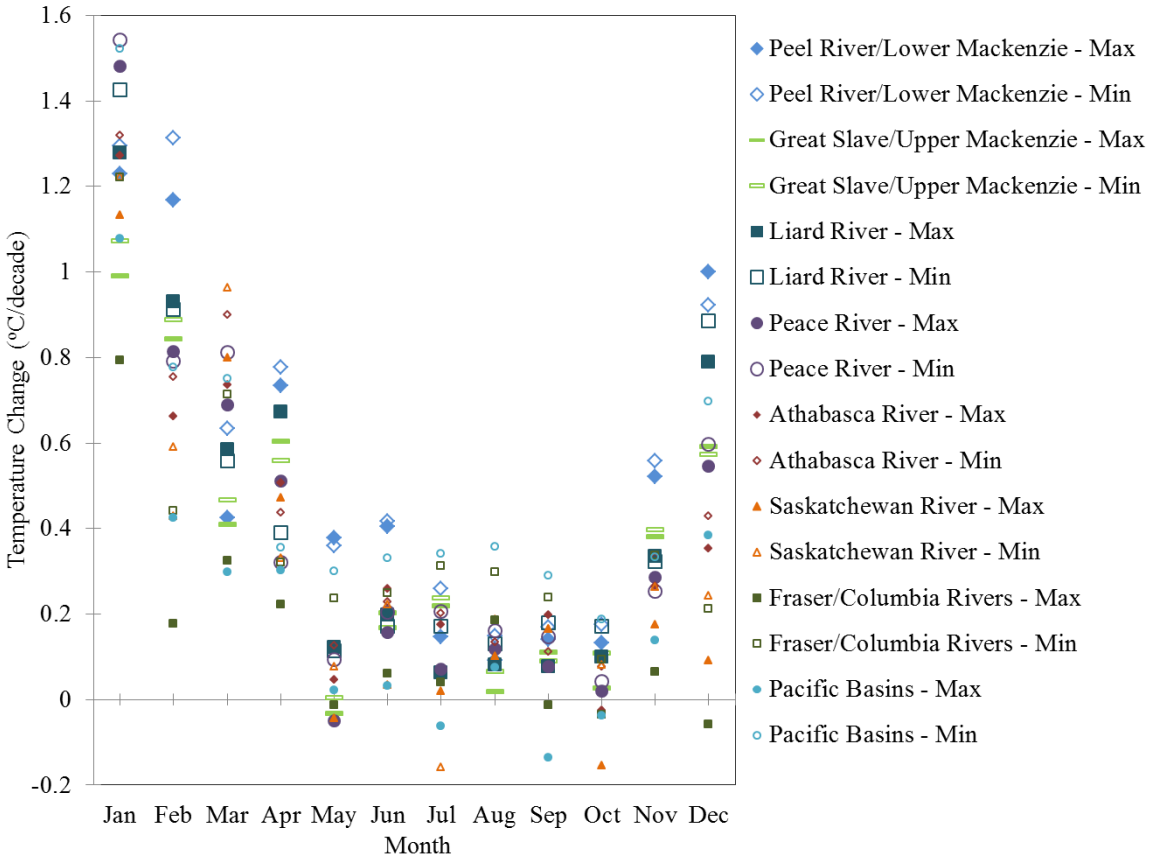

Figure 3.5. Spatially averaged regional rate of change in monthly mean Tmax and Tmin. Results include all calculated trend values. Tmax shown with solid symbols, Tmin shown with unfilled symbols.

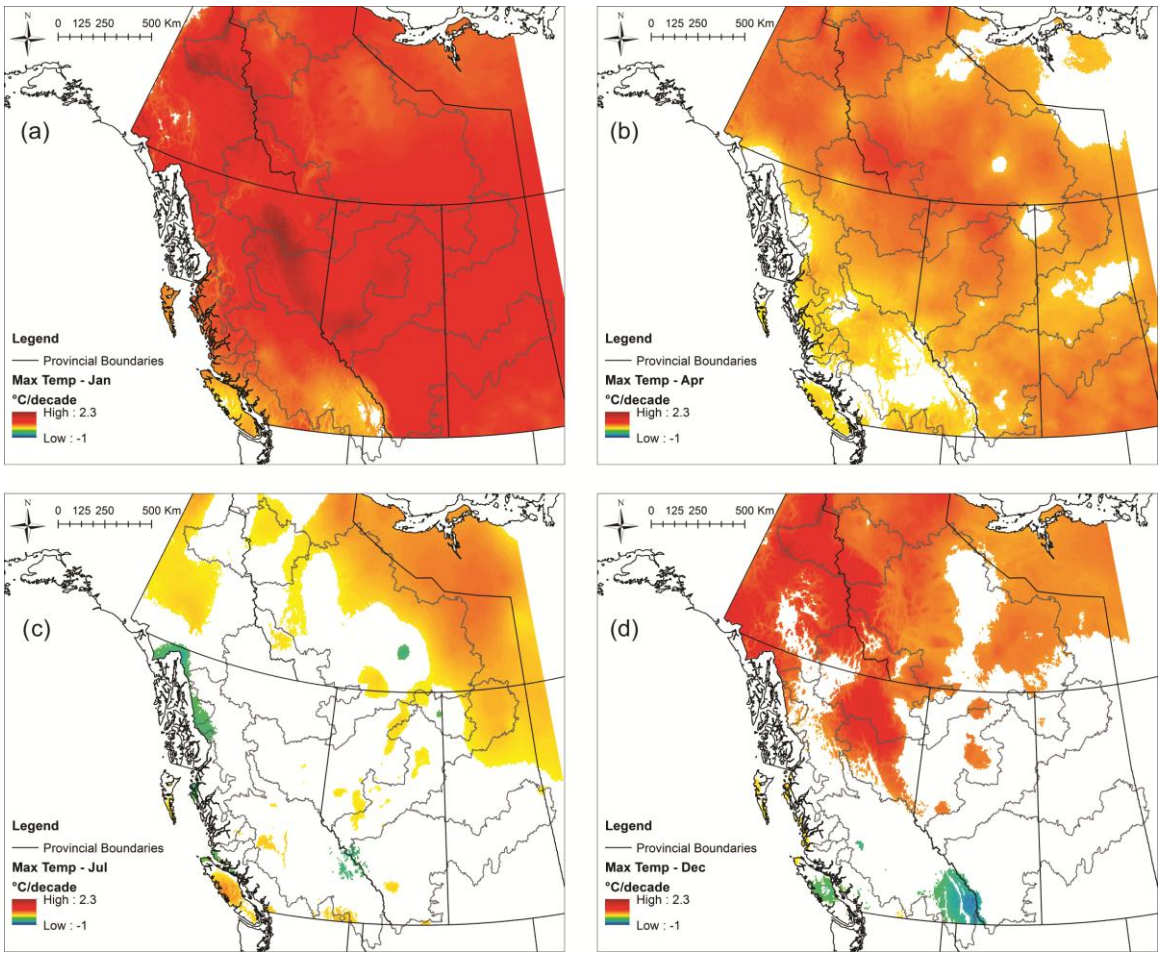

Figure 3.6. Daily Tmax trends in ^{o}C/decade, 1950-2010, for (a) January, (b) April, (c) July, and (d) December. Only trend results statistically significant at 10% or better are shown.

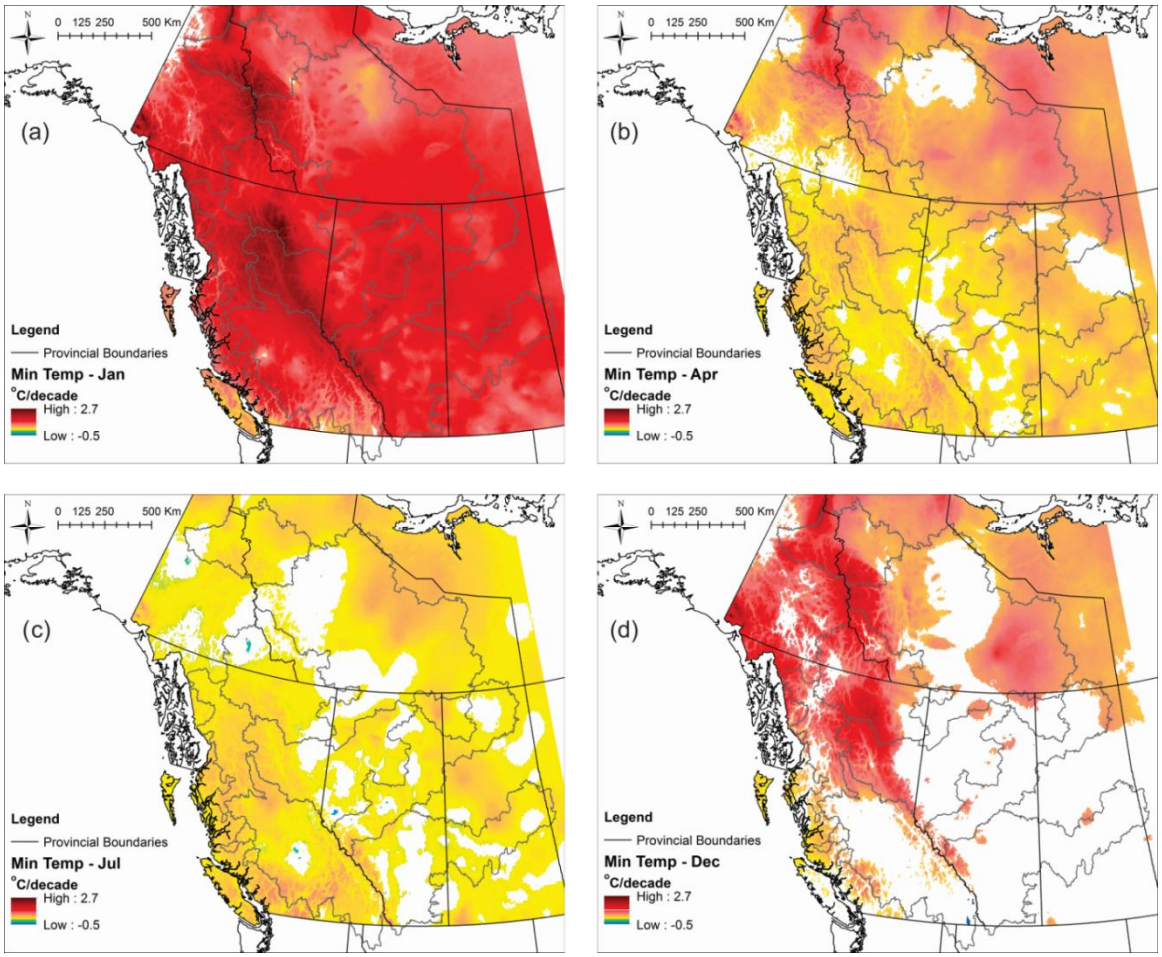

Figure 3.7. Daily Tmin trends in ^{o}C/decade, 1950-2010, for (a) January, (b) April, (c) July, and (d) December. Only trend results statistically significant at 10% or better are shown.

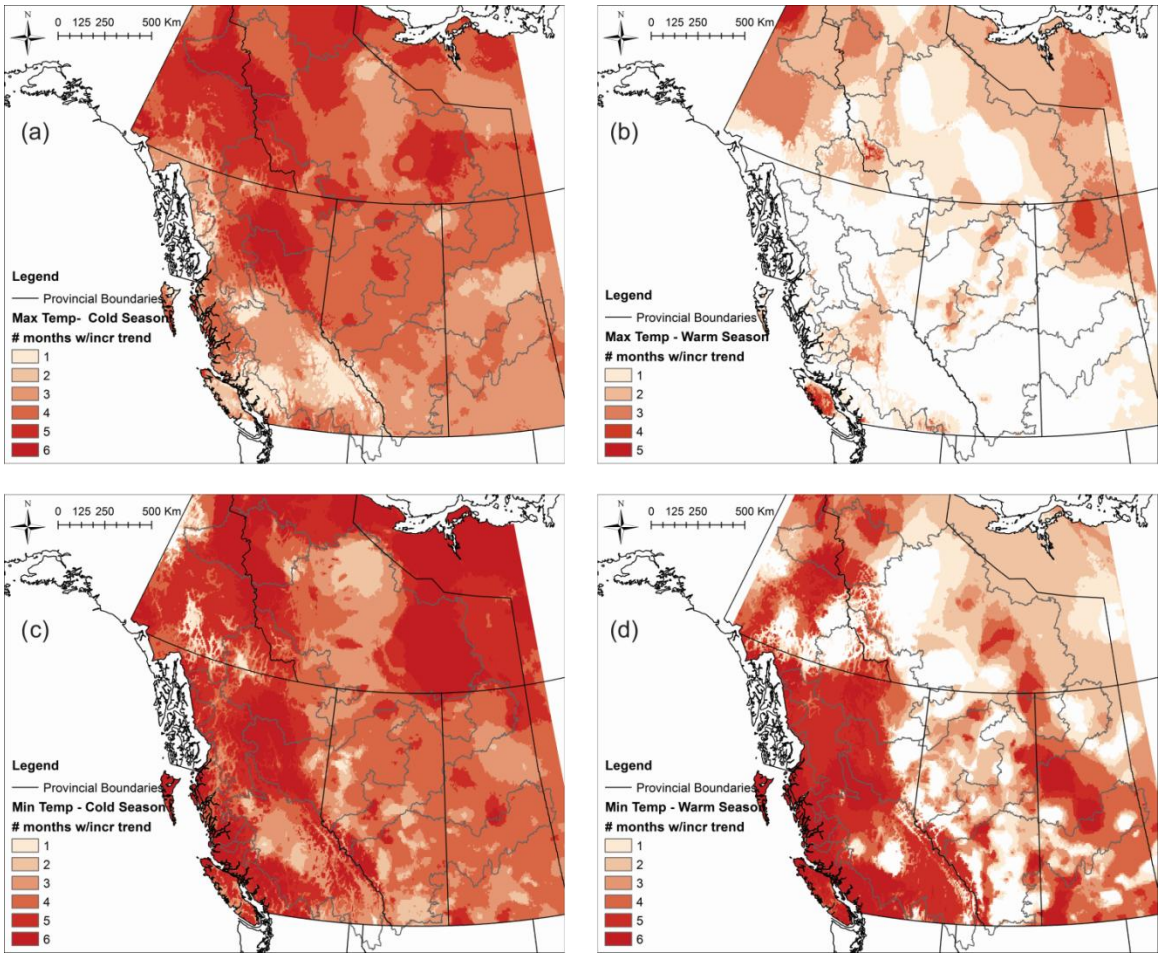

Figure 3.8. Trend persistence maps where colour corresponds to number of months with increasing trend through the cold season (November to April) or the warm season (May to October). (a) Tmax increasing trend persistence through the cold season. (b) Tmax increasing trend persistence through the warm season. (c) Tmin increasing trend persistence through the cold season. (d) Tmin increasing trend persistence through the warm season.

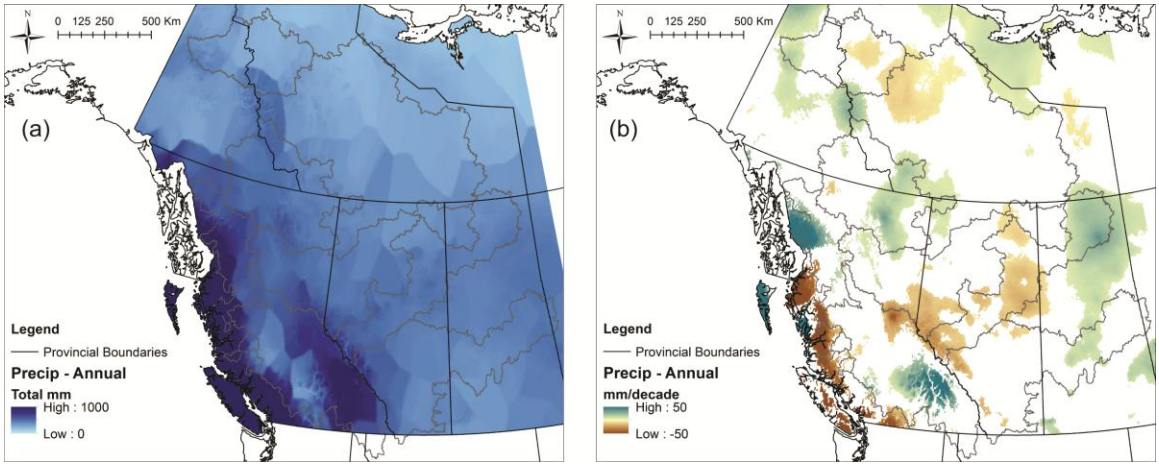

Figure 3.9. Precipitation average annual total and annual trends for 1950-2010. (a) Precipitation average annual total in millimeters, (b) precipitation annual trend in mm/decade. Only trend results statistically significant at 10% or better are shown.

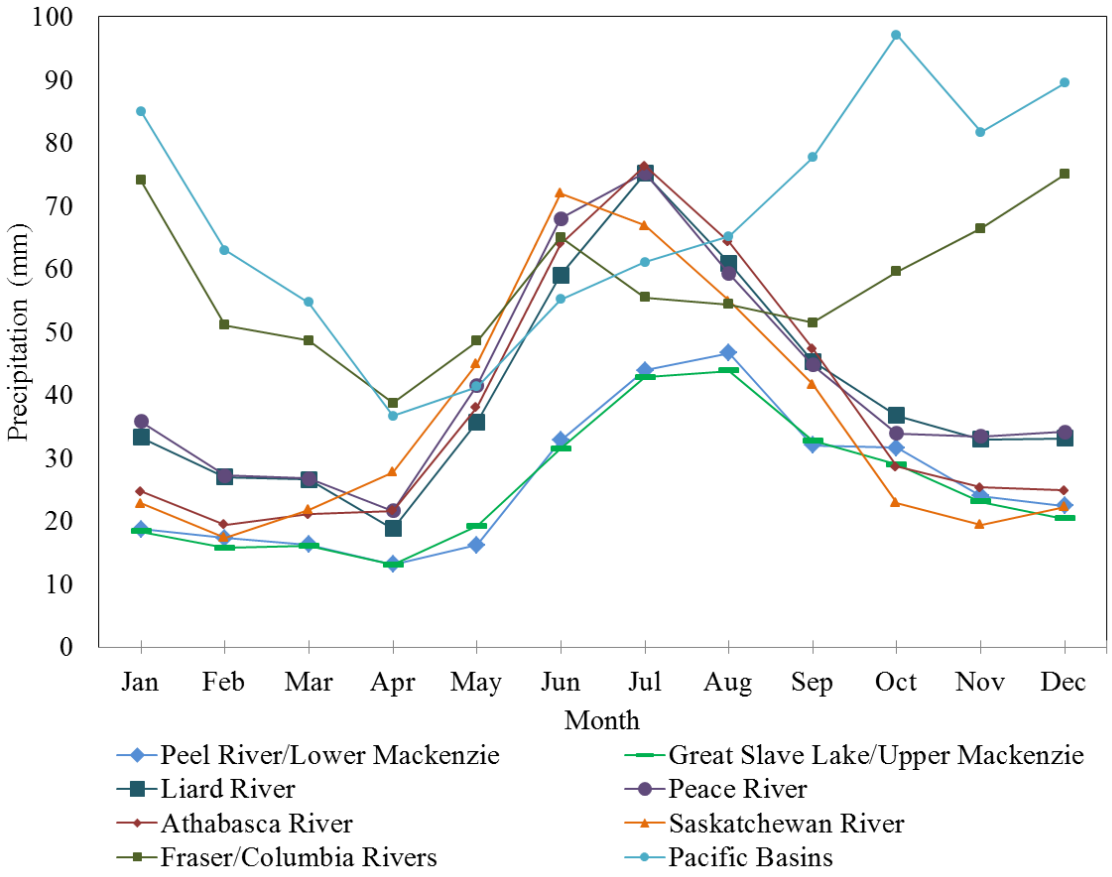

Figure 3.10. Spatially averaged regional precipitation totals for each month.

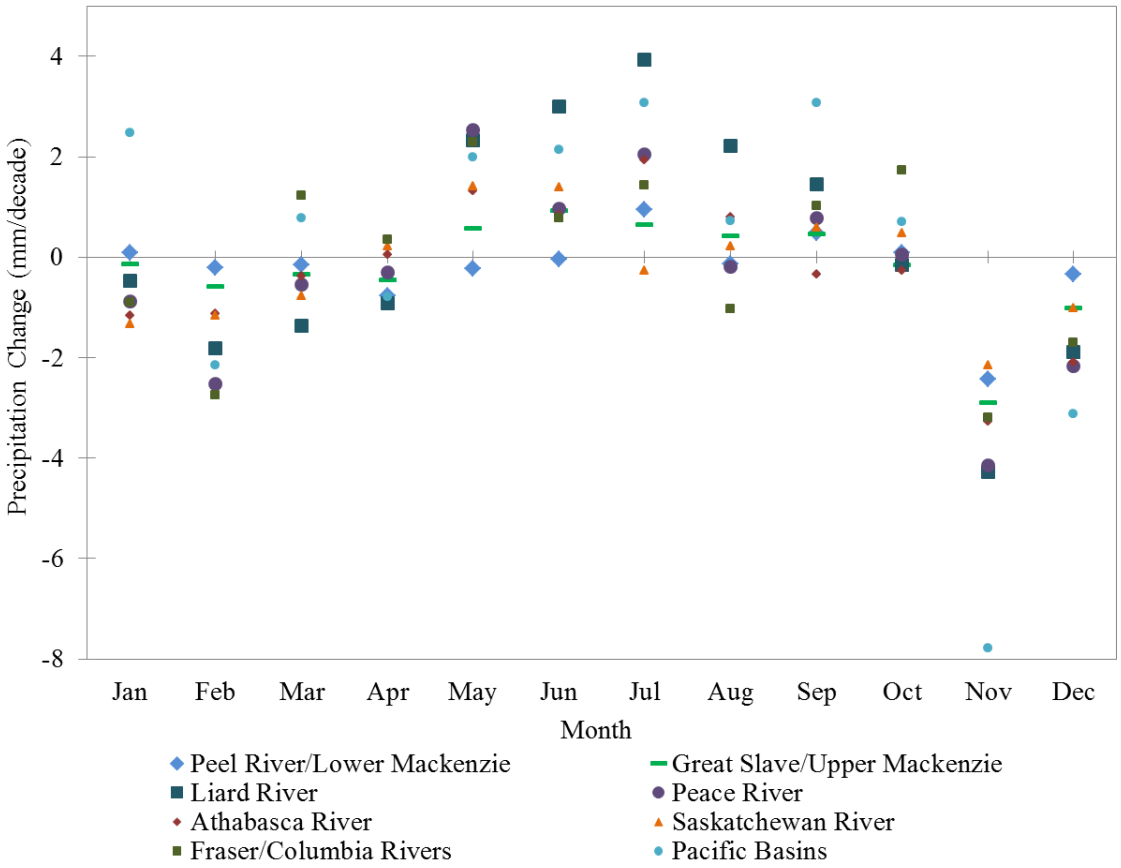

Figure 3.11. Spatially averaged rate of change of monthly total precipitation in mm/decade, from 1950-2010. Results include all calculated trend values.

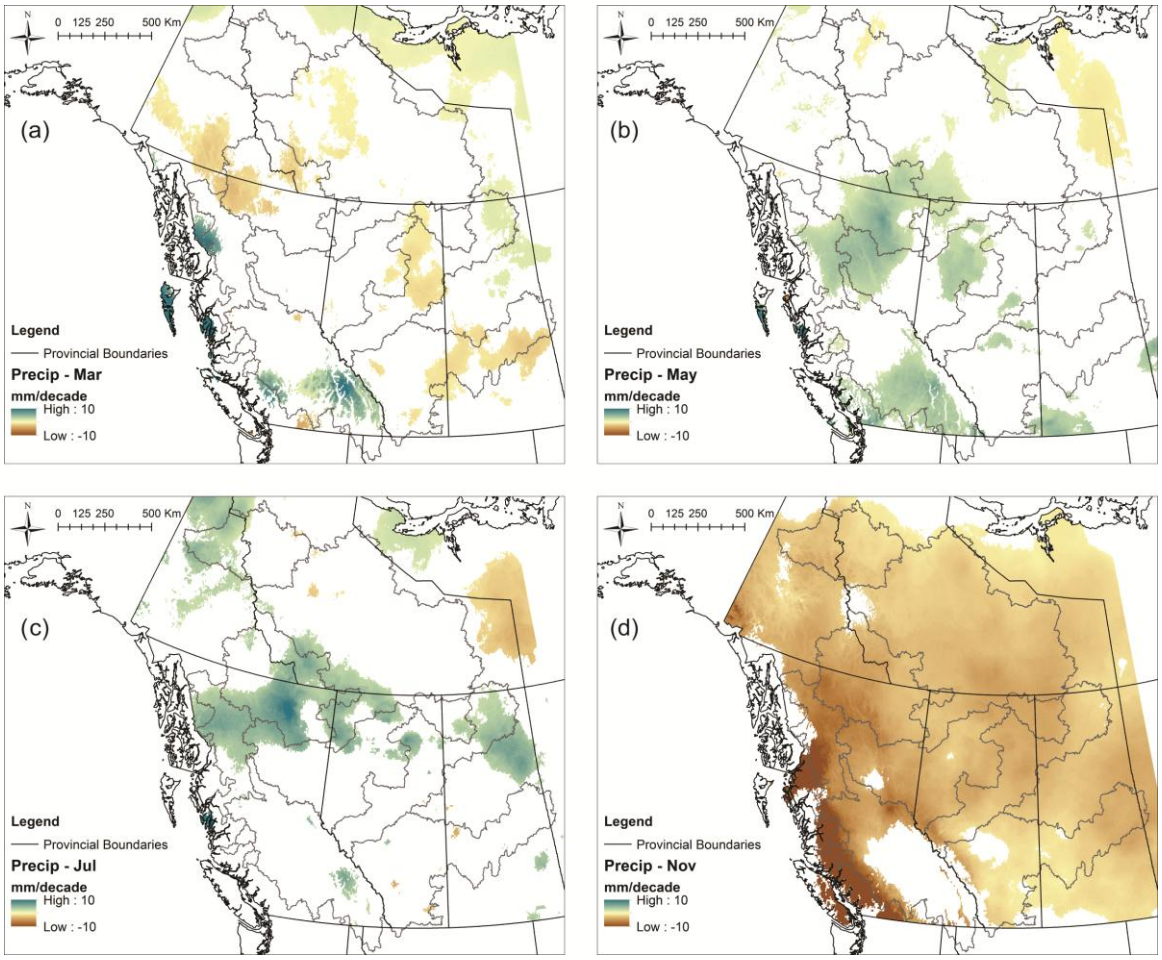

Figure 3.12. Precipitation trends in mm/decade, 1950-2010, for (a) March, (b) May, and (c) July, and (d) November. Only trend results statistically significant at 10% or better are shown.

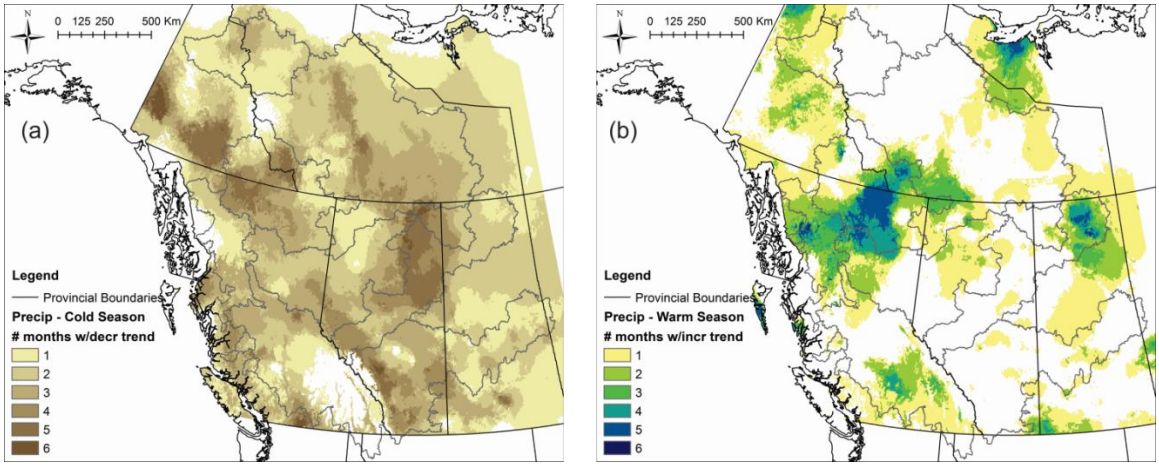

Figure 3.13. Trend persistence maps where colour corresponds to number of months with increasing or decreasing trend through the cold season (November to April) or the warm season (May to October) (a) decreasing precipitation trend persistence through the cold season, (b) increasing precipitation trend persistence through the warm season.

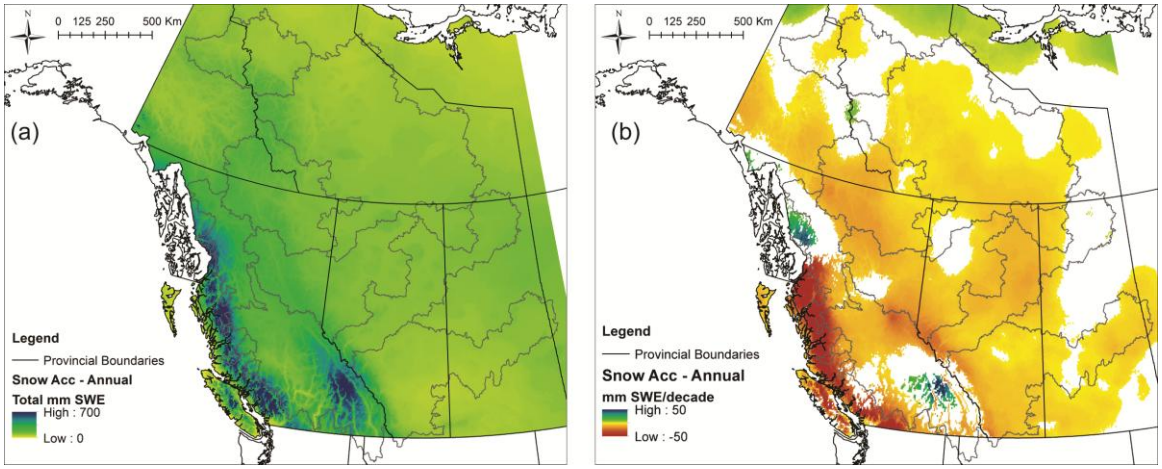

Figure 3.14. Mean annual snow accumulation and trends for 1950-2010. (a) mean annual snow accumulation in mm SWE, (b) annual trend of snow accumulation in mm SWE/decade. Only trend results statistically significant at 10% or better are shown.

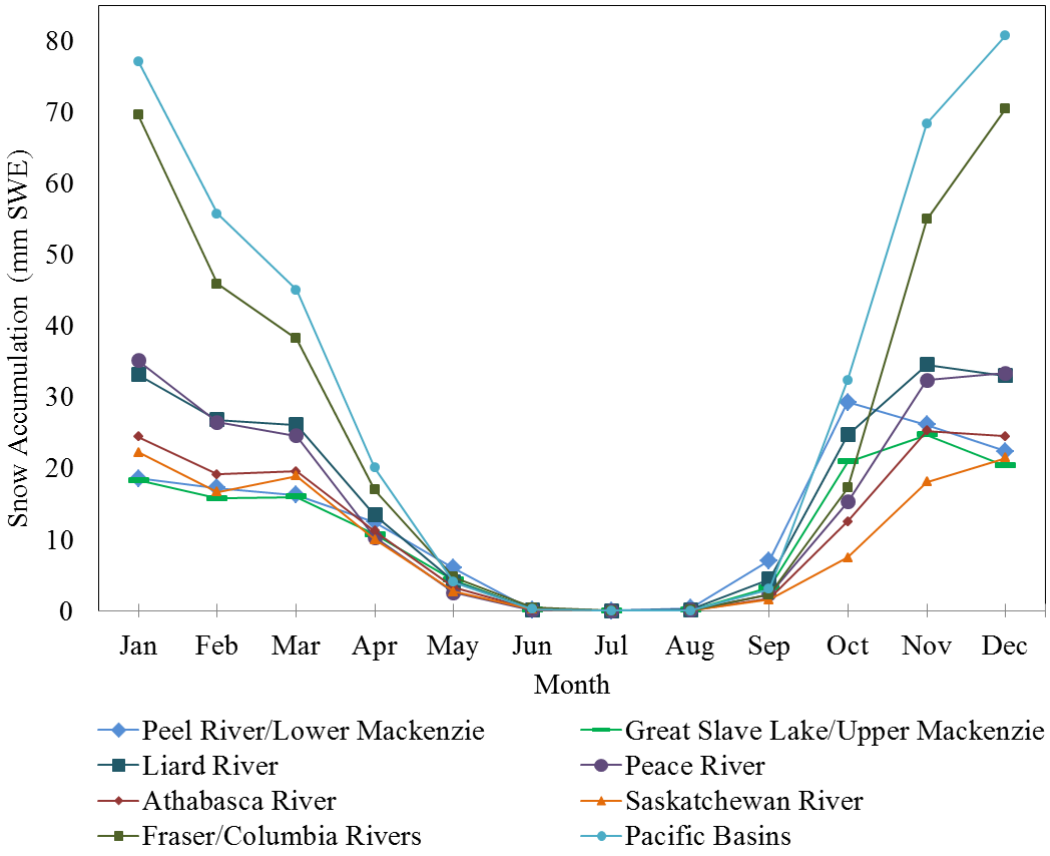

Figure 3.15. Spatially averaged snow accumulation totals for each month.

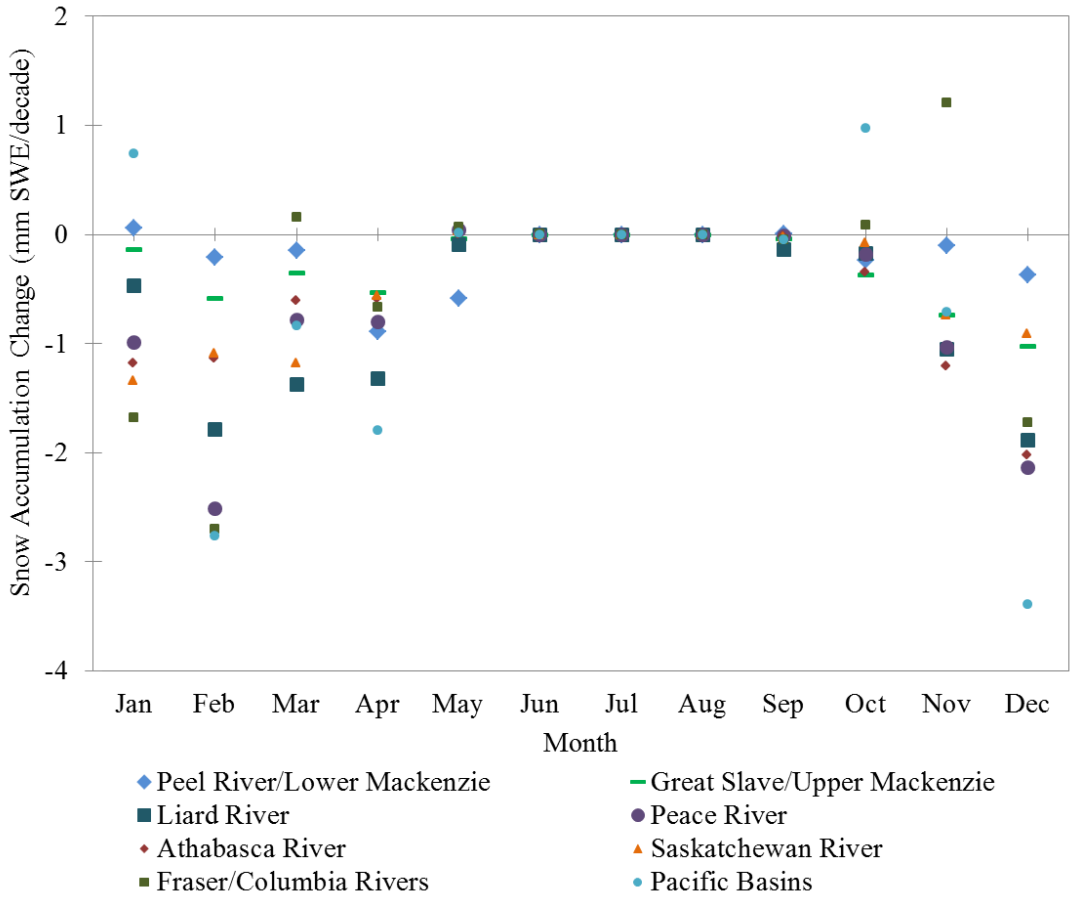

Figure 3.16. Monthly snow accumulation trends in mm SWE/decade spatially averaged for each study region, from 1950-2010. Results include all calculated trend values.

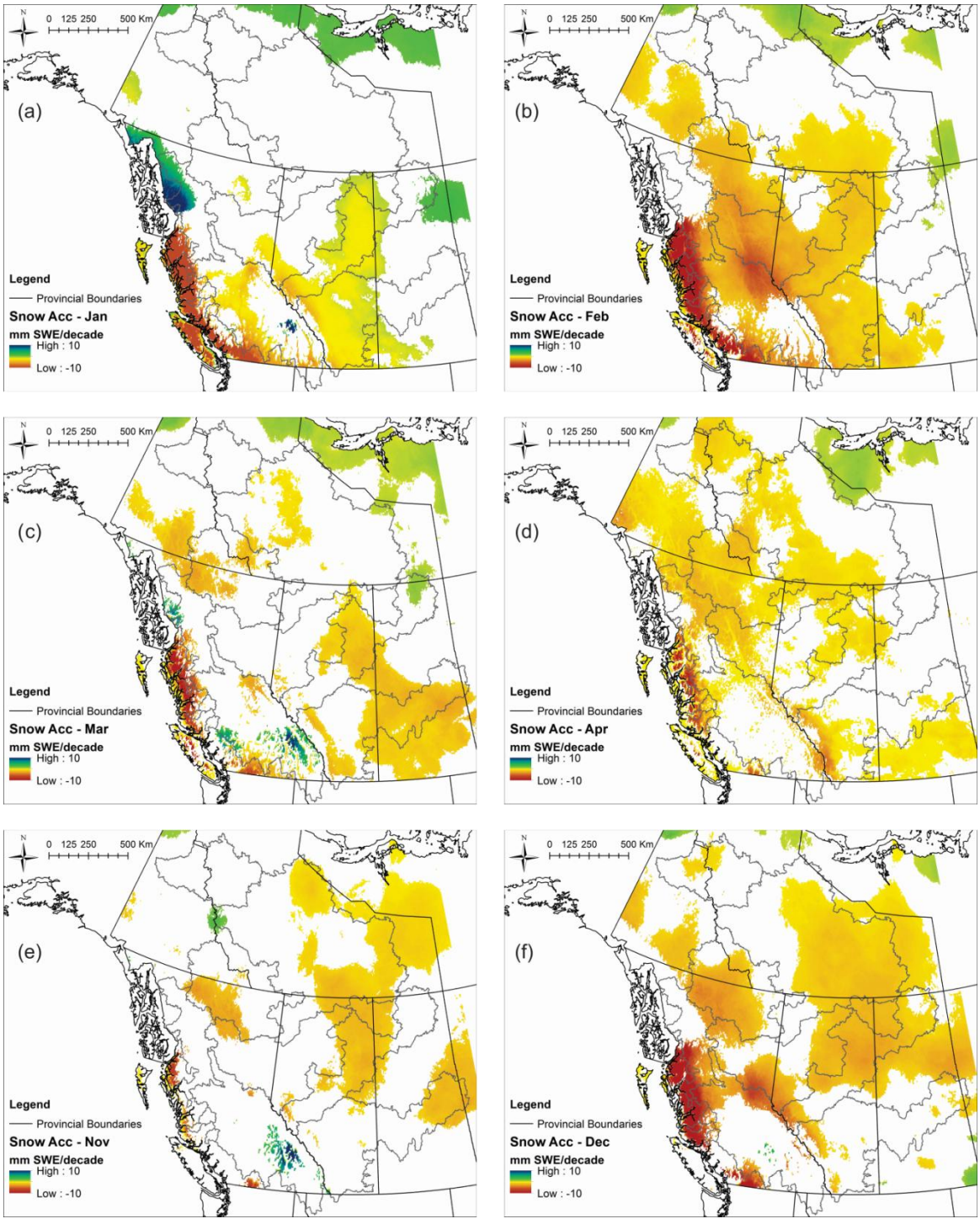

Figure 3.17. Snow accumulation trends in mm SWE/decade, 1950-2010, for (a) January, (b) February, (c) March, (d) April, (e) November, and (f) December. Only trend results statistically significant at 10% or better are shown.

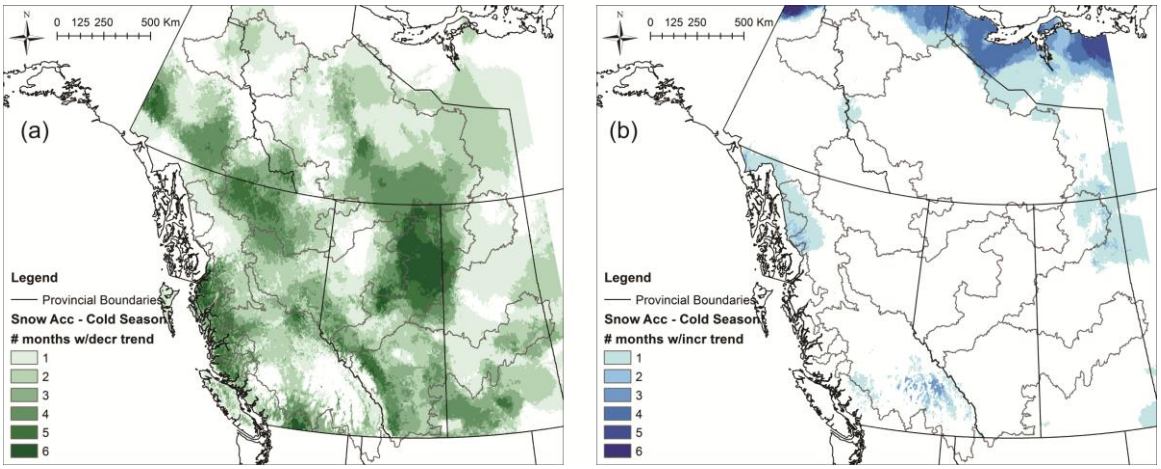

Figure 3.18. Snow accumulation trend persistence through the cold season (November to April). Colour corresponds to number of months with increasing or decreasing trend. (a) decreasing trend persistence, (b) increasing trend persistence.

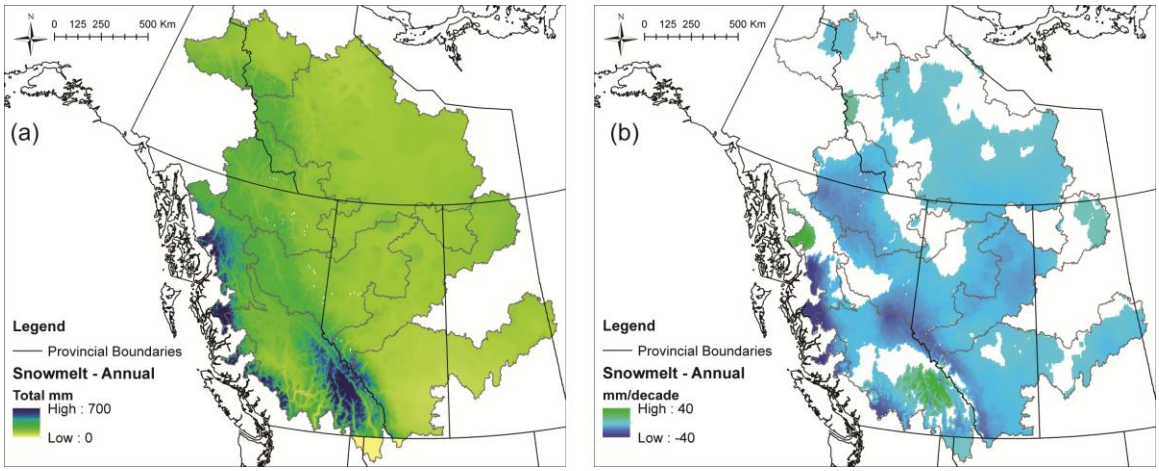

Figure 3.19. Mean annual snowmelt and trends for 1950-2010. (a) Mean annual snowmelt in mm, (b) annual snowmelt trends in mm/decade. Only trend results statistically significant at 10% or better are shown.

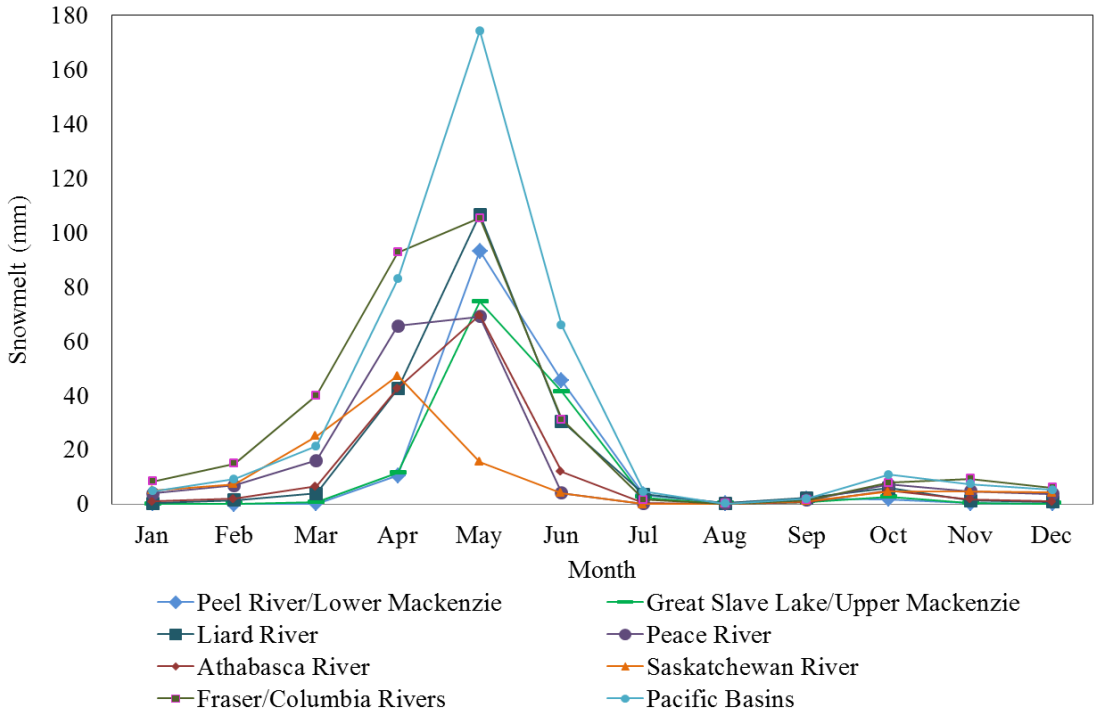

Figure 3.20. Spatially averaged snowmelt totals for each month.

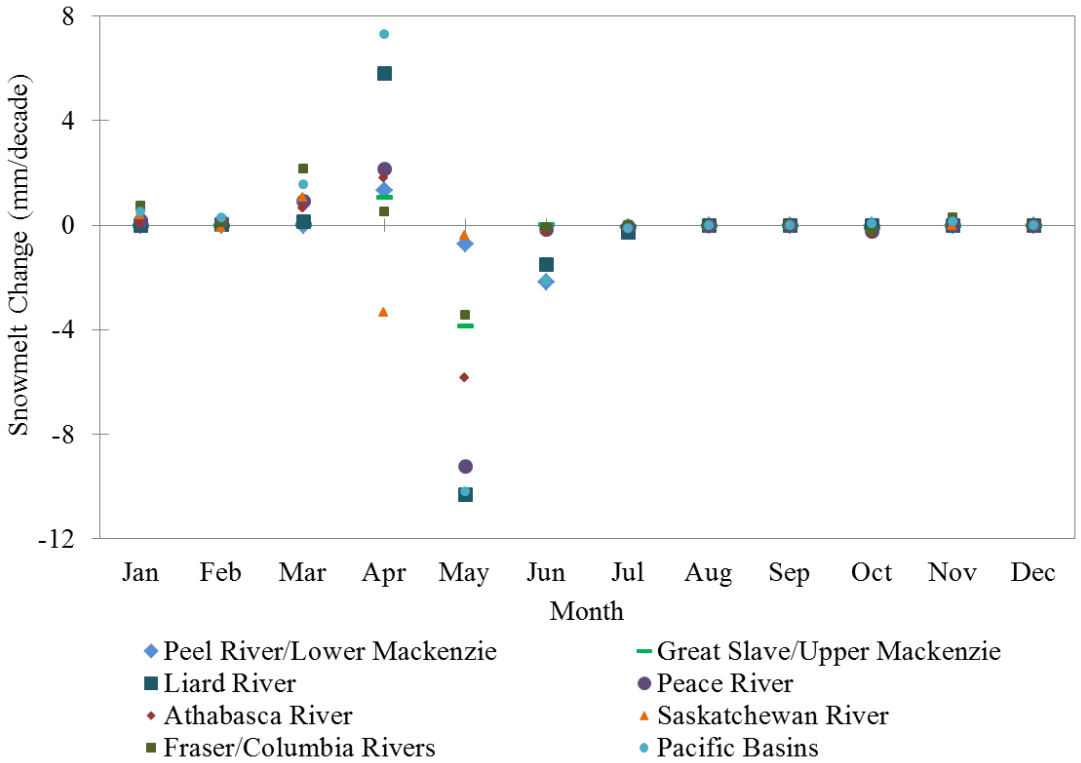

Figure 3.21. Spatially averaged rate of change of monthly total snowmelt in mm/decade, from 1950-2010. Results include all calculated trend values.

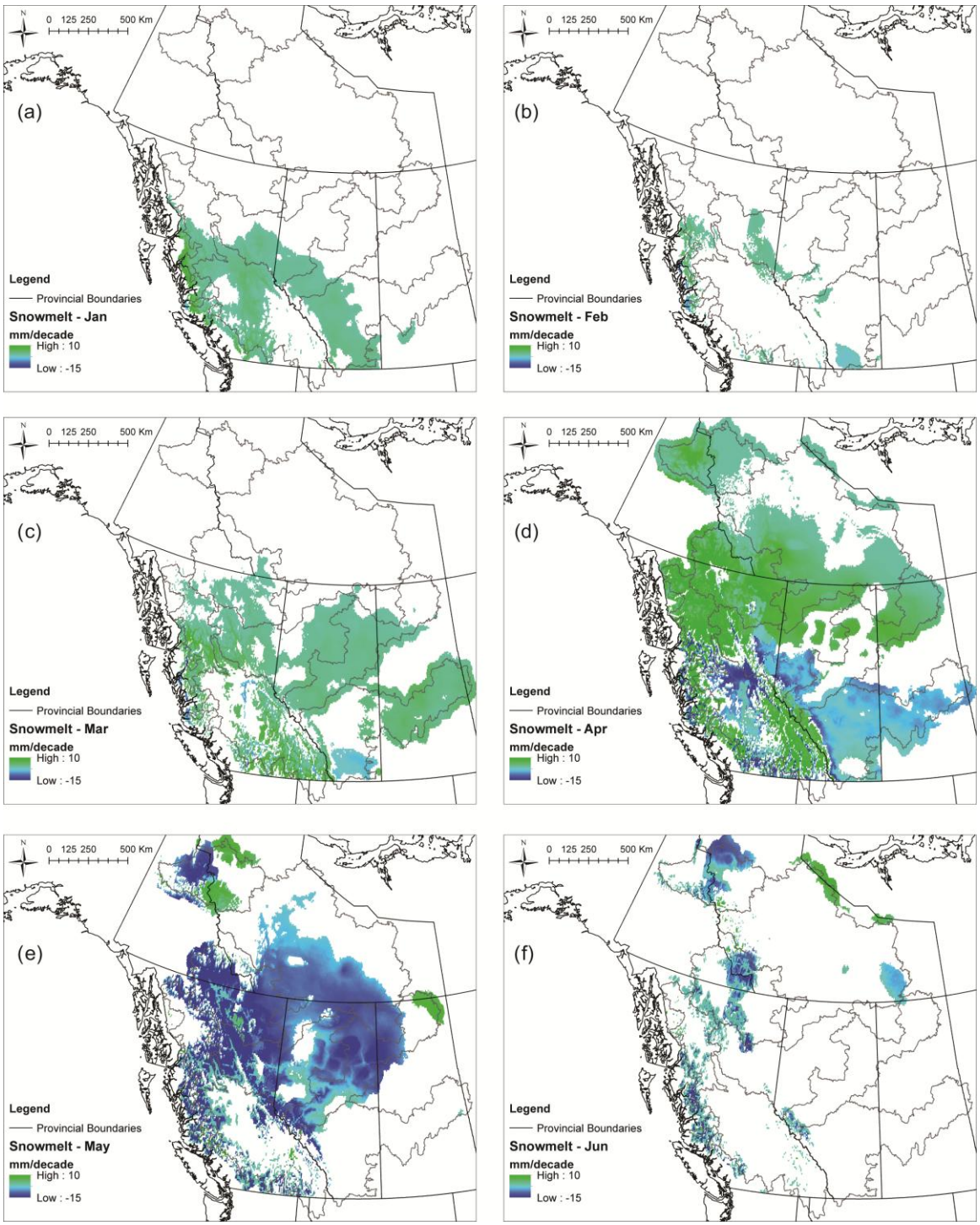

Figure 3.22. Snowmelt trends in mm/decade, 1950-2010, for (a) January, (b) February, (c) March, (d) April, (e) May, and (f) June. Only trend results statistically significant at 10% or better are shown.

4. Chapter 4: Spatial and temporal analysis of projected changes in hydroclimatic variables affecting streamflow in western Canada

Abstract

A large portion of the freshwater in western Canada originates as snowpack from the northern Rocky Mountains. The temperature and precipitation in these areas controls the amount of snow accumulated and stored throughout the winter, and the amount and timing of melt that occurs during the spring freshet. Changes in the extent and timing of snowpack and melt can modify the timing of peak river flow on a continental scale. Changes in temperature, precipitation, snow depth, and snowmelt are examined through comparison of output from the current and future periods of a series of regional climate models covering the time periods 1971-2000 and 2041-2070. The temporal and spatial analyses of these key hydroclimatic variables indicate that changes vary greatly over space and time. Results reveal that minimum temperature is likely to increase more than maximum temperature, particularly during the colder months of the year, possibly contributing to earlier spring melt. Precipitation is projected to increase over most of the study area, particularly in the north, but decrease in the southern half of the study area during the summer. In the coldest months of the year snow depth will potentially increase in high elevation and northern areas while decreasing across the rest of study area. Snowmelt results indicate increases in mid-winter melt events and an earlier onset of the spring freshet. This study provides a summary of potential future climate using key hydroclimatic variables across western Canada with regard to the effects these changes may have on streamflow and the spring freshet, and thus water resources, throughout the study area.

4.1 Introduction

Climate change and variability result in a variety of impacts on the hydrologic regime of a watershed. Such changes to regional water availability will affect many aspects of human society, from agricultural productivity and energy use to flood control, municipal and industrial water supply, and fisheries and wildlife management (Xu & Singh 2004). Examining the linkages between hydrologic and climatic variables, such as air temperature, precipitation, snow depth, and snowmelt, can also supply more information about observed trends in river flow. Numerous changes have been linked to increasing air temperatures, including increasing atmospheric water-vapour content and the resulting changes in precipitation patterns, snow cover reductions, melting of ice, and changes to runoff and soil moisture (Bates et al. 2008). Understanding how such changes in climate affect hydroclimatic conditions in critical water-supply regions is essential for effective water-resource planning (Xu & Singh 2004).

A large portion of the river flow to the Canadian Arctic originates in the mid-latitudes, particularly from alpine snowpacks of the Northern Rocky Mountains, which includes the headwaters of some of the largest river systems in North America, including the Mackenzie, Saskatchewan and Columbia rivers (Stewart et al. 2004; Déry 2005). The boundaries between these major watersheds are in close proximity, so the spatial distribution of snowfall and snowmelt can determine whether melt contributes to the Mackenzie, Saskatchewan or Columbia rivers. Any north-south or east-west shifts in climate, including temperature and precipitation, can have major effects on where the snowfall and snowmelt occur, and thus what water resources are available in each region. Flow from the Mackenzie River to the Arctic Ocean is especially important to ocean

convection, thermohaline circulation, and ultimately to global climate (Min et al. 2008; Holland et al. 2007). Flow from rivers such as the Saskatchewan and Columbia is critical to water-resource use, particularly in the dry, prairie interior of the mid-west. Given that these are primarily nival river regimes and mountain snowpack serves as a natural precipitation reservoir in the cold season, any climate-induced changes that affect the magnitude of their alpine snow accumulations, or the timing and volume of their subsequent melt, can thus have widespread downstream implications (Stewart 2009).

While instrumental observations and paleo-reconstructions have been used to analyze hydroclimatic trends in the past, global and regional climate models provide information with respect to possible future scenarios. In general, the warming trend is expected to continue in the future all across North America, and at a rate greater than the global mean, especially in Arctic regions (Christensen et al. 2007). The higher latitudes and colder months of the year are likely to experience the most warming (Šeparović et al. 2013). Reduced snow cover and decreased albedo are expected to create a positive feedback loop in the Arctic regions, and thus increase the temperature in northern latitudes as much as 10^{o}C by 2099, while temperature increases during the summer months are expected to range from 3-5^{o}C over most of North America (Christensen et al. 2007).

Increases in precipitation are also expected across much of western Canada. The majority of global climate models (GCMs) predict increases in high-latitude precipitation (Min et al. 2008). A warming of surface temperatures, along with an expected cooling of the upper troposphere would increase the instability of the atmosphere and could increase

the occurrence of thunderstorms, which generally bring extreme amounts of precipitation (Kunkel 2003). Zhang et al. (2000) detected increases in annual precipitation up to 35% in the northern regions between 1900 and 1999. Precipitation from extreme events is also expected to increase 5-19% across western Canada (Mladjic et al. 2011). Future precipitation is projected to increase up to 30% in the winter months, and decrease by as much as 20% during the summer between the periods of 1980-1999 and 2080-2099 (Christensen et al. 2007). Though GCMs project both temperature and precipitation to increase overall, decreases to streamflow are expected across most of the Prairies, particularly the Athabasca River (Kerkhoven & Gan 2011; Bawden et al. 2014).

Snowpack in western North America has also declined in recent decades, and is expected to continue declining throughout the 21st century (Pederson et al. 2011a). Increases in spring temperatures as well as warmer winter temperatures are expected to cause decreases in the snowpack which may lead to decreased snowmelt runoff and a decreased spring freshet (Burn & Hag Elnur 2002). The changes in regional water availability that result from the spatial and temporal changes in temperature, precipitation, snow depth, and snowmelt will have effects on global and regional atmospheric circulation, and global and local climate and hydrological cycles (Farmer et al. 2009).

GCM and RCM analyses in a great deal of previous research often focus on large scale, continental or hemispheric changes or individual drainage basins. This approach provides information on individual river systems and watersheds as well as large scale national or continental projections, but does not provide information on the hydroclimatic changes that may modify the spatial distribution of rainfall and snowfall between

drainage basins in western Canada, and thus regional water availability in these major river systems. The research presented in this paper is part of a larger assessment of Canadian water resources that analyzes a range of factors, including atmospheric synoptic patterns, key hydroclimatic variables, and the corresponding streamflows (Prowse et al. 2013). This study aims to identify temporal and spatial variations in future hydroclimatic conditions across western Canada as a continuation of previous research that included spatial and temporal analysis of the historical period from 1950-2010 (located in Chapter 3 and Appendix A). This study includes analysis of possible future scenarios in climatic variables affecting river flows using a series of regional climate models. Analysis was completed on four hydroclimatic variables (maximum and minimum daily air temperature, precipitation, snow depth, and snowmelt) projected with six RCMs for changes between the 1971-2000 and 2041-2070 time periods and spatial variation over the region.

4.2 Study Area

The study area for this project covers western Canada, from the west coast of British Columbia to western Manitoba and from the Canada-United States border to the Mackenzie River Delta in the northernmost reaches of continental Canada (Figure 4.1). This includes the Saskatchewan, Mackenzie, Fraser, and Columbia River Basins, as well as several small basins that drain British Columbia to the Pacific. A companion study (Bawden et al. 2013) has identified a series of hydrometric stations that correspond to distinct hydro-climatic regions within the study area. The identified region is based on drainage areas of 35 hydrometric stations, but these are amalgamated into 8 study regions for the analysis presented in this study.

The identified region incorporates a variety of climatic regions; much of the study area exists within the alpine region, and the remainder is at lower elevations in the boreal plains or prairies (Figure 4.2). The Mackenzie River basin covers several climatic regions, including cold temperate, mountain, sub-Arctic, and Arctic zones (Woo & Thorne 2003). The Athabasca River and Peace River have their headwaters in the Rocky Mountains and then flow across prairie landscapes to the Peace-Athabasca Delta, which drains into Lake Athabasca and then flows north into Great Slave Lake (Burn 2008). The primary outlet of Great Slave Lake is the Mackenzie River, which flows north to the Arctic Ocean. The Slave River, Great Slave Lake, and most of the Mackenzie River are contained within the Great Slave-Upper Mackenzie region, which consists primarily of low elevation boreal forest and Shield catchments characterized by plateaus and lowlands without much topography (Gibson et al. 2006). The Liard River joins the Mackenzie River basin near Great Slave Lake, contributing flows from headwater locations in the Yukon, Northwest Territories, British Columbia, and Alberta (Burn 2008). The Peel River converges with the Mackenzie River basin near the delta.

The Saskatchewan River Basin includes the North and South Saskatchewan Rivers, which are fed by the Red Deer and Bow Rivers. Headwaters originate as glacier and snowmelt in the Rocky Mountains and flow east through the prairie grasslands, where very little runoff is contributed to the streamflow (Cohen 1991). The Fraser River receives flow from snowmelt in spring, glacier melt in summer, and some rainfall throughout the year (Thorne & Woo 2011). The Columbia River Basin covers parts of seven western states and part of British Columbia, and a large portion of the flow is obtained from the Northern Rocky Mountains (Pederson et al. 2011b). The smaller

basins draining to the Pacific consist of several rivers with small watershed areas that drain the Coast Mountains of British Columbia. The landscape consists of steep-sided fjords and valleys with mountain peaks up to 2265m above sea level and alpine ice fields and glaciers occurring at the high elevations (McCuaig & Roberts 2002).

4.3 Data and Methods

Analysis was completed on a monthly basis to identify month to month variation in the selected hydroclimatic variables. Though data was analyzed monthly, results were discussed on a cold/warm season as well as seasonal basis. The cold season includes November through April with the warm season covering May to October. The cold season covers most of the snow accumulation period through to the spring breakup across most of the study area, with the warm season including the end of breakup in the north through the dry summer months to the beginning of freezeup. The seasonal discussion also includes the four seasons: January through March characterized the snow accumulation period, April through June covers the spring breakup across most of the study area, July through September covers the majority of the hot, dry period, and October through December includes the fall freezeup and beginning of the snow accumulation season. The seasons vary across the study area due to variations in elevation as well as the large range of latitudes; however, the seasonal definitions were chosen to represent the cold and warm halves of the year as well as the hydrologic seasons as they exist throughout the majority of the study area. Monthly examples from each season are included in each results section; the full suite of results is located in Appendix B.

Watershed delineations for each of the 8 study regions were created based on a series of latitude-longitude points which correspond to hydrometric stations from Environment Canada's HYDAT database. ArcHydro was used to delineate the contributing areas for each hydrometric station. ArcHydro is an object-oriented model that is capable of establishing a topological network that includes flow direction, connectivity and upstream/downstream relationships of stream segments using a digital elevation model, a stream network, and points to distinguish watershed outlets (Fürst & Hörhan 2009).

The analysis of future climate scenarios was based on the outputs of Regional Climate Models (RCMs) from the North American Regional Climate Change Assessment Program (NARCCAP) (Mearns et al. 2007). NARCCAP is an international research program that provides climate scenario data for the United States, Canada and Mexico. It uses RCMs driven by a set of atmosphere-ocean general circulation models (GCMs) to produce high resolution climate change simulations for generation of future climate change scenarios; these scenarios provide information on local and regional scale processes that are important for understanding impacts of climate variability and change and can be used in impacts research (Mearns 2009; Arritt & Rummukainen 2011).

The GCMs include: Geophysical Fluid Dynamics Laboratory (GFDL) by the National Oceanic and Atmospheric Administration, Canadian Global Climate Model 3 (CGCM3) by Environment Canada, and Community Climate System Model (CCSM) by University Corporation for Atmospheric Research. The regional climate models included are: Canadian Regional Climate Model (CRCM), Regional Climate Model 3 (RCM3) by University Corporation for Atmospheric Research, and Weather Research and

Forecasting (WRFG) by Pacific Northwest National Lab. The combinations of GCMs with RCMs that are considered in the present study are as follows: CRCM-CGCM3, CRCM-CCSM, RCM3-GFDL, RCM3-CGCM3, WRFG-CGCM3, and WRFG-CCSM and all climate model simulation results correspond to the A2 emissions scenario (Nakicenovic et al. 2000).

The RCMs all cover the time periods 1971-2000 for the current period and 2041-2070 for the future (Mearns 2009). The spatial resolution of the RCMs is 50km x 50km, with results recorded at 3-hour intervals. Climate models are computer-based simulations of geophysical processes; however, there are many uncertainties in these simulations and they all contain biases which skew the results to some extent. One way to attempt to compensate for some of the model bias is to use a multi-model mean, or weighted average of available models (Sain & Furrer 2010). This research utilized a series of models and used an ensemble approach to view potential changes on a monthly and annual basis.

These six models were chosen because they provided the appropriate spatial and temporal coverage, as well as the required variables of maximum and minimum daily air temperature, precipitation, snow depth (in snow water equivalent, or SWE), and snowmelt. These variables were chosen for study due to their strong influence on streamflow, particularly the spring freshet. There are many other climatic variables that also affect streamflow, but the scope of the research was not large enough to include all possible variables. There were also many other regional climate models available, but those listed previously were the only ones that contained the required variables.

However, the datasets were not always complete. For example, the current period of all CCSM-driven models ends in December 1999 instead of December 2000, providing 29 years of data instead of the expected 30 years and the WRFG-CGCM3 future time period was missing every fifth year of data for SWE and snowmelt. The RCM3-CGCM3 and RCM3-GFDL models were missing all snowmelt data, so model comparisons for this variable contain only 4 models instead of 6.

Pixel trajectory analysis was used to track temporal changes in each climate variable at each pixel through time, and then map the results over the study area. Each data point (50km x 50km pixel) received a unique spatial identifier, and each point was analyzed individually for temporal changes in each variable. Each model contains a future and current time period, so the potential future change was determined using a delta method (Future - Current = Change) for each pixel. The 30-year average value for the current time period was subtracted from the average value for the future time period to determine the change in mean values. The change in monthly average values between the two time periods from the different RCMs were combined to create a multi-model mean. Monthly or annual values for precipitation and temperature were calculated as cumulative and average values over each period respectively. Due to snow depth being provided as an instantaneous measure, the April 1st SWE was used in the annual analysis while snowmelt was accumulated over each analysis period. The change in average values for both annual and monthly results was mapped for visual interpretation. The monthly data analysis was completed on each model output individually to view the range of possible future scenarios but only the multi-model mean for representative months from each season are discussed, with the entire suite of results placed in Appendix B. Additionally,

the RCMs used in this analysis all cover different spatial windows, and so the northernmost reaches of the study area show jagged lines that are an artefact of the data.

Rates of change for each model for both the current and future time periods were also compared to assess the agreement of potential change between the models. The Mann Kendall (MK) non-parametric test was used to calculate a trend value for each 50km x 50km pixel, then the MK results were used to determine rate of change per decade using Sen's slope method (Mann 1945; Kendall 1975; Sen 1968). Rates of change for the current and future time periods were reclassified into positive and negative values, with rates of change greater than 0.1 or less than -0.1 ^{o}C/decade or mm/decade changed to 1 and all other values changed to zero. The number of models with such changes were then summed to determine the total number of models with positive or negative rates of change for each time period. The values 0.1 and -0.1 ^{o}C/decade or mm/decade were chosen for the reclassification because it allows inclusion of most moderate or strong positive or negative rates of change, without including the weak changes close to zero.

4.4 Results and Discussion

4.4.1 Maximum and Minimum Temperature

Average annual modelled maximum daily temperature (Tmax) for the current period ranges from -5 to 15^{o}C (Figures 4.3a and 4.3b) while minimum daily temperature (Tmin) ranges from -15 to 5^{o}C (Figure 4.4a and 4.4b) with the average calculated from all six RCMs. The difference between the 30-year means of the current and future time periods shows an expected Tmax increase of 1.5 to 2.5^{o}C (Figure 4.3c) and a Tmin increase of 3^{o}C (Figure 4.4c) across the study area. The temperature increases for minimum

temperature are greater than that of maximum temperature, indicating a decrease in the daily temperature range.

During the winter Tmax values range from -18 to -1^{o}C and Tmin values range from -26 to -10^{o}C while during the summer Tmax ranges from 11 to 22^{o}C and Tmin ranges from 3 to 10^{o}C throughout the current period (Figures 4.5 and 4.6). Tmax and Tmin are expected to increase in the future in all study regions through all months of the year with the greatest increases during the cold season (Figure 4.7).

Tmax during the winter is projected to increase 3 to 5^{o}C and Tmin is expected to increase 4 to 5^{o}C between the current and future time periods throughout the study area (Figure 4.8a and 4.9a). The non-coastal regions show the greatest increases for both Tmax and Tmin, while slightly less warming is predicted in the southwest. The models mostly agree on the locations of increasing and decreasing trends during the current and future time periods. Most models are in agreement that rates of change were positive in the current period for Tmax and Tmin through the western half of the study area. The future period shows 4-6 models in agreement that trends will be positive for both Tmax and Tmin during the winter months (Figures 4.10 and 4.11).

During the spring, Tmax is projected to increase by 1-3^{o}C over most of the study area, with the higher values located in the northern half of the study area (Figure 4.8b). Tmin shows a similar pattern but with increases of 2-4^{o}C (Figure 4.9b). 4-6 models agree that Tmax and Tmin rates of change are positive through the current period and will be (Projected to) positive in the future in the early spring, though both show slightly less model agreement later in the spring (Figures 4.12 and 4.13).

Tmax increases of 1-3^{o}C are predicted in summer, with the largest increases located in the southwest and the remainder of the study area expecting values of 1-2^{o}C (Figure 4.8c). Most models show similar results, but the WRFG models predict decreased future maximum temperature in some parts of the study area during all summer months; the individual model results can be seen in Appendix B. Results for Tmin are similar, with expected increases of 1-4^{o}C and the majority of projected values between 2 and 3^{o}C (Figure 4.9c). The models show less consensus regarding rates of change compared to the winter and spring for both Tmax and Tmin. Consensus is slightly greater in the current period compared to the future, though most models agree on positive trends in both time periods through the southern half of the study area (Figures 4.14 and 4.15).

Fall is expected to experience Tmax increases of 1-4^{o}C between the current and future periods with the greatest increases in the northeast of the study area (Figure 4.8d). Predictions show that Tmin is expected to increase slightly more than Tmax, with values of 2-4^{o}C, with much of the study area showing values around 4^{o}C (Figure 4.9d). The highest Tmin changes are located in non-coastal regions and lower elevations. 4-6 models agree that rates of change are positive in both time periods, indicating that Tmax and Tmin are likely to continue increasing into the future (Figures 4.16 and 4.17). In contrast to most of the study area, the southeast of the study area contains some pockets of 1-3 models in agreement that rates of change may be negative in the future for both Tmax and Tmin.

The greatest Tmax and Tmin increases are expected to occur during the fall and winter, with some models predicting Tmax values to rise as much as 5^{o}C and Tmin values to

increase up to 6 or 7^{o}C. GCM and RCM analyses conducted in other studies also show the cold season is likely to experience greater temperature increases than the warm season with a north-south gradient (e.g., de Elía et al. 2013; Šeparović et al. 2013). Warming is predicted to be slightly less during the spring and summer which may further decrease the temperature range, both on a daily basis as well as throughout the year. The cold season (November to April) also shows generally greater model agreement for both Tmax and Tmin rates of change with most months showing 4-6 models in agreement that rates of change are positive, both for the current and future time periods. The warm season (May to October) also shows most models in agreement; though to a lesser degree than during the cold season. Negative rates of change were rarely agreed upon by more than 2 or 3 models, so it seems unlikely that temperature decreases will occur during the future period, since increases were so readily agreed upon throughout most months of the year.

4.4.1.1 Hydrologic Relevance of Temperature Changes

Air temperature is an important factor in local and downstream water availability through its influence on evaporation and evapotranspiration in a watershed. Temperature is also a primary controlling factor of whether or not precipitation occurs as rain or snow, and influences the rate and timing of snowmelt. Therefore, the expected increases in daily temperature will modify the proportion of rainfall to snowfall in the study area and also result in a shorter cold season and earlier start to the spring melt season. During the current period, the proportion of rainfall to snowfall already shows a transition towards more rainfall, particularly in western mountainous areas (Davis et al. 1999; Burn et al. 2004; Knowles et al. 2006), and earlier spring melt has also been detected in several

previous studies, trends that are likely to continue into the future (Brown & Braaten 1998; Burn & Hag Elnur 2002; Stewart et al. 2005; Schindler & Donahue 2006; Burn 2008).

Temperature increases during the summer also contribute to less water being available for streamflow due to higher evaporation rates. Although predicted increases are lower in the warm season than the cold season, any decreases to streamflow in dry areas such as the Prairies could be a pose an issue for water availability. Streamflow decreases have already been detected in the Saskatchewan River basin in the current period (Rood et al. 2008; Bawden et al. 2013), but the continued increase in temperature indicates that further flow decreases may occur in the future as well. Throughout the colder months of the year, the predicted temperature increases will likely contribute to more frequent mid-winter melt events in areas of lower elevation throughout the study area.

4.4.2 Precipitation

Total annual precipitation ranges from 350mm to over 1200mm per year, with the average calculated from all six RCMs (Figures 4.18a and 4.18b). The difference between the 30-year means of the current and future time periods shows that annual precipitation is expected to increase across the study area by as much as 190mm (Figure 4.18c). The greatest increases of over 100mm occur in the western half of the study area, with increases of 20-70mm expected through the east.

Precipitation varies greatly throughout the year; most study regions receive the greatest quantities of precipitation during the late spring and summer, though coastal areas receive the most during the winter (Figure 4.19). The regional averages show that differences between the current and future periods are likely to be mostly positive throughout the

year in all study regions (Figure 4.20). The changes range from values slightly above zero to over 25mm each month. Decreases are also expected in many months, though the regional averages do not always reflect the variations within each region.

Precipitation during the winter is likely to increase by 2 to 5mm east of the Rocky Mountains, with values of 15mm or greater near the coast (Figure 4.21a). Decreases of -5 to -20mm are expected as well by some models in the southern half of the study area, though this change is more evident in the individual model results than in the multi-model mean. 3-6 models agree that trends during the current period were positive in coastal and northern areas while lower elevations in non-coastal areas show most models in agreement that rates of change will be negative in the future (Figure 4.22). Negative trends in the future show particularly strong agreement east of the Rocky Mountains, in the headwaters of the Saskatchewan and Athabasca River regions.

Spring precipitation is expected to increase up to 15mm each month. The largest projected increases are located in the southwest, with minimal increases and slight decreases of -5mm in the north (Figure 4.21b). Model agreement patterns are more scattered through the spring months, but the models are mostly in agreement that rates of change were positive throughout the current period, with the future period showing positive trends in the north and some negative trends in the south (Figure 4.23).

Throughout the summer, precipitation is expected to increase up to 15mm across the Upper Liard and Pacific regions, and decrease by -5 to -12mm in the Fraser-Columbia and headwaters of the Athabasca and Saskatchewan regions (Figure 4.21c). Model

agreement also varies greatly across the study area, though in the future period most rates of change are predicted to be positive in the north and negative in the south (Figure 4.24).

The models predict precipitation increases of 2 to 5mm during the fall in non-coastal regions, with larger increases expected in coastal and high elevation areas (Figure 4.21d). Individual models show more variation, including decreases of -5 to -10mm expected through the Prairies. The current period contains good model agreement that the study area experienced positive rates of change, but 3-6 models agree that the future period will experience negative trends over most of the study area (Figure 4.25).

Overall, the models show more spatial variation in precipitation scenarios than for Tmax and Tmin, likely due to the high spatial variability of precipitation patterns. This variation is apparent in the differences in total precipitation and the model agreement of current and future rates of change. All seasons contain some projected increases to precipitation, with the greatest increases expected in coastal regions during the cold season. Predicted changes in the interior during the cold season are either slight increases or slight decreases, indicating minimal change in the future. Projections for the warm season indicate a continuation of the northward shift in precipitation discussed in Chapter 3, with decreased precipitation in the south. The models mostly agree that the future period will experience negative precipitation trends through the study area in the cold season and through the southern half of the study area during the warm season.

4.4.2.1 Hydrologic Relevance of Precipitation Changes

Precipitation is one of the primary contributing factors to streamflow. Changes to the amount and timing of precipitation affect streamflow. The predicted increases in summer

precipitation through the northern half of the study area may contribute to higher summer streamflow in these regions. In contrast, summer precipitation in the south is expected to decrease, particularly in the Saskatchewan and Athabasca River regions, decreasing the available water resources in these important agricultural areas. The Prairie regions of western Canada already experience dry summers, that have become drier in the current period, but results from this study and from previous research show that the dryness will likely intensify in the future (e.g., Sushama et al. 2010).

The predicted increases during the fall months, mostly located in coastal areas, are consistent with previous RCM and GCM analyses that predict modest precipitation increases at this time of year (e.g., Mote et al. 2010). These increases are likely to increase streamflow, since the increased temperatures during the current period have already contributed to increased snowmelt and decreased snowpacks during the fall and winter (Brown & Braaten 1998; Burn & Hag Elnur 2002). The winter months show strong model agreement on negative trends east of the Rocky Mountains, indicating that most of the oceanic moisture traveling inland may be falling in the mountains and intensifying the rain shadow effect of the Prairies during the winter months.

4.4.3 Snow Water Equivalent (SWE)

The April 1st SWE ranges from 20-200mm SWE across the study area in both the current and future periods (Figures 4.26a and 4.26b). The difference between the current and future periods shows that the south is anticipated to decrease by -5 to -20mm SWE while the north is expected to increase by 5 - 20mm SWE (Figure 4.26c). The greatest

increases and decreases are located in mountainous regions, where snow depth is generally largest.

SWE varies greatly depending on location and time of year, and is mostly expected to decrease in the future. Peak values range from 50mm SWE in the Saskatchewan River region to over 500mm SWE in the Pacific region (Figure 4.27). Some increases up to 20mm SWE are expected throughout the cold season at northern latitudes, though SWE across the remainder of the study area is likely to decrease during all months of the year (Figure 4.28).

During winter, the multi-model mean predicts increases of 10-20mm SWE in the northern half of the study area, and decreases as low as -20mm SWE in the Fraser-Columbia and Pacific regions (Figure 4.29a). The models agree that the northernmost parts of the study area experienced positive rates of change during the current period while the southern half experienced mostly negative rates of change. However, 3-6 models are generally in agreement that most of the study area will experience negative rates of change in SWE in the future (Figure 4.30).

Predicted decreases of -10 to -20mm SWE may occur throughout the spring, with the most widespread decreases during April (Figure 4.29b) and the decreases covering progressively less area through May and June. The greatest decreases are located throughout BC during all spring months, with smaller values located in the interior and northern regions. Most models are in agreement that trends in SWE during the current period were negative and will remain so in the future (Figure 4.31). The later spring

months show some areas with no model agreement due to snow no longer being present at that time of year.

During the summer months, no snow is present over the majority of the study area, but projected decreases of -10 to -20mm SWE are expected during September in the west and north of the study area (Figure 4.29c). The models predict mostly decreased SWE during the fall, but some increases in the north. The largest decreases of -10 to -20mm SWE are located in the western half of the study area with values around -5mm SWE in the interior regions (Figure 4.29d). Very few SWE increases are projected for October, but during November and December increases of 5-20mm SWE are expected in the north. Throughout the current period, most models agree that the north of the study area contains positive trends while the remainder of the study area contains mostly negative rates of change. However, the future period shows most models in agreement that rates of change will be negative throughout the study area (Figure 4.32).

The cold season months all show very similar patterns of change in SWE; the high elevation areas near the coast are expected to receive less snow in the future, with smaller decreases across the Prairies, and increases throughout the north. The winter months all show this pattern for all models, and some fall months show a similar pattern as well. This pattern is consistent with other RCM and GCM studies of snow distribution in the northern hemisphere (e.g., Krasting et al. 2013). This is likely due in part to the increased temperatures in the north leading to greater water vapour availability in the air, creating more precipitation (Davis et al. 1999). The model agreement during the cold season also shows similar patterns through most months. The current period generally shows some

models in agreement that the northernmost parts of the study area contain positive rates of change with the remainder showing negative rates of change, and the future period generally shows most models in agreement that rates of change will be negative across most of the study area, indicating the likelihood that SWE will be decreased in the future, probably as a result of further increased temperatures.

4.4.4 Snowmelt

Total annual snowmelt ranges from 100-900mm each year in both the current and future periods, with the greatest values located in the mountainous western half of the study area (Figures 4.33a and 4.33b). Snowmelt totals in the future are expected to be slightly lower in the west and slightly higher in the north and interior regions. The difference between the current and future periods shows decreases of -20 to -60mm in the Fraser-Columbia and Pacific regions, with snowmelt increases of 10-50mm expected in interior and northern regions (Figure 4.33c).

Snowmelt values are low throughout much of the year, with monthly totals of 0-40mm, and then during April and May snowmelt peaks with values up to 225mm during the spring melt (Figure 4.34). According to the projected changes in total monthly snowmelt, values will increase during the cold season while decreasing through the warm season in nearly all study regions (Figure 4.35).

During the winter months snowmelt is predicted to increase 5-20mm, mostly in the southwest and interior regions, particularly in January (Figure 4.36a). During February and March (Figures 4.36b and 4.36c), some decreases of -5 to -20mm are located in the lower elevations of the southwest, particularly where the increases were located in

January. The models mostly agree that rates of change in the southern half of the study area are positive through both the current and future periods during the winter months (Figures 4.37).

During early spring, snowmelt increases up to 20mm across most of the study area are predicted by the multi-model mean, though some decreases of -10mm are expected in the Saskatchewan River region, likely due to snow having melted in previous months (Figure 4.36d). Later in the spring, projected decreases of -5 to -20mm across most of the study area may occur, while the southeast of the study area shows no changes likely due to very little or no snow being left on the ground (Figures 4.36e and 4.36f). Early in the spring, model agreement is strong, with 2-4 models in agreement that rates of change are positive in both time periods (Figure 4.38). Later in the spring, model agreement shifts from positive rates of change in the current period toward negative rates of change in the future or no agreement due to lack of snow (Figures 4.39).

Snowmelt during the summer months is not likely to change much due to lack of snow on the ground. The exception to this is September; snowmelt is expected to decrease by -5 to -20mm, mostly in the western half of the study area. This is likely due to the decrease in SWE during September, so there is less snow available for melt. Early in the fall, some decreases of -5 to -10 mm are predicted in the southern half of the study area while snowmelt in the remainder of the study area is predicted to increase 2-5mm. Later in the fall, snowmelt increases up to 20mm are expected throughout the study area, with the greatest increases in the coastal and mountainous areas and smaller increases throughout the east and north. The current and future periods show similar patterns of model

agreement in the early fall, with the northern half of the study area showing 2-4 models in agreement that rates of change are positive and the southern half showing 2-3 models in agreement that rates of change are negative. The positive rates of change in the north are likely related to the increased temperatures allowing for more melt while the negative rates of change in the south are likely related to increased temperatures and decreased snowfall.

Snowmelt patterns are highly variable throughout the study are and throughout the year, though some patterns are visible. The southwest is likely to experience more instances of midwinter melt, with January showing greater total snowmelt values at low elevations and in coastal mountainous areas and the melt increases located at greater elevations and more northern latitudes each month until April. These midwinter melt events may contribute to decreased freshet volume in the spring due to less snow being present on the ground. Spring melt is also expected to occur earlier in the year (Salathé 2005), with results for March and April showing many areas of increased snowmelt across the study area, with March containing mostly increases to lower latitudes and April displaying increasing at higher latitudes and decreases to lower latitudes. Snowmelt decreases occur throughout the spring, particularly in May and June, mostly in higher elevation areas and at northern latitudes, likely due to less and less snow available for melt each year during these months. Snowmelt in late summer and throughout the fall is likely to decrease in the future, potentially due to the reduced snowfall expected in these months. Precipitation is expected to increase during these months, but warmer temperatures are likely to have contributed to the decrease in snowfall and snowmelt.

4.4.4.1 Hydrologic Relevance of SWE and Snowmelt Changes

A large portion of the streamflow in western Canada originates in the Rocky Mountains and is dependent upon winter snow accumulation and spring melt. The Rocky Mountains store water in the form of snow and ice all winter, then as the snow melts during the spring it provides flow to the Fraser and Columbia Rivers which flow to the Pacific, the Saskatchewan River which flows across the Prairies and eventually to Hudson Bay, and to the Peace, Athabasca, and Liard Rivers which feed the Mackenzie River and eventually the Arctic Ocean. The spring freshet volume is highly dependent upon winter snow; therefore changes to winter snow accumulation will alter the spring freshet volume through much of the study area. The widespread decreases to winter SWE in the southern half of the study area will likely contribute to decreased spring freshet volume as well as decreased summer streamflow throughout western Canada in the future.

The timing of the spring freshet is important as well, since it generally peaks in the spring and then the snowmelt continues slowly throughout the summer, providing flow to much of western Canada during the driest times of year. Results indicate that snowmelt has been occurring earlier in the year during the current period, a trend that has been well documented (e.g., Zhang et al. 2001; Whitfield 2001) and is likely to continue into the future. This shift toward earlier snowmelt leads to decreased snowmelt during the late spring and early summer, which contributes to decreased summer streamflow throughout much of the study area. In addition to an earlier spring freshet, the results also predict increased mid-winter snowmelt at lower elevations in the western regions of the study area, leading to an increase in winter streamflow, particularly in the Fraser-Columbia,

Pacific, and Peace River regions. Greater winter streamflow in these areas has already been detected in the current period by Rood et al. (2008) and Bawden et al. (2013).

4.4.5 Hydrologic Relevance of Predicted Changes in Climate

The variables analysed in this research are all individually important factors in hydroclimate of a watershed and all have their own impacts on streamflow, but they also interact in numerous ways to produce changes to both small and large scale watersheds. The expected increases to both Tmax and Tmin will contribute to a further shortened cold season, so while SWE is expected to decrease throughout the fall and winter in the southern half of the study area, it will also have a shorter period of time to accumulate. In addition to being dependent upon precipitation, SWE and snowmelt are also dependent upon temperature, since the temperature determines whether the precipitation accumulates as snow or becomes streamflow.

The fall and winter seasons are expected to experience slightly more precipitation, but decreased SWE in the southern half of the study area, likely related to the warmer temperatures. The northern half of the study area is an exception, since increased temperatures in these areas can increase water vapour storage in the air and thus more precipitation can occur, but if temperatures have not risen enough to remain above zero then SWE can increase. The expected increases to precipitation during the late spring and early summer, particularly in the Liard River region, and to a lesser extent, the Peace River and Pacific regions may increase summer streamflow in these watersheds as well as the downstream areas of the Mackenzie River. During the current period, a similar trend was identified in the same region and is mentioned in Chapter 3.4.5.

The shortening of the cold season also means that snowmelt will occur earlier in the year, with increased snowmelt values in March and April and decreases during May and June. Snowmelt is also expected to increase during the winter at lower elevations, likely as a result of the temperature increases predicted during the winter. An increase in mid-winter melt will likely contribute to increased winter streamflow in some parts of the study area, primarily the Fraser-Columbia and Pacific regions; previous analysis of RCMs shows runoff in the Upper Columbia and Peace Rivers may increase as much as 30mm during the winter (Schnorbus et al. 2014).

The changes and interactions between hydroclimatic variables within the study area combine to point out several potential changes in the future. The cold season is likely to decrease in length, which may cause the snowmelt and spring freshet to occur earlier in the year. The shortened cold season length along with projected decreases in SWE are likely to lead to less snowmelt and a decreased spring freshet volume. Precipitation is predicted to shift more toward spring months and more northern latitudes, with less precipitation occurring in the driest parts of the study area, so summer streamflow is expected to be greater in the northern watersheds of the study area while the southern watersheds show less streamflow during the warm season.

4.5 Conclusion

This study utilized a series of RCMs to analyze the potential changes to future climate in western Canada. This included spatial and temporal analysis of a series of hydroclimatic variables (maximum and minimum daily air temperature, precipitation, SWE, and

snowmelt) for changes between the 1971-2000 and 2041-2070 time periods and spatial variation both over time as well as within the year.

The greatest increases in Tmax and Tmin are expected to occur during the cold season (November to April). The projected Tmax increases during all months of the year are generally less than the Tmin increases; these increases indicate a potential decrease of temperature range across most of the study area. Analysis of the 1950-2010 period in Chapter 3 also revealed similar trends in temperature, so it appears likely that the detected decrease in temperature range will continue into the future. The projected increases in Tmax and Tmin will likely contribute to later freeze-up, increased instances of mid-winter melt, earlier break-up and an earlier spring freshet. The shorter cold season combined with expected decreases to winter precipitation across much of the study area indicate a possible decreased spring freshet volume, particularly in the south. However, all models predict an overall increase in SWE throughout the northern half of the study area in the future. Summer results show some decreases in Prairie precipitation, which is likely to increase summer dryness, decreasing the available water resources in these areas and downstream. Lower precipitation amounts were also detected across the Prairies between 1950 and 2010 in Chapter 3; past reductions in warm season precipitation in addition to the likelihood of less precipitation occurring in the future indicates that water management in the Prairies is likely to become even more difficult in the future.

The research presented in this chapter could be continued for better understanding of potential change patterns. Seasonal and cold/warm season analysis would offer more

information about seasonal shifts in these hydroclimatic variables than the monthly results alone can provide.

References

Arritt, R. W., & Rummukainen, M. 2011. Challenges in Regional-Scale Climate Modeling. *Bulletin of the American Meteorological Society*, *92*(3), 365–368. doi:10.1175/2010BAMS2971.1

Bates, B.C., Kundzewicz, Z.W., Wu S. & Palutikof, J.P. Eds. 2008. *Climate Change and Water: IPCC Technical Paper VI*, Geneva: IPCC Secretariat.

Bawden, A.J., Burn, D.H. & Prowse, T.D. 2013. Recent changes in patterns of western Canadian river flow and association with climatic drivers: A CROCWR component. M.A.Sc Thesis. University of Waterloo, Ontario, Canada.

Bawden, A.J., Linton, H.C., Burn, D.H. & Prowse, T.D. 2014. A spatiotemporal analysis of hydrological trends and variability in the Athabasca River region, Canada. *Journal of Hydrology, 509*, 333-342.

Brown & Braaten. 1998. Spatial and Temporal Variability of Canadian Monthly Snow Depths , 1946-1995. Atmosphere-Ocean, 36(1), 37-54.

Burn D.H., Abdul Aziz, O.I., Pietroniro, A. 2004. A comparison of trends in hydrological variables for two watersheds in the Mackenzie River Basin. *Canadian Water Resources Journal*, 29(4), 283-298.

Burn, D.H. 2008. Climatic influences on streamflow timing in the headwaters of the Mackenzie River Basin. *Journal of Hydrology,* 352, 225- 238.

Burn, D.H. & Hag Elnur, M.A. 2002. Detection of hydrologic trends and variability. *Journal of Hydrology*, 255.

Christensen, J.H. Hewitson, B. , Busuioc, A., Chen, A., Gao, X., Held, I., Jones, R., Kolli, R.K., Kwon, W.-T., Laprise, R., Magaña Rueda, V., Mearns, L., Menéndez, C.G., Räisänen, J., Rinke, A., Sarr, A.& Whetton, P. 2007. Regional Climate Projections. In *Climate Change 2007: The Physical Science Basis. Contribution of Working Group I to the Fourth Assessment Report of the Intergovernmental Panel on Climate Change*. Cambridge, United Kingdom: Cambridge University Press.

Cohen, S.J. 1991. Possible impacts of climatic warming scenarios on water resources in the Saskatchewan River sub-basin, Canada. *Climatic Change*, 19, 291-317.

Coppin, P., Jonckheere, I., Nackaerts, K., Muys, B., & Lambin, E. 2004. Digital change detection methods in ecosystem monitoring: A review. *International Journal of Remote Sensing*, 25(9), 1565-1596.

Davis, Lowit, Knappenberger & Legates. 1999. A climatology of snowfall-temperature relationships in Canada. *Journal of Geophysical Research*, *104*(10), 11,985–11,994.

de Elía, R., Biner, S. & Frigon, A. 2013. Interannual variability and expected regional climate change over North America. Climate Dynamics, 41(5-6), 1245-1267.

Déry, S.J. 2005. Decreasing river discharge in northern Canada. *Geophysical Research Letters, 32*(10), L10401

Farmer, C.J.Q., Nelson, T.A., Wulder, M.A. & Derksen, C. 2009. Spatial-temporal patterns of snow cover in western Canada. Canadian Geographer, 4, 473-487.

Fürst, J. & Hörhan, T. 2009. Coding of watershed and river hierarchy to support GIS-based hydrological analyses at different scales. Computers & Geosciences, 35(3), 688–696.

Gibson, J., Prowse, T., & Peters, D. 2006. Hydroclimatic controls on water balance and water level variability in Great Slave Lake. *Hydrological Processes*, 20, 4155-4172.

Holland, M.M., Finnis, J., Barrett, A.P. & Serreze, M.C. 2007. Projected changes in Arctic Ocean freshwater budgets. *Journal of Geophysical Research, 112*, doi:10.1029/2006JG000354.

Kendall, M.D. 1975. *Rank correlation measures*, Charles Griffin, London, UK.

Kerkhoven, E., & Gan, T.Y. 2011. Differences and sensitivities in potential hydrologic impact of climate change to regional-scale Athabasca and Fraser River basins of the leeward and windward sides of the Canadian Rocky Mountains respectively. *Climatic Change, 106*(4), 583–607. doi:10.1007/s10584-010-9958-7

Knowles, N., Dettinger, M. & Cayan, D. 2006. Trends in snowfall versus rainfall in the Western United States. *Journal of Climate, 19*, 4545-4559.

Krasting, J.P., Broccoli, A.J., Dixon, K.W. & Lanzante, J.R. 2013. Future changes in Northern Hemisphere snowfall. *Journal of Climate, 26*(20), 7813-7828.

Kunkel, K.E. 2003. North American Trends in Extreme Precipitation. *Natural Hazards, 29*, 291–305.

Mann, H.B. 1945. Non-parametric tests against trend. *Econometrica*, *13*, 245-259.

McCuaig, S.J. & Roberts, M.C. 2002. Topographically-independent ice flow in northwestern British Columbia: implications for Cordilleran Ice Sheet reconstruction. Journal of Quaternary Science, 17(4): 341-348.

Mearns, L.O., Gutowski, W.J., Jones, R., Leung, L.-Y., McGinnis, S., Nunes, A.M.B.& Qian Y. 2009. A regional climate change assessment program for North America. *EOS, 90*(36), 311-312.

Min, S.K., Zhang, X. & Zwiers, F. 2008. Human-induced Arctic moistening. *Science*, 320: 518-520.

Mladjic, B., Sushama, L., Khaliq, M. N., Laprise, R., Caya, D., & Roy, R. 2011. Canadian RCM Projected Changes to Extreme Precipitation Characteristics over Canada. *Journal of Climate*, *24*(10), 2565–2584. doi:10.1175/2010JCLI3937.1

Mote, P.W. & Salathé, E.P. 2010. Future climate in the Pacific Northwest. *Climatic Change, 102*(1-2), 29-50.

Nakicenovic, N. & Swart, R. (Eds.). 2000. *Special Report on Emissions Scenarios*. Geneva, Switzerland: IPCC Secretariat.

Pederson, G.T., Gray, S.T., Woodhouse, C.A., Betancourt, J.L., Fagre, D.B., Littell, J.S., Watson, E., Luckman, B.H. & Graumlich, L.J. 2011a. The unusual nature of recent snowpack declines in the North American cordillera. *Science*, 333: 332-335.

Pederson, G.T., Gray, S.T., Ault, T., Marsh, W., Fagre, D.B., Bunn, A.G., Woodhouse, C.A. & Graumlich, L.J. 2011b. Climatic controls on the snowmelt hydrology of the Northern Rocky Mountains. *Journal of Climate*, 24(6): 1666-1687.

Prowse, T.D., Bonsal, B.R., Burn, D.H., Dibike, Y.B., Edwards, T., Ahmed, R., Bawden, A.J., Linton, H.C., Newton, B.W. & Walker, G.S. 2013. Climatic Redistribution of Canada's Western Water Resources (CROCWR). Proceedings of the 19th International Northern Research Basins Symposium and Workshop, Southcentral Alaska, USA, August 11-17th, 2013.

Rood, S.B., Pan, J., Gill, K.M., Franks, C.G., Samuelson, G.M., Shepherd, A. 2008. Declining summer flows of Rocky Mountain rivers: Changing seasonal hydrology and probable impacts on floodplain forests. *Journal of Hydrology*, 349, 397-410.

Sain, S. R., & Furrer, R. 2010. Combining climate model output via model correlations. *Stochastic Environmental Research and Risk Assessment*, *24*(6), 821–829. doi:10.1007/s00477-010-0380-5

Salathé, E. 2005. Downscaling simulations of future global climate with application to hydrologic modelling. *International Journal of Climatology*, *25*(4), 419-436.

Schindler, D. & Donahue, W. 2006. An impending water crisis in Canada's western prairie provinces. *Proceedings of the National Academy of Sciences*, 103(19), 7210-7216.

Schnorbus, M., Werner, A. & Bennett, K. 2014. Impacts of climate change in three hydrologic regimes in British Columbia, Canada. *Hydrological Processes, 28*(3), 1170-1189.

Sen, P.K. 1968. Estimates of the regression coefficient based on Kendall's Tau. *Journal of the American Statistical Association*, 63(324), 1379-1389.

Šeparović, L., Alexandru, A., Laprise, R., Martynov, A., Sushama, L., Winger, K., Tete, K., & Valin, M. 2013. Present climate and climate change over North America as simulated by the fifth-generation Canadian regional climate model. *Climate Dynamics, 41*(11-12), 3167-3201.

Stewart, I.T., Cayan, D. & Dettinger, M. 2004. Changes in snowmelt runoff timing in western North America under a 'business as usual' climate change scenario. *Climate Change, 62*, 217-232.

Stewart, I.T., Cayan, D., & Dettinger, M. 2005. Changes toward earlier streamflow timing across western North America. *Journal of Climate,* 18(8), 1136-1155.

Stewart, I.T. 2009. Changes in snowpack and snowmelt runoff for key mountain regions. *Hydrological Processes*, 23: 78-94.

Sushama, L., Khaliq, N. & Laprise, R. 2010. Dry spell characteristics over Canada in a changing climate as simulated by the Canadian RCM. *Global and Planetary Change, 74*(1), 1–14. doi:10.1016/j.gloplacha.2010.07.004

Thorne, R. & Woo, M. 2011. Streamflow response to climatic variability in a complex mountainous environment: Fraser River Basin, British Columbia, Canada. *Hydrological Processes*, 25, 3076-3085.

Whitfield, P.H. 2001. Linked hydrologic and climate variations in British Columbia and Yukon. *Environmental Monitoring and Assessment, 67*(1-2), 217-238.

Woo, M. & Thorne, R. 2003. Streamflow in the Mackenzie Basin, Canada. *Arctic Institute of North America*, 56(4), pp.328-340.

Xu, C.Y. & Singh, V.P. 2004. Review on regional water resources assessment models under stationary and changing climate. *Water Resources Management*, 18, 591-612.

Zhang, X., Vincent, L., Hogg, W., & Niitsoo, A. 2000. Temperature and precipitation trends in Canada during the 20th century. *Atmosphere-Ocean*, 38(3), 395-429.

Zhang, X., Harvey, K.D, Hogg, W.D., Yuzyk, T.R. 2001. Trends in Canadian streamflow. *Water Resources Research*, 37(4), 987-998.

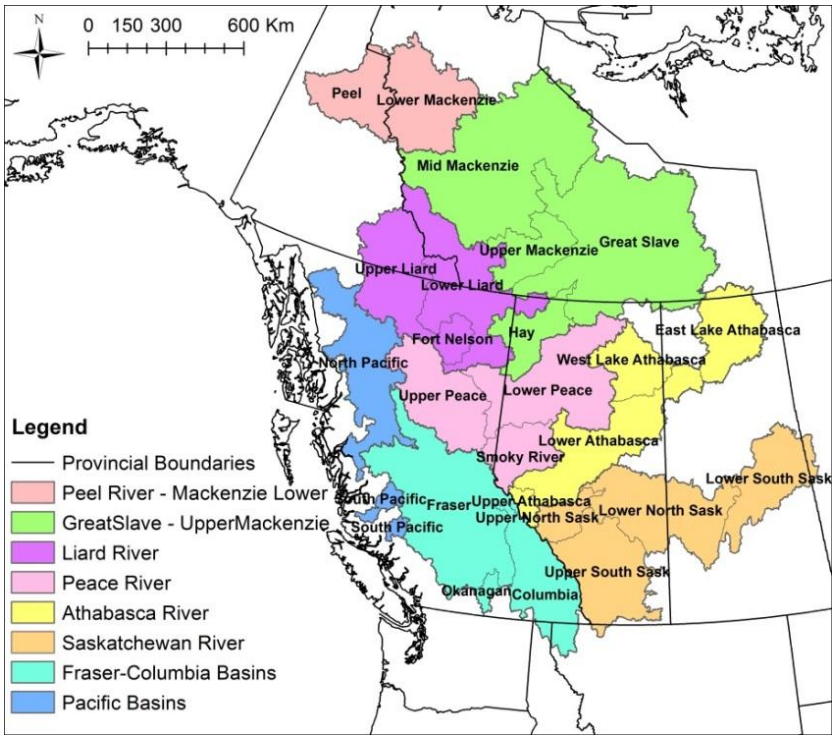

Figure 4.1. CROCWR study area with watersheds labeled by name and study regions identified by colour.

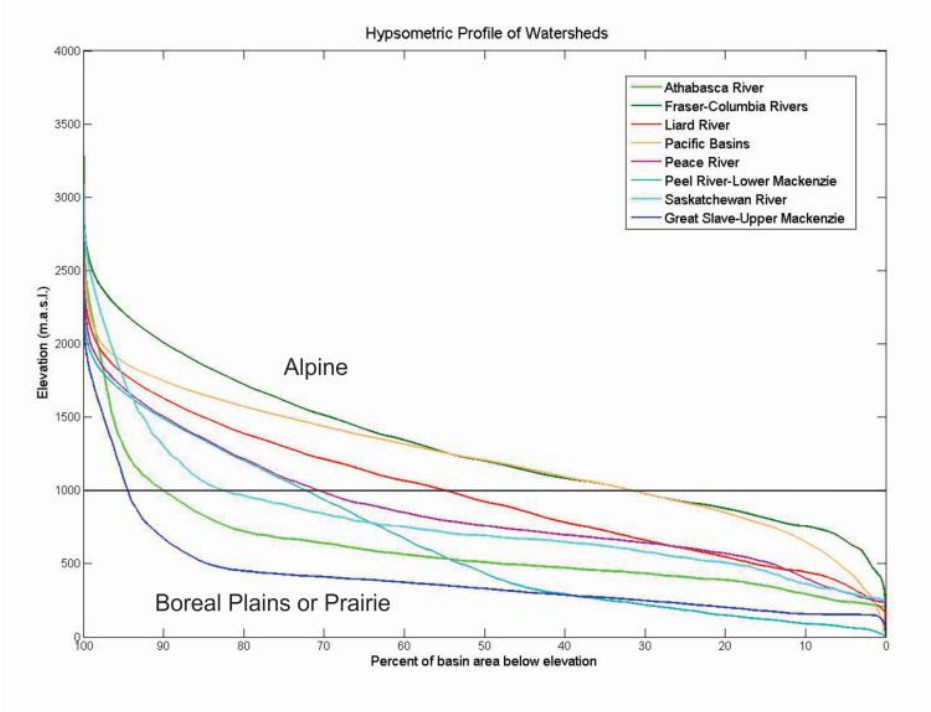

Figure 4.2. Hypsometric curves of each study region.

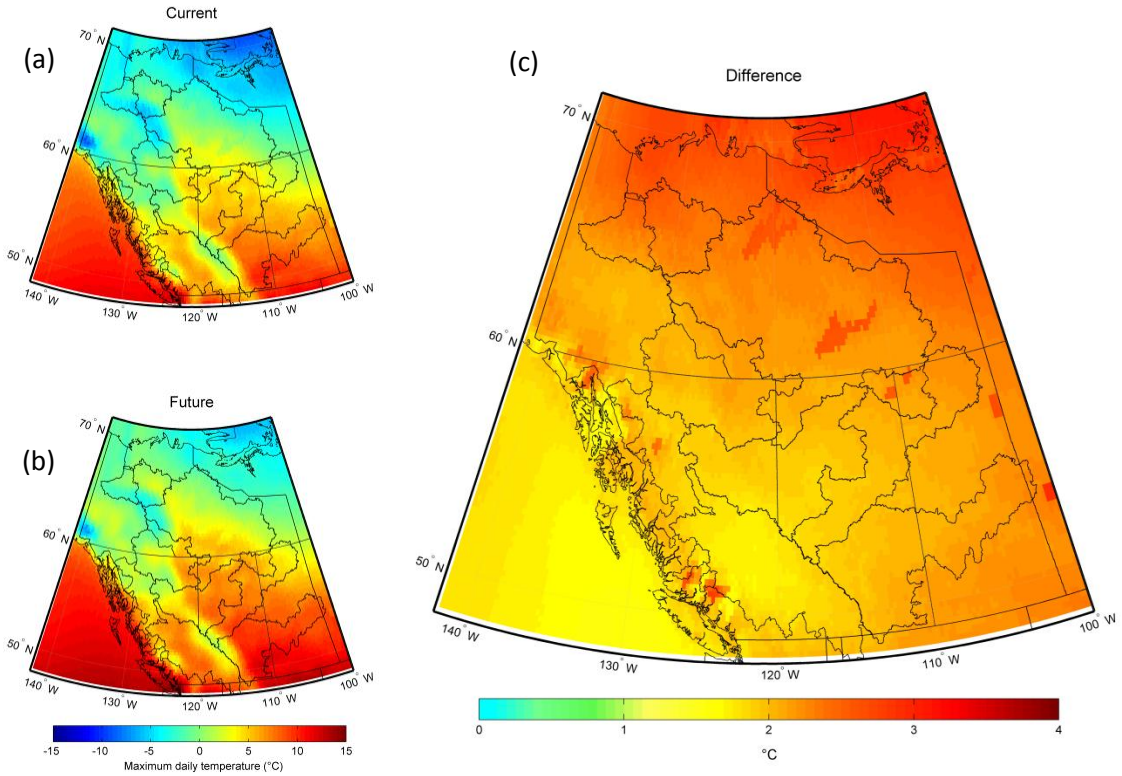

Figure 4.3. Multi-model mean of mean annual maximum temperature for the current and future time periods, and the expected difference. (a) Current, (b) future, (c) difference.

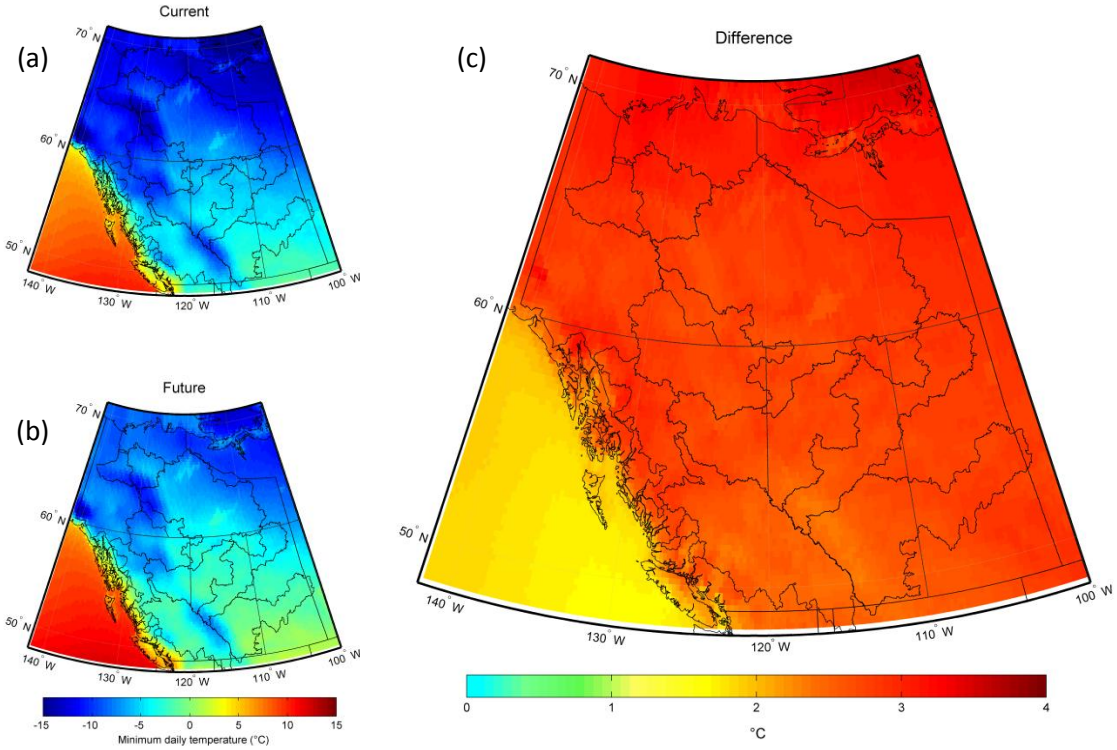

Figure 4.4. Multi-model mean of mean annual minimum temperature for the current and future time periods, and the expected difference. (a) Current, (b) future, (c) difference.

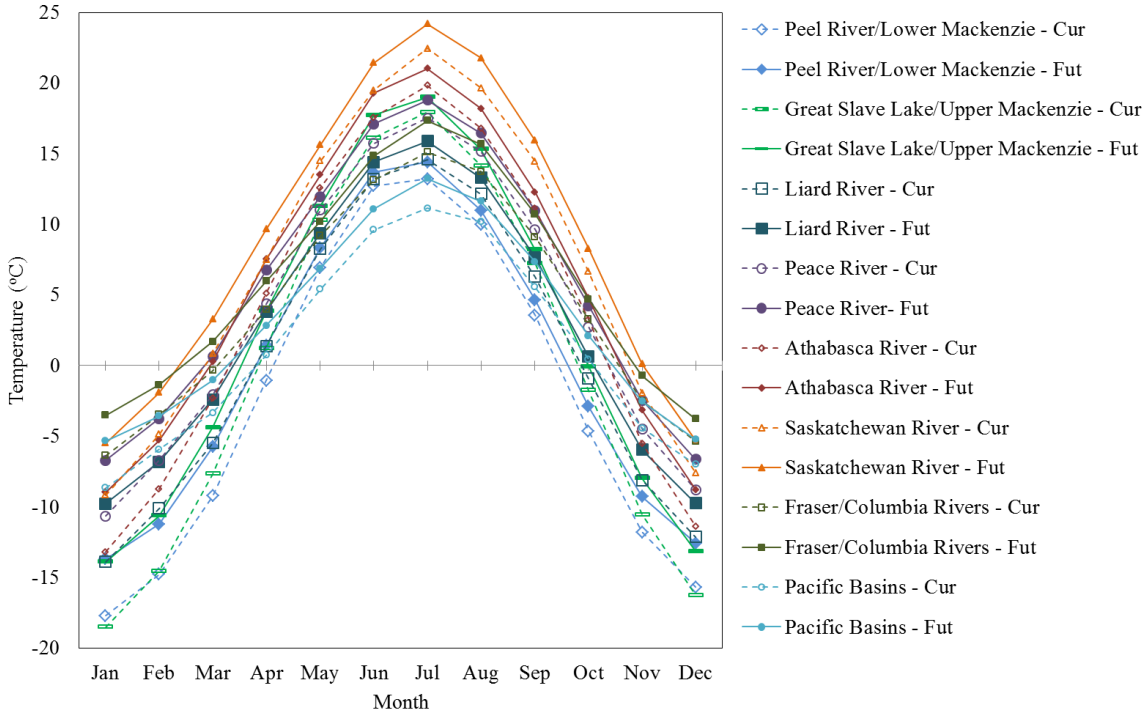

Figure 4.5. Daily average Tmax for each month during the current and future periods spatially averaged for each study region. Current period shown with unfilled symbols and dashed lines, future period shown with solid symbols and lines.

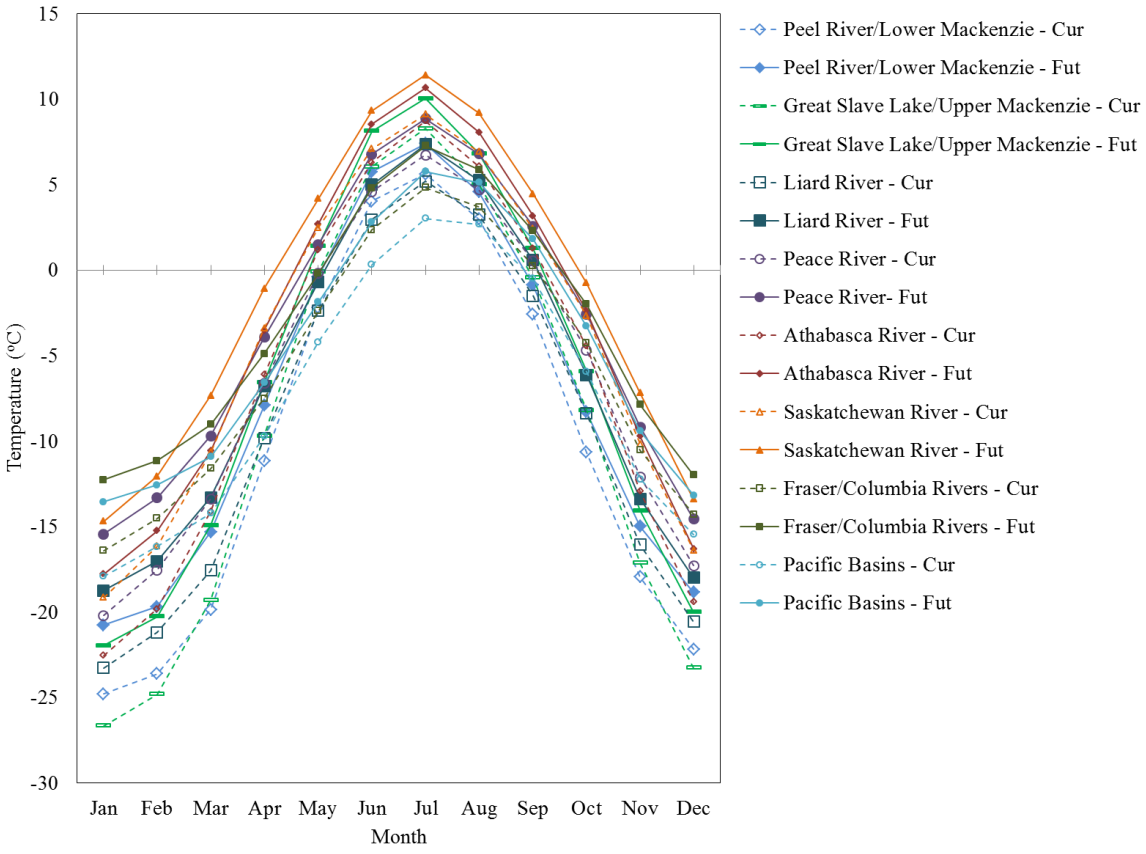

Figure 4.6. Daily average Tmin for each month during the current and future periods spatially averaged for each study region. Current period shown with unfilled symbols and dashed lines, future period shown with solid symbols and lines.

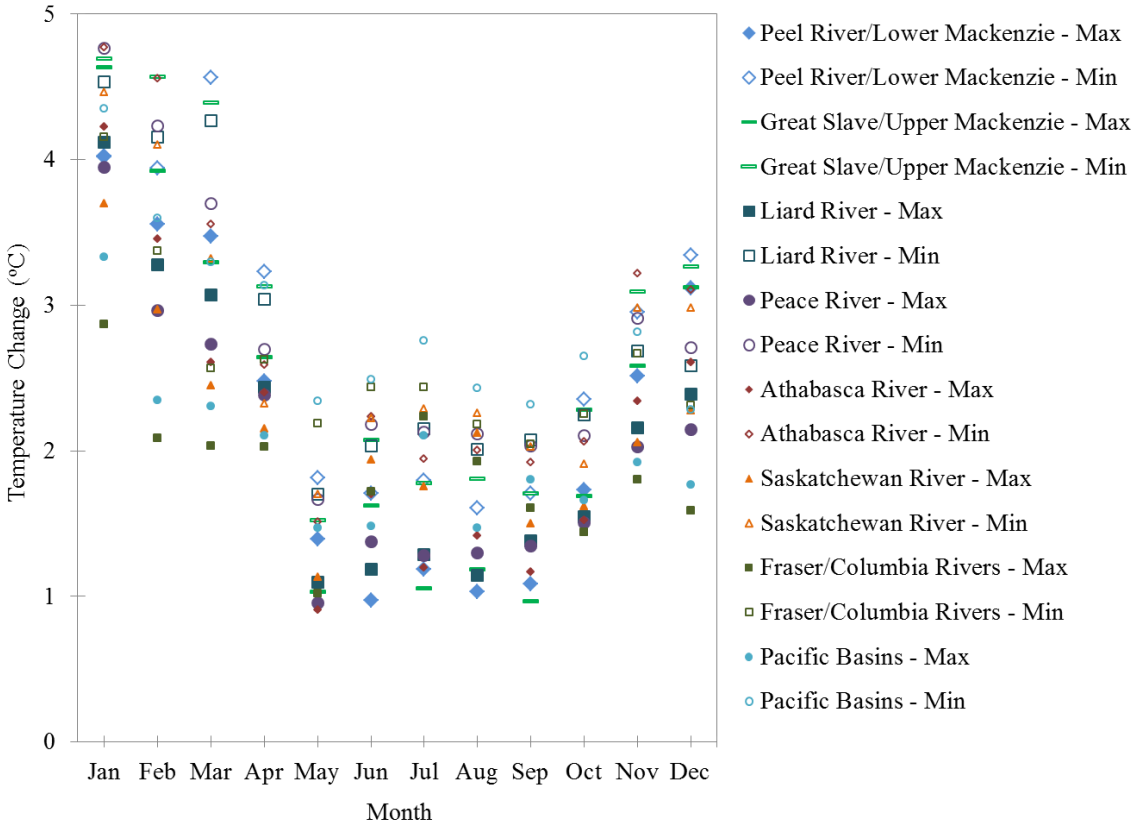

Figure 4.7. Spatially averaged regional change in monthly mean Tmax and Tmin between the current and future periods. Tmax shown with solid symbols, Tmin shown with unfilled symbols.

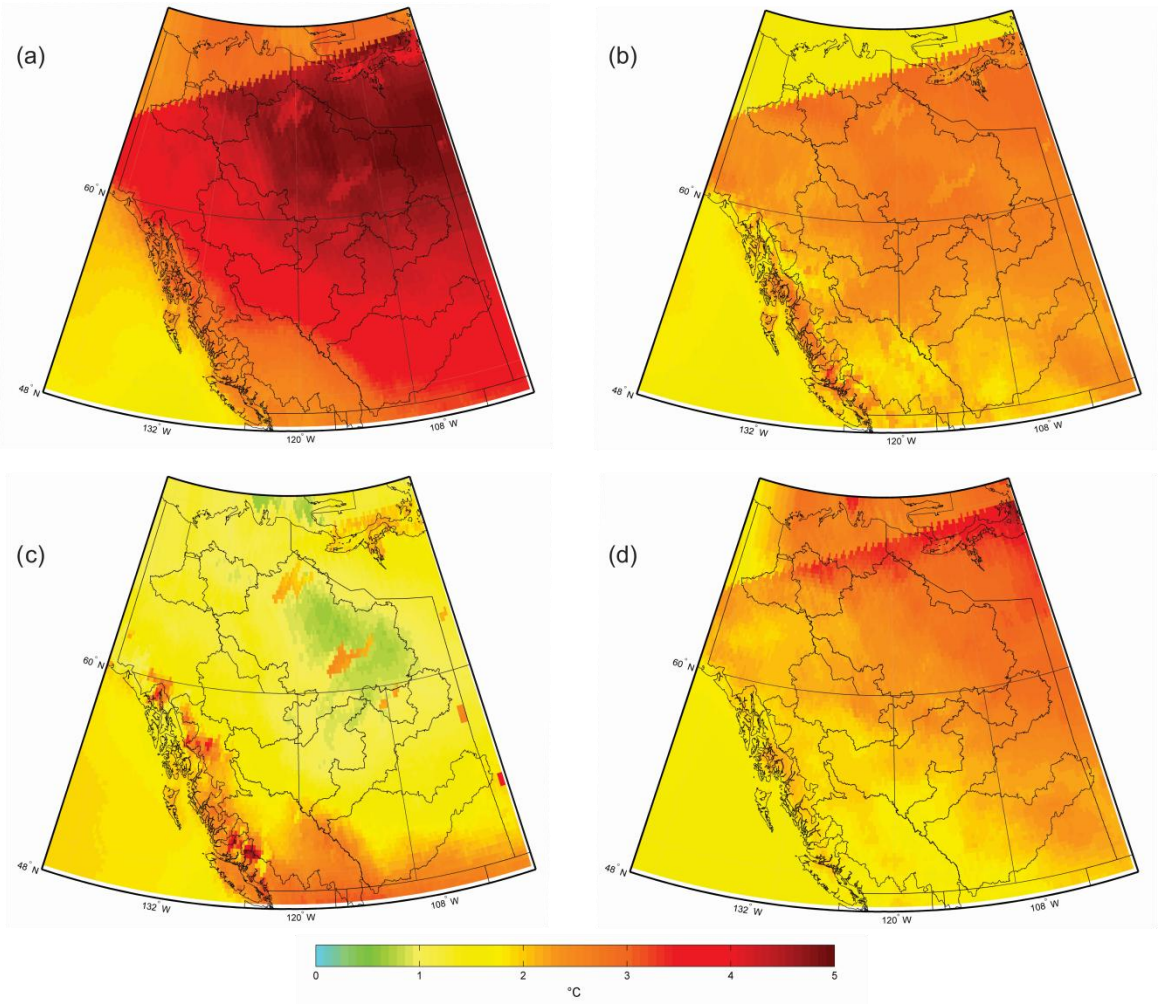

Figure 4.8. Multi-model mean difference in Tmax values between the current and future periods during (a) January, (b) April, (c) July, and (d) November.

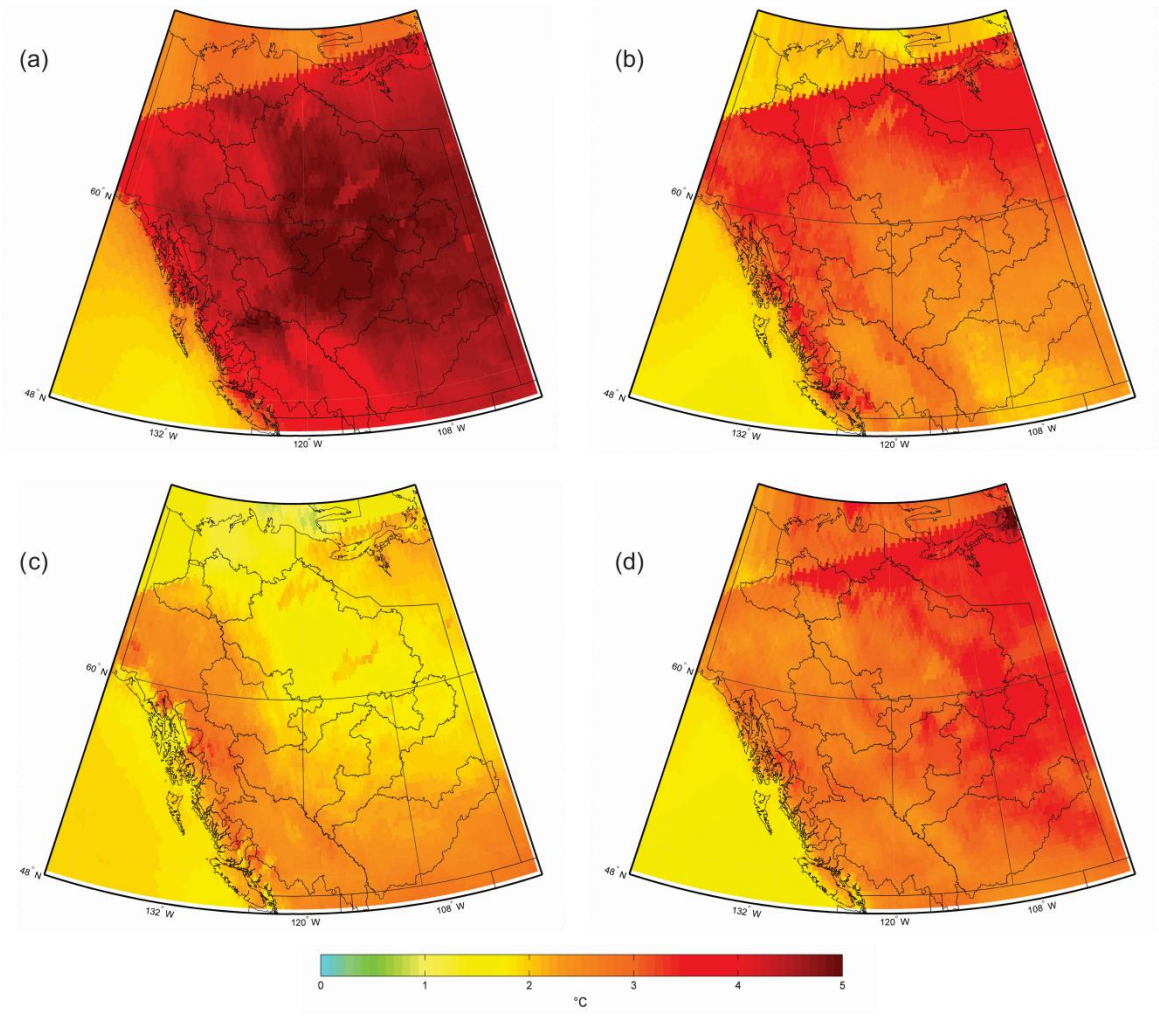

Figure 4.9. Multi-model mean difference in Tmin values between the current and future periods during (a) January, (b) April, (c) July, and (d) November.

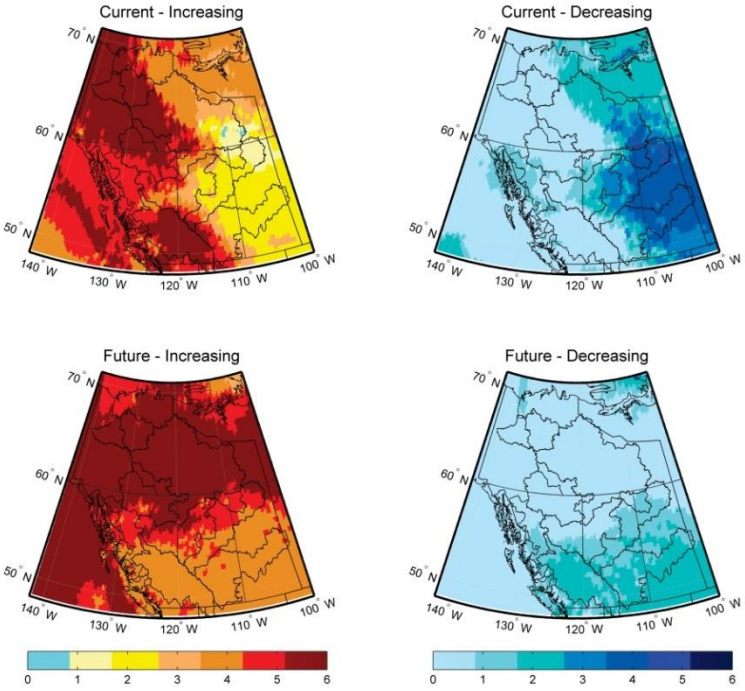

Figure 4.10. Number of models showing increasing or decreasing rates of change in Tmax during the current and future time periods during January.

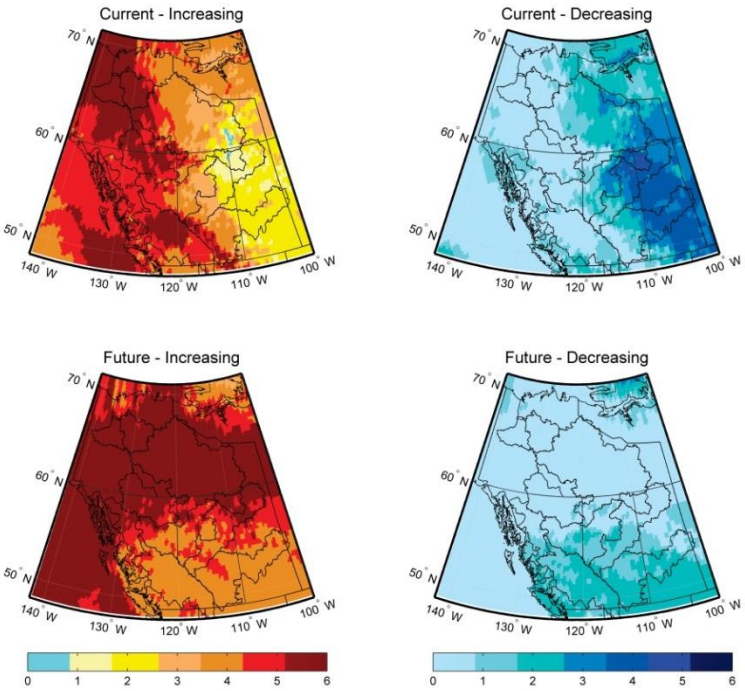

Figure 4.11. Number of models showing increasing or decreasing rates of change in Tmin during the current and future time periods during January.

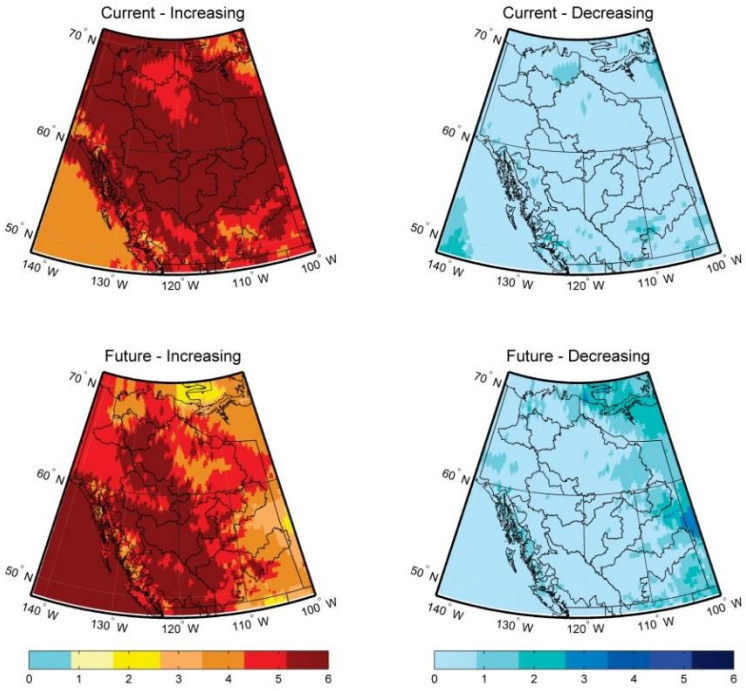

Figure 4.12. Number of models showing increasing or decreasing rates of change in Tmax during the current and future time periods during April.

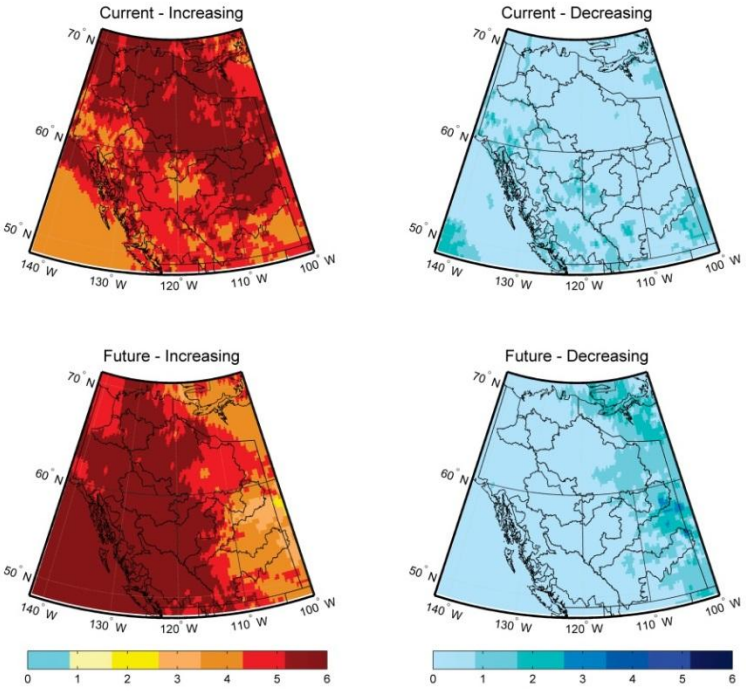

Figure 4.13. Number of models showing increasing or decreasing rates of change in Tmin during the current and future time periods during April.

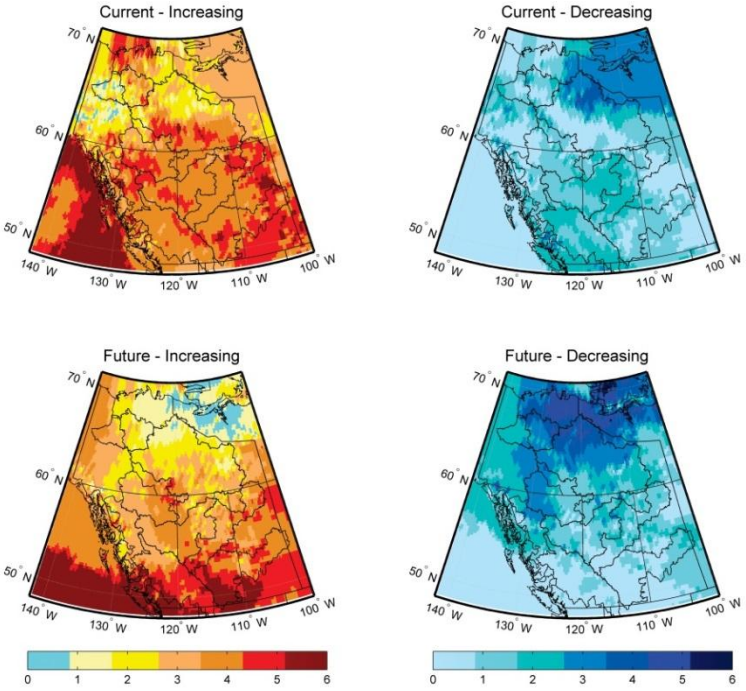

Figure 4.14. Number of models showing increasing or decreasing rates of change in Tmax during the current and future time periods during July.

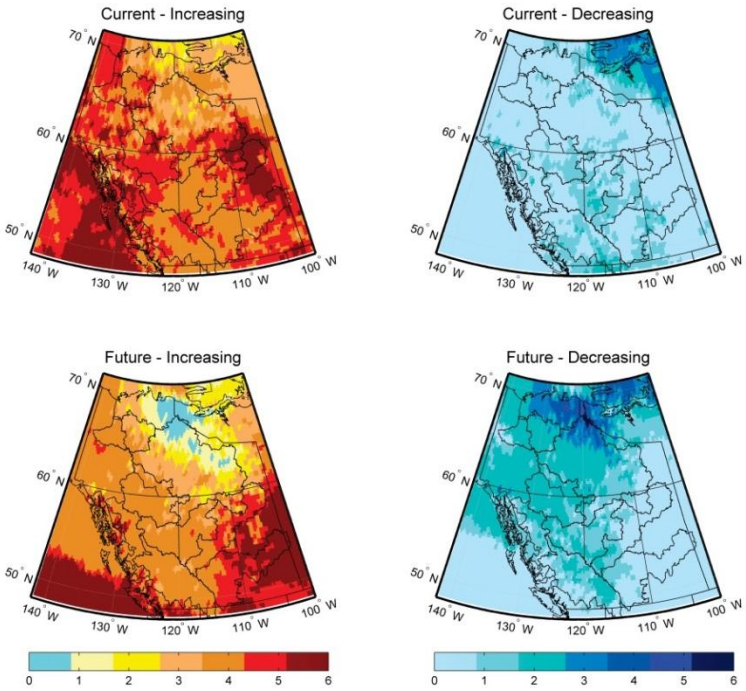

Figure 4.15. Number of models showing increasing or decreasing rates of change in Tmin during the current and future time periods during July.

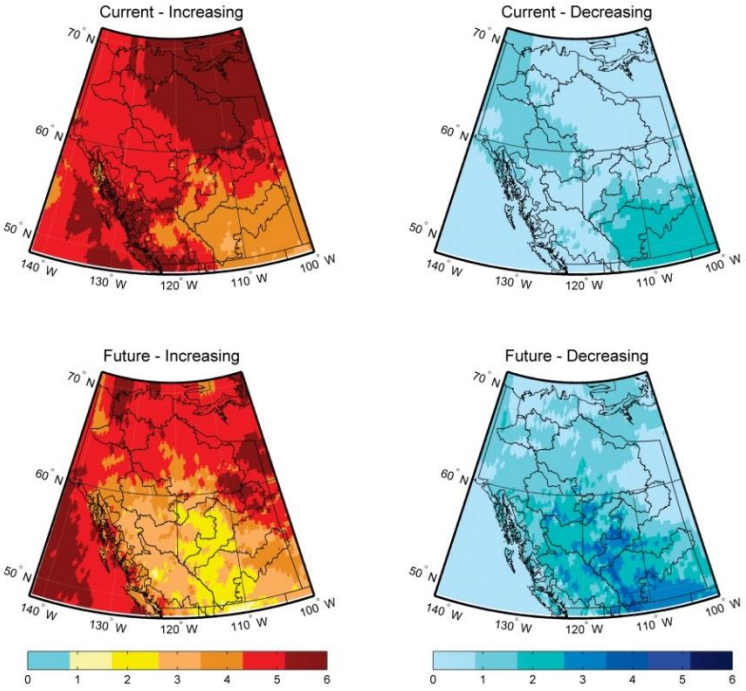

Figure 4.16. Number of models showing increasing or decreasing rates of change in Tmax during the current and future time periods during November.

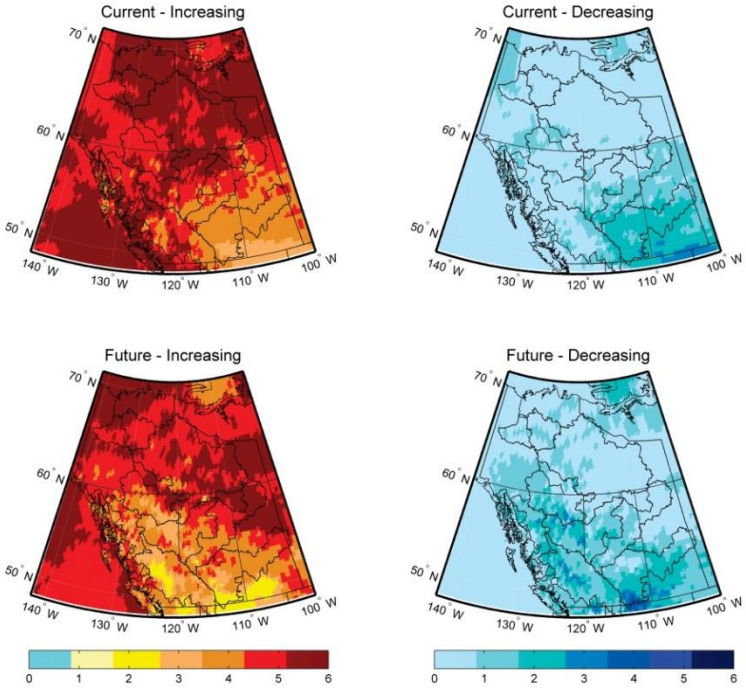

Figure 4.17. Number of models showing increasing or decreasing rates of change in Tmin during the current and future time periods during November.

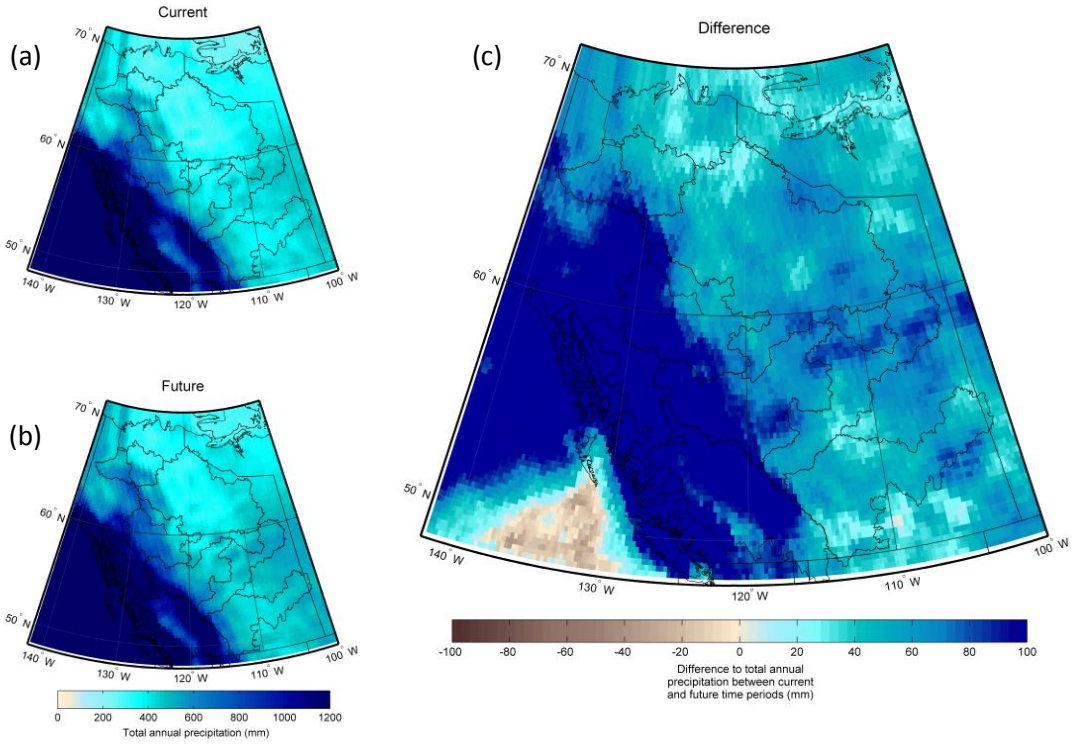

Figure 4.18. Multi-model mean of mean annual precipitation for the current and future time periods, and the expected difference. (a) Current, (b) future, (c) difference.

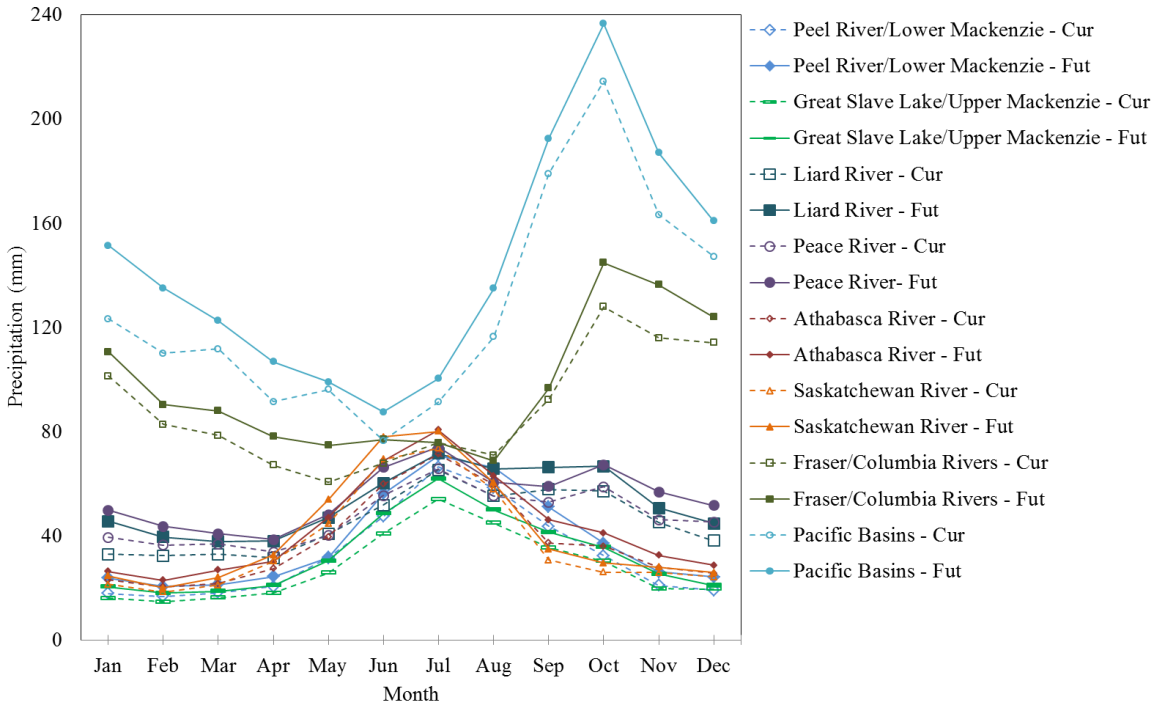

Figure 4.19. Precipitation during each month in the current and future periods spatially averaged for each study region. Current period shown with unfilled symbols and dashed lines, future period shown with solid symbols and lines.

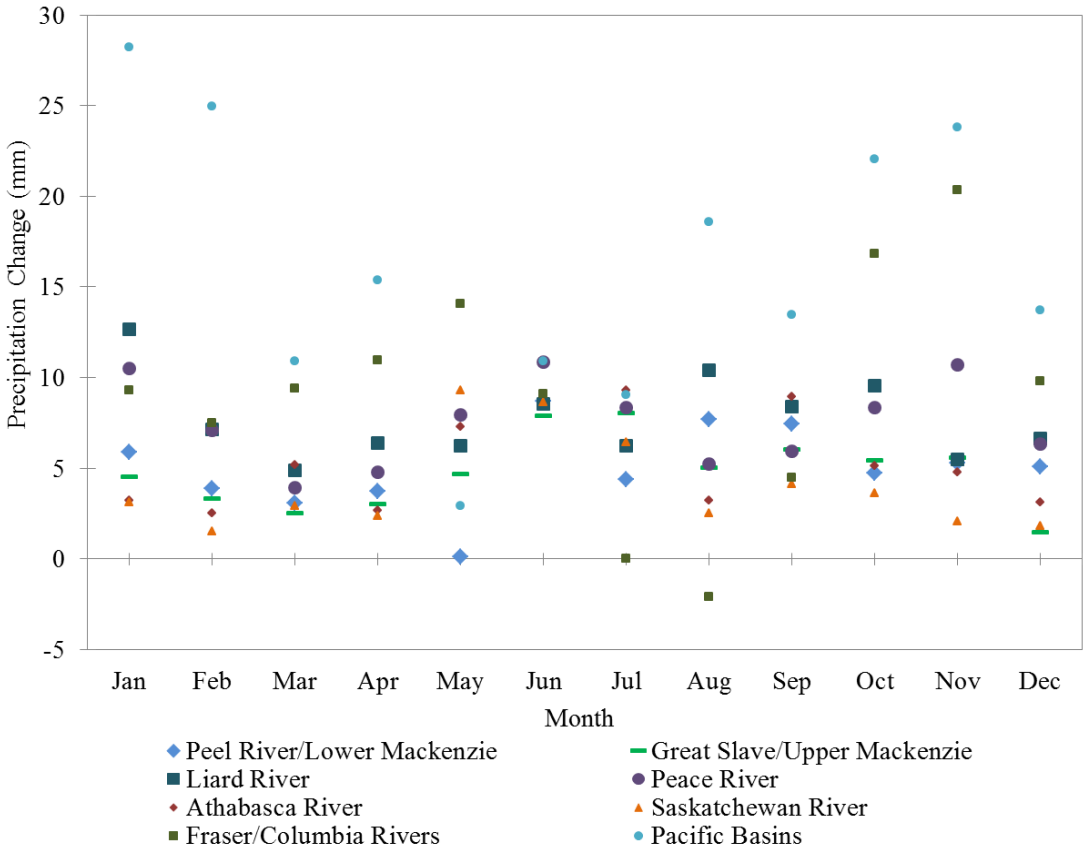

Figure 4.20. Spatially averaged regional change in monthly precipitation between the current and future periods.

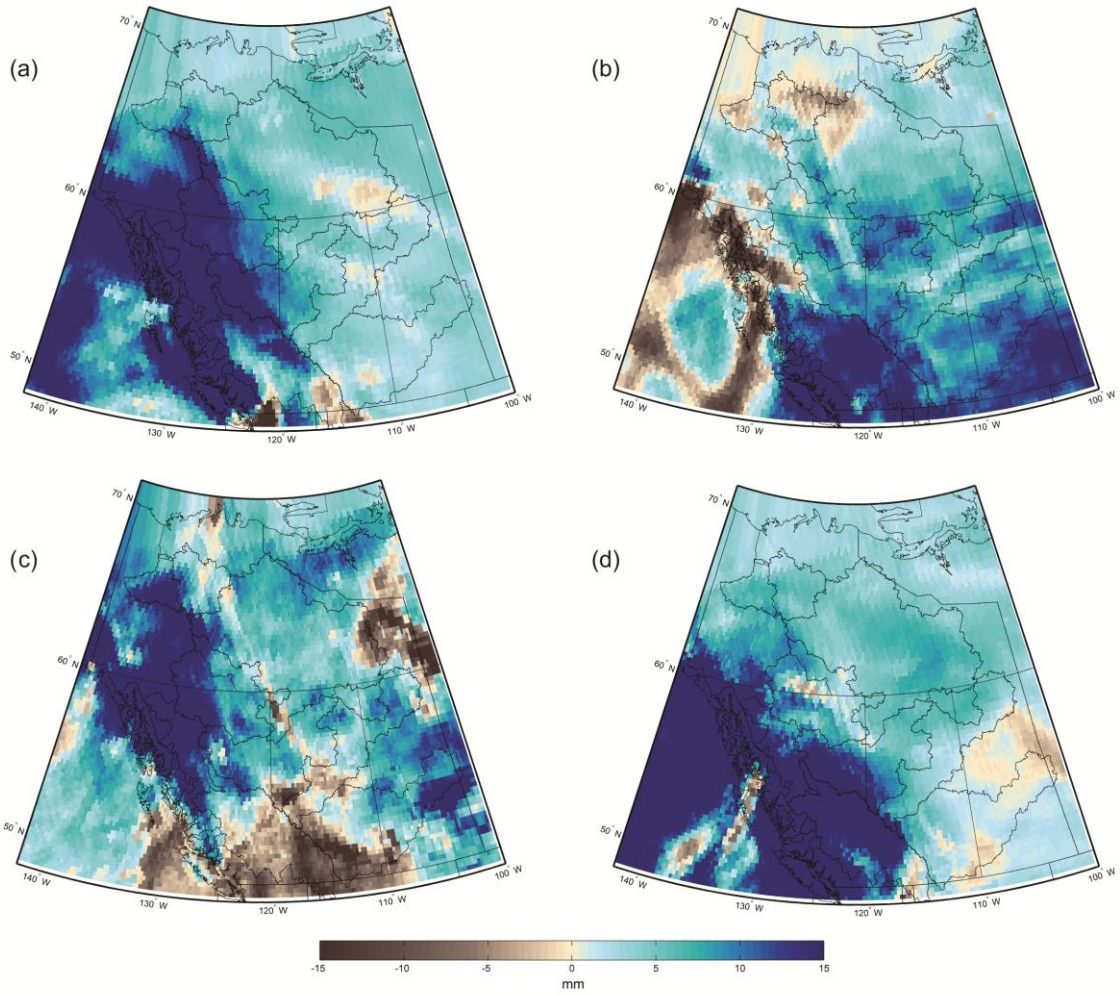

Figure 4.21. Multi-model mean difference in monthly precipitation between the current and future periods during (a) January, (b) May, (c) August, and (d) November.

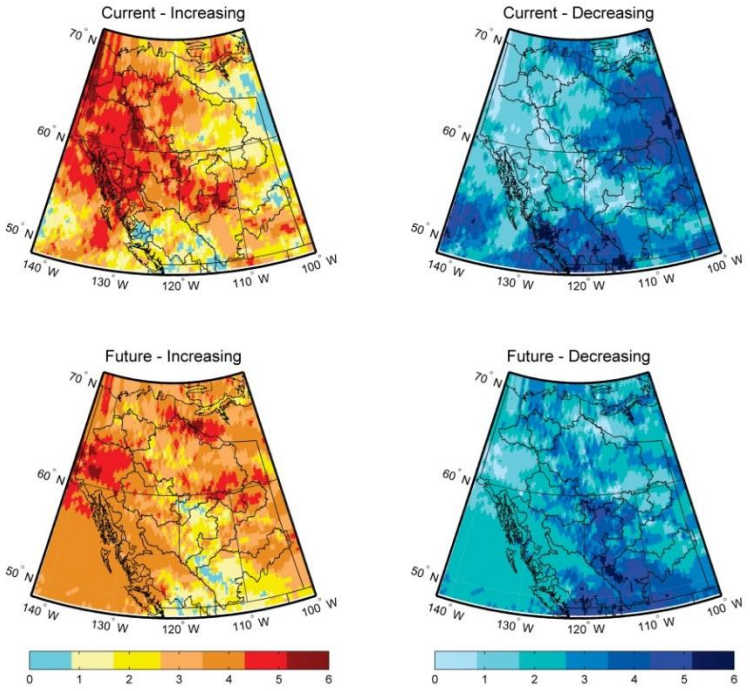

Figure 4.22. Number of models showing increasing or decreasing rates of change in precipitation during the current and future time periods during January.

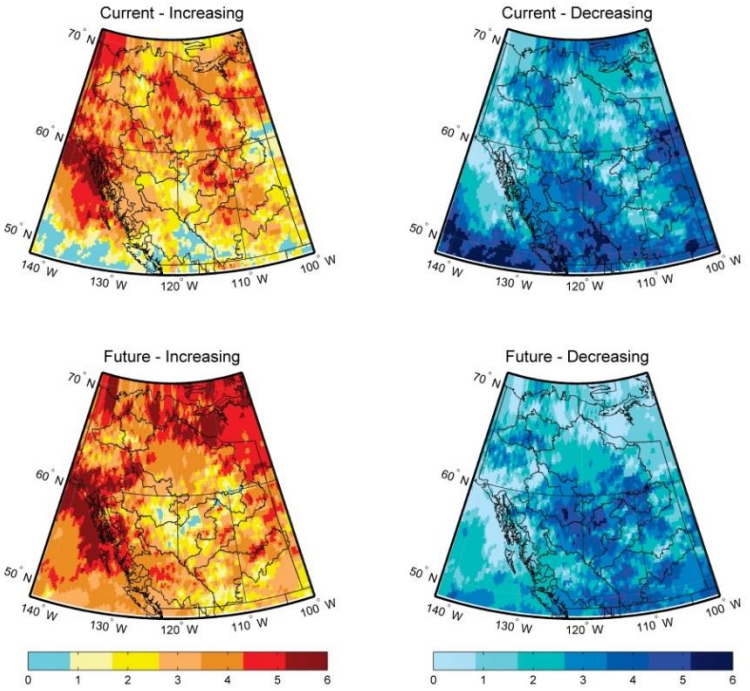

Figure 4.23. Number of models showing increasing or decreasing rates of change in precipitation during the current and future time periods during May.

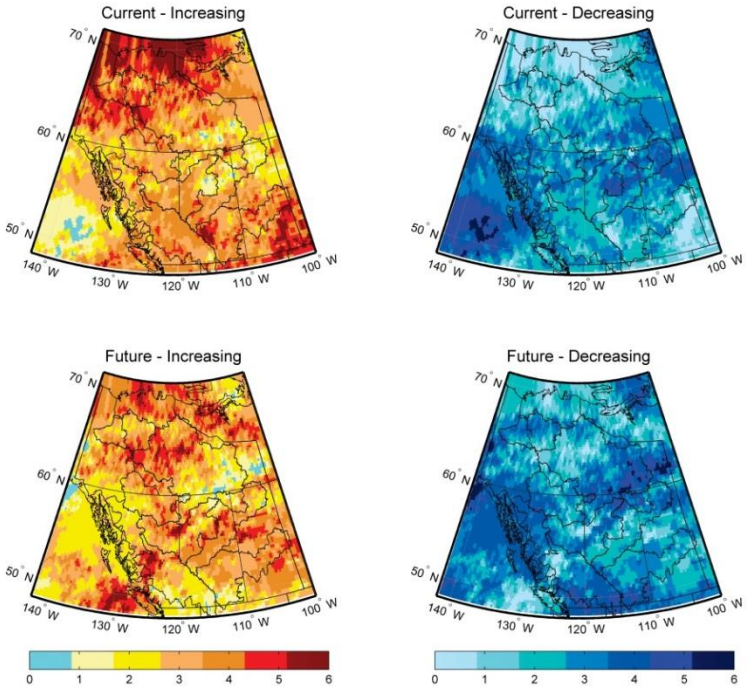

Figure 4.24. Number of models showing increasing or decreasing rates of change in precipitation during the current and future time periods during August.

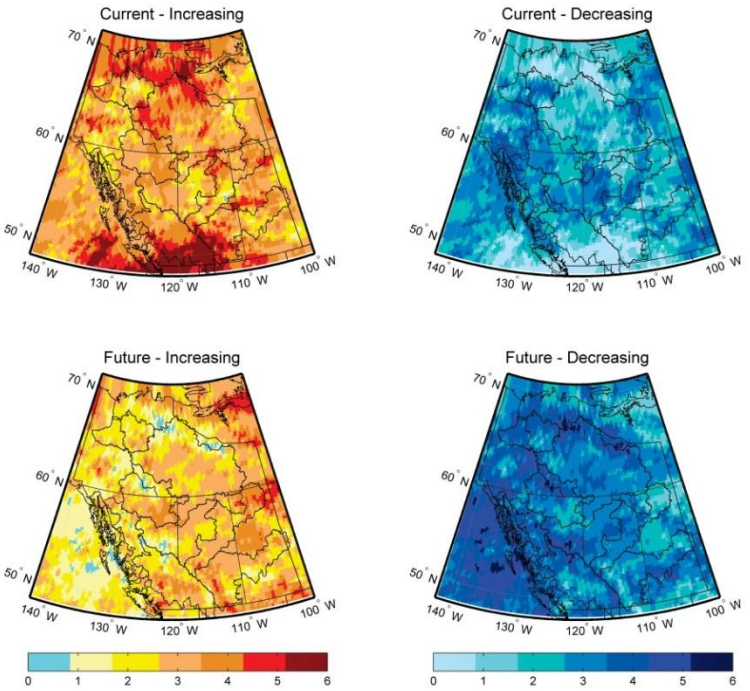

Figure 4.25. Number of models showing increasing or decreasing rates of change in precipitation during the current and future time periods during November.

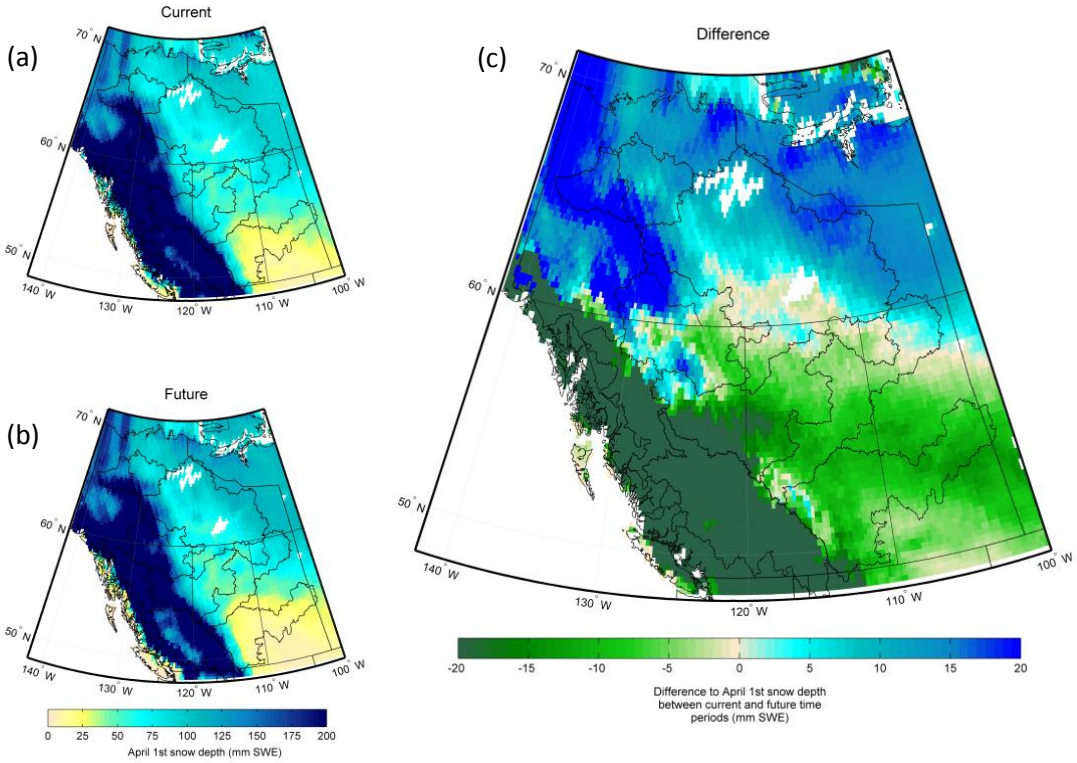

Figure 4.26. Multi-model mean of April 1st SWE for the current and future time periods, and the expected difference. (a) Current, (b) future, (c) difference.

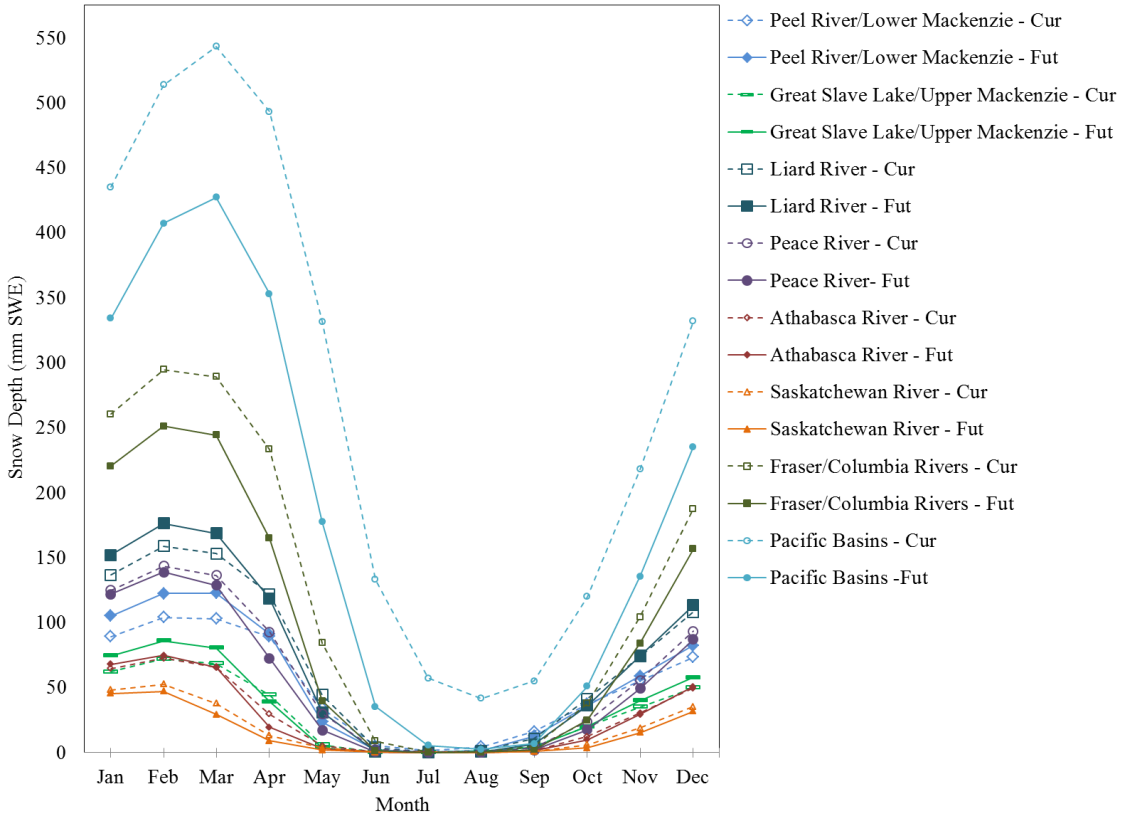

Figure 4.27. SWE at the end of each month in the current and future periods spatially averaged for each study region. Current period shown with unfilled symbols and dashed lines, future period shown with solid symbols and lines.

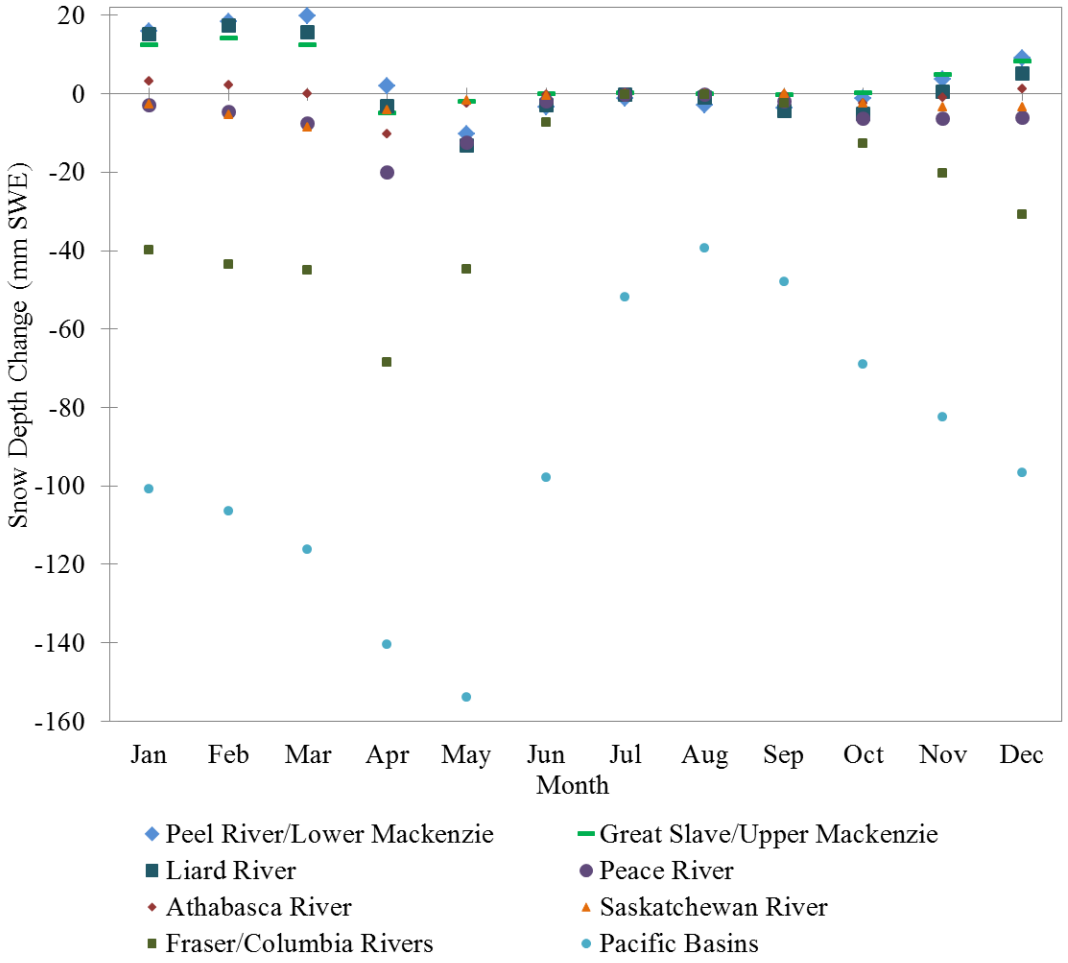

Figure 4.28. Spatially averaged regional change in monthly SWE between the current and future periods.

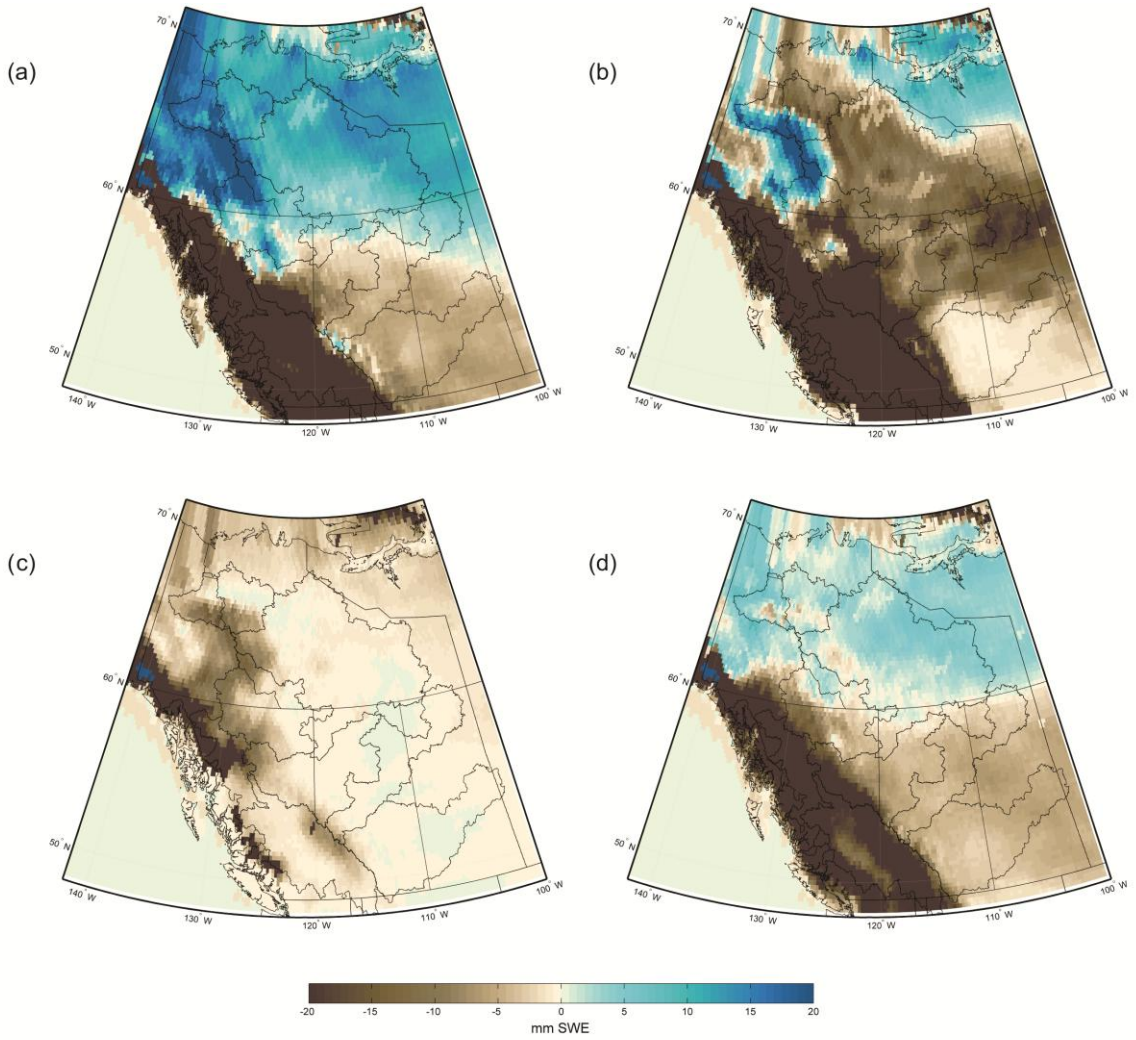

Figure 4.29. Multi-model mean difference in monthly SWE between the current and future periods during (a) January, (b) April, (c) September, and (d) November.

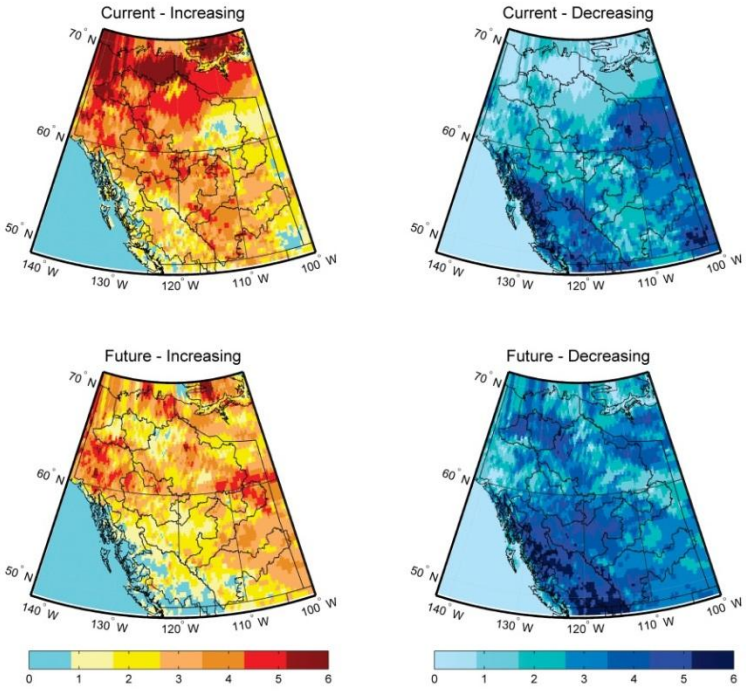

Figure 4.30. Number of models showing increasing or decreasing rates of change in SWE during the current and future time periods during January.

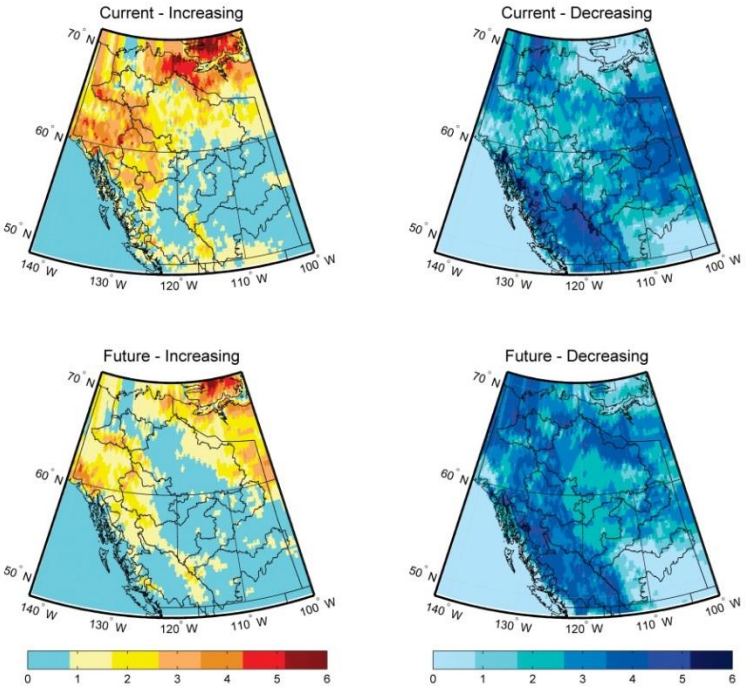

Figure 4.31. Number of models showing increasing or decreasing rates of change in SWE during the current and future time periods during April.

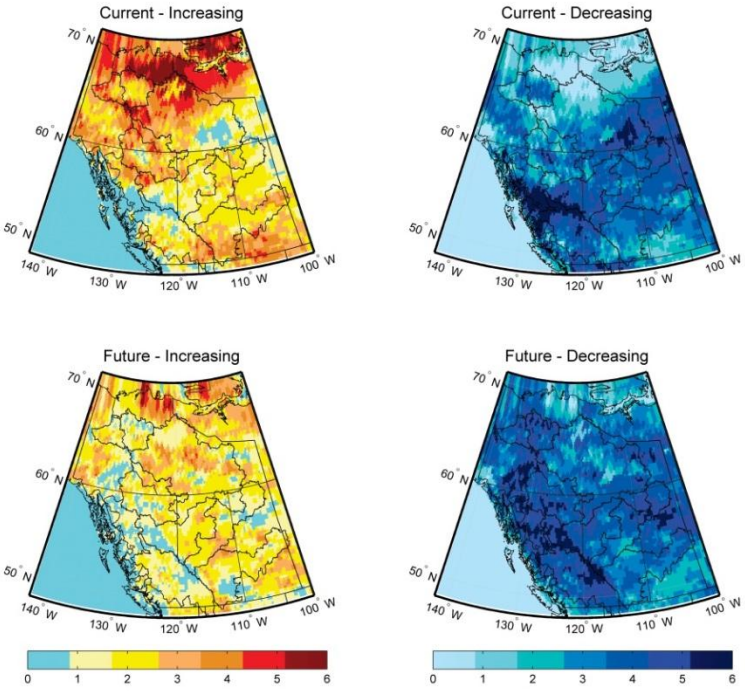

Figure 4.32. Number of models showing increasing or decreasing rates of change in SWE during the current and future time periods during November.

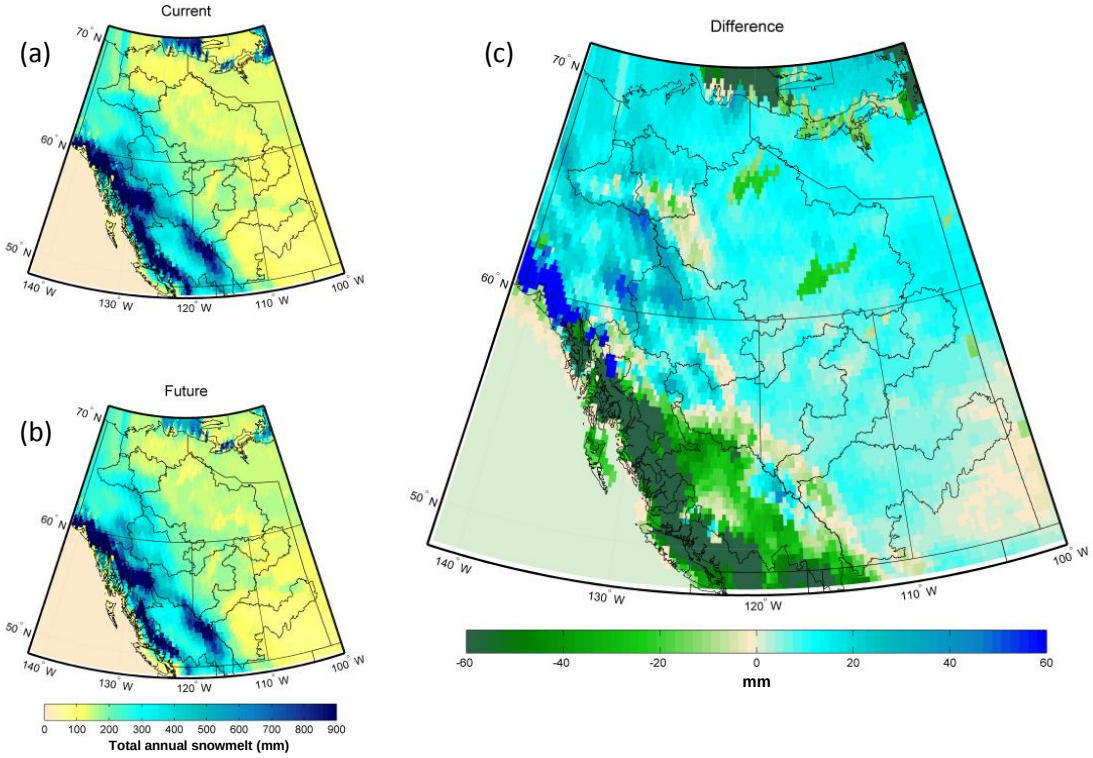

Figure 4.33. Multimodel mean of annual snowmelt for the current and future time periods, and the expected difference. (a) Current, (b) future, (c) difference.

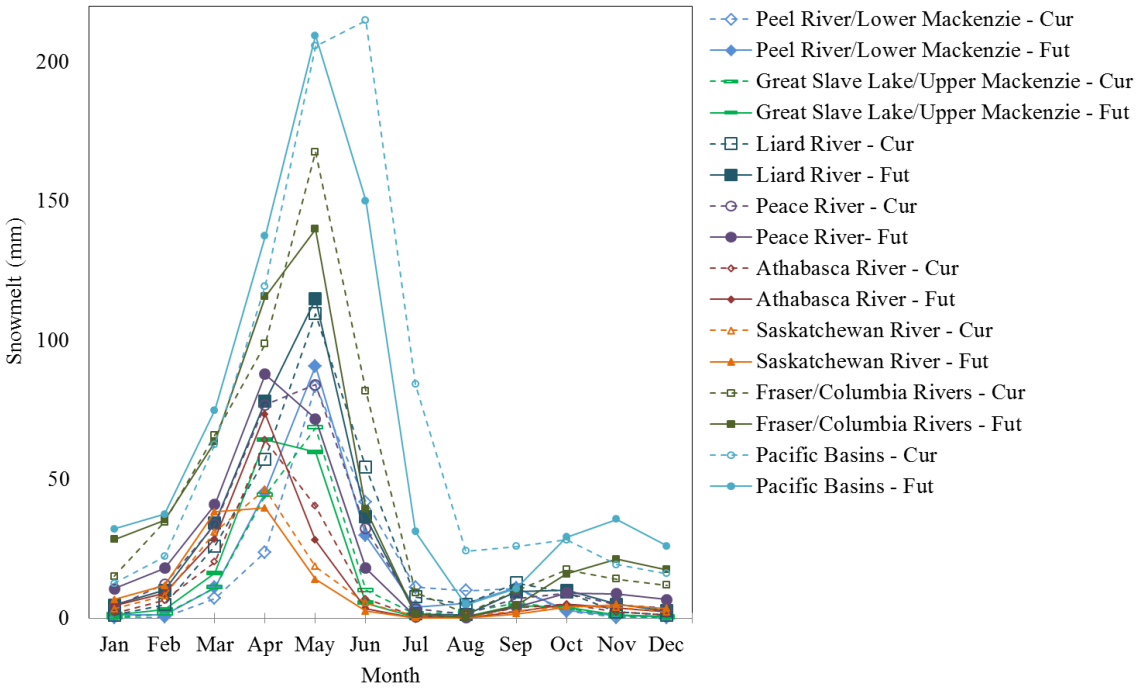

Figure 4.34. Monthly snowmelt in the current and future periods spatially averaged for each study region. Current period shown with unfilled symbols and dashed lines, future period shown with solid symbols and lines.

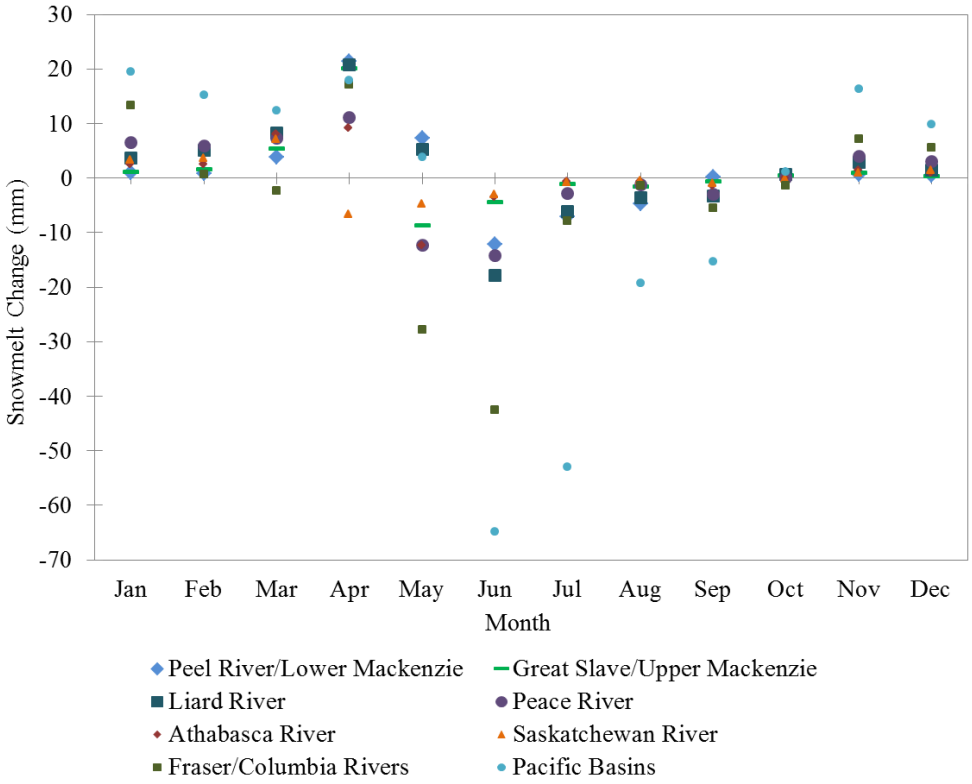

Figure 4.35. Spatially averaged regional change in monthly snowmelt between the current and future periods.

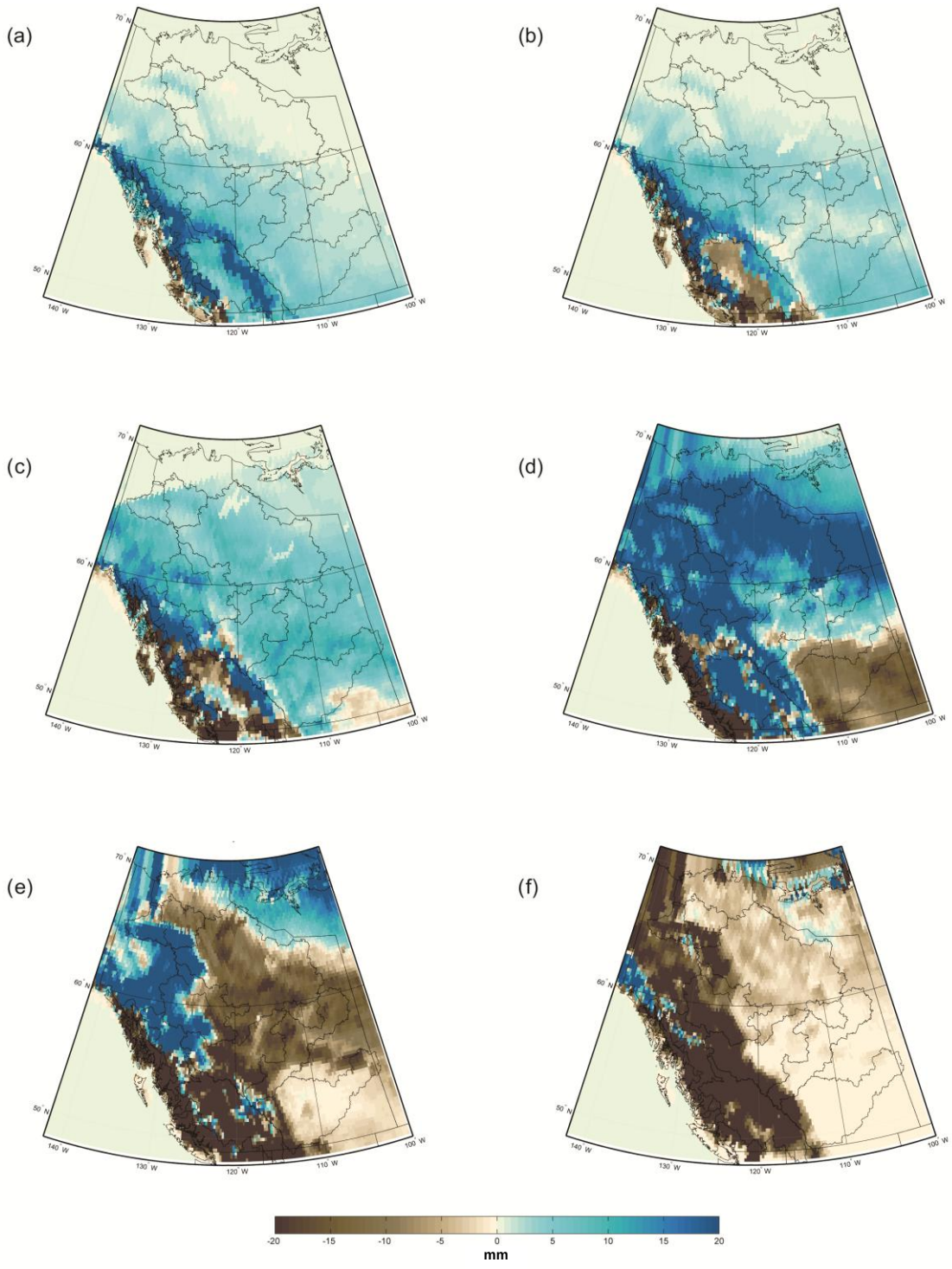

Figure 4.36. Multimodel mean difference in monthly snowmelt between the current and future periods during (a) January, (b) February, (c) March, (d) April, (e) May, and (f) June.

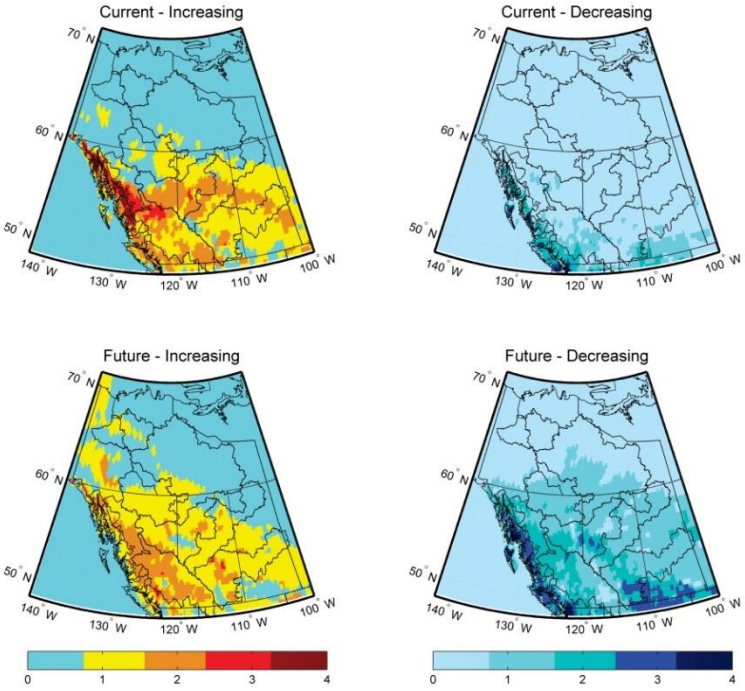

Figure 4.37. Number of models showing increasing or decreasing rates of change in snowmelt during the current and future time periods during January.

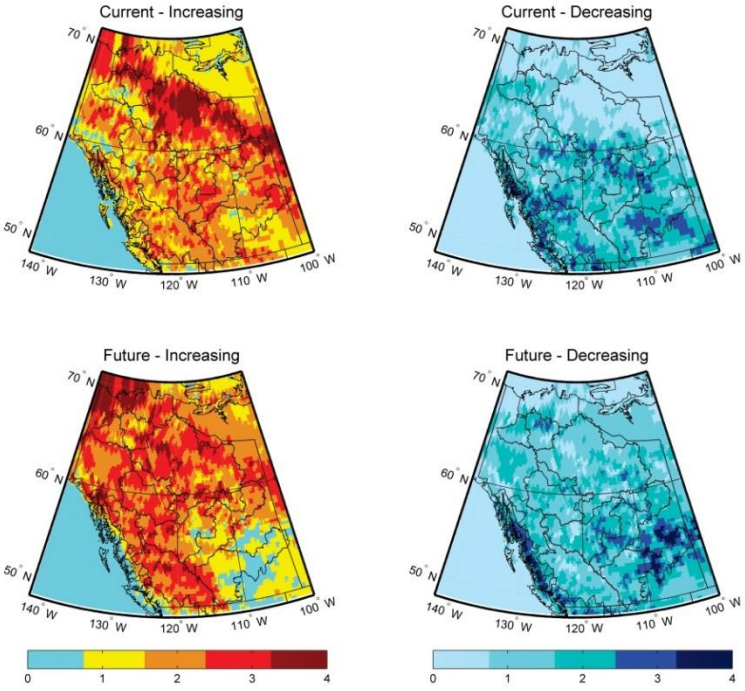

Figure 4.38. Number of models showing increasing or decreasing rates of change in snowmelt during the current and future time periods during April.

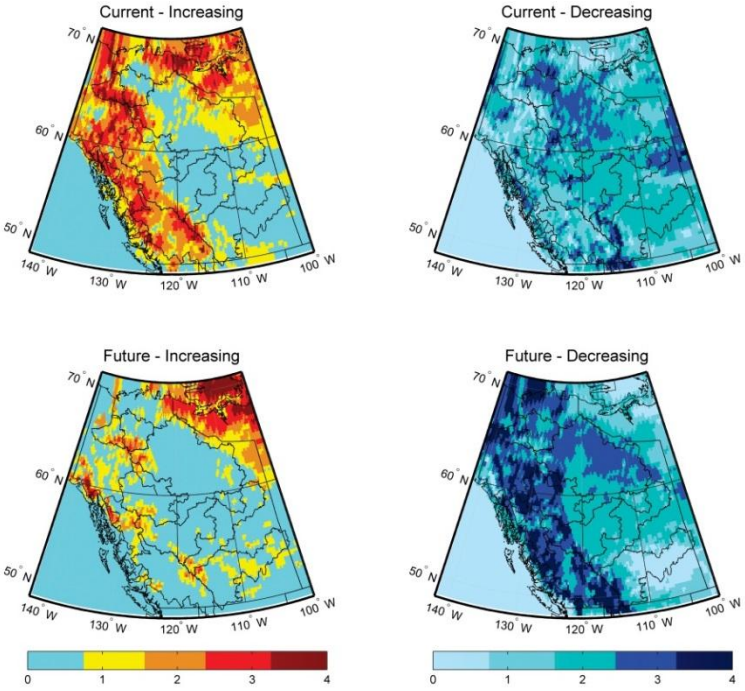

Figure 4.39. Number of models showing increasing or decreasing rates of change in snowmelt during the current and future time periods during May.

5. Chapter 5: Conclusion

This research evaluated the spatial variations in hydroclimatic trends throughout western Canada for the historic and future time periods using a combination of interpolated, gridded climate data and regional climate models, and is one component of the multi-disciplinary CROCWR project. The objectives identified for this study included assessment of historical trends, future scenarios, and spatial variation in historical trends and possible future change of the selected hydroclimatic variables: temperature, precipitation, snow depth, and snowmelt. This study is the first to analyze high resolution historical climate data over such a large area as western Canada and to also assess future scenarios on a monthly basis using RCMs in this region.

Chapter 2 included a literature review of previously identified trends and changes to the hydroclimatic variables selected for study along with a description of the study area, potential sources of historical and future projection data, and statistical and spatial analysis techniques to be used in this research. Chapter 3 met objectives 1 and 3 as outlined in Chapter 1 while Chapter 4 met objectives 2 and 3, with both chapters presented as journal-style manuscripts.

Results from the historical analysis were presented in Chapter 3. The gridded, interpolated climate dataset, referred to as the NRCan 2012 dataset, included maximum and minimum temperature and precipitation at a daily timestep which allowed snow depth and snowmelt to be modelled using a temperature-index model. Pixel trajectory analysis was then used in conjunction with the Mann-Kendall non-parametric test and Sen's slope estimator to calculate monthly and annual trend values for each data point on the 10km x 10km grid for each variable between 1950 and 2010 and map the results.

Chapter 4 presented the results of the future scenario analysis. Future climate data consisted of six regional climate models from the North American Regional Climate Change Assessment Program. Pixel trajectory analysis along with a multi-model mean approach was used to assess potential future change in temperature, precipitation, SWE, and snowmelt between the current and future periods using a delta method on an annual and monthly basis.

The multiple datasets used in this research show some variation in results, though the major changes are apparent through both the historical and future periods. The NRCan 2012 dataset as well as the suite of RCMs all agree that minimum temperature has increased more consistently and at a greater rate than maximum temperature and is likely to continue to do so in the future; diurnal temperature range is decreasing, and is expected to continue to decrease in the future. The greatest temperature increases were detected during the cold season in both time periods. Temperature increases were also greatest at northern latitudes, as well as at higher elevations in the mountain ranges located within the study area. Large scale precipitation decreases were also detected in both datasets. Cold season precipitation decreases were detected across much of the study area through both time periods, though some increases across the northern half of the study area are expected in the form of snow depth, indicating a potential northward shift in winter precipitation in the future. A northward shift in summer precipitation was also detected, particularly in the Liard River and surrounding regions. In the southern half of the study area the decreases to winter precipitation in the current period and increases to more northern and high latitude area precipitation in summer indicates precipitation shifting away from Prairie areas and more to northern latitude areas during the summer. This

may further exacerbate the drought issues that occur over the Prairies in the warm season in the future. Consistent with the detected precipitation changes, snow accumulation decreased through the cold season across most of the southern half of the study area and SWE is expected to continue decreasing into the future as well. Snowmelt results indicate increases throughout most winter and spring months in both time periods, indicating greater mid-winter melt and an earlier spring freshet. This trend is particularly apparent in the southern half of the study area and at lower elevations. The shorter cold season combined with expected decreases to winter precipitation across much of the study area indicate a possible decreased spring freshet volume, particularly in the south.

This study has provided some insight into historical trends and potential future changes of hydroclimatic variables affecting streamflow, but further analysis is required for improving understanding of these phenomena. Seasonal and cold season/warm season analysis in addition to the monthly analysis already completed would provide more insight into seasonal shifts in the selected hydroclimatic variables. Further integration of the individual components of the CROCWR project would also create a more complete, multidisciplinary product that can explain how atmospheric circulation pattern and teleconnections have affected hydroclimatic variables, streamflow, and spring freshet volume and timing. In addition, the CROCWR project focused on western Canada, but further study of northern or eastern Canada would offer a more complete view of hydroclimatic variations across Canada.

This research provides a summary of detected trends and potential future scenarios in hydroclimatic variables throughout western Canada that can be combined with CROCWR project analyses on atmospheric circulation patterns, streamflow trends, and

spring freshet timing and volume to evaluate the spatial and temporal distribution of water resources in this region.

APPENDICES

APPENDIX A – Supplementary material for Chapter 3

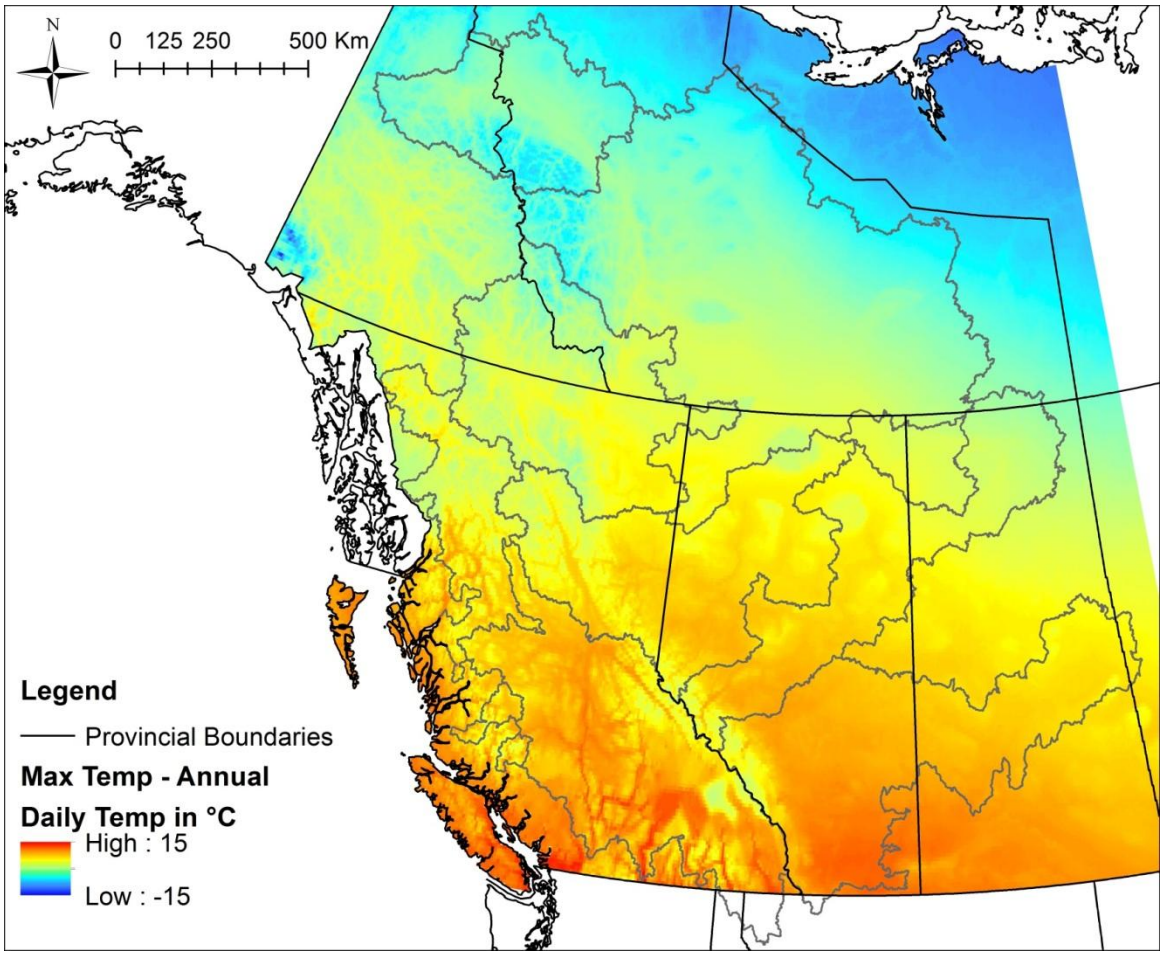

Figure A.1. Mean annual Tmax in ^{o}C. Averaged from 1950-2010.

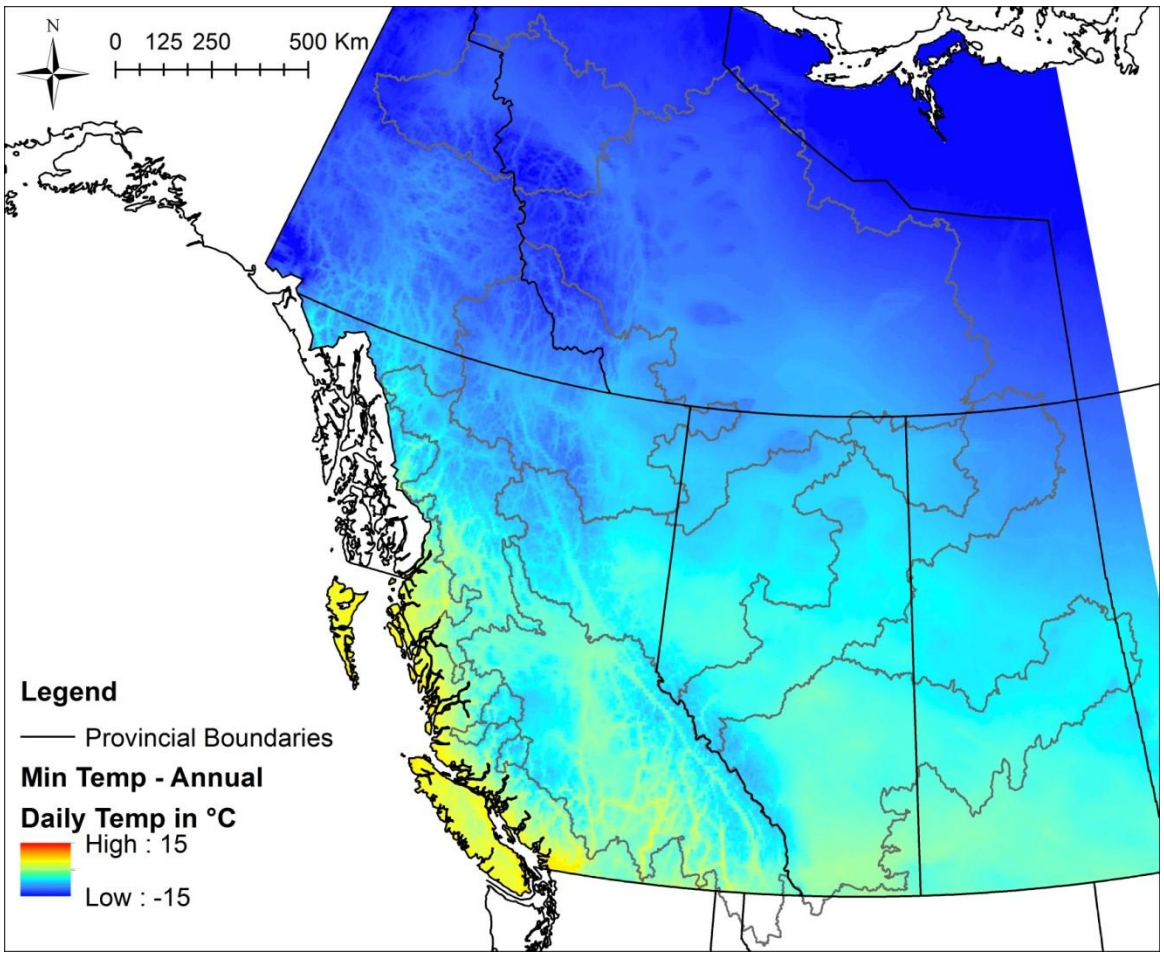

Figure A.2. Mean annual Tmin in ^{o}C. Averaged from 1950-2010.

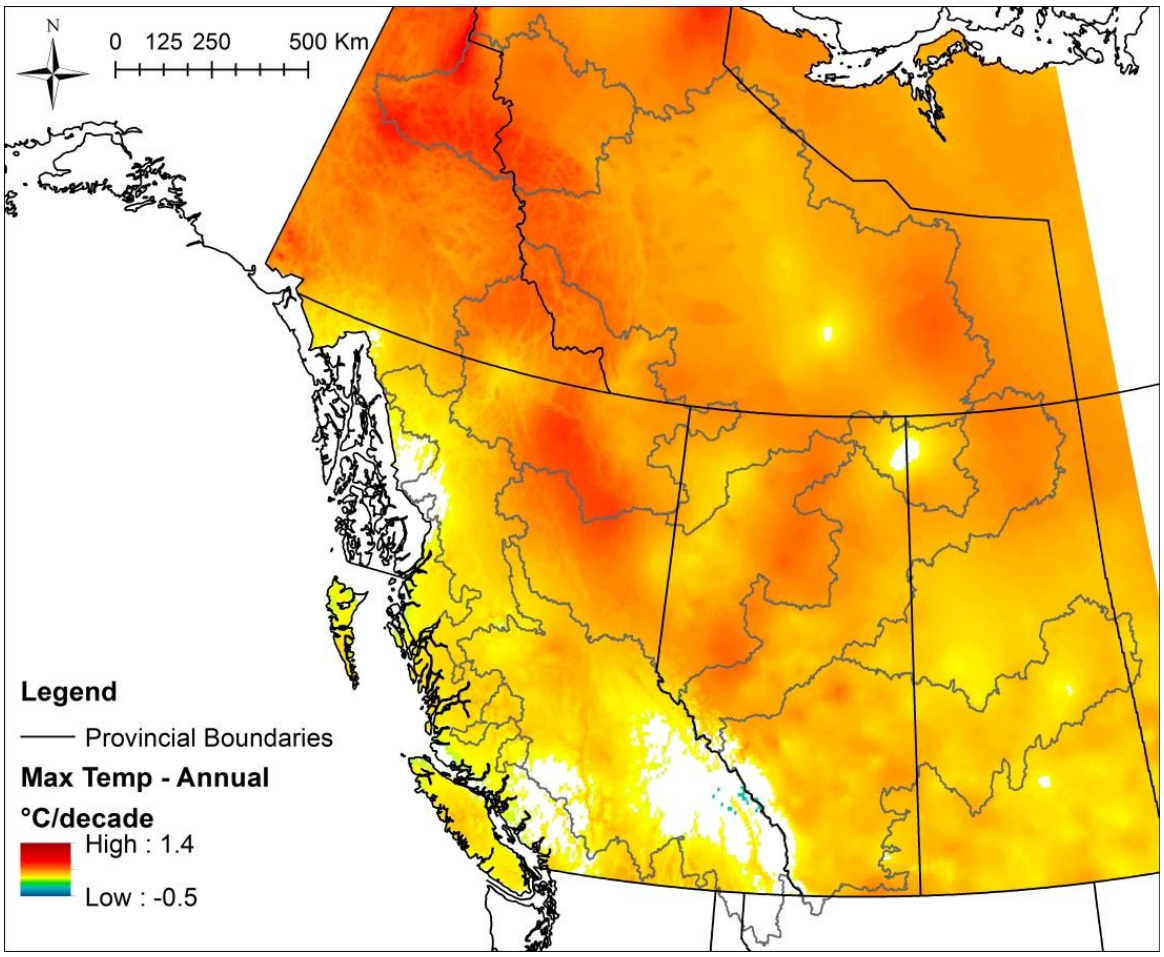

Figure A.3. Annual Tmax trends, in ^{o}C/decade. 1950-2010.

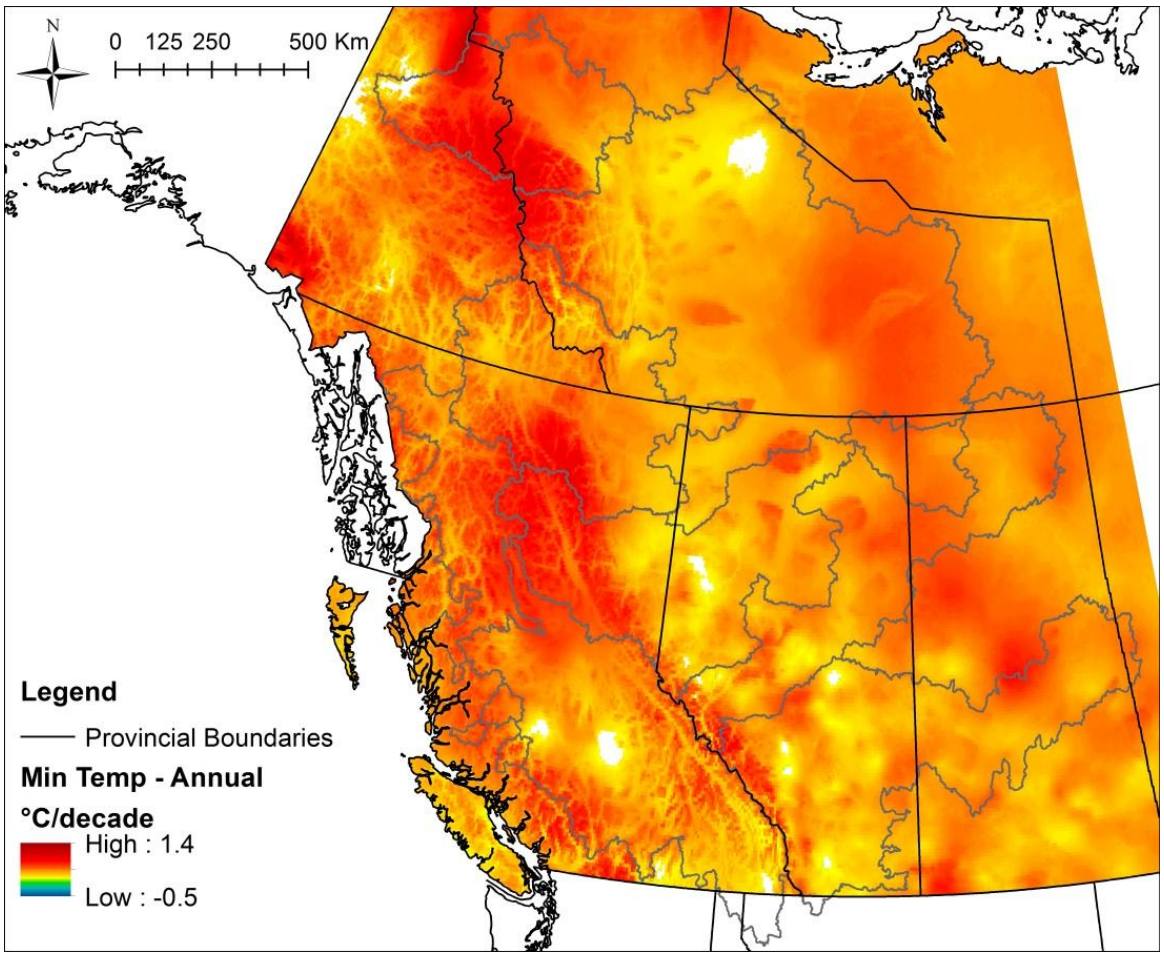

Figure A.4. Annual Tmin trends, in ^{o}C/decade. 1950-2010.

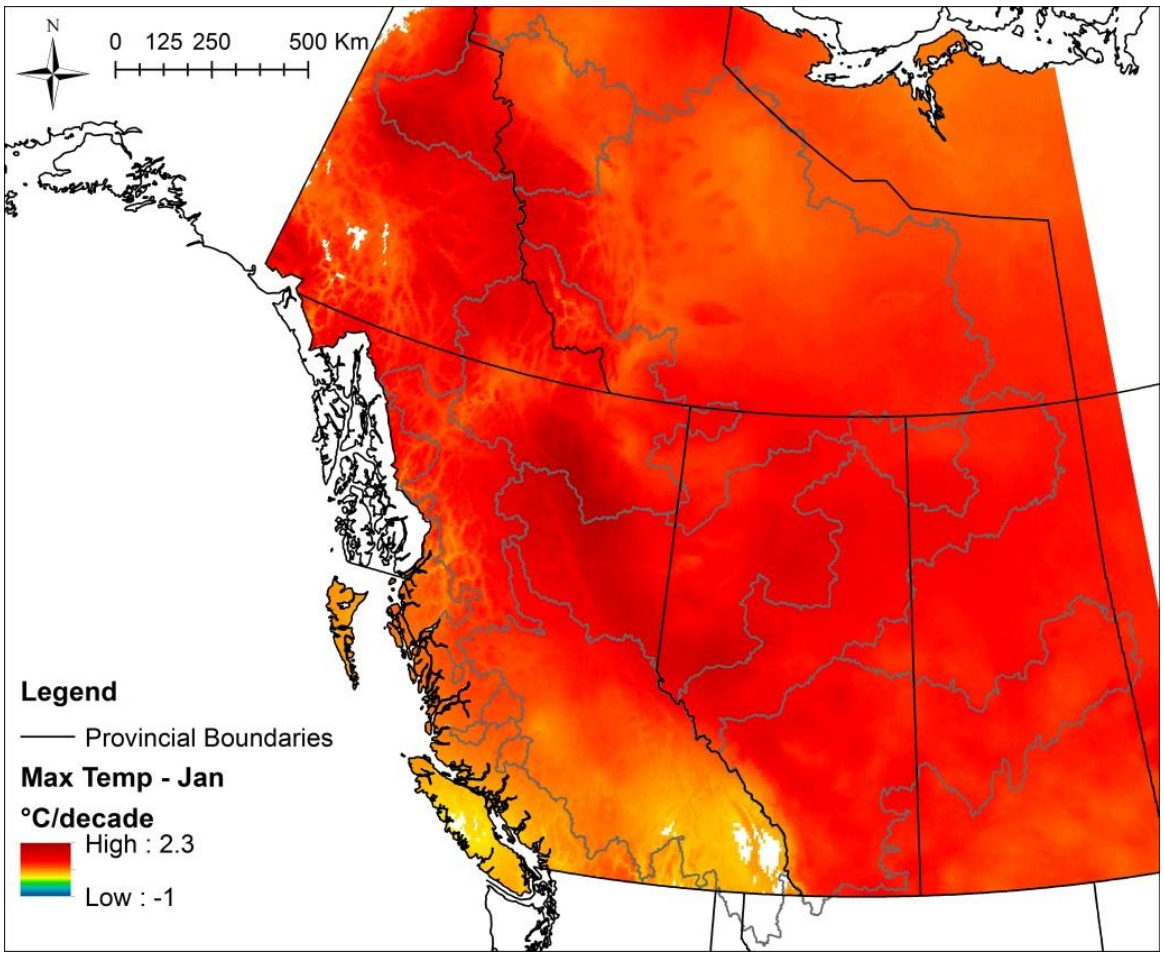

Figure A.5. January Tmax trends in ^{o}C/decade, 1950-2010.

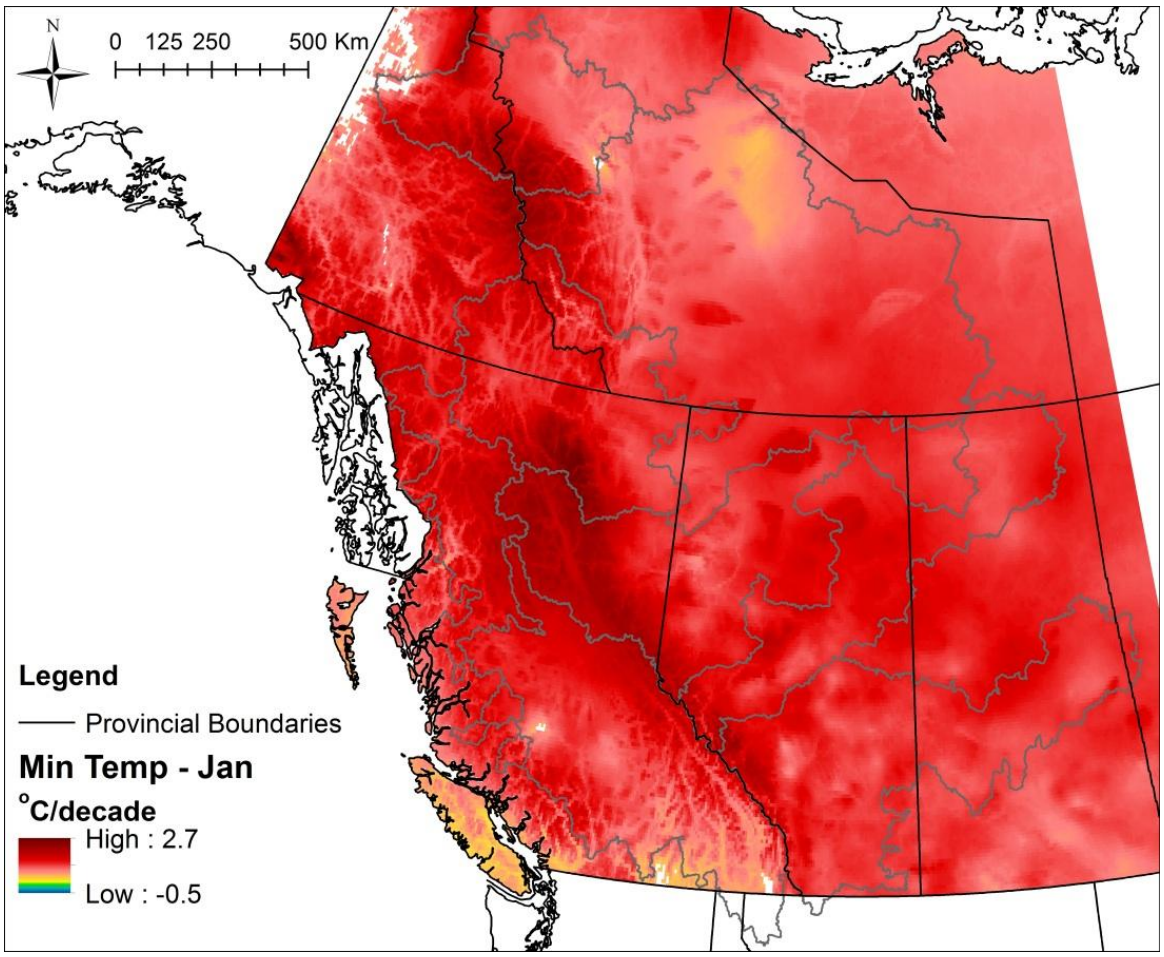

Figure A.6. January Tmin trends in ^{o}C/decade, 1950-2010.

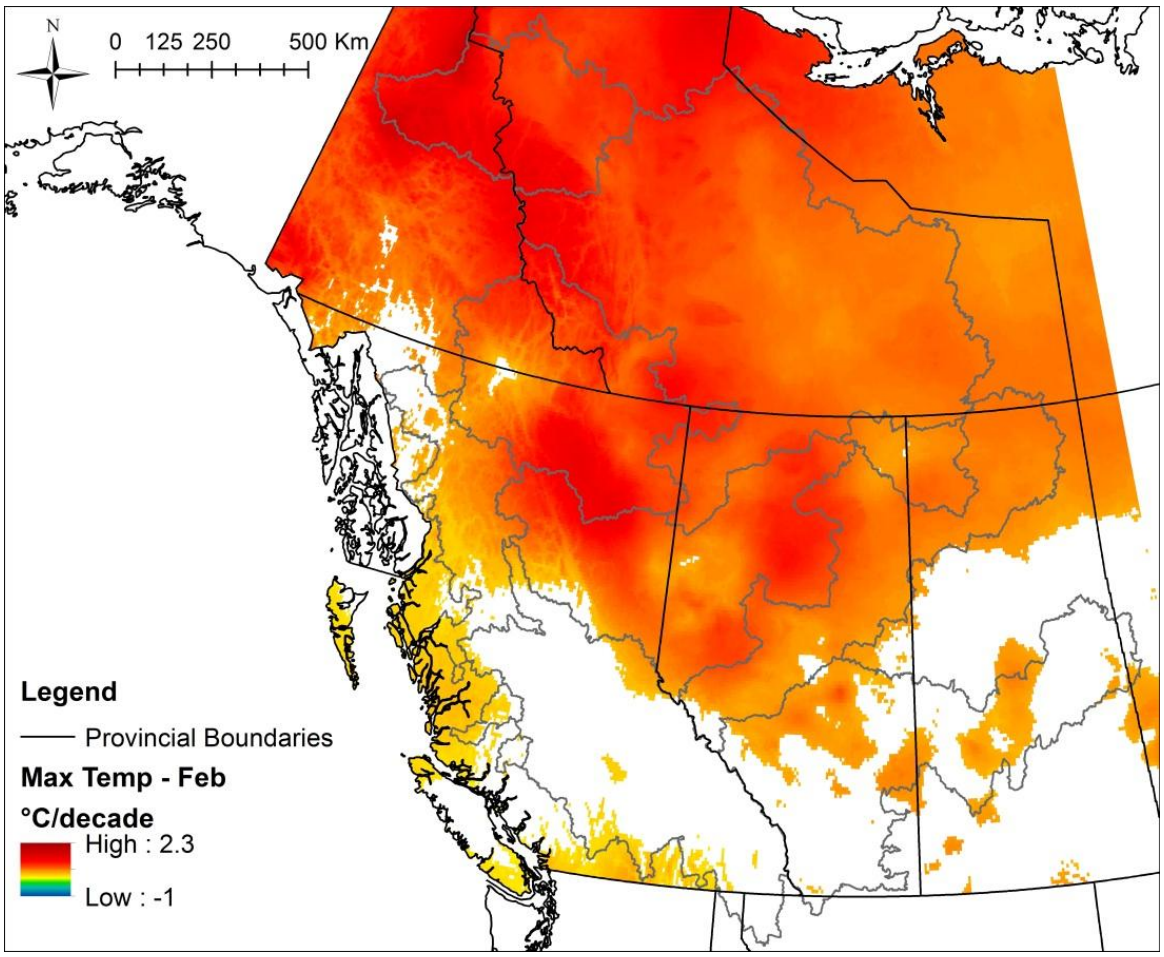

Figure A.7. February Tmax trends in ^{o}C/decade, 1950-2010.

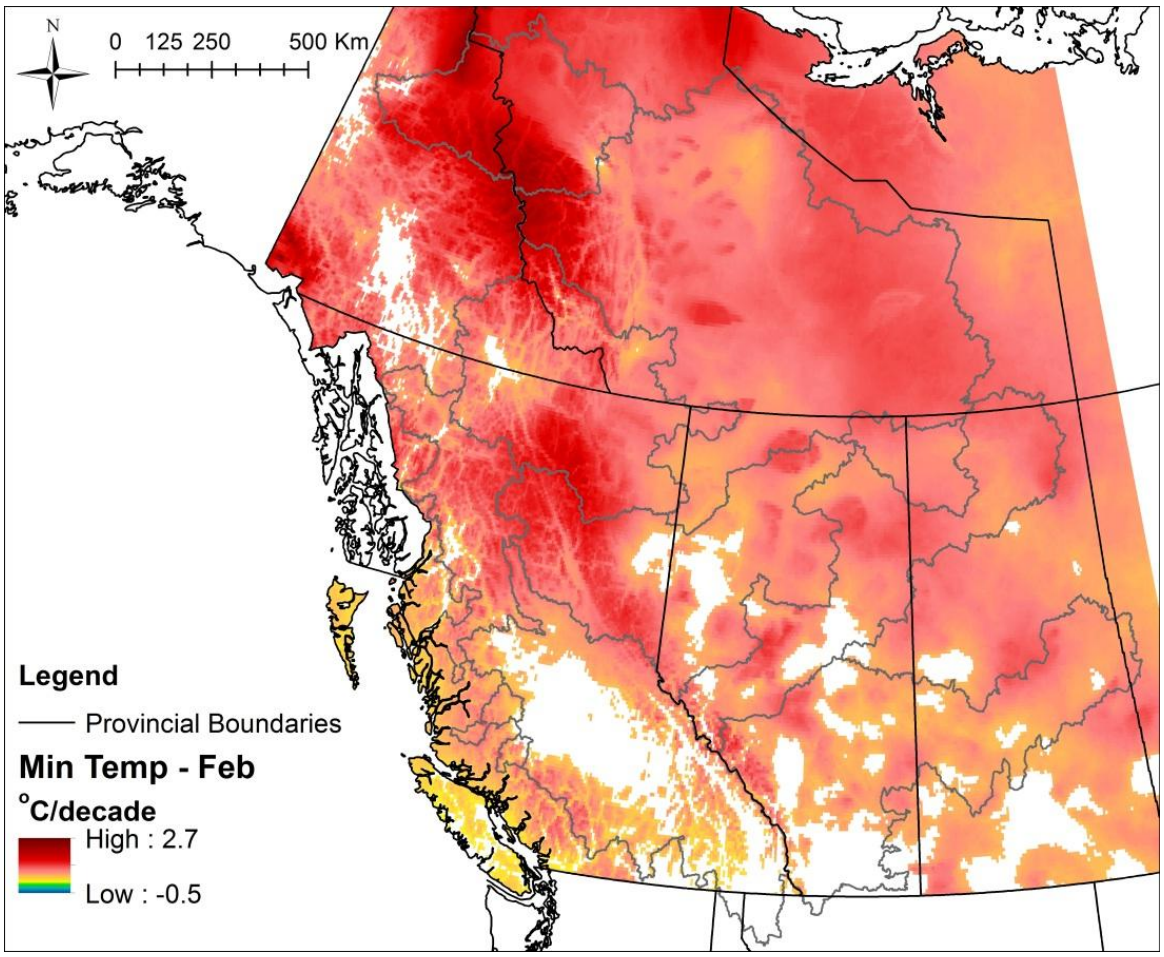

Figure A.8. February Tmin trends in ^{o}C/decade, 1950-2010.

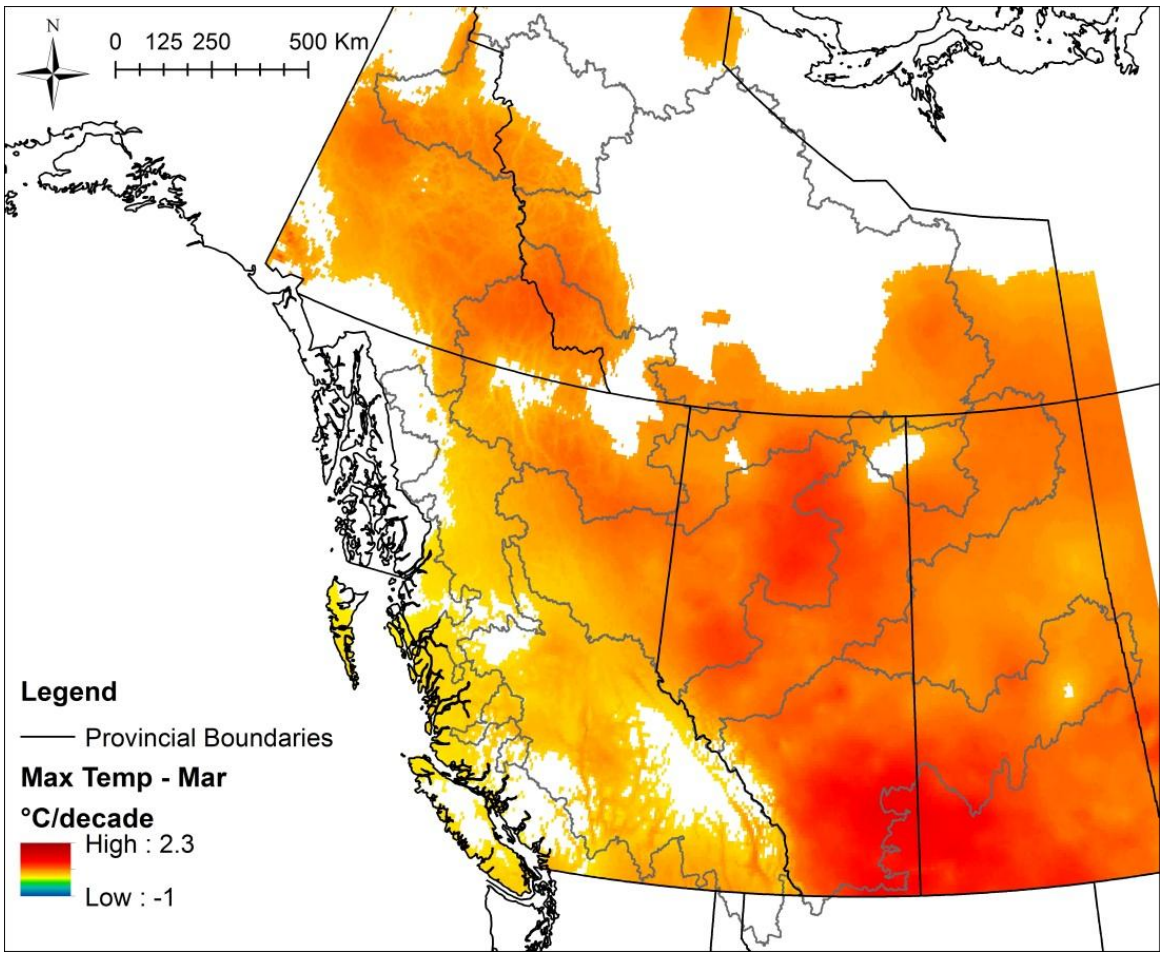

Figure A.9. March Tmax trends in ^{o}C/decade, 1950-2010.

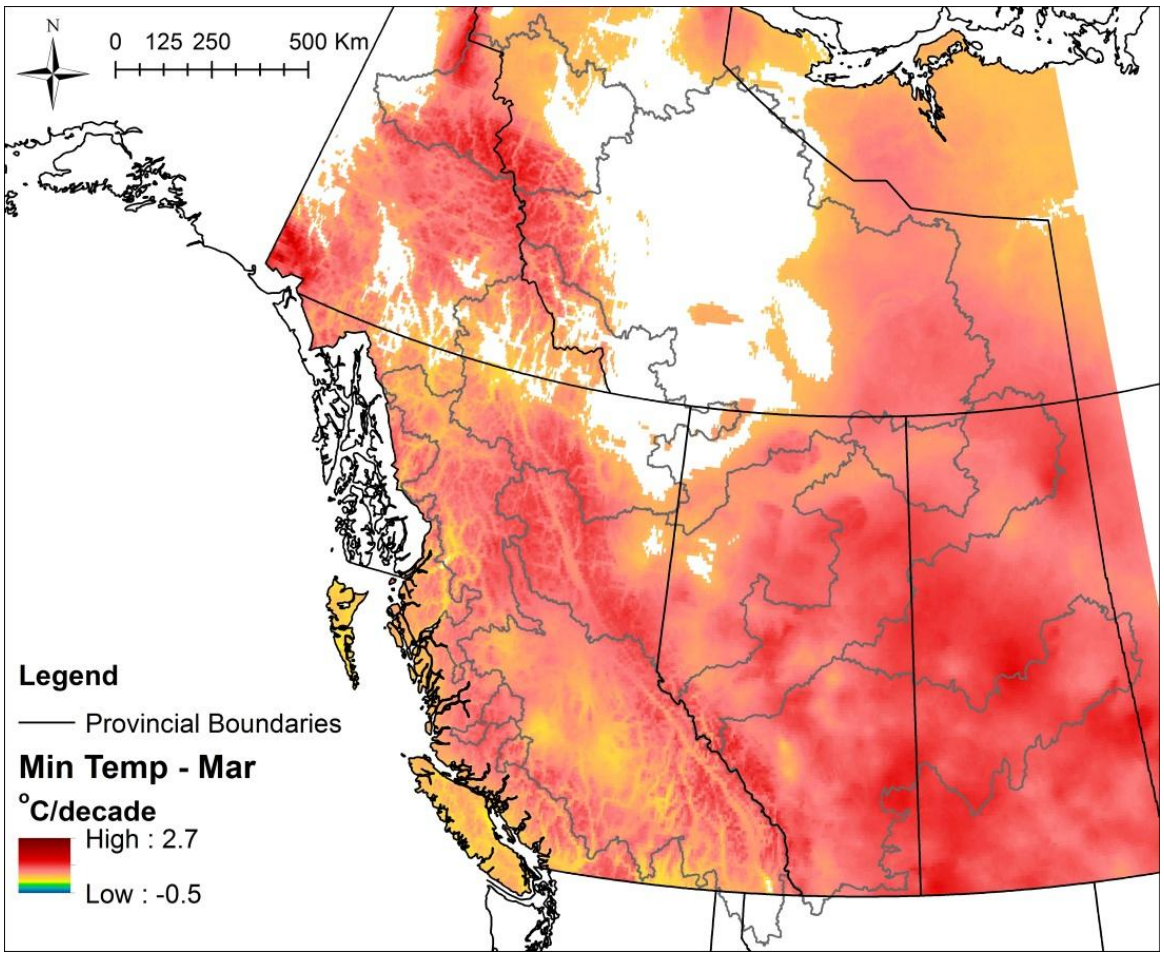

Figure A.10. March Tmin trends in ^{o}C/decade, 1950-2010.

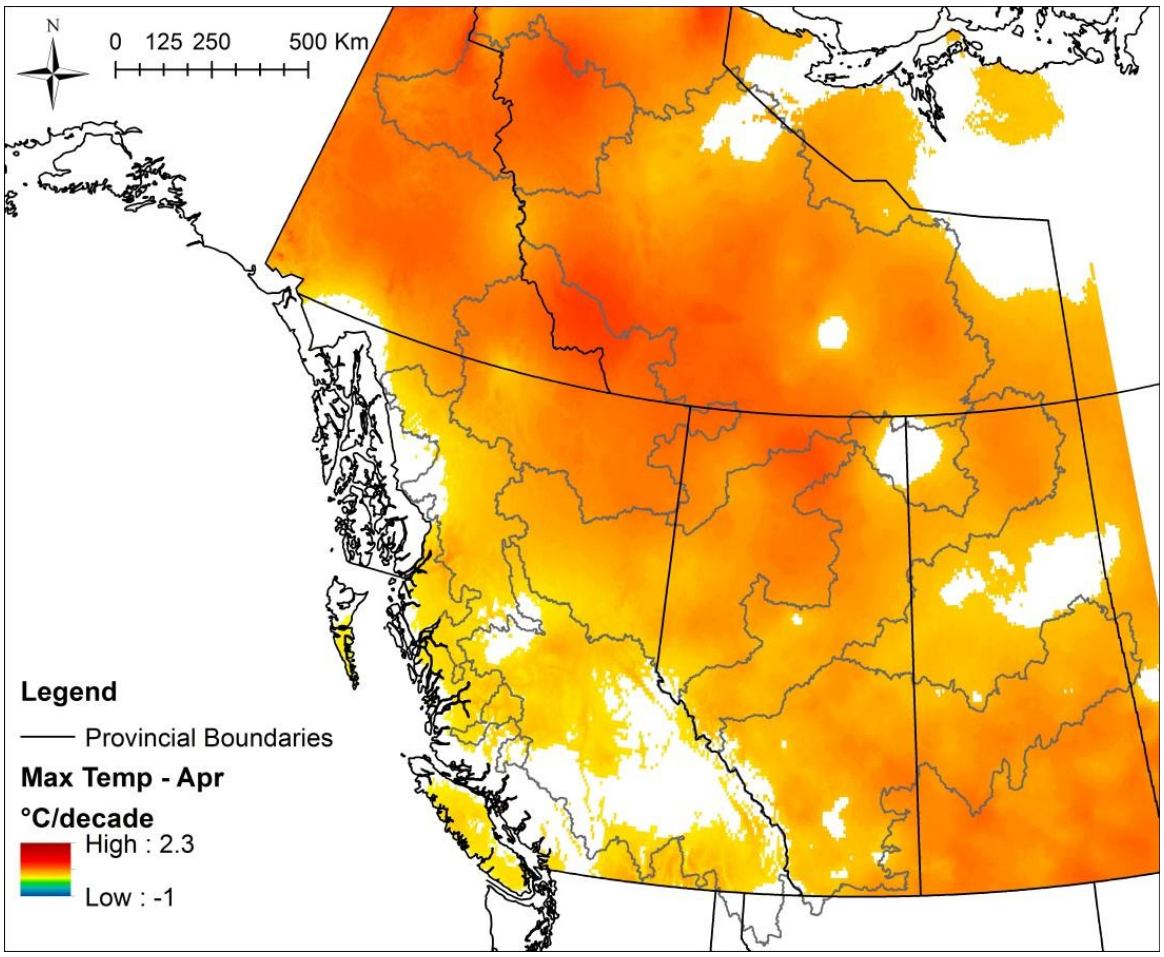

Figure A.11. April Tmax trends in ^{o}C/decade, 1950-2010.

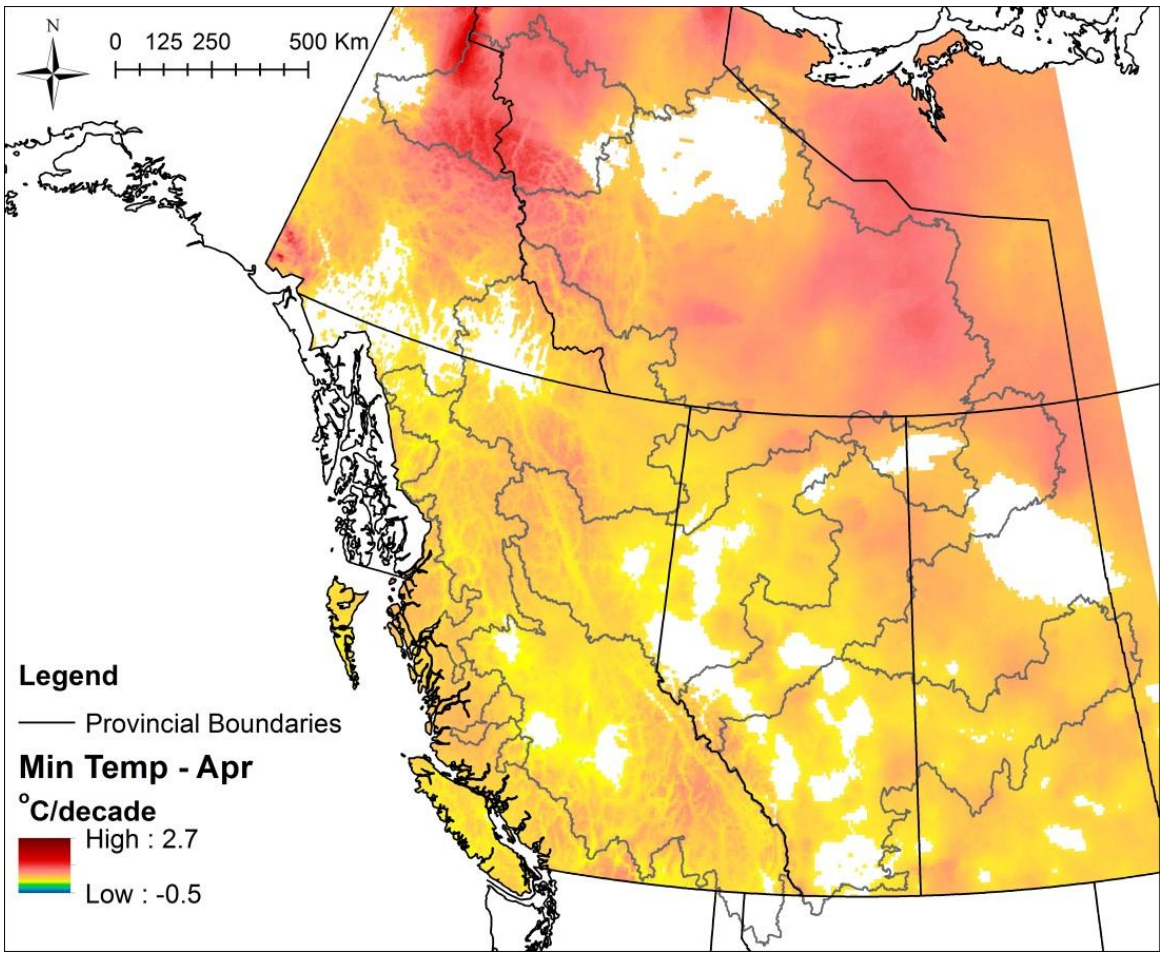

Figure A.12. April Tmin trends in ^{o}C/decade, 1950-2010.

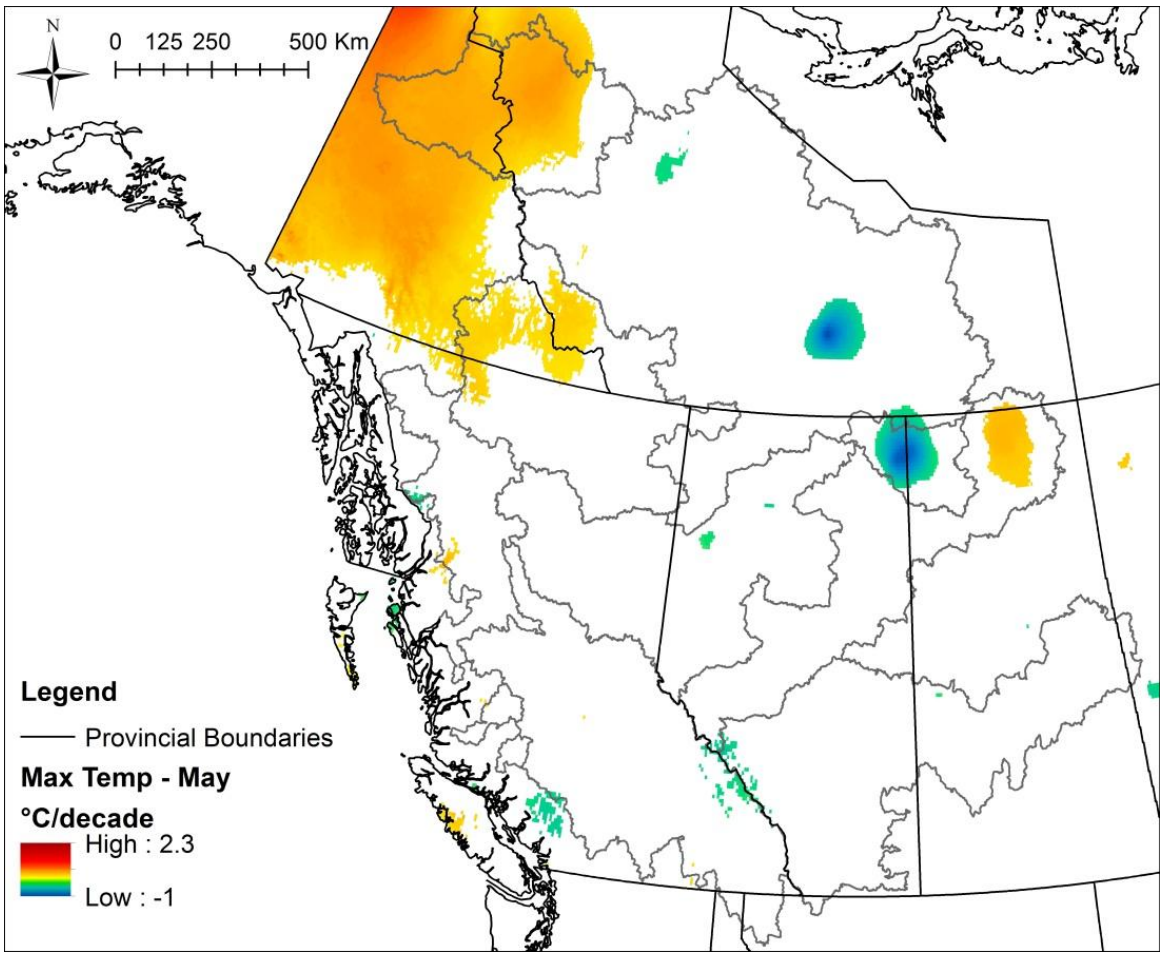

Figure A.13. May Tmax trends in ^{o}C/decade, 1950-2010.

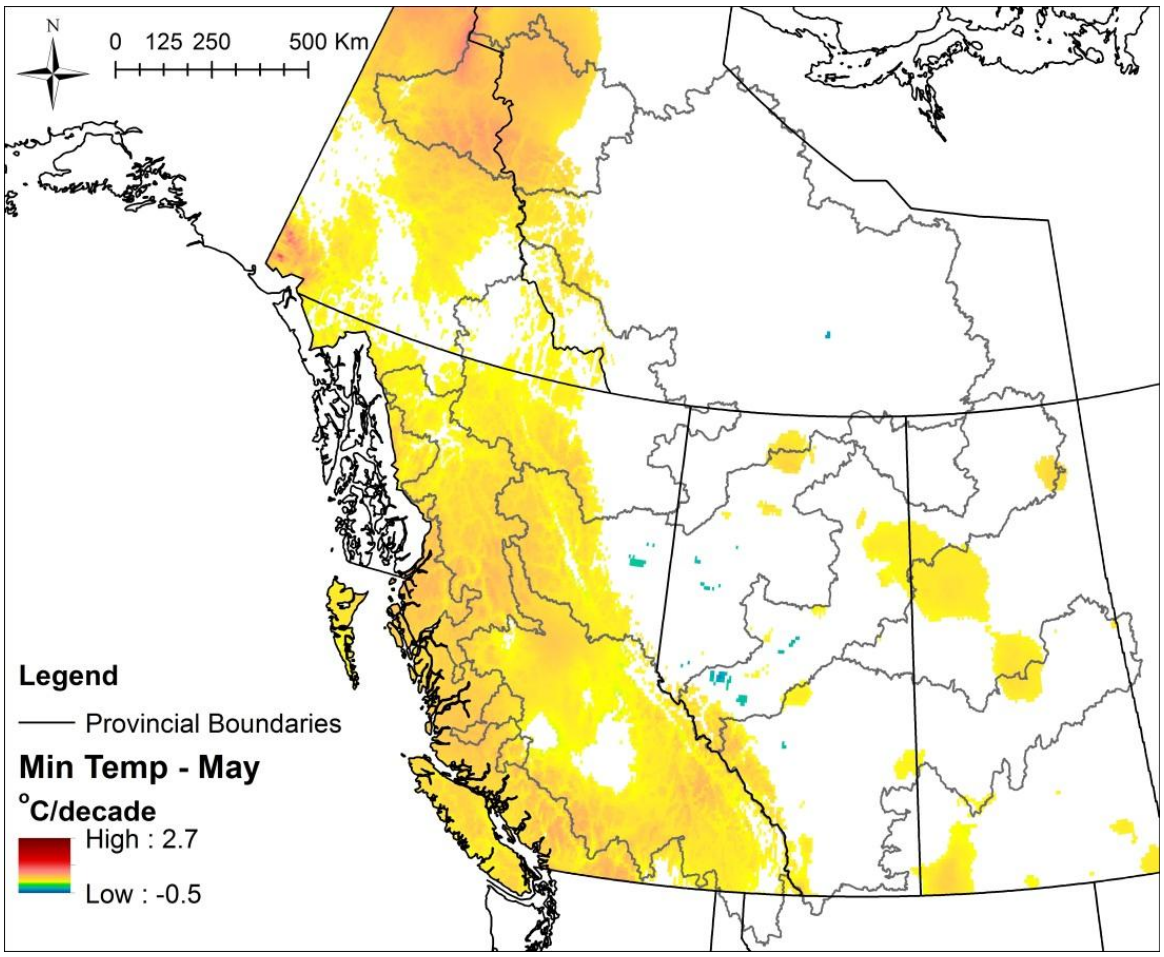

Figure A.14. May Tmin trends in ^{o}C/decade, 1950-2010.

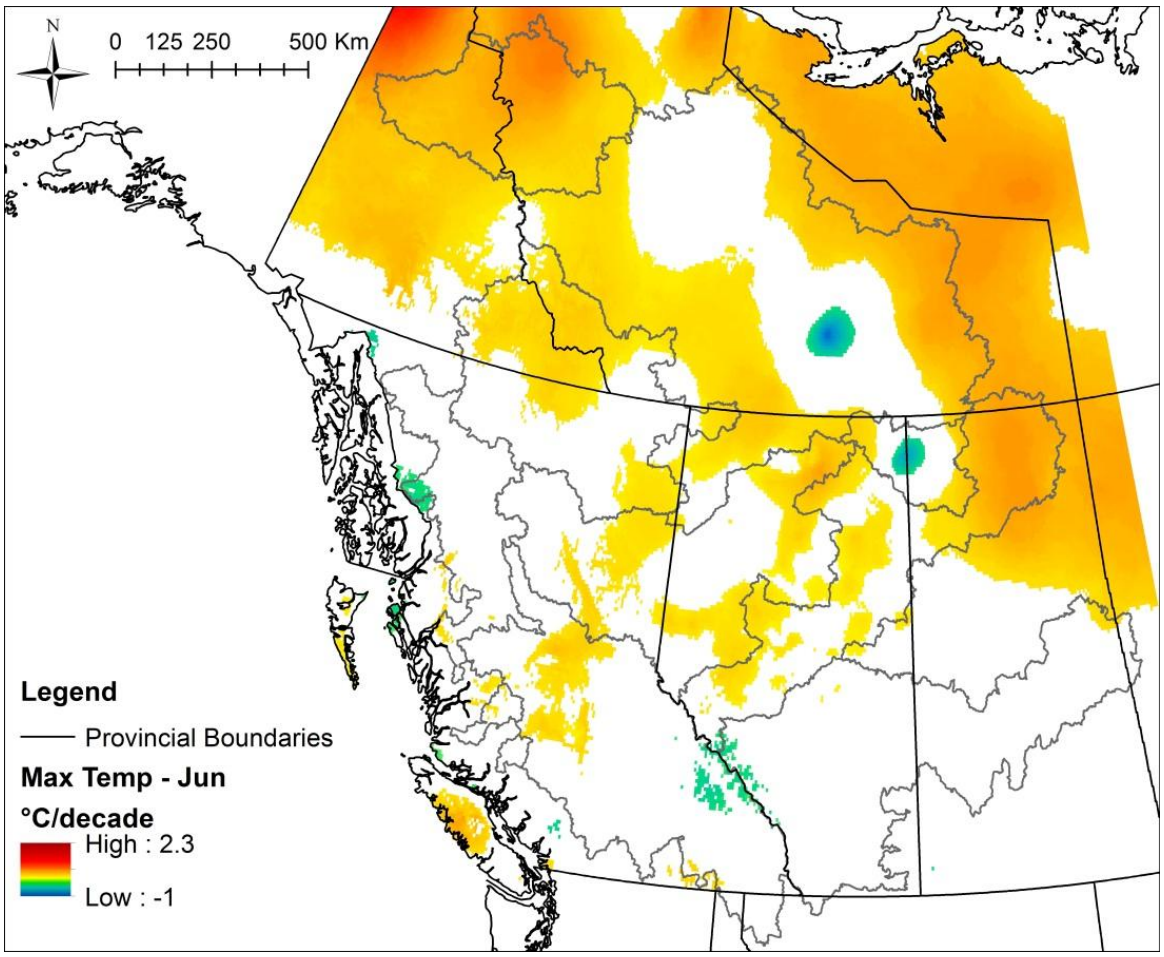

Figure A.15. June Tmax trends in ^{o}C/decade, 1950-2010.

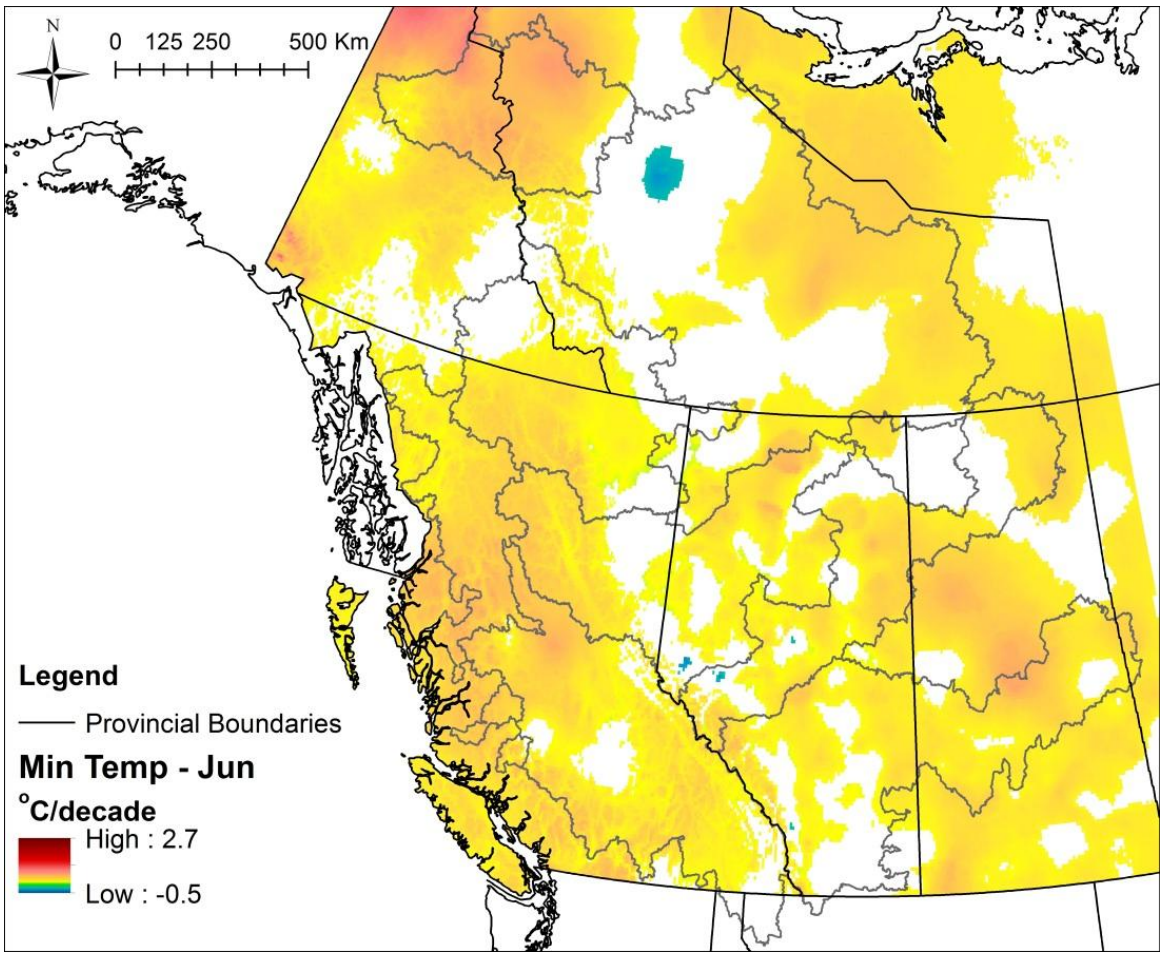

Figure A.16. June Tmin trends in ^{o}C/decade, 1950-2010.

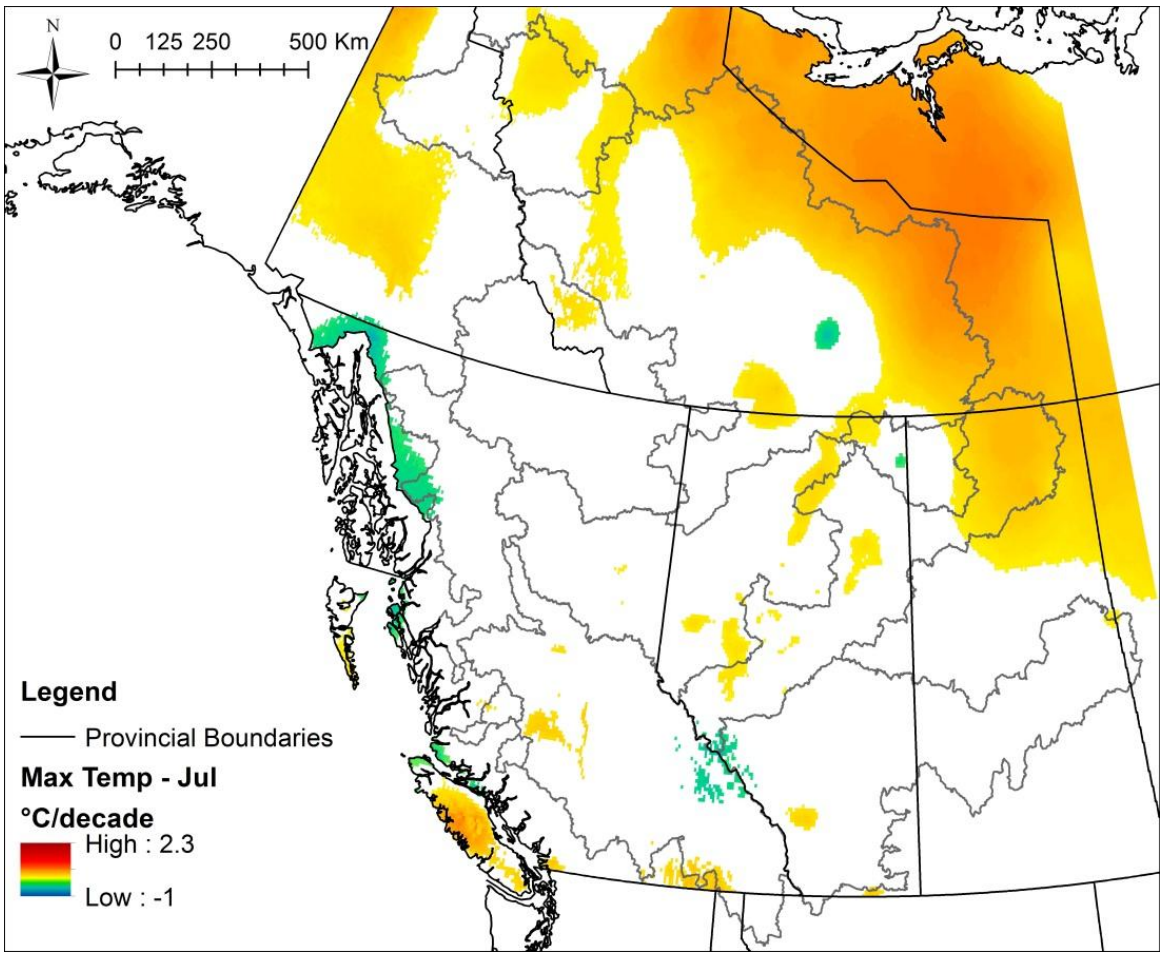

Figure A.17. July Tmax trends in ^{o}C/decade, 1950-2010.

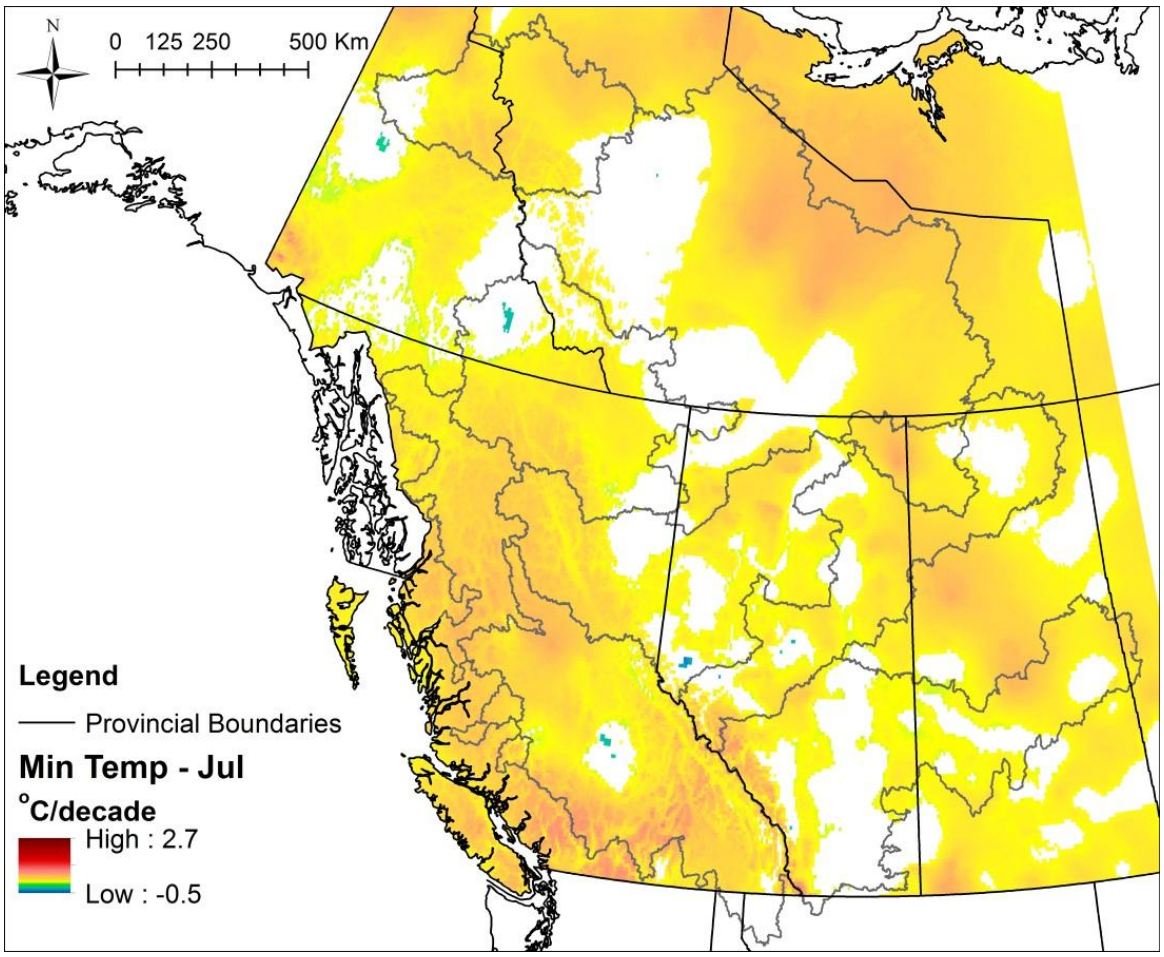

Figure A.18. July Tmin trends in ^{o}C/decade, 1950-2010.

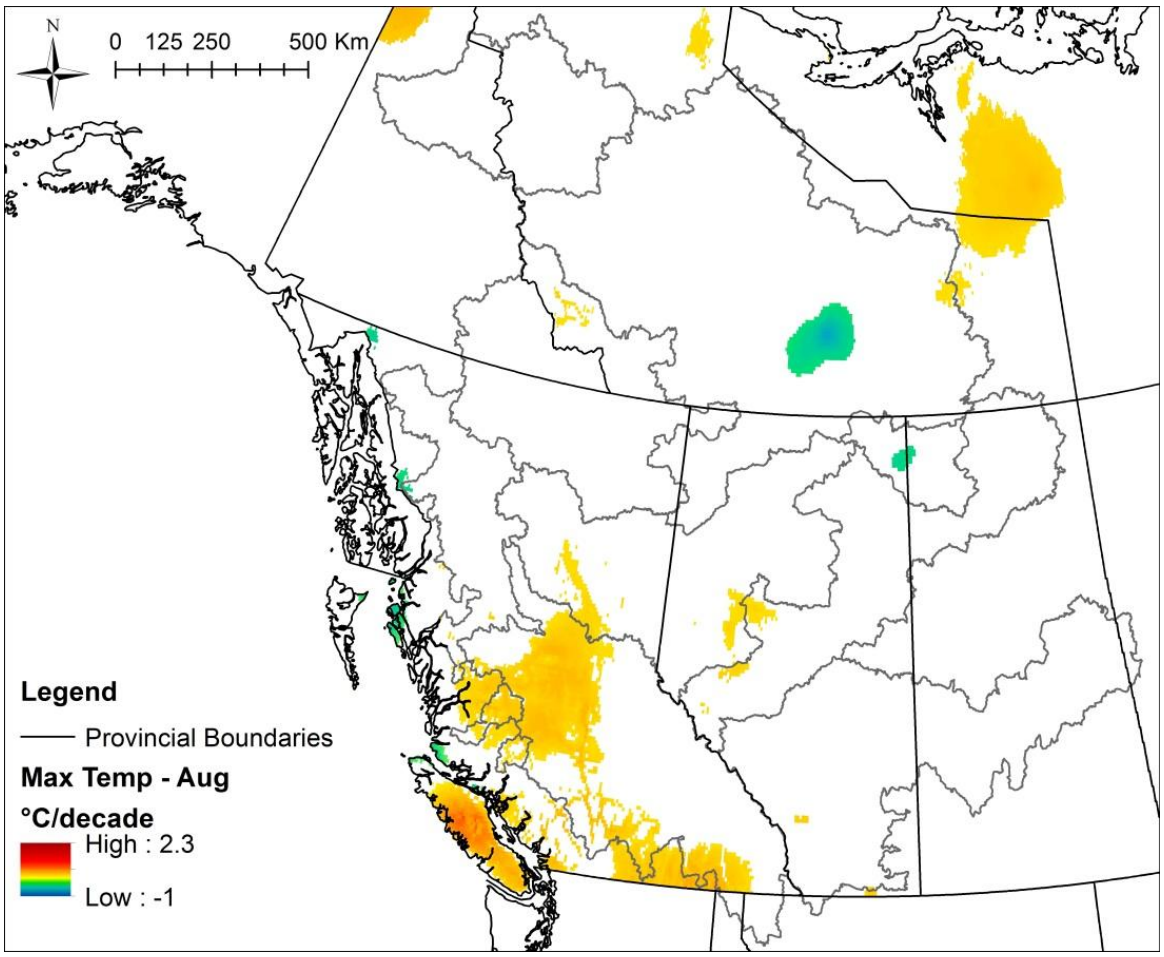

Figure A.19. August Tmax trends in ^{o}C/decade, 1950-2010.

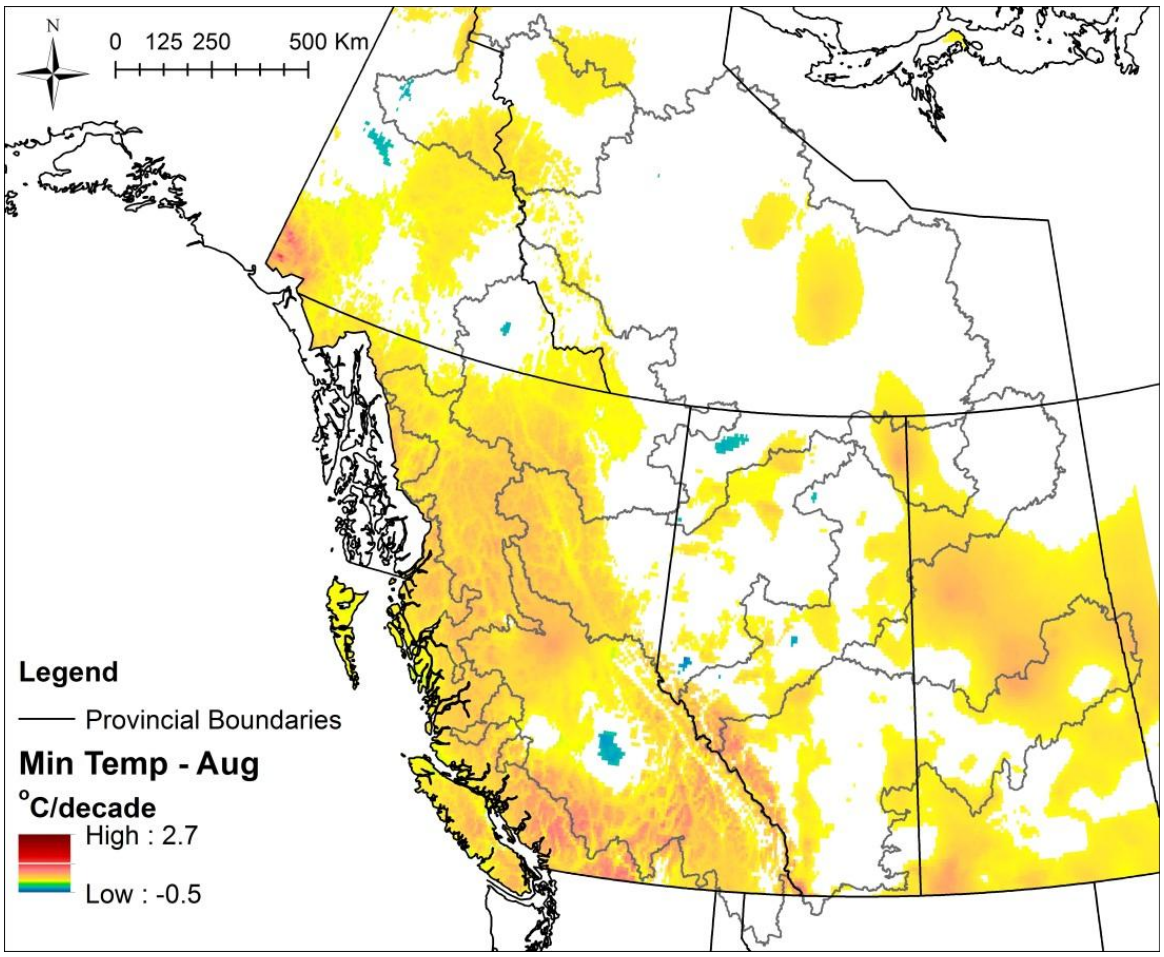

Figure A.20. August Tmin trends in ^{o}C/decade, 1950-2010.

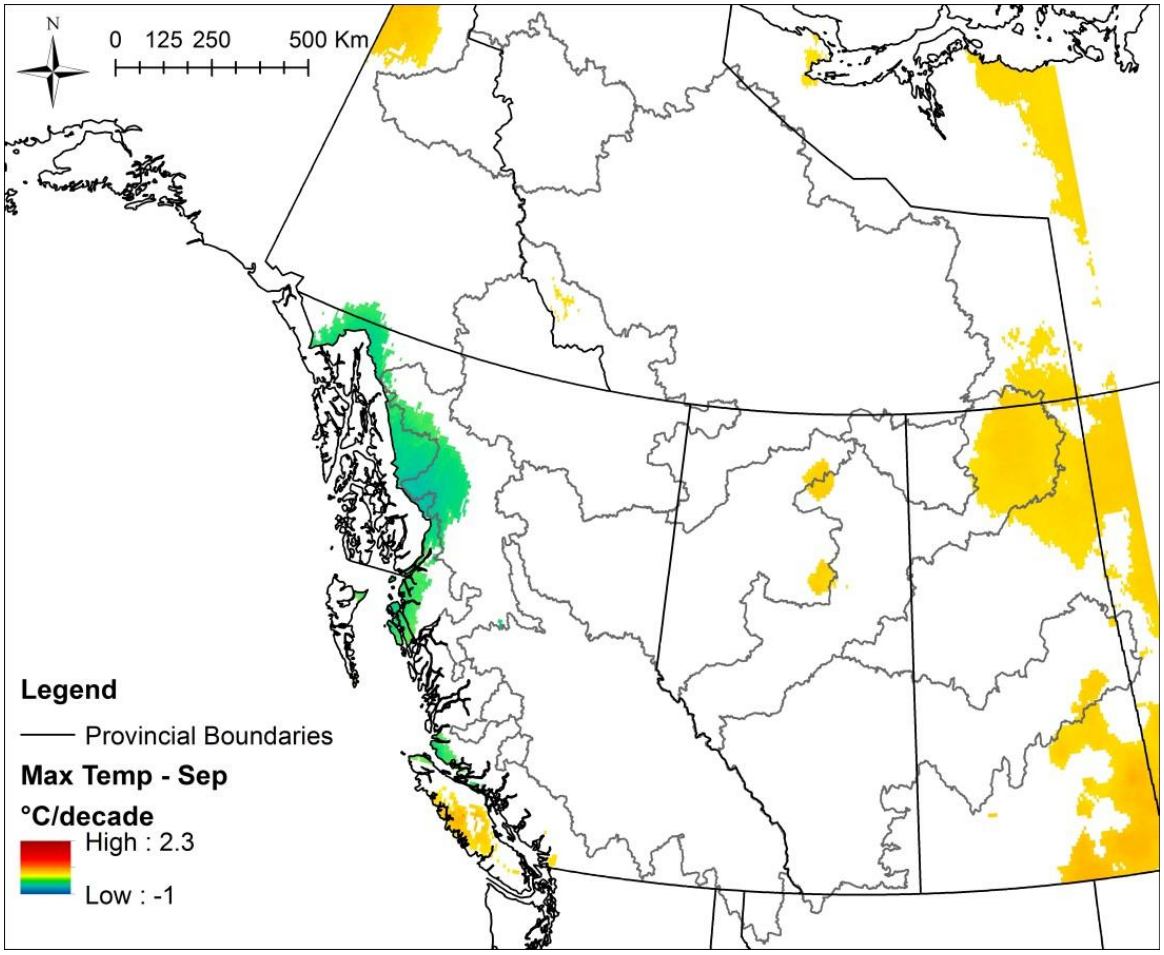

Figure A.21. September Tmax trends in ^{o}C/decade, 1950-2010.

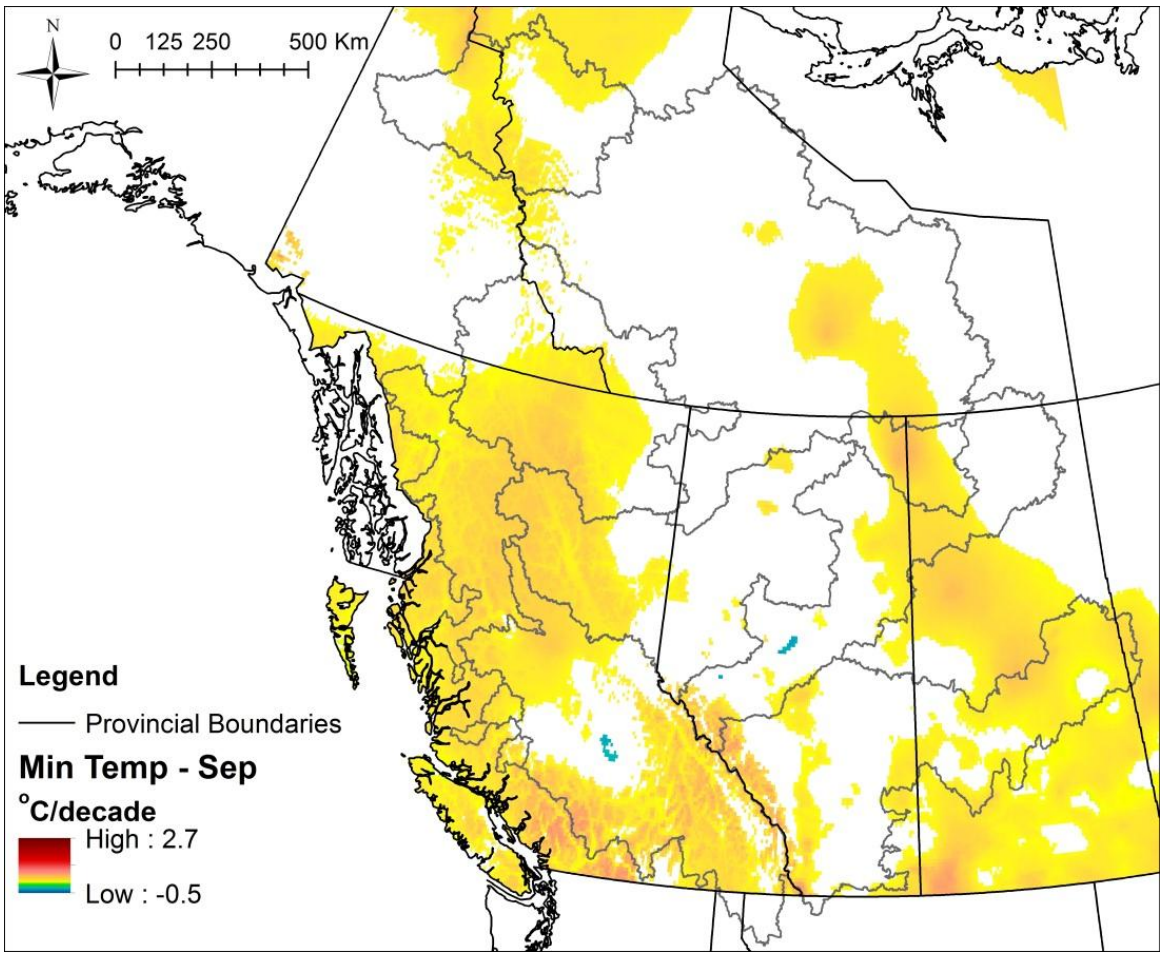

Figure A.22. September Tmin trends in ^{o}C/decade, 1950-2010.

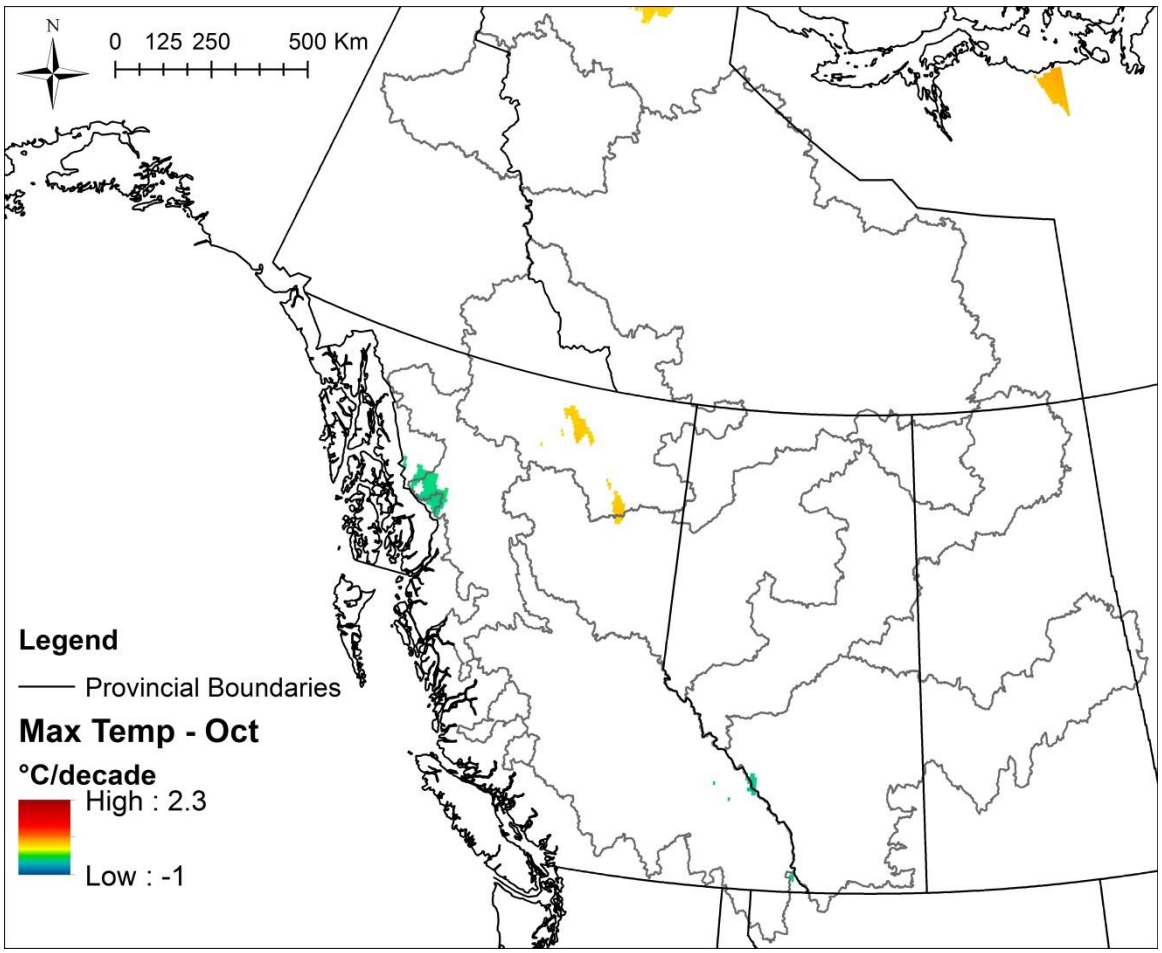

Figure A.23. October Tmax trends in ^{o}C/decade, 1950-2010.

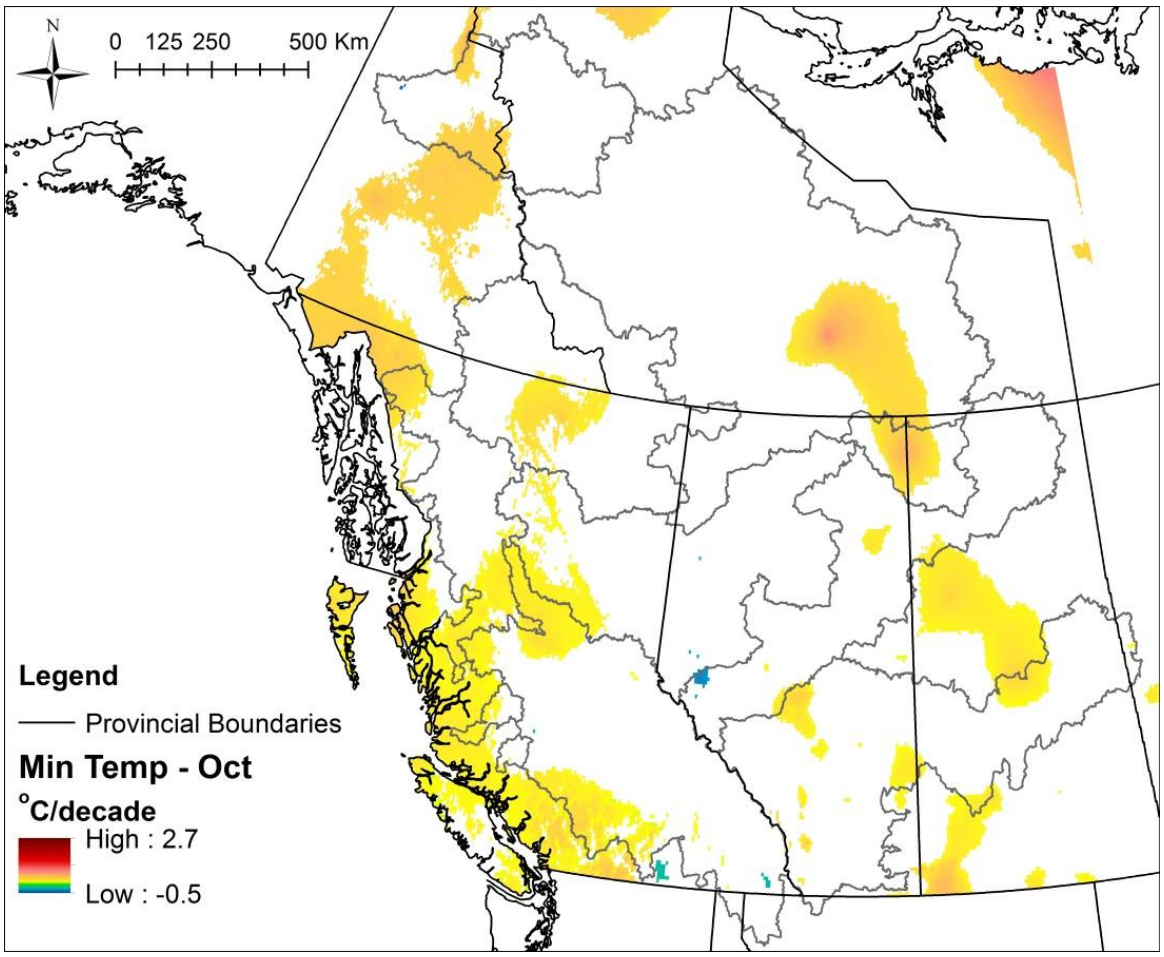

Figure A.24. October Tmin trends in ^{o}C/decade, 1950-2010.

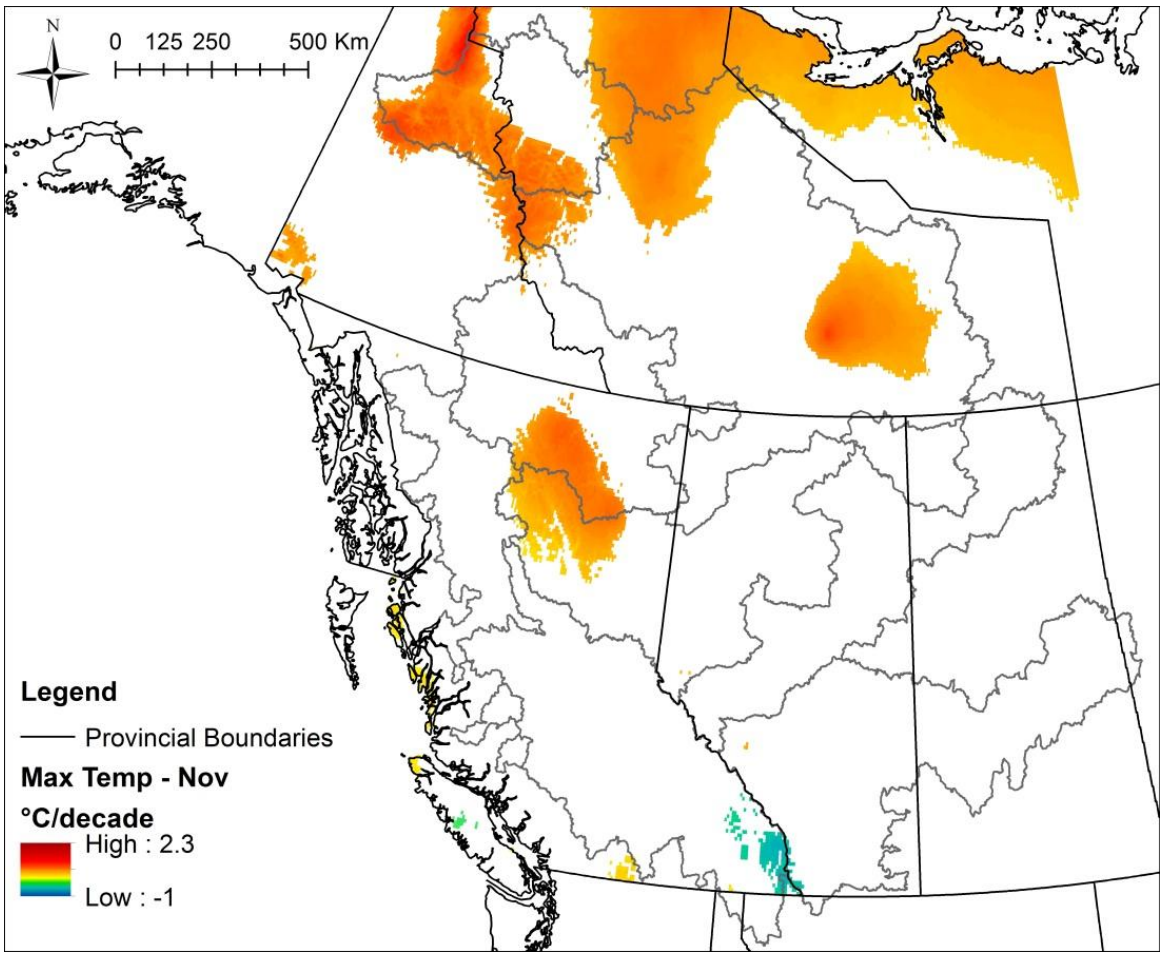

Figure A.25. November Tmax trends in ^{o}C/decade, 1950-2010.

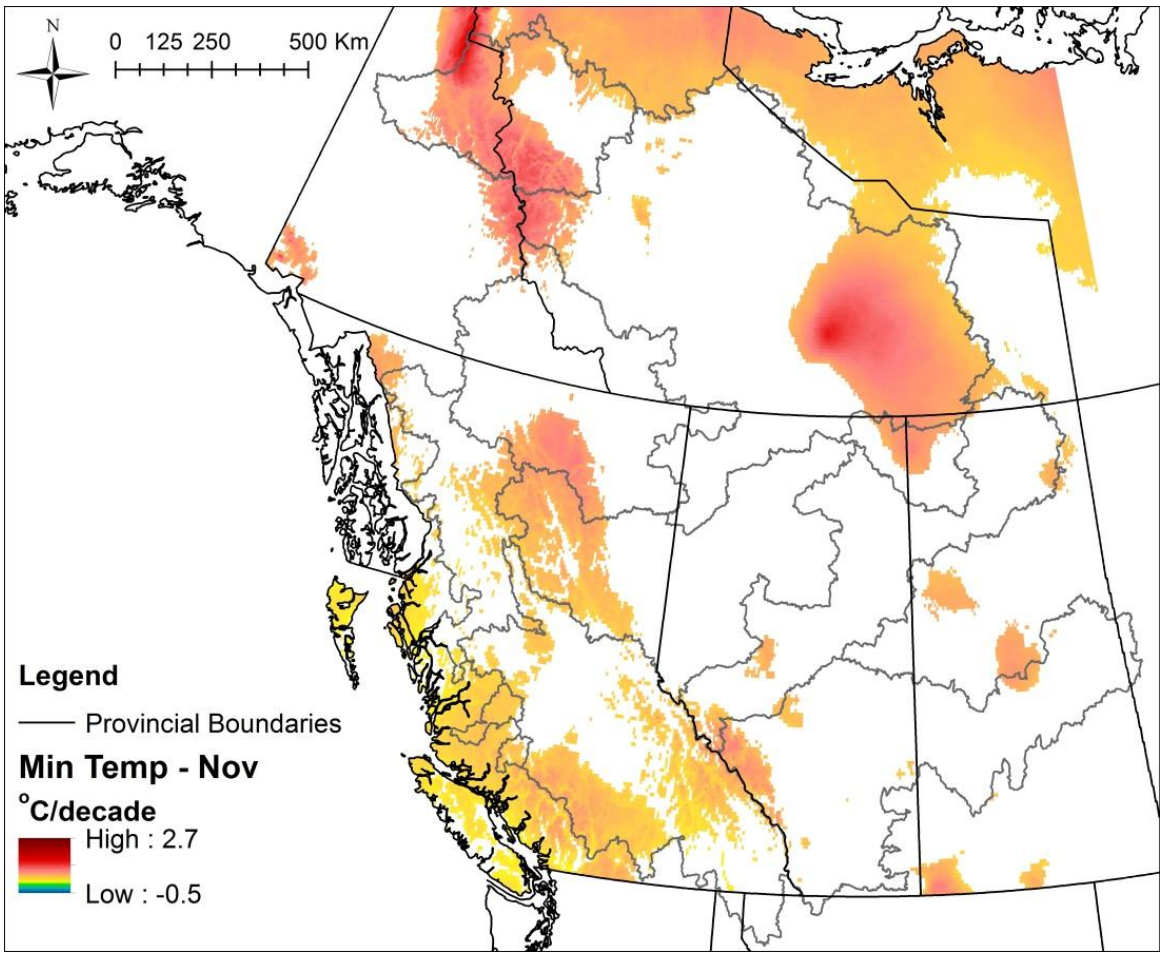

Figure A.26. November Tmin trends in ^{o}C/decade, 1950-2010.

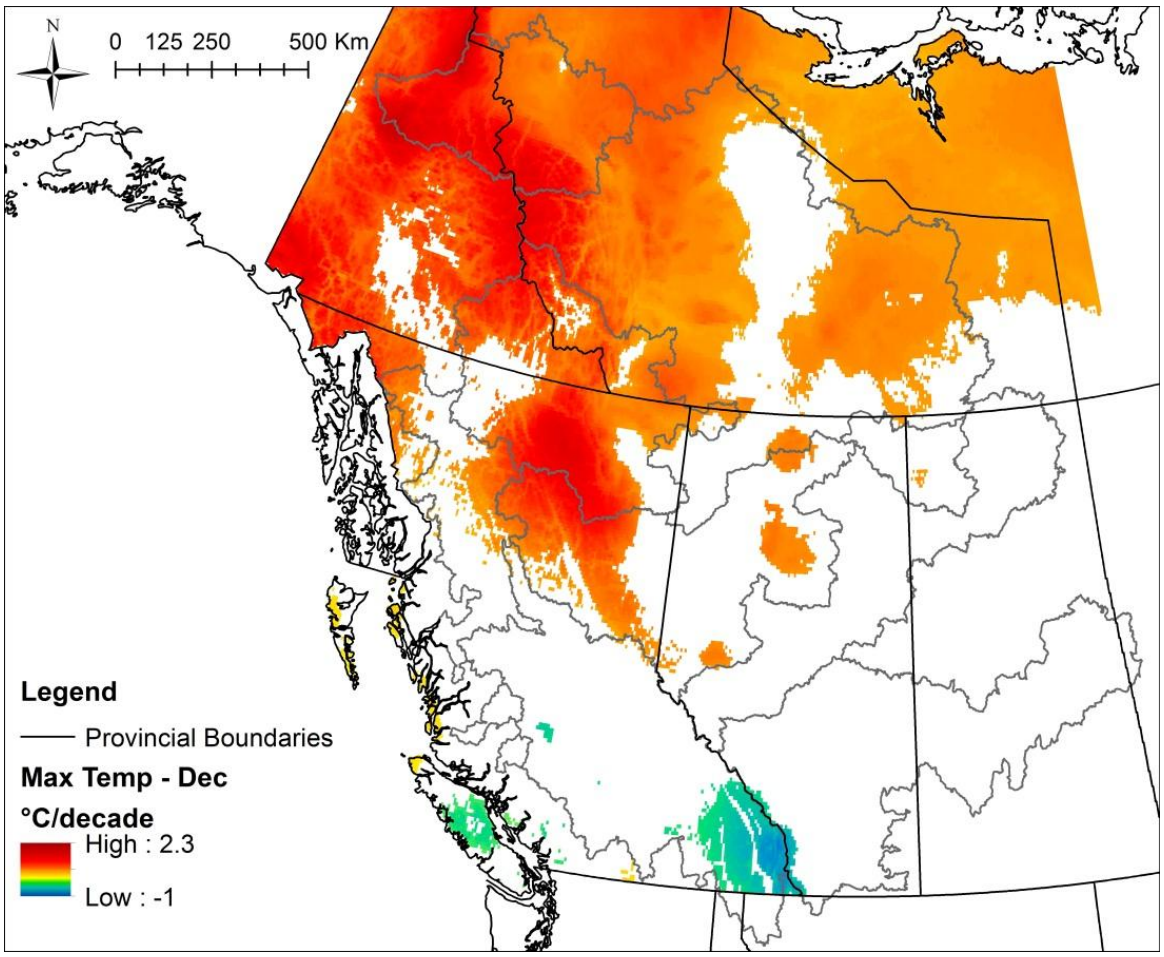

Figure A.27. December Tmax trends in ^{o}C/decade, 1950-2010.

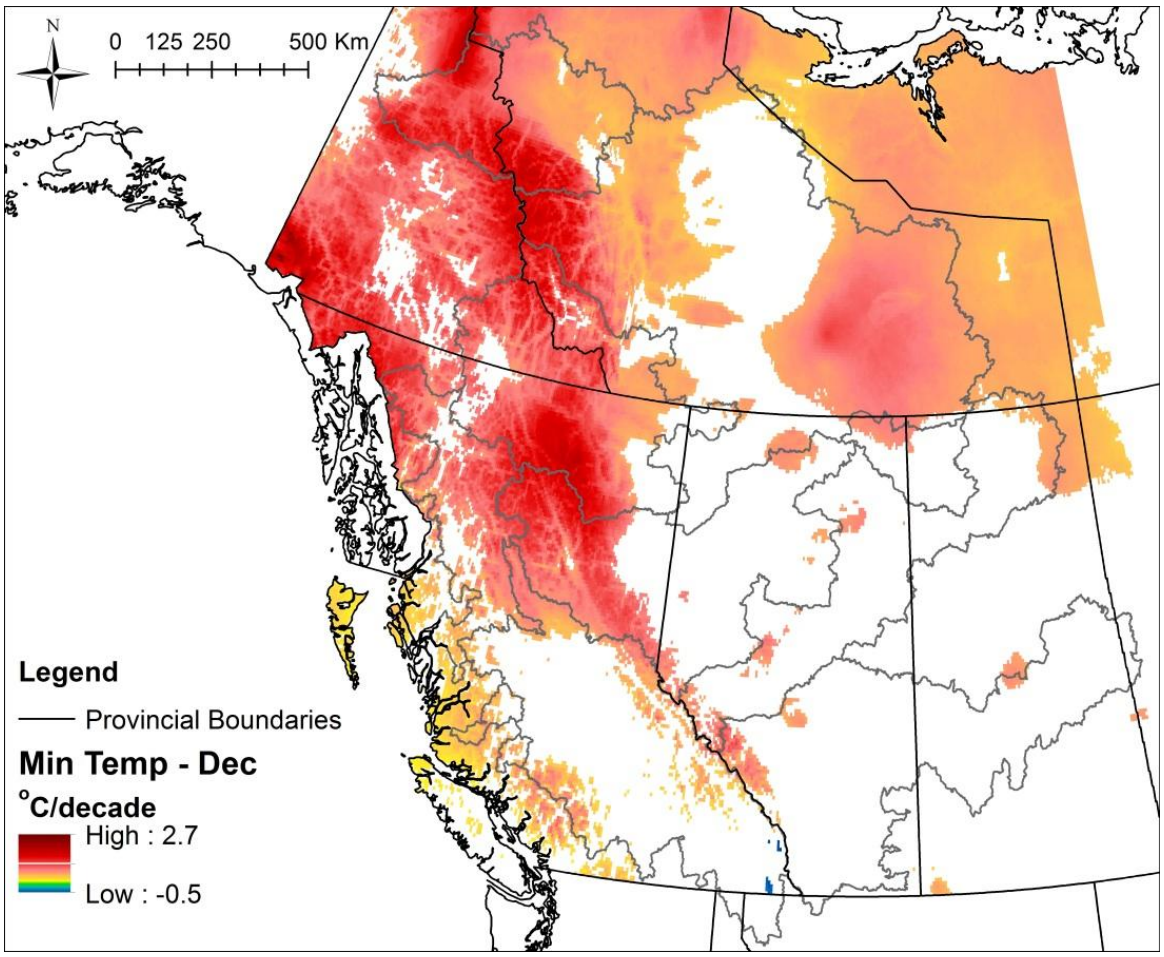

Figure A.28. December Tmin trends in ^{o}C/decade, 1950-2010.

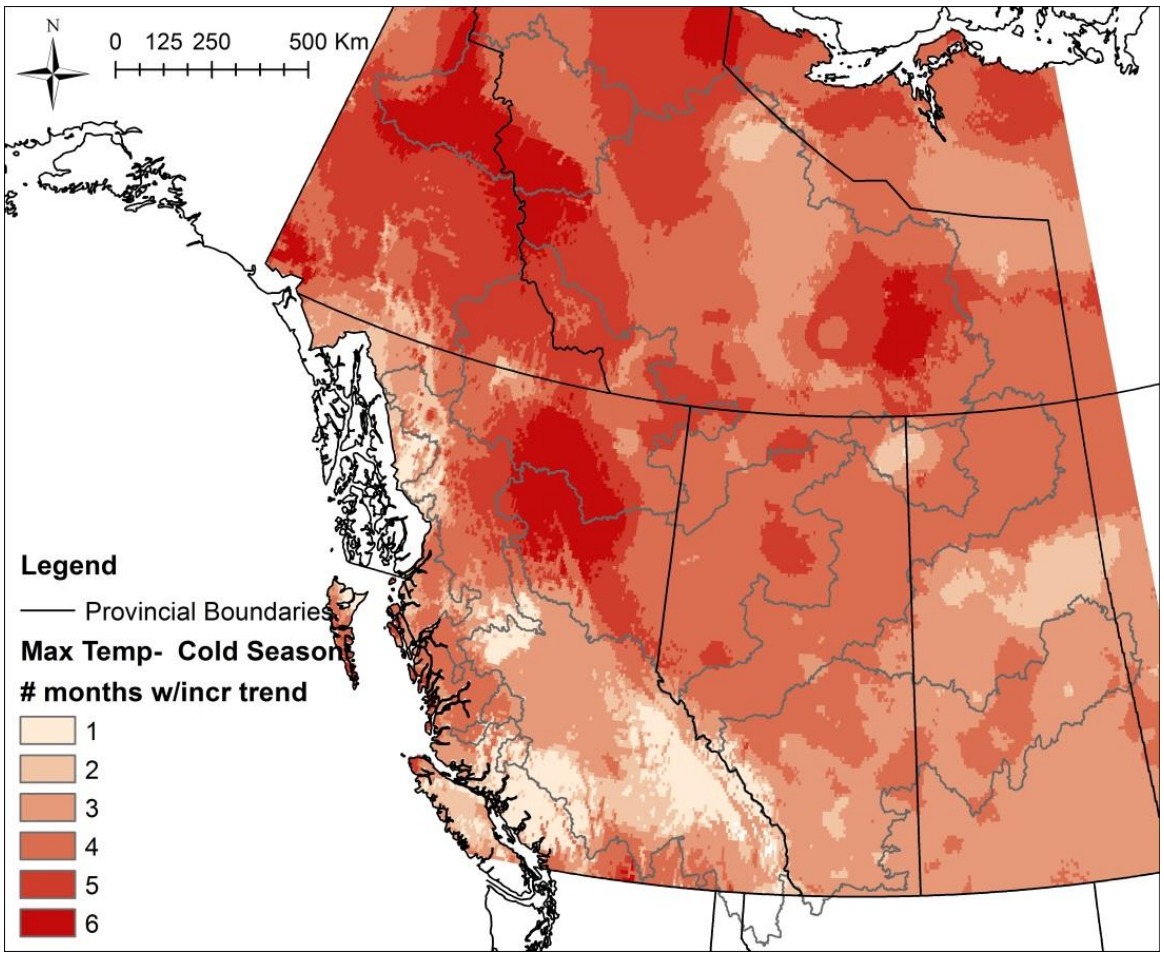

Figure A.29. Tmax increasing trend persistence through the cold season (November to April). Colour corresponds to number of months with increasing trend.

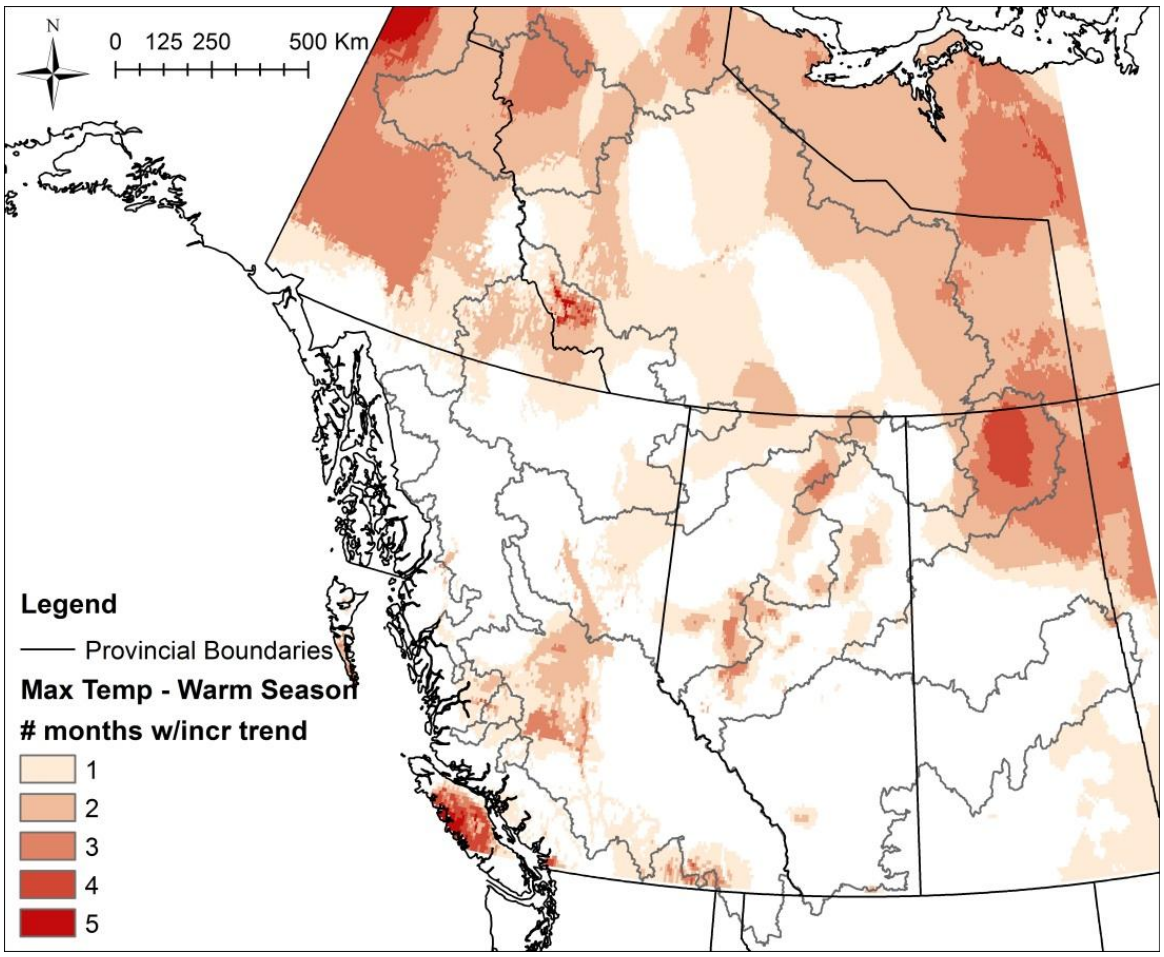

Figure A.30. Tmax increasing trend persistence through the warm season (May to October). Colour corresponds to number of months with increasing trend.

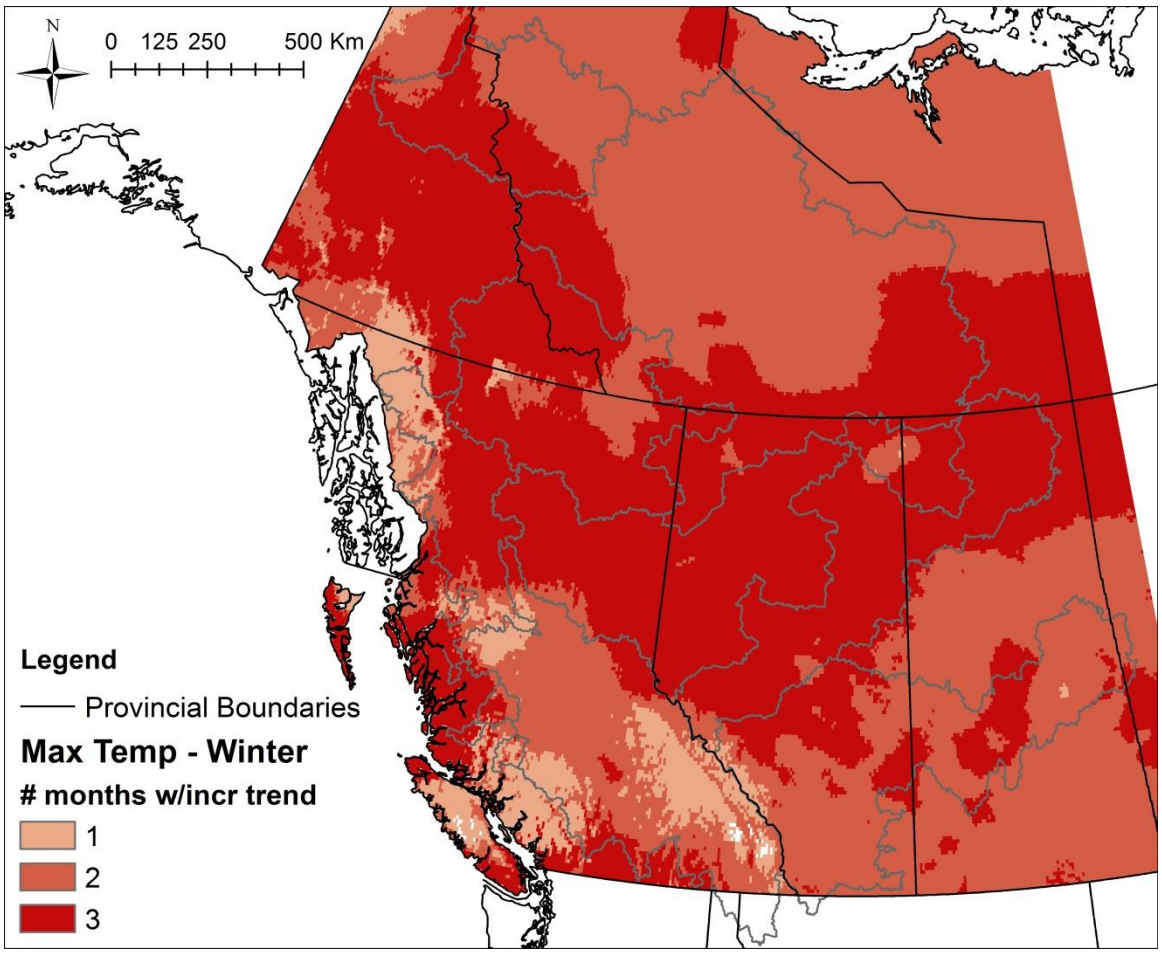

Figure A.31. Tmax increasing trend persistence through winter (January to March). Colour corresponds to number of months with increasing trend.

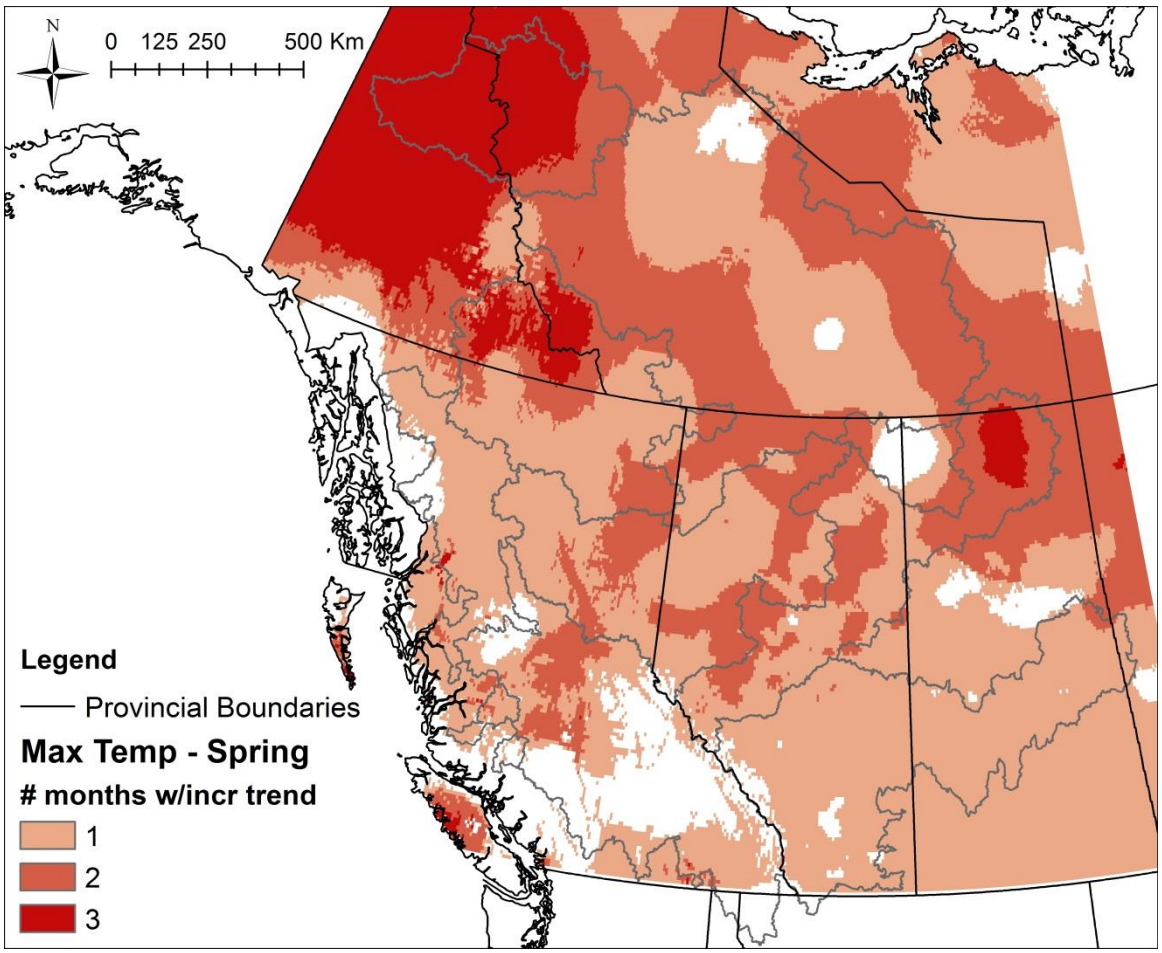

Figure A.32. Tmax increasing trend persistence through spring (April to June). Colour corresponds to number of months with increasing trend.

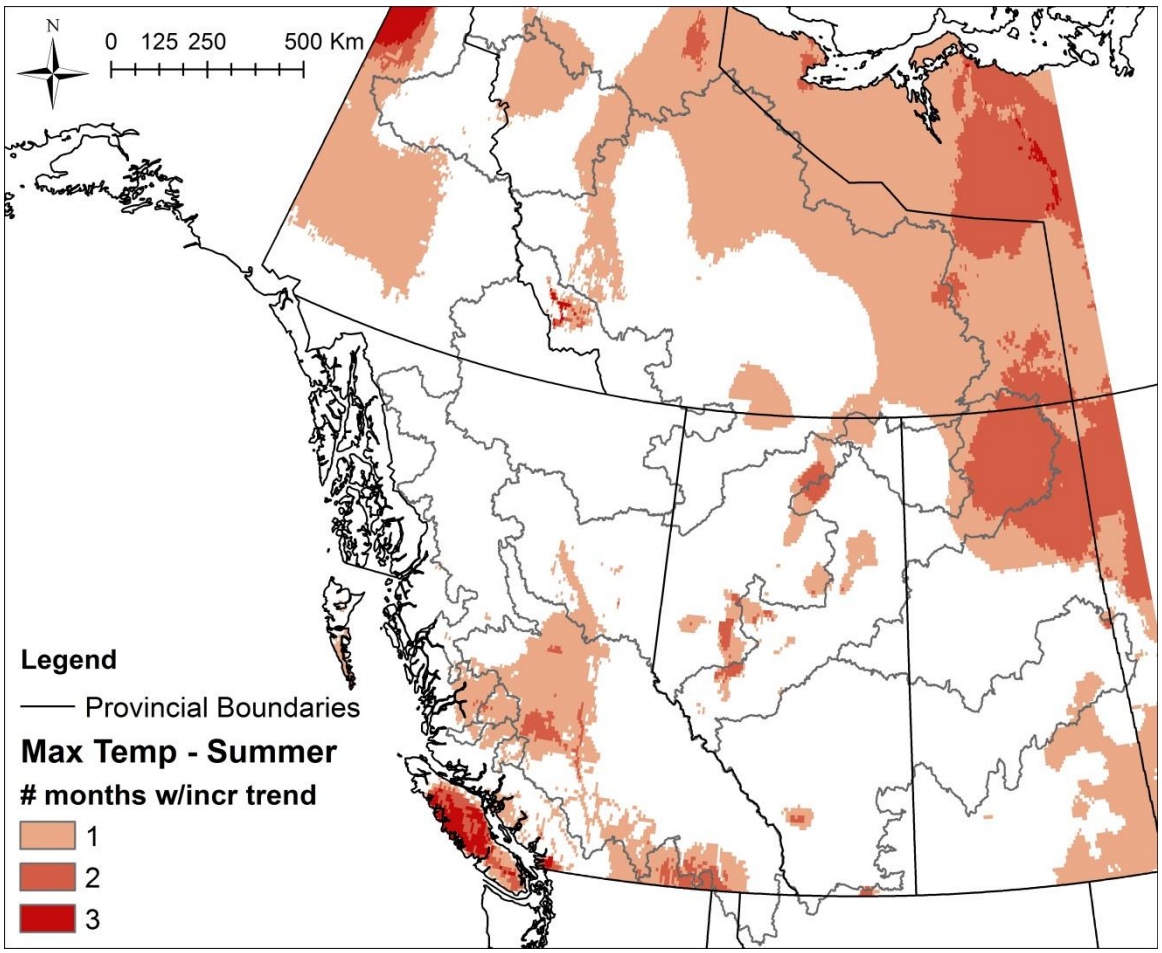

Figure A.33. Tmax increasing trend persistence through summer (July to September). Colour corresponds to number of months with increasing trend.

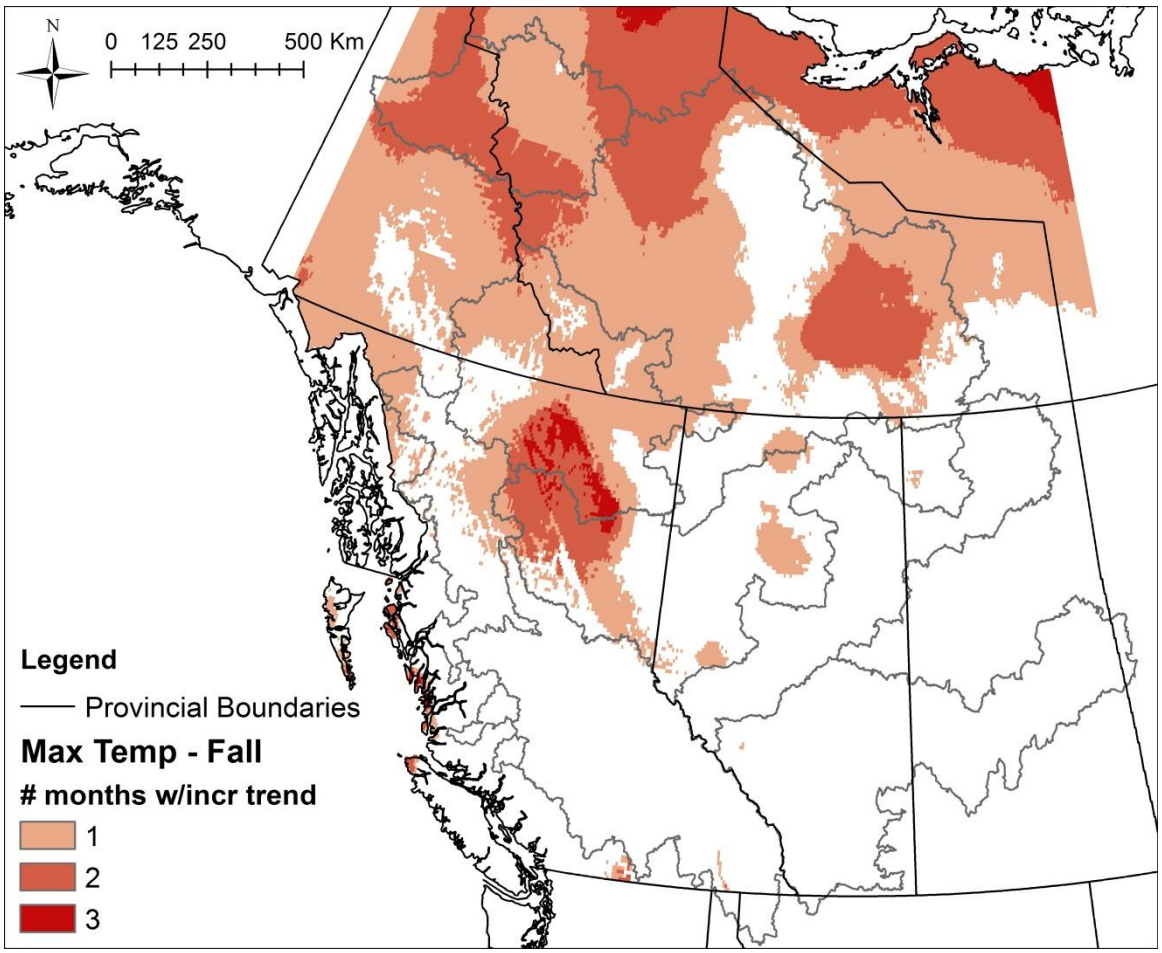

Figure A.34. Tmax increasing trend persistence through fall (October to December). Colour corresponds to number of months with increasing trend.

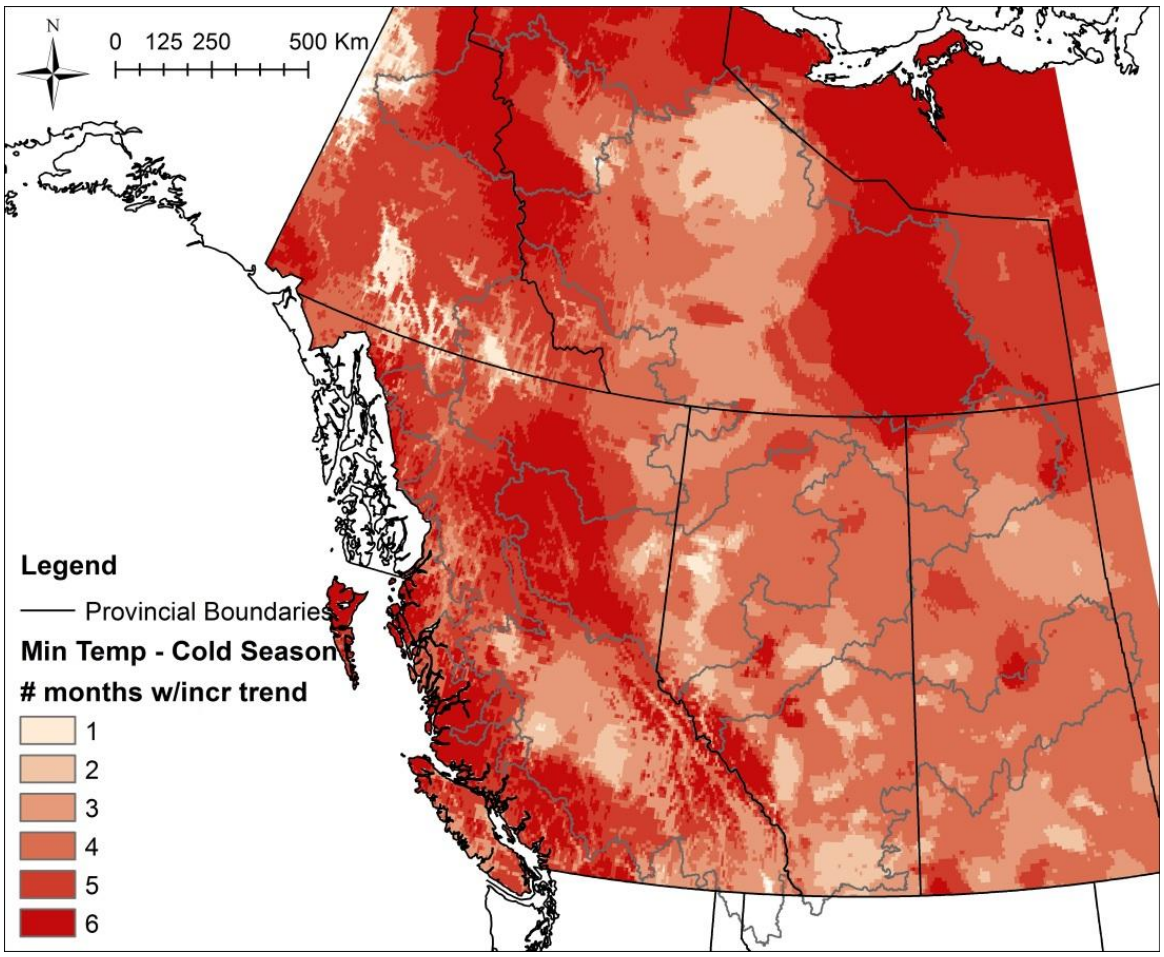

Figure A.35. Tmin increasing trend persistence through the cold season (November to April). Colour corresponds to number of months with increasing trend.

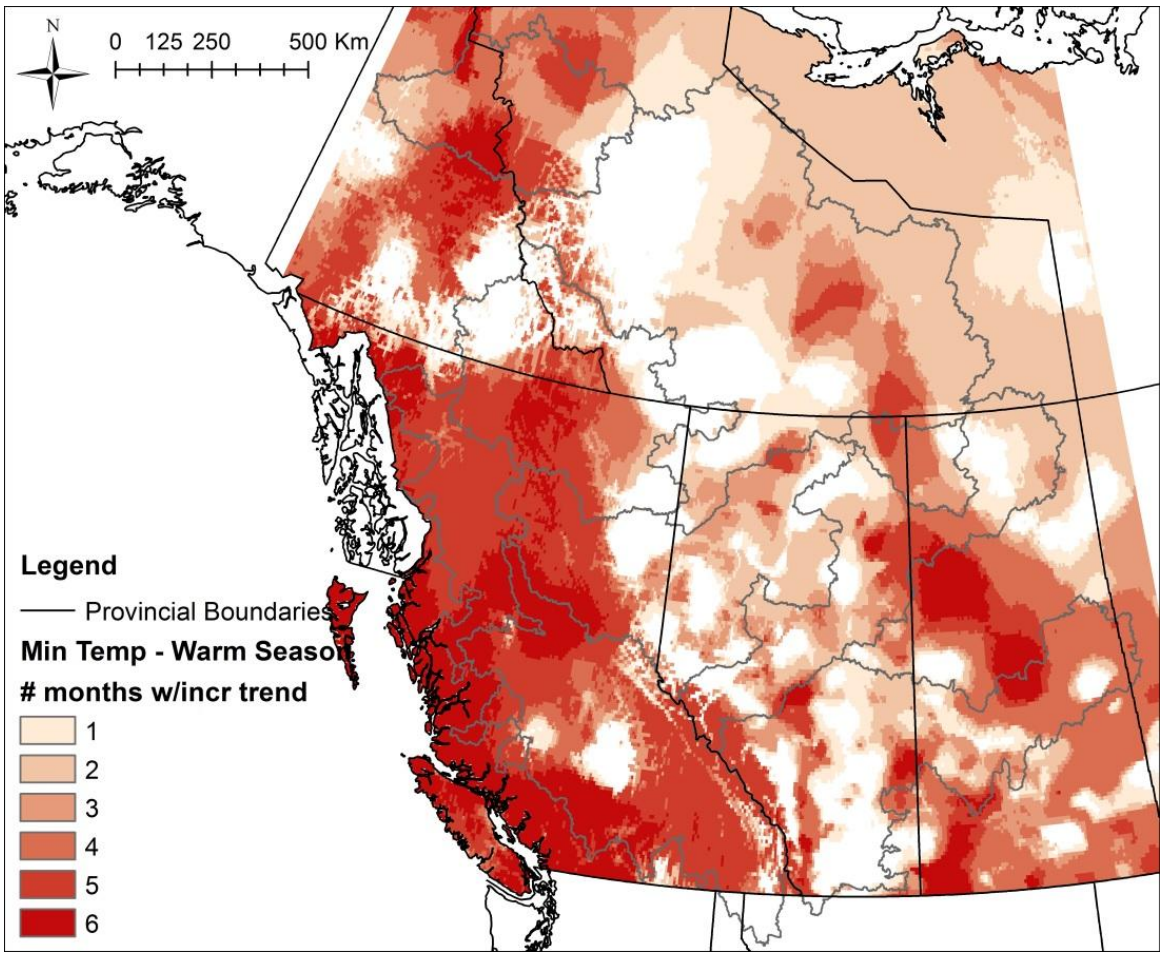

Figure A.36. Tmin increasing trend persistence through the warm season (May to October). Colour corresponds to number of months with increasing trend.

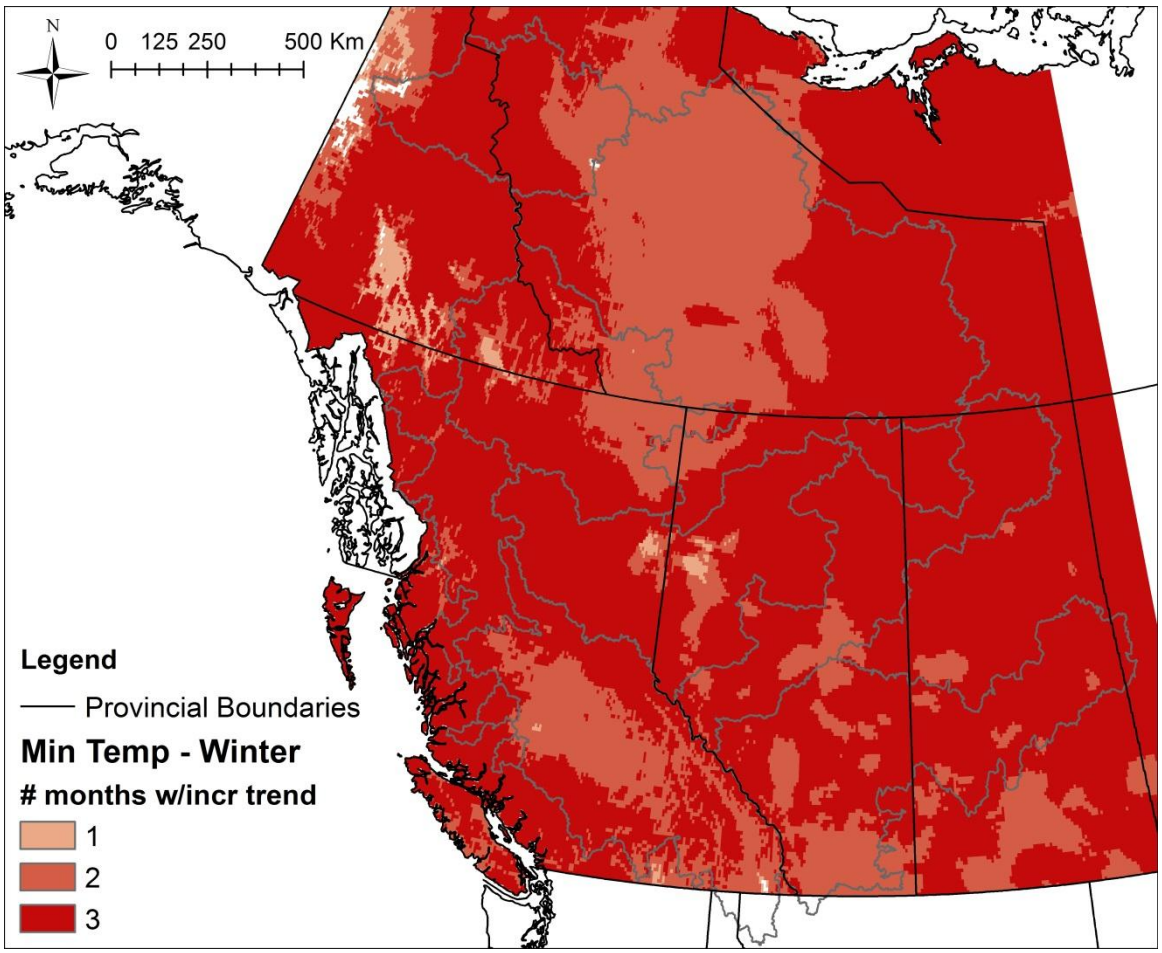

Figure A.37. Tmin increasing trend persistence through winter (January to March). Colour corresponds to number of months with increasing trend.

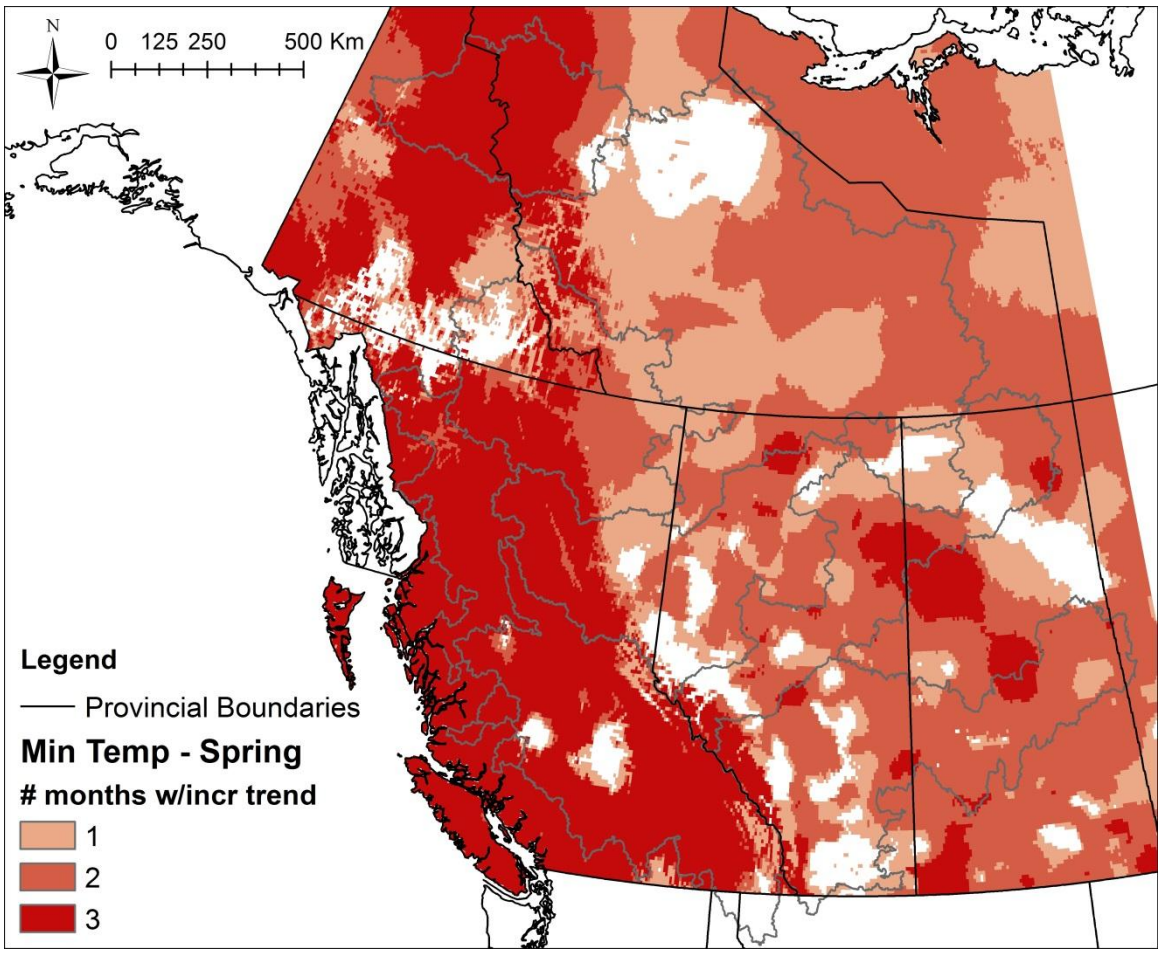

Figure A.38. Tmin increasing trend persistence through spring (April to June). Colour corresponds to number of months with increasing trend.

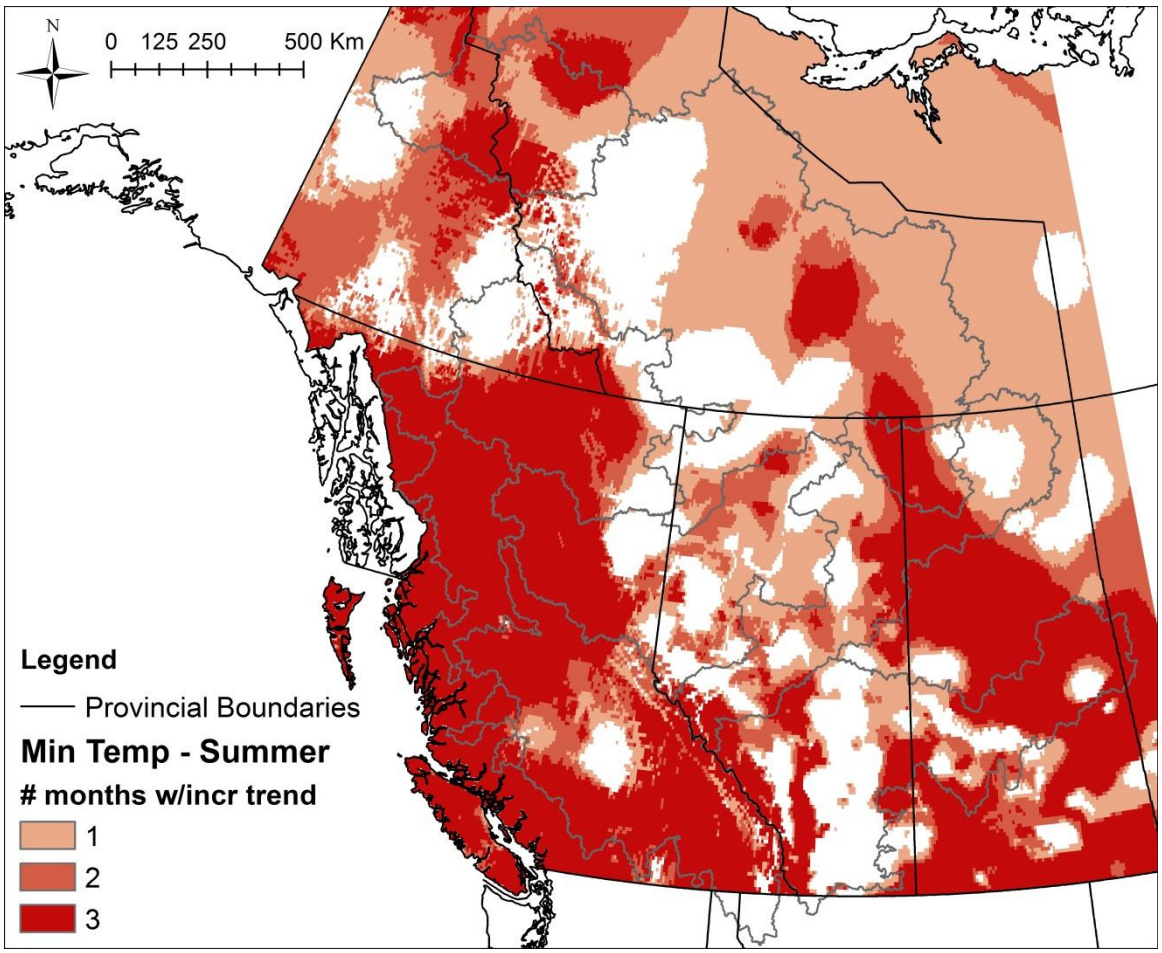

Figure A.39. Tmin increasing trend persistence through summer (July to September). Colour corresponds to number of months with increasing trend.

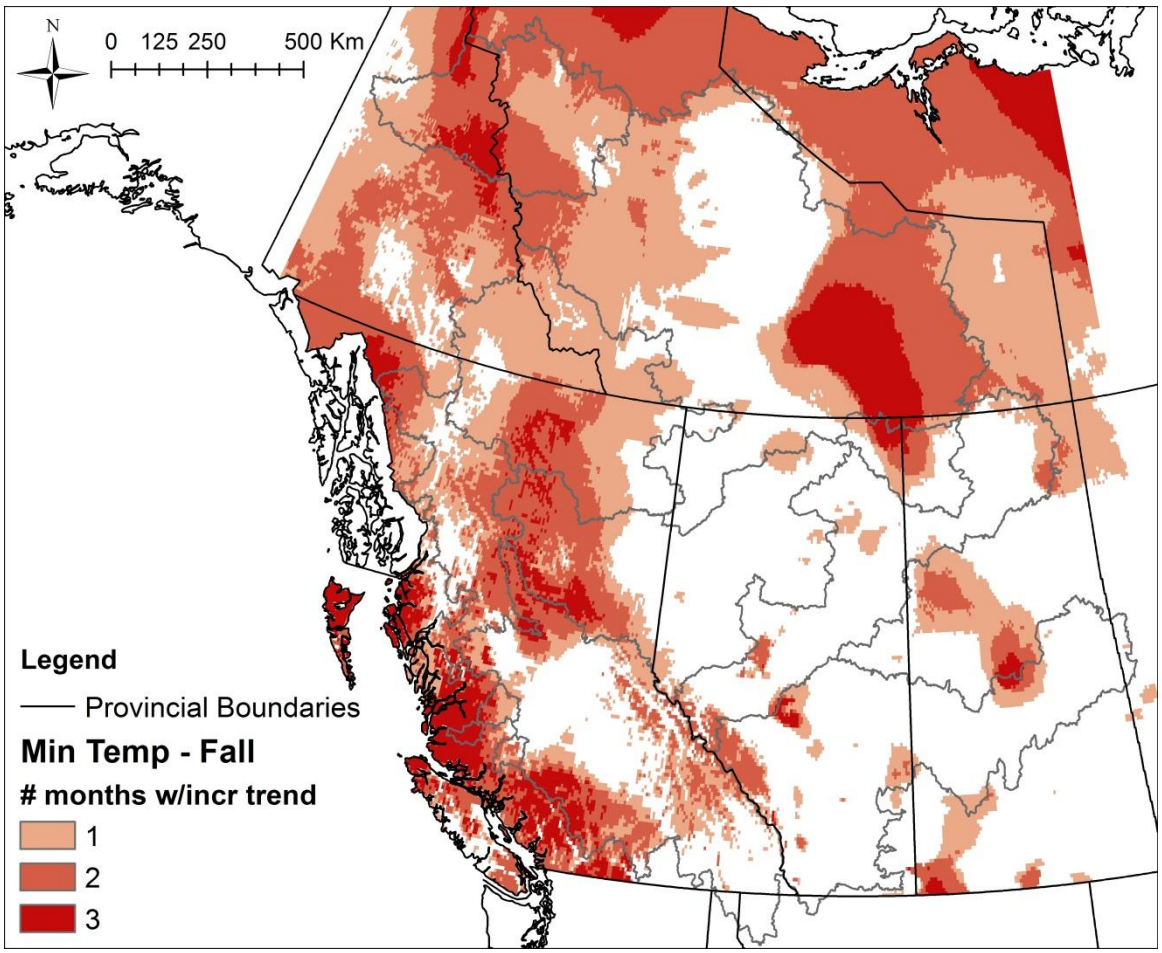

Figure A.40. Tmin increasing trend persistence through fall (October to December). Colour corresponds to number of months with increasing trend.

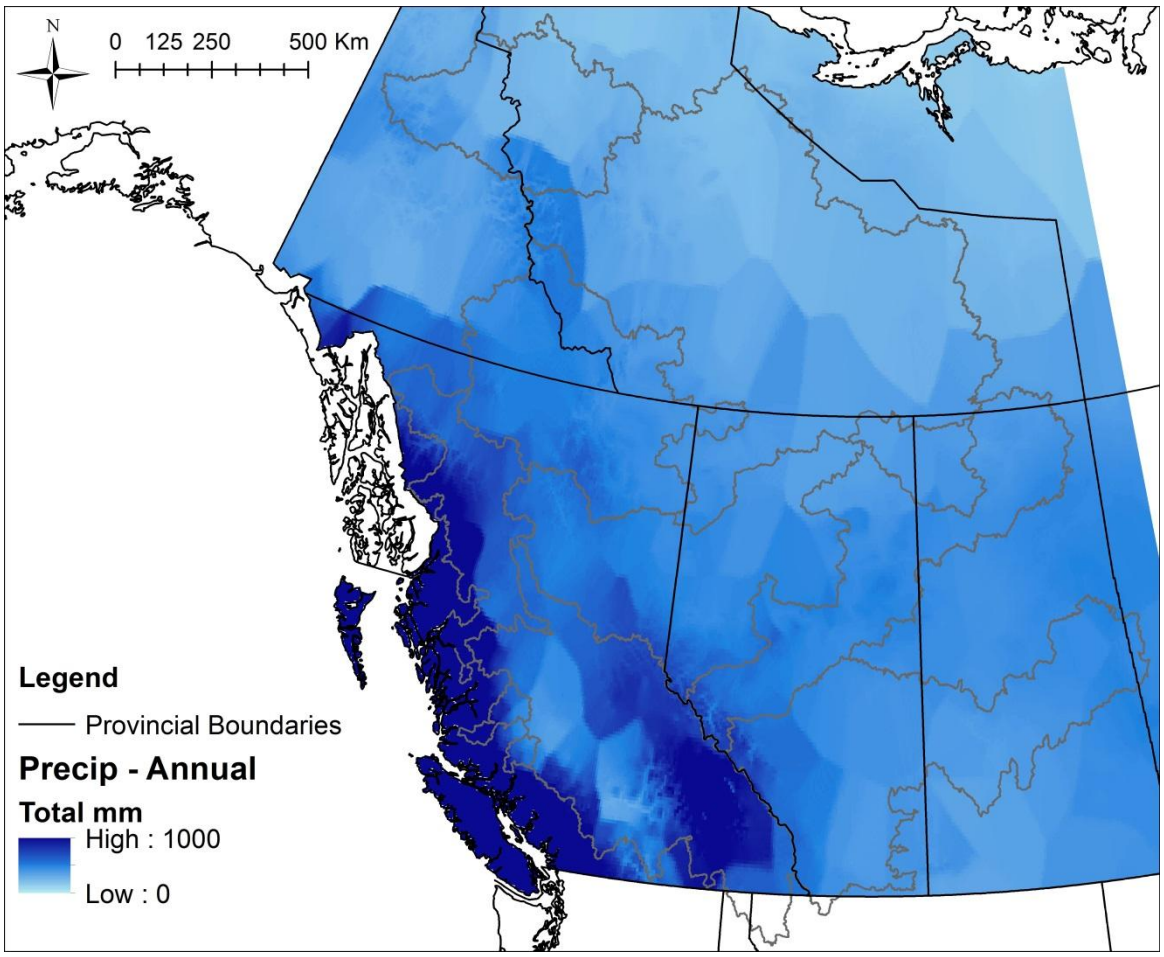

Figure A.41. Annual total precipitation in mm. Averaged from 1950-2010.

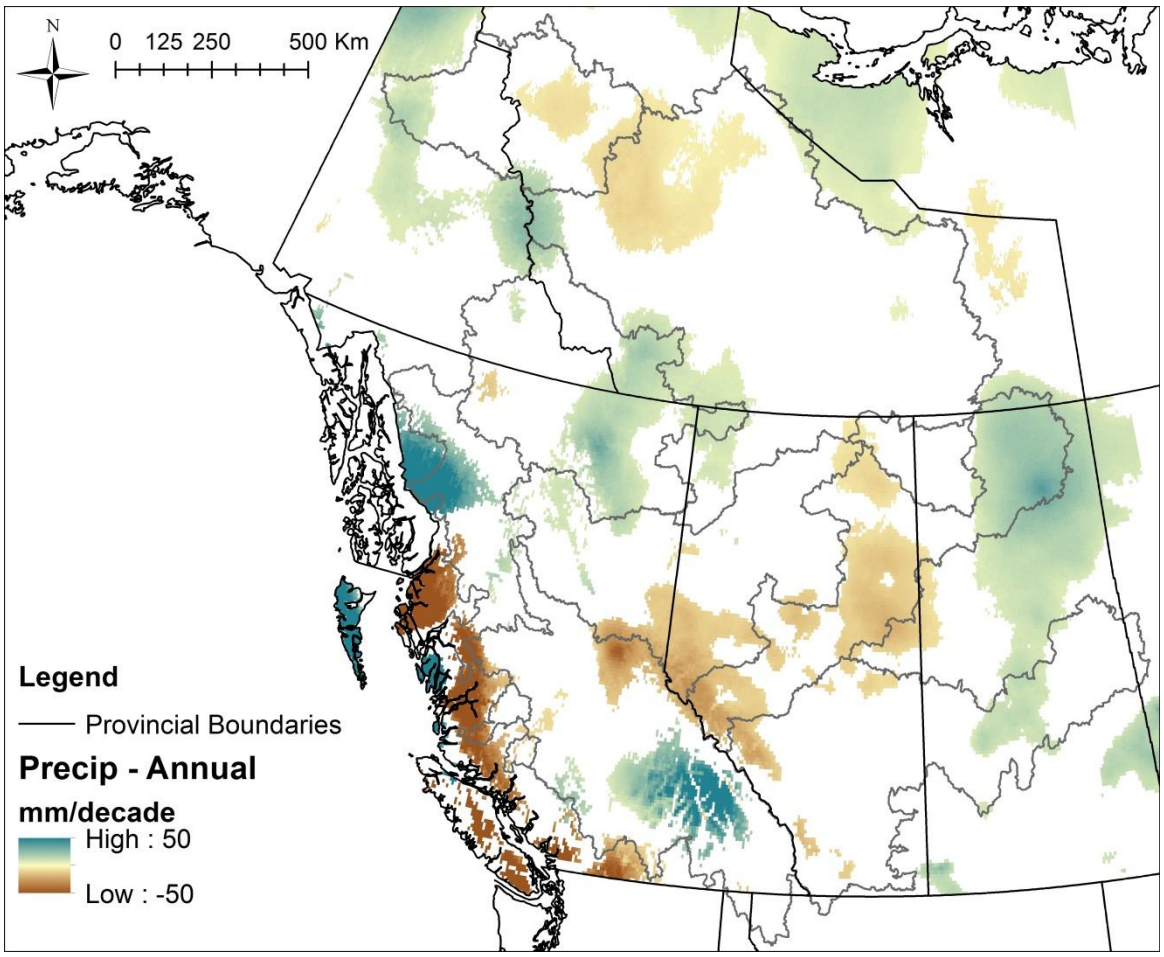

Figure A.42. Annual precipitation trend results showing rate of change in mm/decade, from 1950-2010. Only trends significant at 10% or better are shown.

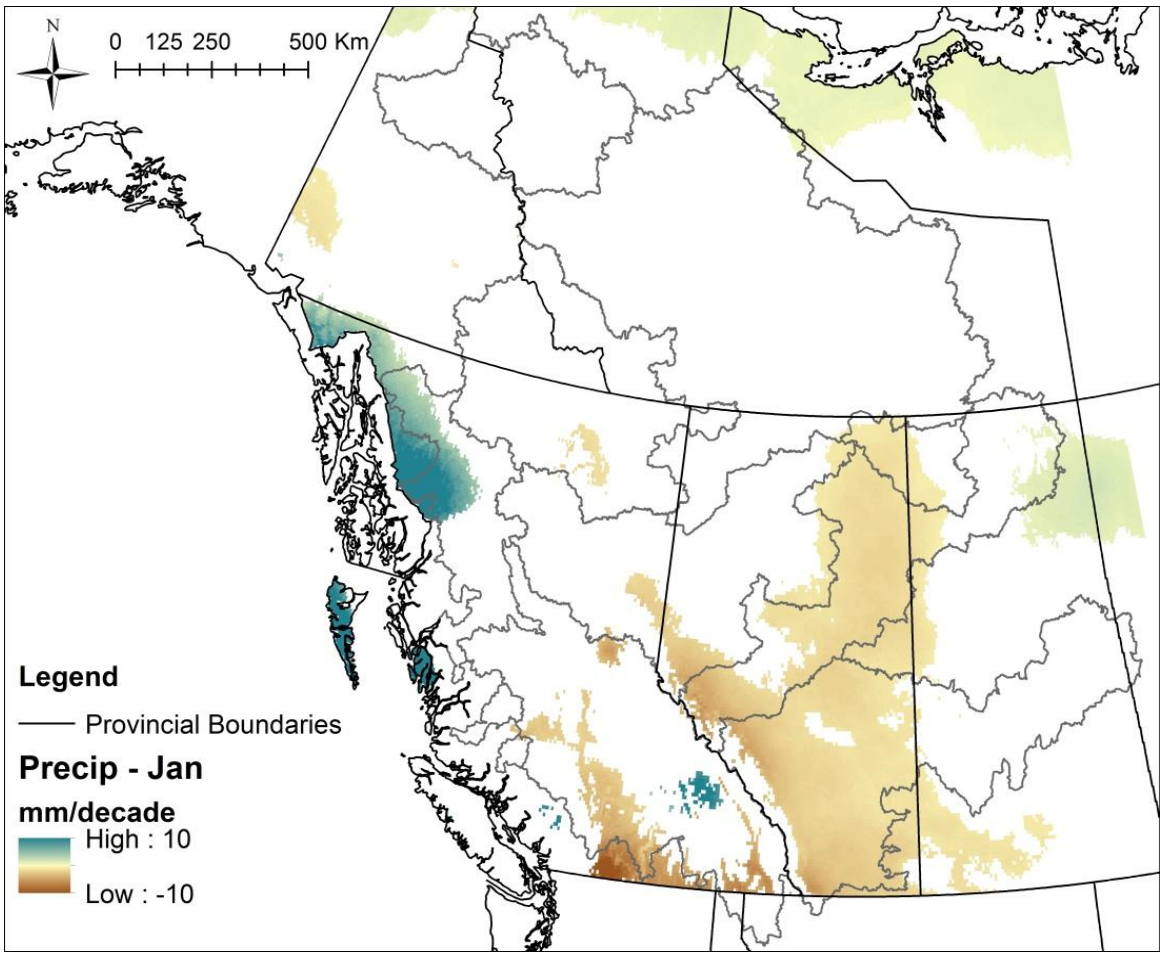

Figure A.43. January precipitation trend results showing rate of change in mm/decade, from 1950-2010. Only trends significant at 10% or better are shown.

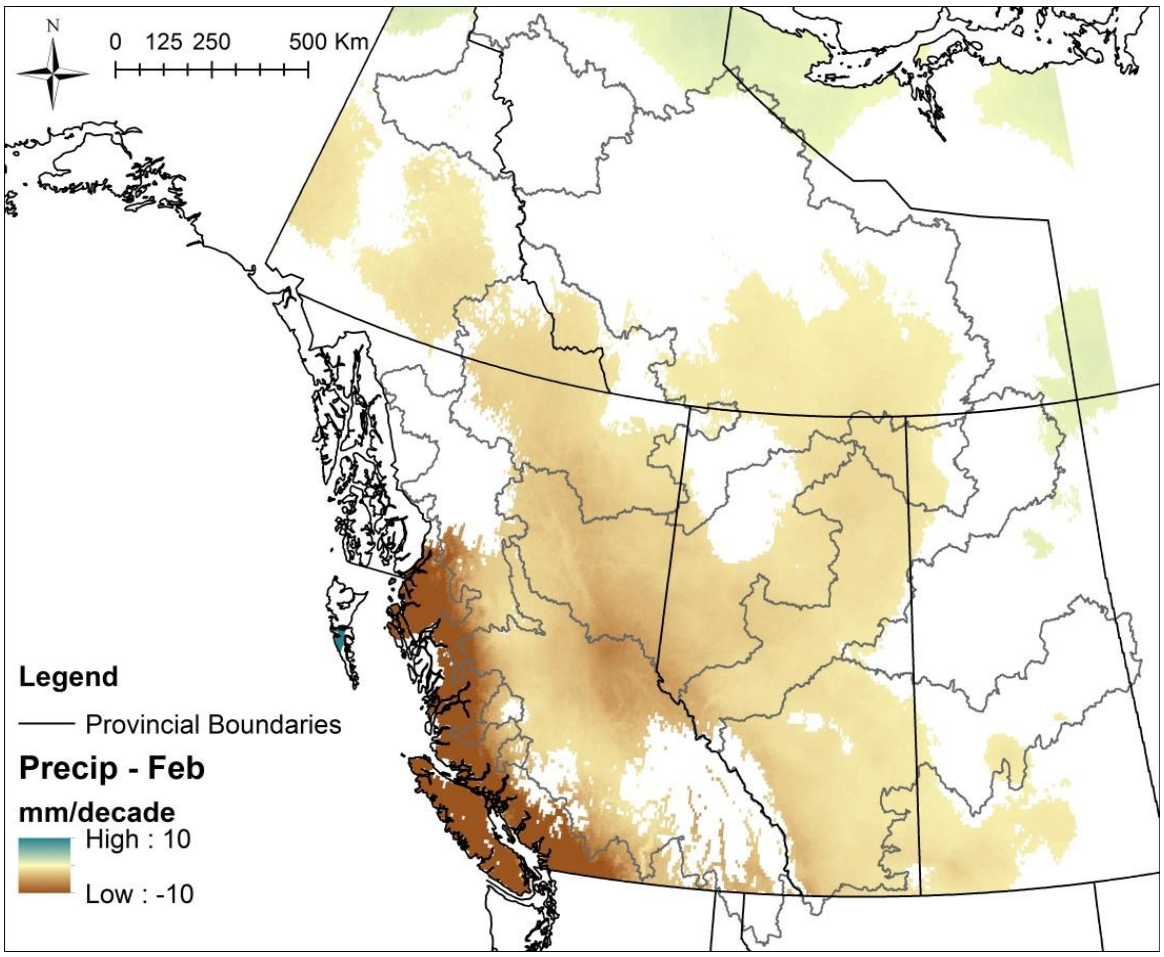

Figure A.44. February precipitation trend results showing rate of change in mm/decade, from 1950-2010. Only trends significant at 10% or better are shown.

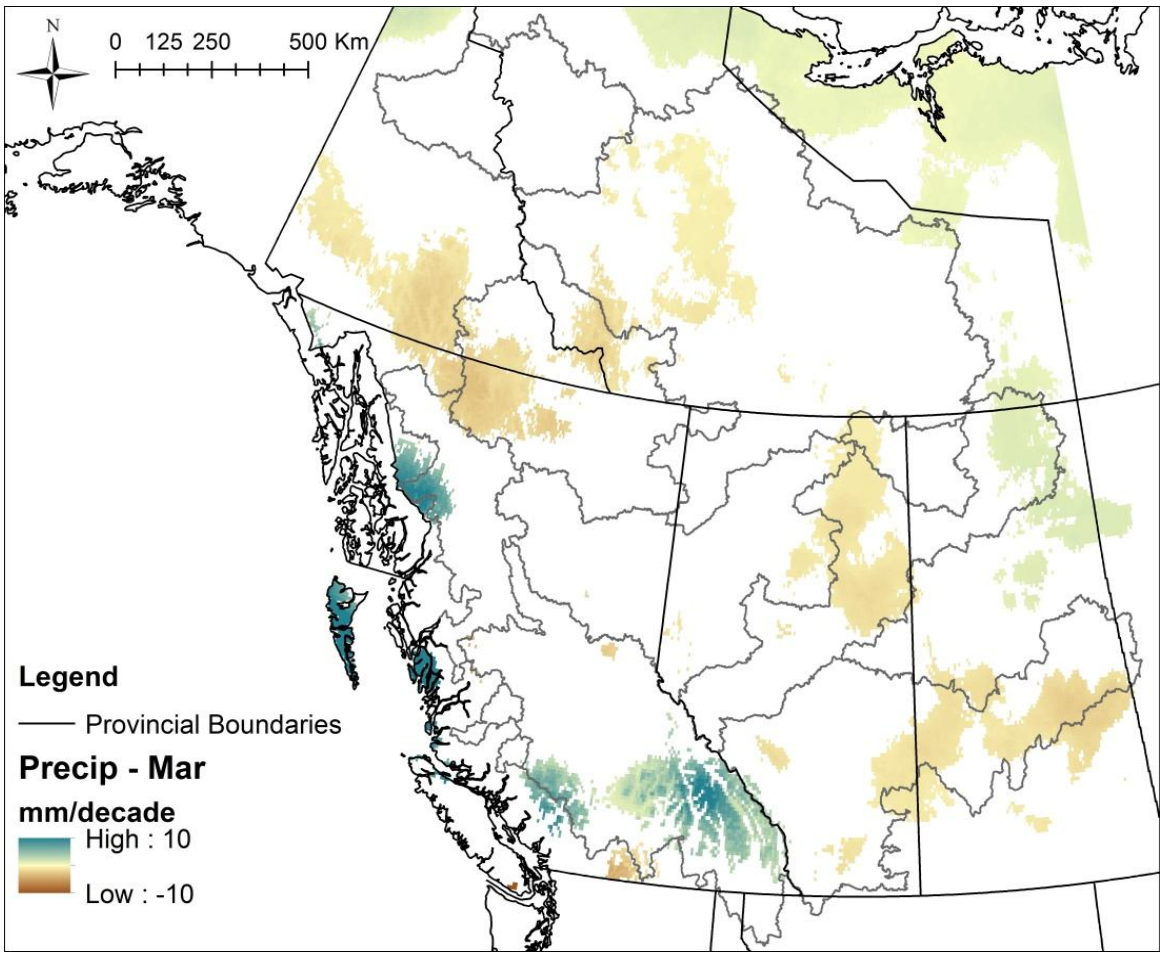

Figure A.45. March precipitation trend results showing rate of change in mm/decade, from 1950-2010. Only trends significant at 10% or better are shown.

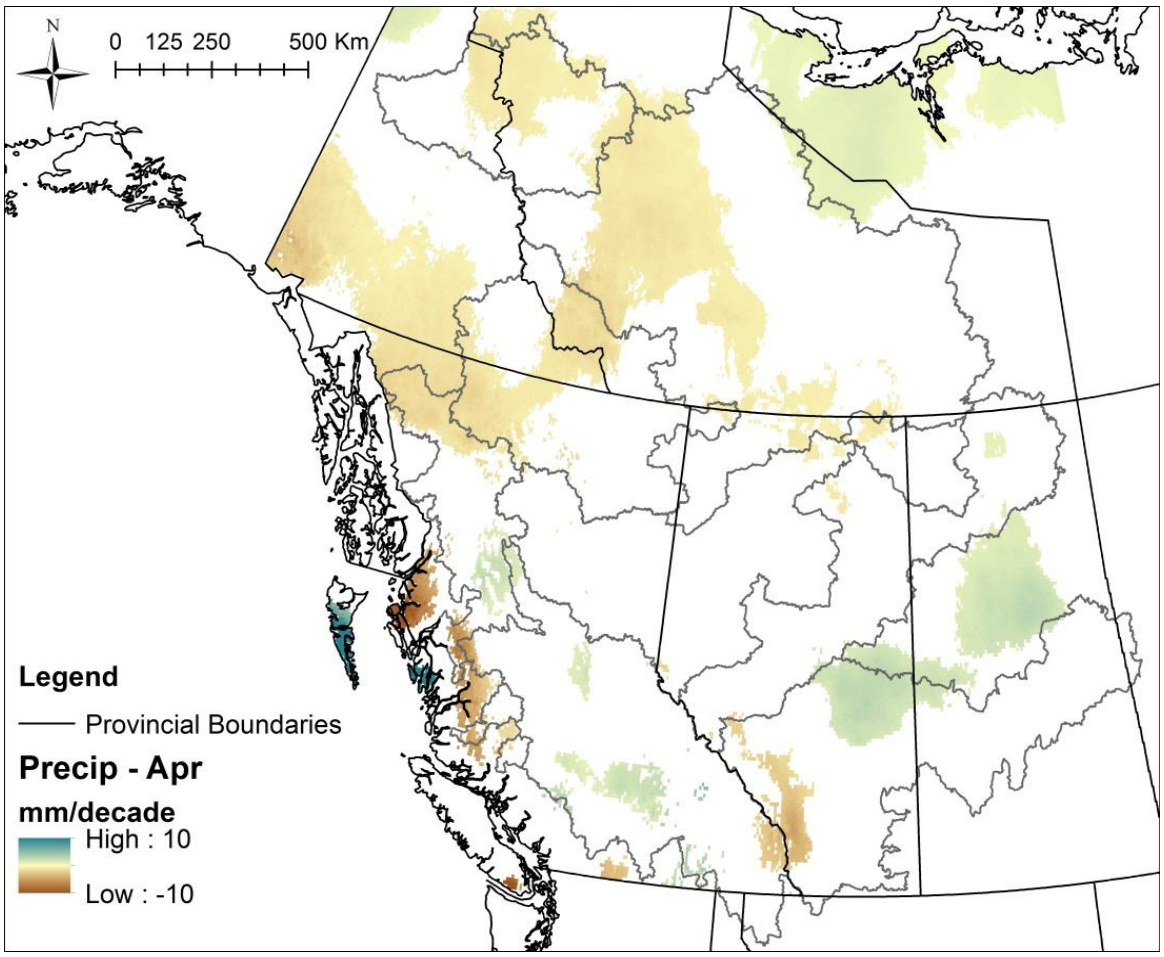

Figure A.46. April precipitation trend results showing rate of change in mm/decade, from 1950-2010. Only trends significant at 10% or better are shown.

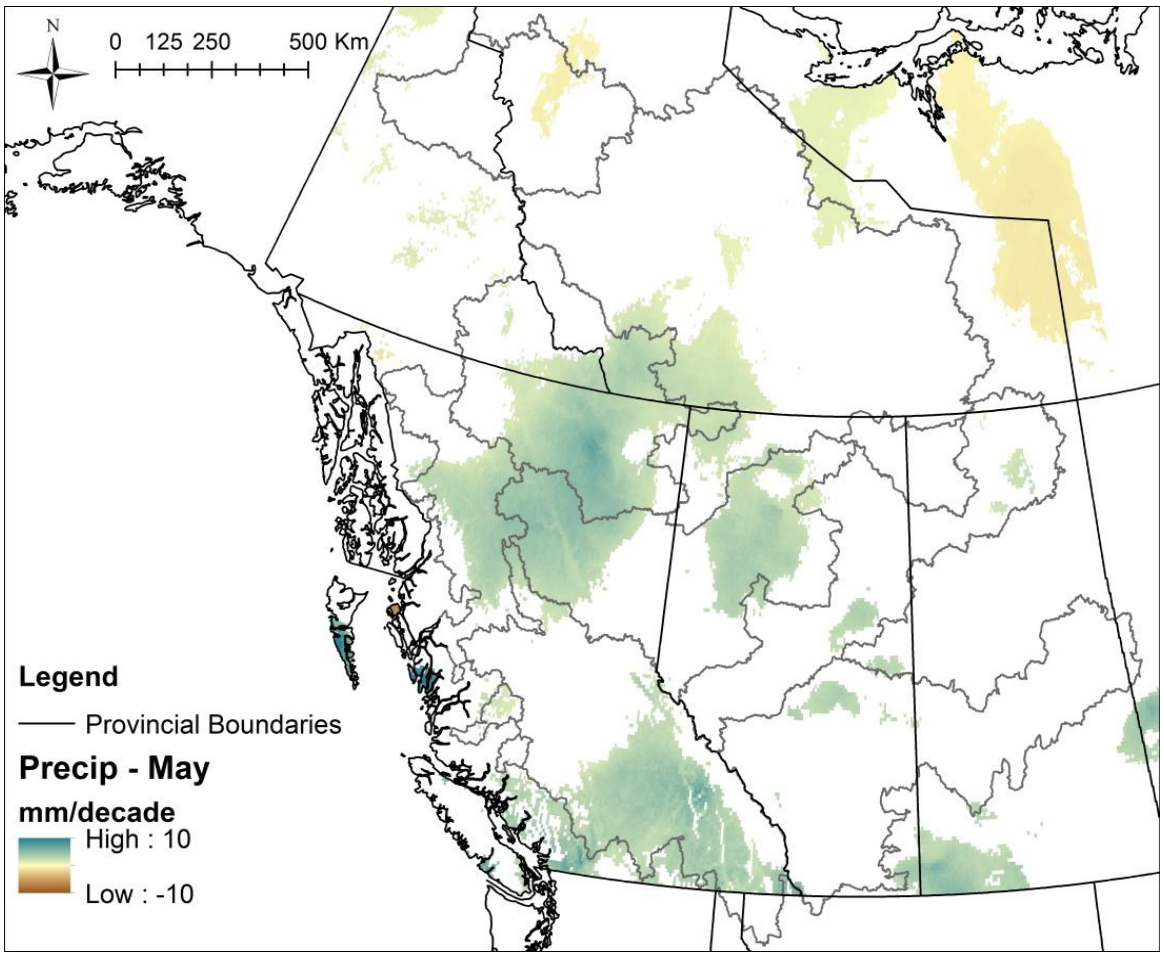

Figure A.47. May precipitation trend results showing rate of change in mm/decade, from 1950-2010. Only trends significant at 10% or better are shown.

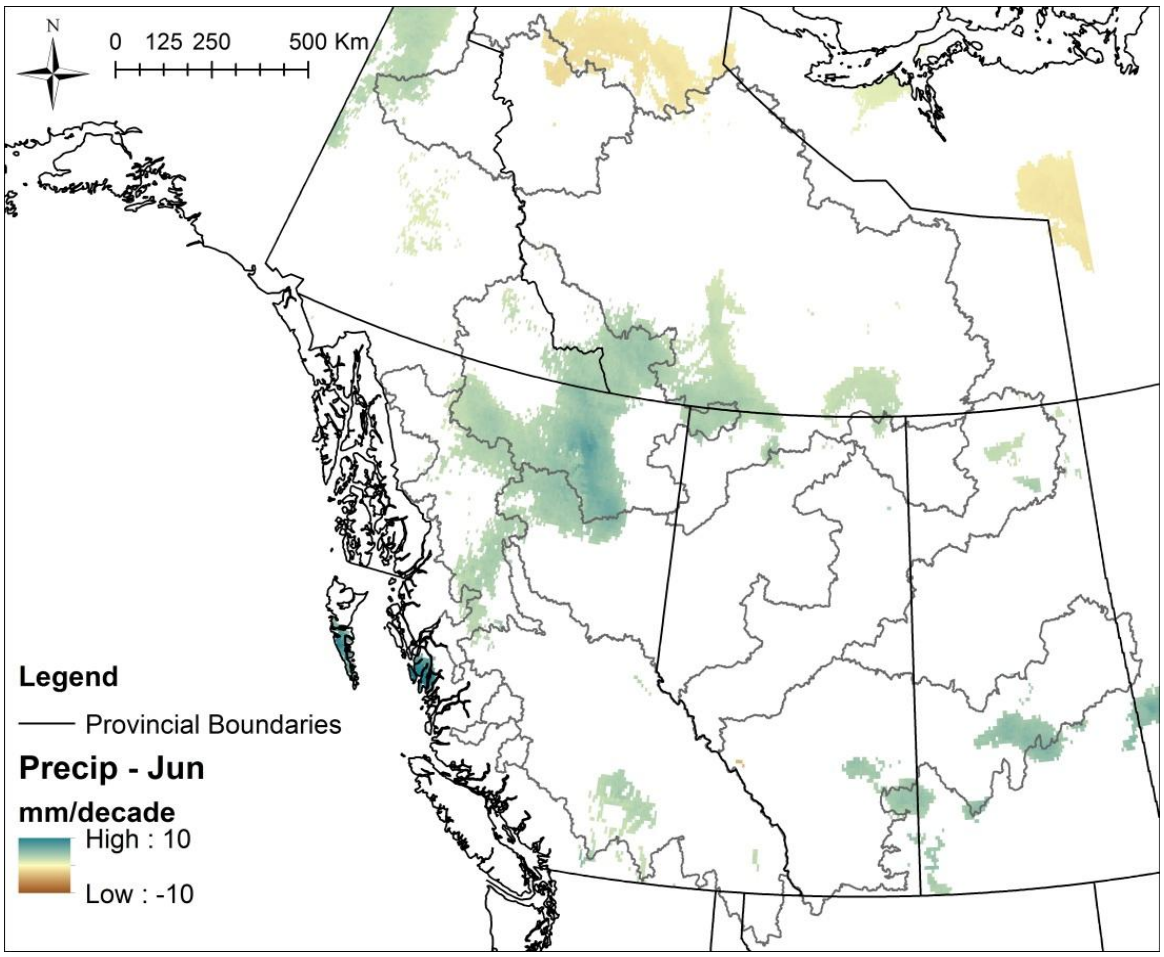

Figure A.48. June precipitation trend results showing rate of change in mm/decade, from 1950-2010. Only trends significant at 10% or better are shown.

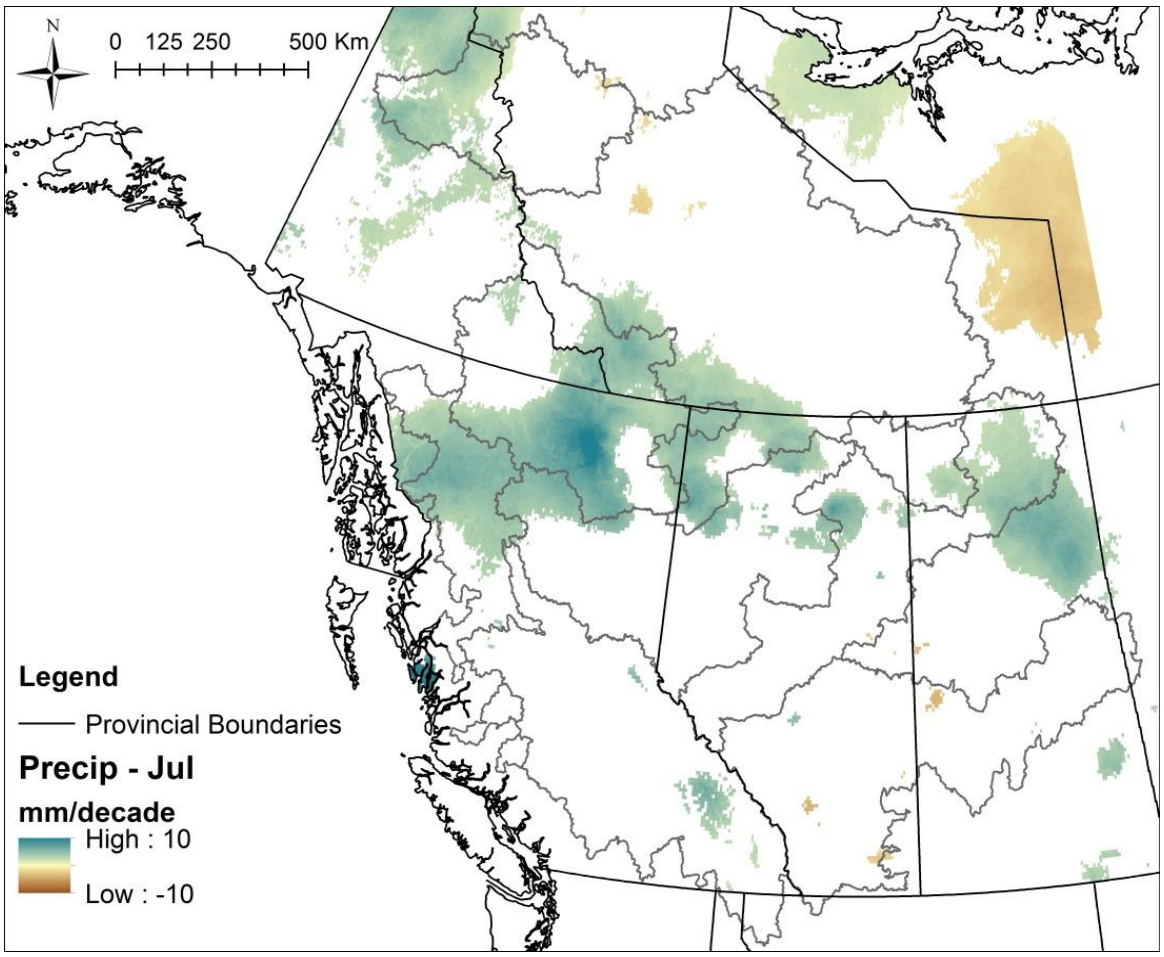

Figure A.49. July precipitation trend results showing rate of change in mm/decade, from 1950-2010. Only trends significant at 10% or better are shown.

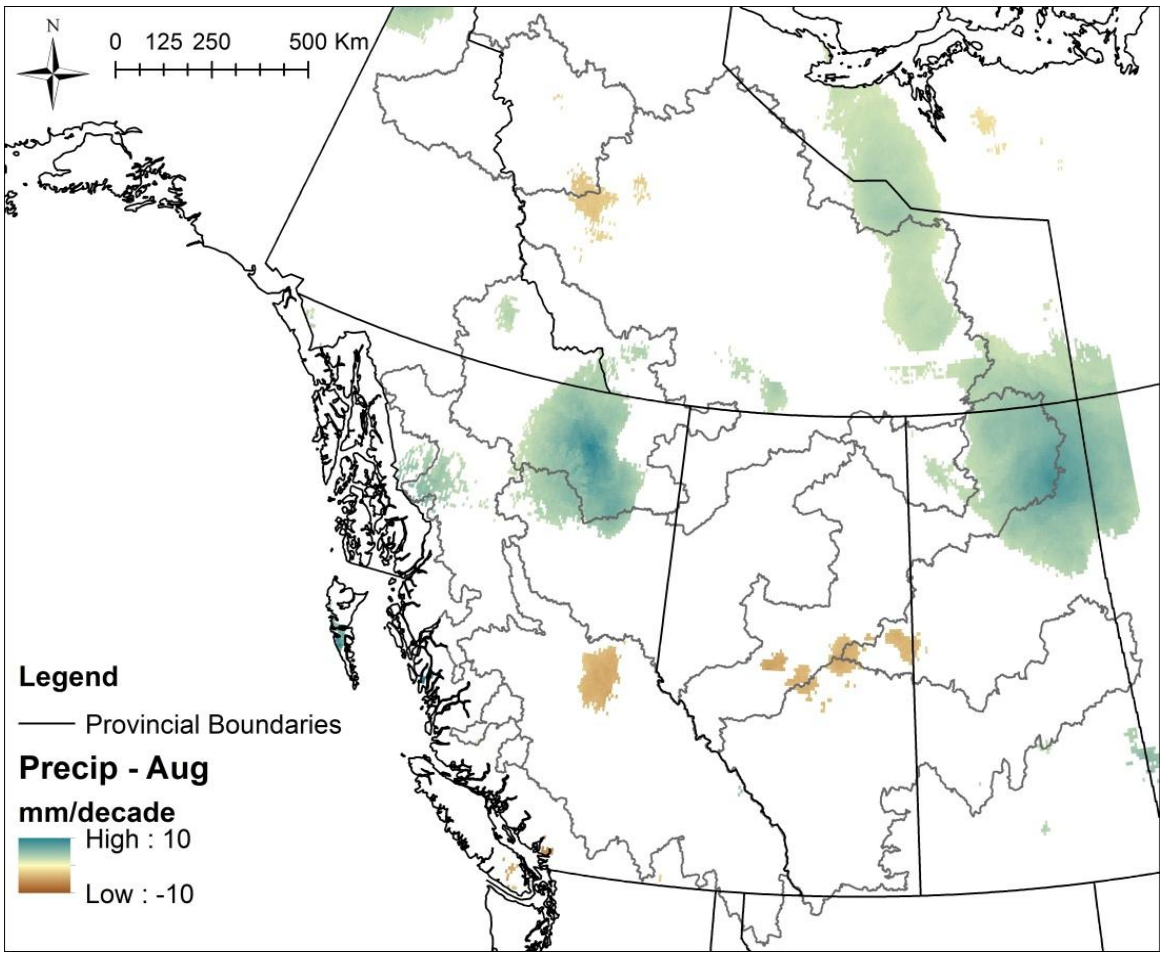

Figure A.50. August precipitation trend results showing rate of change in mm/decade, from 1950-2010. Only trends significant at 10% or better are shown.

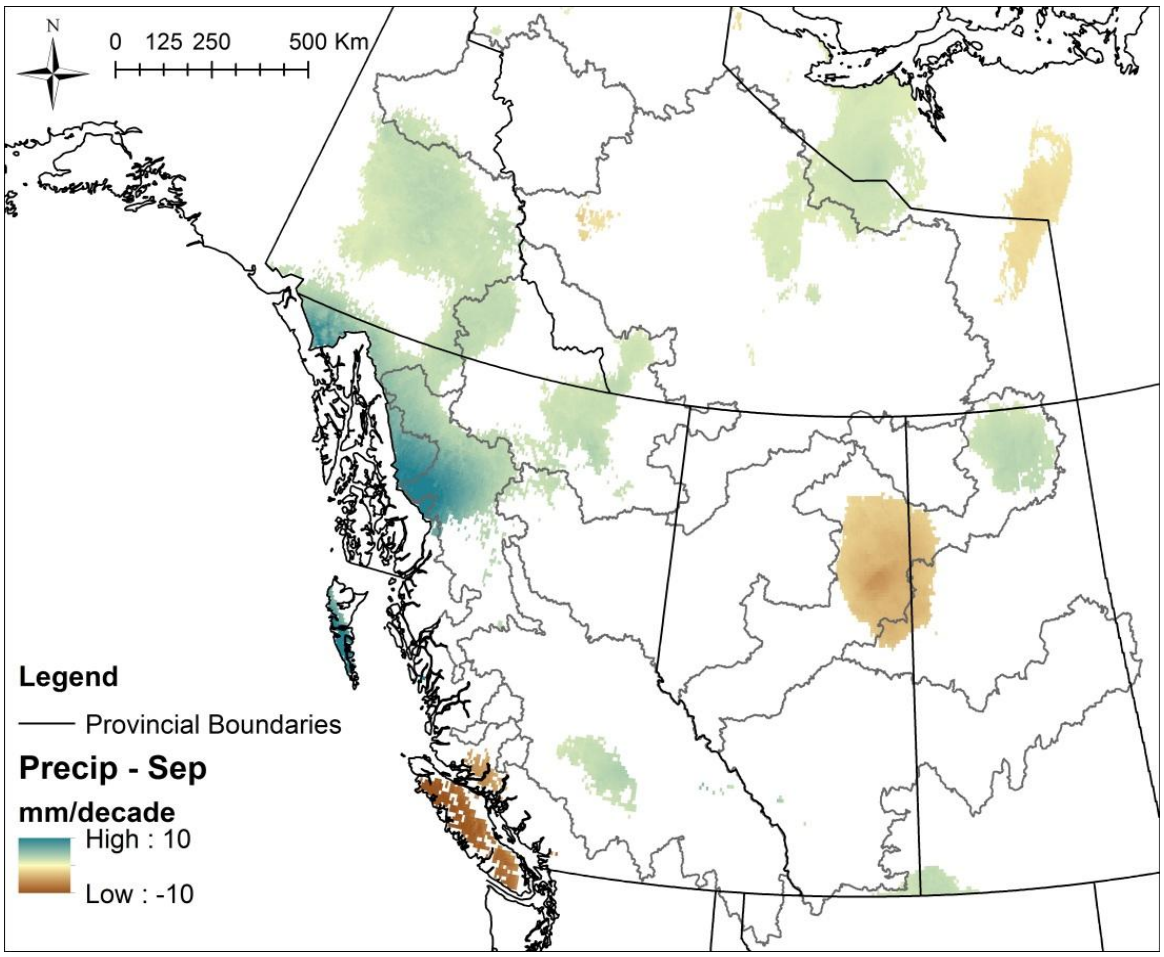

Figure A.51. September precipitation trend results showing rate of change in mm/decade, from 1950-2010. Only trends significant at 10% or better are shown.

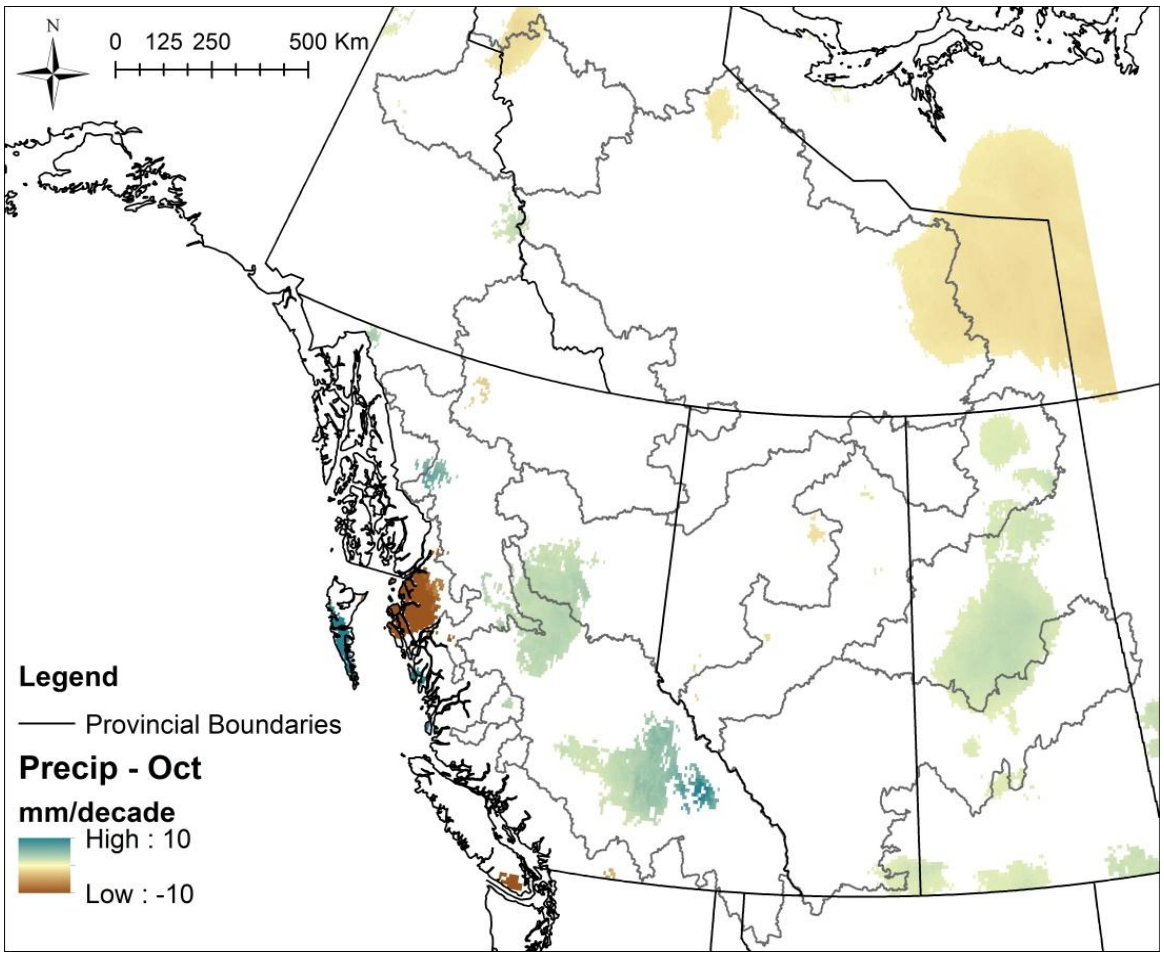

Figure A.52. October precipitation trend results showing rate of change in mm/decade, from 1950-2010. Only trends significant at 10% or better are shown.

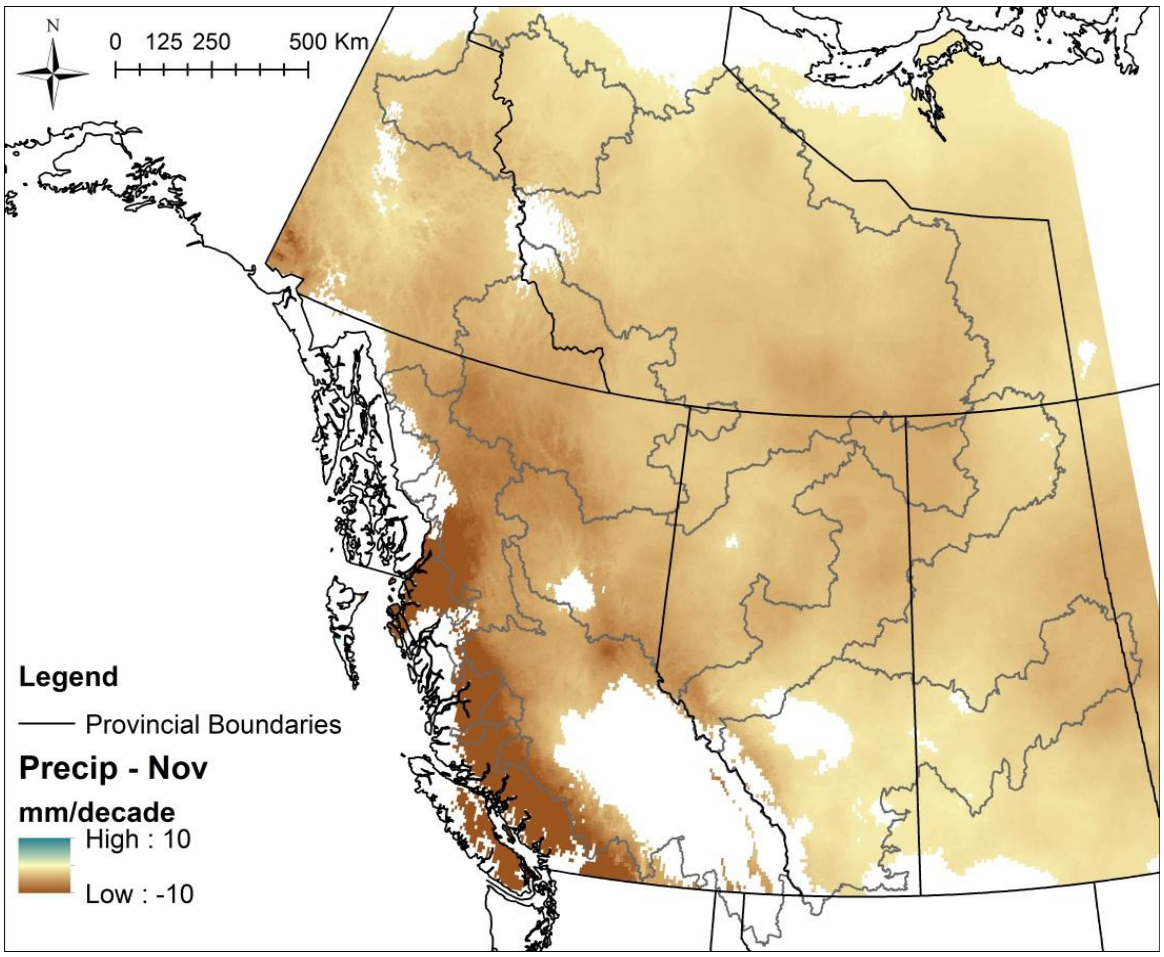

Figure A.53. November precipitation trend results showing rate of change in mm/decade, from 1950-2010. Only trends significant at 10% or better are shown.

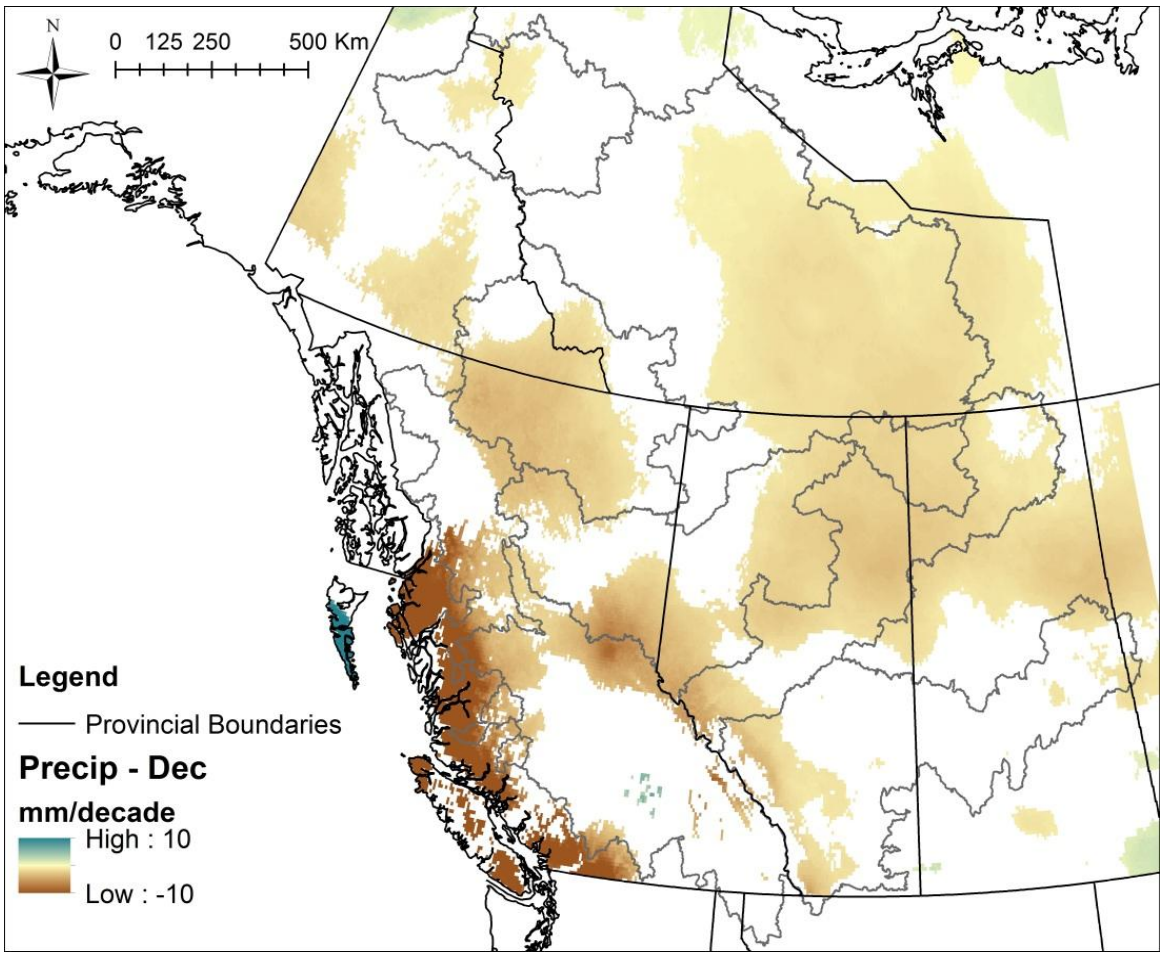

Figure A.54. December precipitation trend results showing rate of change in mm/decade, from 1950-2010. Only trends significant at 10% or better are shown.

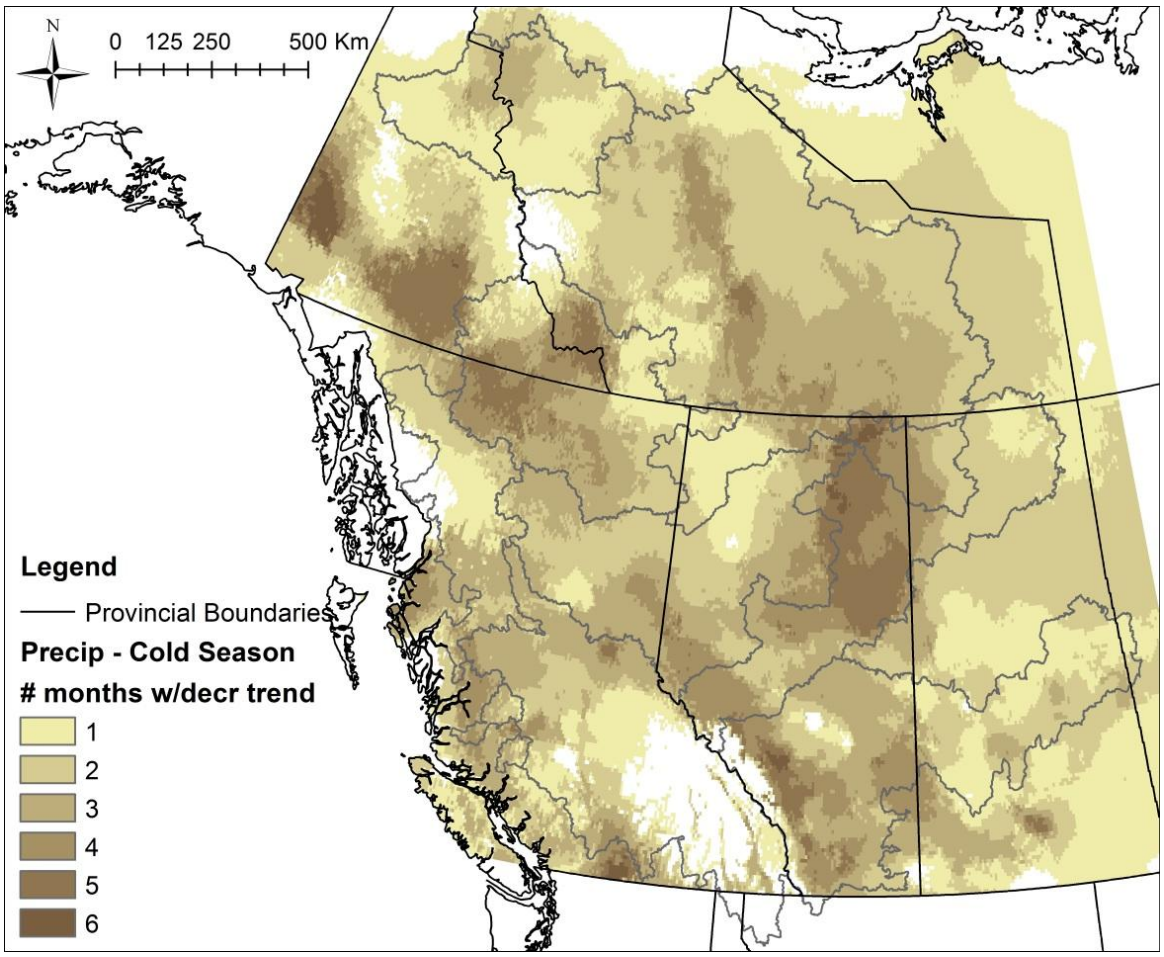

Figure A.55. Precipitation decreasing trend persistence through the cold season (November to April). Colour corresponds to number of months with decreasing trend.

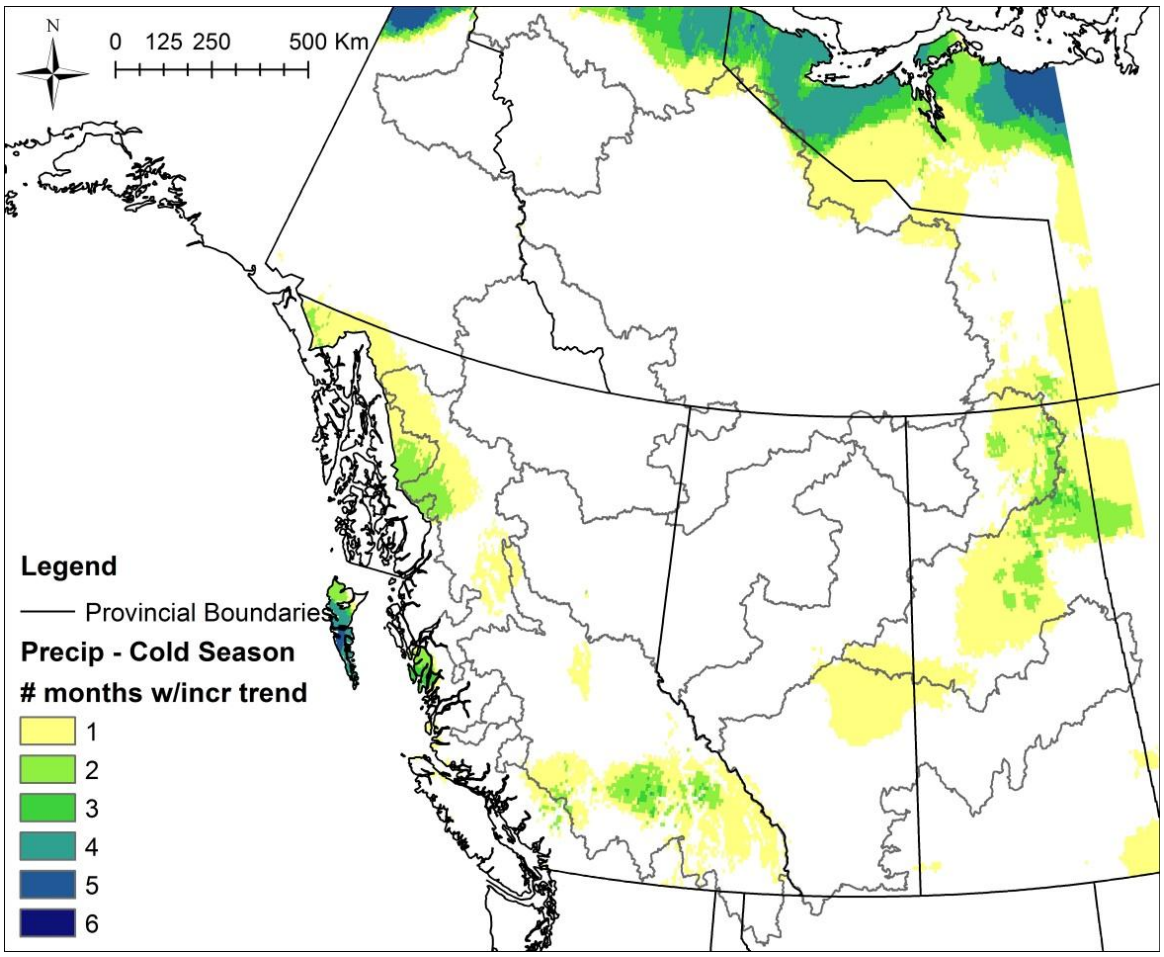

Figure A.56. Precipitation increasing trend persistence through the cold season (November to April). Colour corresponds to number of months with increasing trend.

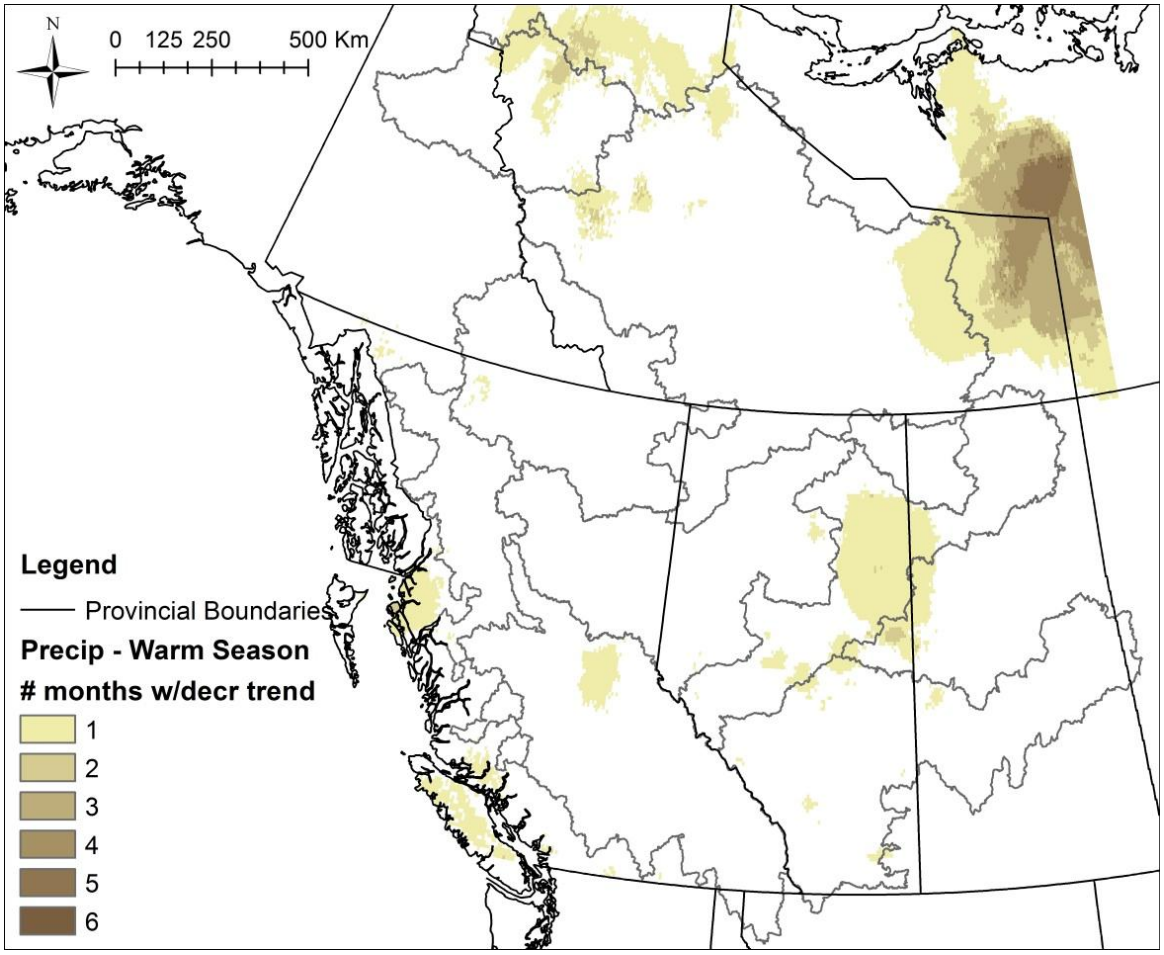

Figure A.57. Precipitation decreasing trend persistence through the warm season (May to October). Colour corresponds to number of months with decreasing trend.

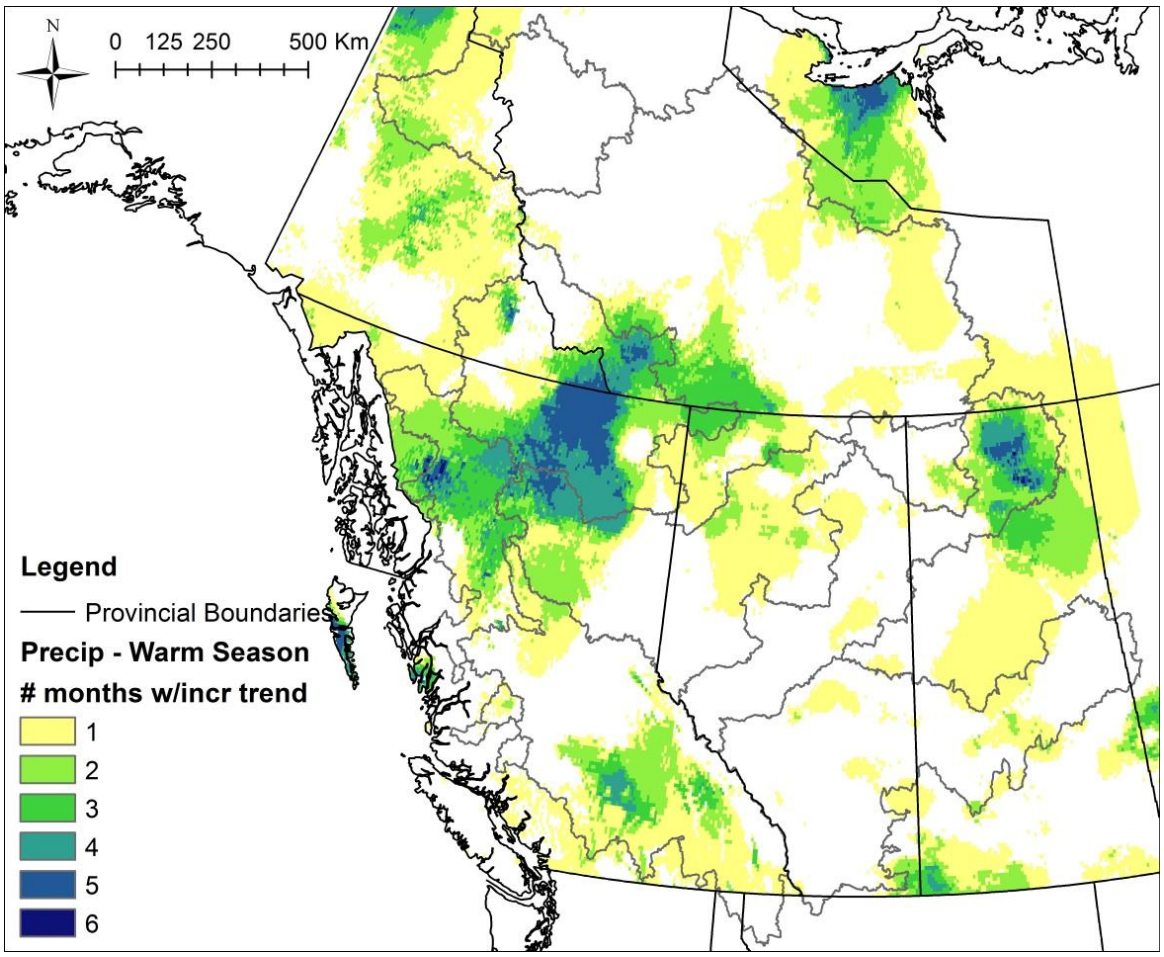

Figure A.58. Precipitation increasing trend persistence through the warm season (May to October). Colour corresponds to number of months with increasing trend.

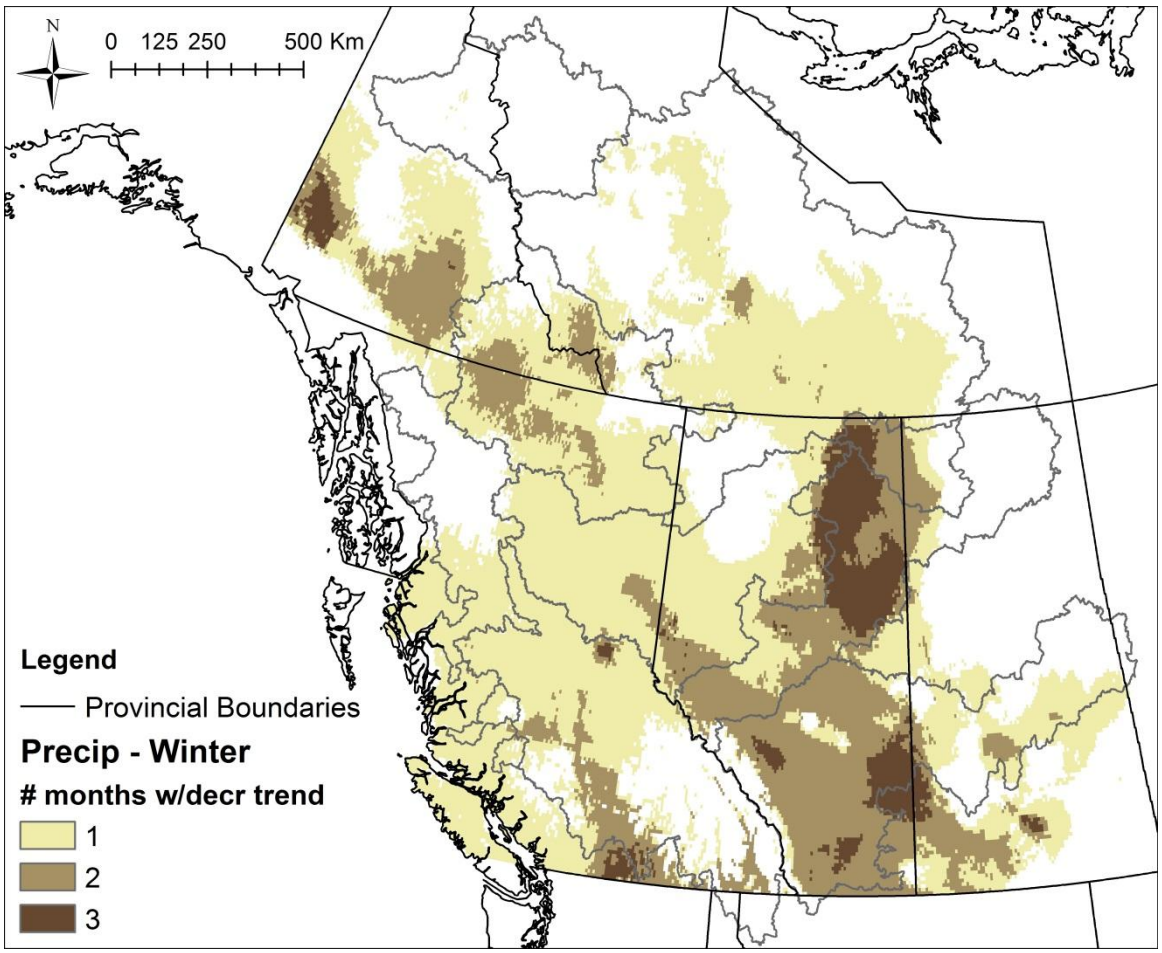

Figure A.59. Precipitation decreasing trend persistence during winter (January to March). Colour corresponds to number of months with decreasing trend.

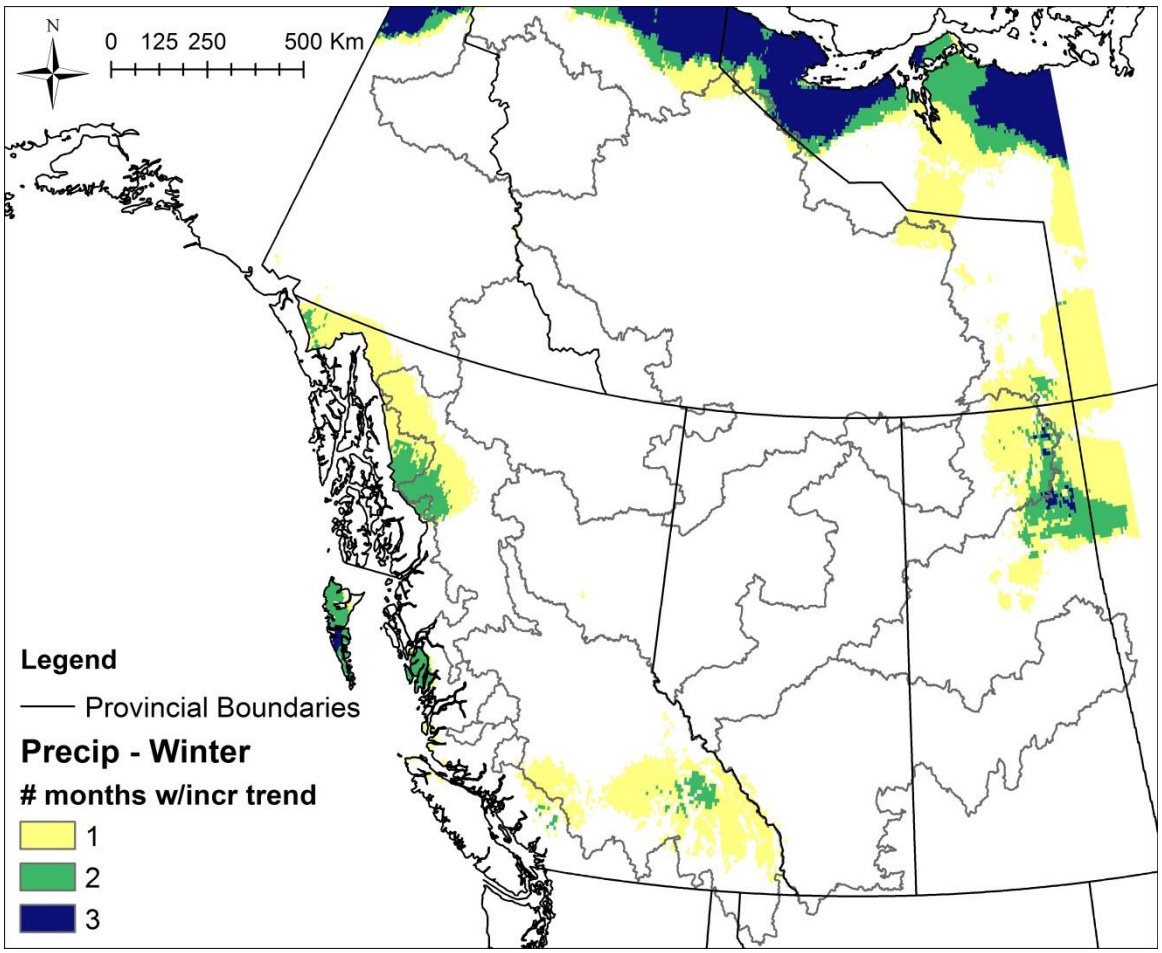

Figure A.60. Precipitation increasing trend persistence during winter (January to March). Colour corresponds to number of months with decreasing trend.

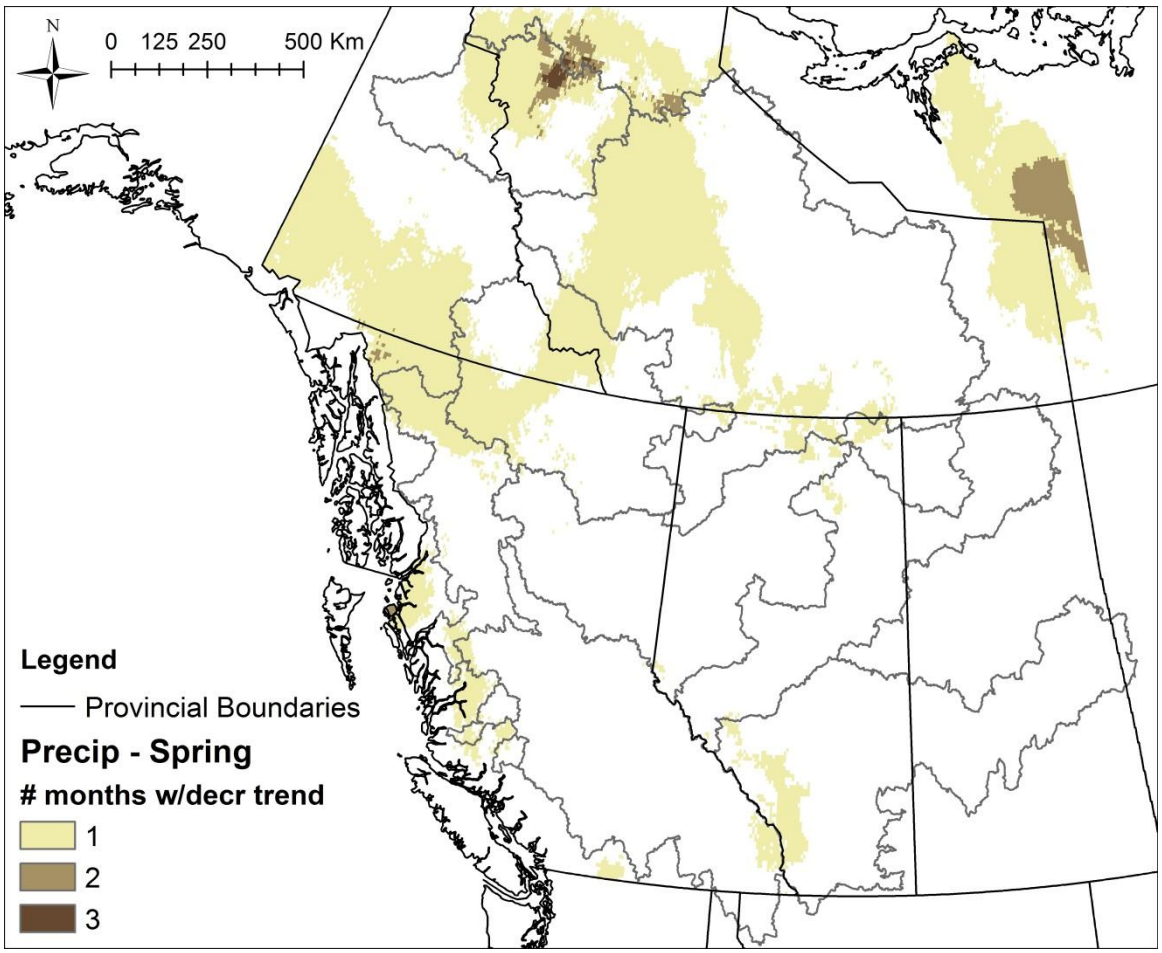

Figure A.61. Precipitation decreasing trend persistence during spring (April to June). Colour corresponds to number of months with decreasing trend.

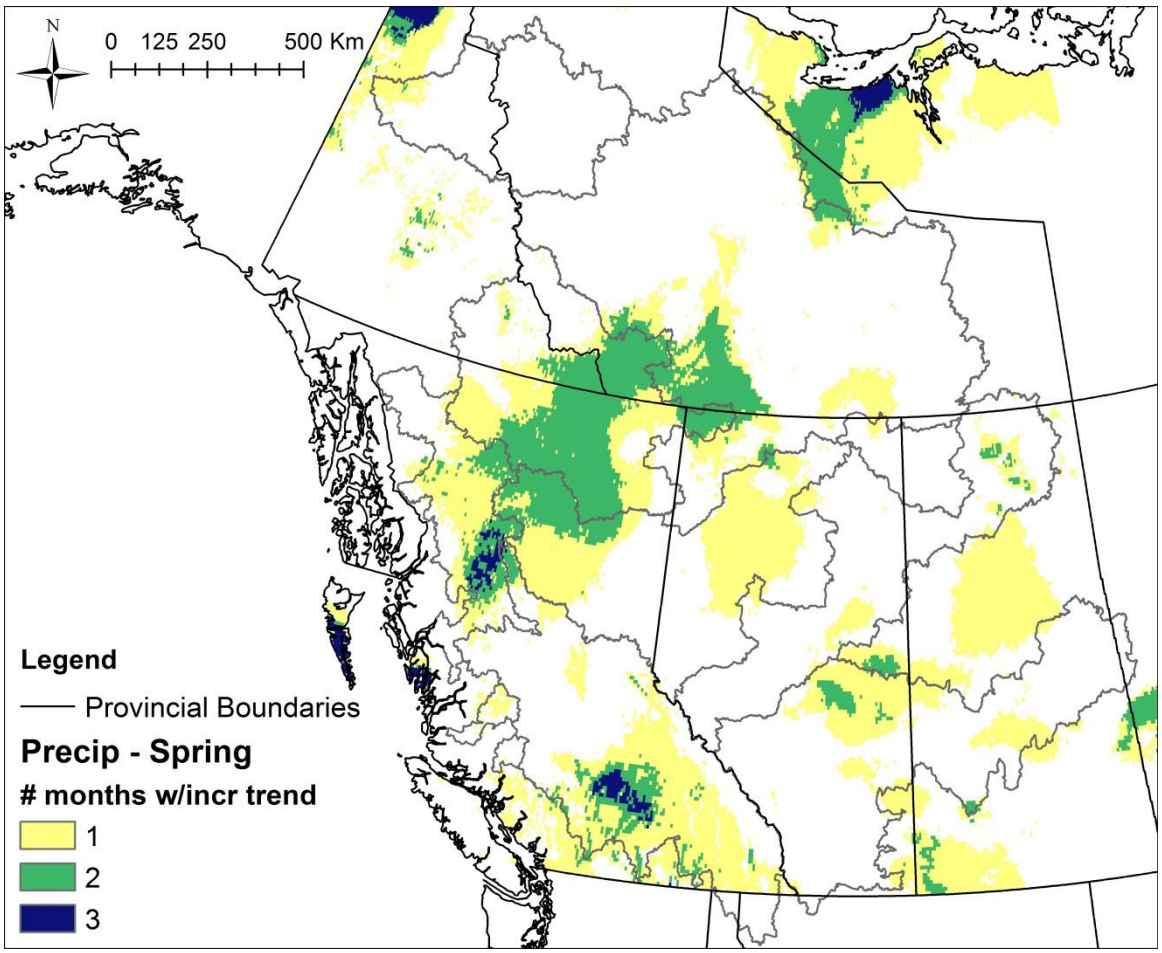

Figure A.62. Precipitation increasing trend persistence during spring (April to June). Colour corresponds to number of months with decreasing trend.

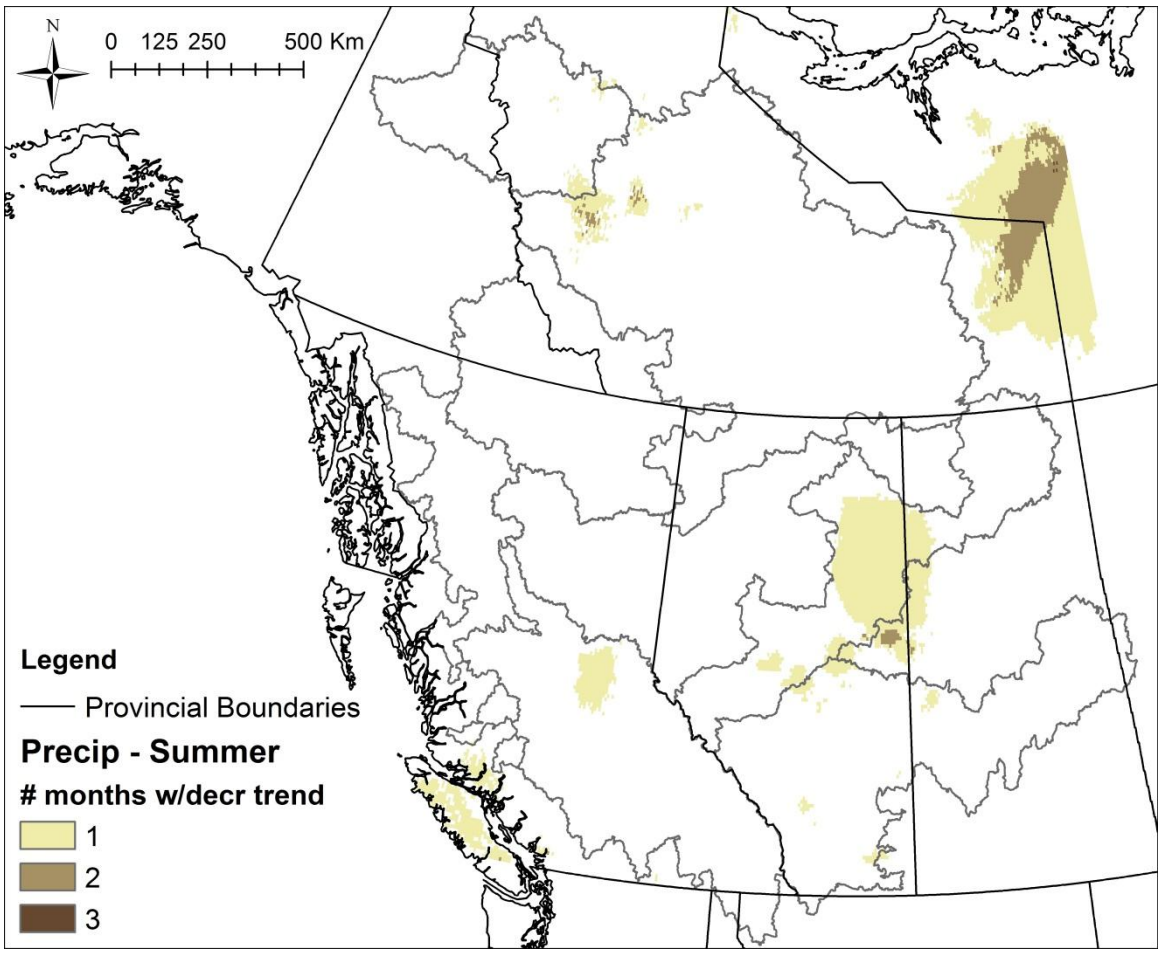

Figure A.63. Precipitation decreasing trend persistence during summer (July to September). Colour corresponds to number of months with decreasing trend.

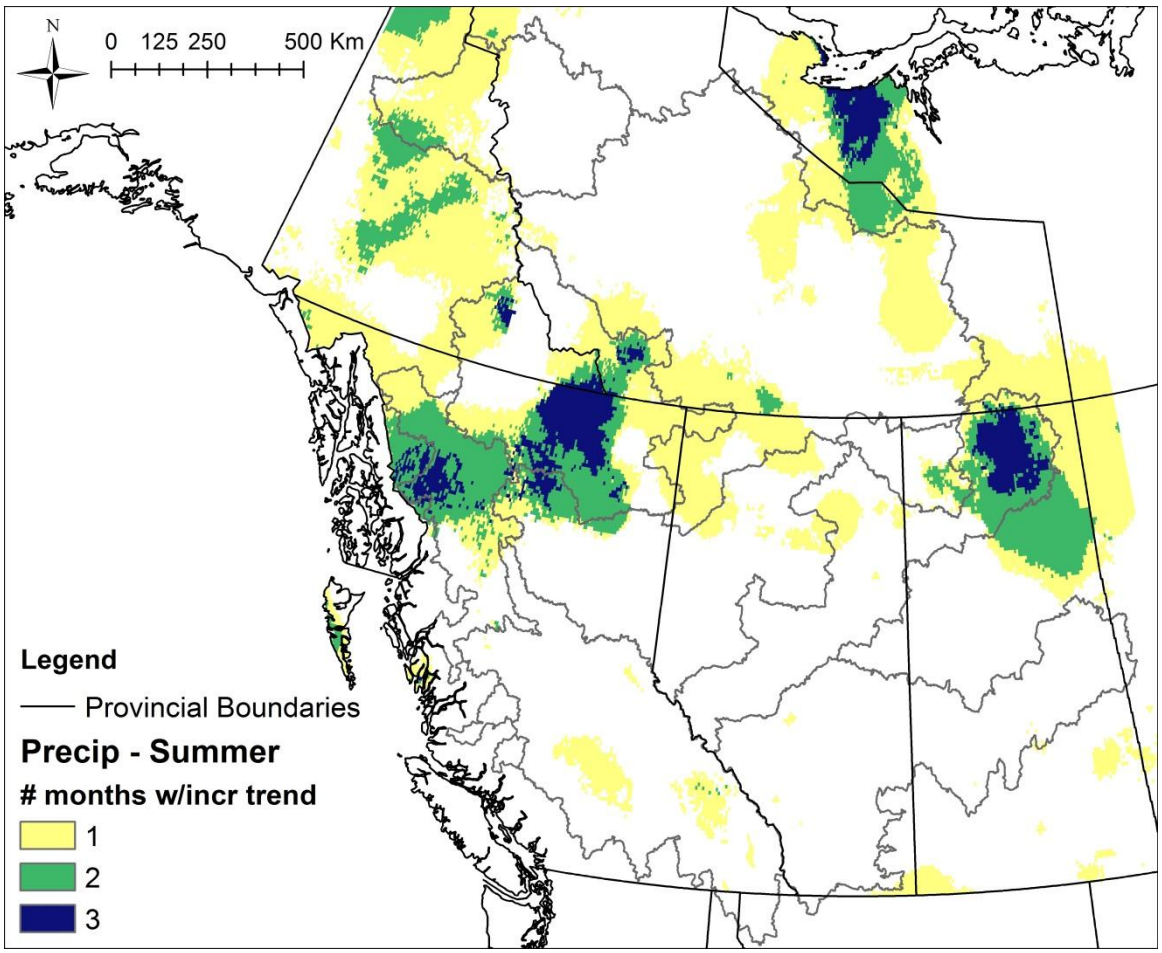

Figure A.64. Precipitation increasing trend persistence during summer (July to September). Colour corresponds to number of months with decreasing trend.

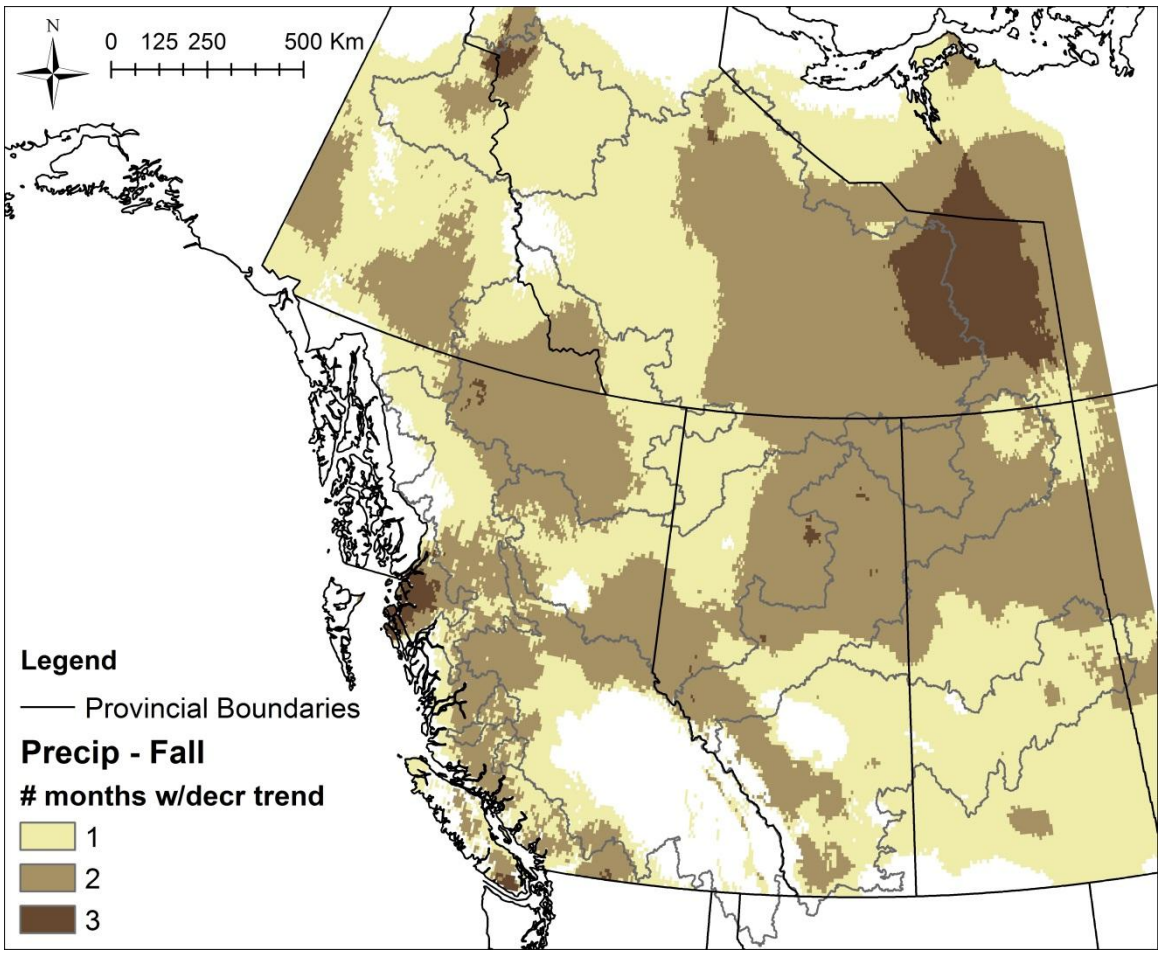

Figure A.65. Precipitation decreasing trend persistence during fall (October to December). Colour corresponds to number of months with decreasing trend.

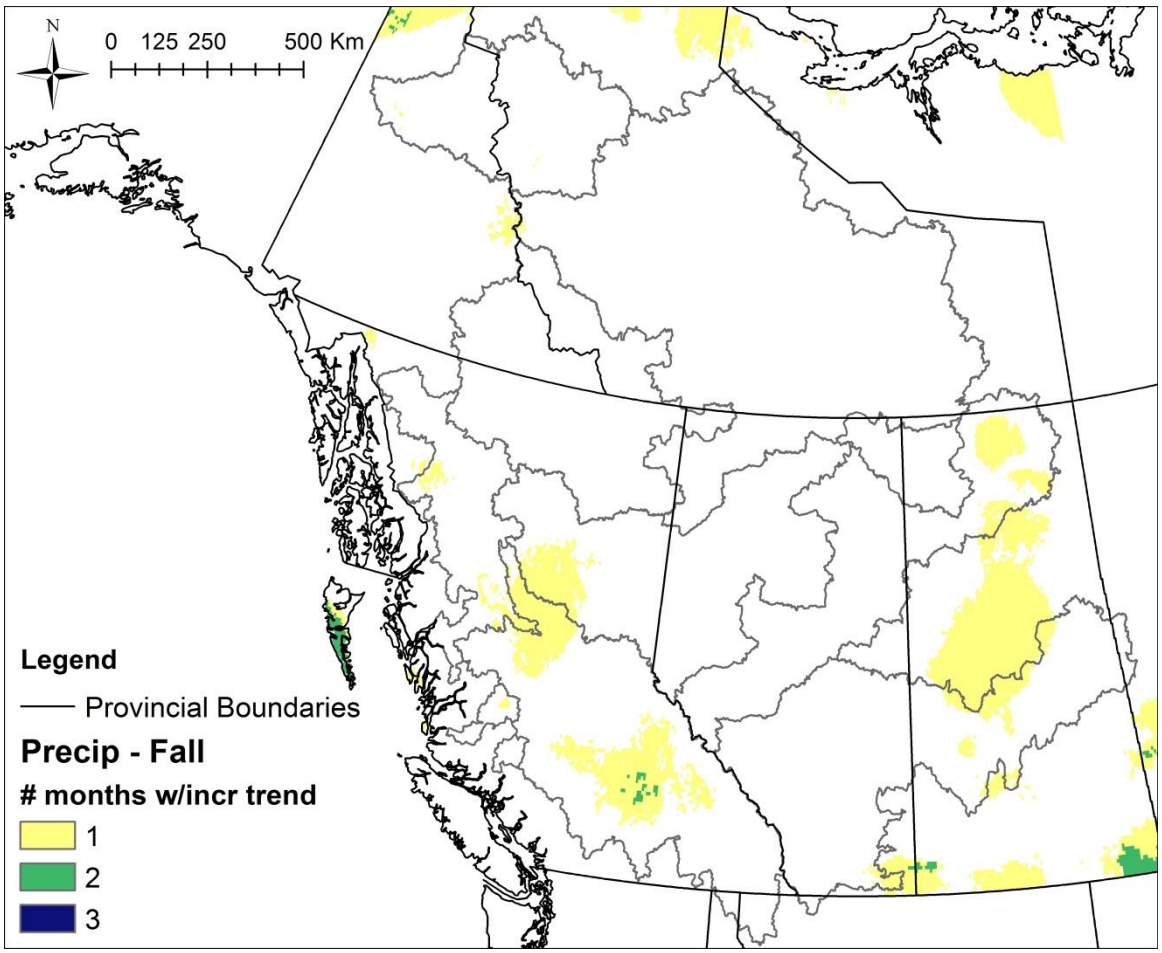

Figure A.66. Precipitation increasing trend persistence during fall (October to December). Colour corresponds to number of months with decreasing trend.

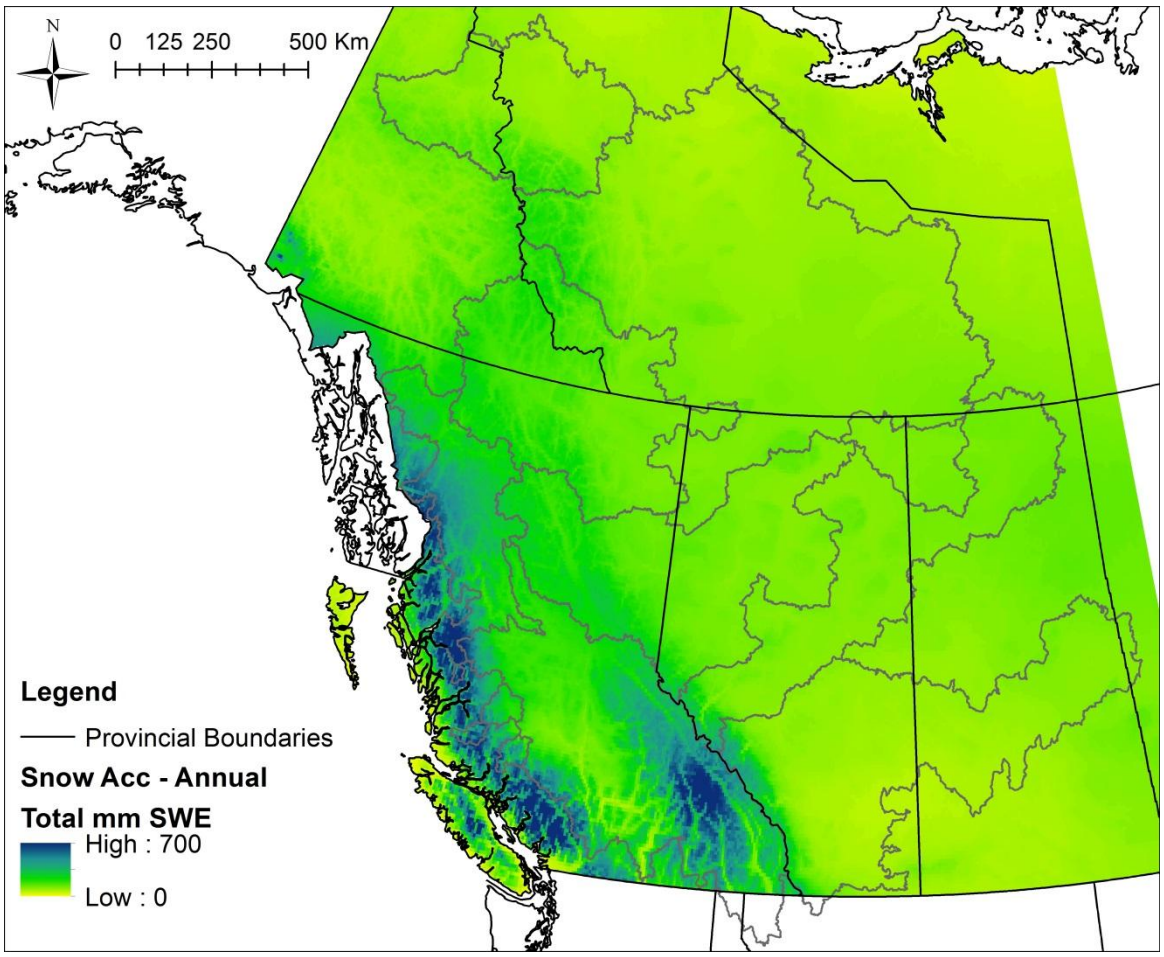

Figure A.67. Annual total snow accumulation in mm SWE, from 1950-2010. Only trends significant at 10% or better are shown.

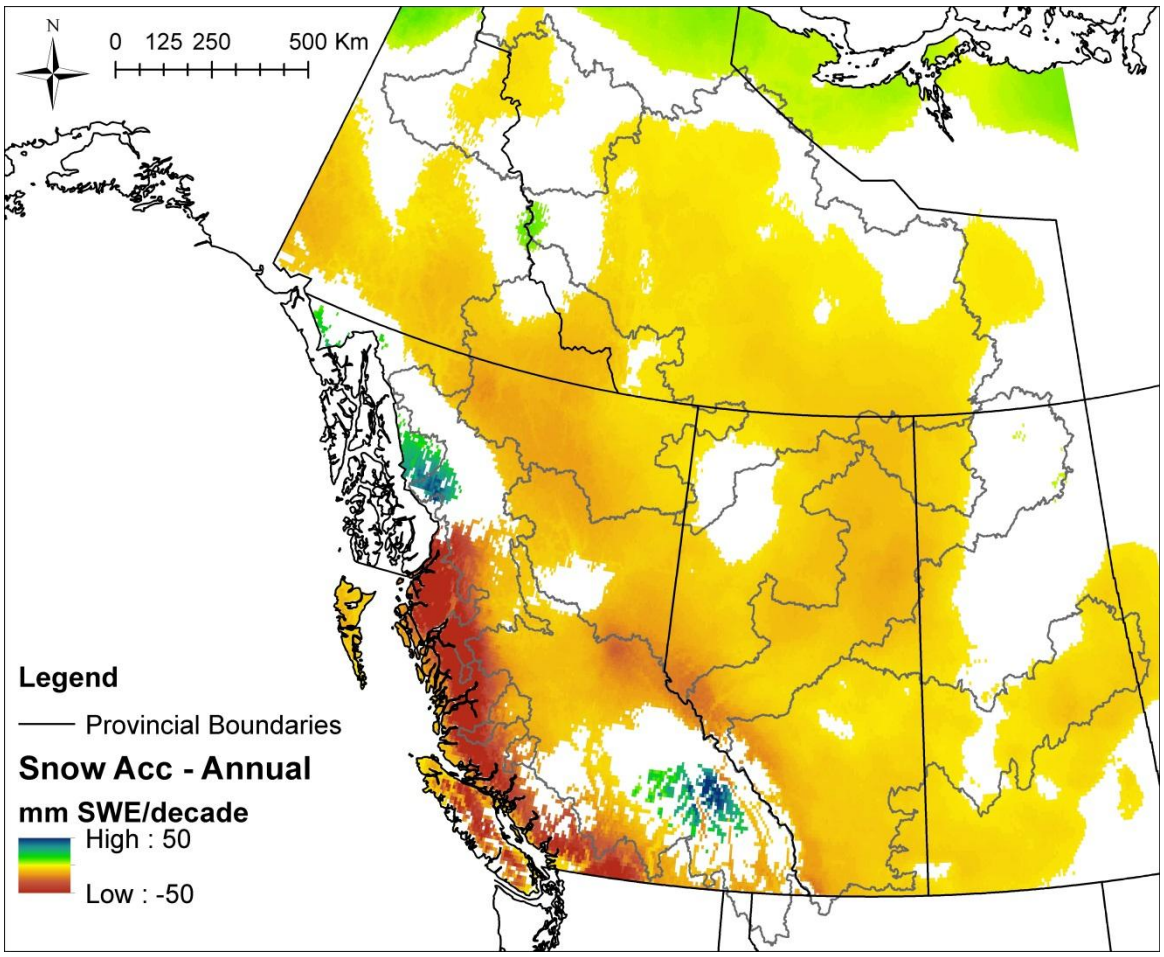

Figure A.68. Annual total snow accumulation trend results showing rate of change in mm SWE/decade, from 1950-2010. Only trends significant at 10% or better are shown.

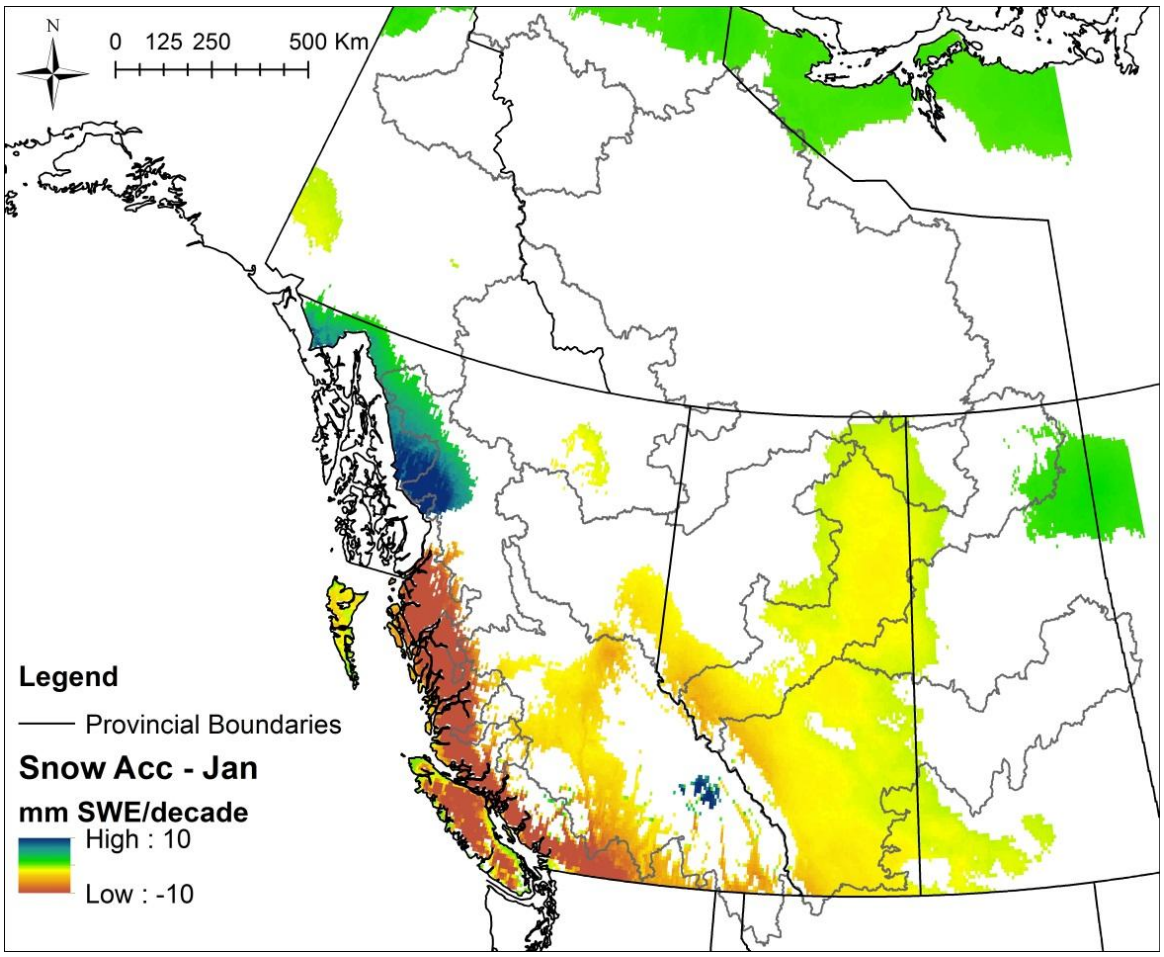

Figure A.69. January snow accumulation trend results showing rate of change in mm SWE/decade, from 1950-2010. Only trends significant at 10% or better are shown.

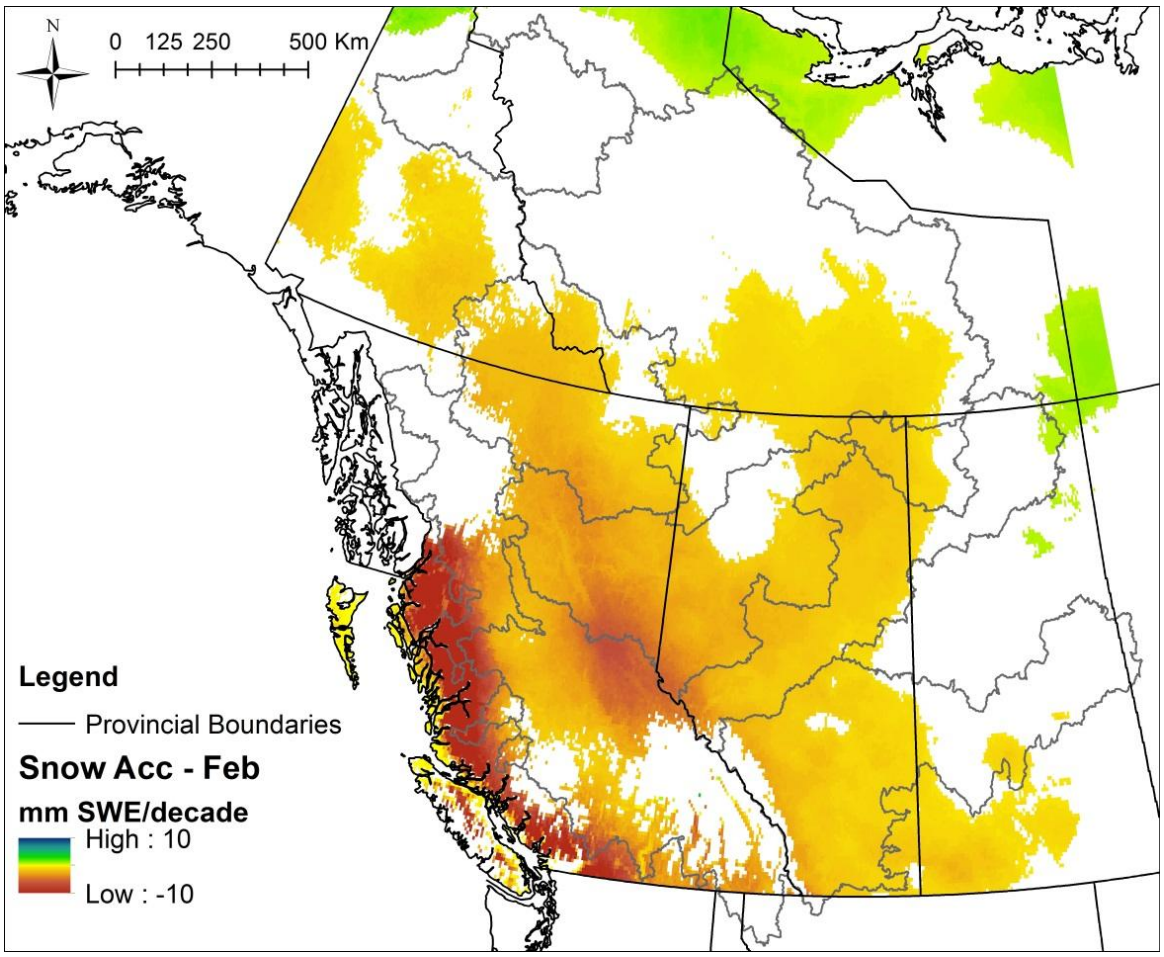

Figure A.70. February snow accumulation trend results showing rate of change in mm SWE/decade, from 1950-2010. Only trends significant at 10% or better are shown.

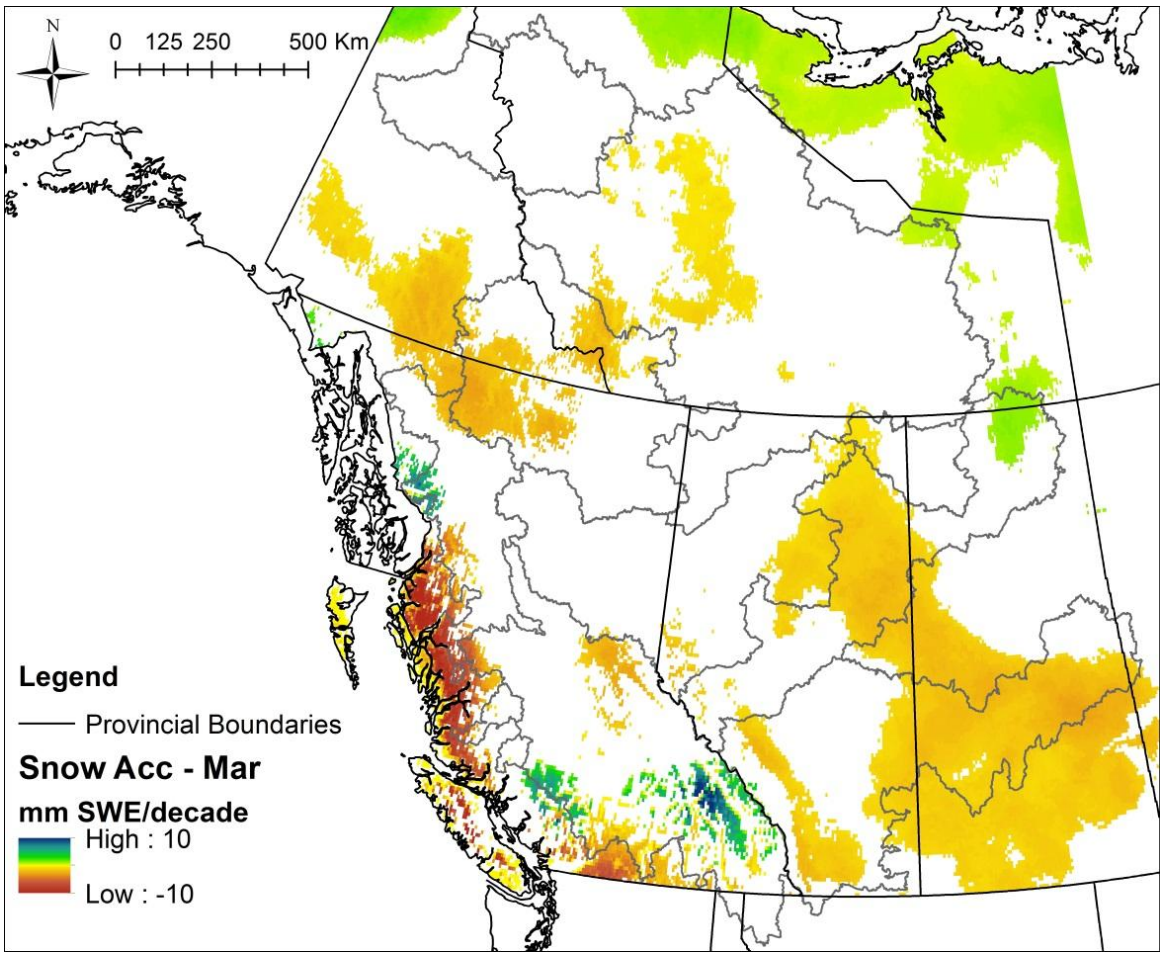

Figure A.71. March snow accumulation trend results showing rate of change in mm SWE/decade, from 1950-2010. Only trends significant at 10% or better are shown.

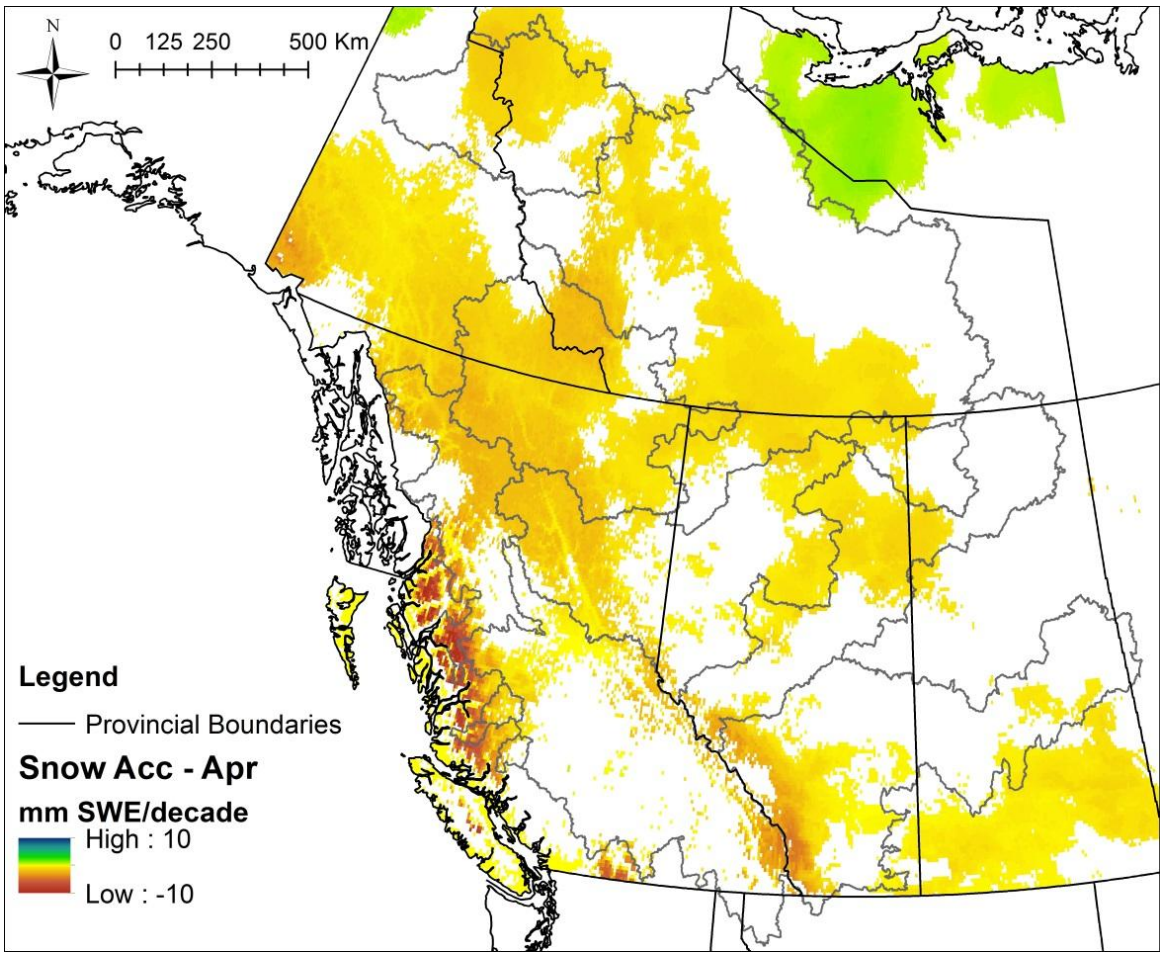

Figure A.72. April snow accumulation trend results showing rate of change in mm SWE/decade, from 1950-2010. Only trends significant at 10% or better are shown.

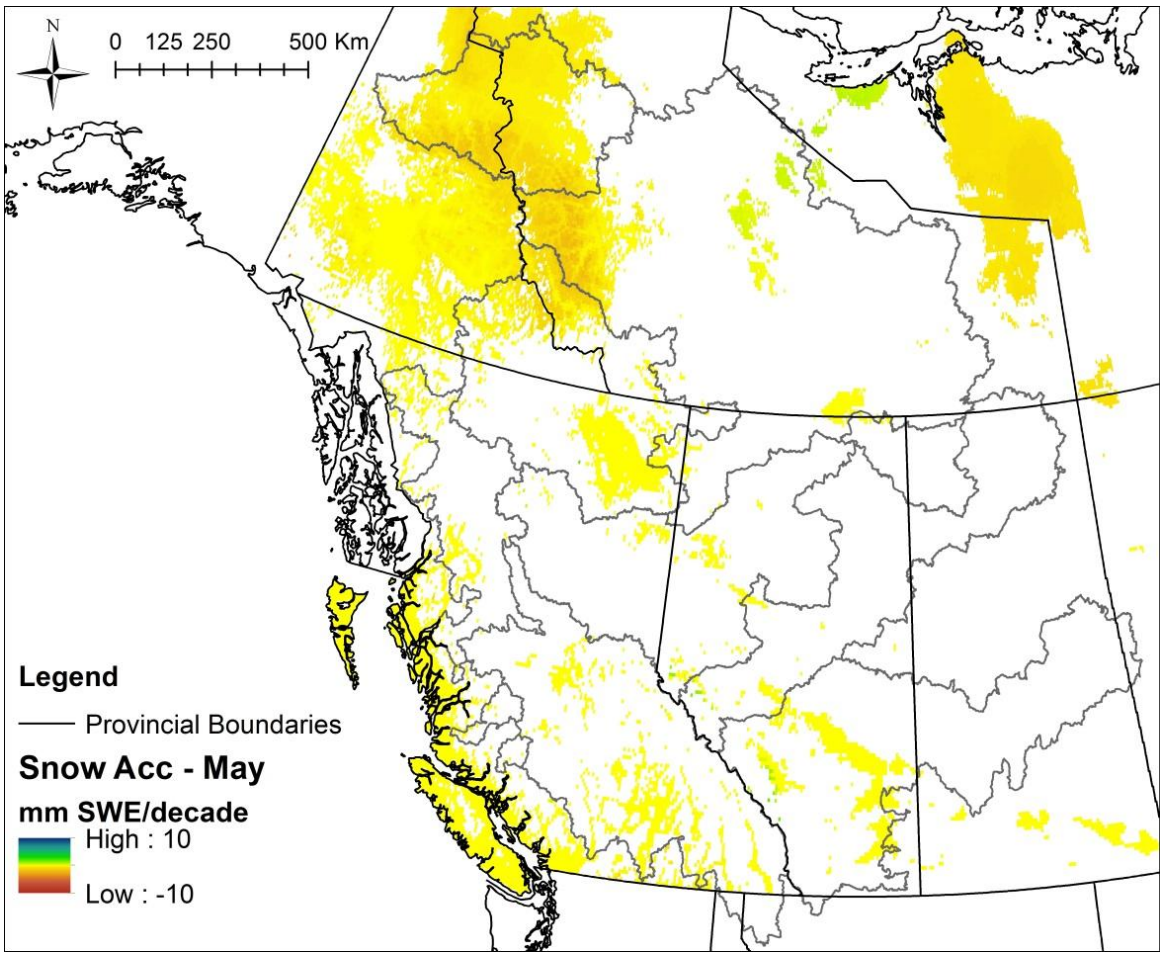

Figure A.73. May snow accumulation trend results showing rate of change in mm SWE/decade, from 1950-2010. Only trends significant at 10% or better are shown.

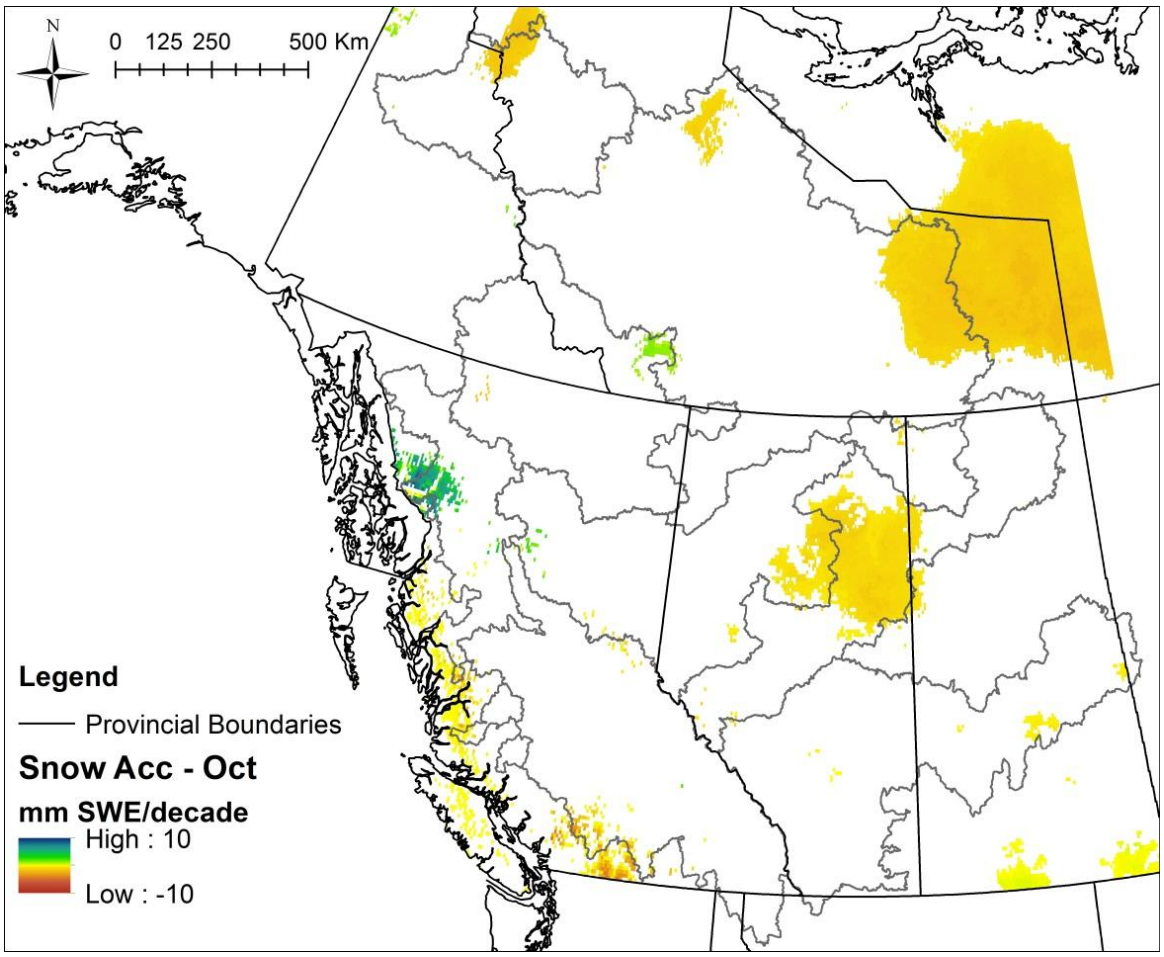

Figure A.74. October snow accumulation trend results showing rate of change in mm SWE/decade, from 1950-2010. Only trends significant at 10% or better are shown.

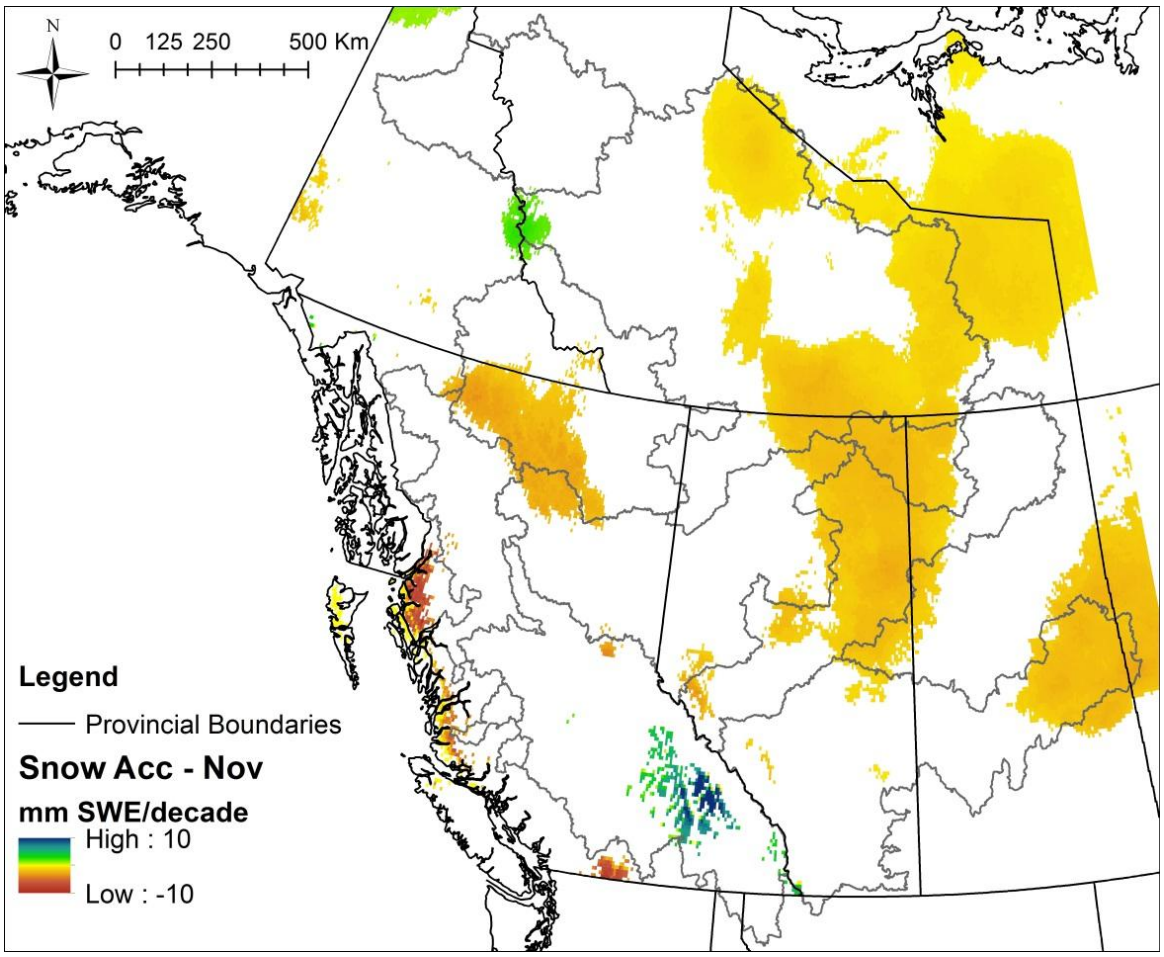

Figure A.75. November snow accumulation trend results showing rate of change in mm SWE/decade, from 1950-2010. Only trends significant at 10% or better are shown.

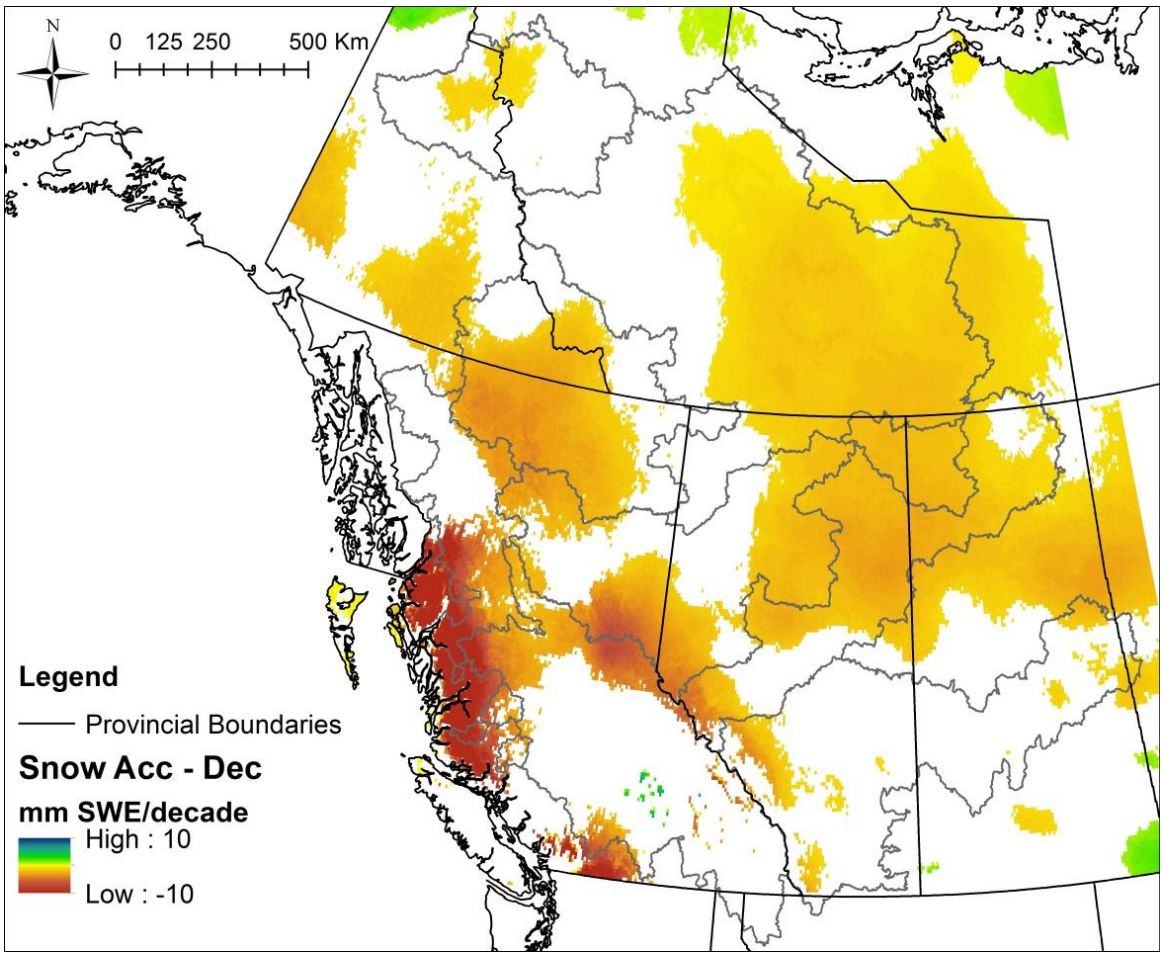

Figure A.76. December snow accumulation trend results showing rate of change in mm SWE/decade, from 1950-2010. Only trends significant at 10% or better are shown.

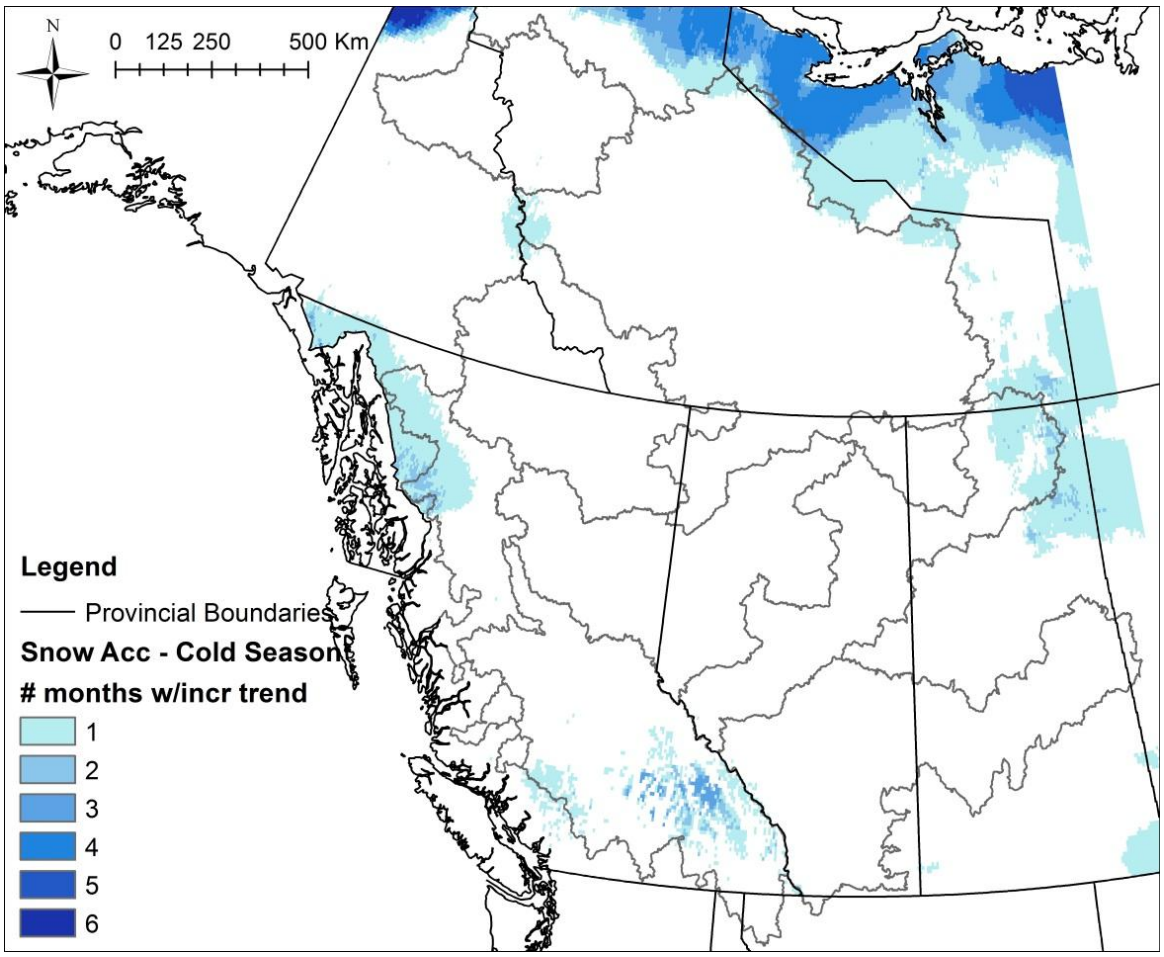

Figure A.77. Snow accumulation increasing trend persistence through the cold season (November to April). Colour corresponds to number of months with increasing trend.

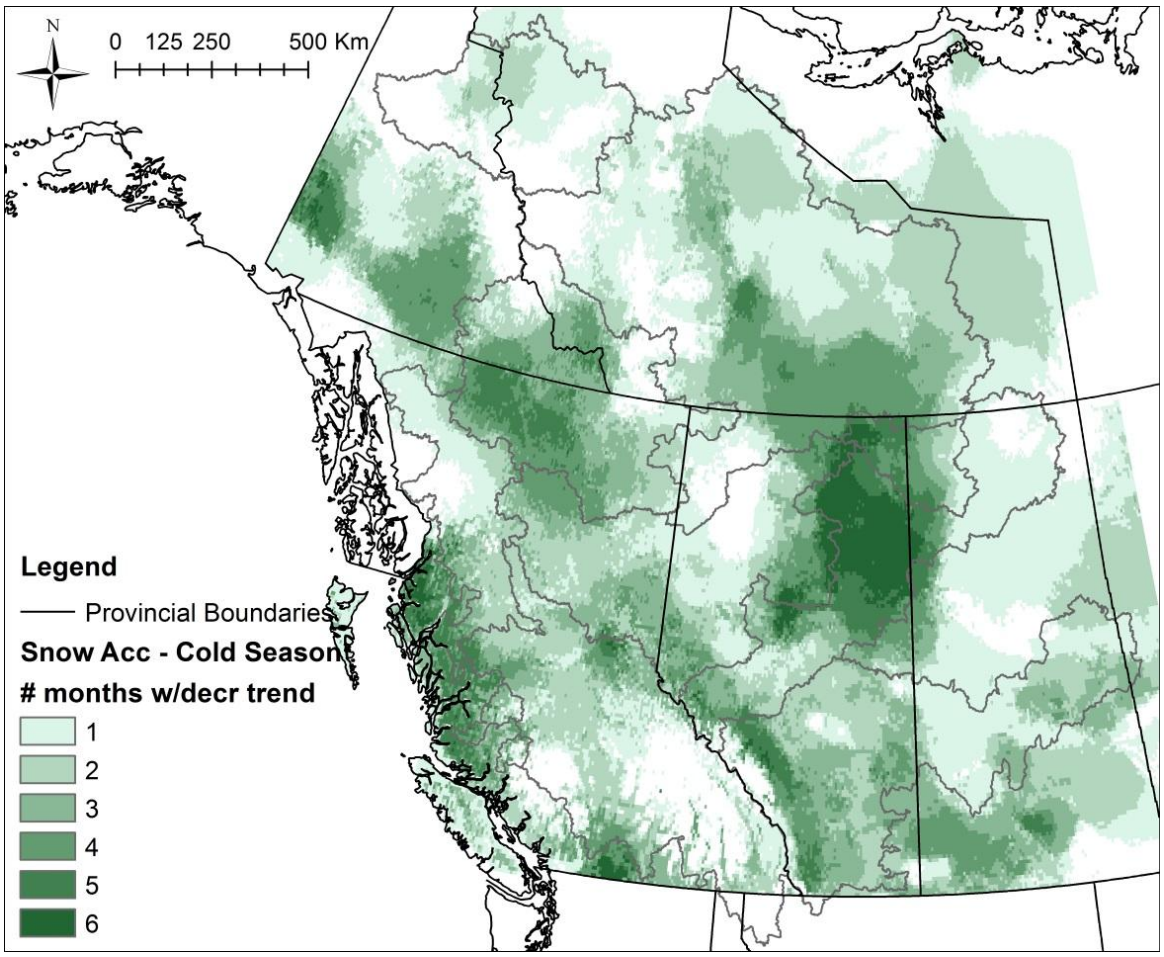

Figure A.78. Snow accumulation decreasing trend persistence through the cold season (November to April). Colour corresponds to number of months with decreasing trend.

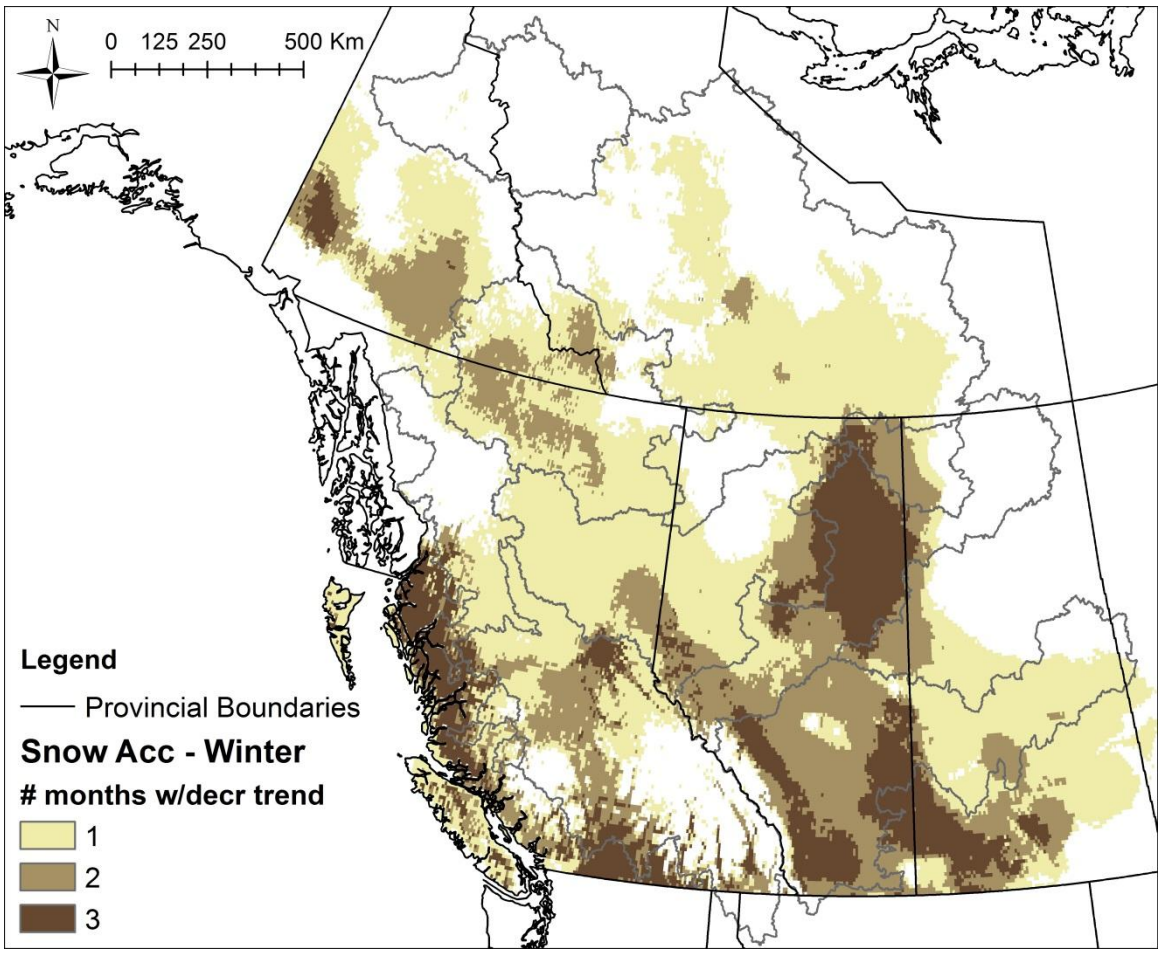

Figure A.79. Snow accumulation decreasing trend persistence during winter (January to March). Colour corresponds to number of months with decreasing trend.

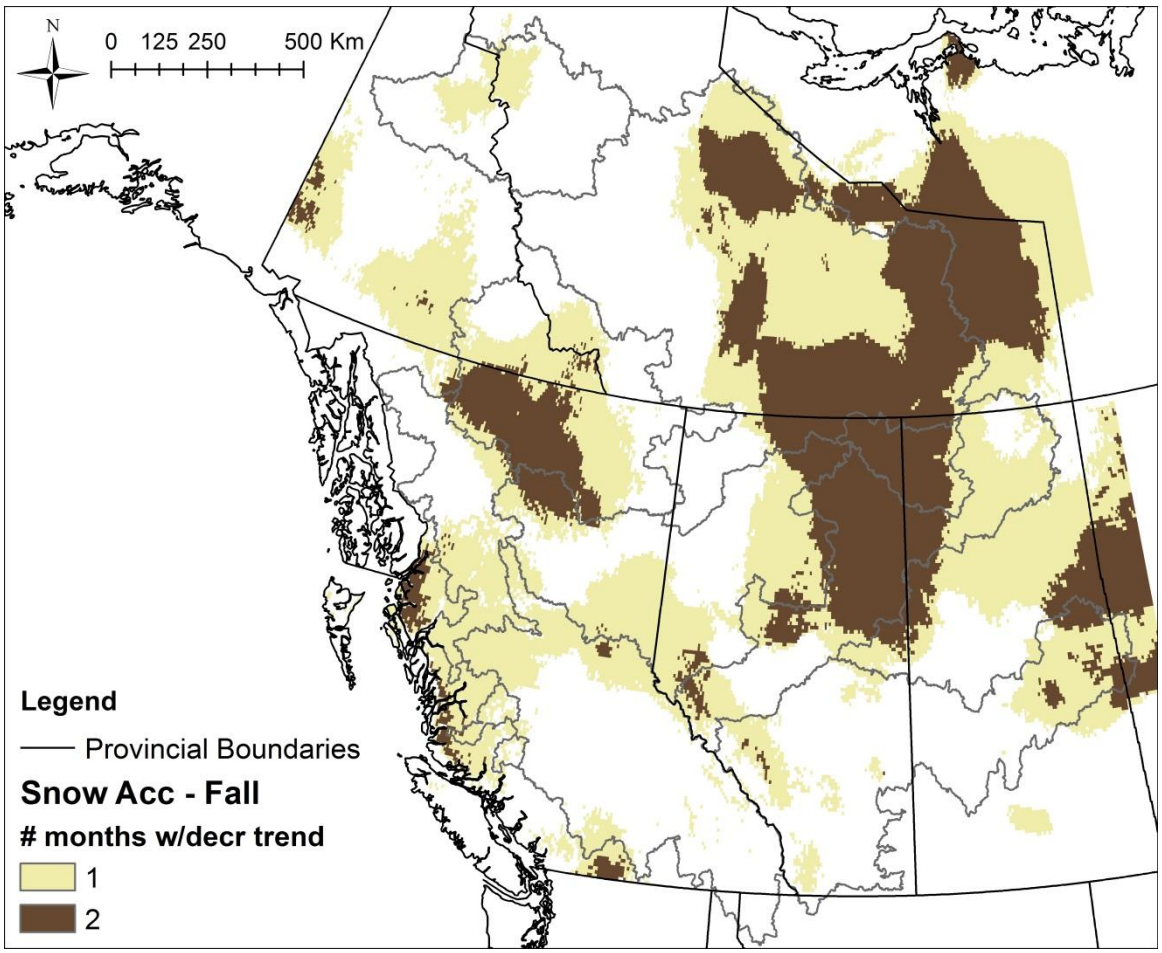

Figure A.80. Snow accumulation decreasing trend persistence during fall (October to December). Colour corresponds to number of months with decreasing trend.

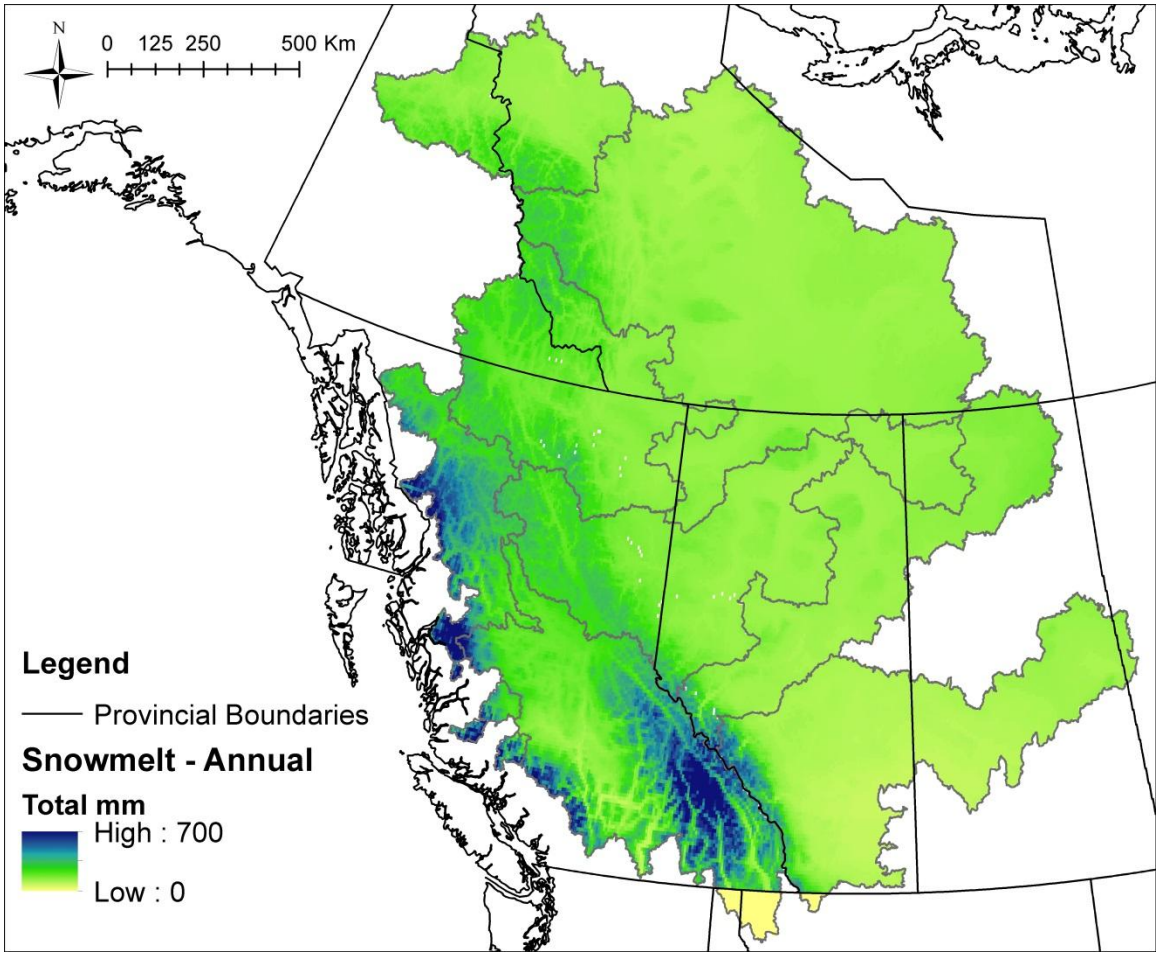

Figure A.81. Annual total snowmelt in mm, from 1950-2010. Only trends significant at 10% or better are shown.

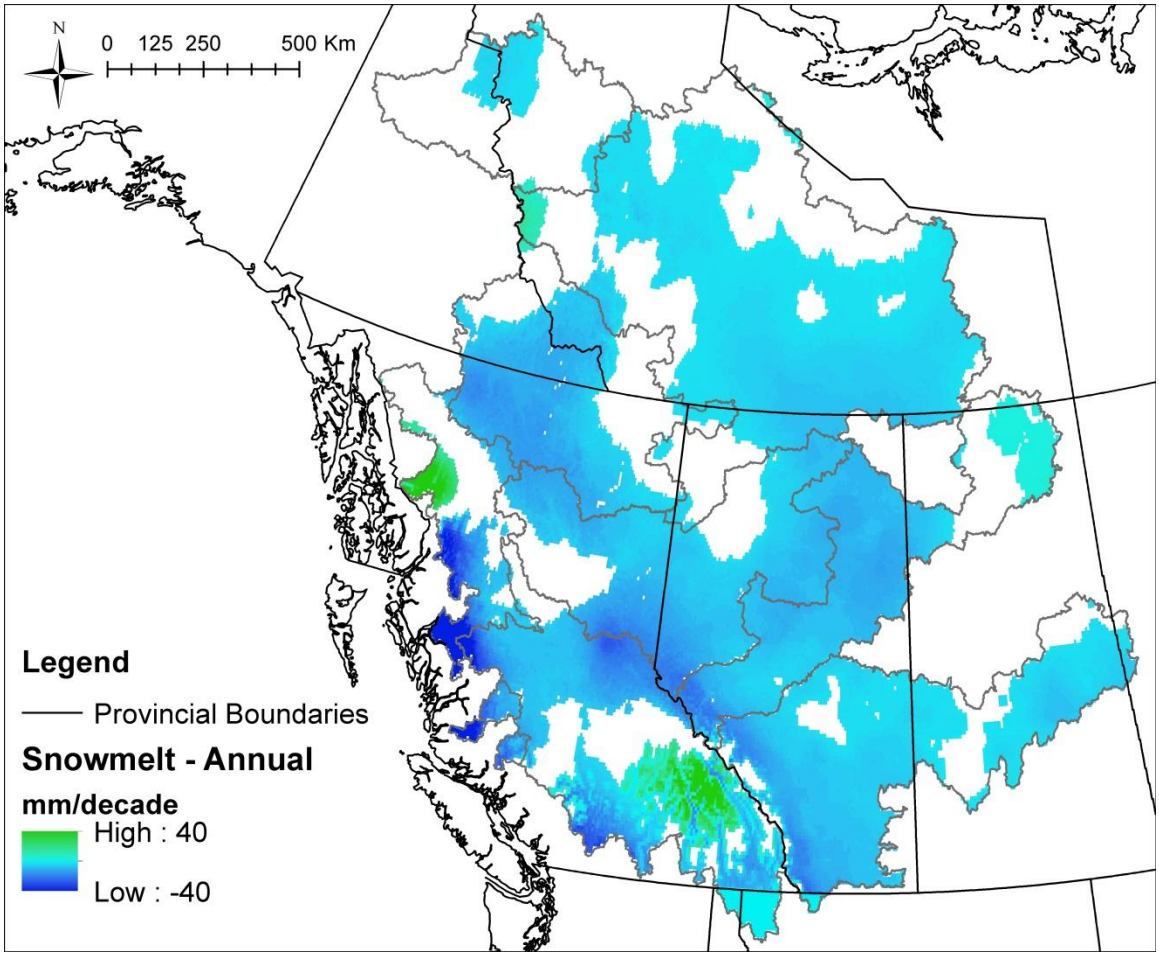

Figure A.82. Annual total snowmelt trend results showing rate of change in mm/decade, from 1950-2010. Only trends significant at 10% or better are shown.

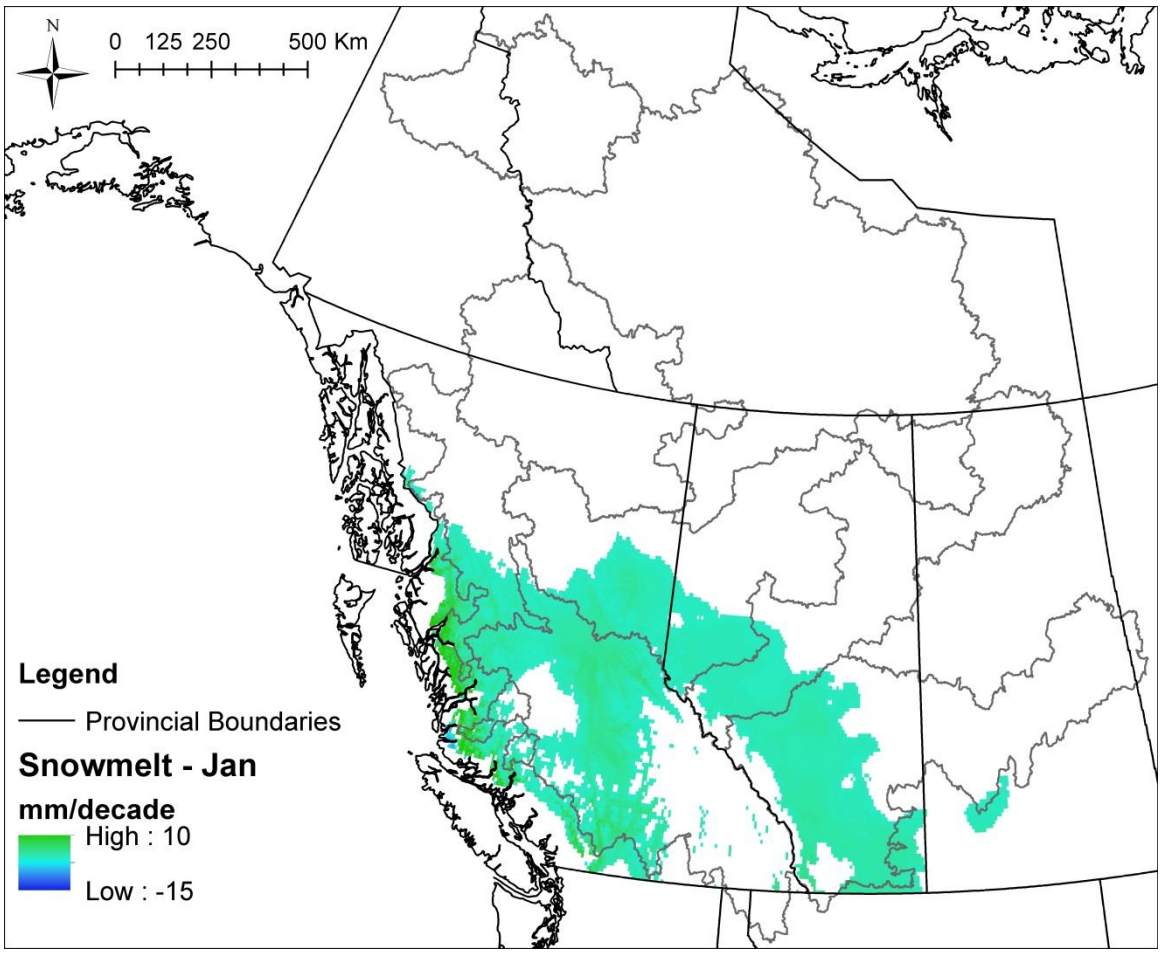

Figure A.83. January snowmelt trend results showing rate of change in mm/decade, from 1950-2010. Only trends significant at 10% or better are shown.

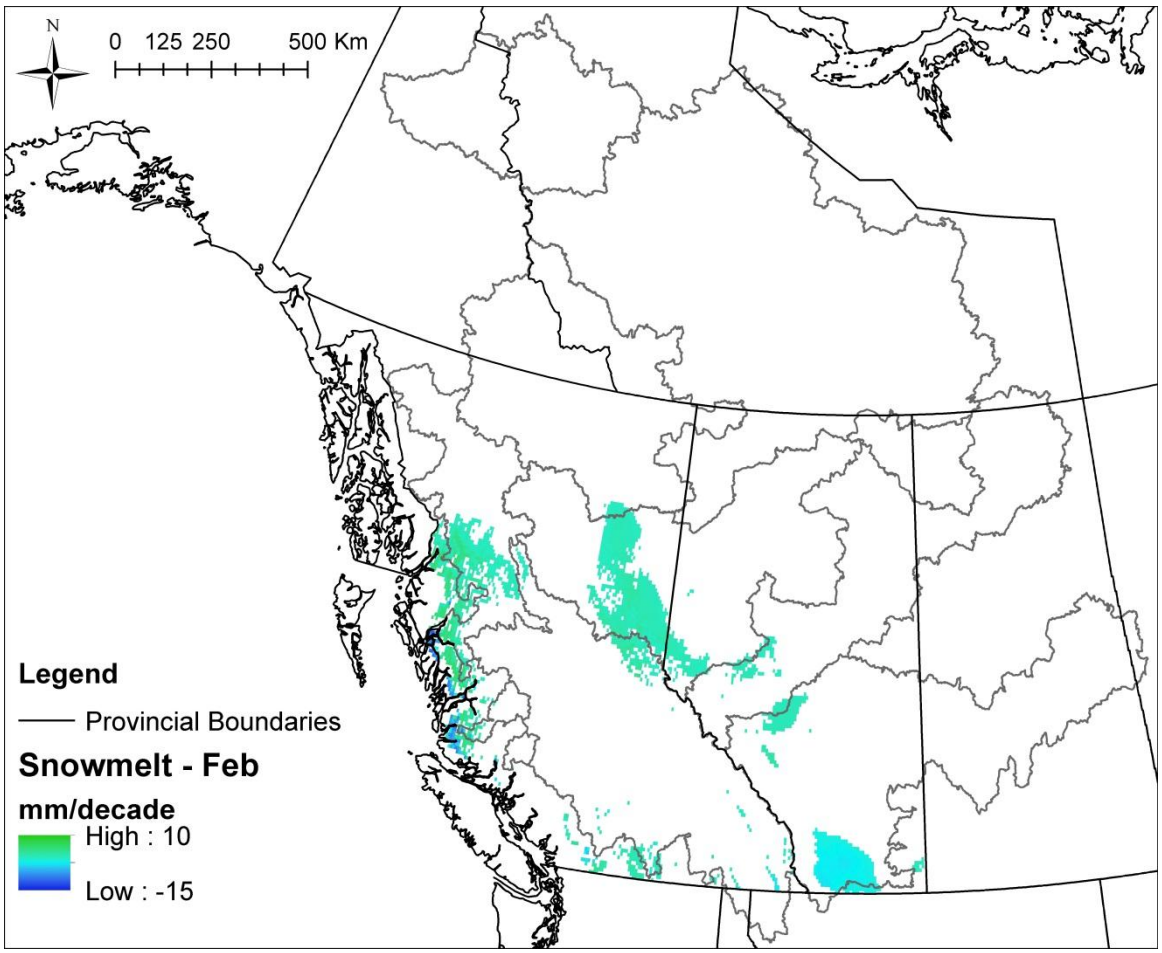

Figure A.84. February snowmelt trend results showing rate of change in mm/decade, from 1950-2010. Only trends significant at 10% or better are shown.

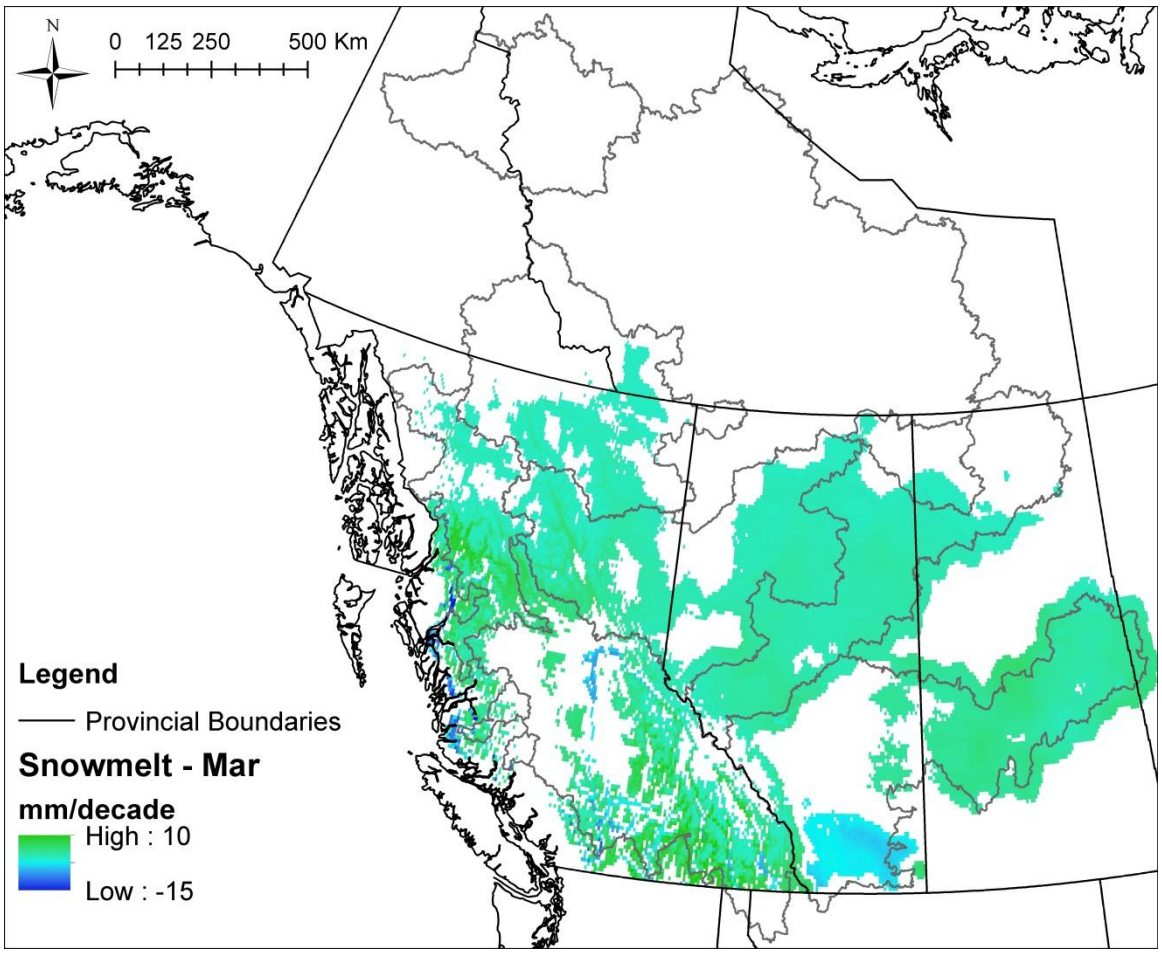

Figure A.85. March snowmelt trend results showing rate of change in mm/decade, from 1950-2010. Only trends significant at 10% or better are shown.

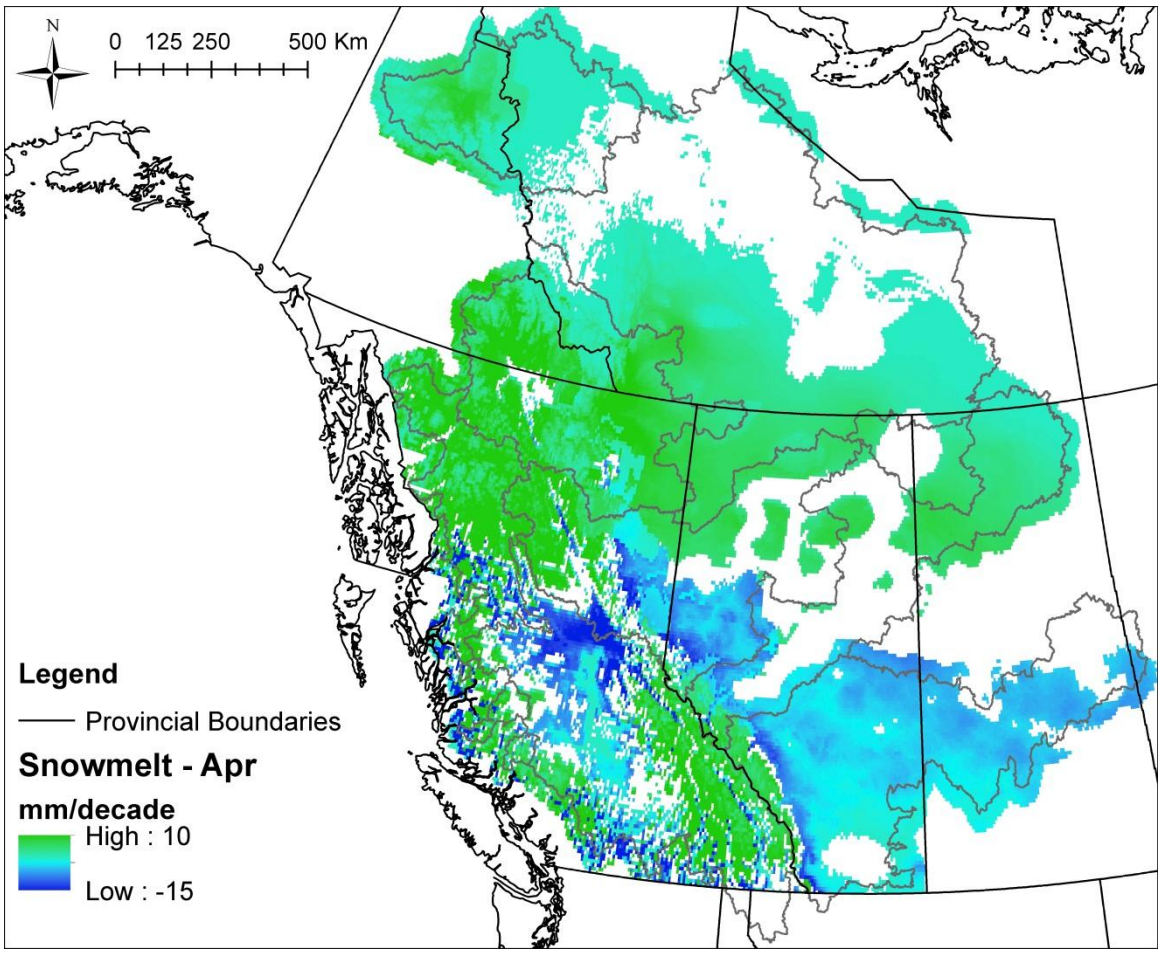

Figure A.86. April snowmelt trend results showing rate of change in mm/decade, from 1950-2010. Only trends significant at 10% or better are shown.

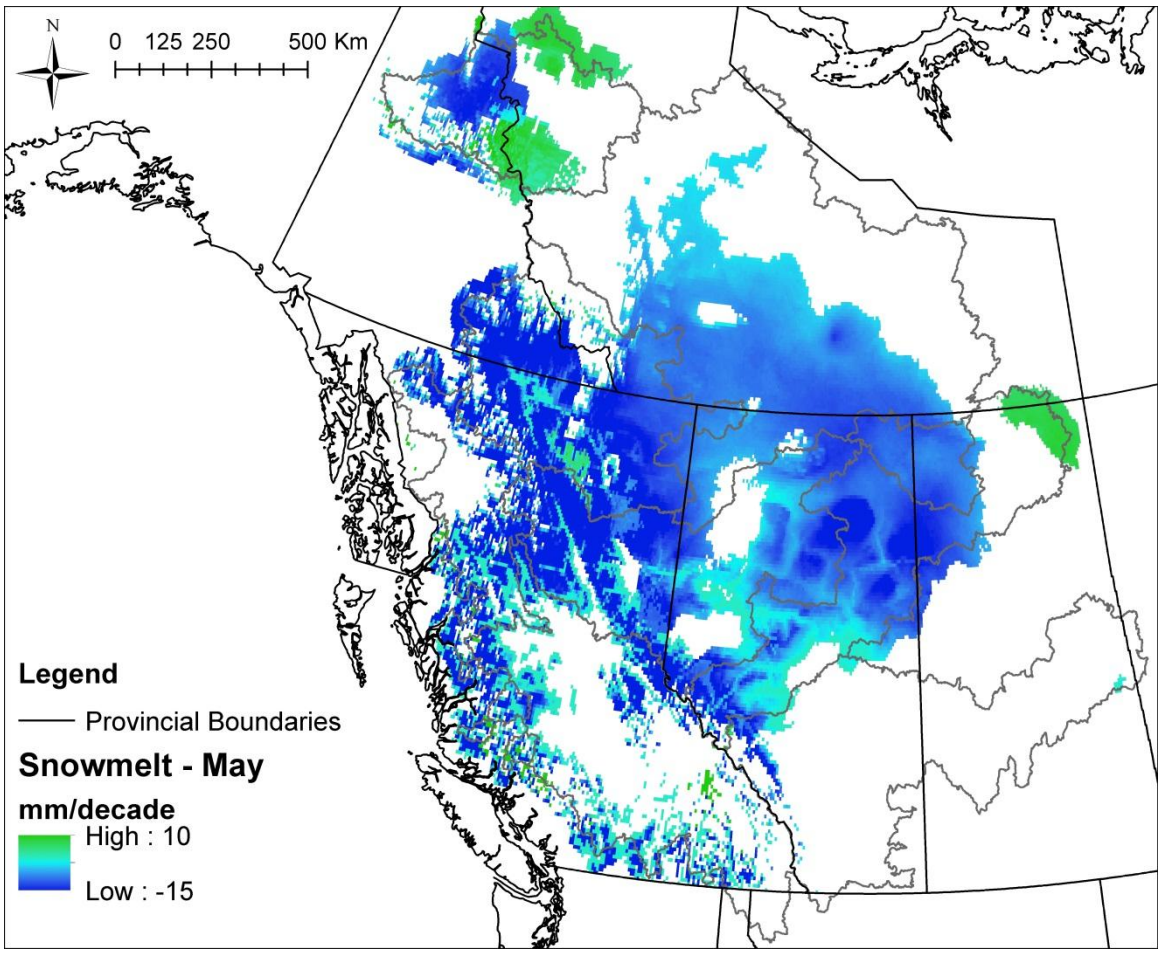

Figure A.87. May snowmelt trend results showing rate of change in mm/decade, from 1950-2010. Only trends significant at 10% or better are shown.

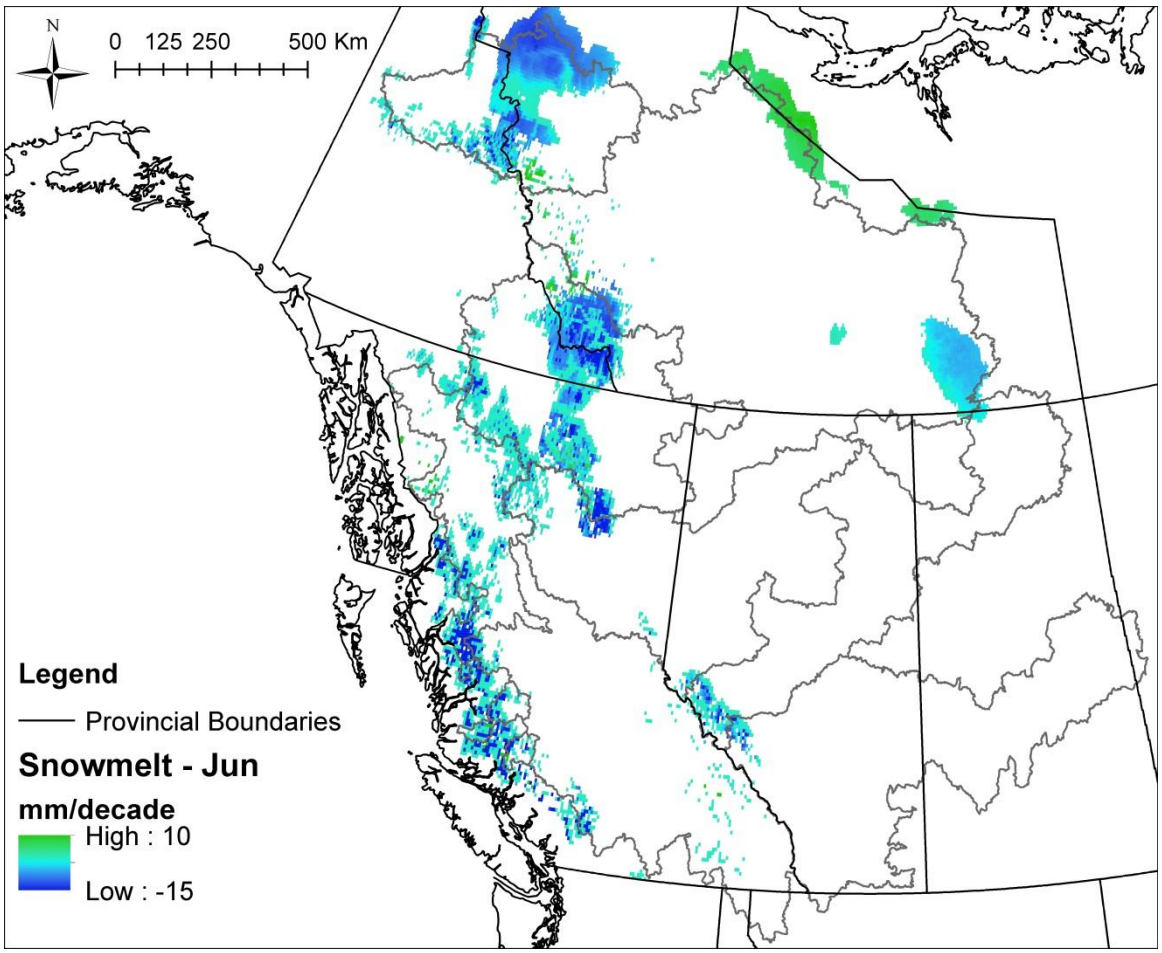

Figure A.88. June snowmelt trend results showing rate of change in mm/decade, from 1950-2010. Only trends significant at 10% or better are shown.

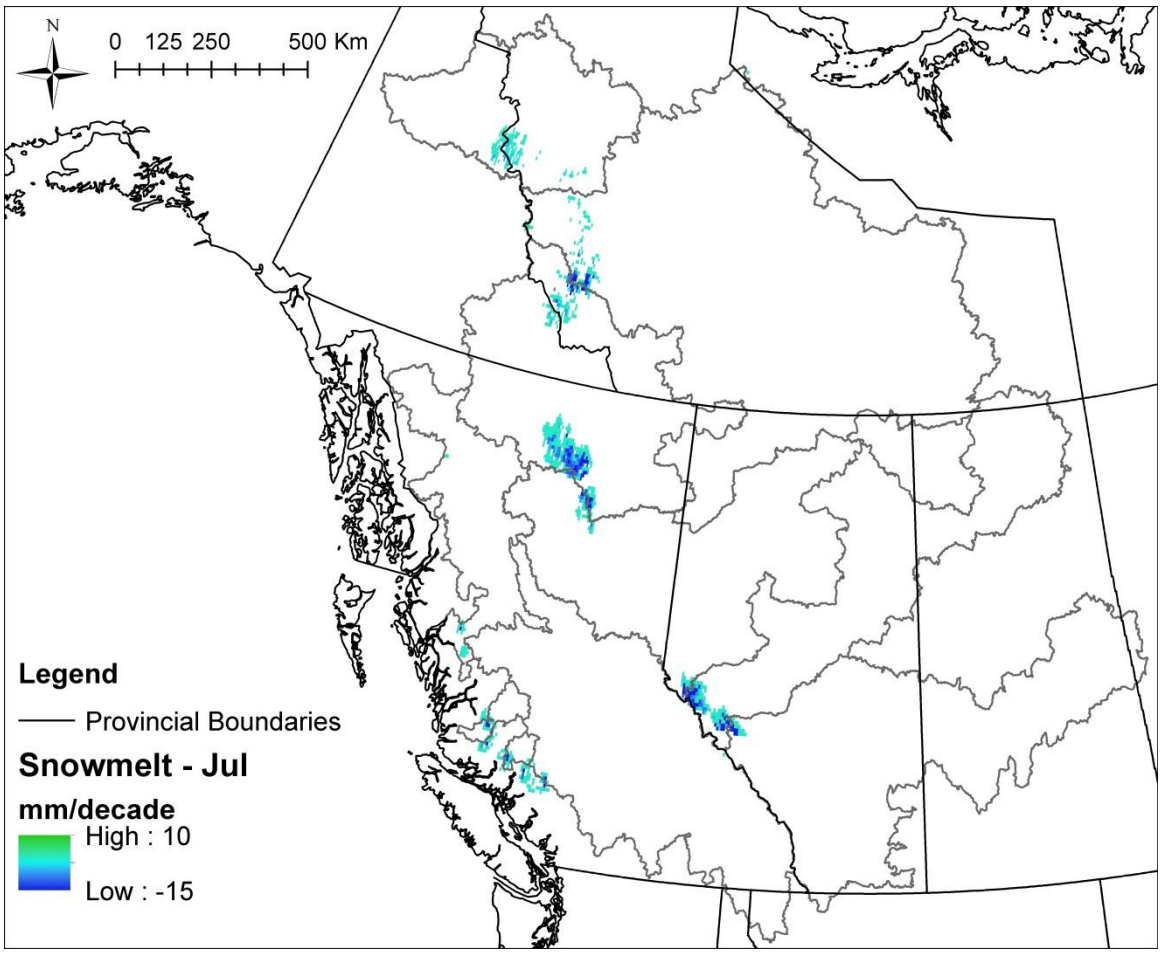

Figure A.89. July snowmelt trend results showing rate of change in mm/decade, from 1950-2010. Only trends significant at 10% or better are shown.

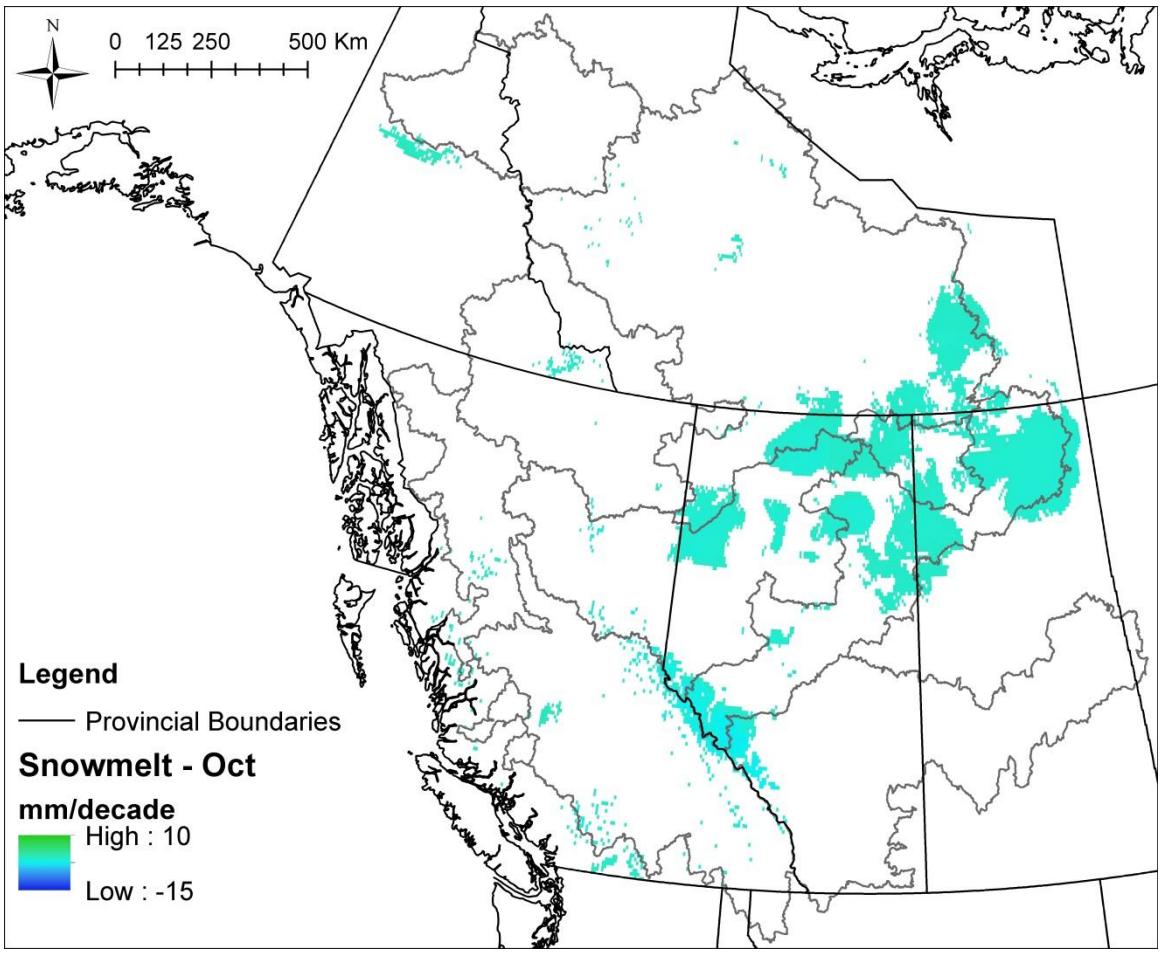

Figure A.90. October snowmelt trend results showing rate of change in mm/decade, from 1950-2010. Only trends significant at 10% or better are shown.

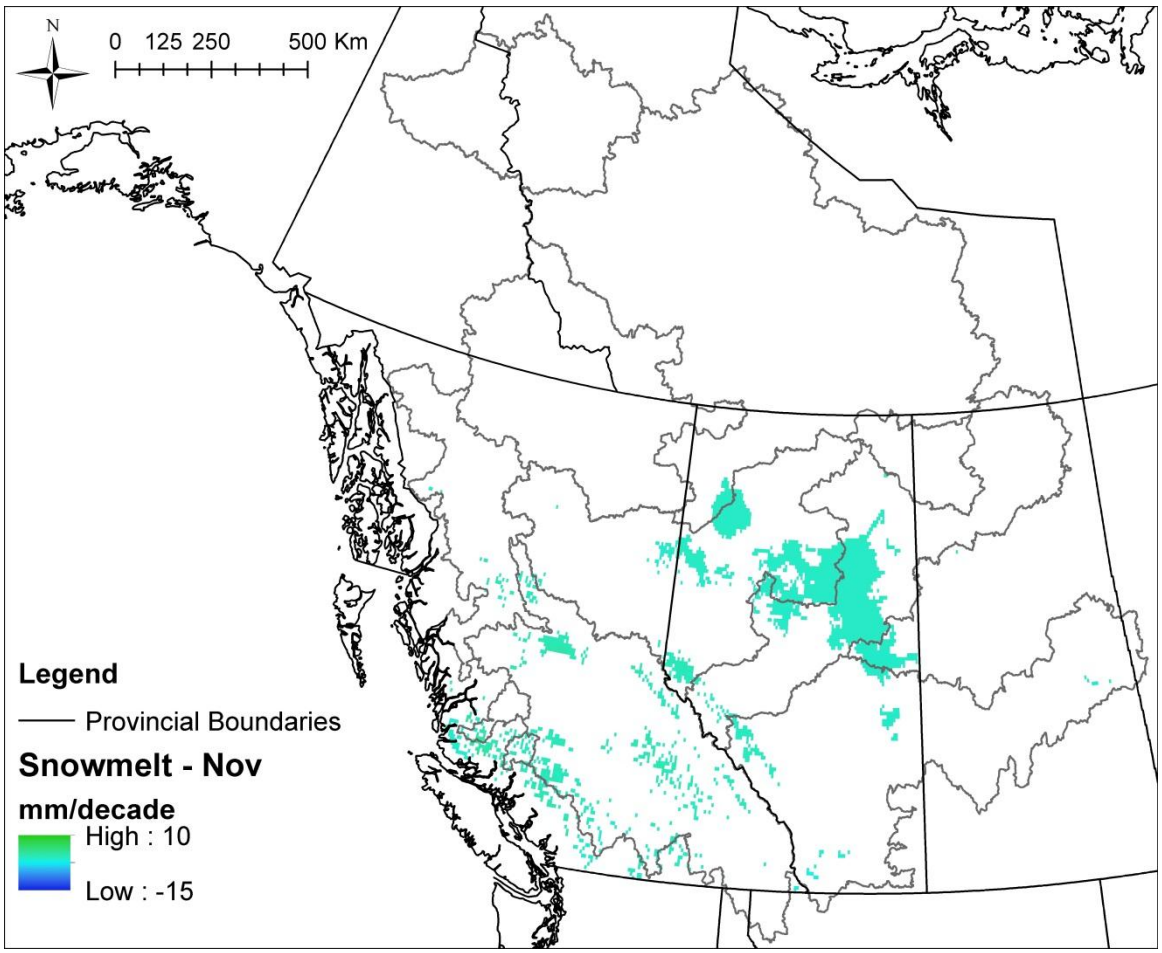

Figure A.91. November snowmelt trend results showing rate of change in mm/decade, from 1950-2010. Only trends significant at 10% or better are shown.

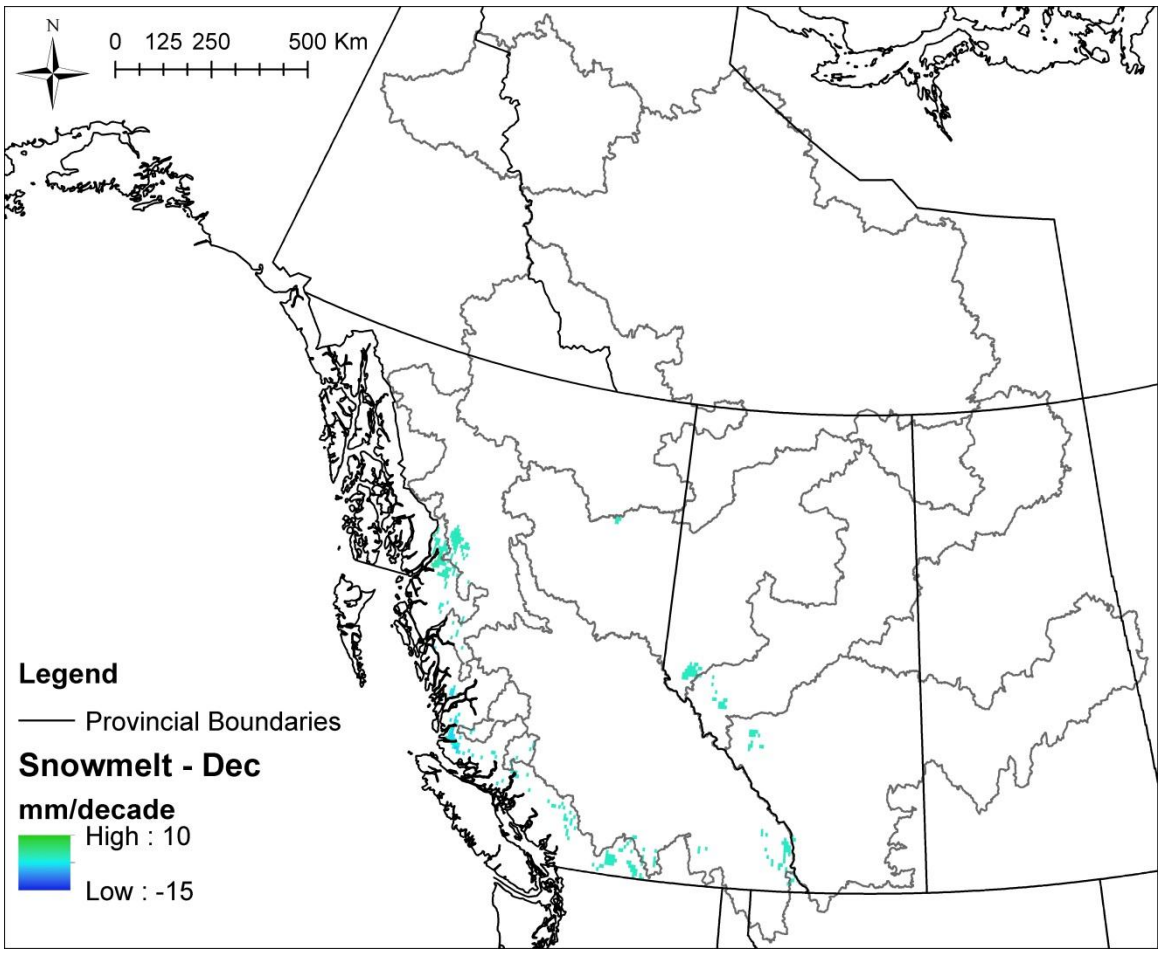

Figure A.92. December snowmelt trend results showing rate of change in mm/decade, from 1950-2010. Only trends significant at 10% or better are shown.

APPENDIX B – Supplementary material for Chapter 4

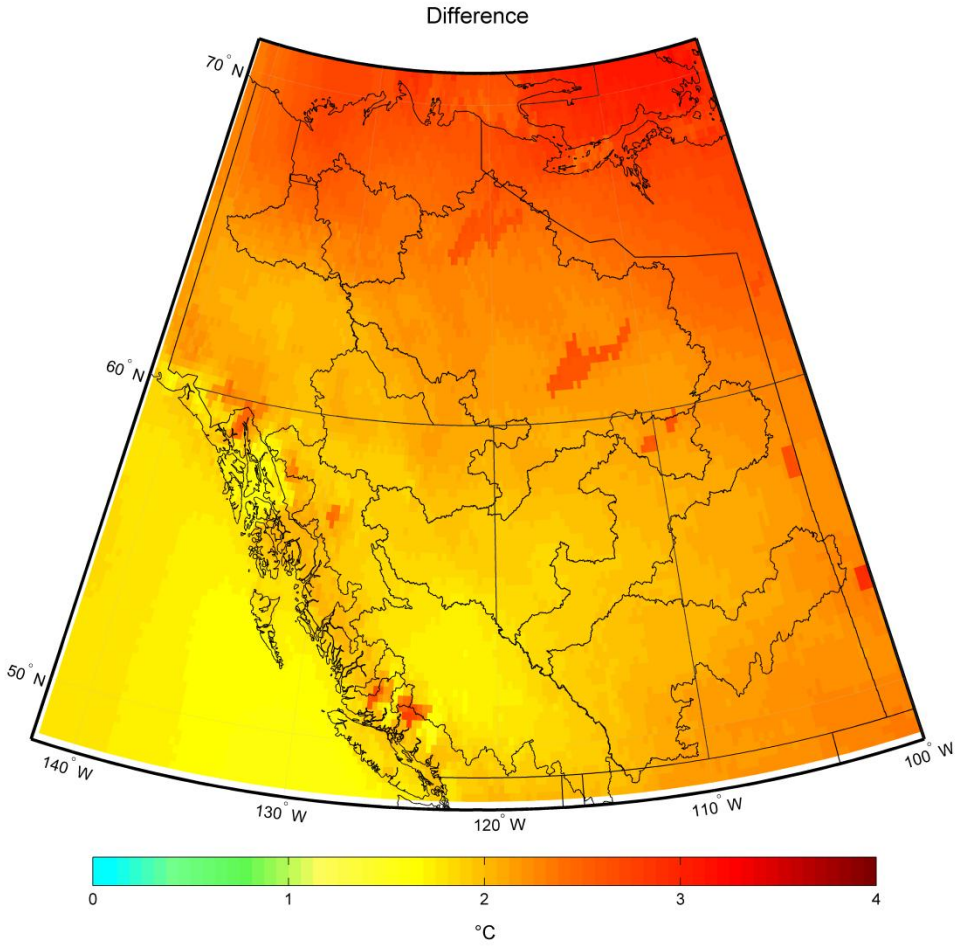

Figure B.1. Multimodel mean difference in annual Tmax between the current and future periods.

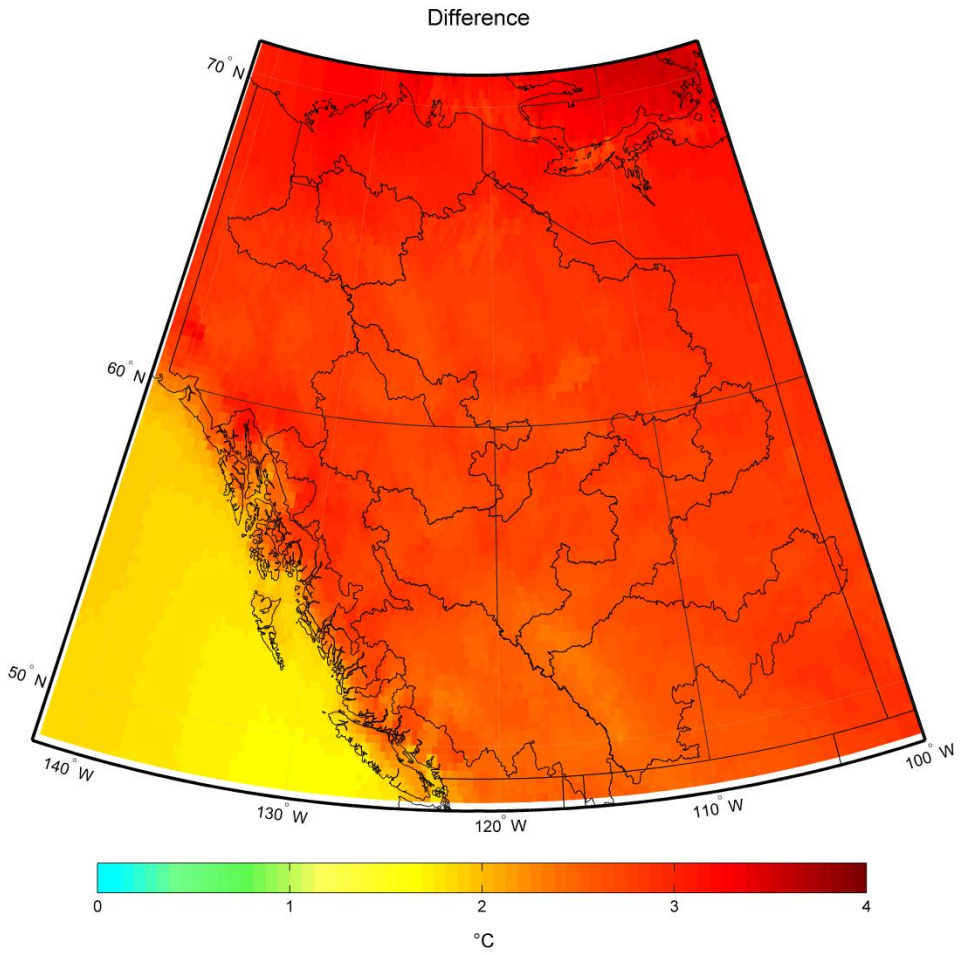

Figure B.2. Multimodel mean difference in annual Tmin between the current and future periods.

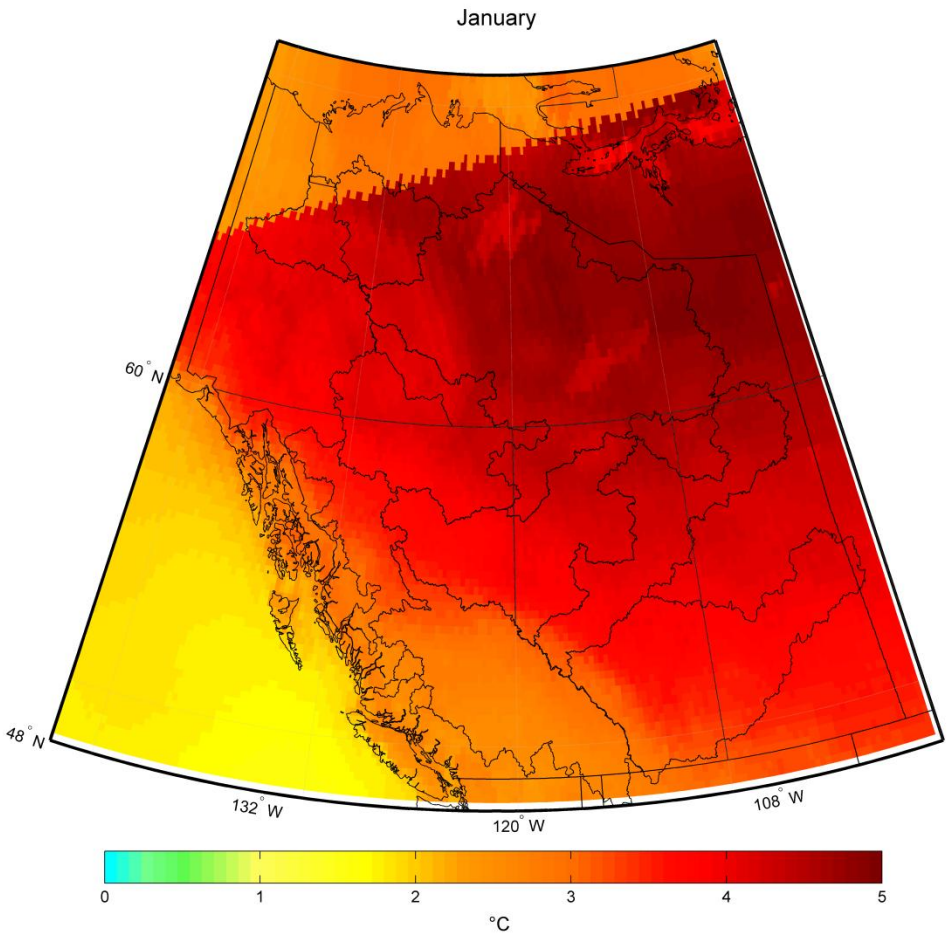

Figure B.3. Multimodel mean difference in monthly Tmax between the current and future periods during January.

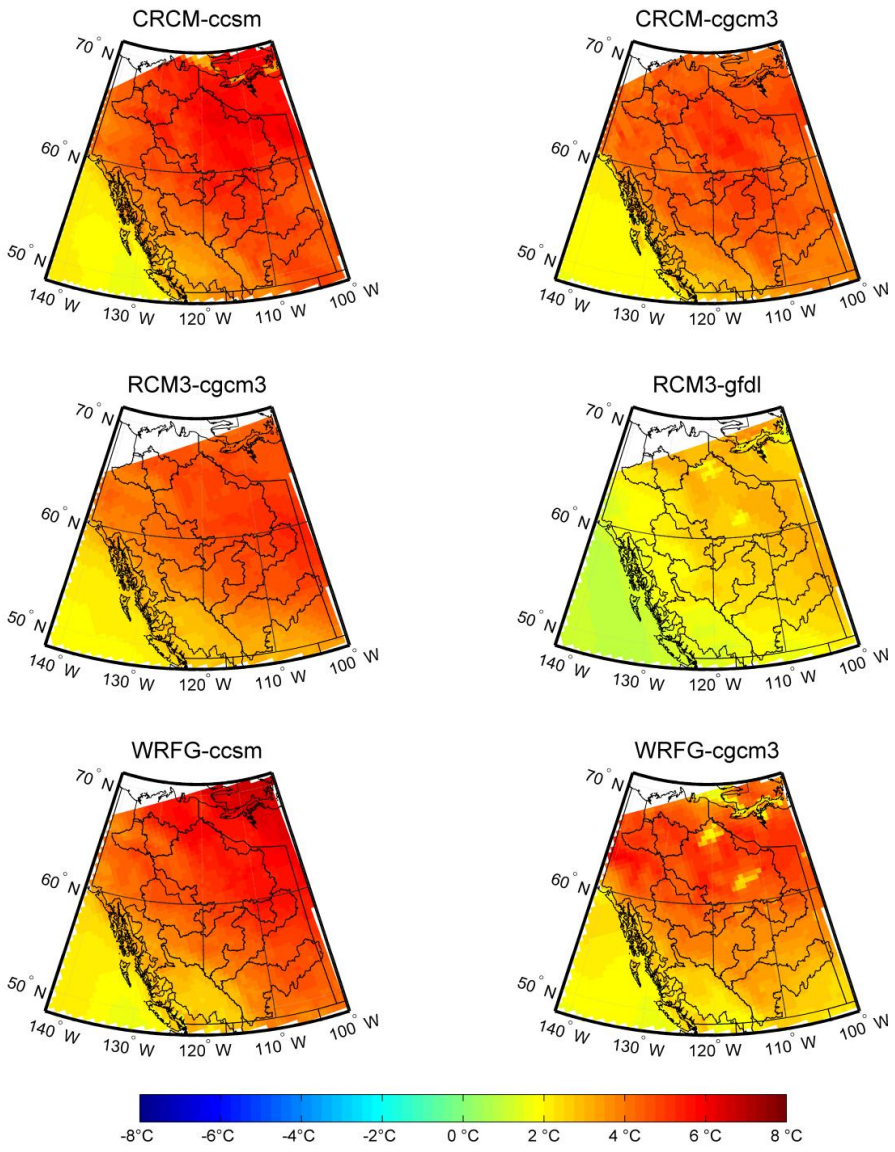

Figure B.4. Difference in Tmax values between 1971-2000 and 2041-2070 during January.

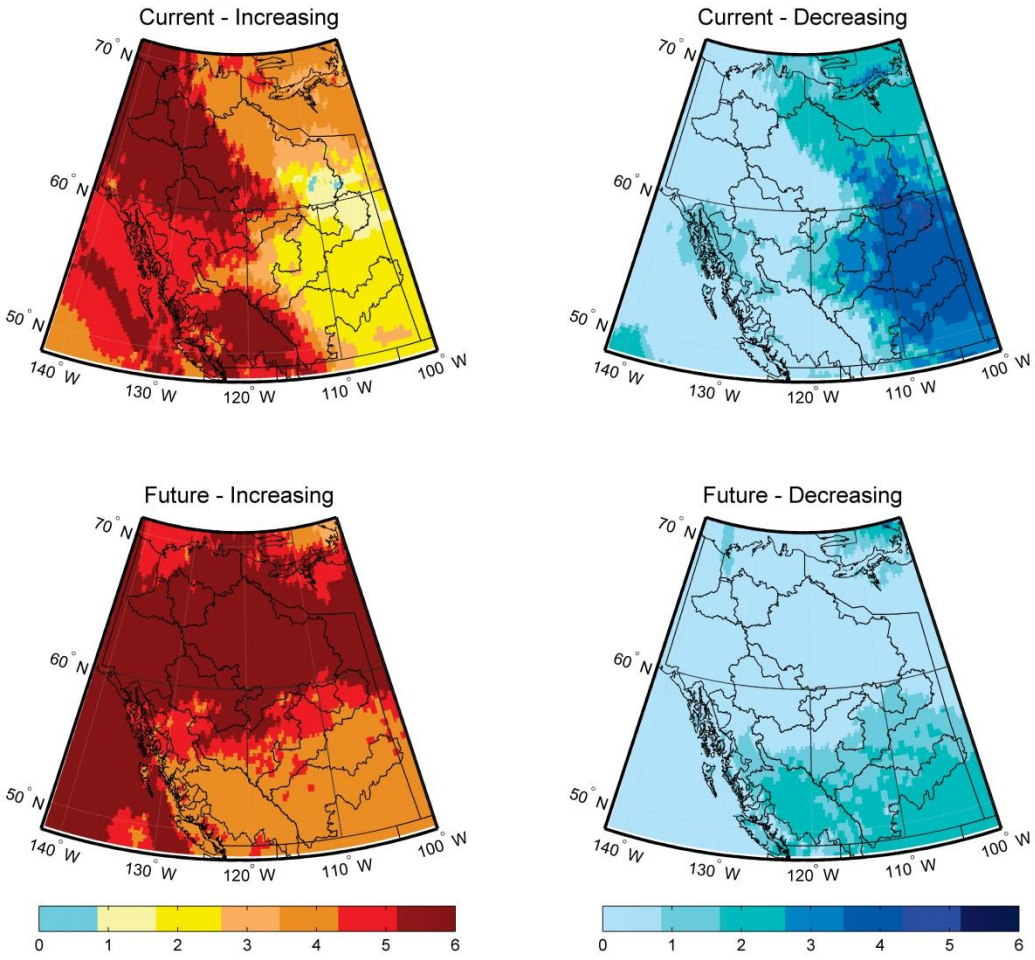

Figure B.5. Number of models showing increasing or decreasing rates of change in Tmax during the current (1971-2000) and future (2041-2070) time periods during January.

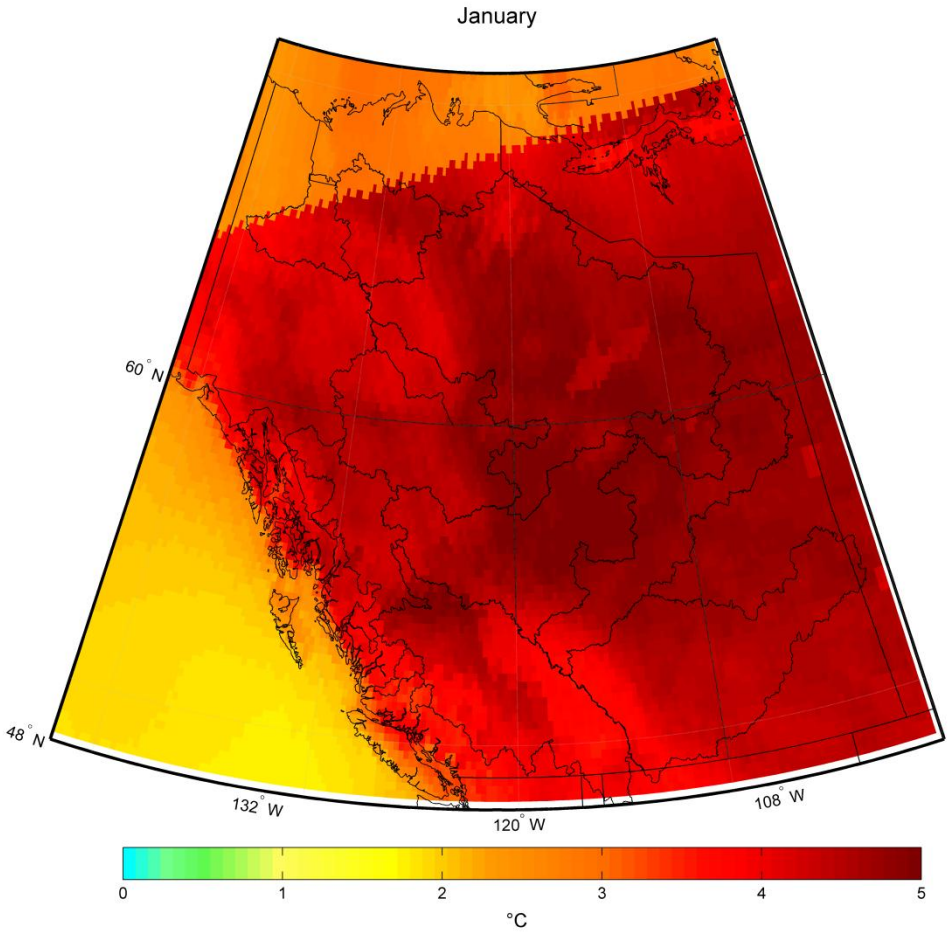

Figure B.6. Multimodel mean difference in monthly Tmin between the current and future periods during January.

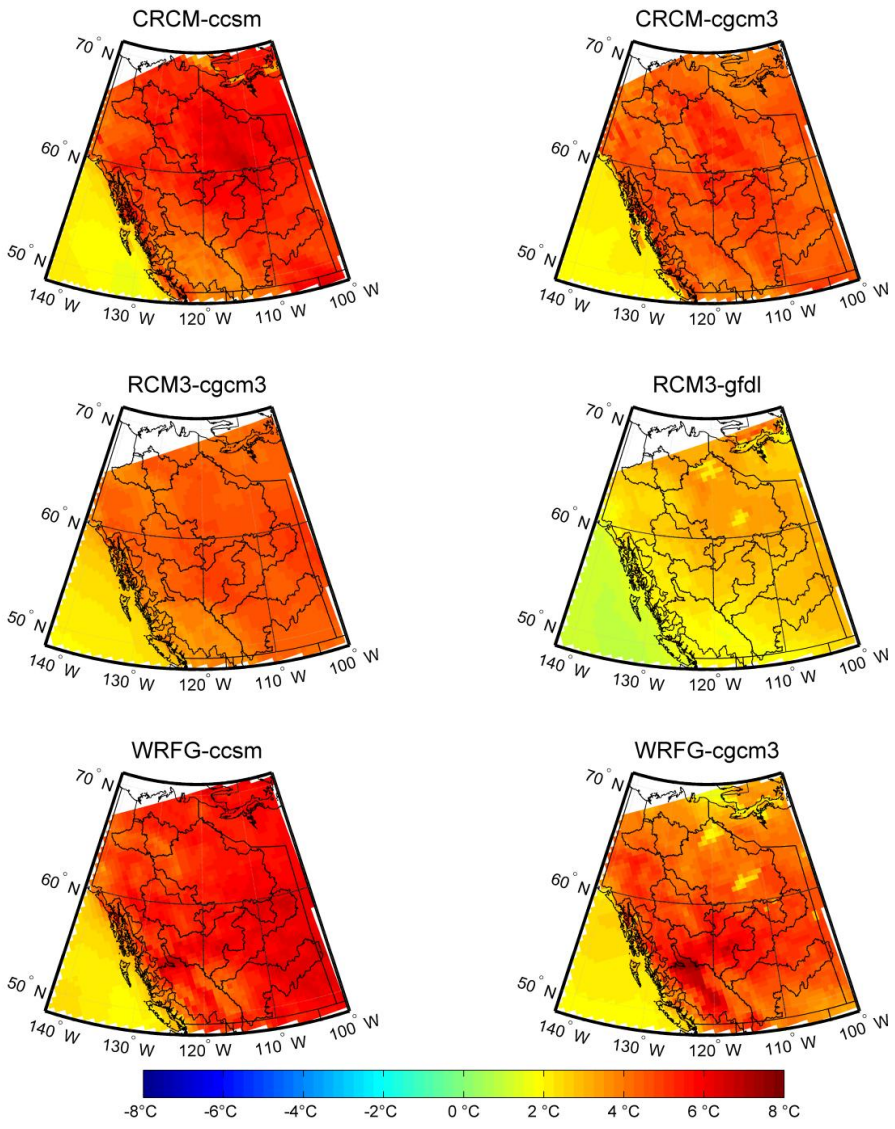

Figure B.7. Difference in Tmin values between 1971-2000 and 2041-2070 during January.

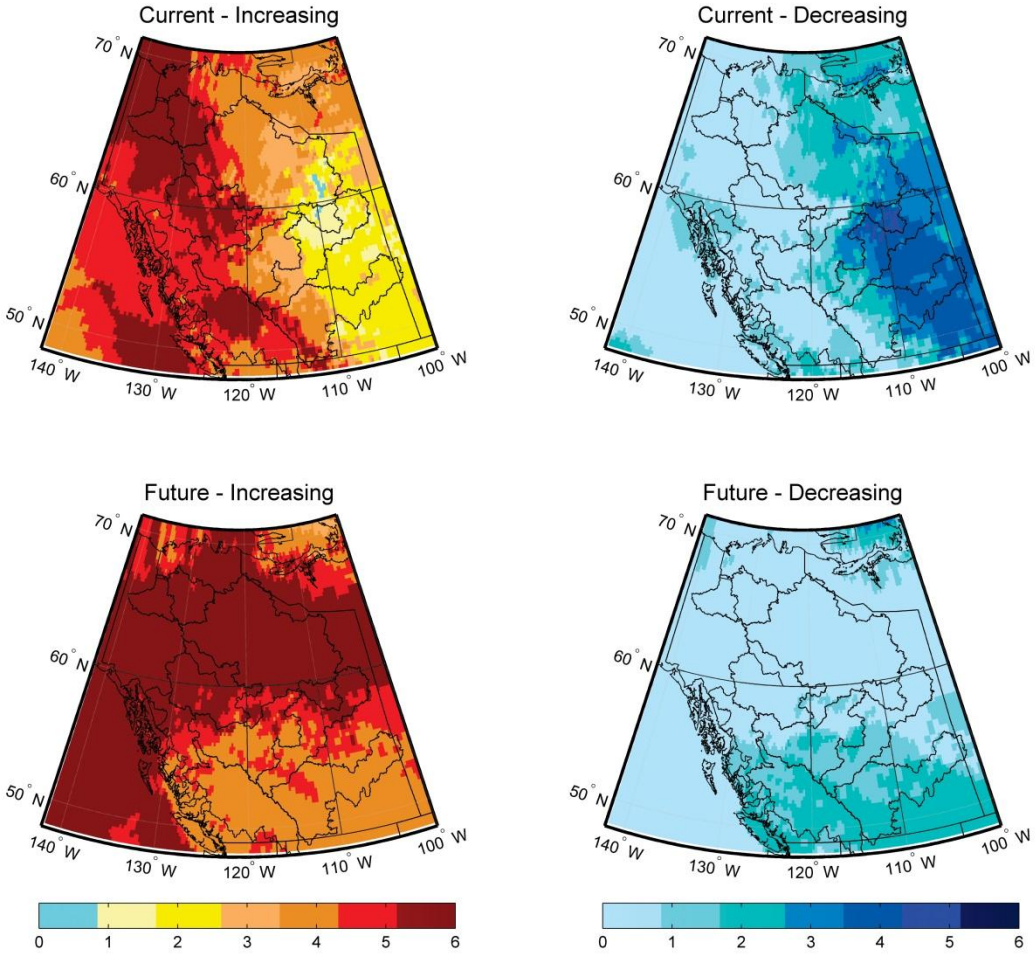

Figure B.8. Number of models showing increasing or decreasing rates of change in Tmin during the current (1971-2000) and future (2041-2070) time periods during January.

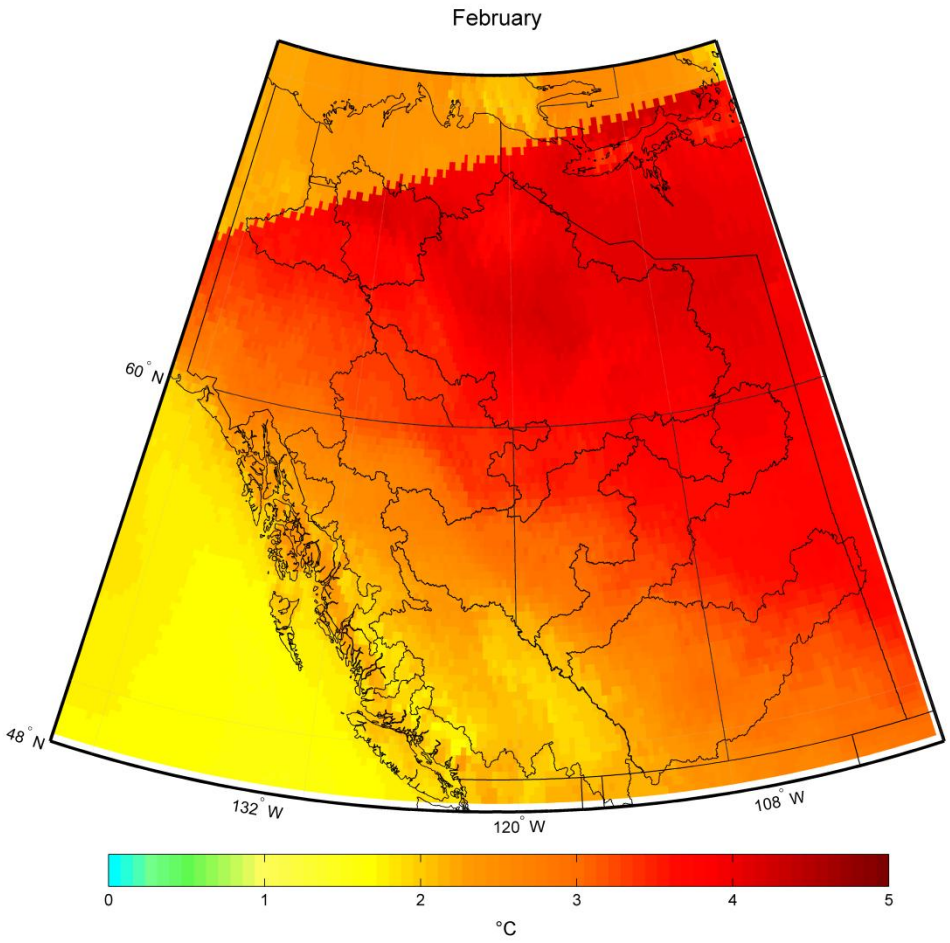

Figure B.9. Multimodel mean difference in monthly Tmax between the current and future periods during February.

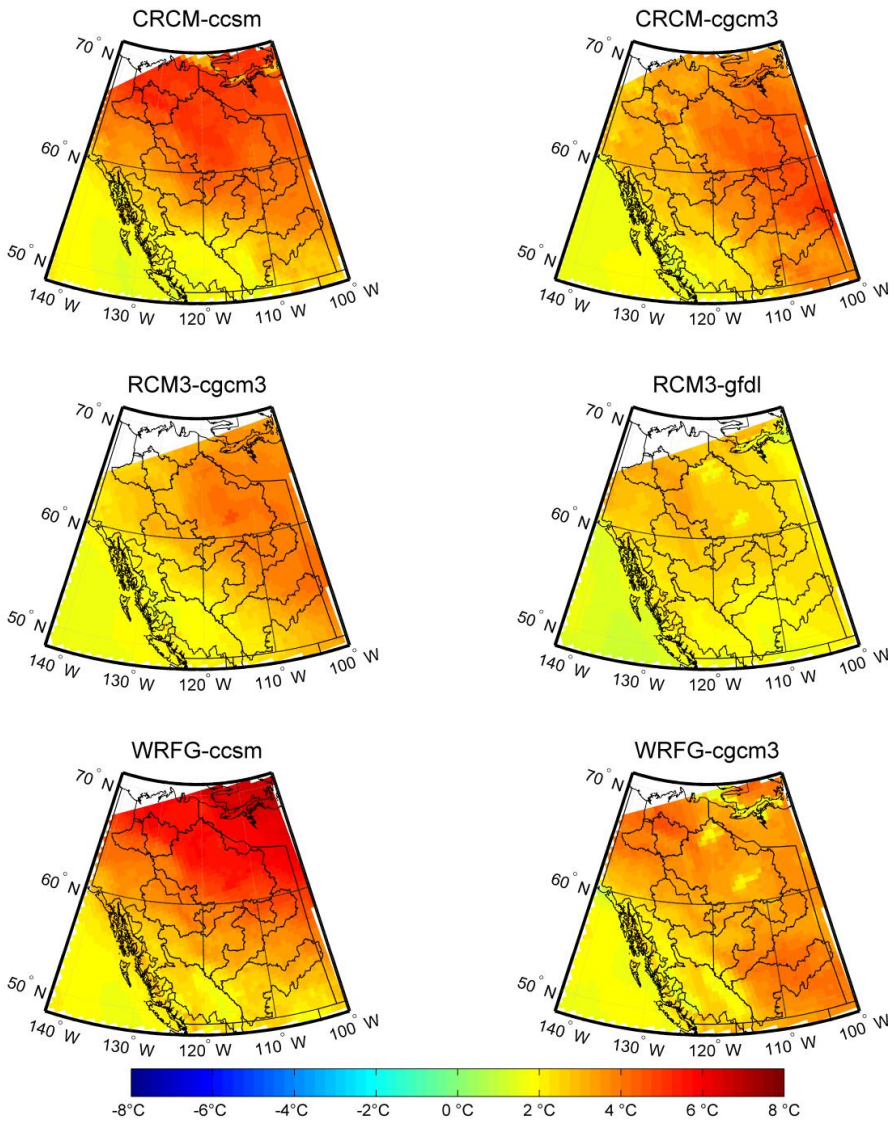

Figure B.10. Difference in Tmax values between 1971-2000 and 2041-2070 during February.

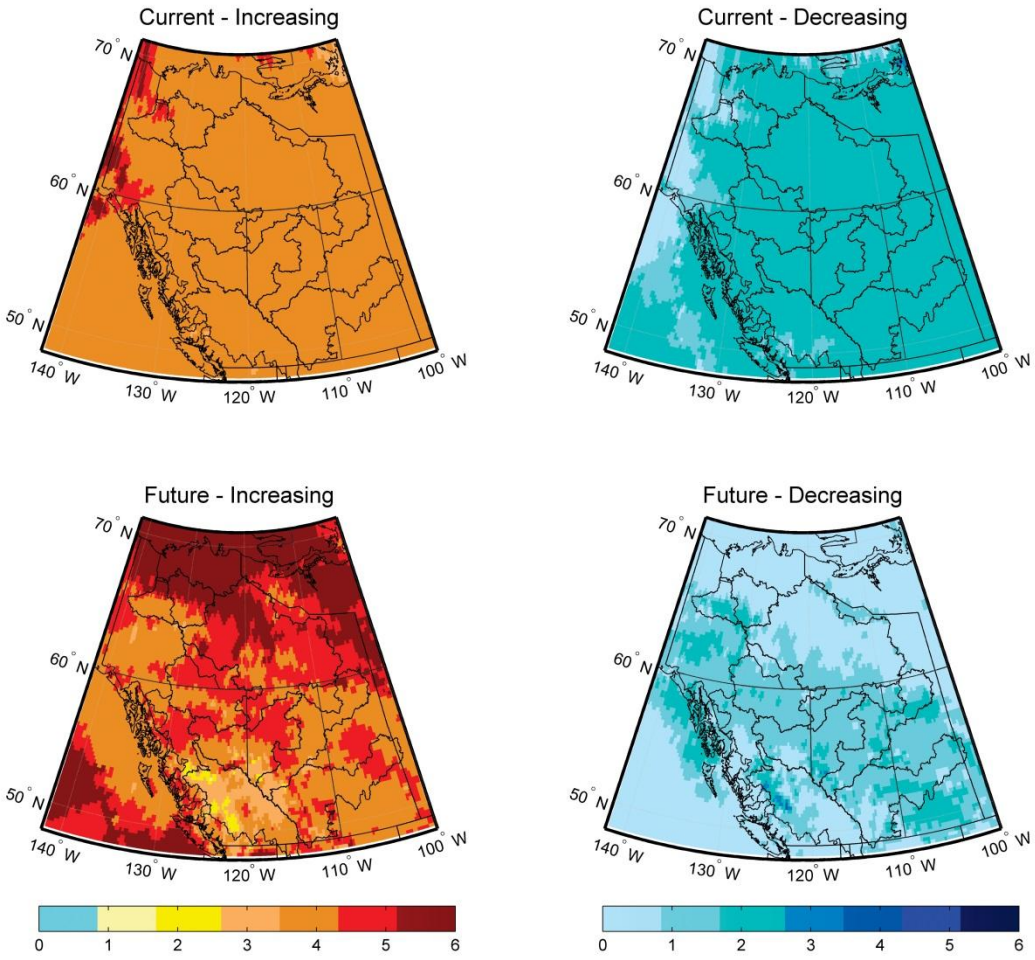

Figure B.11. Number of models showing increasing or decreasing rates of change in Tmax during the current (1971-2000) and future (2041-2070) time periods during February.

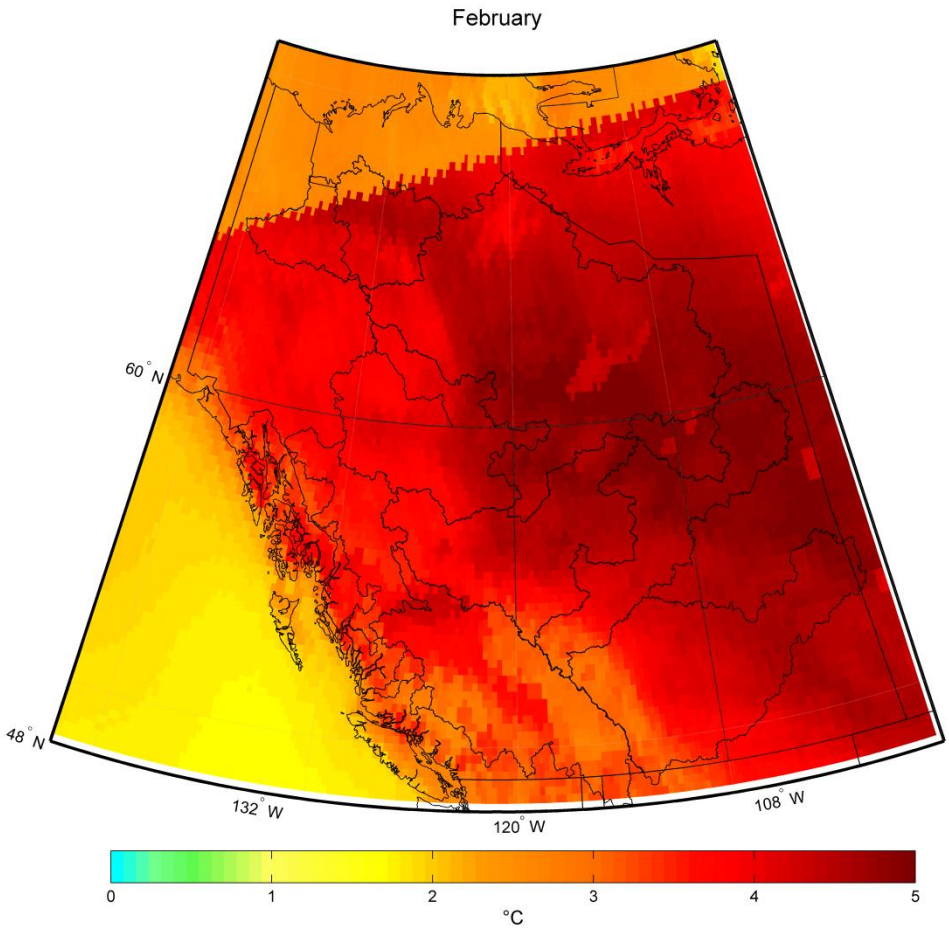

Figure B.12. Multimodel mean difference in monthly Tmin between the current and future periods during February.

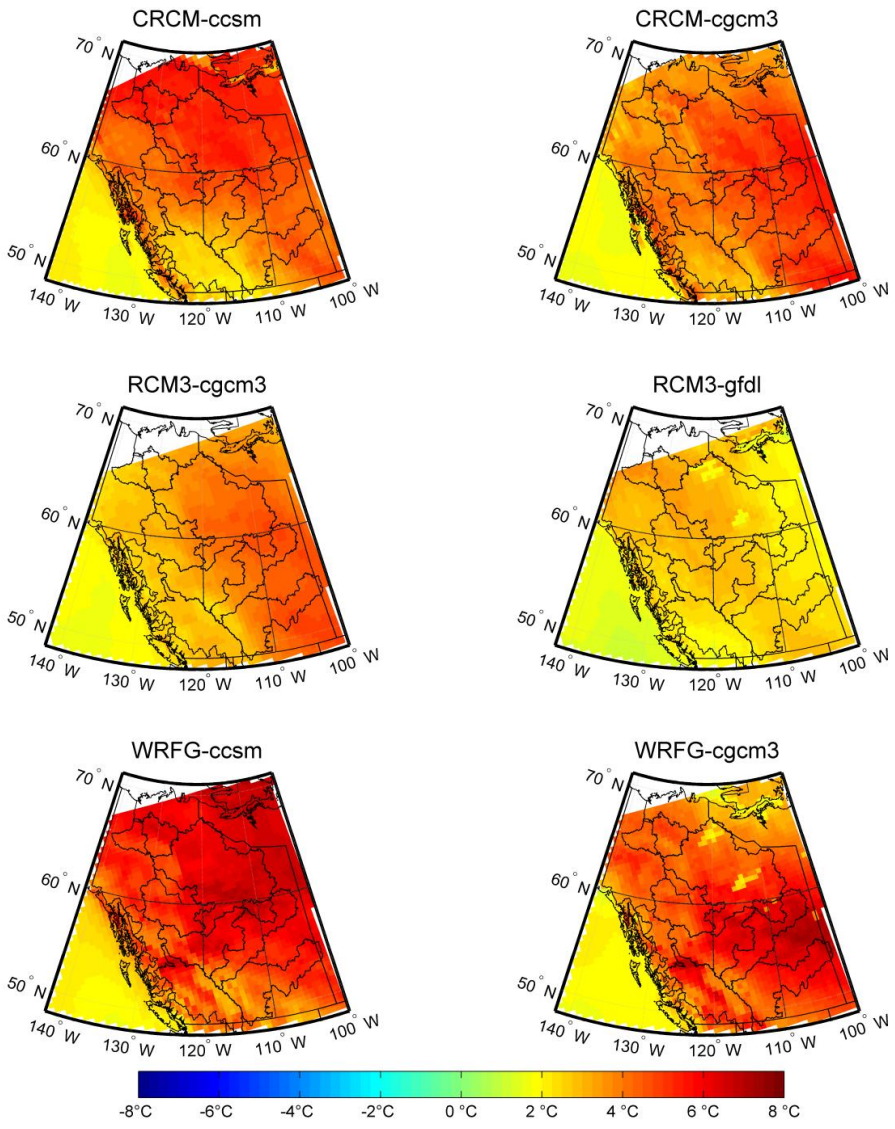

Figure B.13. Difference in Tmin values between 1971-2000 and 2041-2070 during February.

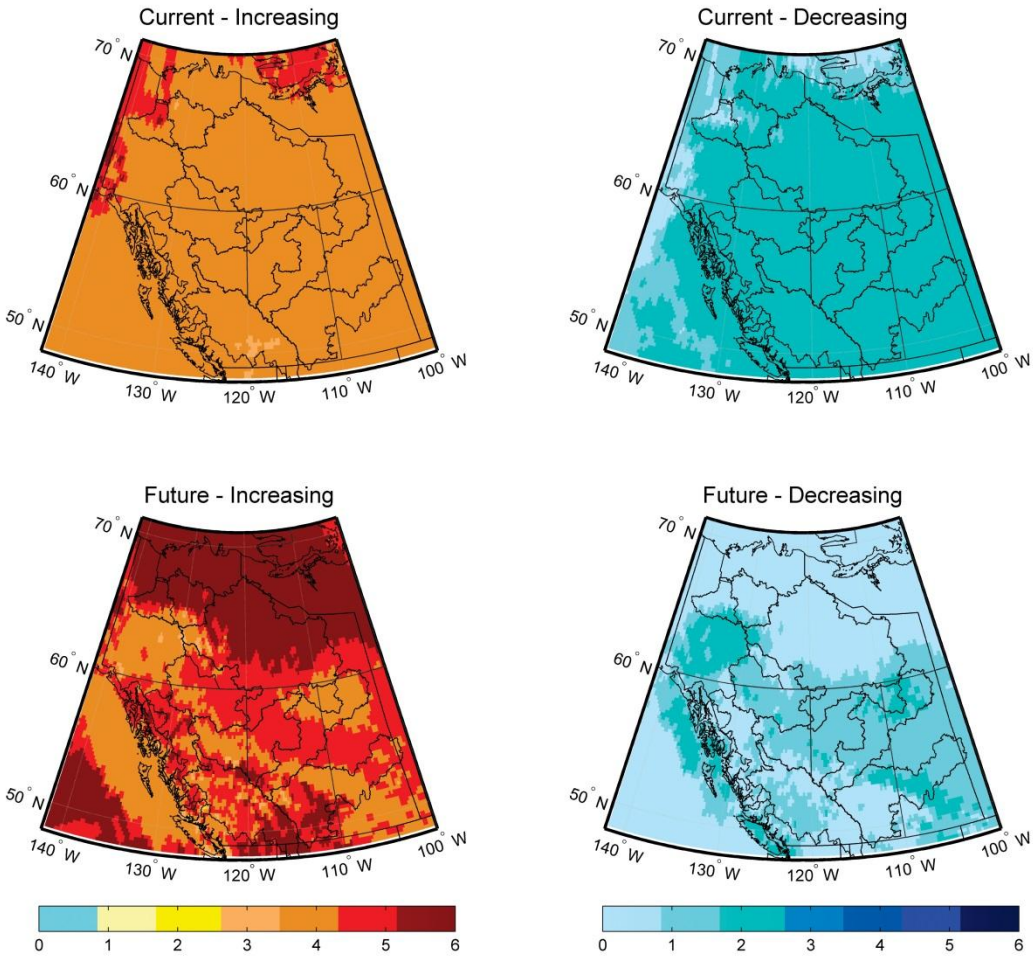

Figure B.14. Number of models showing increasing or decreasing rates of change in Tmin during the current (1971-2000) and future (2041-2070) time periods during February.

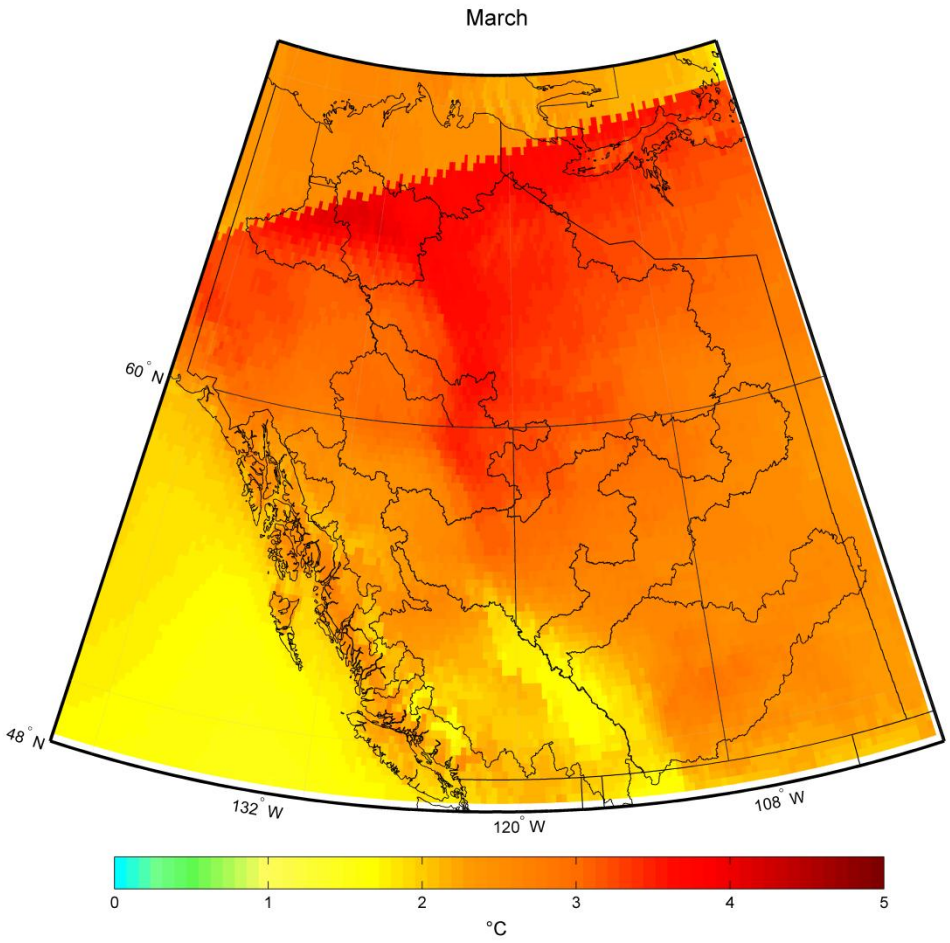

Figure B.15. Multimodel mean difference in monthly Tmax between the current and future periods during March.

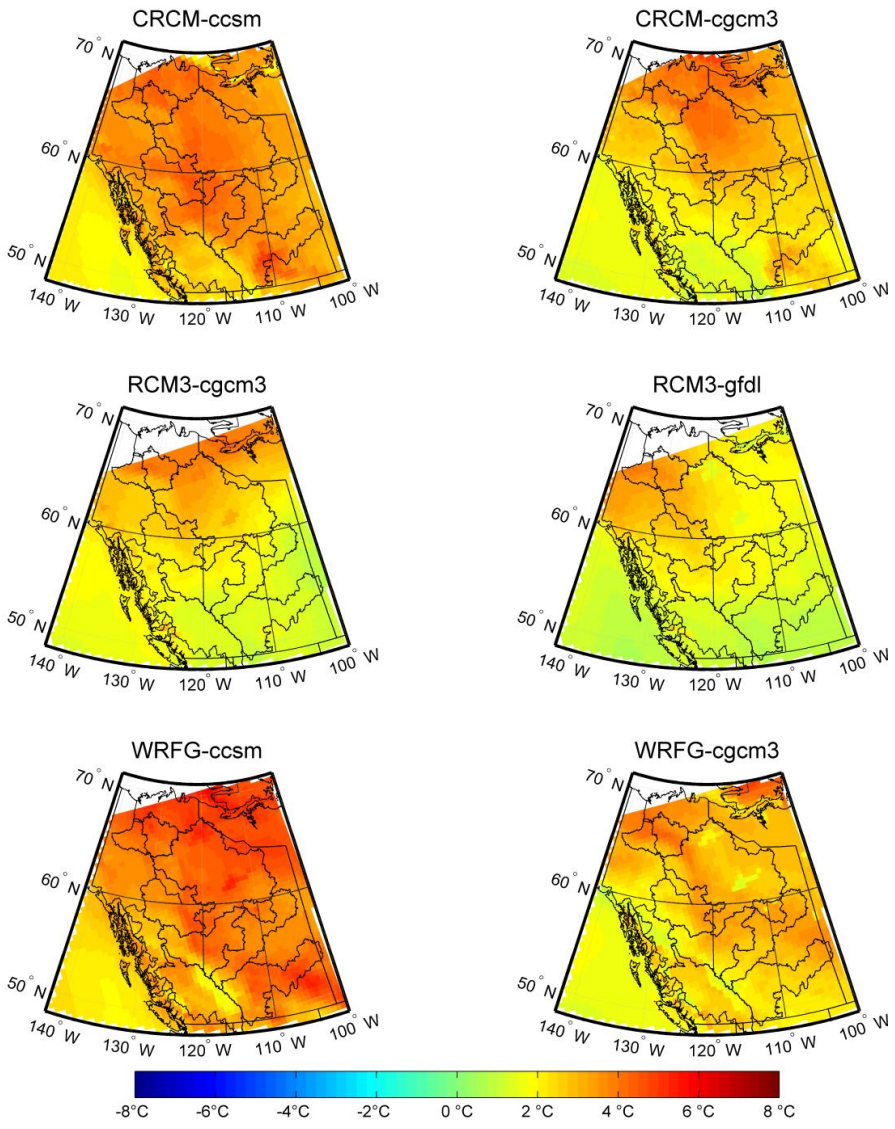

Figure B.16. Difference in Tmax values between 1971-2000 and 2041-2070 during March.

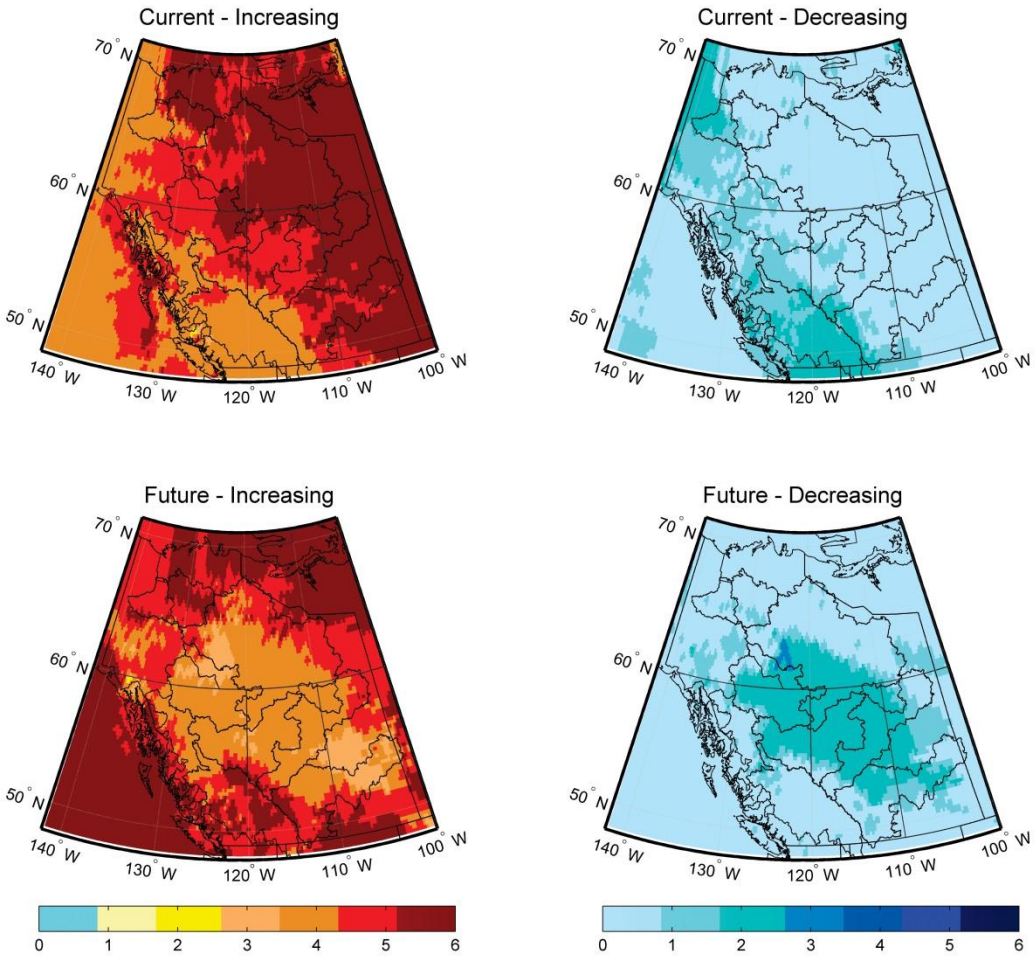

Figure B.17. Number of models showing increasing or decreasing rates of change in Tmax during the current (1971-2000) and future (2041-2070) time periods during March.

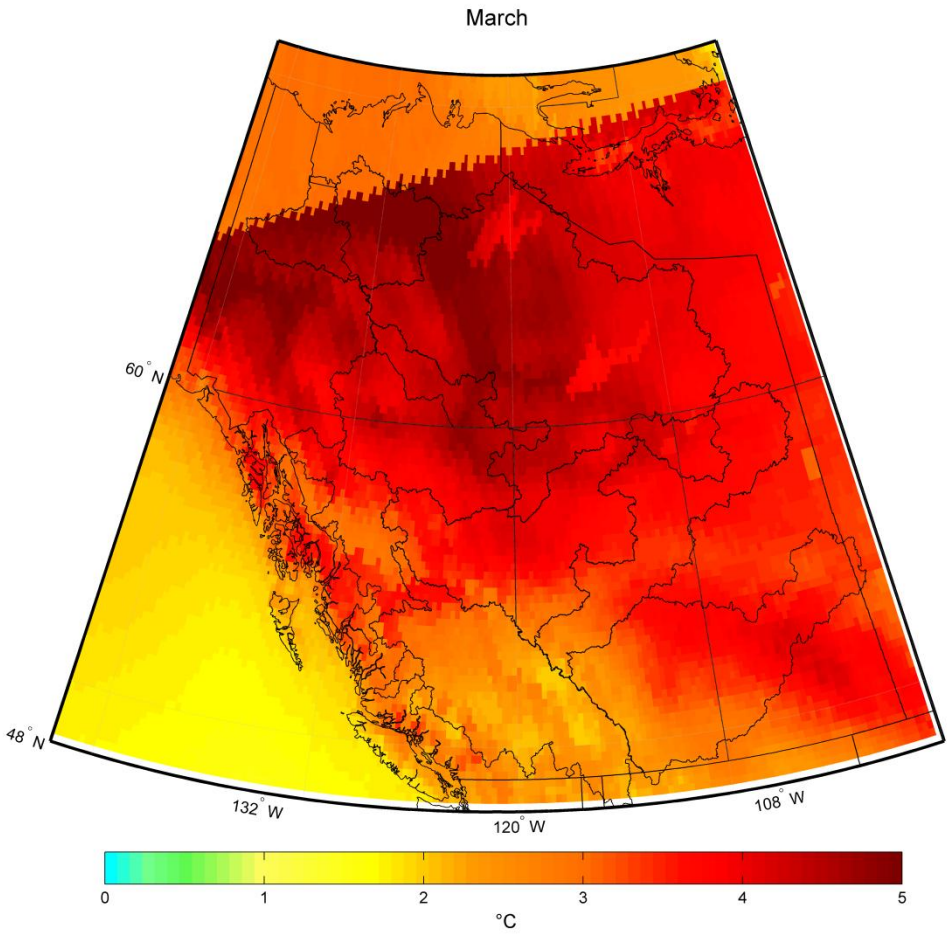

Figure B.18. Multimodel mean difference in monthly Tmin between the current and future periods during March.

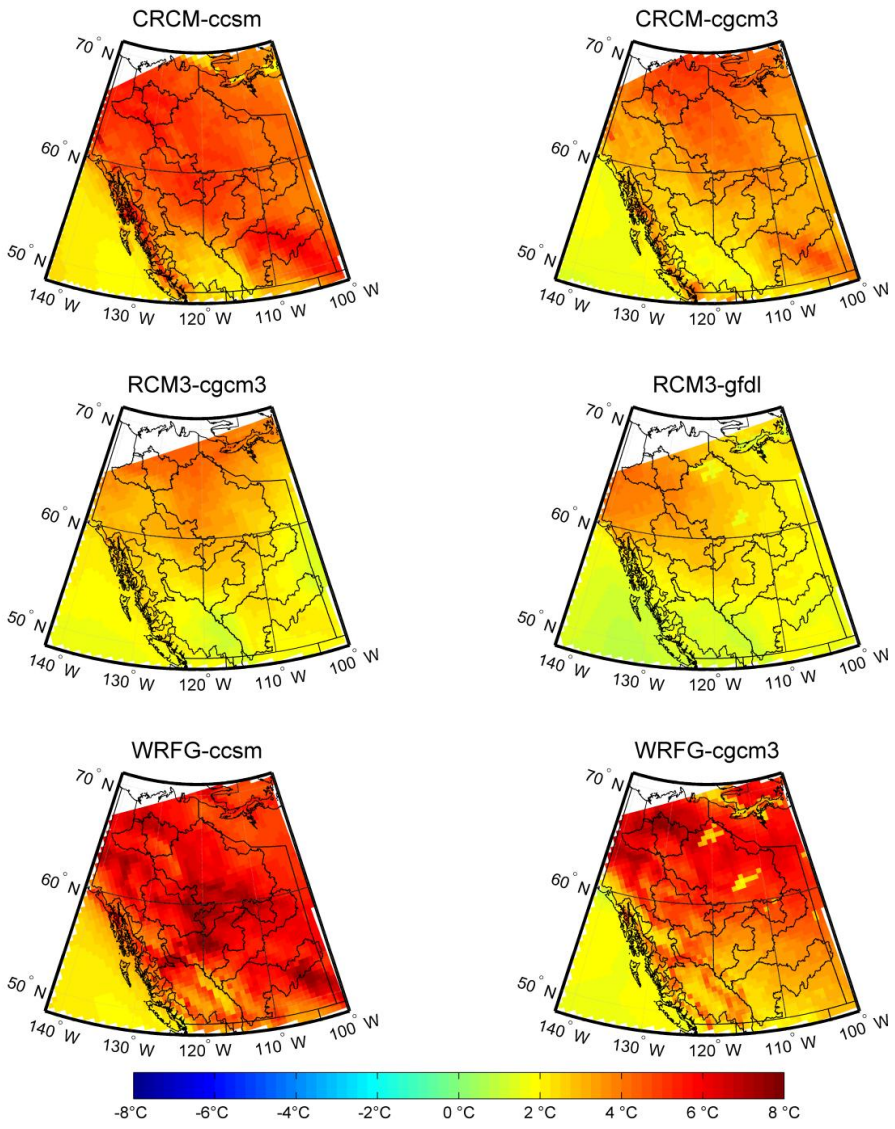

Figure B.19. Difference in Tmin values between 1971-2000 and 2041-2070 during March.

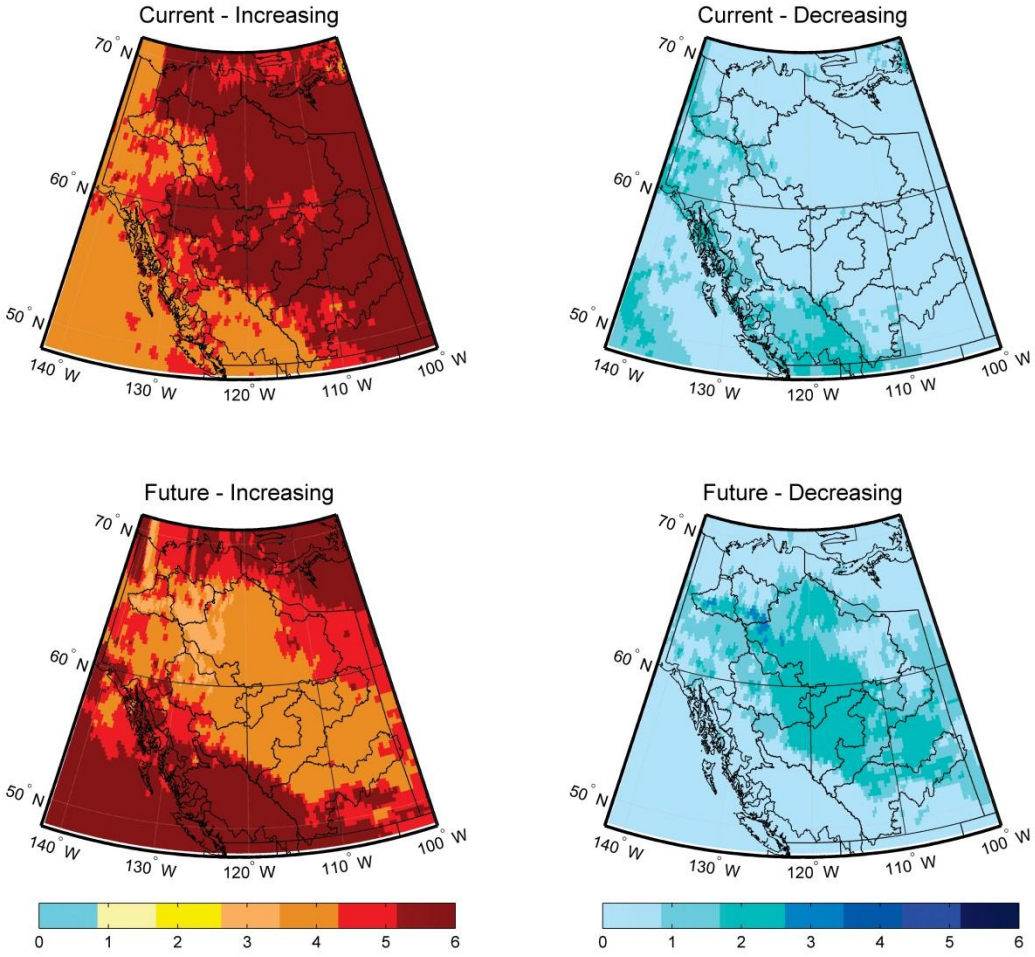

Figure B.20. Number of models showing increasing or decreasing rates of change in Tmin during the current (1971-2000) and future (2041-2070) time periods during March.

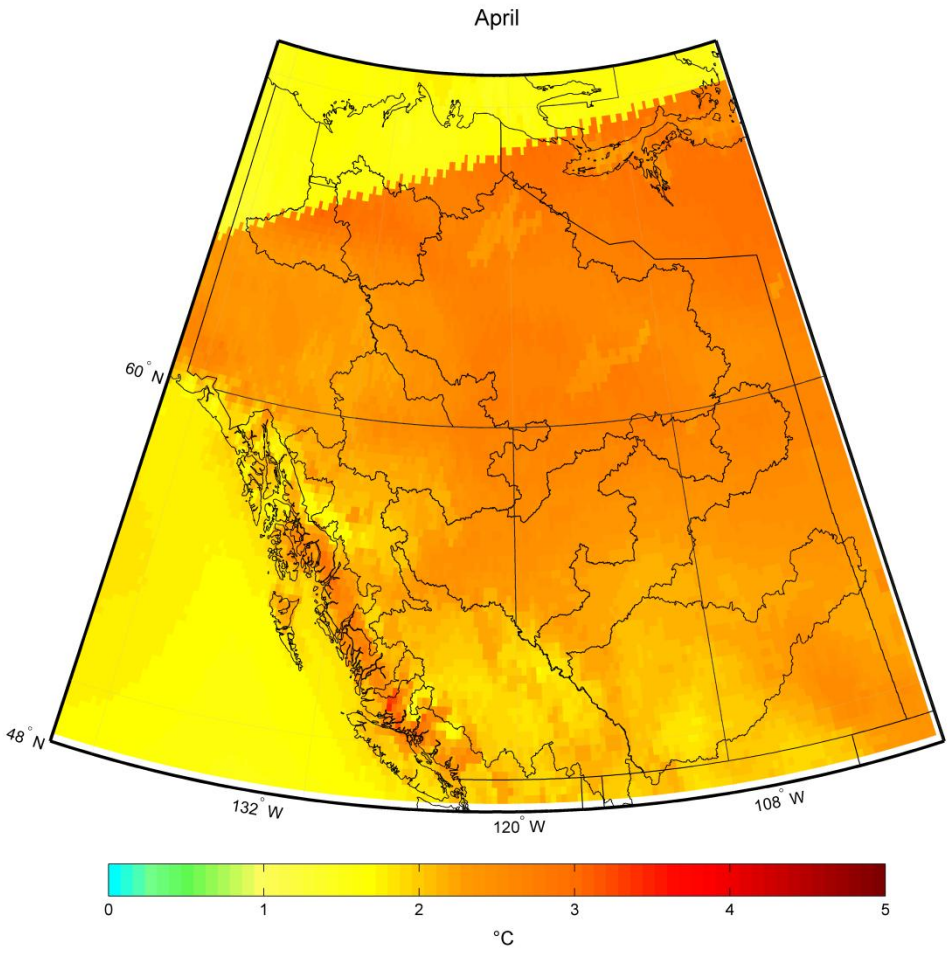

Figure B.21. Multimodel mean difference in monthly Tmax between the current and future periods during April.

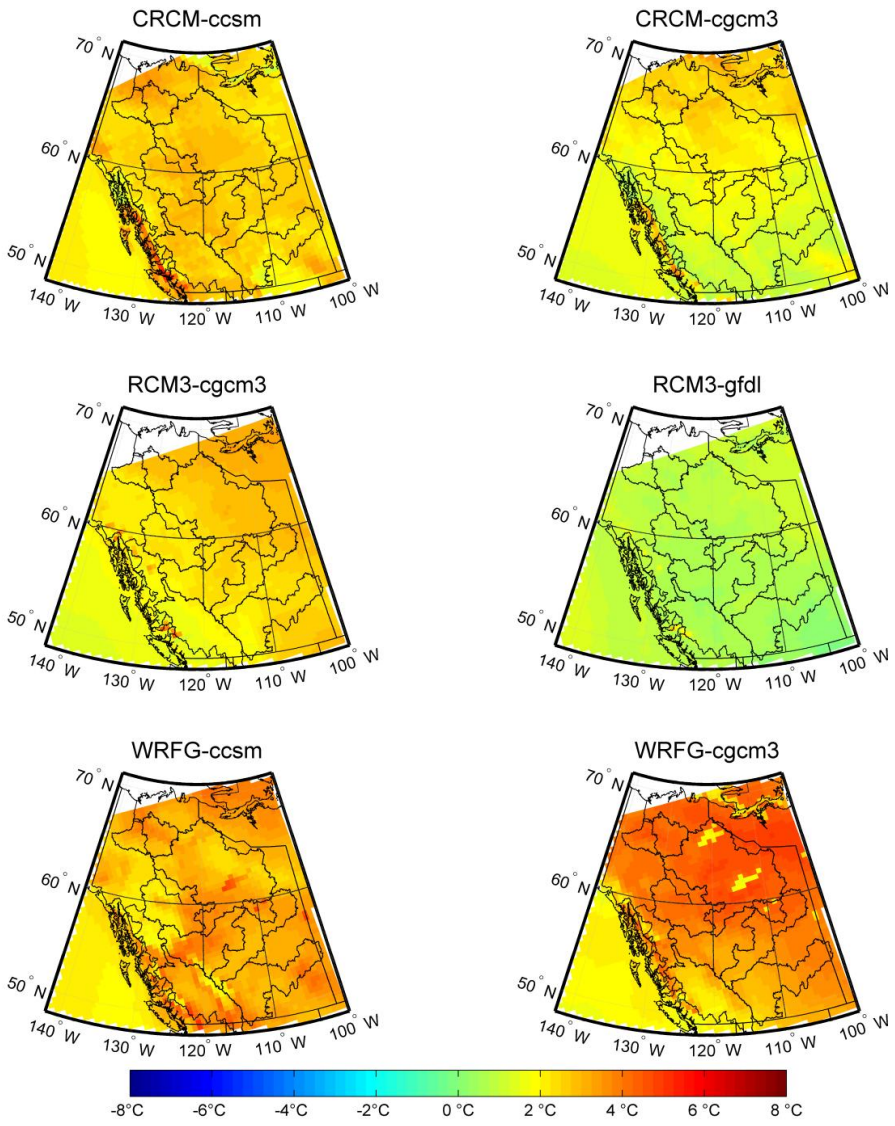

Figure B.22. Difference in Tmax values between 1971-2000 and 2041-2070 during April.

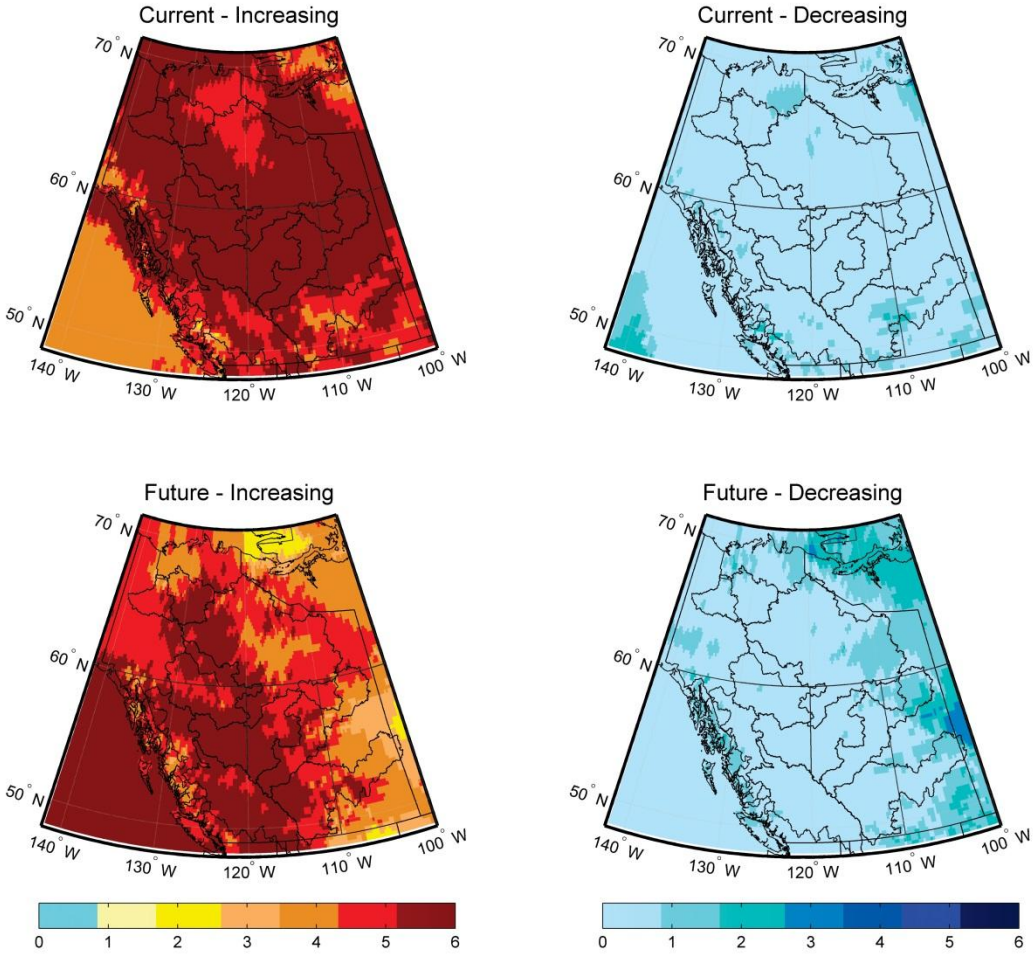

Figure B.23. Number of models showing increasing or decreasing rates of change in Tmax during the current (1971-2000) and future (2041-2070) time periods during April.

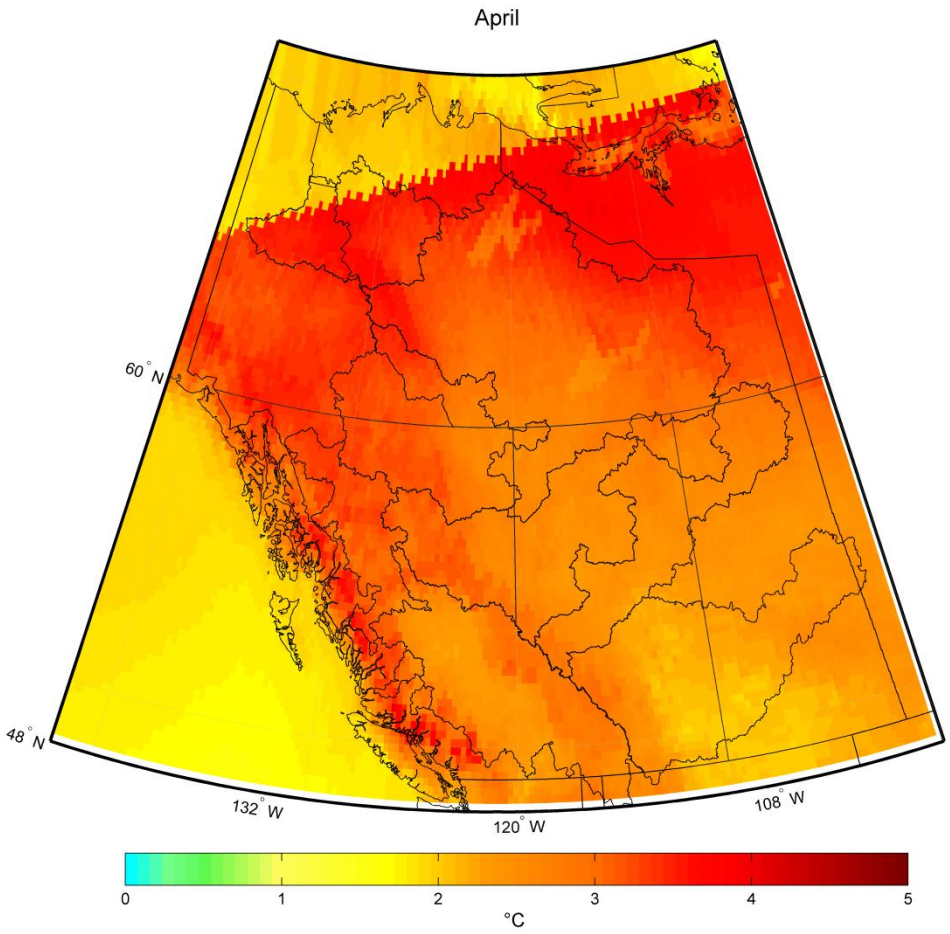

Figure B.24. Multimodel mean difference in monthly Tmin between the current and future periods during April.

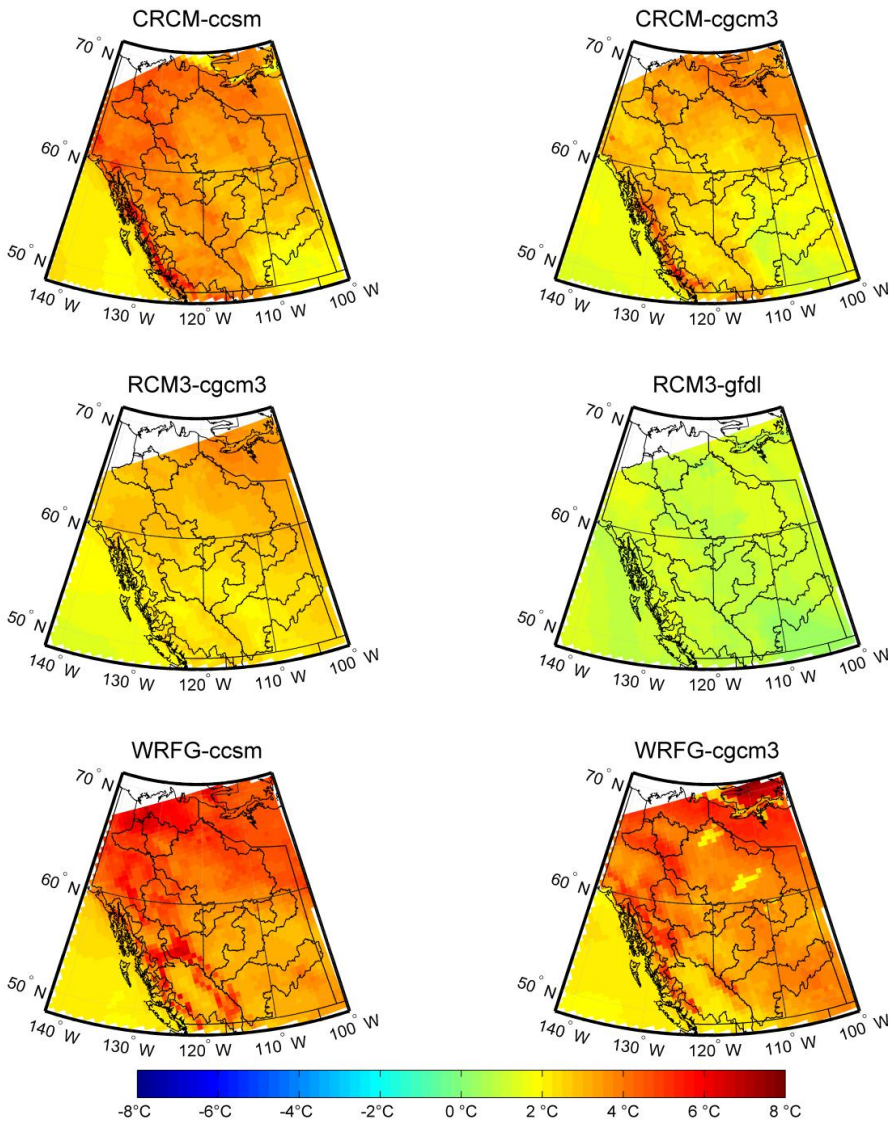

Figure B.25. Difference in Tmin values between 1971-2000 and 2041-2070 during April.

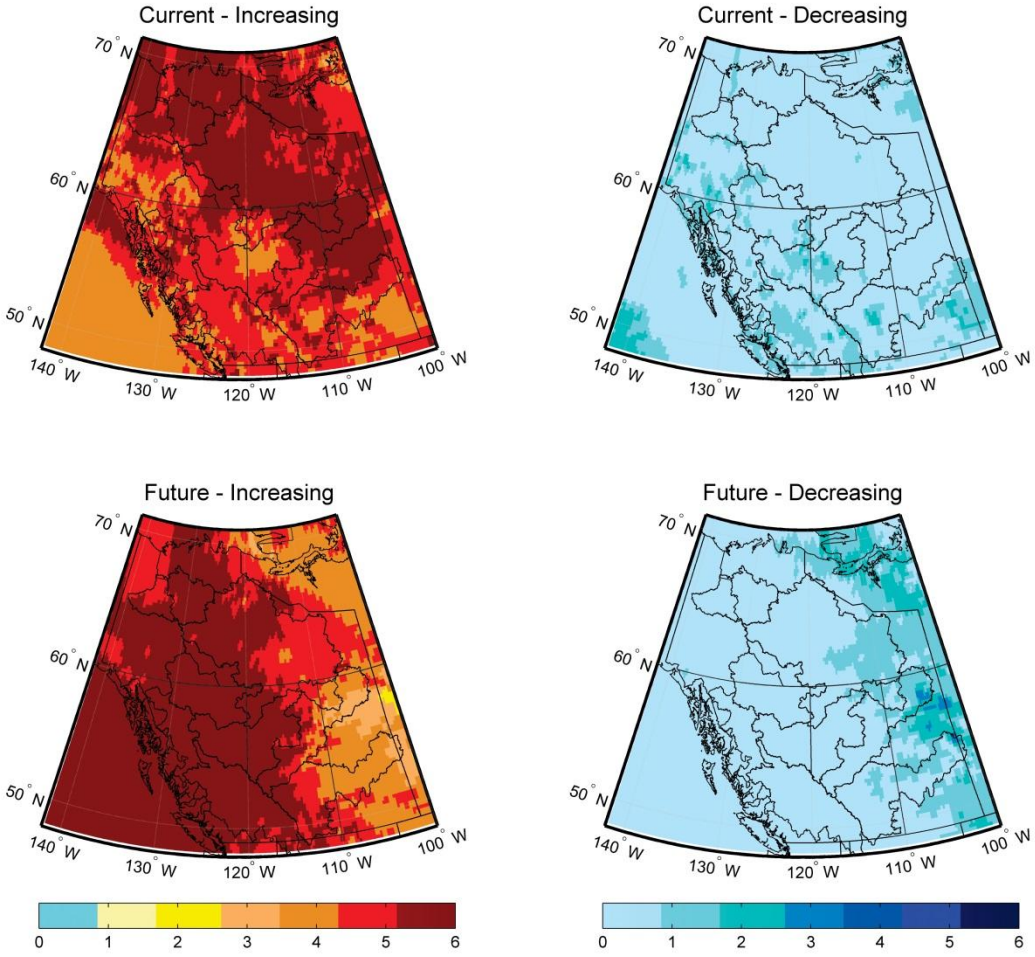

Figure B.26. Number of models showing increasing or decreasing rates of change in Tmin during the current (1971-2000) and future (2041-2070) time periods during April.

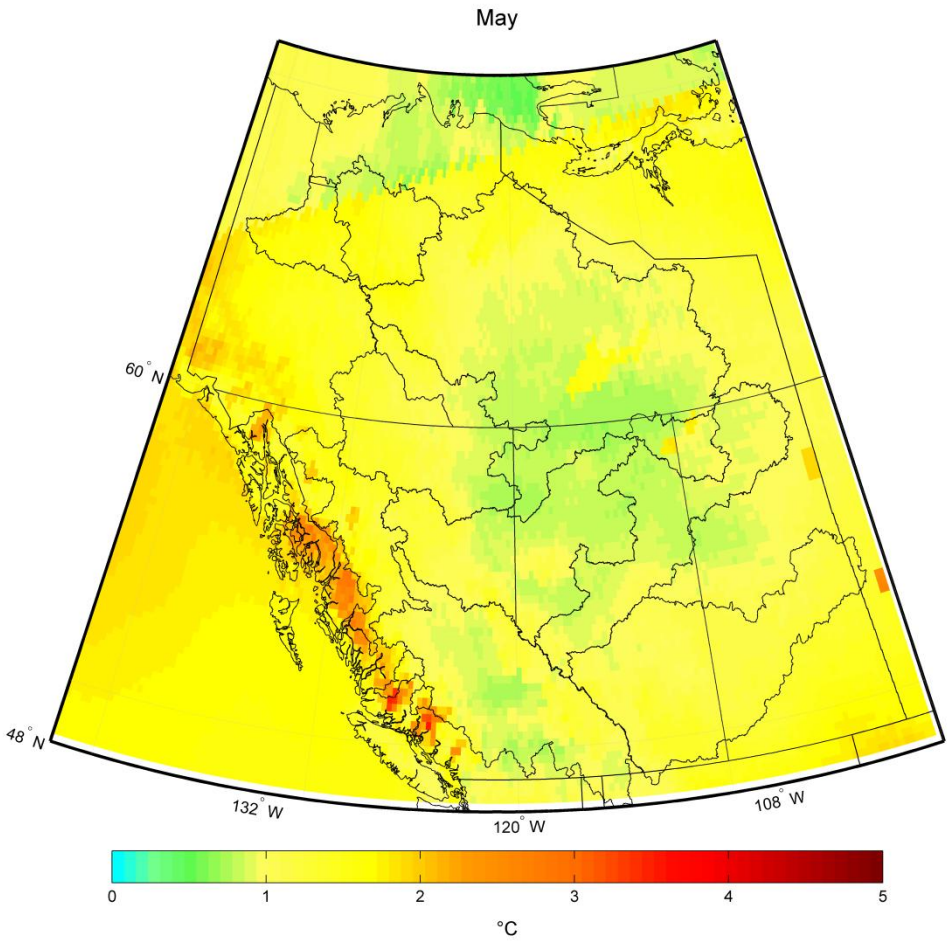

Figure B.27. Multimodel mean difference in monthly Tmax between the current and future periods during May.

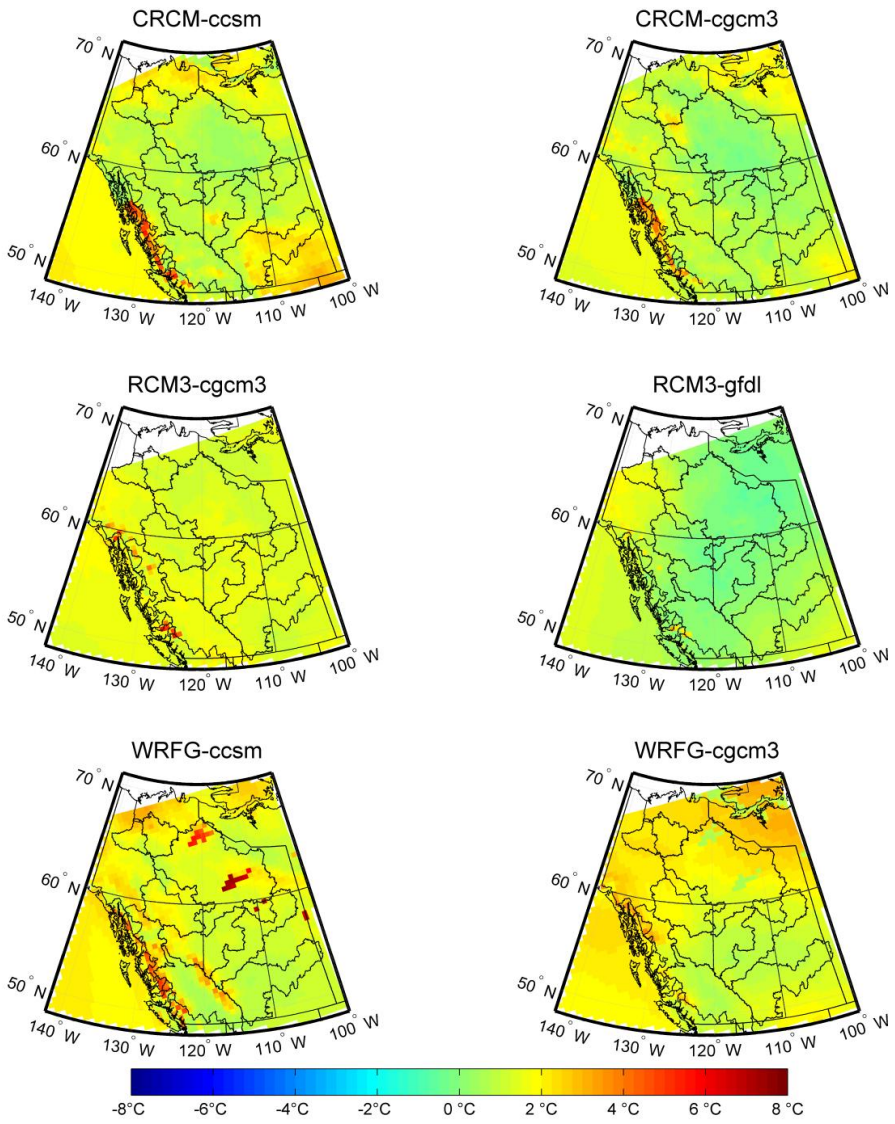

Figure B.28. Difference in Tmax values between 1971-2000 and 2041-2070 during May.

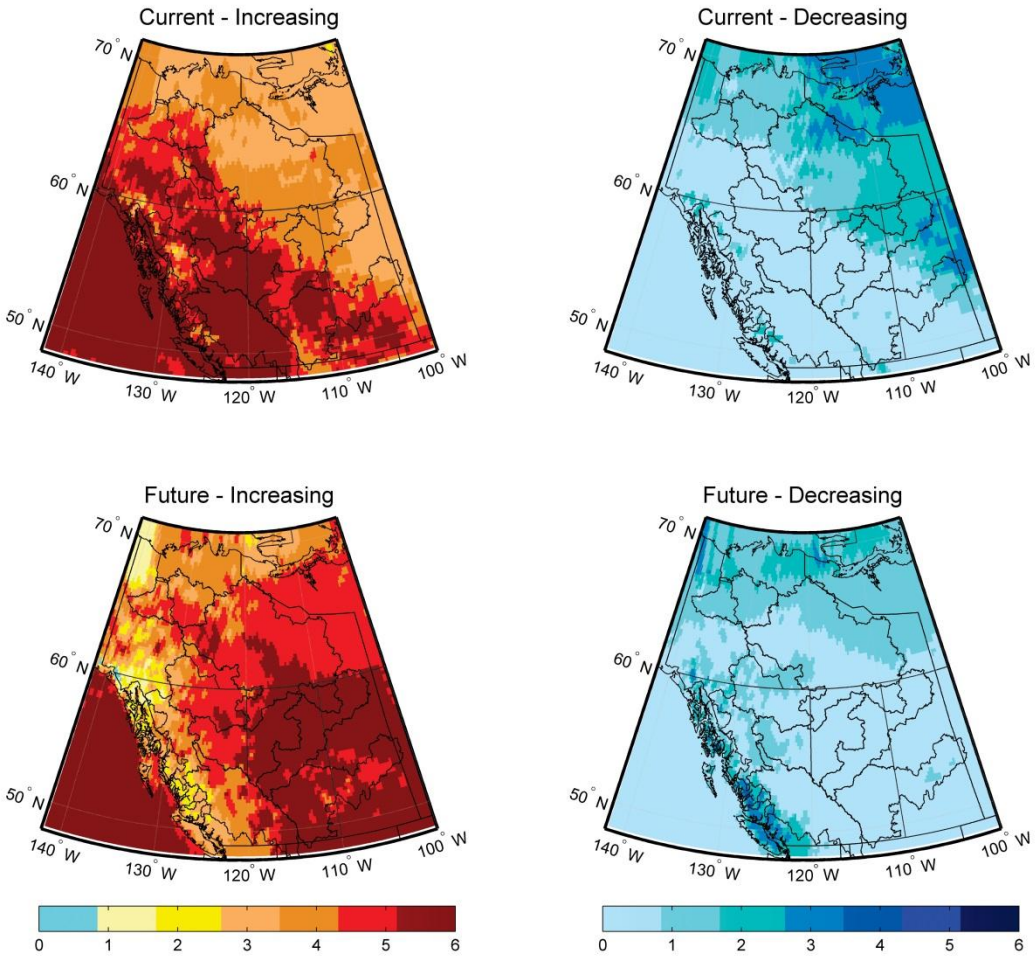

Figure B.29. Number of models showing increasing or decreasing rates of change in Tmax during the current (1971-2000) and future (2041-2070) time periods during May.

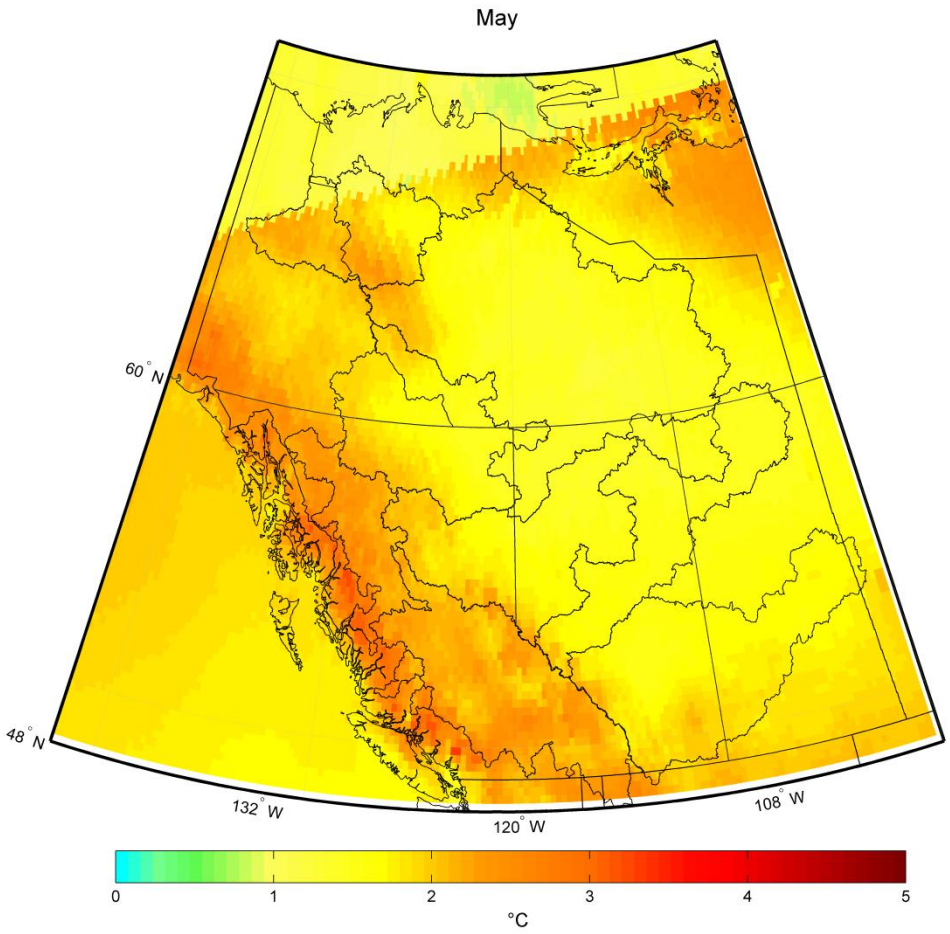

Figure B.30. Multimodel mean difference in monthly Tmin between the current and future periods during May.

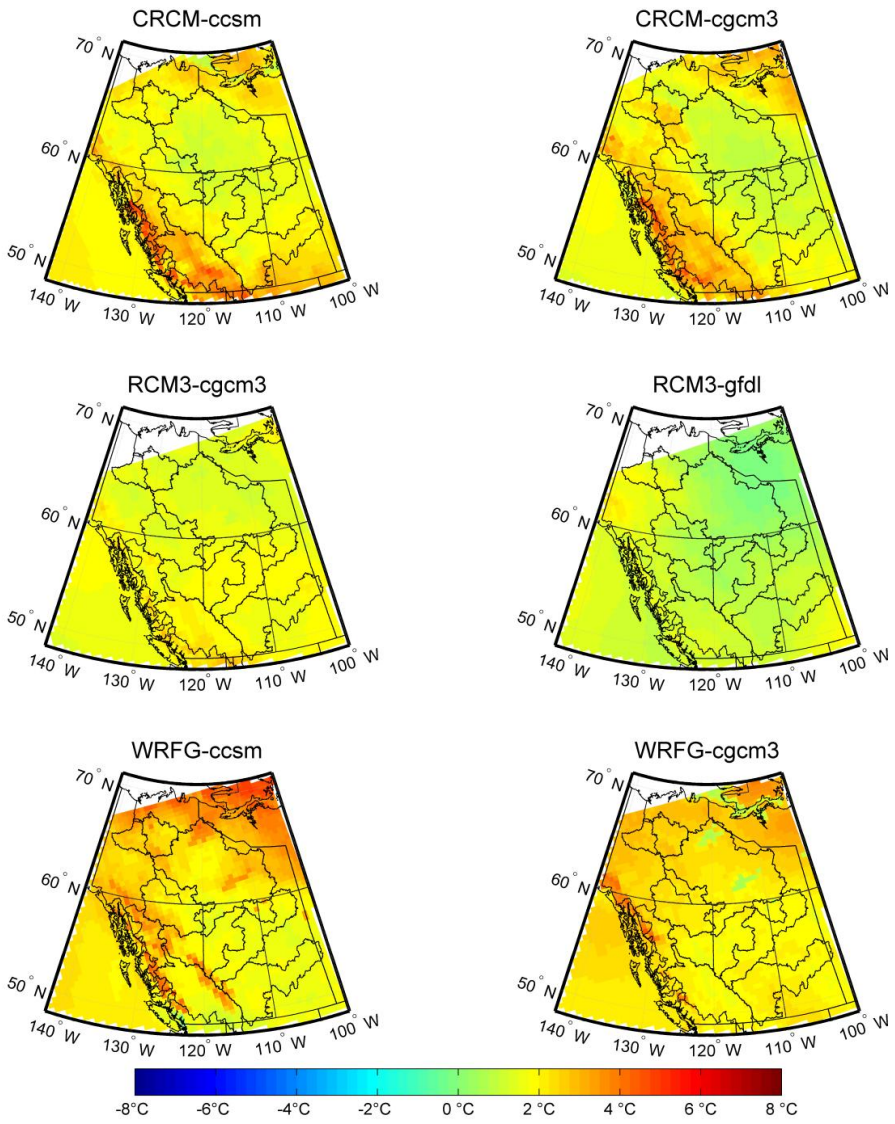

Figure B.31. Difference in Tmin values between 1971-2000 and 2041-2070 during May.

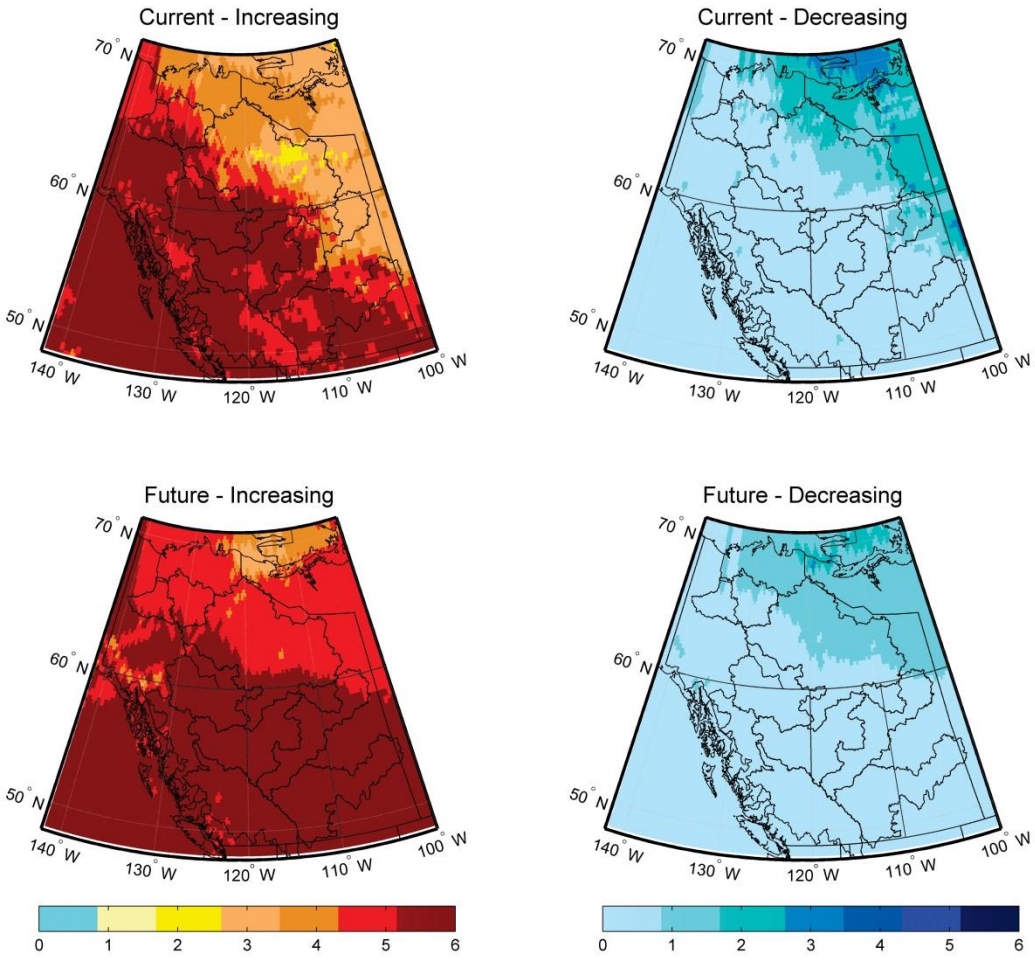

Figure B.32. Number of models showing increasing or decreasing rates of change in Tmin during the current (1971-2000) and future (2041-2070) time periods during May.

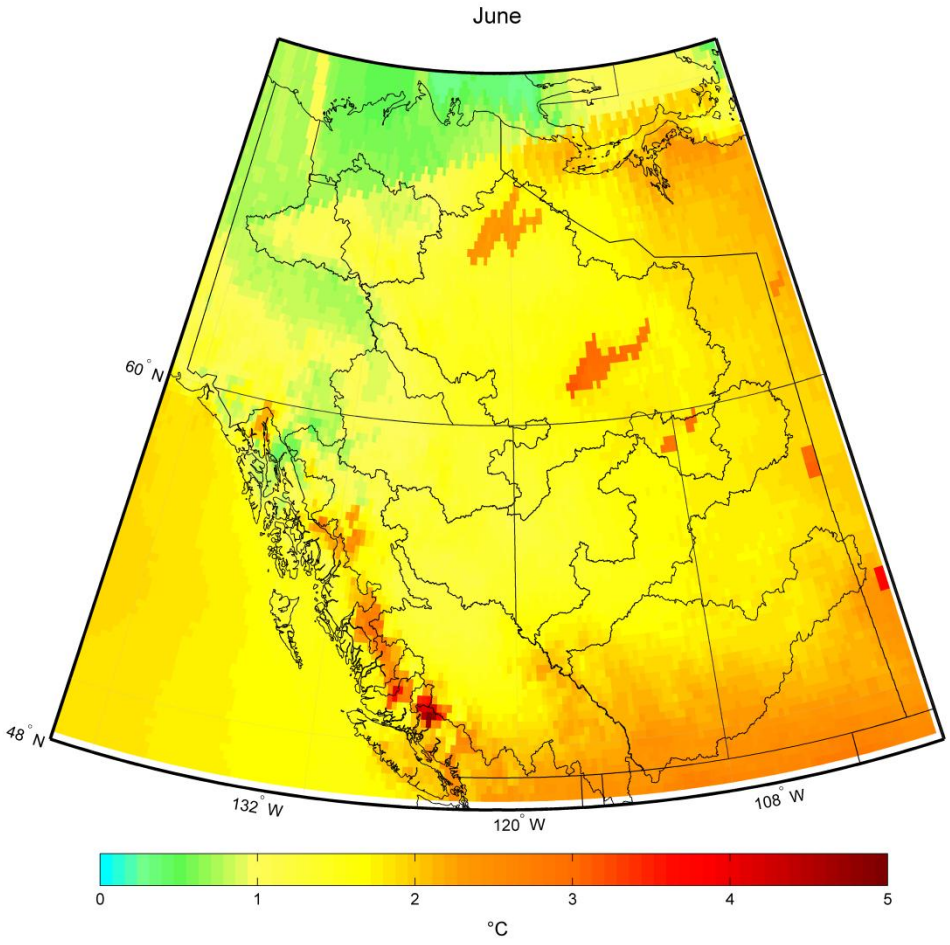

Figure B.33. Multimodel mean difference in monthly Tmax between the current and future periods during June.

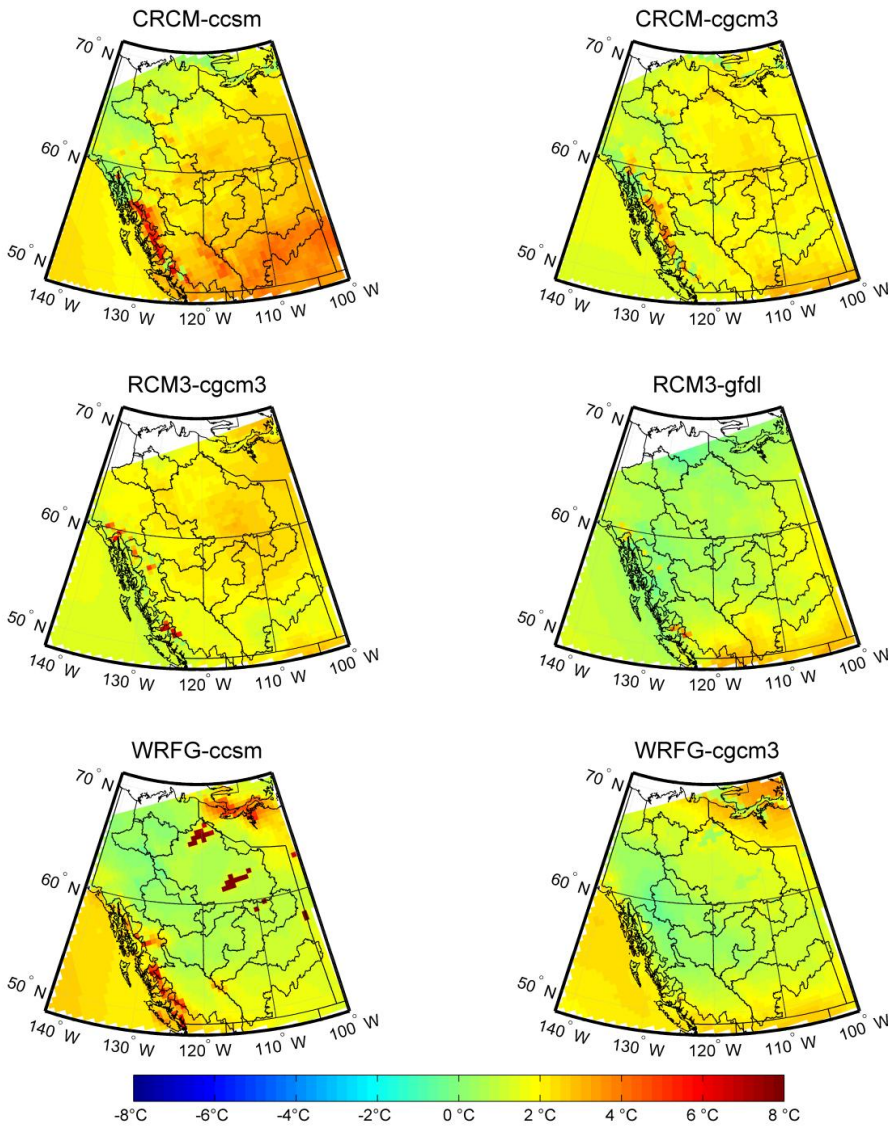

Figure B.34. Difference in Tmax values between 1971-2000 and 2041-2070 during June.

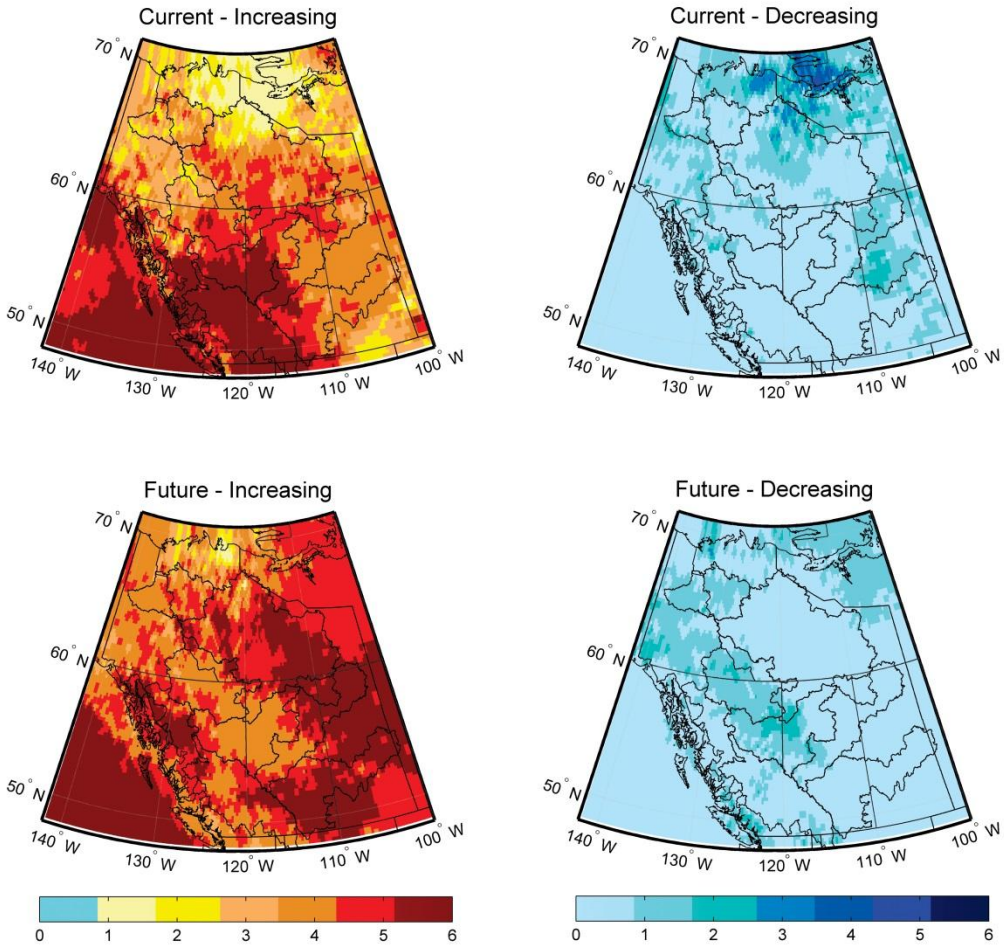

Figure B.35. Number of models showing increasing or decreasing rates of change in Tmax during the current (1971-2000) and future (2041-2070) time periods during June.

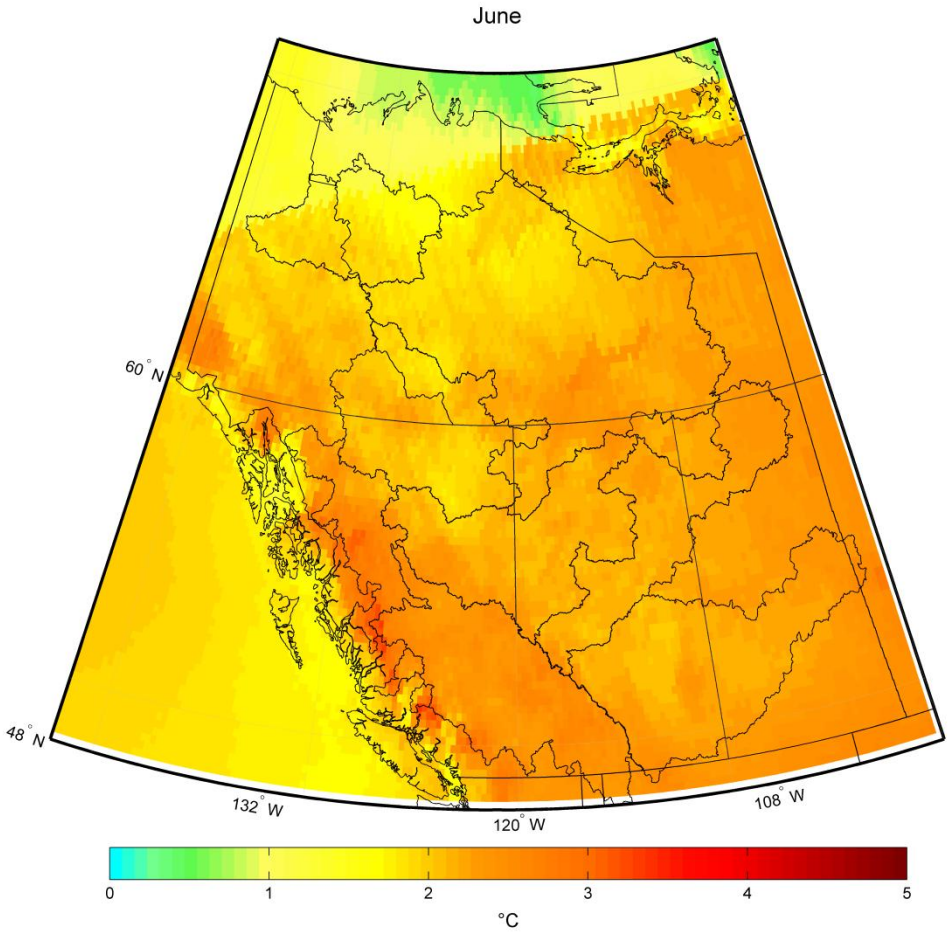

Figure B.36. Multimodel mean difference in monthly Tmin between the current and future periods during June.

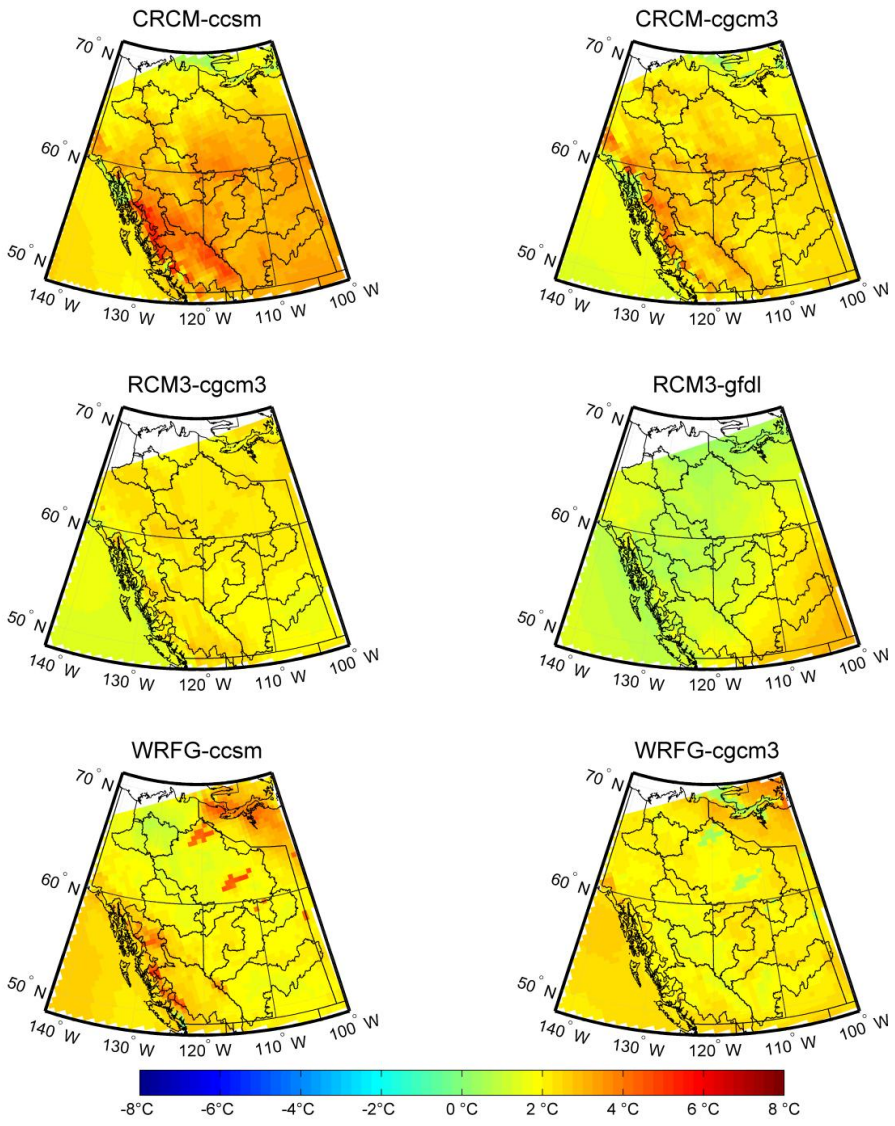

Figure B.37. Difference in Tmin values between 1971-2000 and 2041-2070 during June.

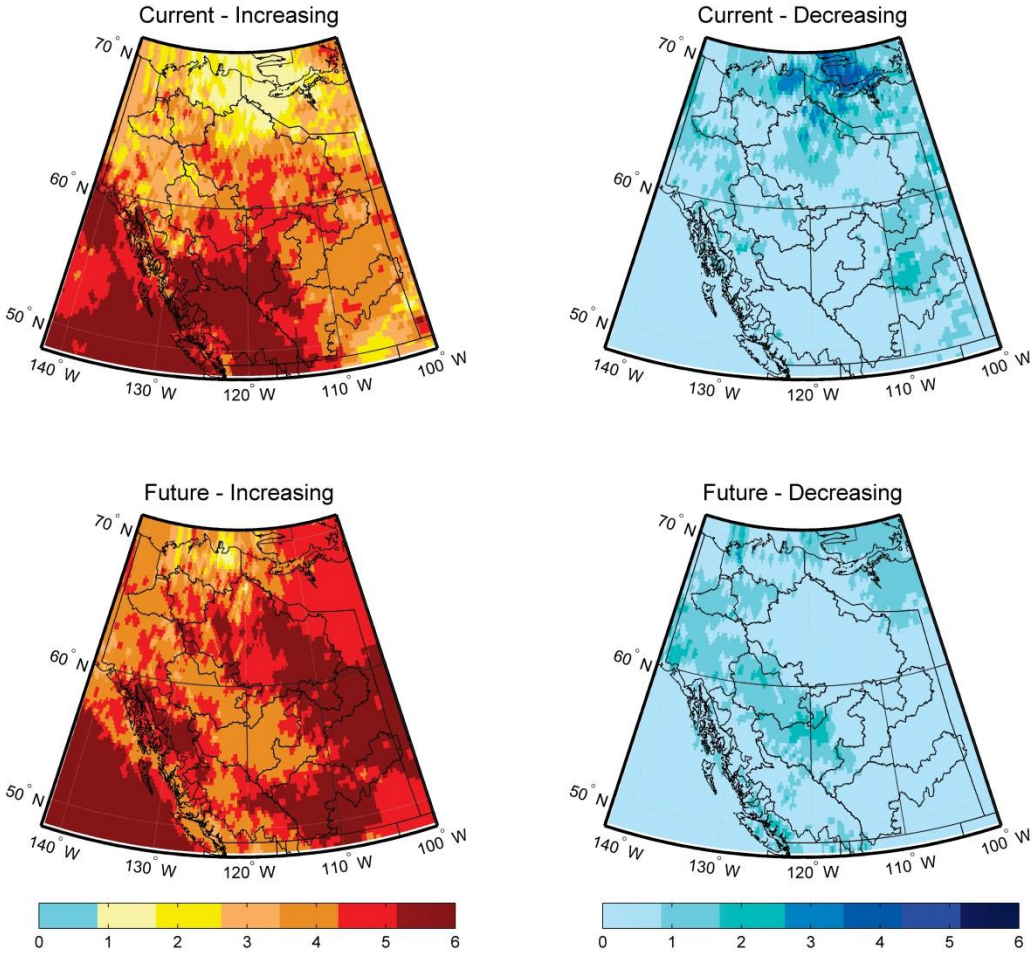

Figure B.38. Number of models showing increasing or decreasing rates of change in Tmin during the current (1971-2000) and future (2041-2070) time periods during June.

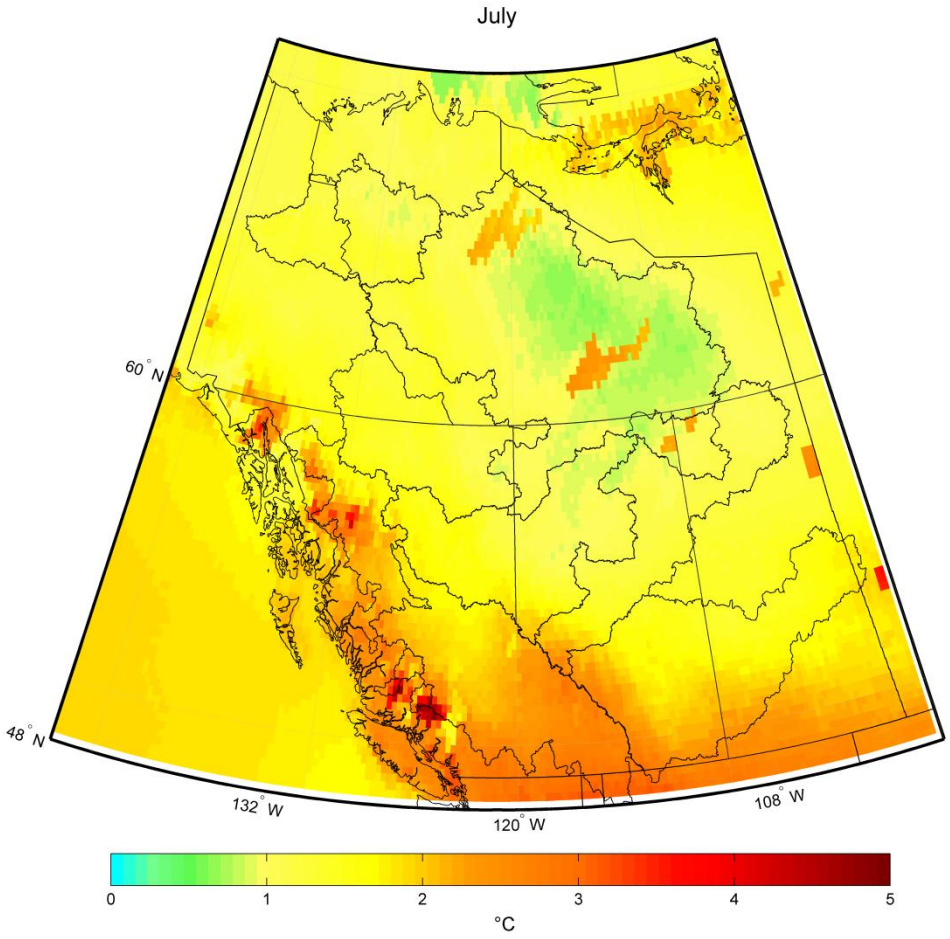

Figure B.39. Multimodel mean difference in monthly Tmax between the current and future periods during July.

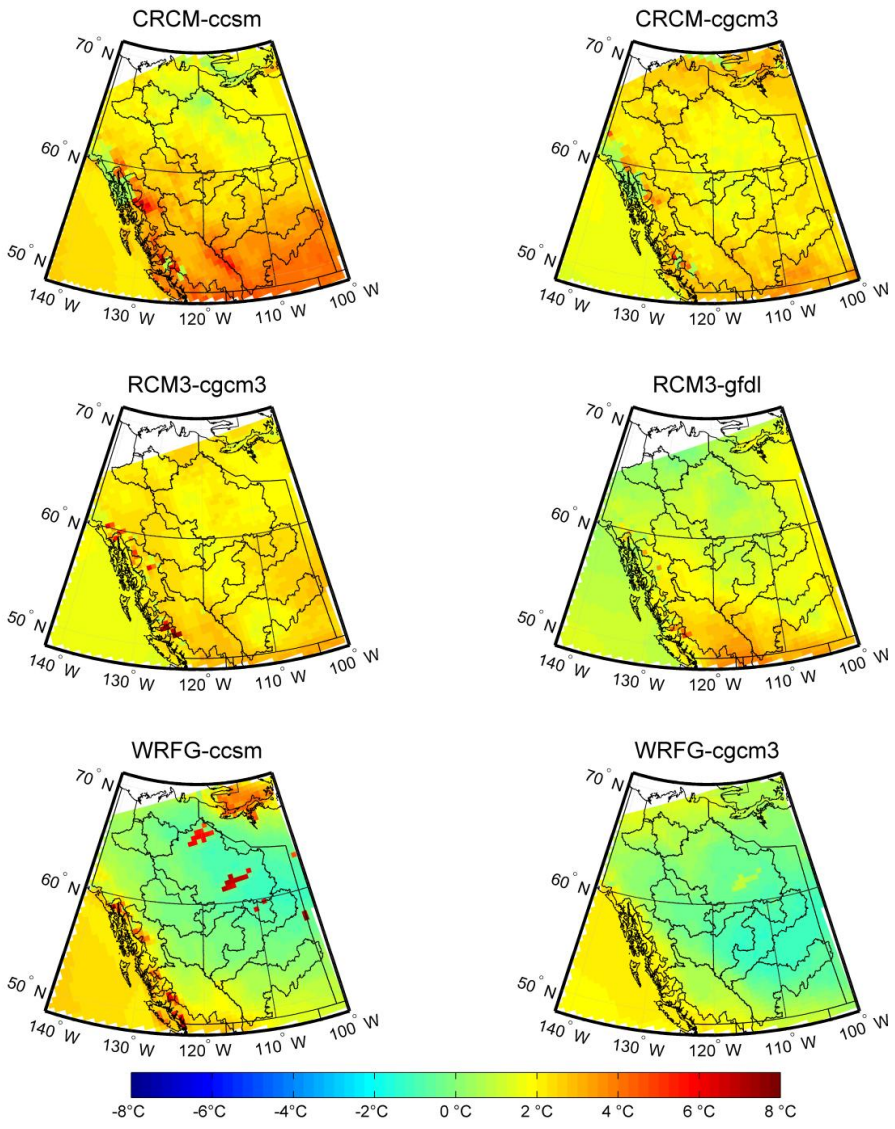

Figure B.40. Difference in Tmax values between 1971-2000 and 2041-2070 during July.

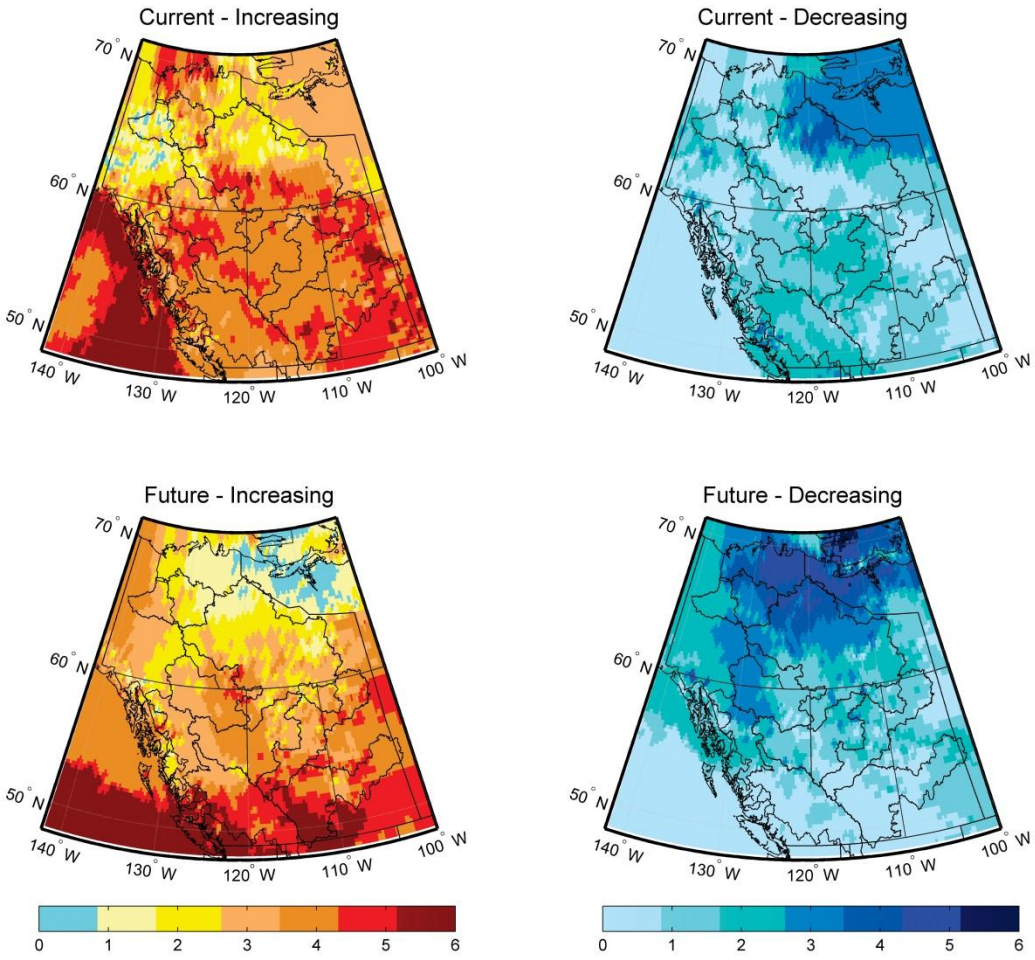

Figure B.41. Number of models showing increasing or decreasing rates of change in Tmax during the current (1971-2000) and future (2041-2070) time periods during July.

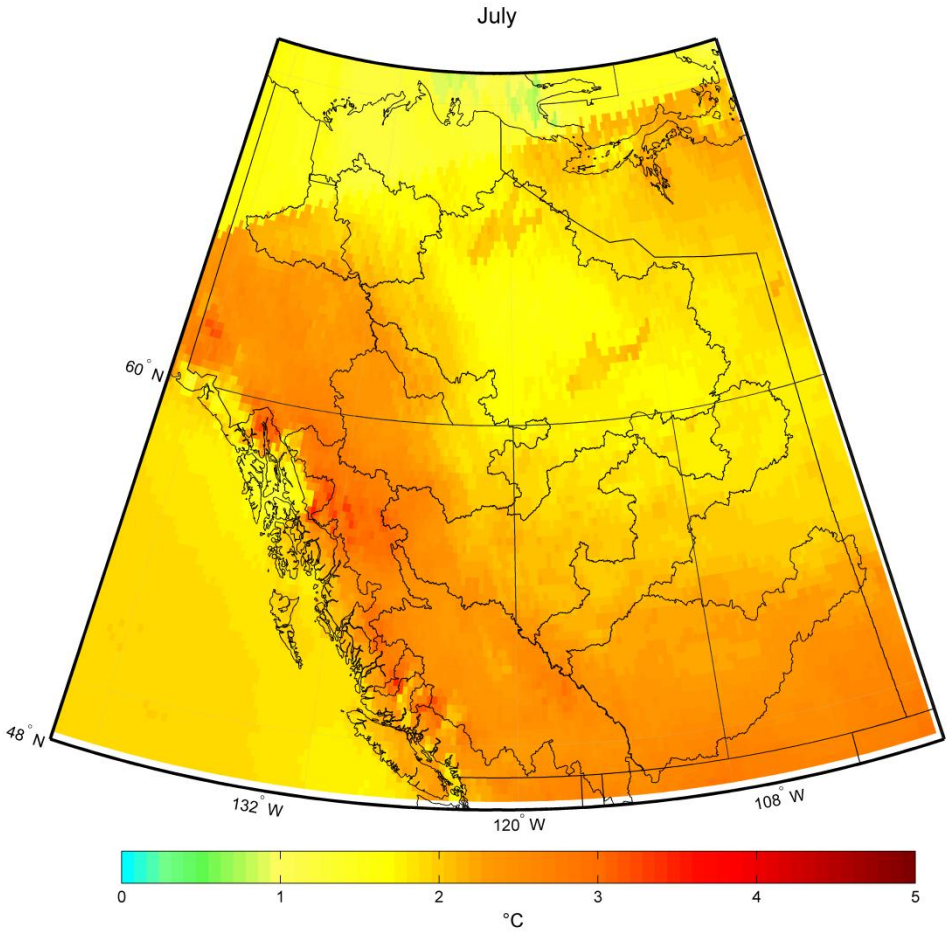

Figure B.42. Multimodel mean difference in monthly Tmin between the current and future periods during July.

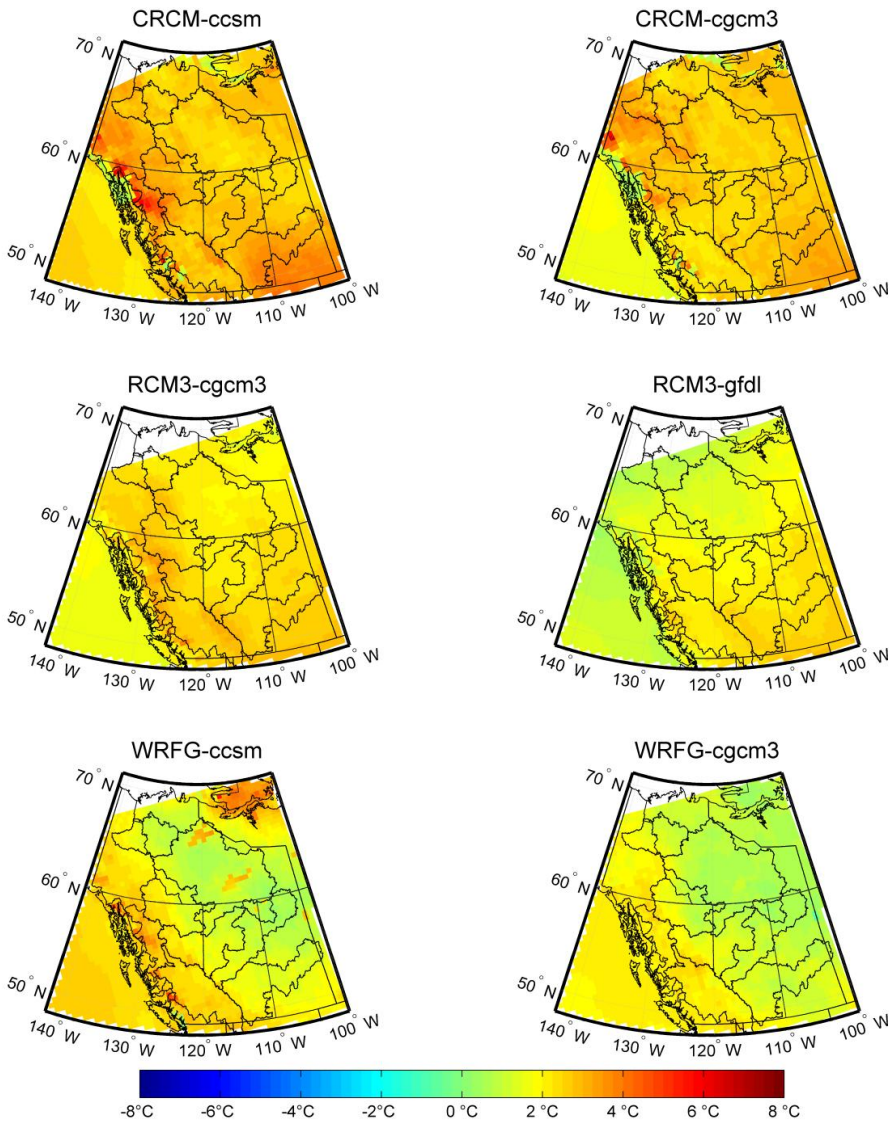

Figure B.43. Difference in Tmin values between 1971-2000 and 2041-2070 during July.

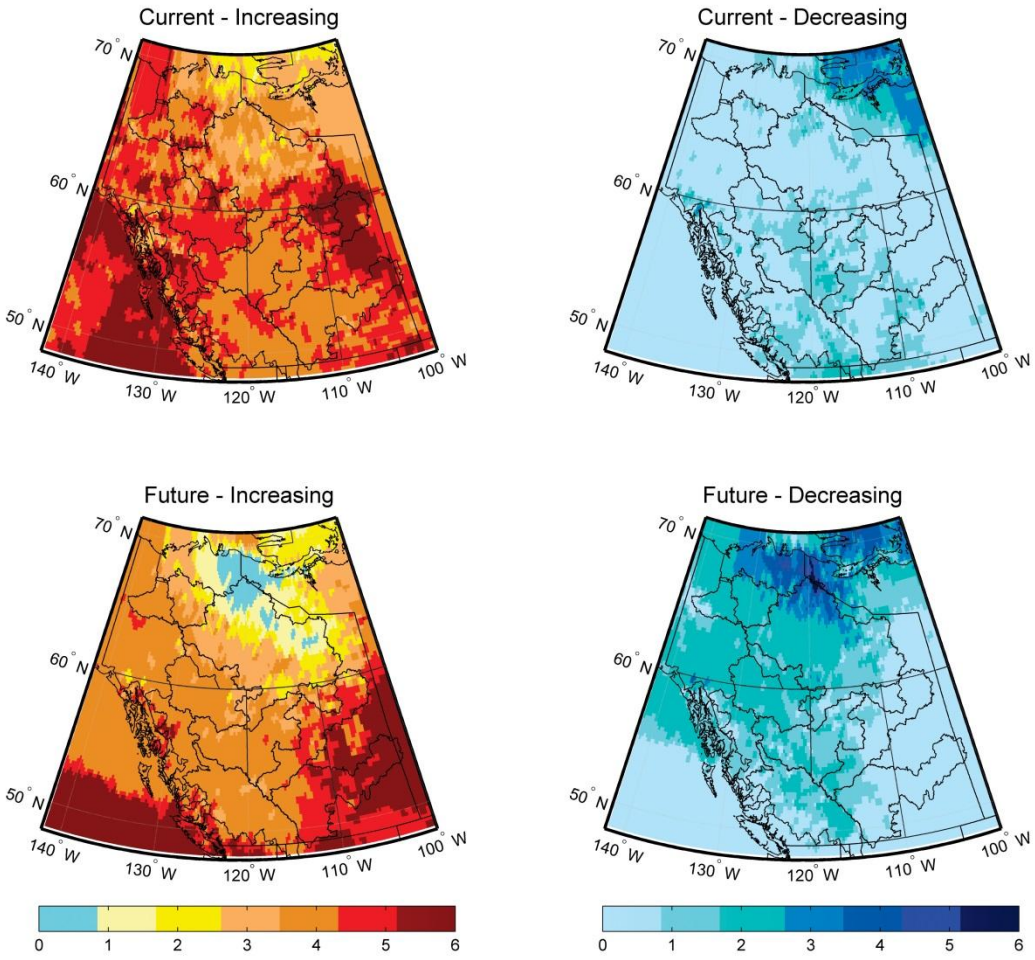

Figure B.44. Number of models showing increasing or decreasing rates of change in Tmin during the current (1971-2000) and future (2041-2070) time periods during July.

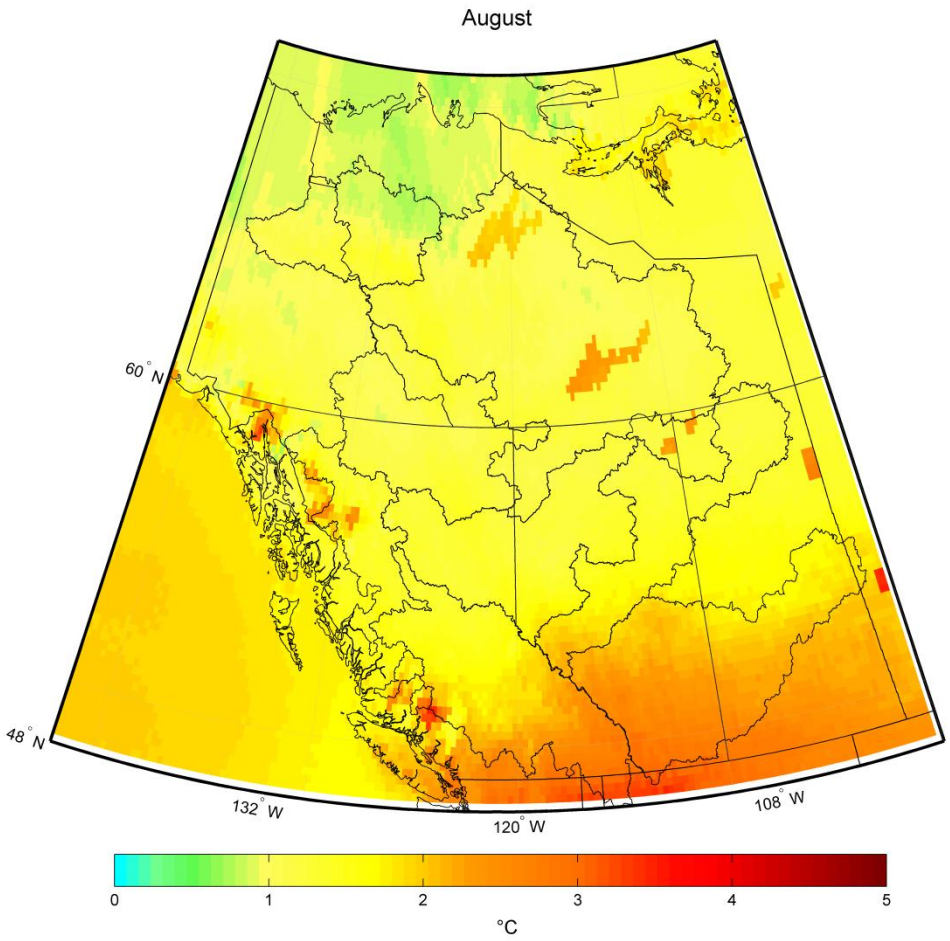

Figure B.45. Multimodel mean difference in monthly Tmax between the current and future periods during August.

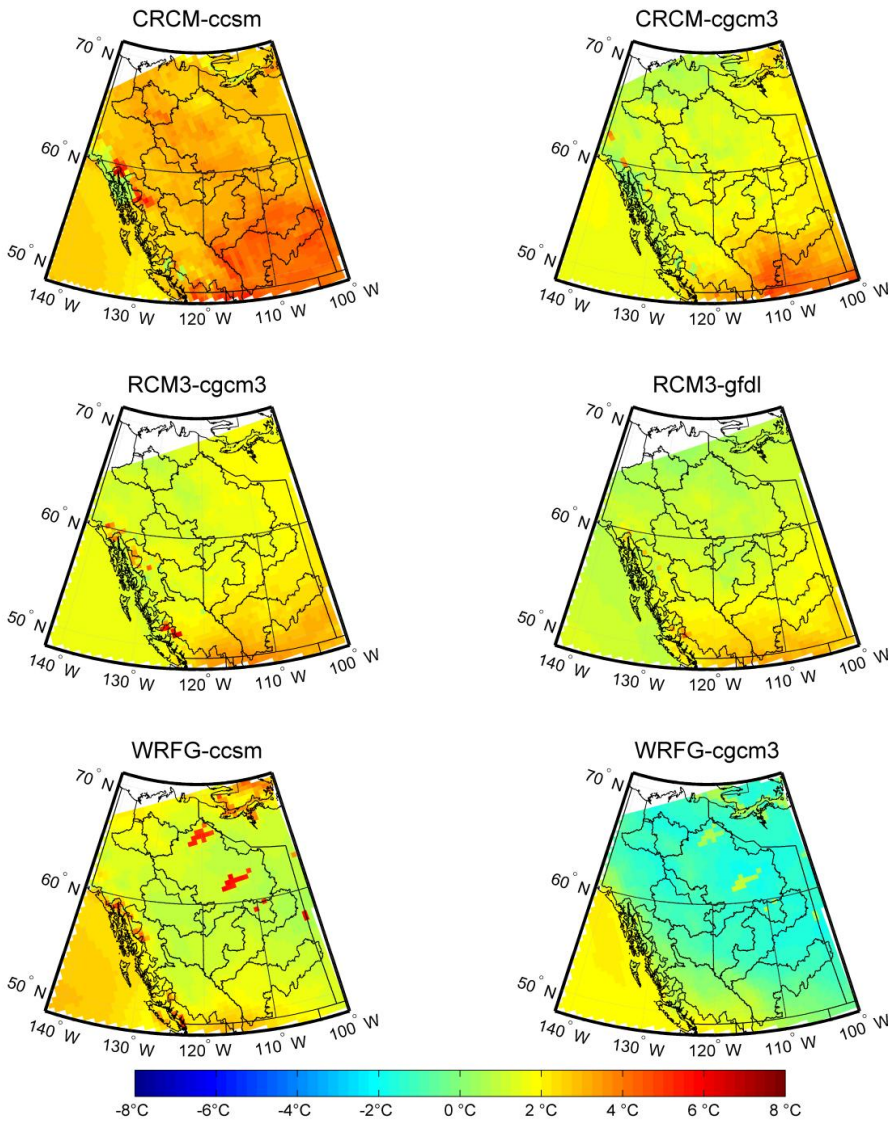

Figure B.46. Difference in Tmax values between 1971-2000 and 2041-2070 during August.

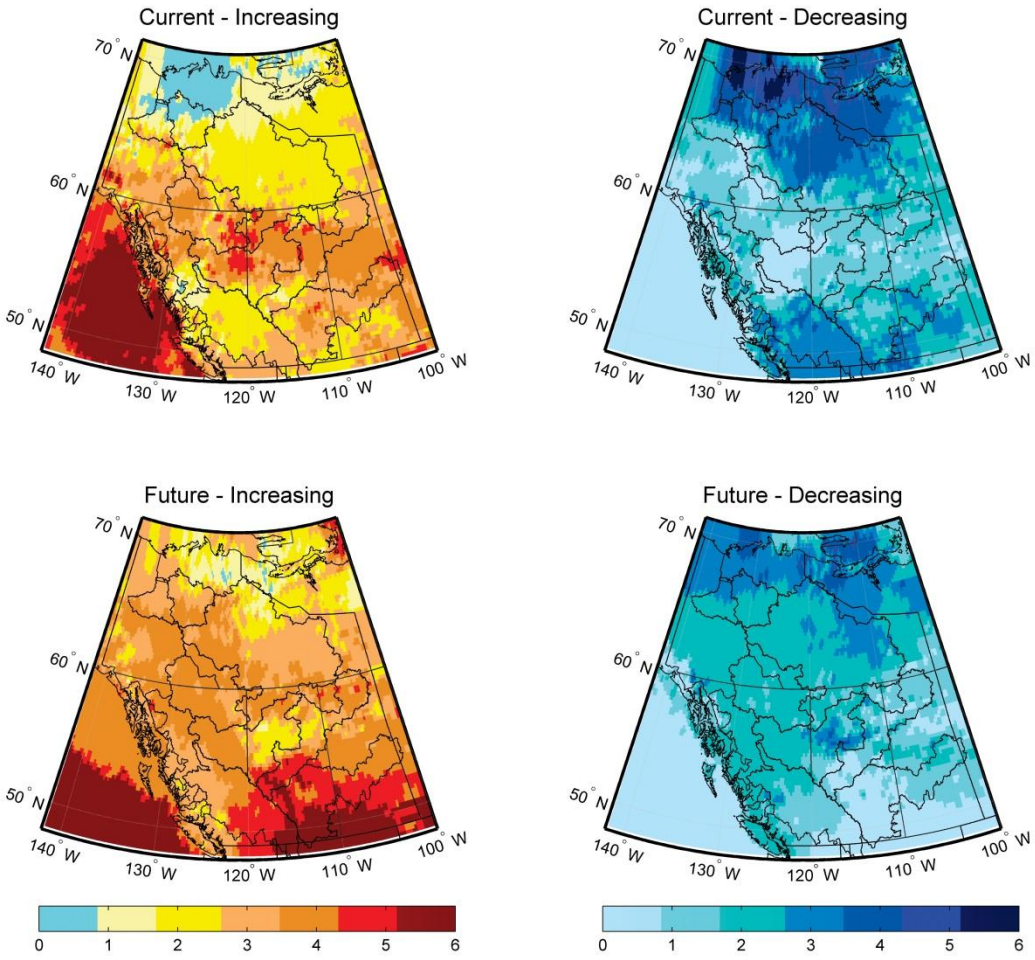

Figure B.47. Number of models showing increasing or decreasing rates of change in Tmax during the current (1971-2000) and future (2041-2070) time periods during August.

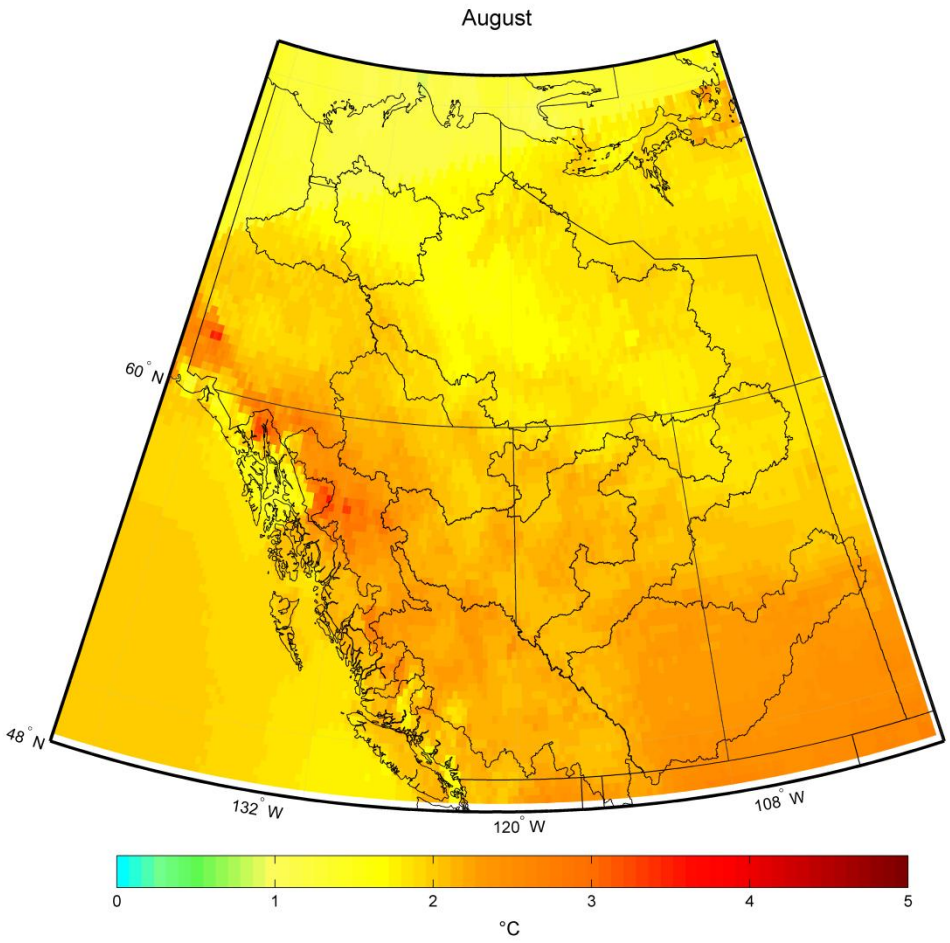

Figure B.48. Multimodel mean difference in monthly Tmin between the current and future periods during August.

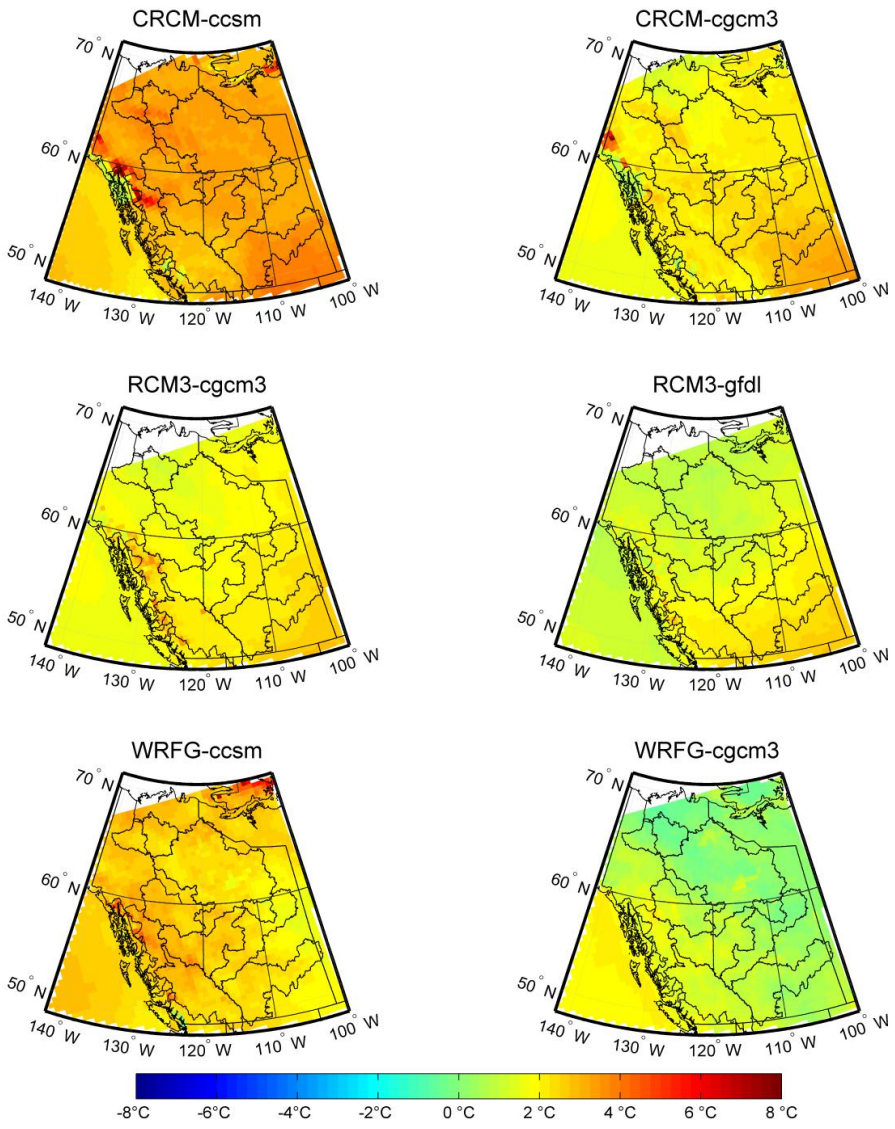

Figure B.49. Difference in Tmin values between 1971-2000 and 2041-2070 during August.

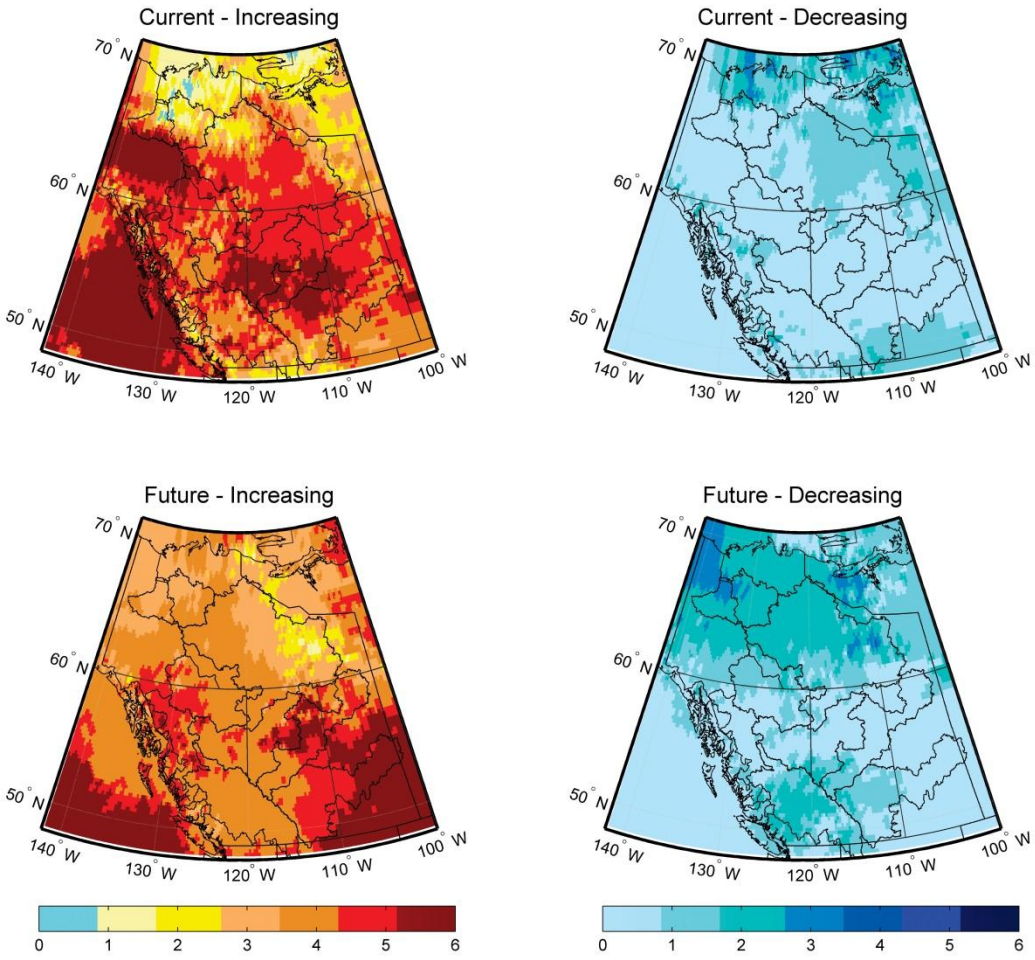

Figure B.50. Number of models showing increasing or decreasing rates of change in Tmin during the current (1971-2000) and future (2041-2070) time periods during August.

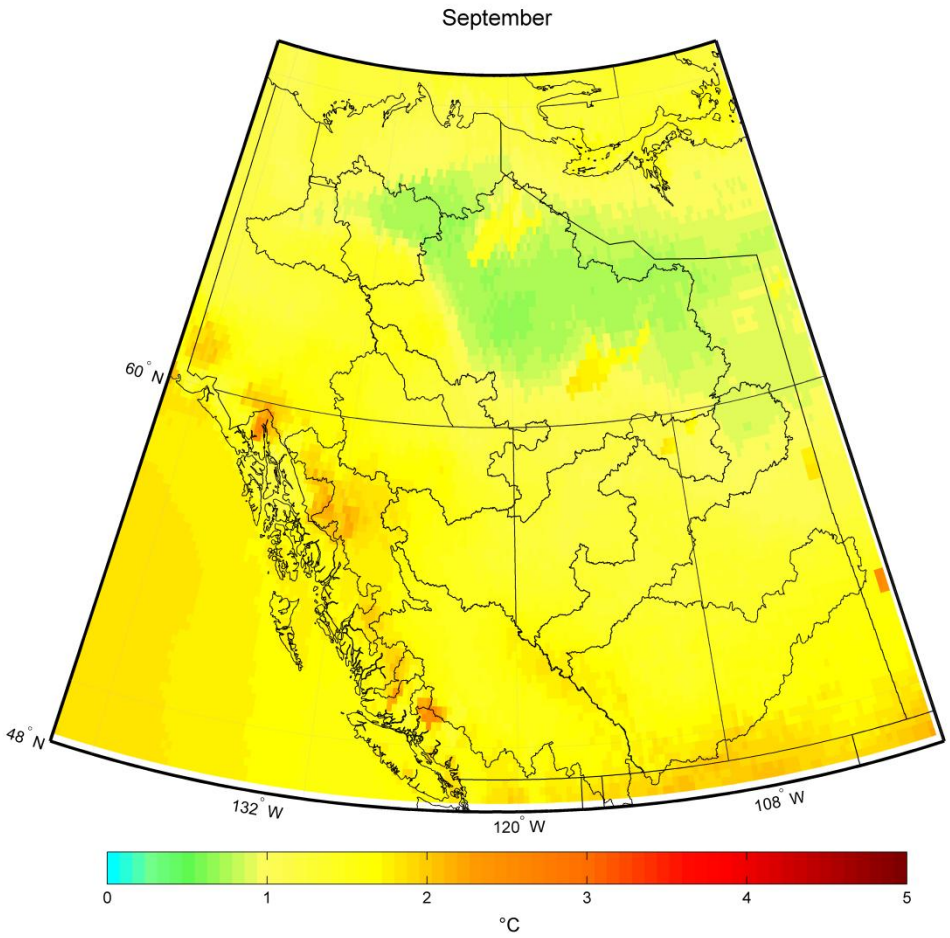

Figure B.51. Multimodel mean difference in monthly Tmax between the current and future periods during September.

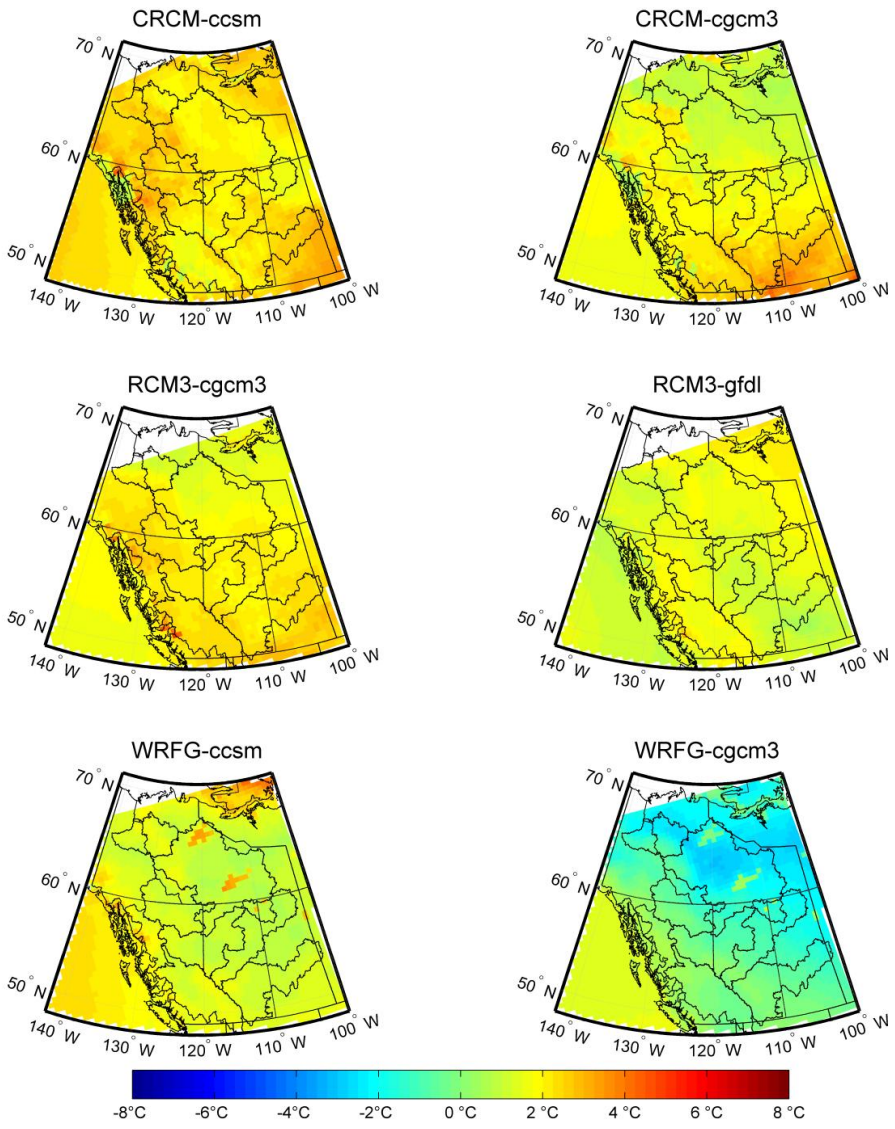

Figure B.52. Difference in Tmax values between 1971-2000 and 2041-2070 during September.

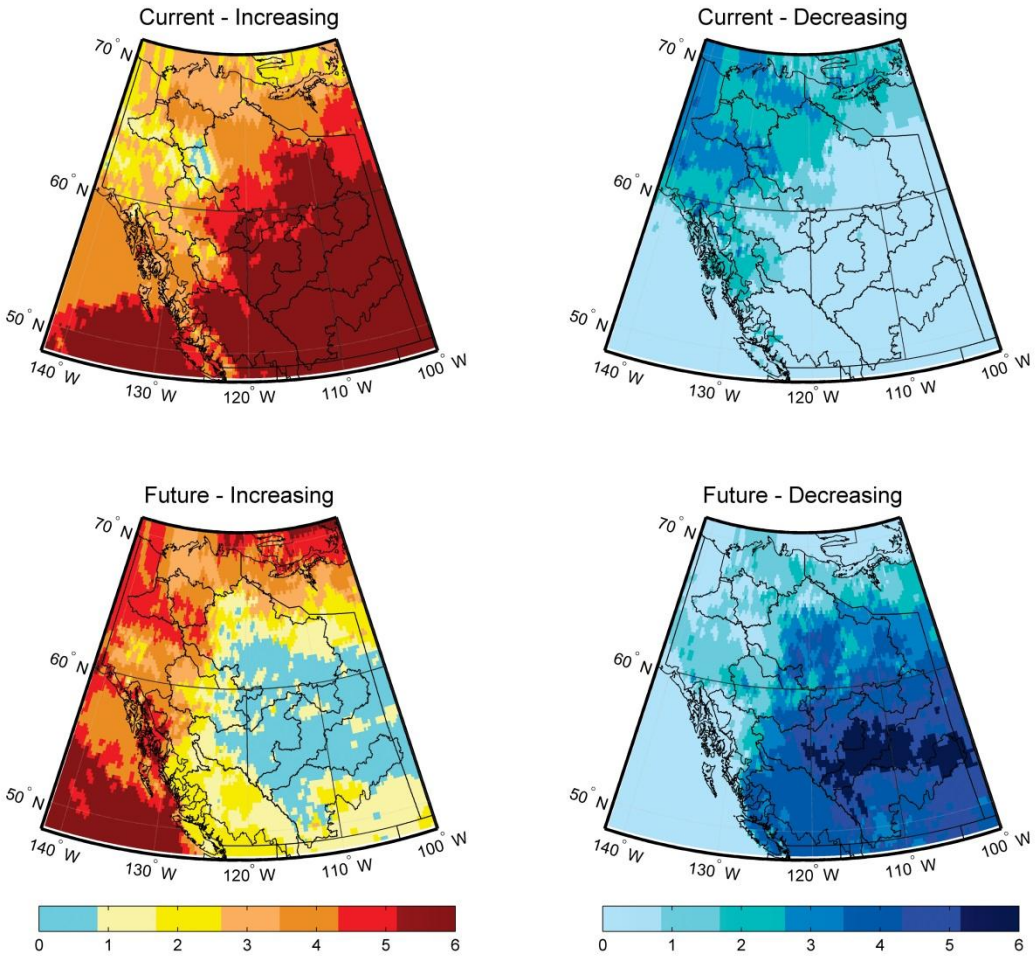

Figure B.53. Number of models showing increasing or decreasing rates of change in Tmax during the current (1971-2000) and future (2041-2070) time periods during September.

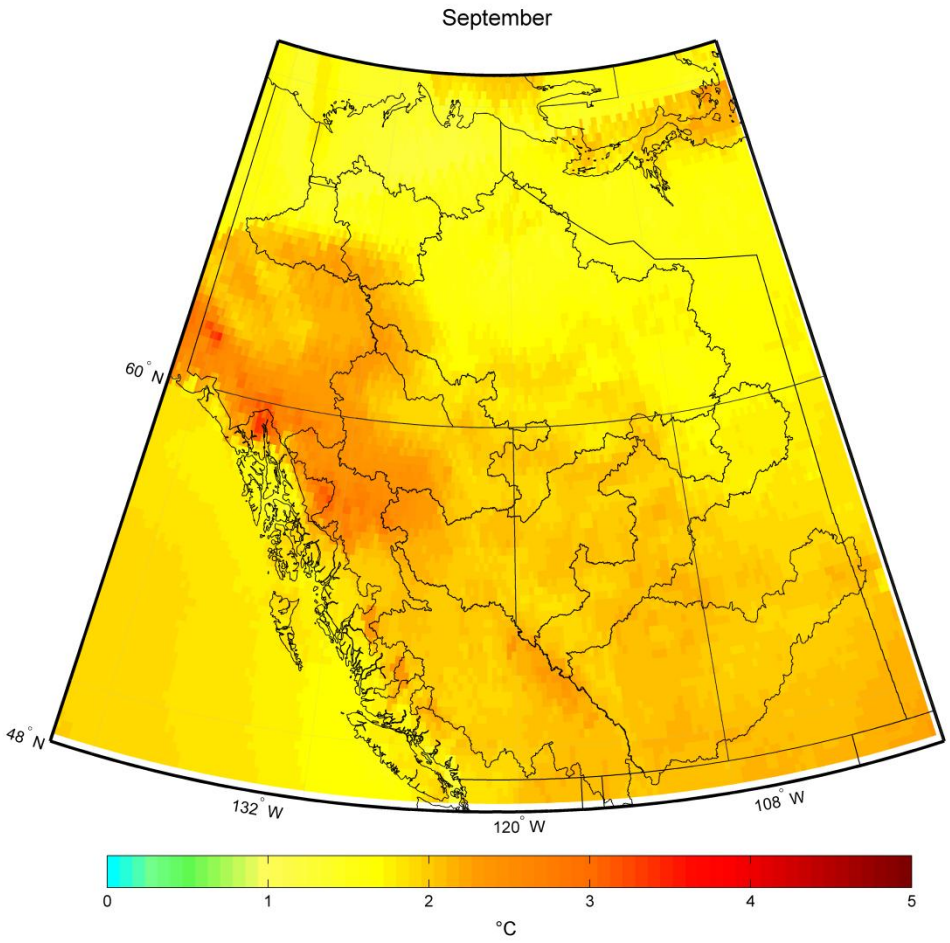

Figure B.54. Multimodel mean difference in monthly Tmin between the current and future periods during September.

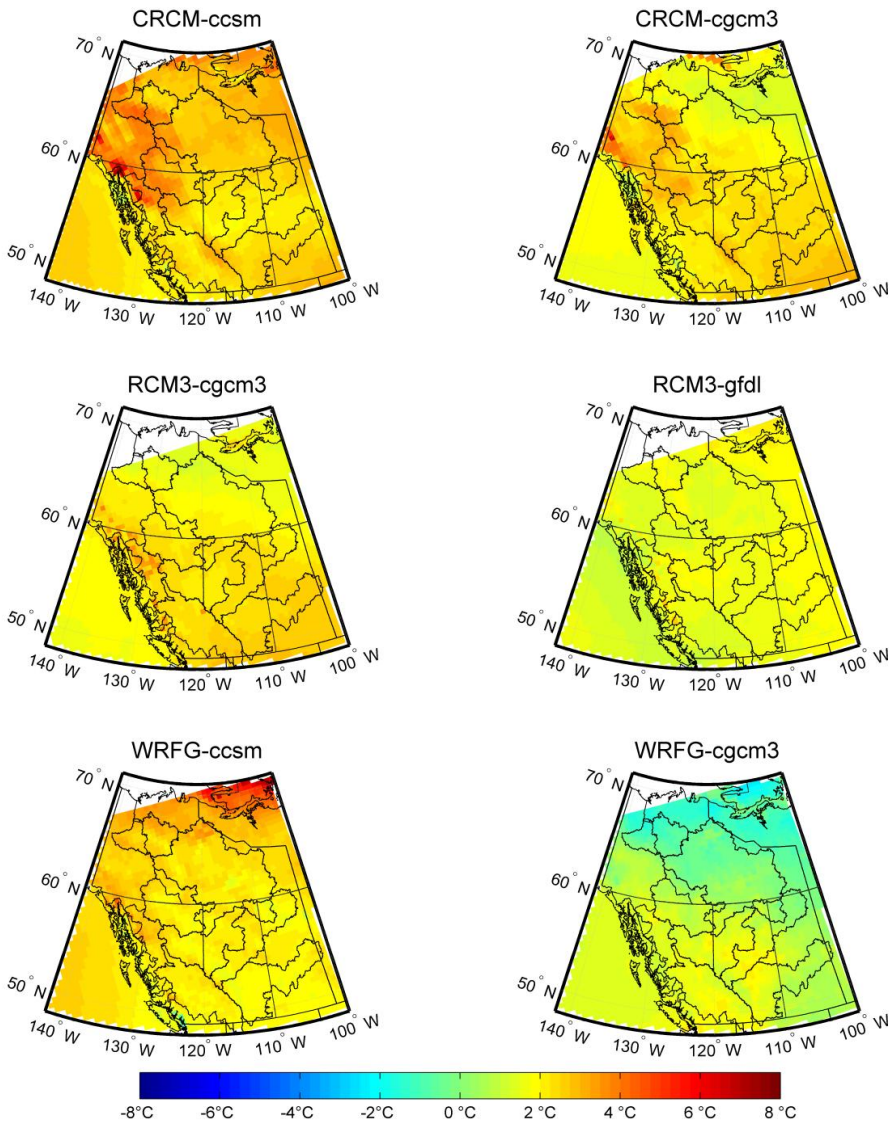

Figure B.55. Difference in Tmin values between 1971-2000 and 2041-2070 during September.

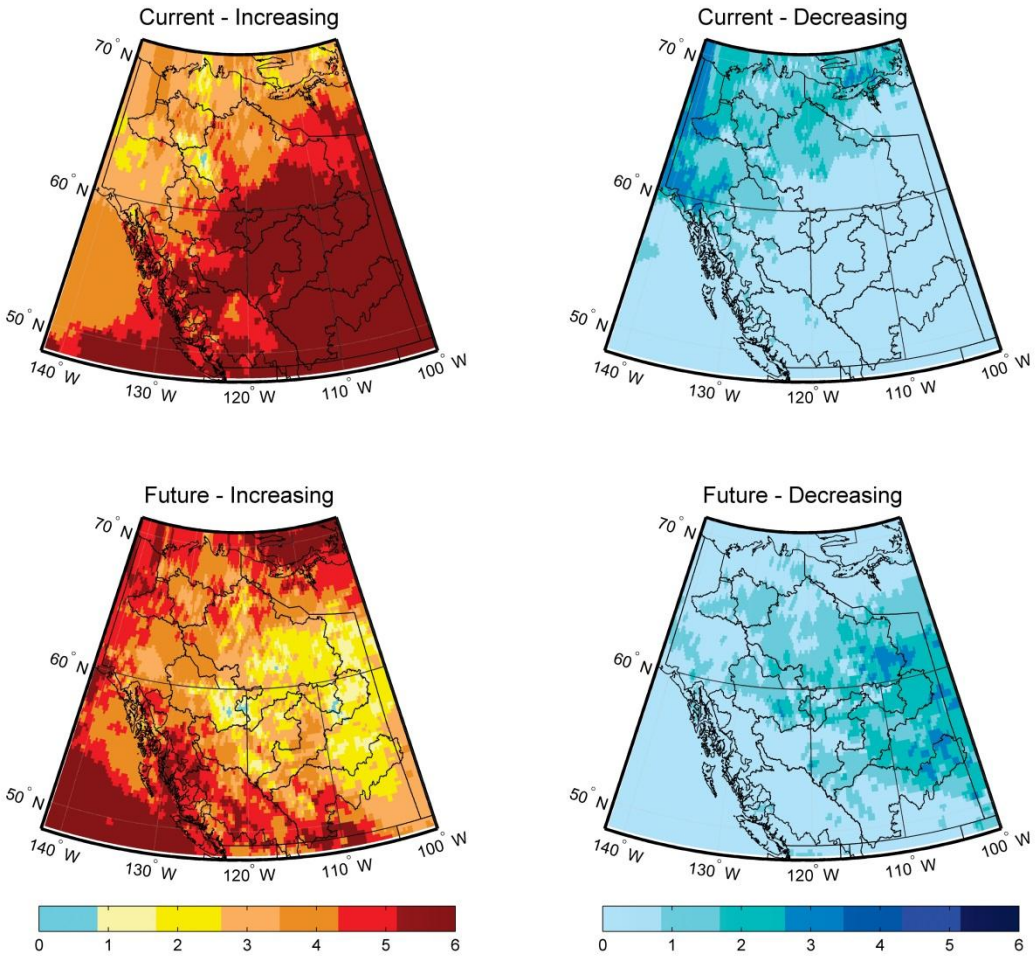

Figure B.56. Number of models showing increasing or decreasing rates of change in Tmin during the current (1971-2000) and future (2041-2070) time periods during September.

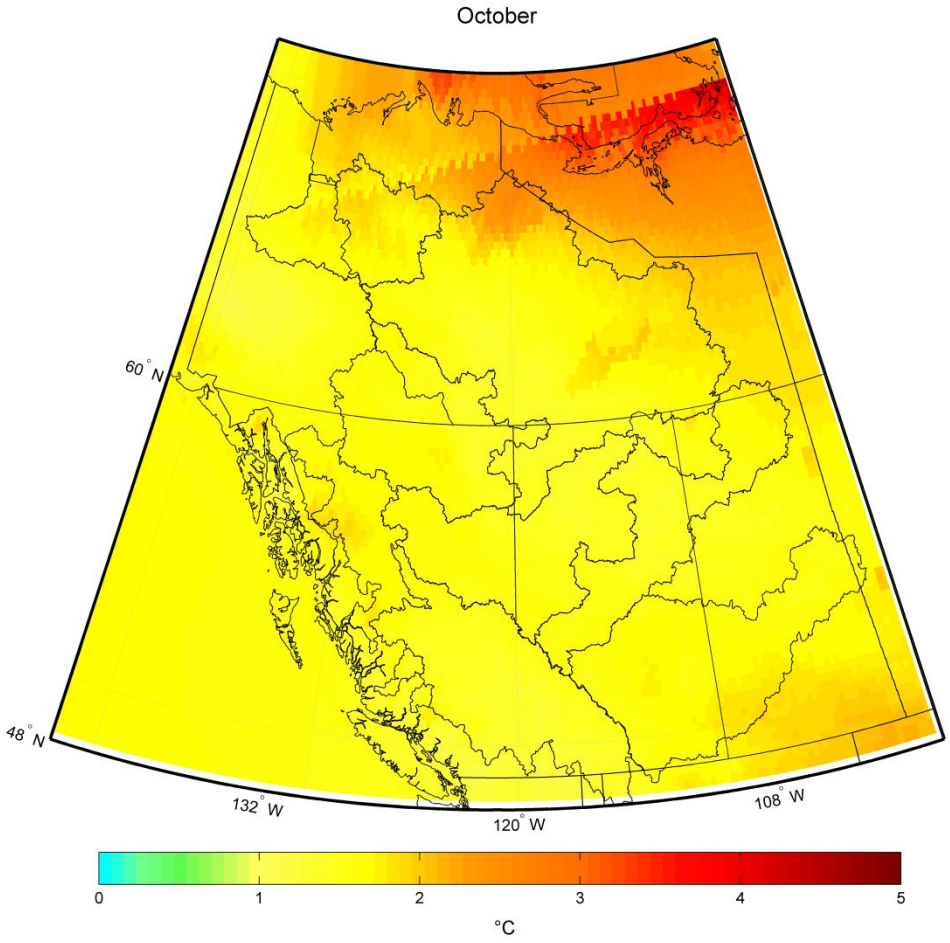

Figure B.57. Multimodel mean difference in monthly Tmax between the current and future periods during October.

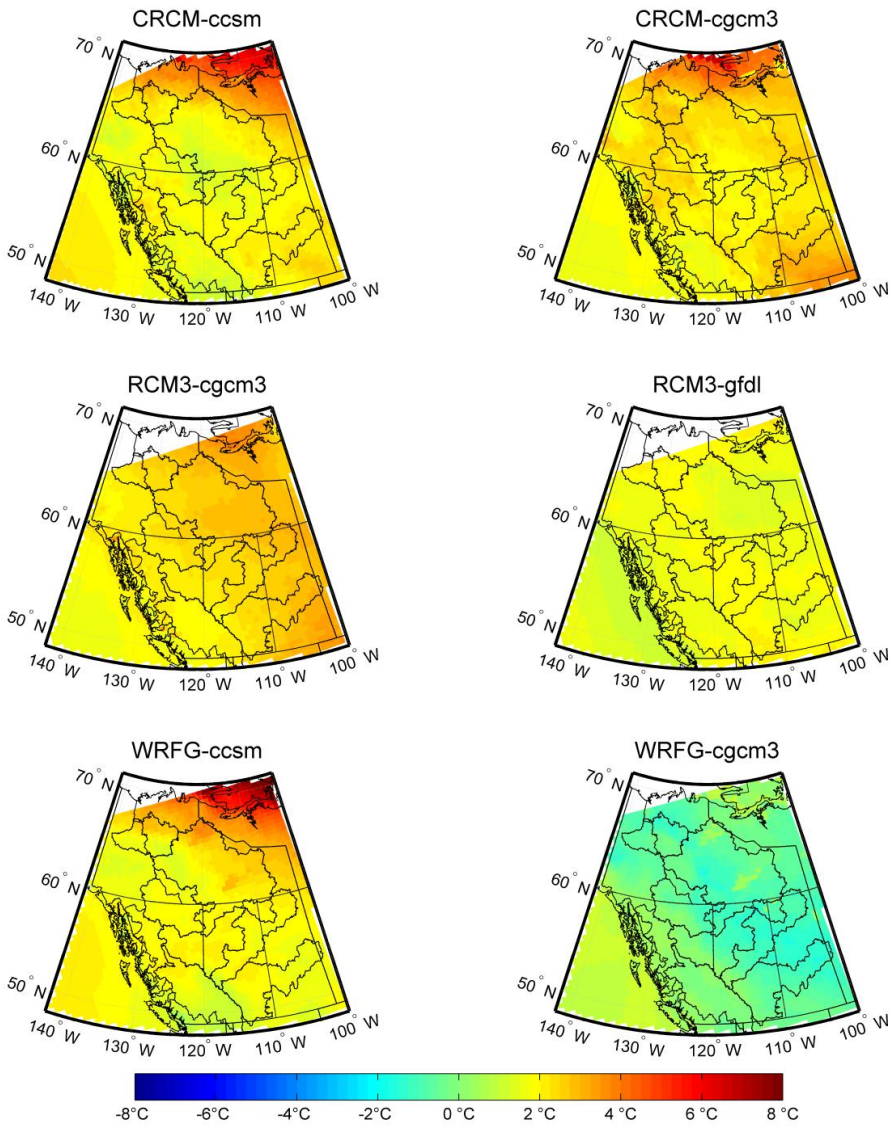

Figure B.58. Difference in Tmax values between 1971-2000 and 2041-2070 during October.

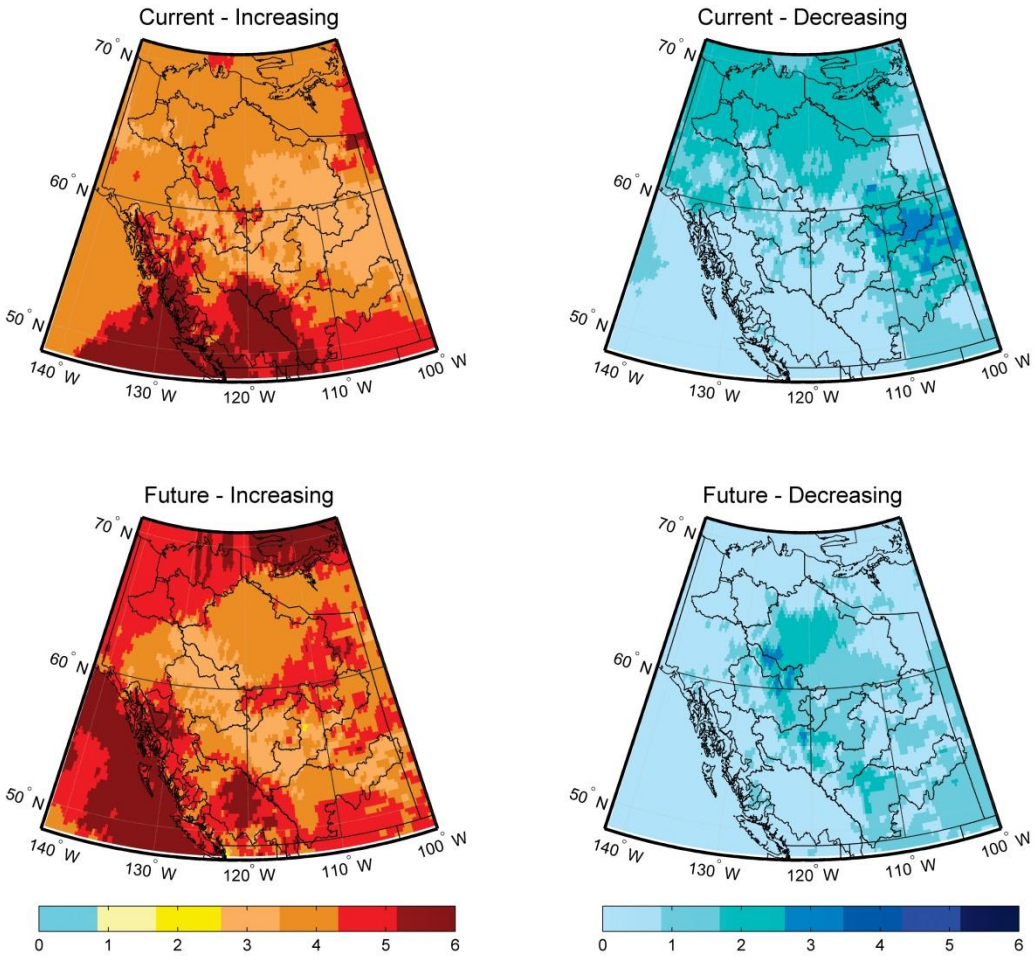

Figure B.59. Number of models showing increasing or decreasing rates of change in Tmax during the current (1971-2000) and future (2041-2070) time periods during October.

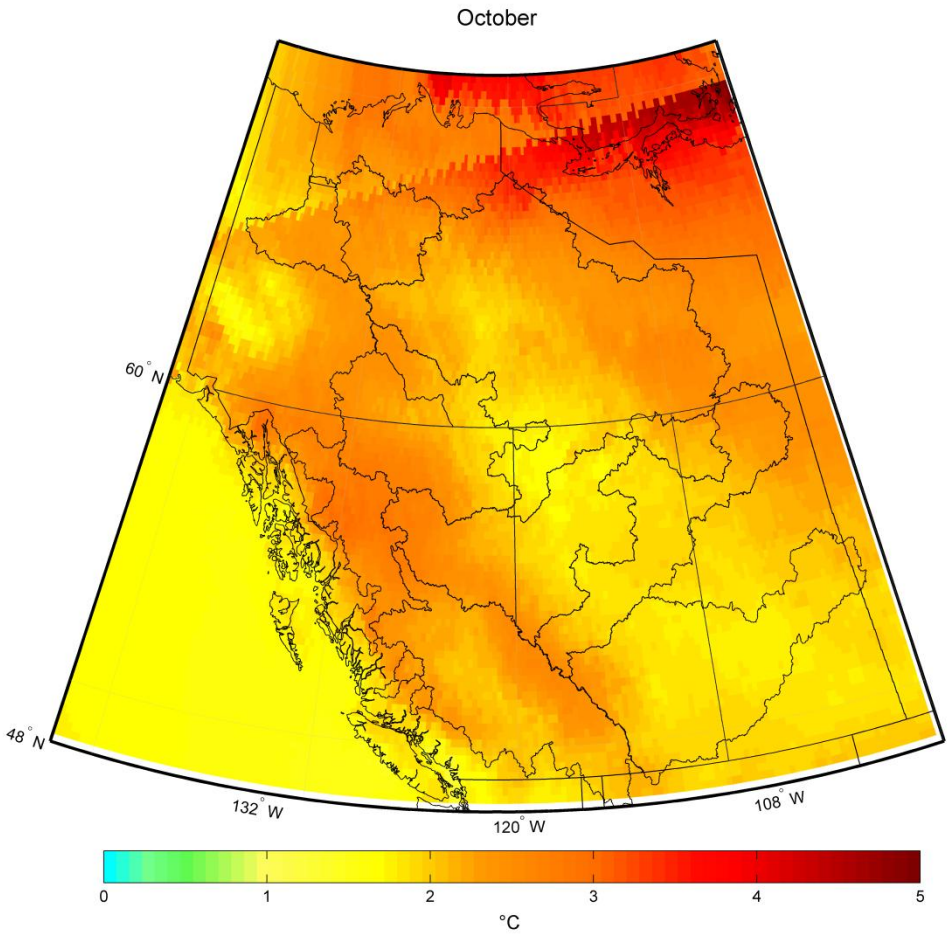

Figure B.60. Multimodel mean difference in monthly Tmin between the current and future periods during October.

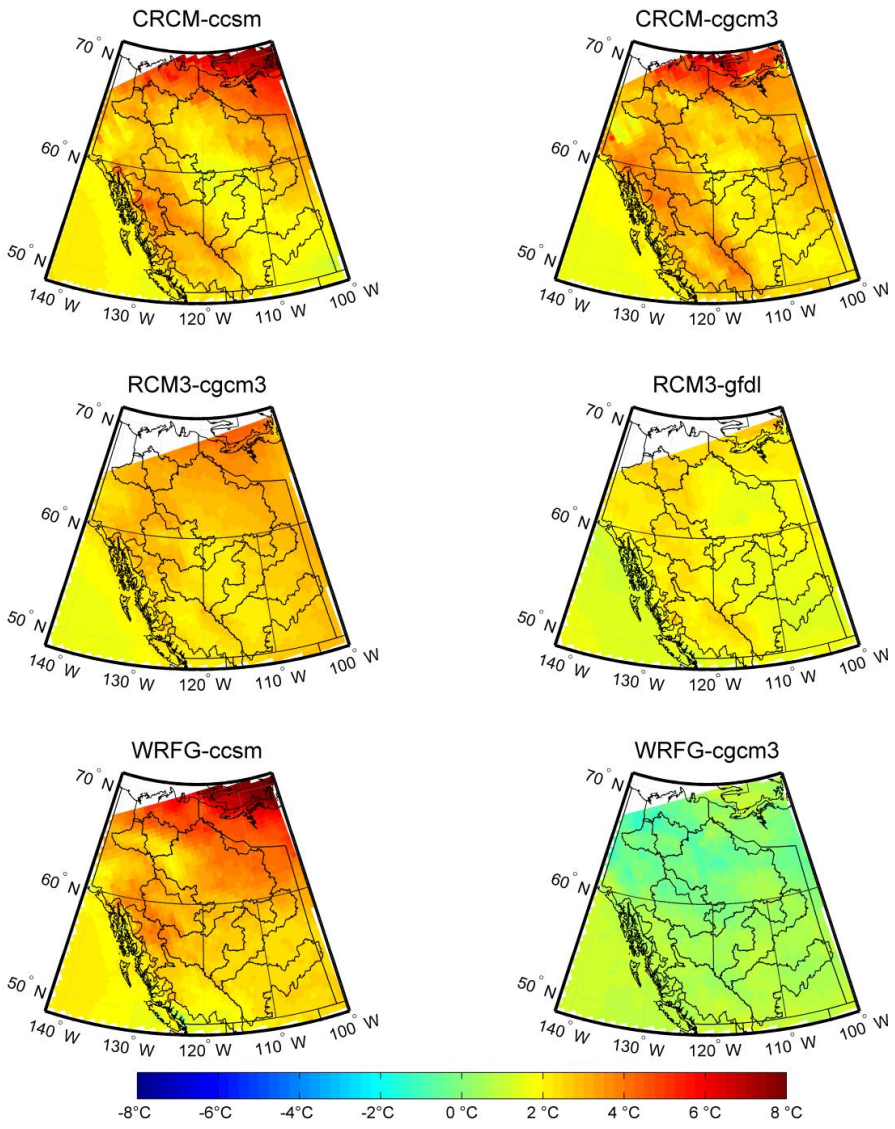

Figure B.61. Difference in Tmin values between 1971-2000 and 2041-2070 during October.

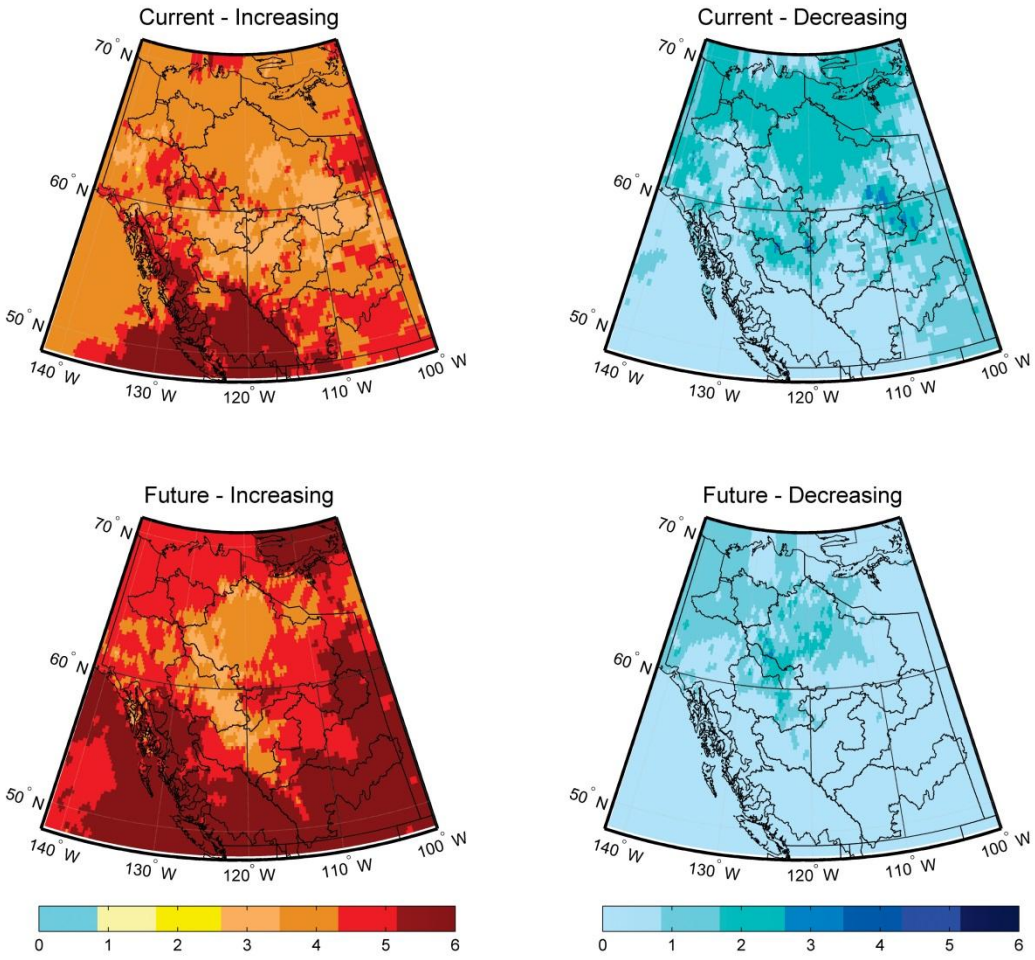

Figure B.62. Number of models showing increasing or decreasing rates of change in Tmin during the current (1971-2000) and future (2041-2070) time periods during October.

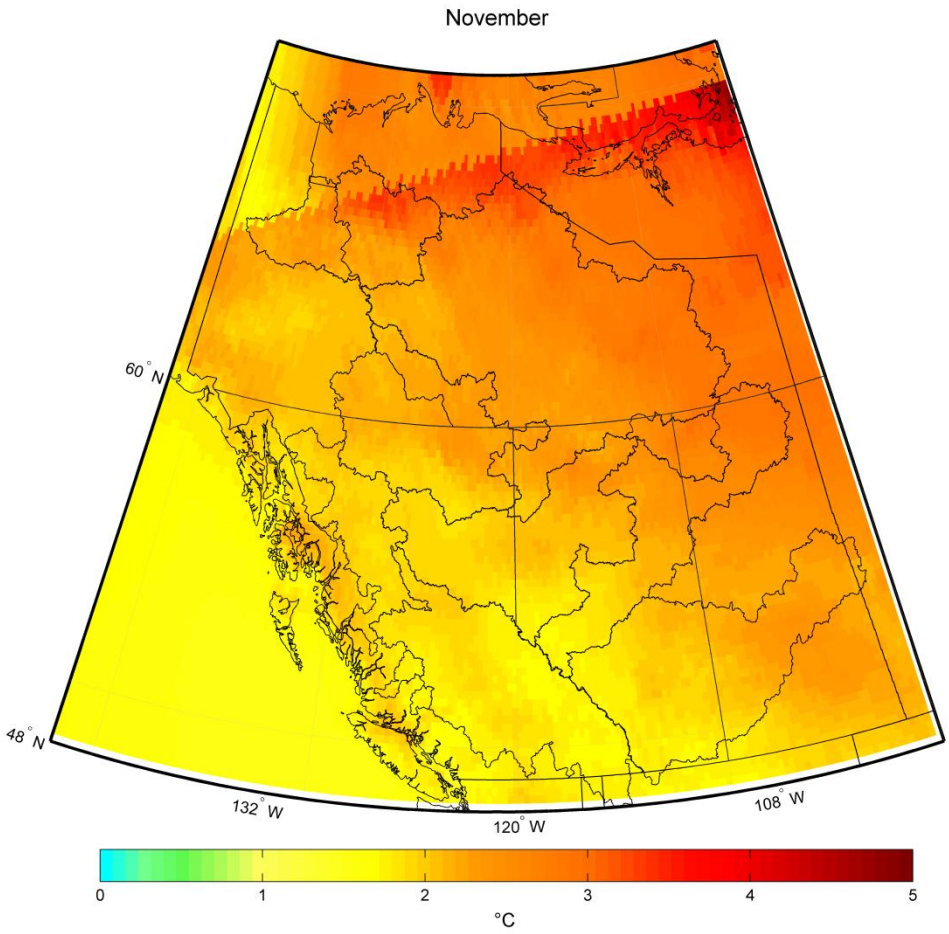

Figure B.63. Multimodel mean difference in monthly Tmax between the current and future periods during November.

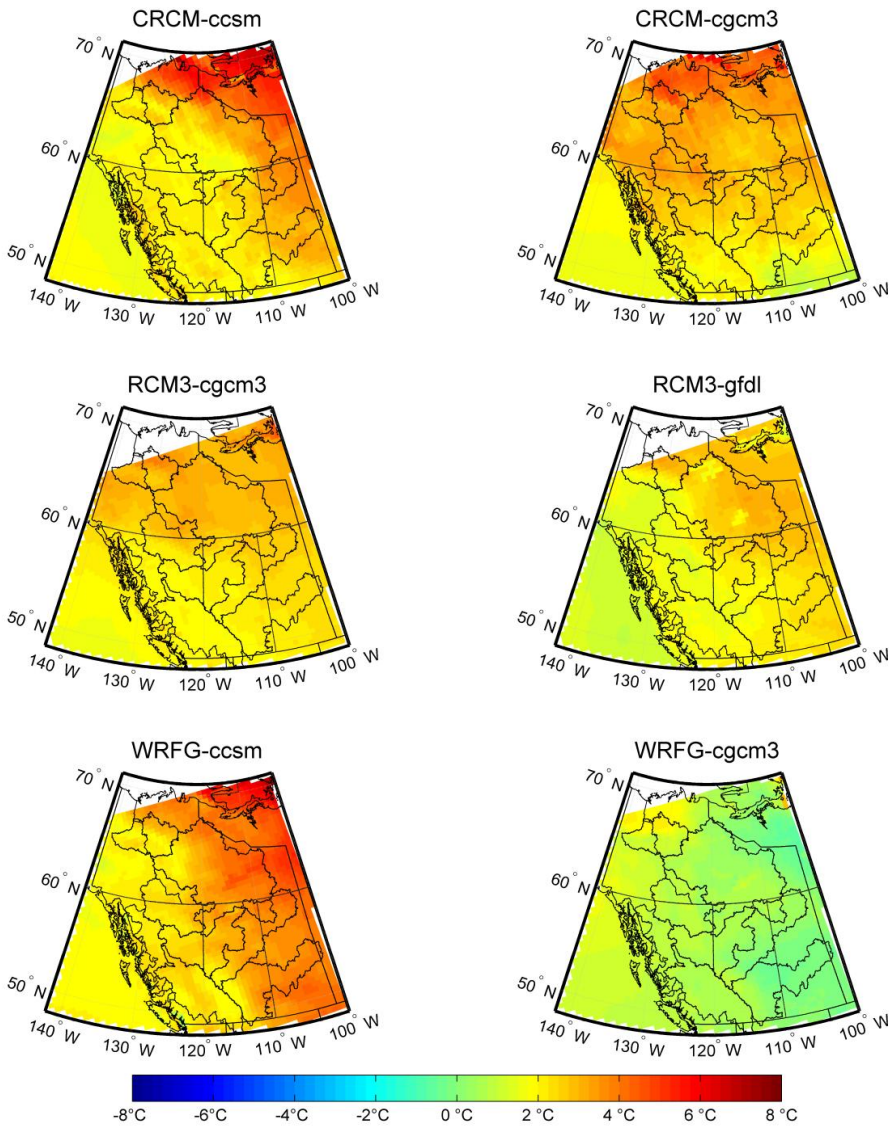

Figure B.64. Difference in Tmax values between 1971-2000 and 2041-2070 during November.

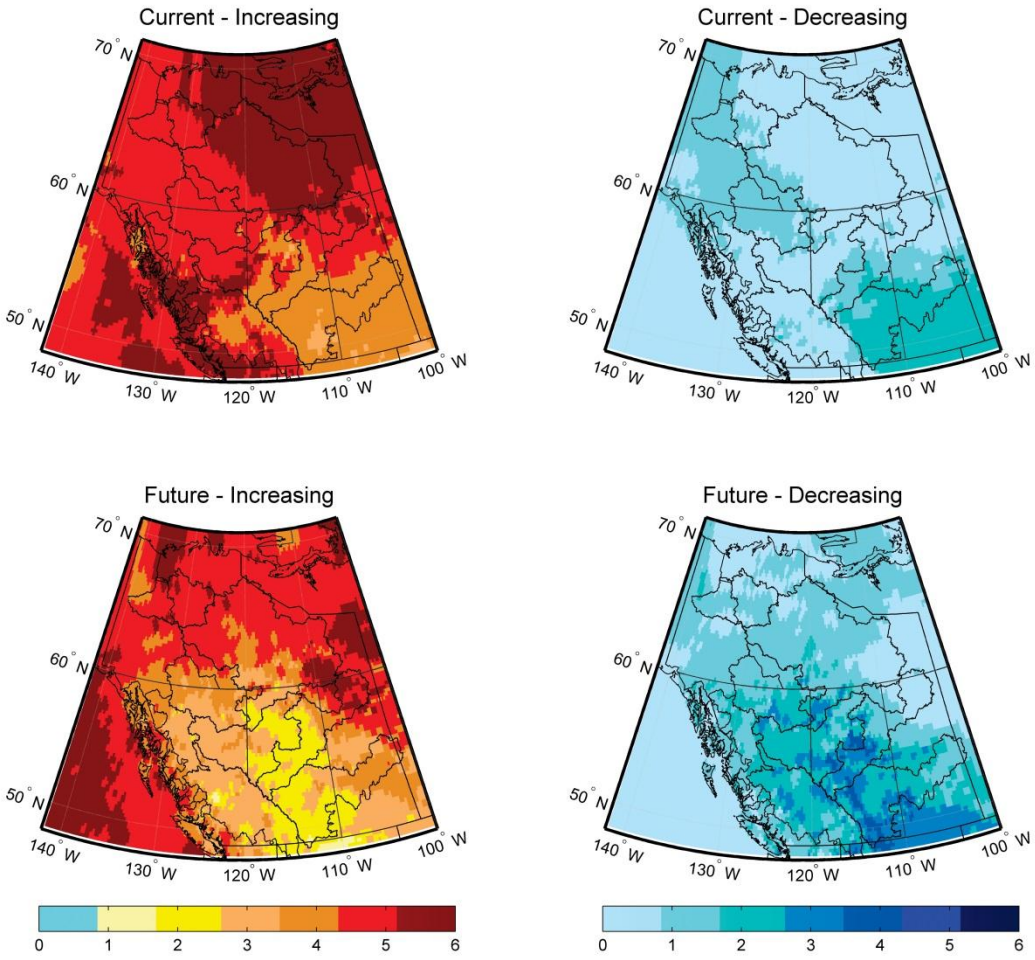

Figure B.65. Number of models showing increasing or decreasing rates of change in Tmax during the current (1971-2000) and future (2041-2070) time periods during November.

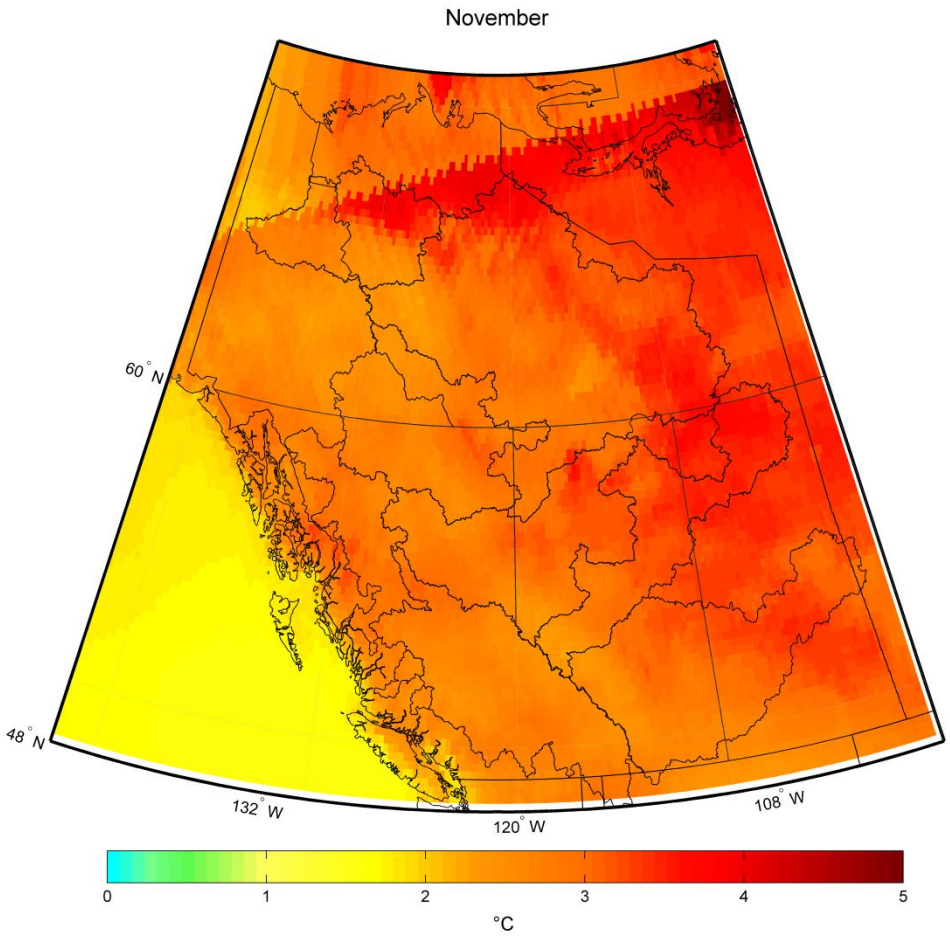

Figure B.66. Multimodel mean difference in monthly Tmin between the current and future periods during November.

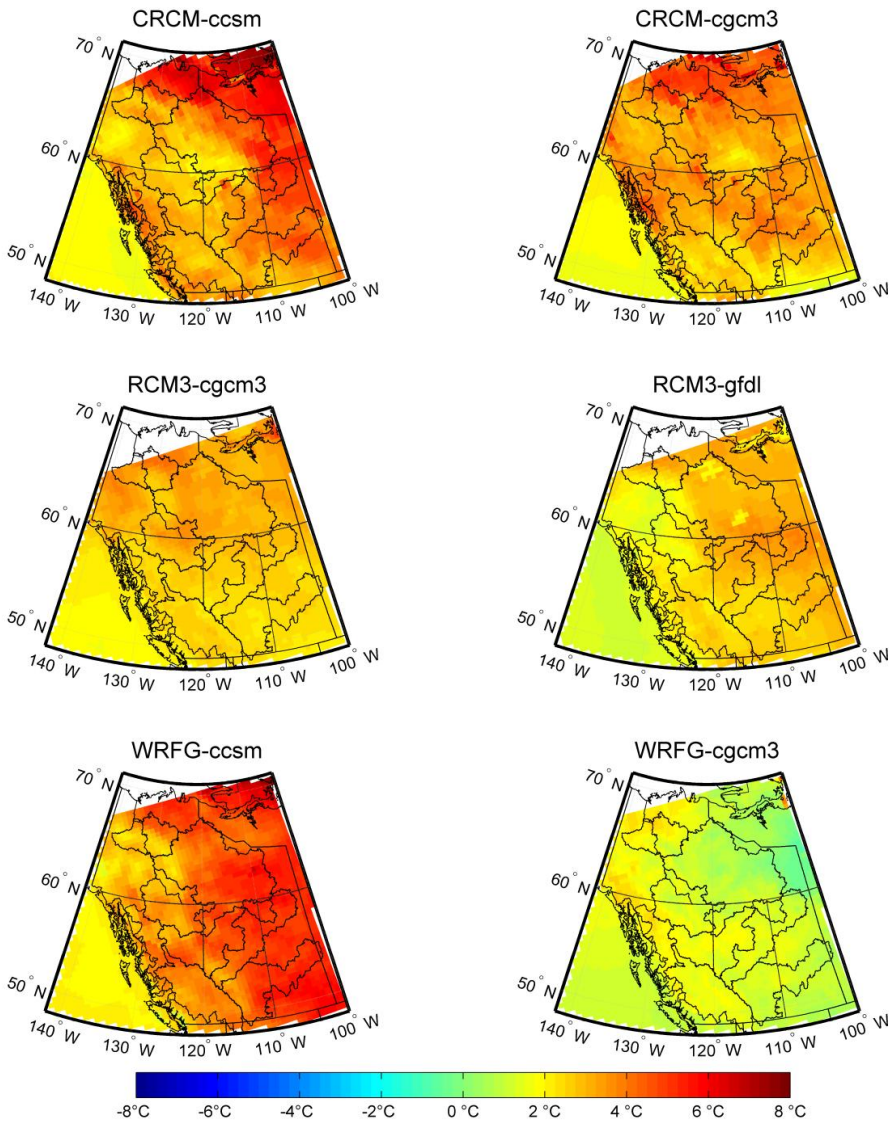

Figure B.67. Difference in Tmin values between 1971-2000 and 2041-2070 during November.

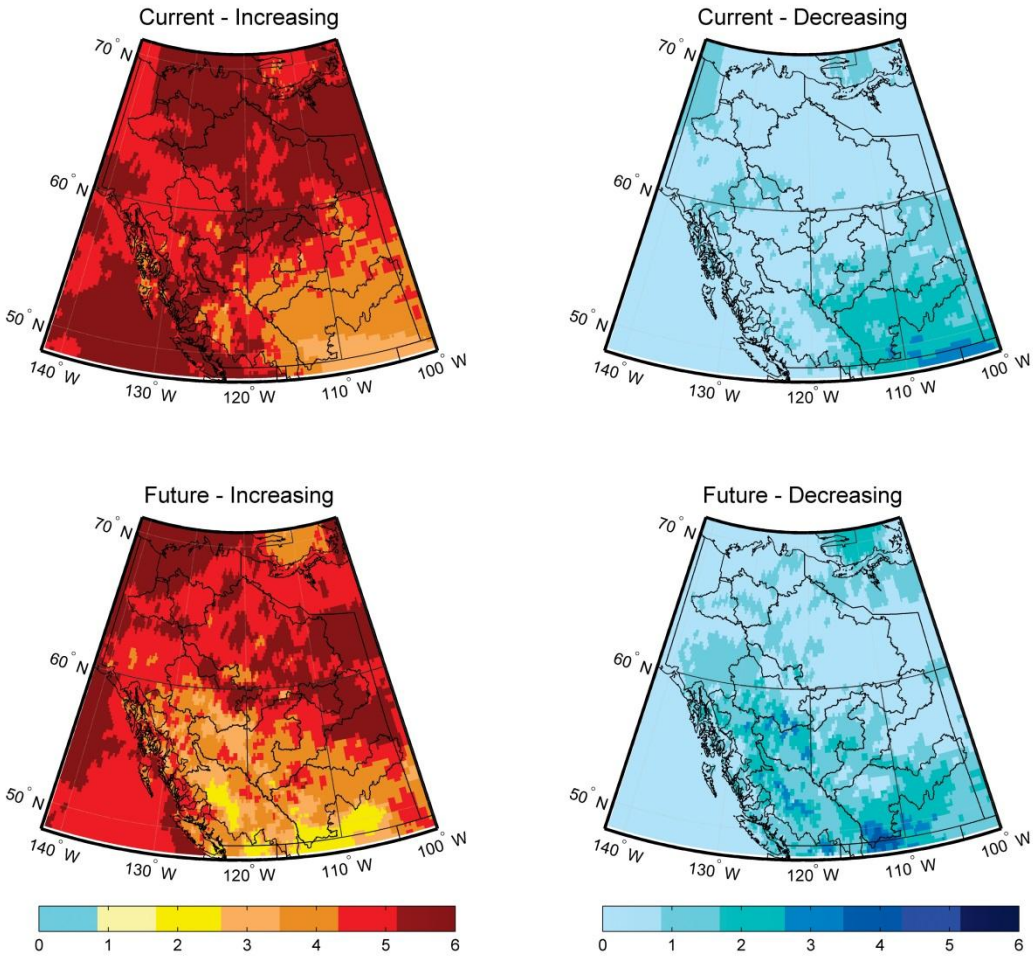

Figure B.68. Number of models showing increasing or decreasing rates of change in Tmin during the current (1971-2000) and future (2041-2070) time periods during November.

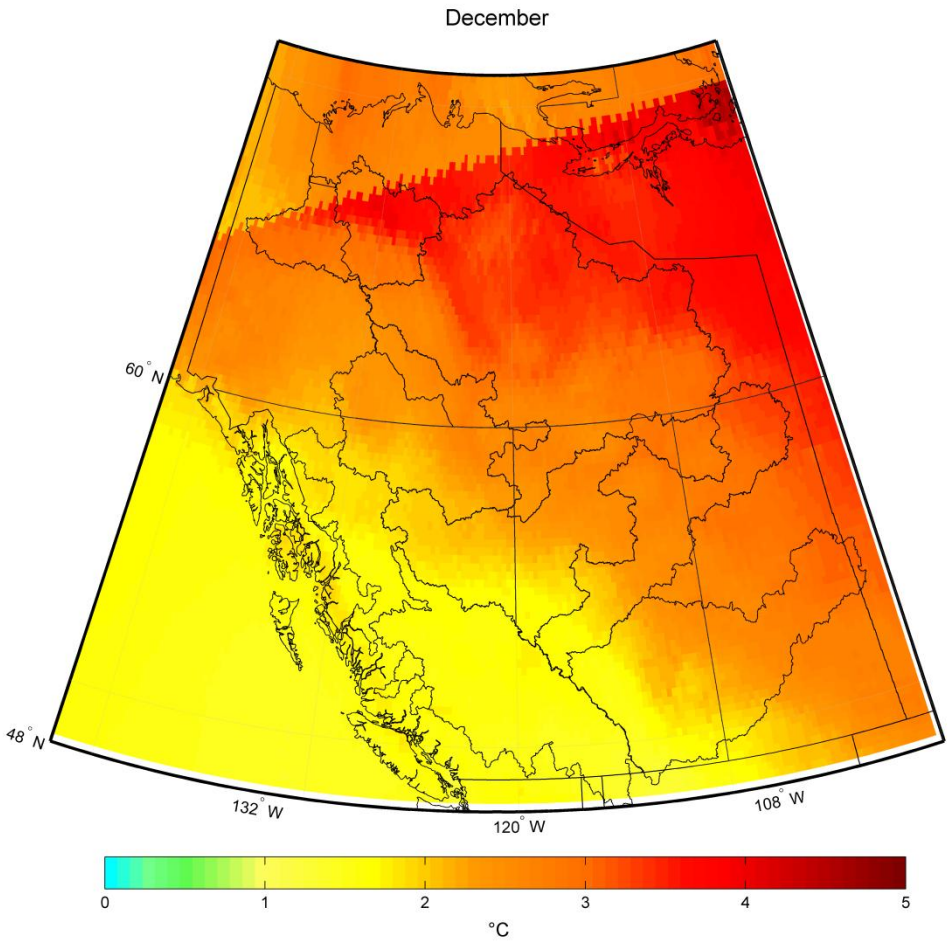

Figure B.69. Multimodel mean difference in monthly Tmax between the current and future periods during December.

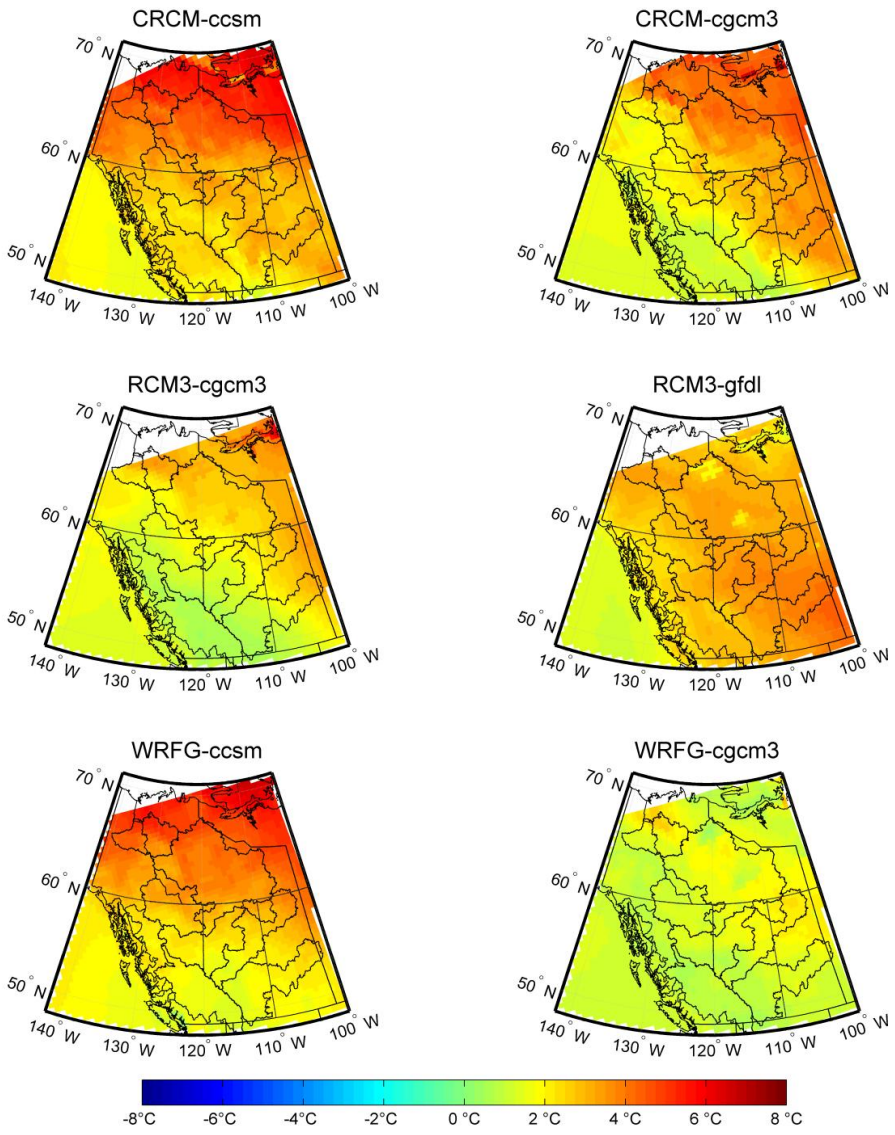

Figure B.70. Difference in Tmax values between 1971-2000 and 2041-2070 during December.

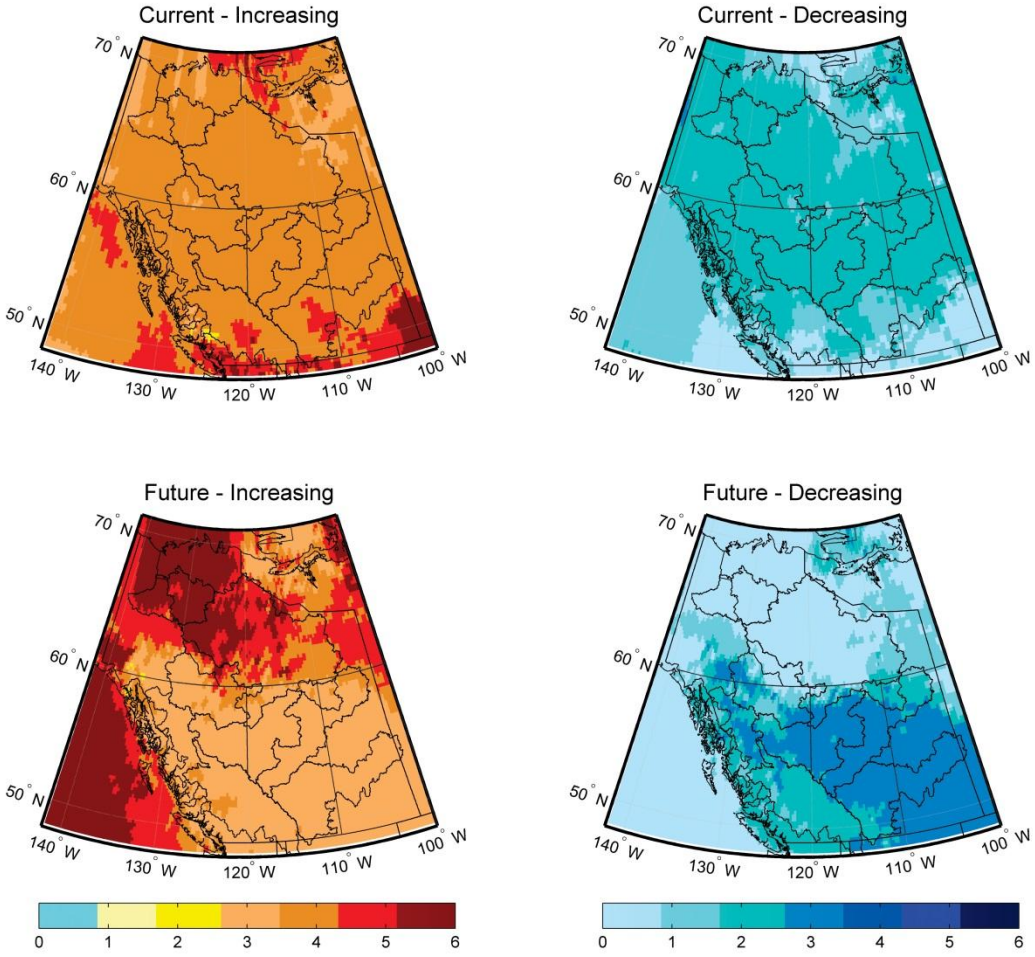

Figure B.71. Number of models showing increasing or decreasing rates of change in Tmax during the current (1971-2000) and future (2041-2070) time periods during December.

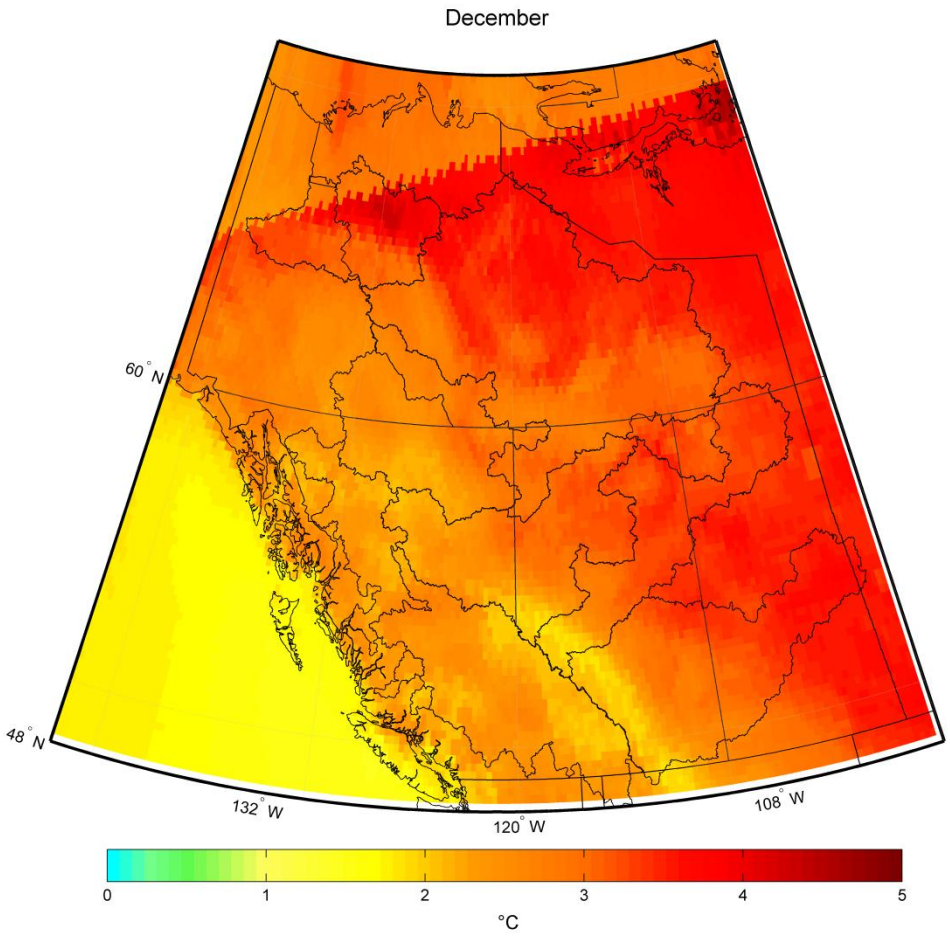

Figure B.72. Multimodel mean difference in monthly Tmin between the current and future periods during December.

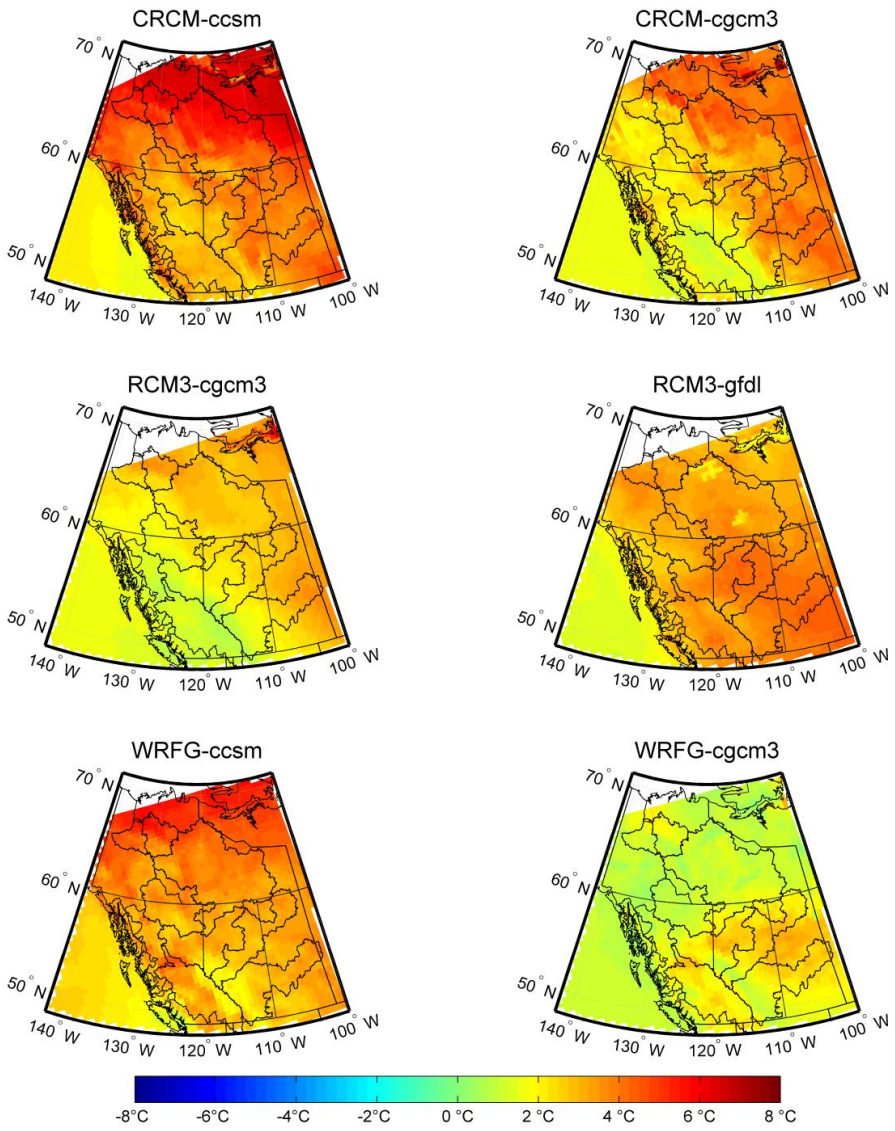

Figure B.73. Difference in Tmin values between 1971-2000 and 2041-2070 during December.

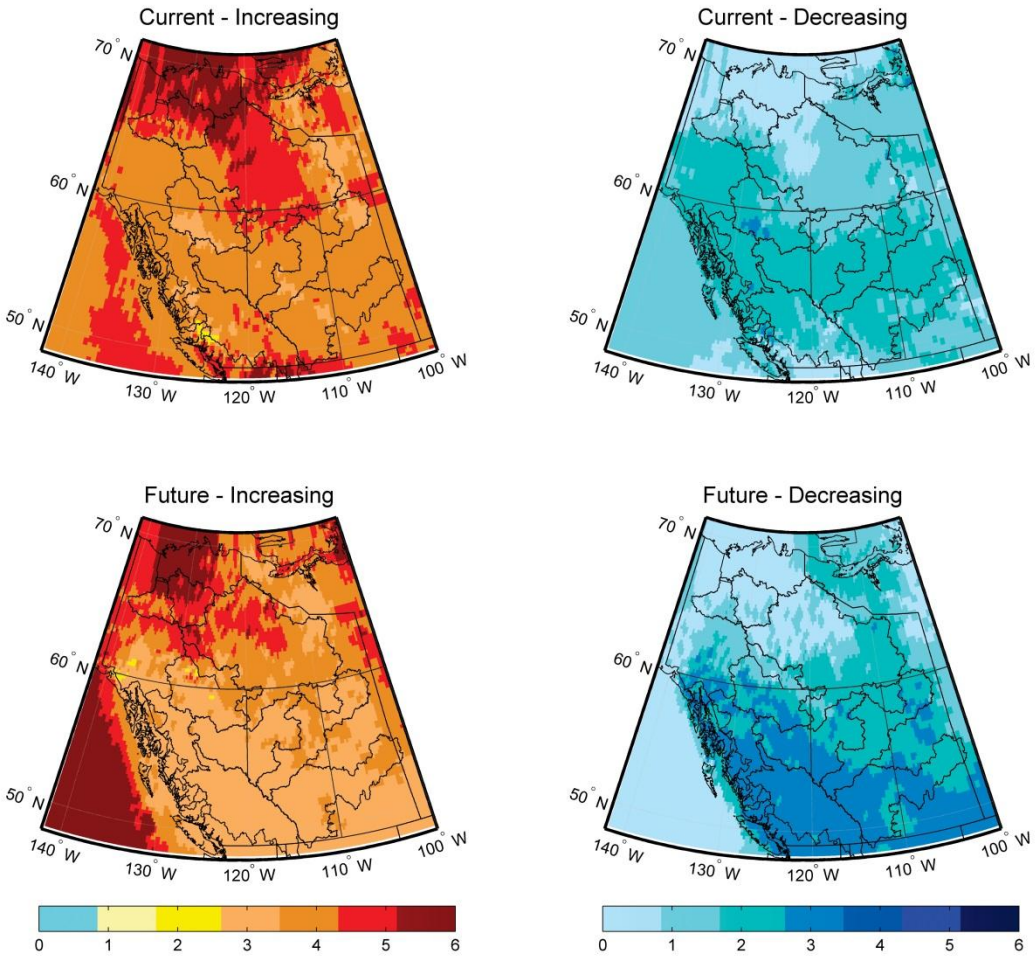

Figure B.74. Number of models showing increasing or decreasing rates of change in Tmin during the current (1971-2000) and future (2041-2070) time periods during December.

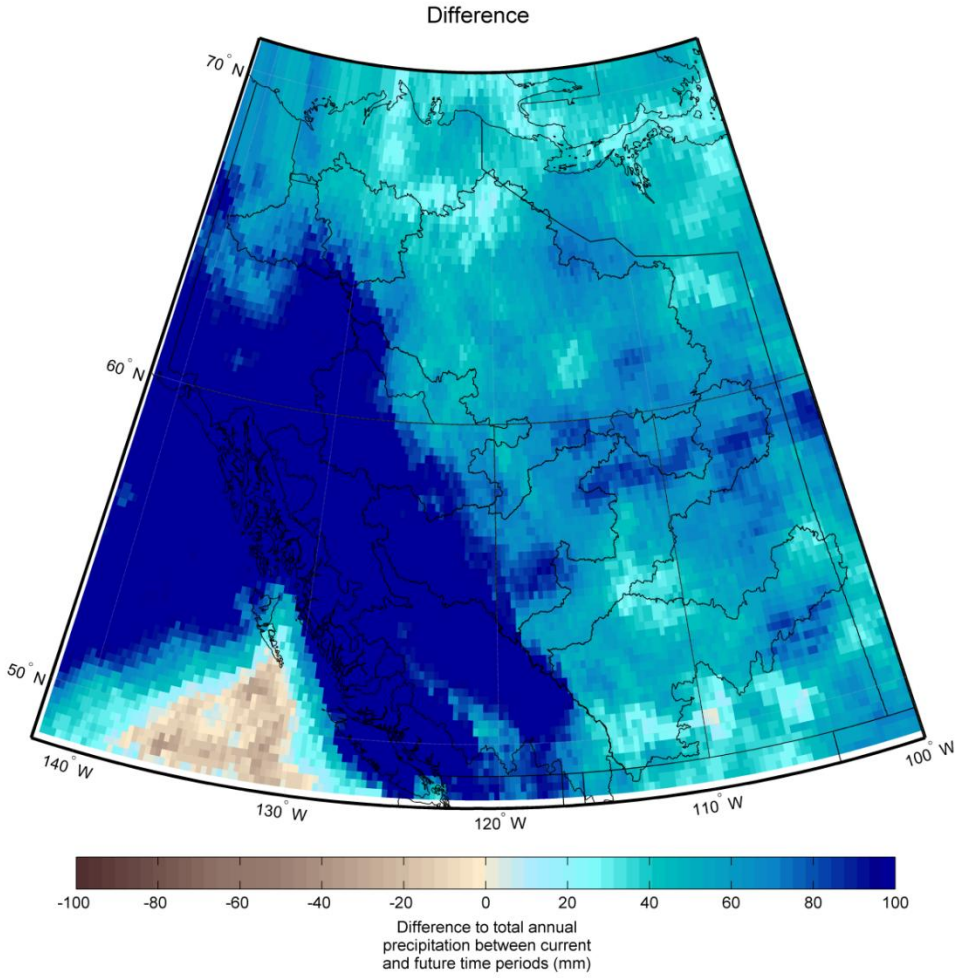

Figure B.75. Multimodel mean difference in annual precipitation between the current and future periods.

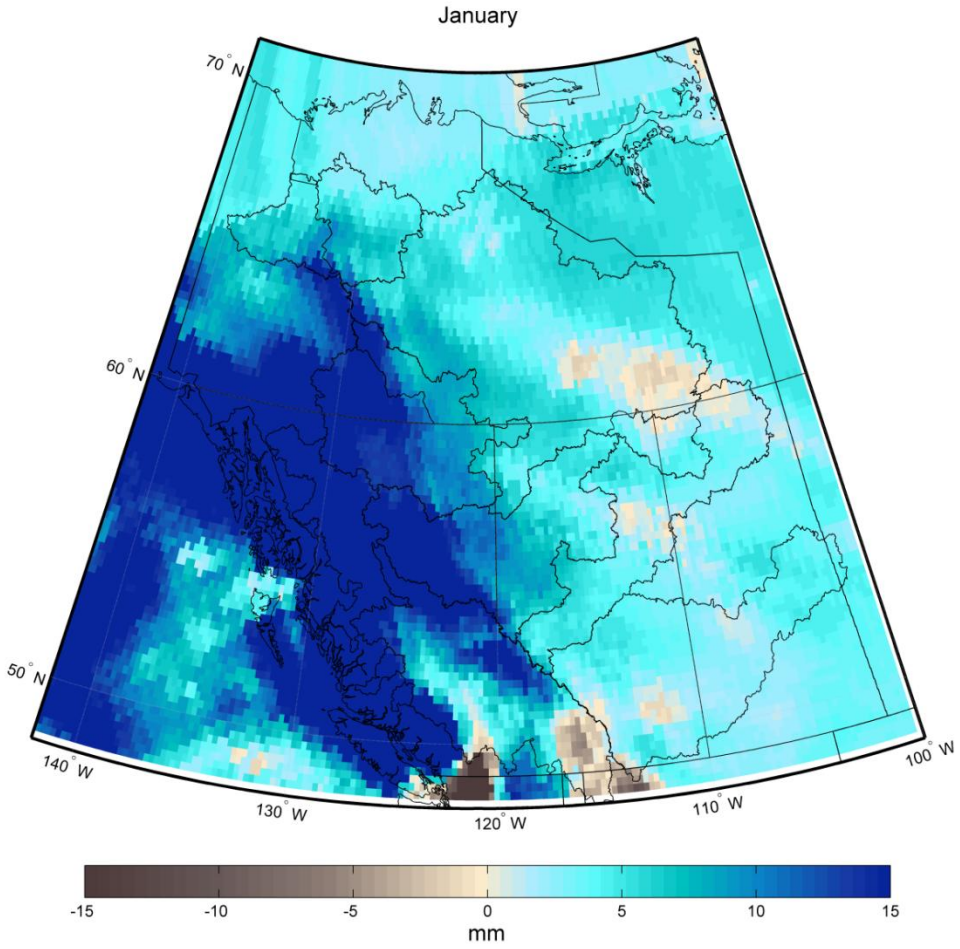

Figure B.76. Multimodel mean difference in monthly precipitation between the current and future periods during January.

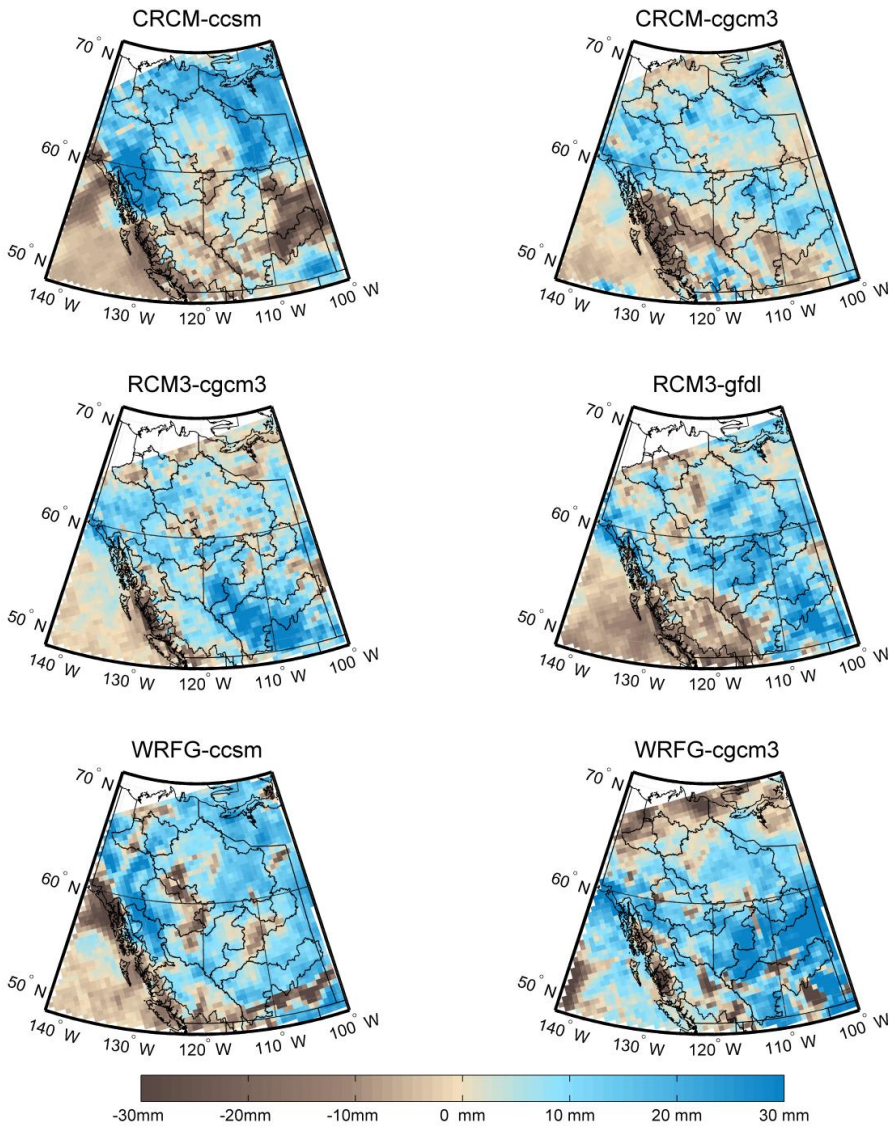

Figure B.77. Difference in precipitation totals between 1971-2000 and 2041-2070 during January.

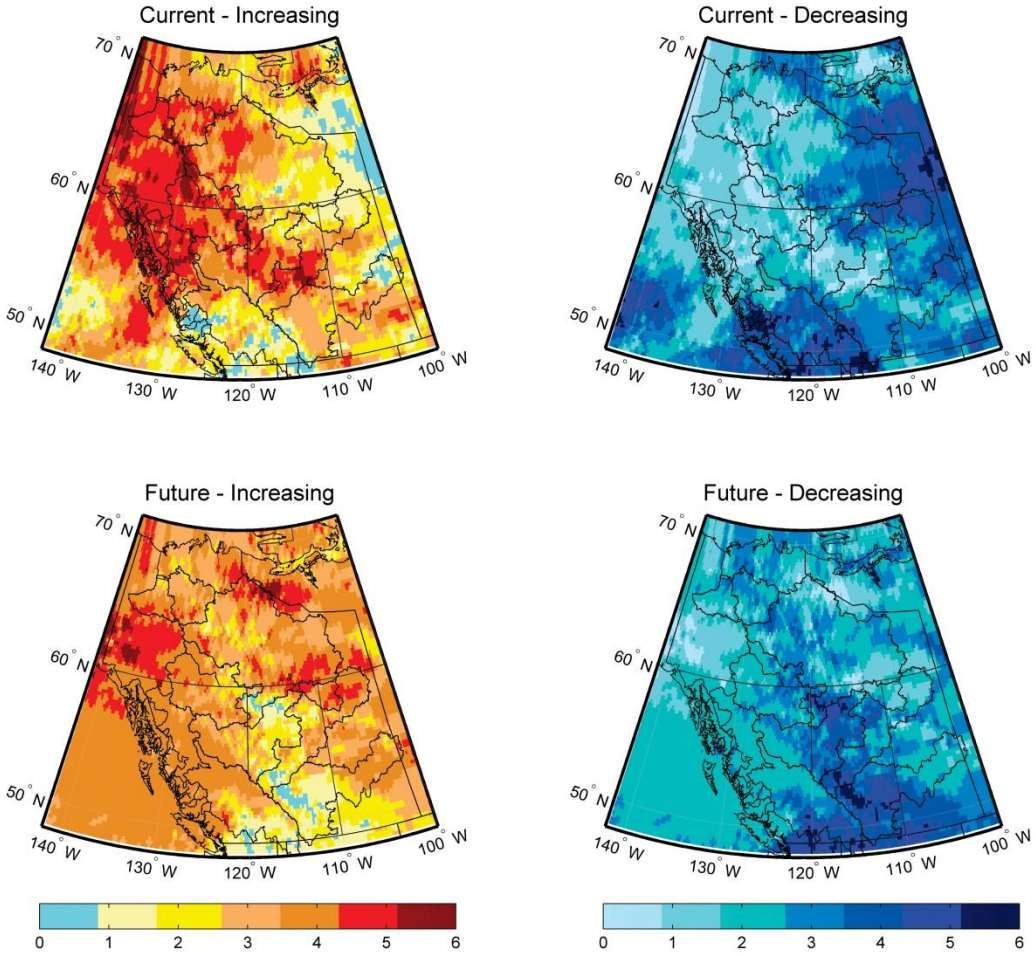

Figure B.78. Number of models showing increasing or decreasing rates of change in precipitation during the current (1971-2000) and future (2041-2070) time periods during January.

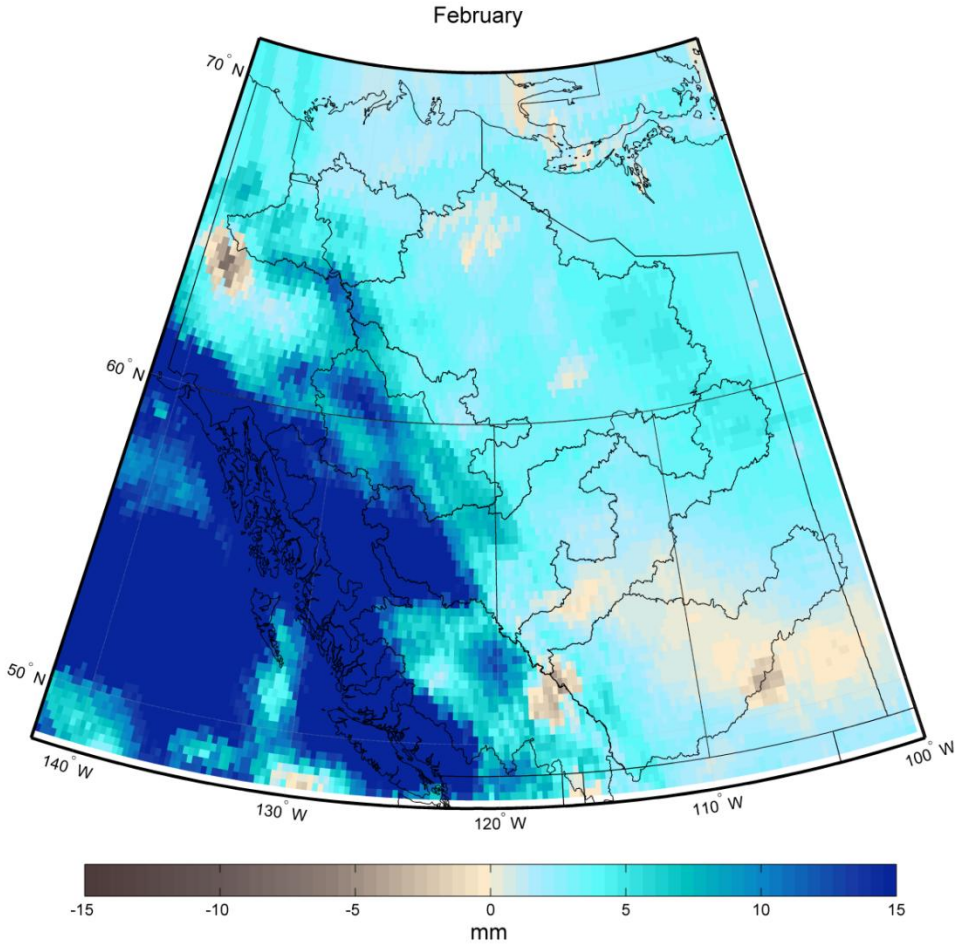

Figure B.79. Multimodel mean difference in monthly precipitation between the current and future periods during February.

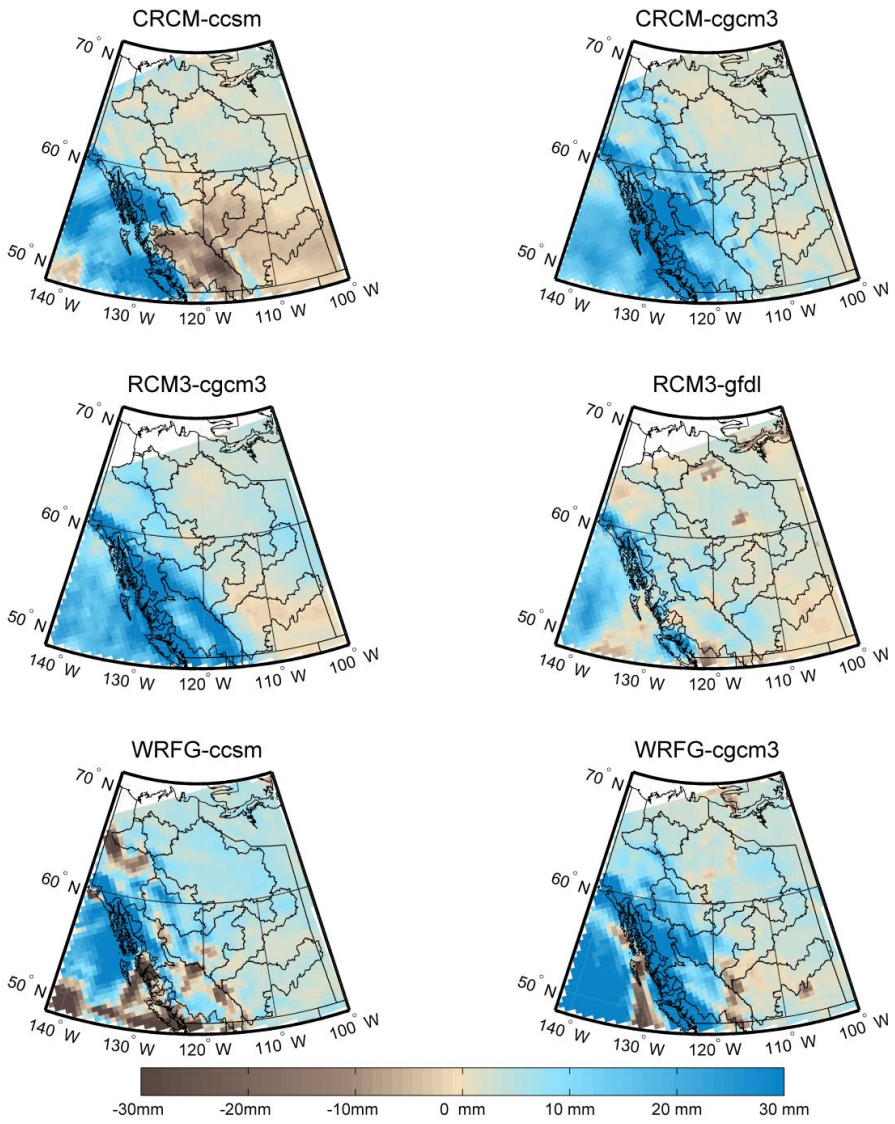

Figure B.80. Difference in precipitation totals between 1971-2000 and 2041-2070 during February.

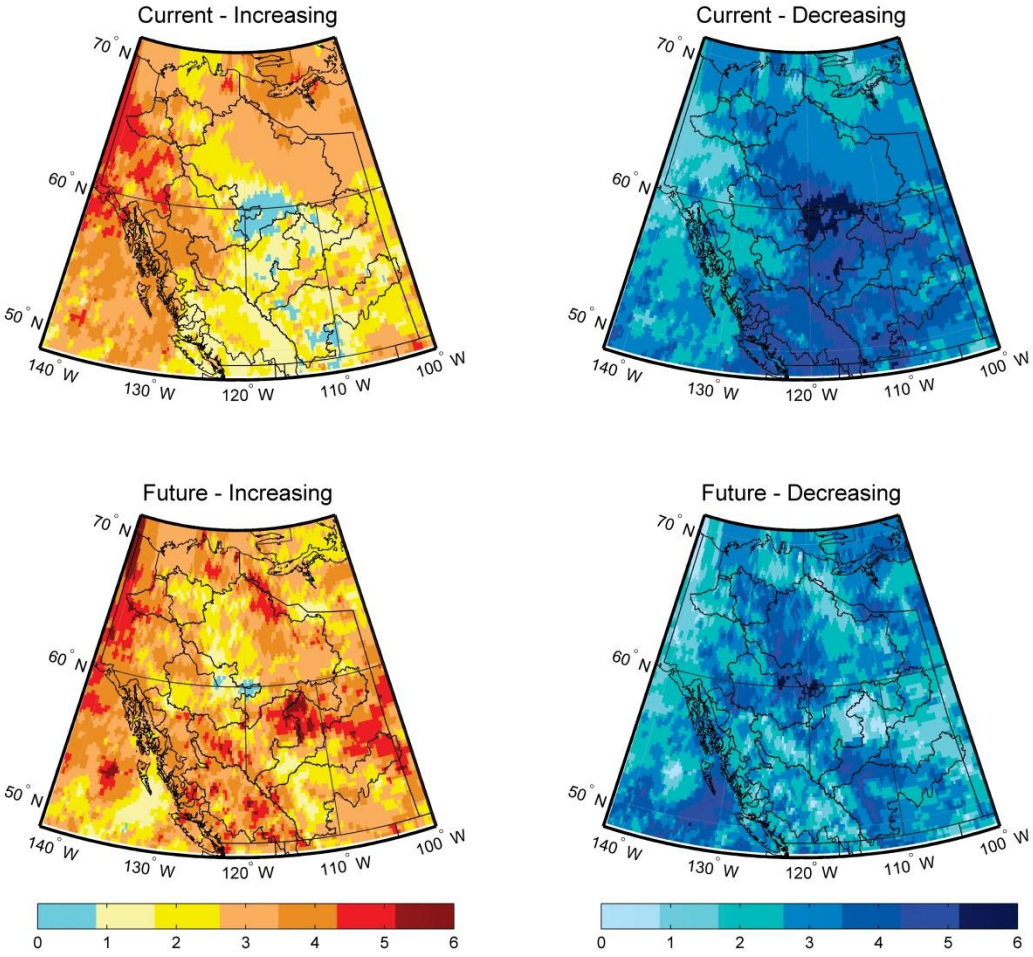

Figure B.81. Number of models showing increasing or decreasing rates of change in precipitation during the current (1971-2000) and future (2041-2070) time periods during February.

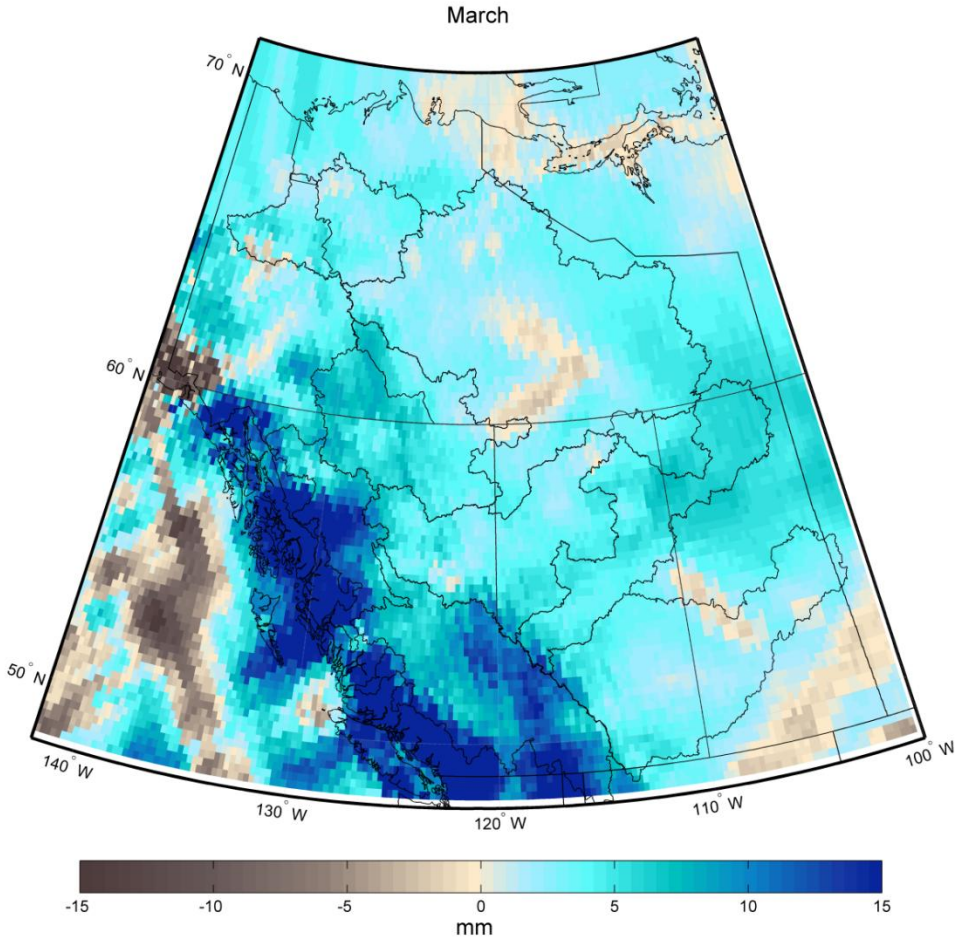

Figure B.82. Multimodel mean difference in monthly precipitation between the current and future periods during March.

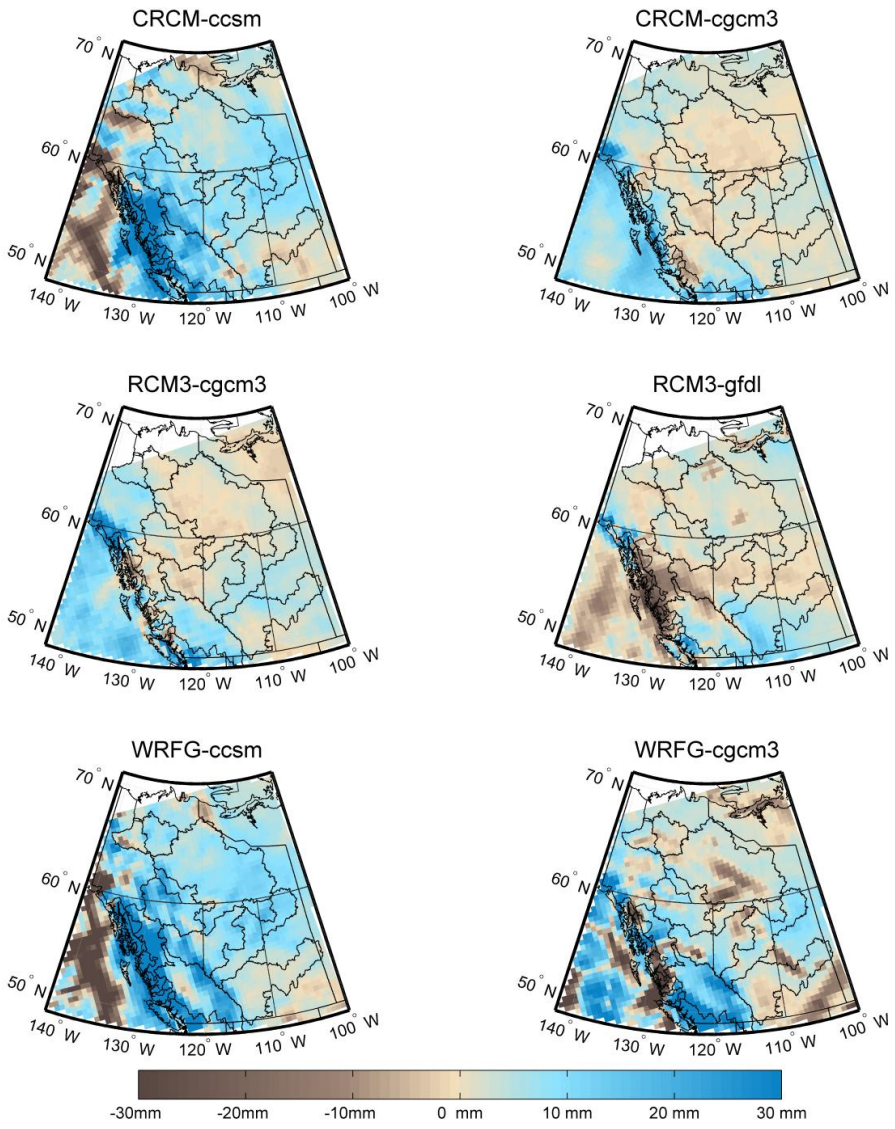

Figure B.83. Difference in precipitation totals between 1971-2000 and 2041-2070 during March.

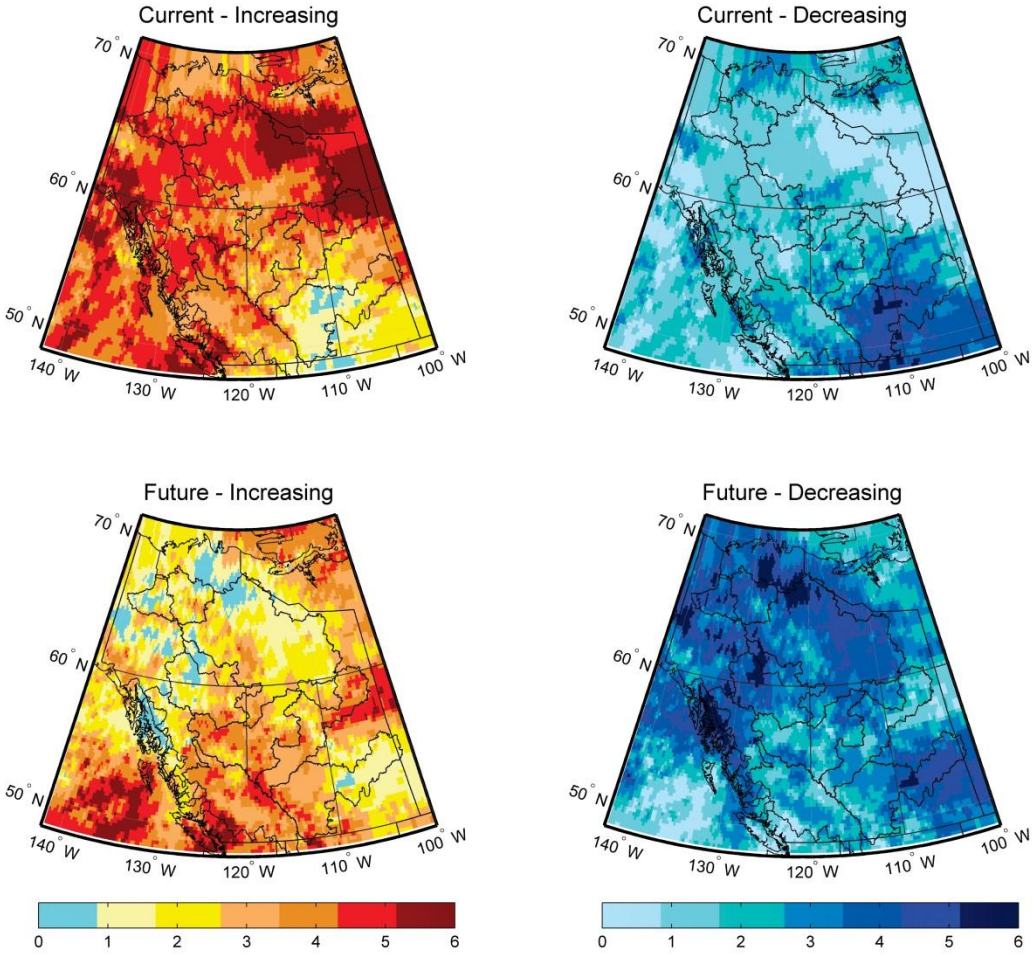

Figure B.84. Number of models showing increasing or decreasing rates of change in precipitation during the current (1971-2000) and future (2041-2070) time periods during March.

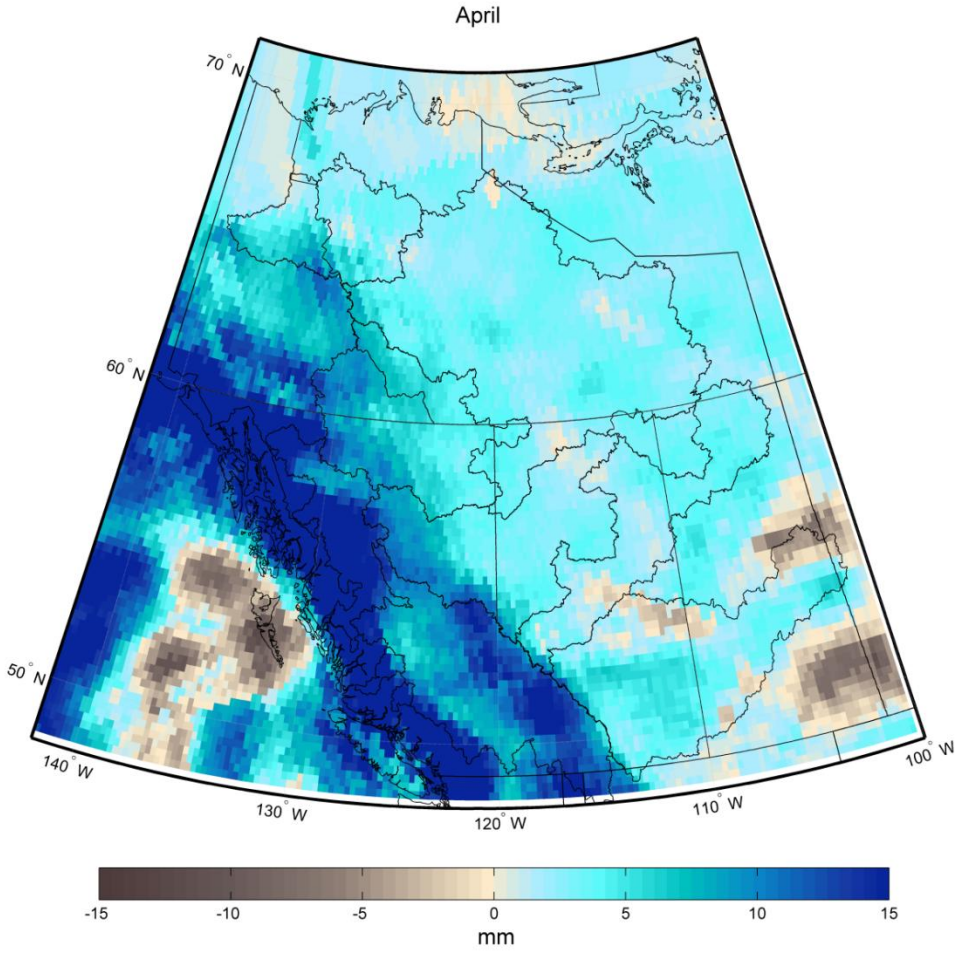

Figure B.85. Multimodel mean difference in monthly precipitation between the current and future periods during April.

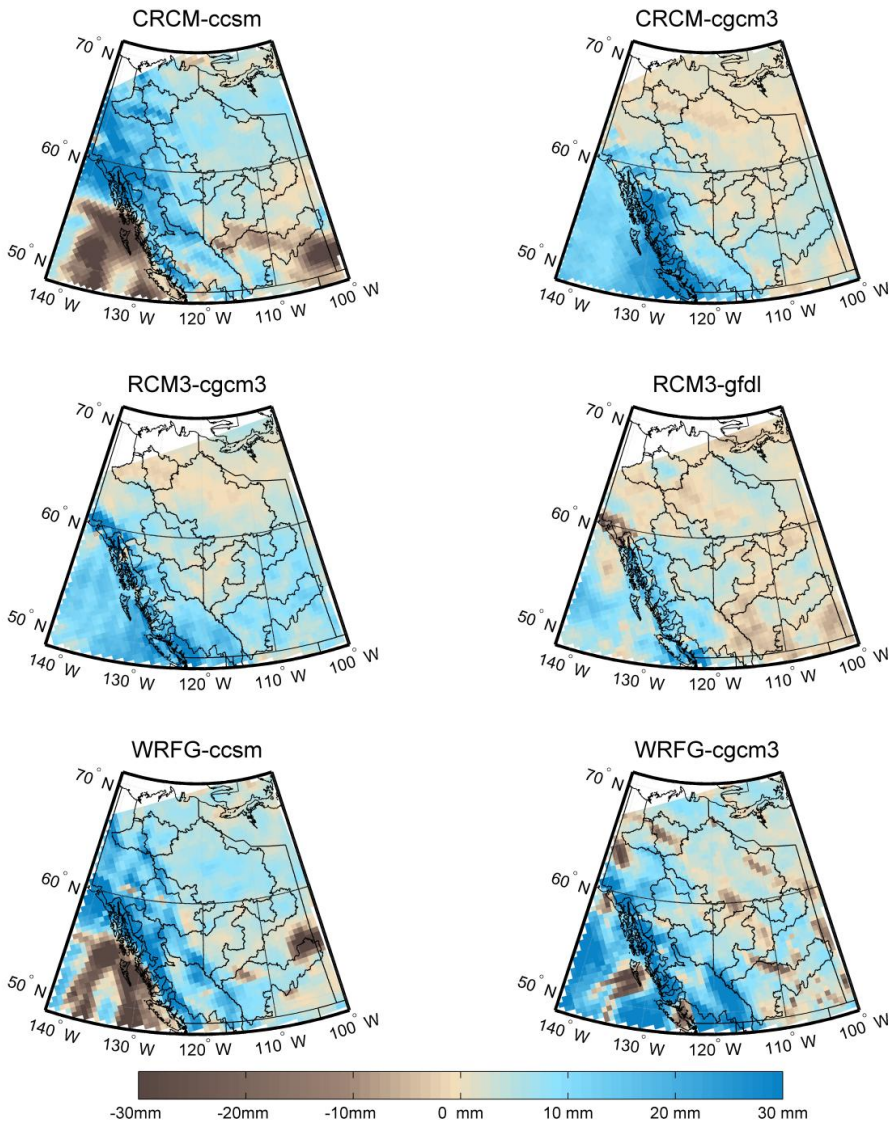

Figure B.86. Difference in precipitation totals between 1971-2000 and 2041-2070 during April.

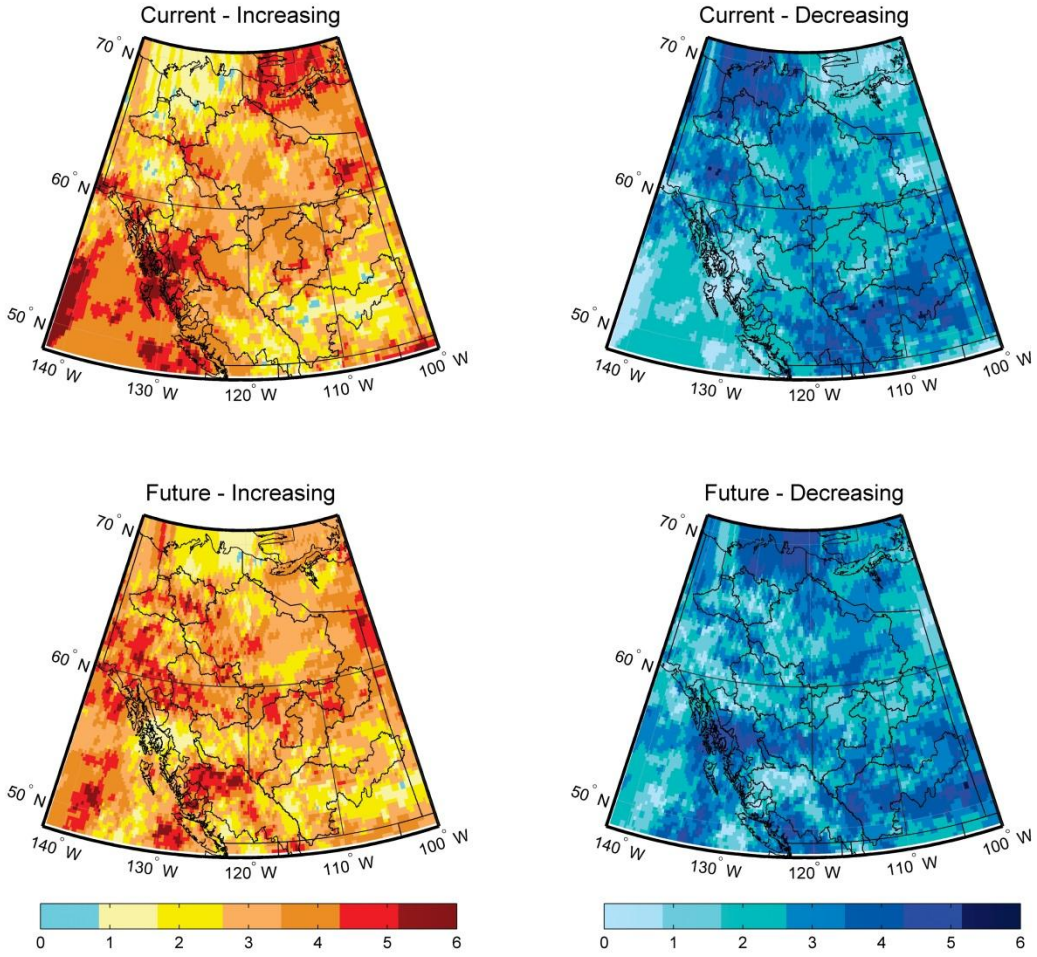

Figure B.87. Number of models showing increasing or decreasing rates of change in precipitation during the current (1971-2000) and future (2041-2070) time periods during April.

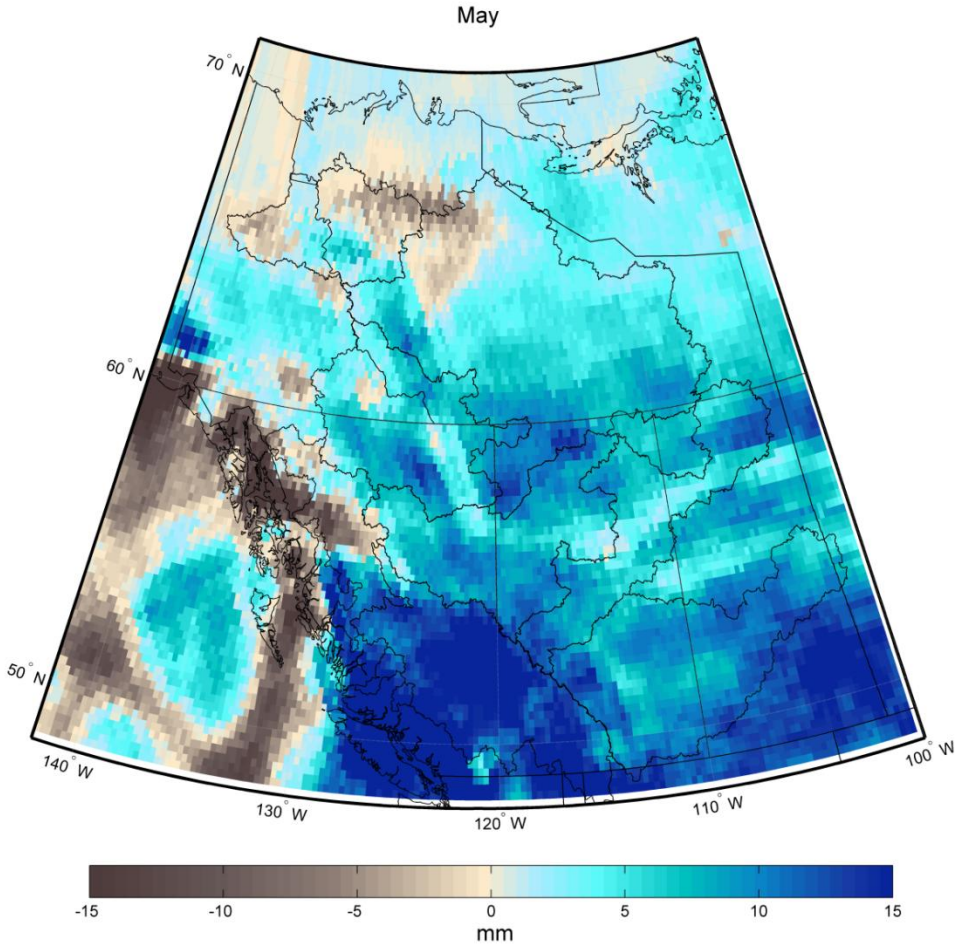

Figure B.88. Multimodel mean difference in monthly precipitation between the current and future periods during May.

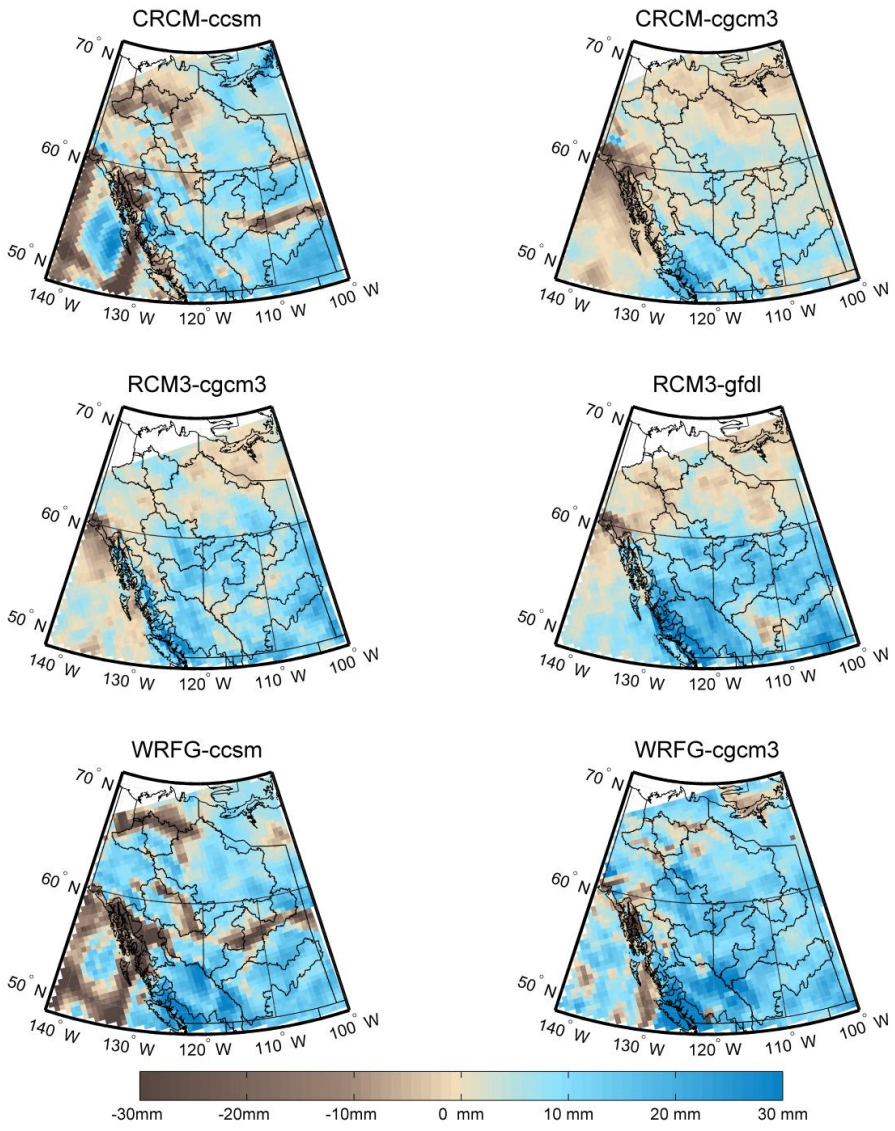

Figure B.89. Difference in precipitation totals between 1971-2000 and 2041-2070 during May.

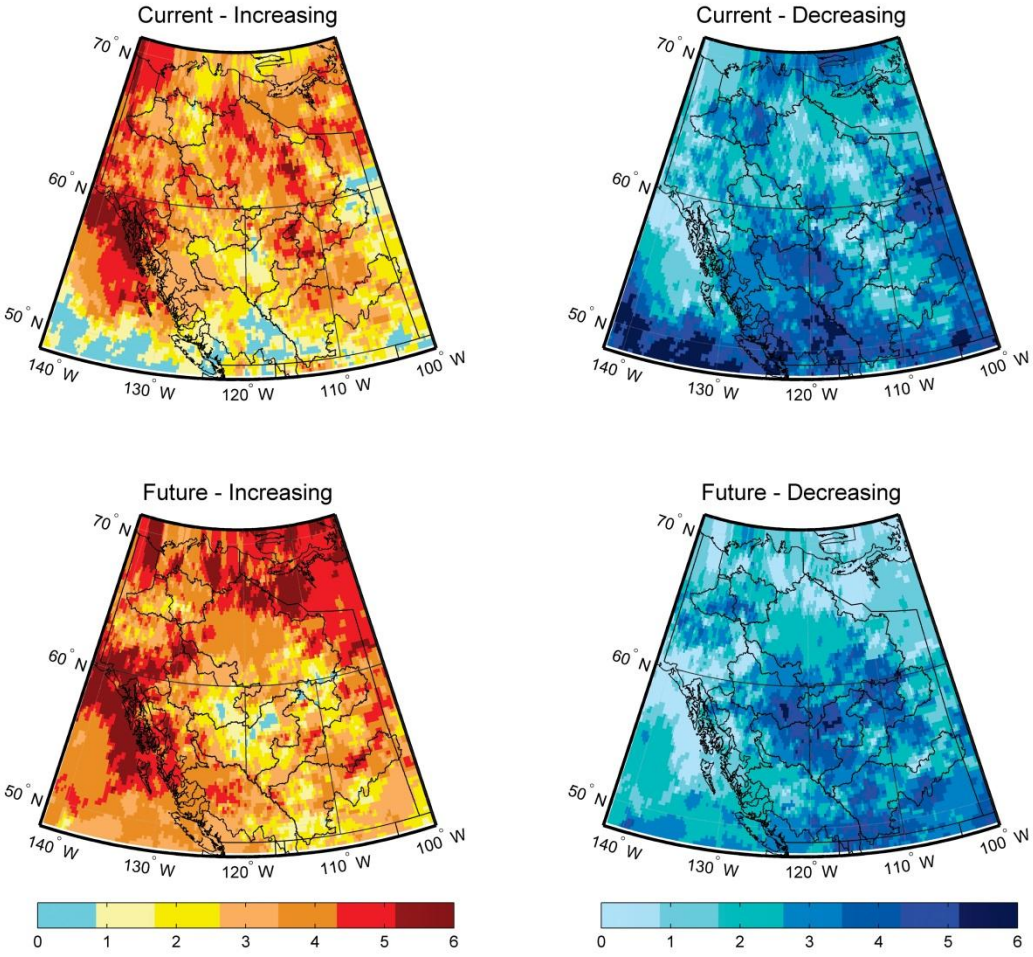

Figure B.90. Number of models showing increasing or decreasing rates of change in precipitation during the current (1971-2000) and future (2041-2070) time periods during May.

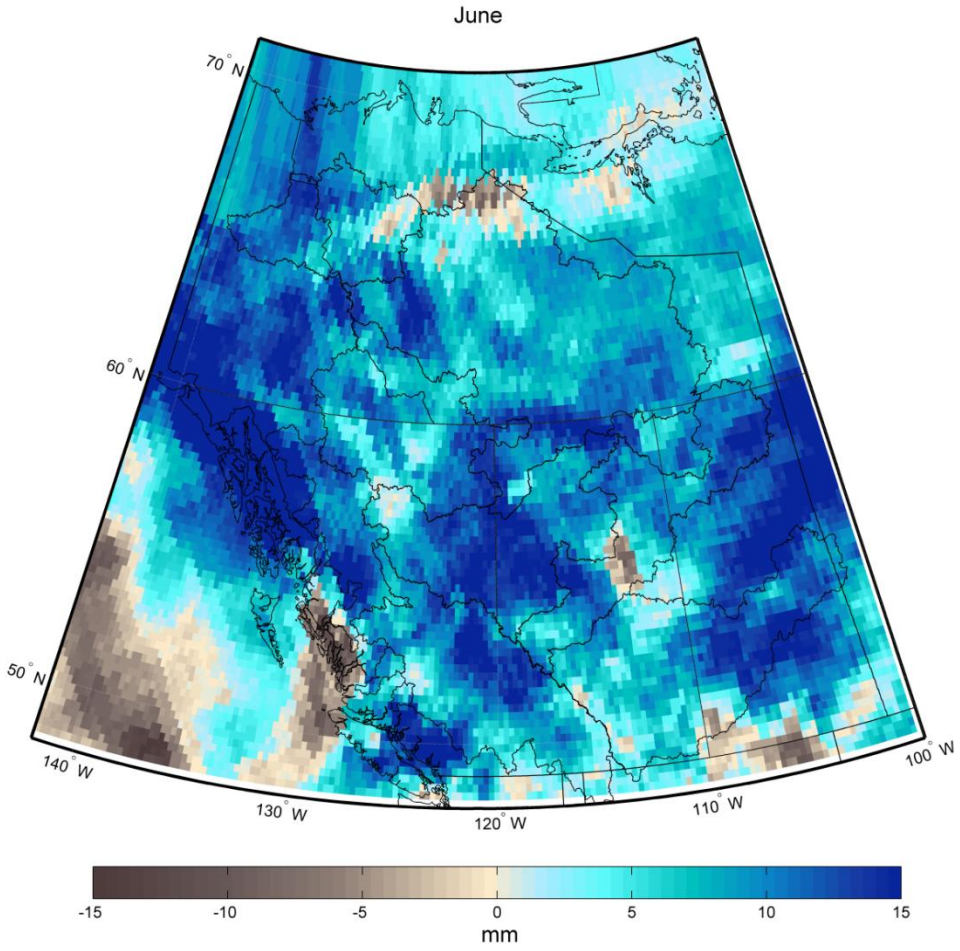

Figure B.91. Multimodel mean difference in monthly precipitation between the current and future periods during June.

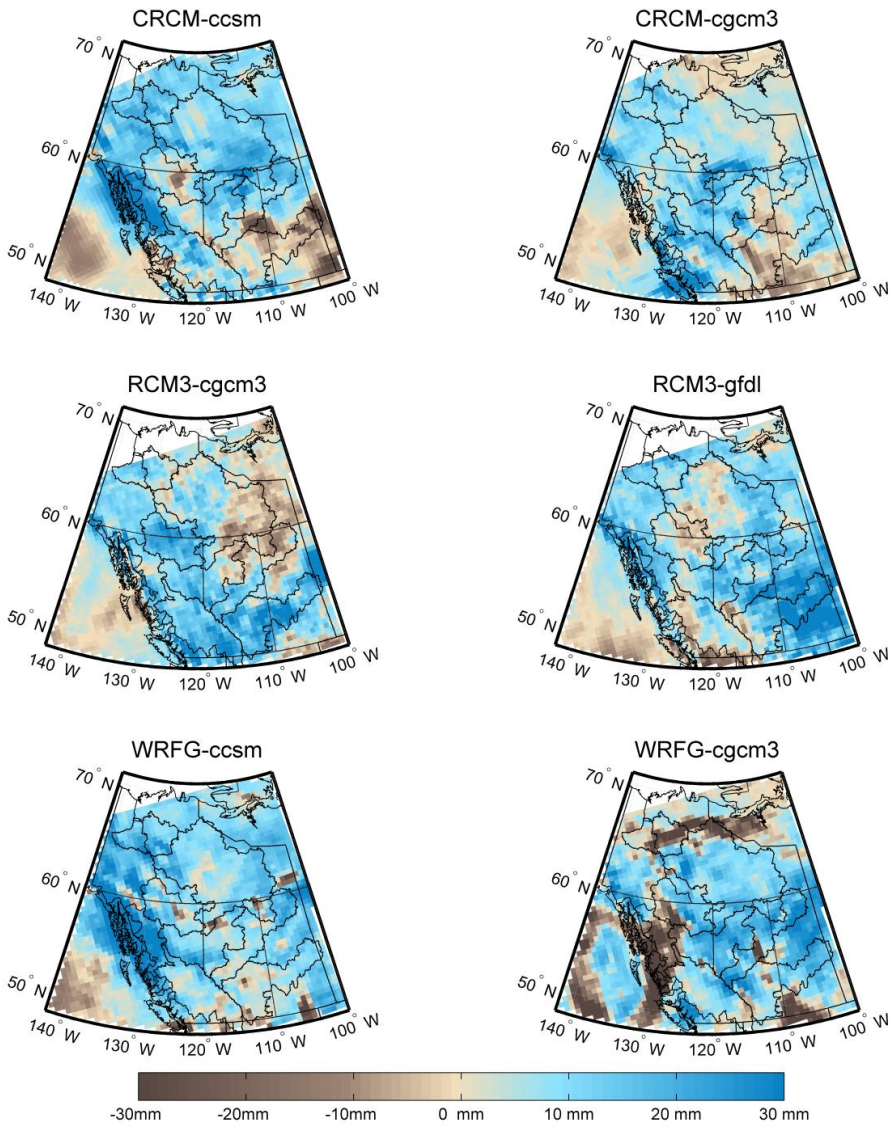

Figure B.92. Difference in precipitation totals between 1971-2000 and 2041-2070 during June.

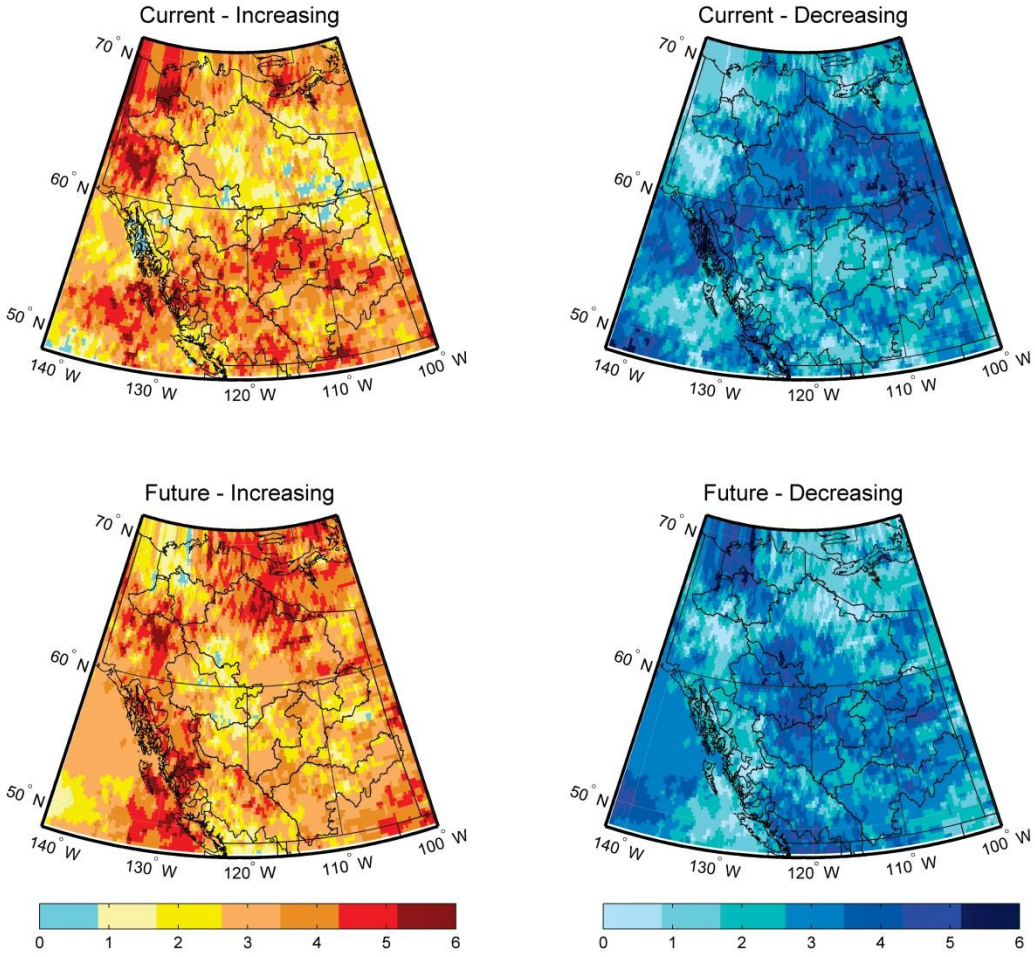

Figure B.93. Number of models showing increasing or decreasing rates of change in precipitation during the current (1971-2000) and future (2041-2070) time periods during June.

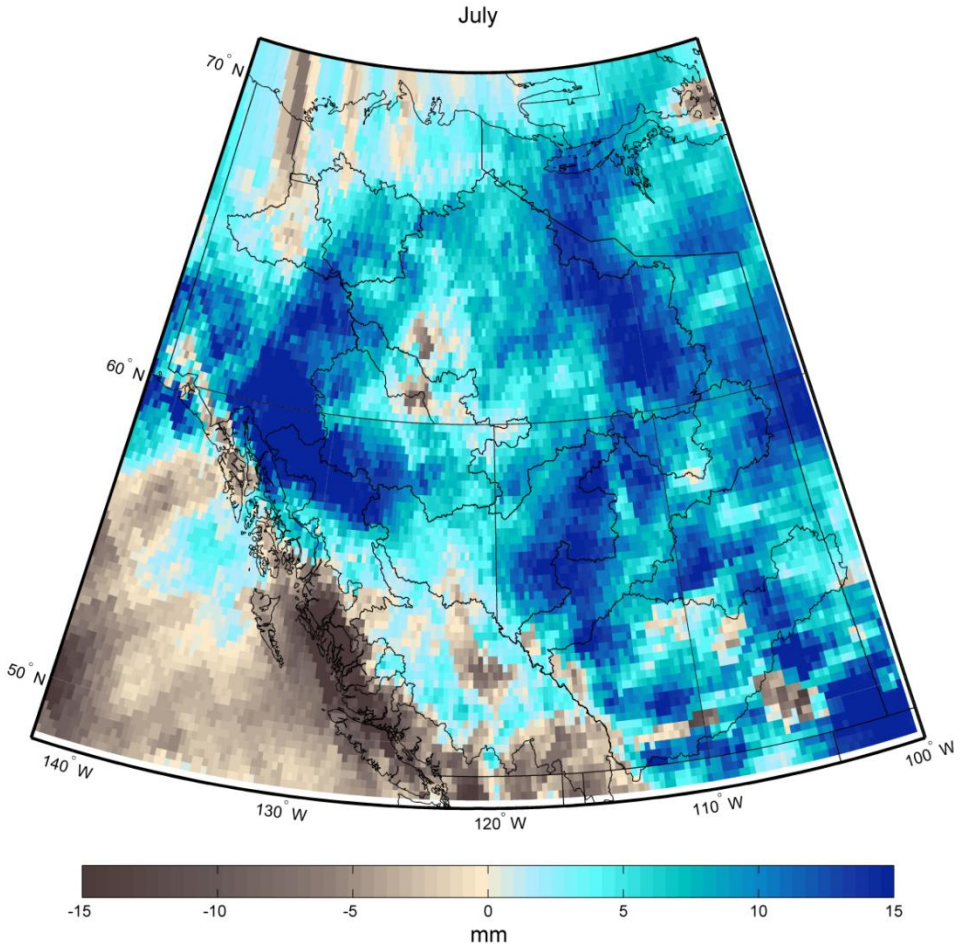

Figure B.94. Multimodel mean difference in monthly precipitation between the current and future periods during July.

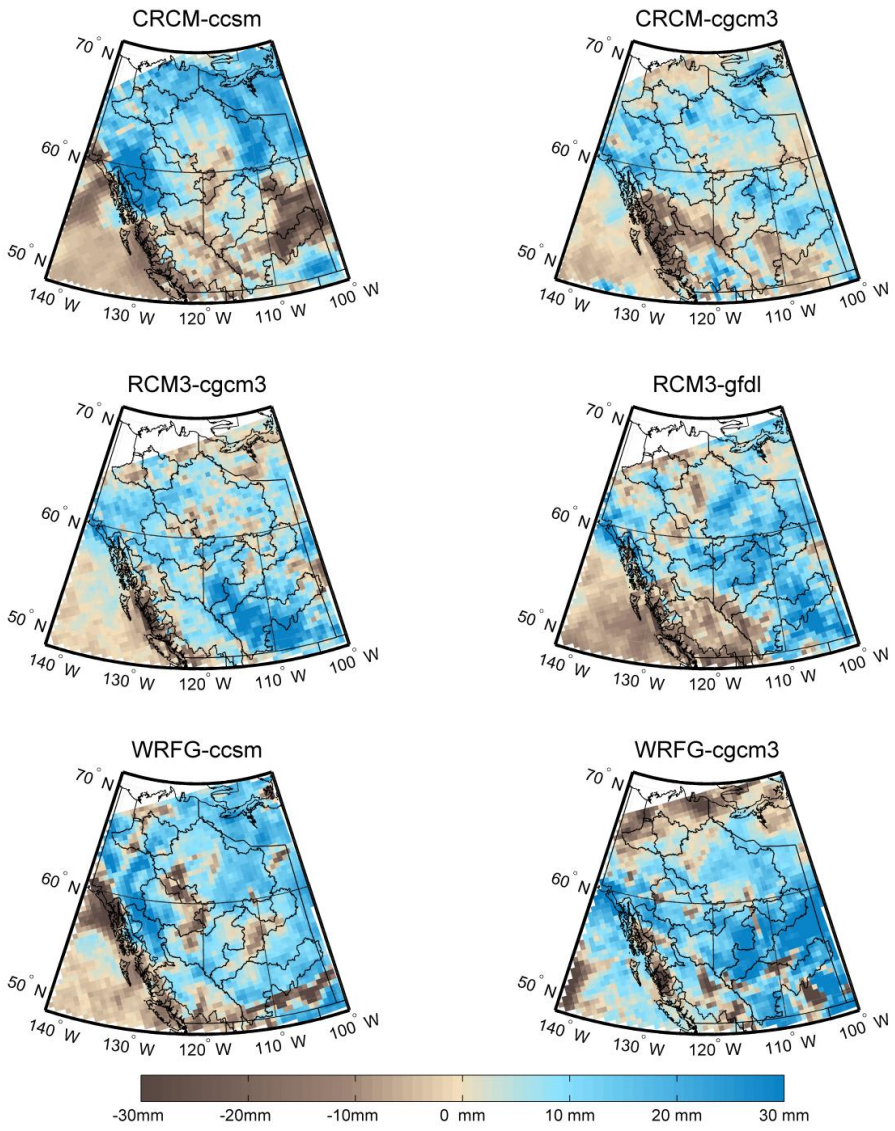

Figure B.95. Difference in precipitation totals between 1971-2000 and 2041-2070 during July.

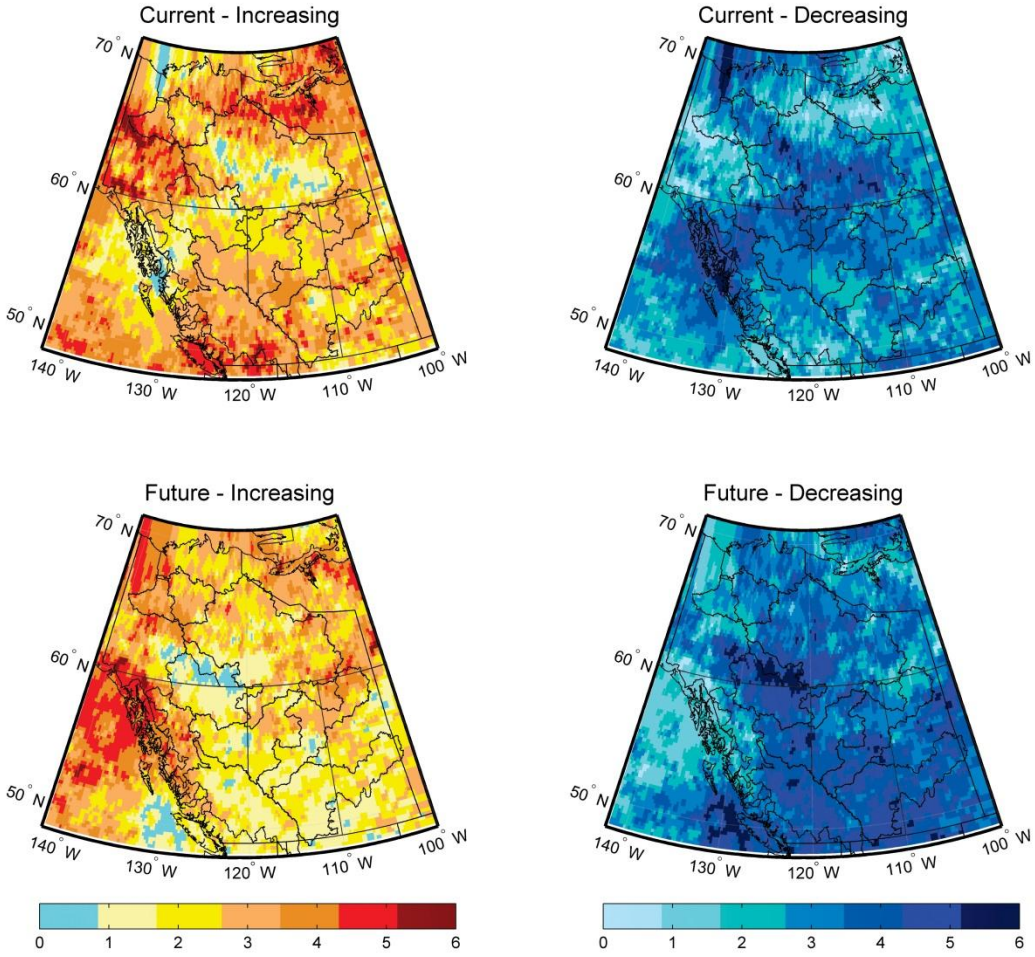

Figure B.96. Number of models showing increasing or decreasing rates of change in precipitation during the current (1971-2000) and future (2041-2070) time periods during July.

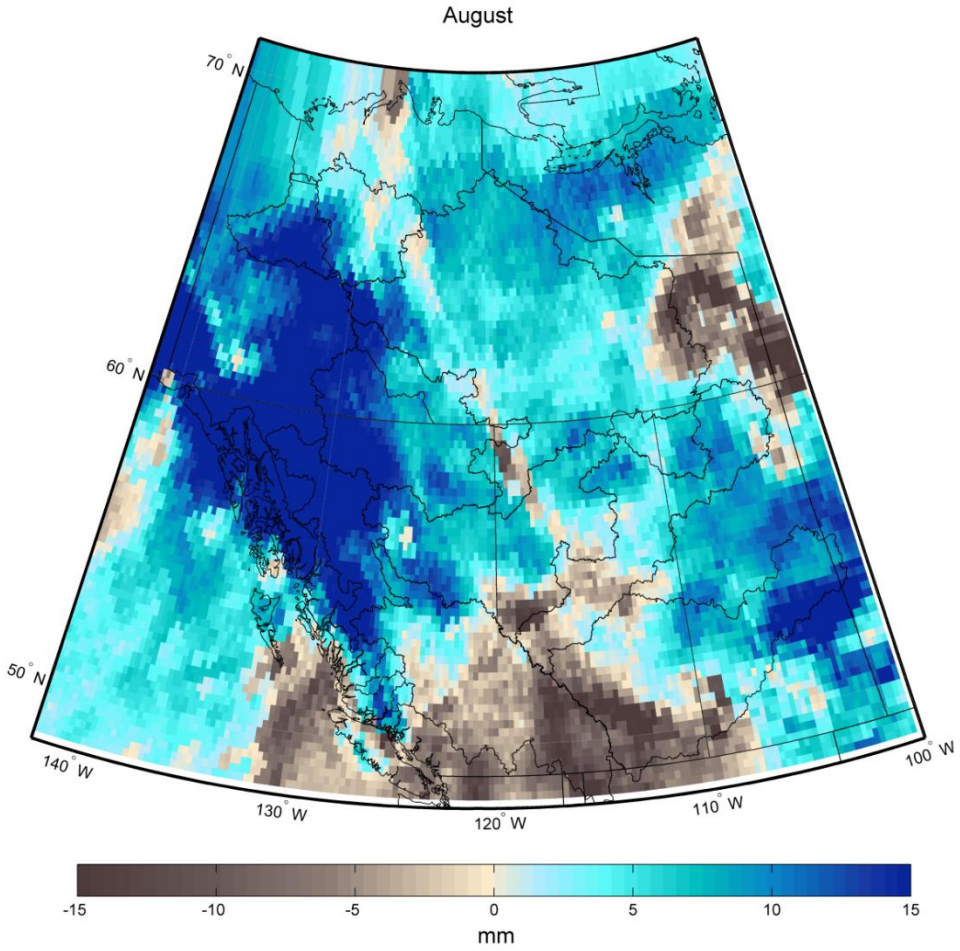

Figure B.97. Multimodel mean difference in monthly precipitation between the current and future periods during August.

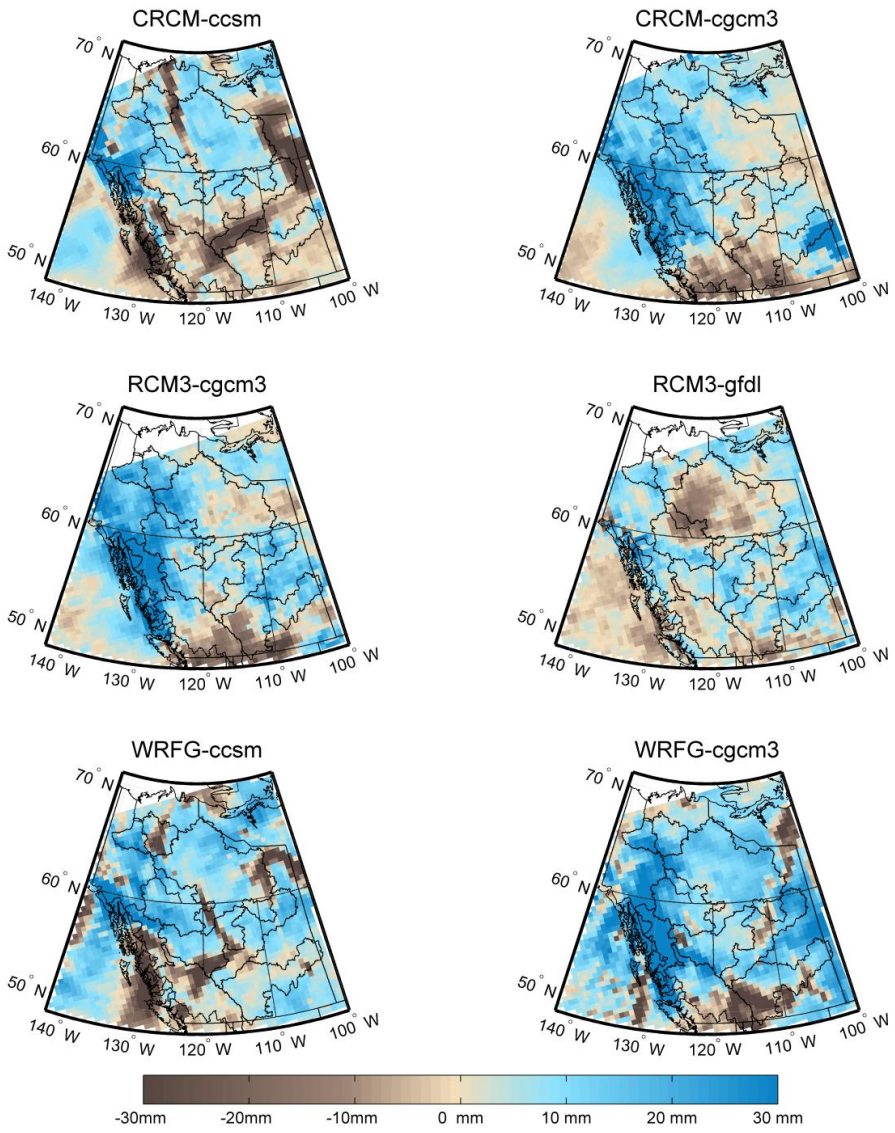

Figure B.98. Difference in precipitation totals between 1971-2000 and 2041-2070 during August.

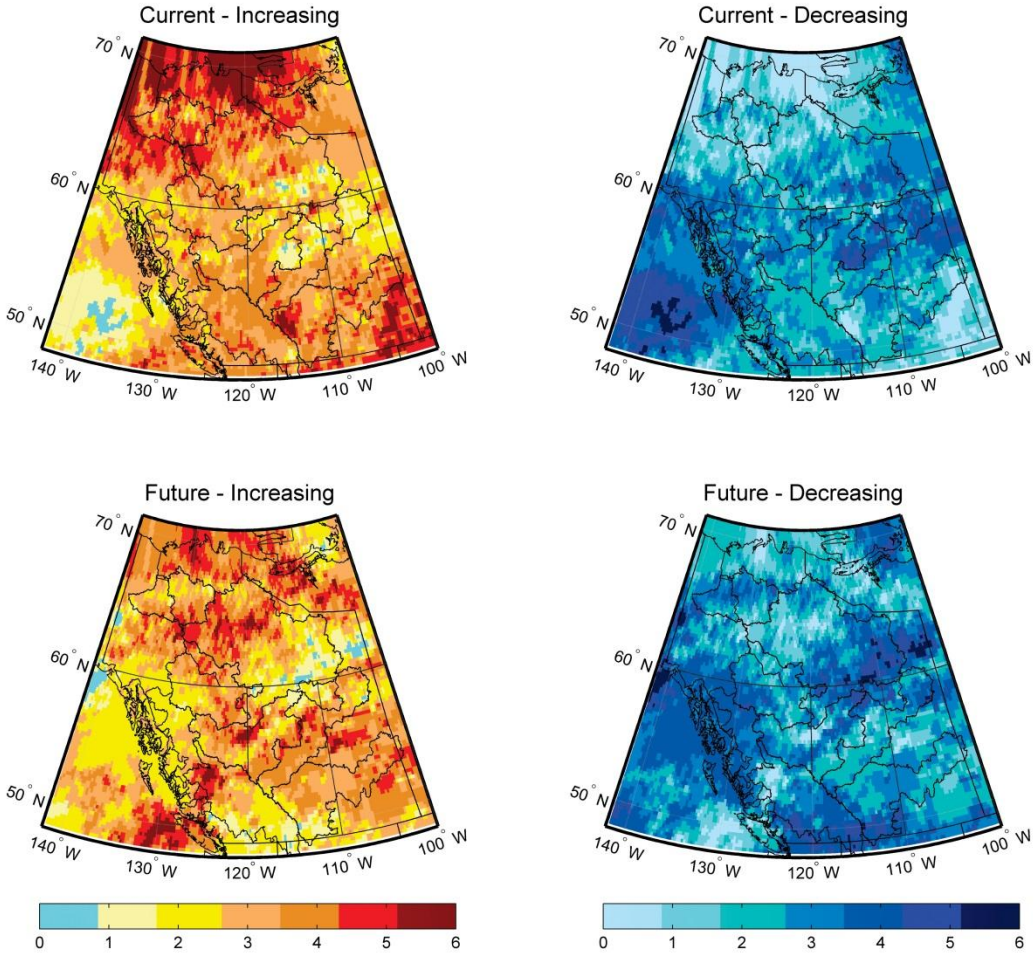

Figure B.99. Number of models showing increasing or decreasing rates of change in precipitation during the current (1971-2000) and future (2041-2070) time periods during August.

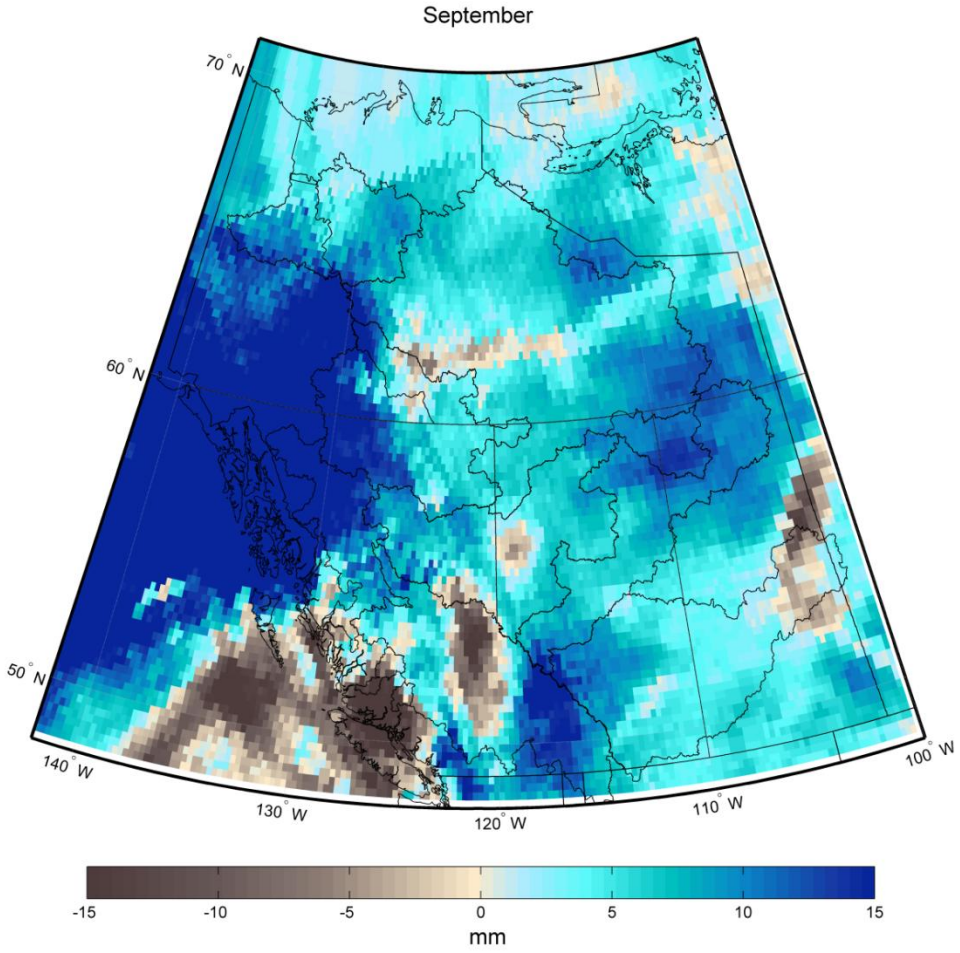

Figure B.100. Multimodel mean difference in monthly precipitation between the current and future periods during September.

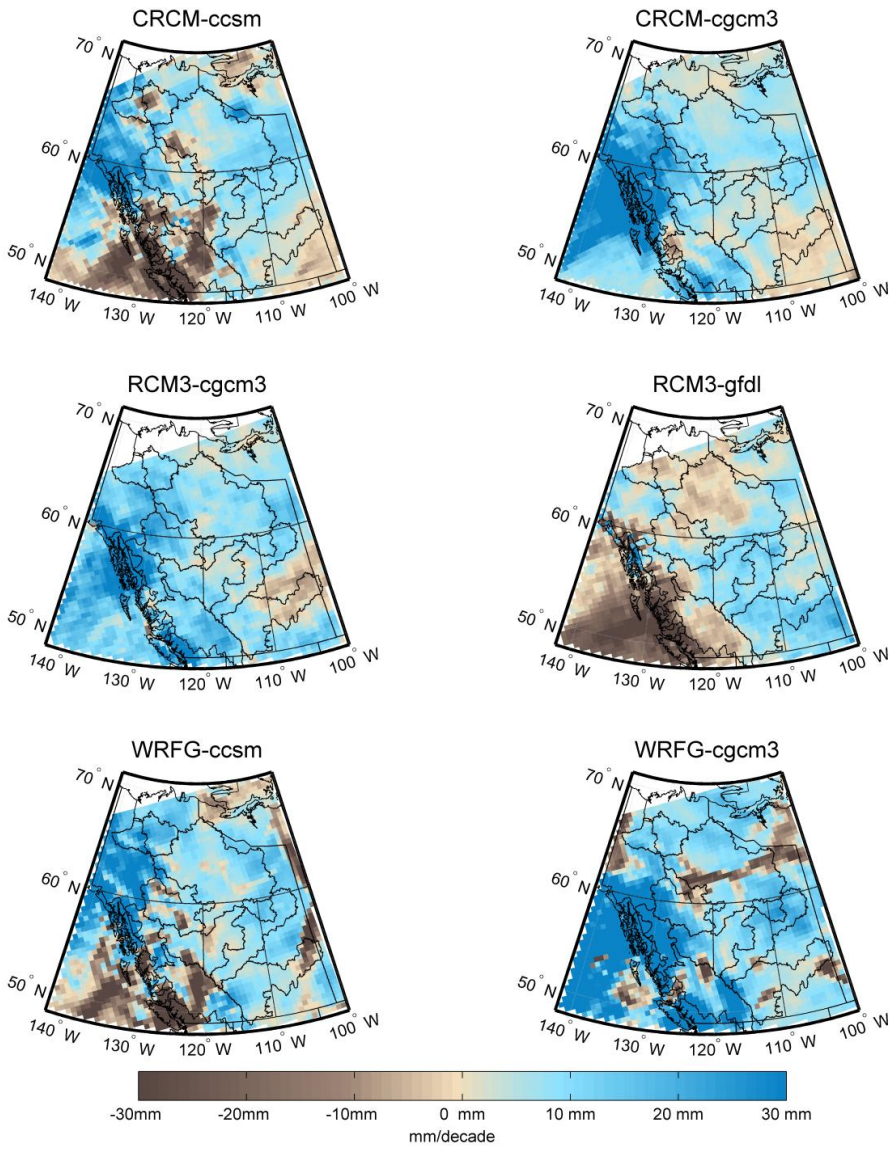

Figure B.101. Difference in precipitation totals between 1971-2000 and 2041-2070 during September.

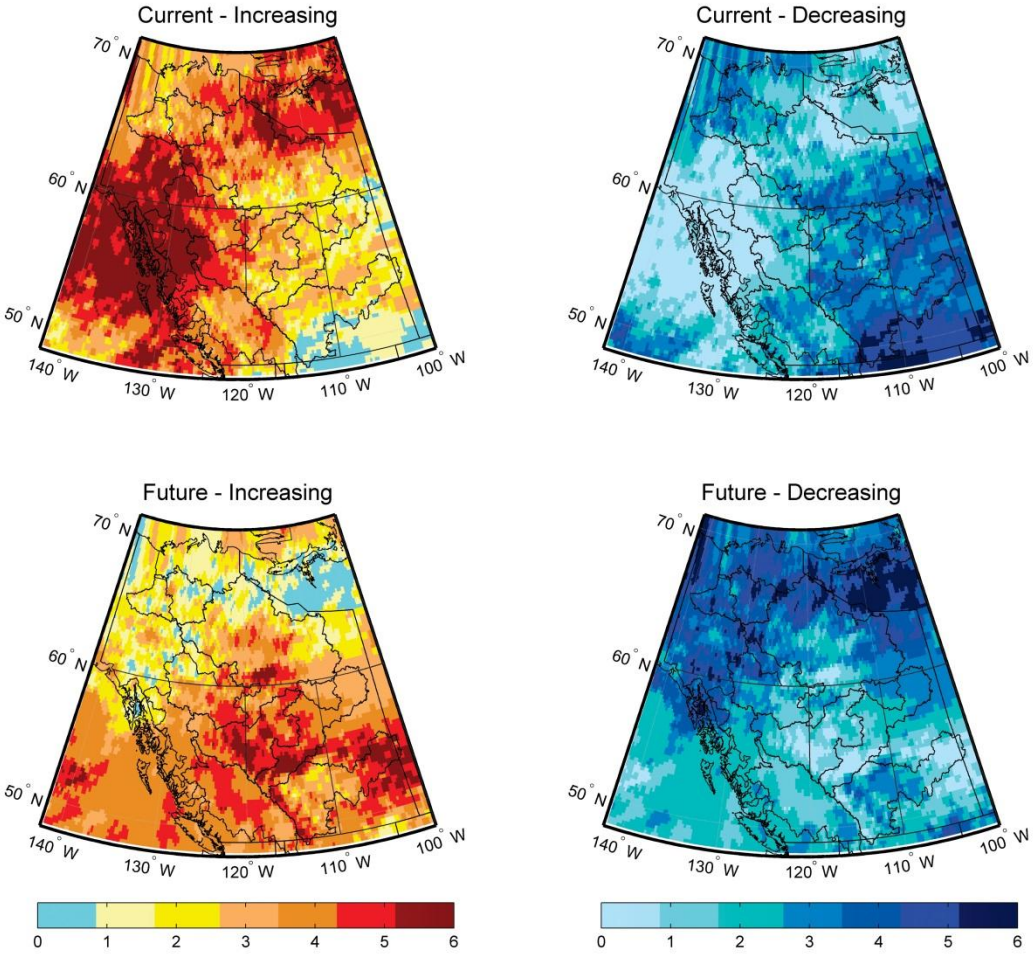

Figure B.102. Number of models showing increasing or decreasing rates of change in precipitation during the current (1971-2000) and future (2041-2070) time periods during September.

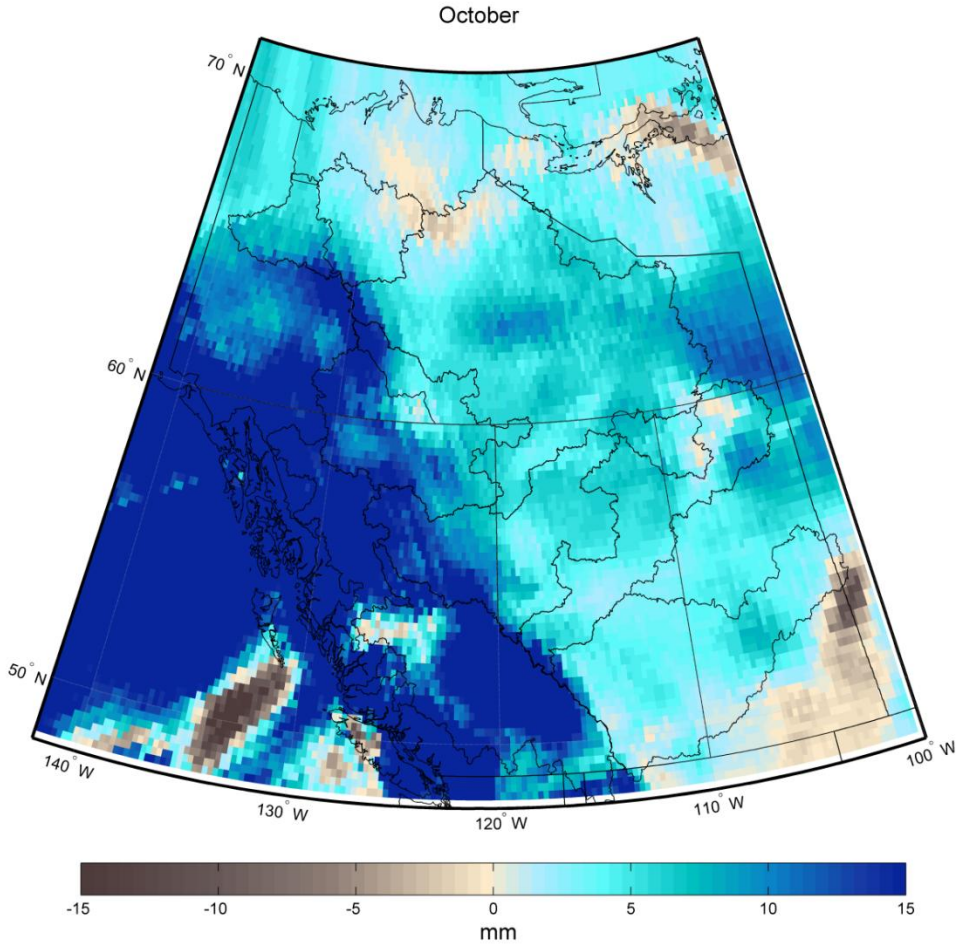

Figure B.103. Multimodel mean difference in monthly precipitation between the current and future periods during October.

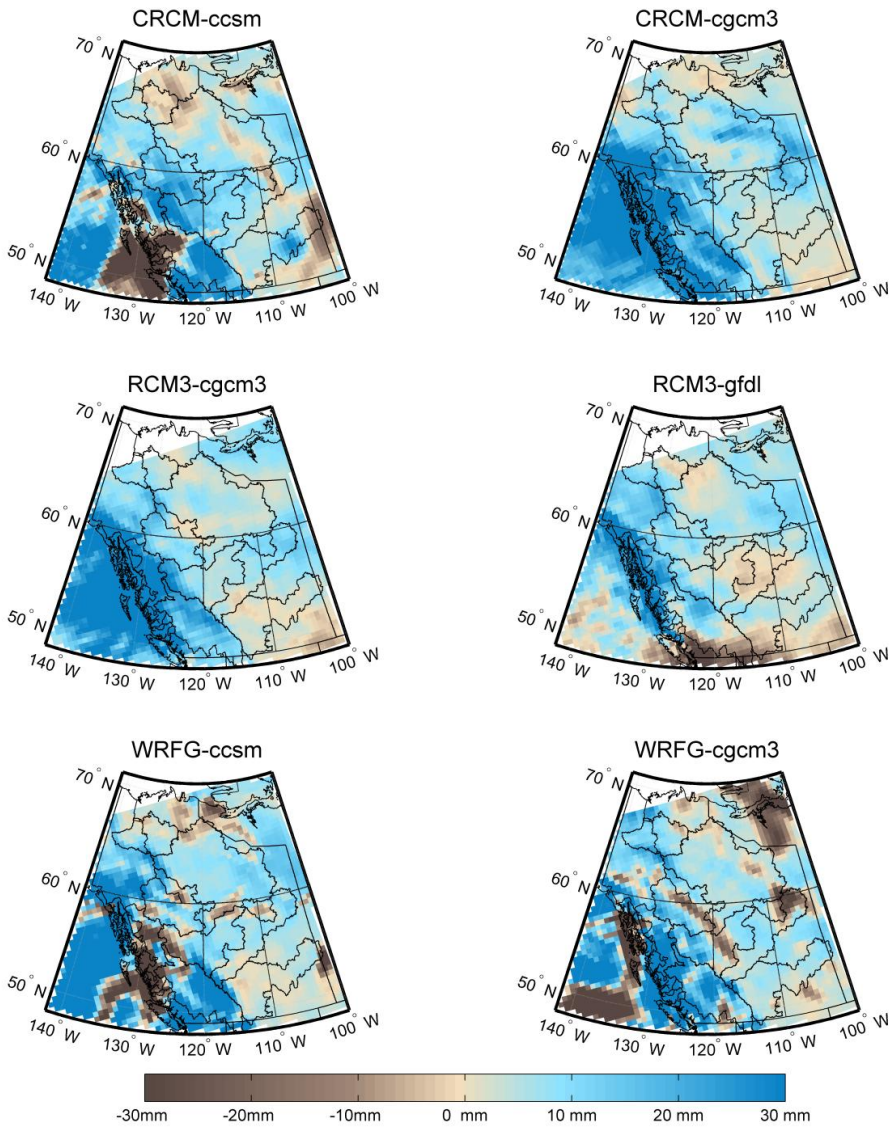

Figure B.104. Difference in precipitation totals between 1971-2000 and 2041-2070 during October.

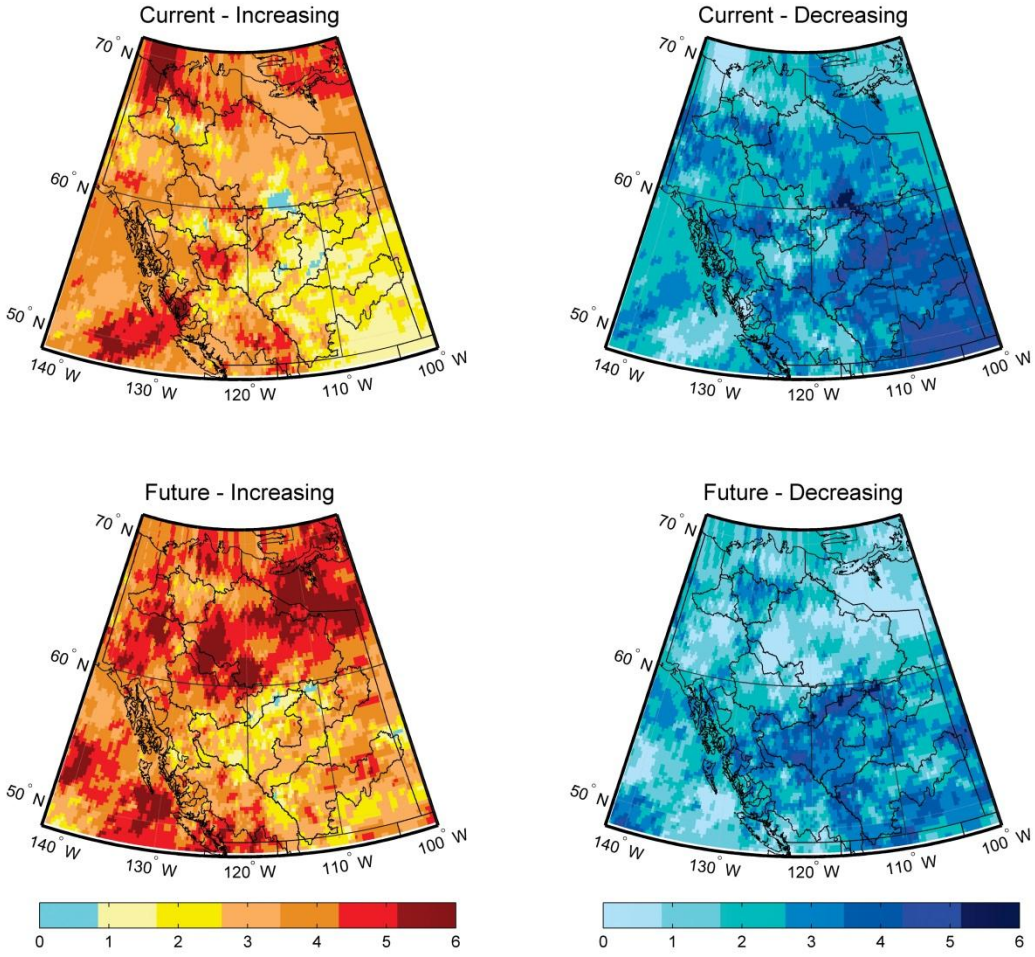

Figure B.105. Number of models showing increasing or decreasing rates of change in precipitation during the current (1971-2000) and future (2041-2070) time periods during October.

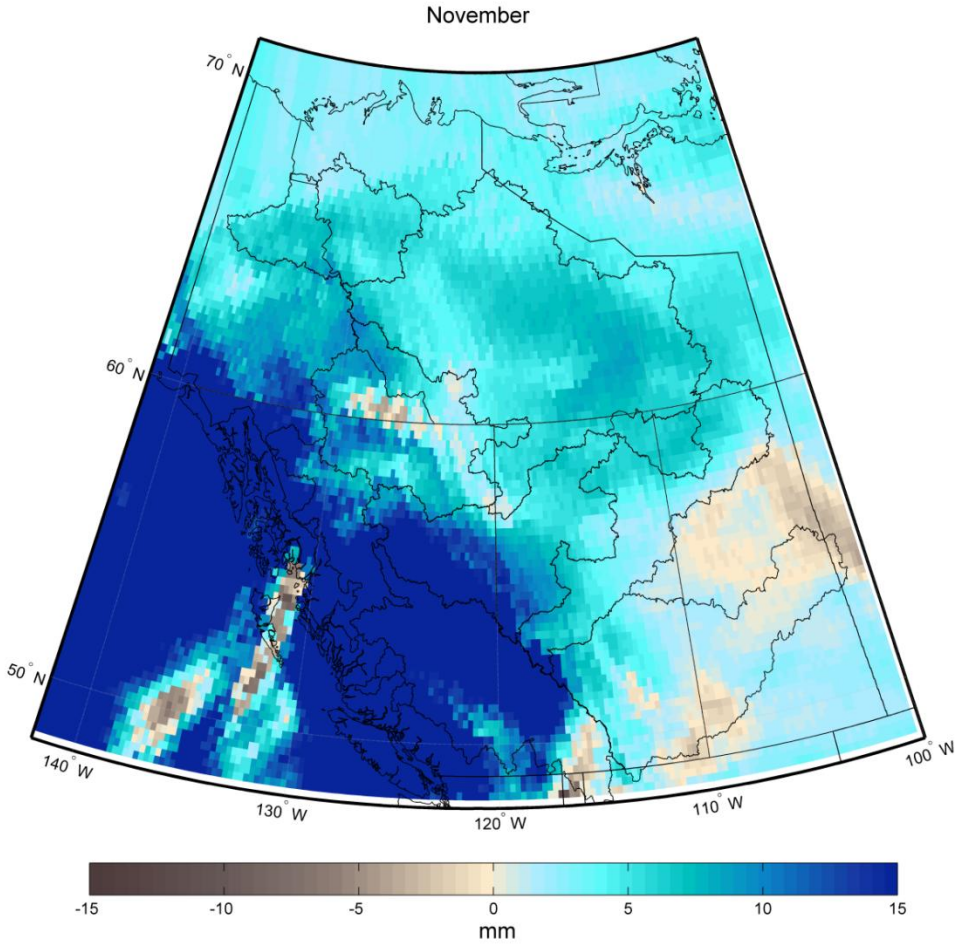

Figure B.106. Multimodel mean difference in monthly precipitation between the current and future periods during November.

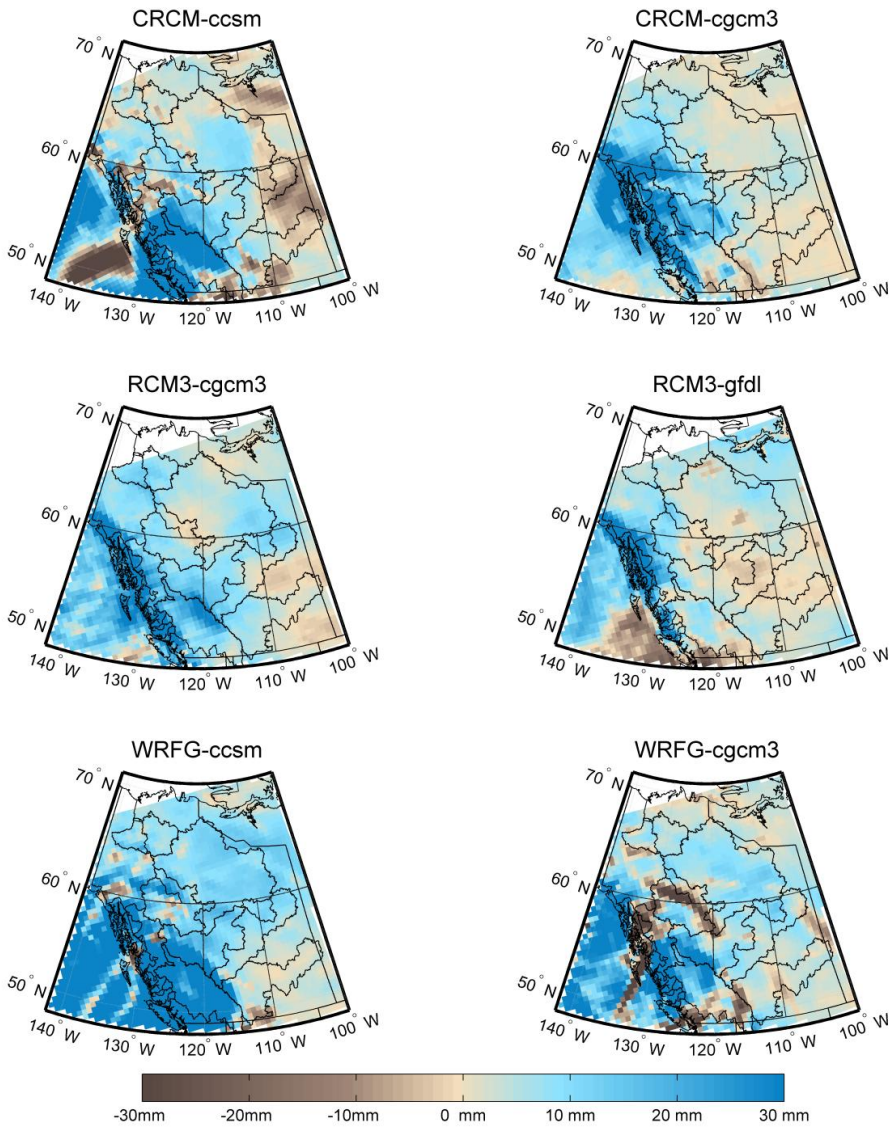

Figure B.107. Difference in precipitation totals between 1971-2000 and 2041-2070 during November.

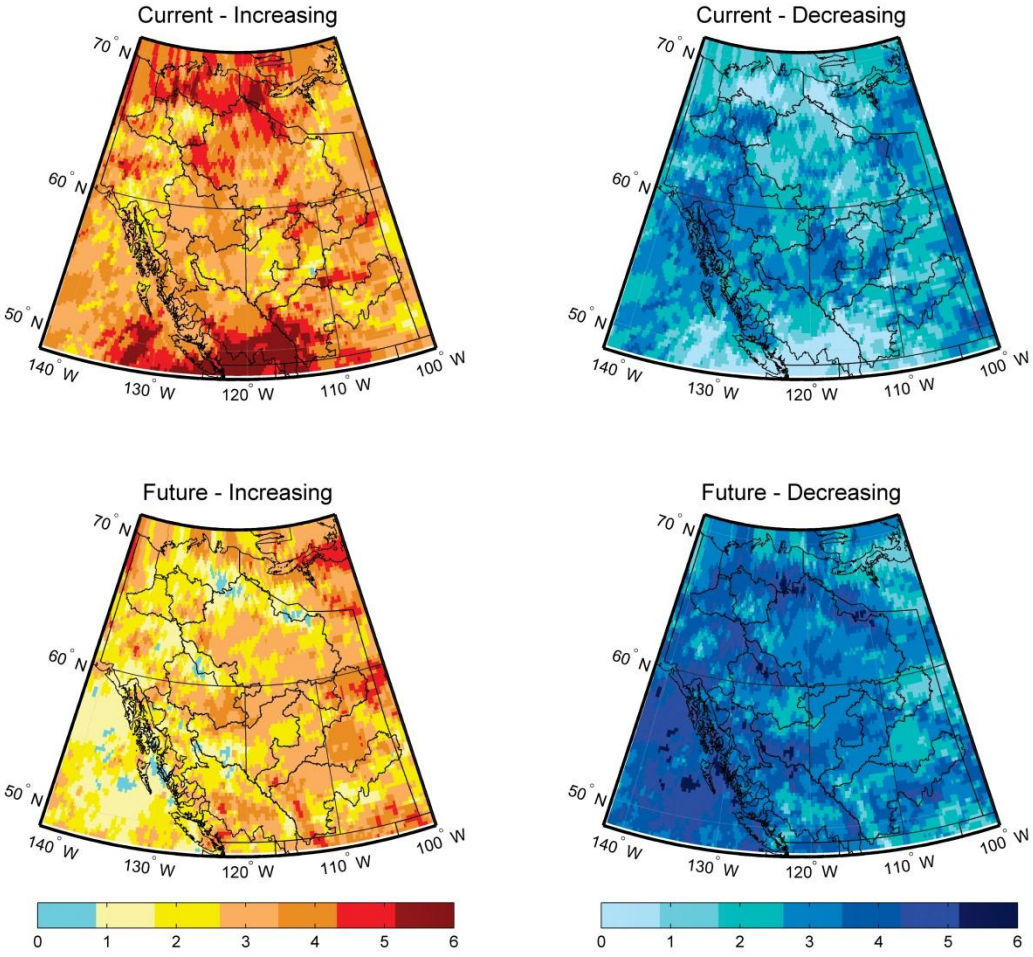

Figure B.108. Number of models showing increasing or decreasing rates of change in precipitation during the current (1971-2000) and future (2041-2070) time periods during November.

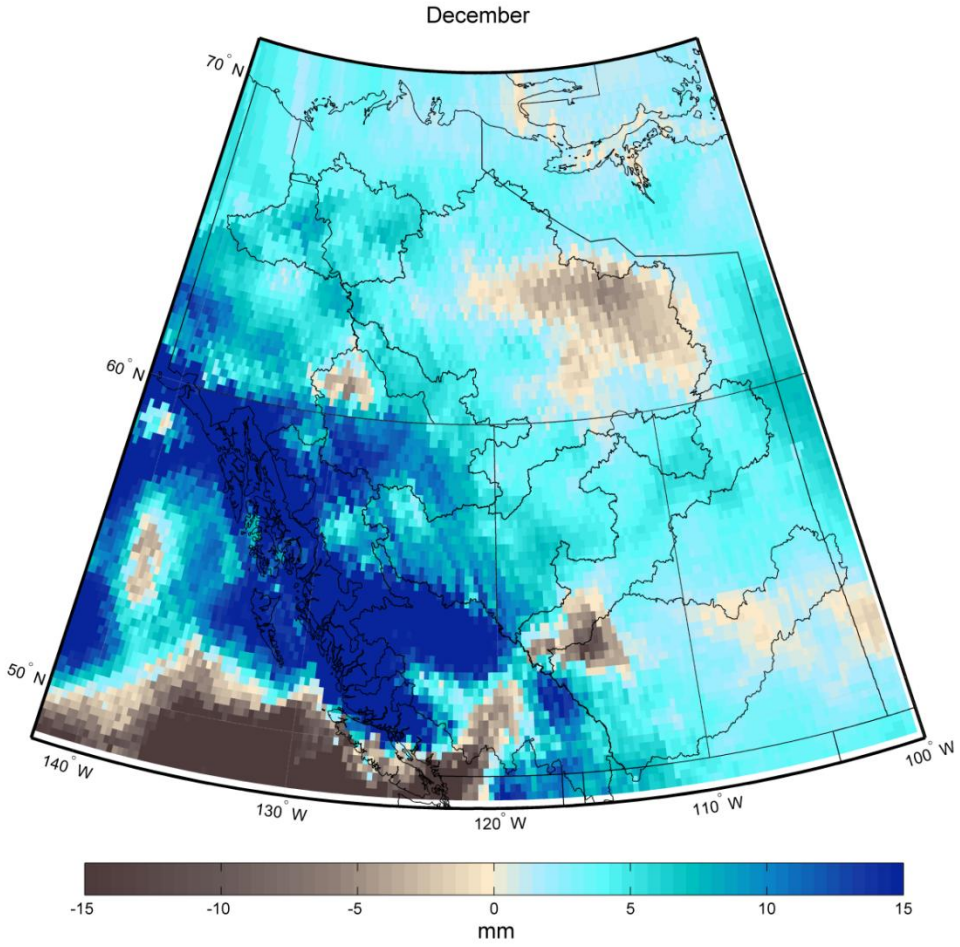

Figure B.109. Multimodel mean difference in monthly precipitation between the current and future periods during December.

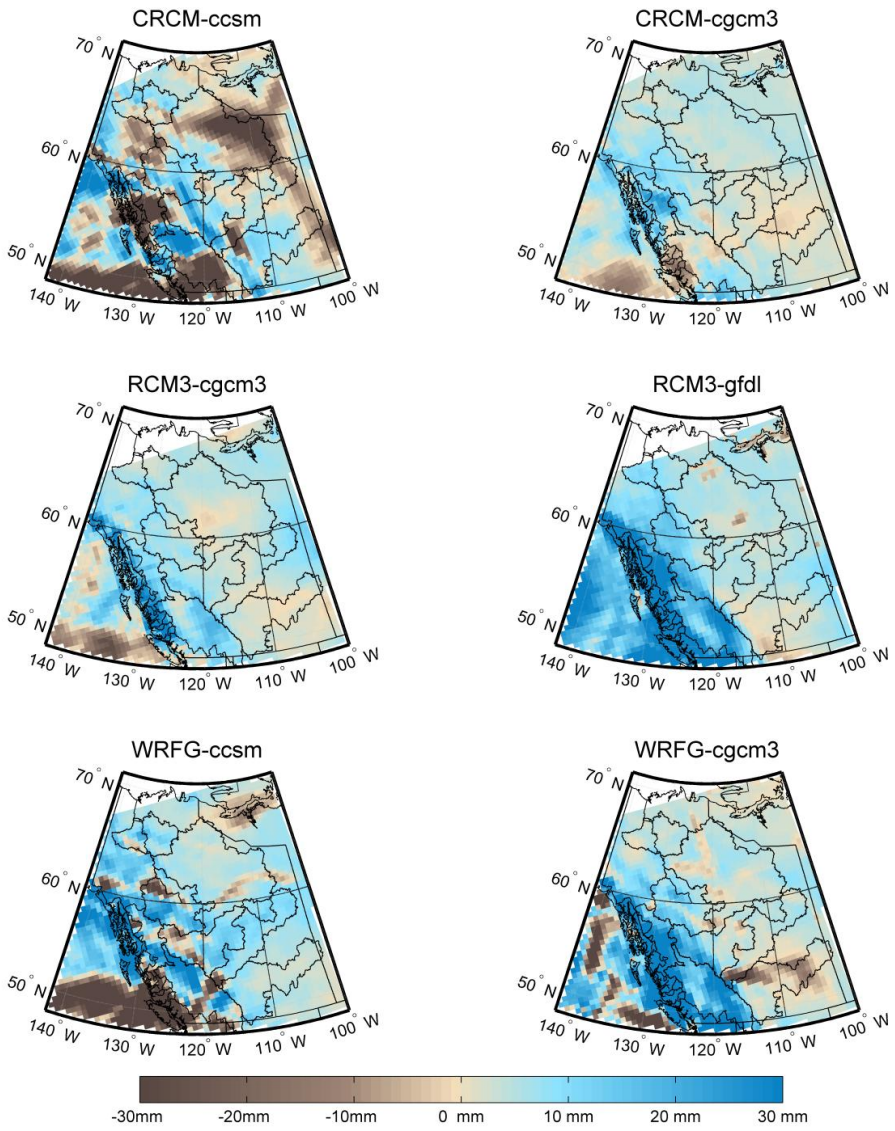

Figure B.110. Difference in precipitation totals between 1971-2000 and 2041-2070 during December.

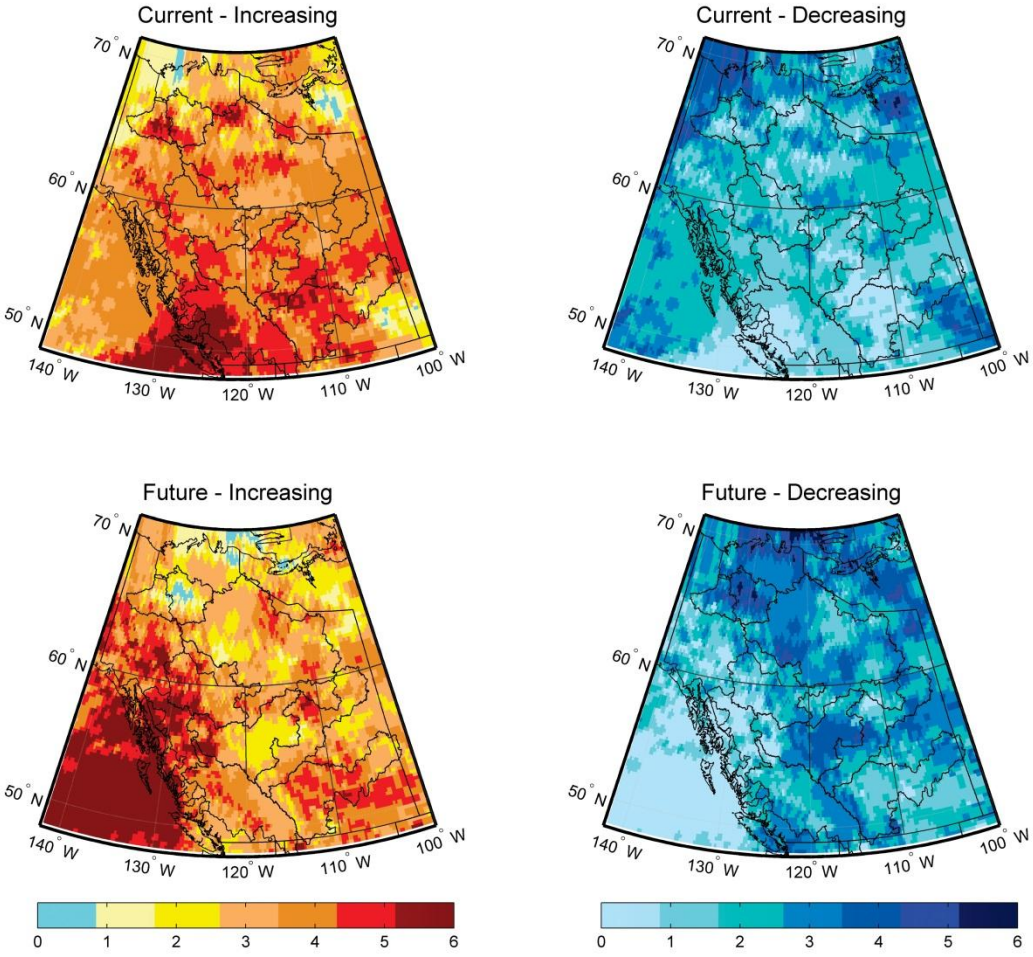

Figure B.111. Number of models showing increasing or decreasing rates of change in precipitation during the current (1971-2000) and future (2041-2070) time periods during December.

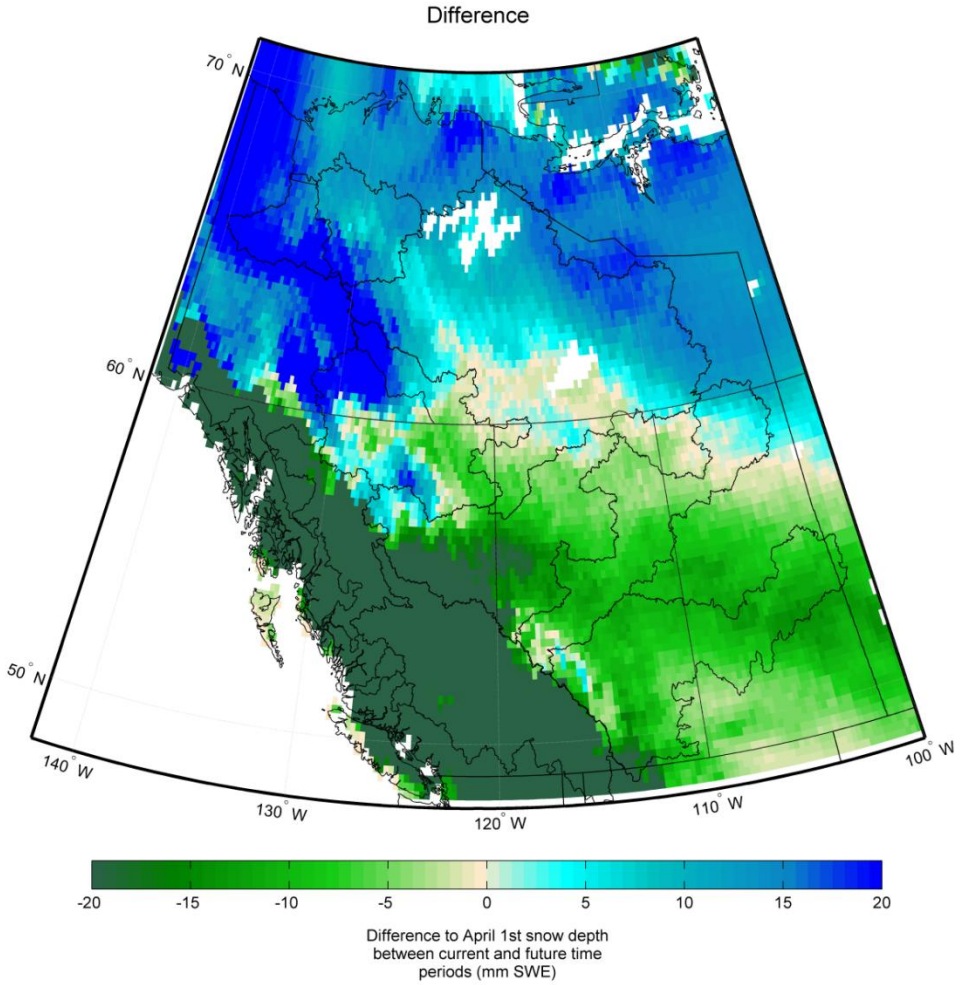

Figure B.112. Multimodel mean difference in April 1st SWE between the current and future periods.

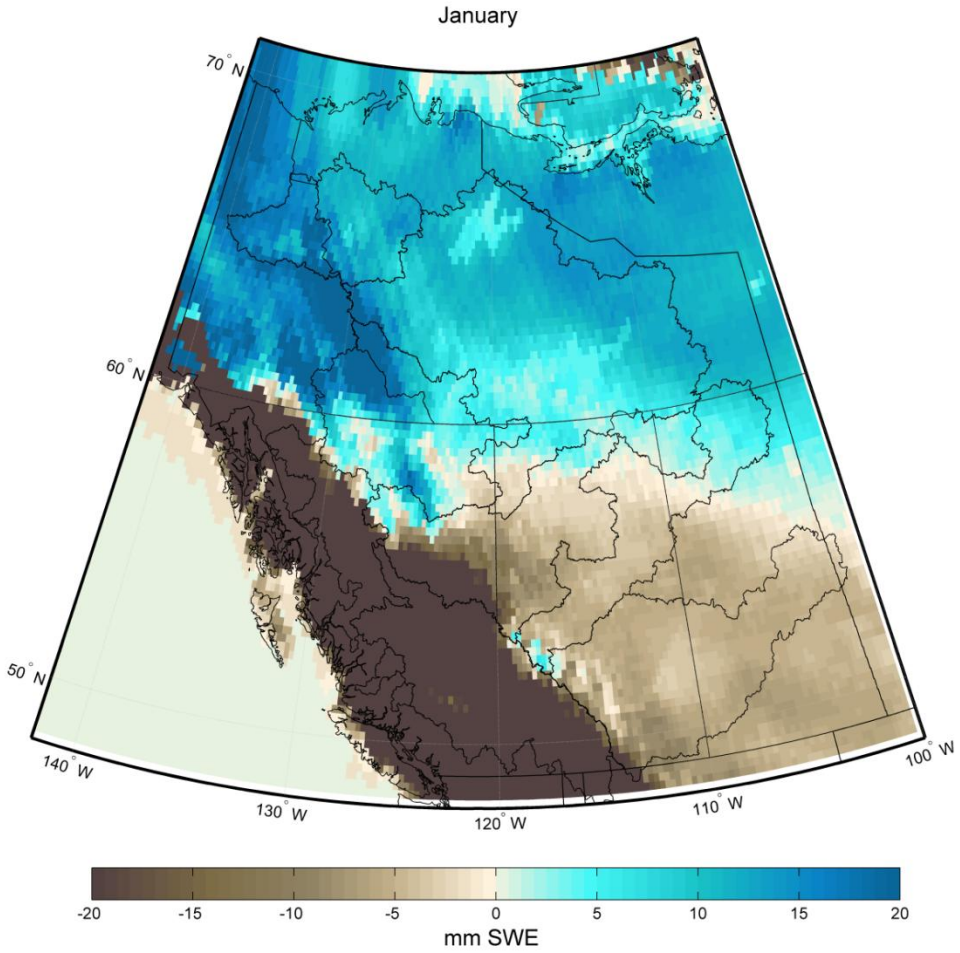

Figure B.113. Multimodel mean difference in monthly SWE between the current and future periods during January.

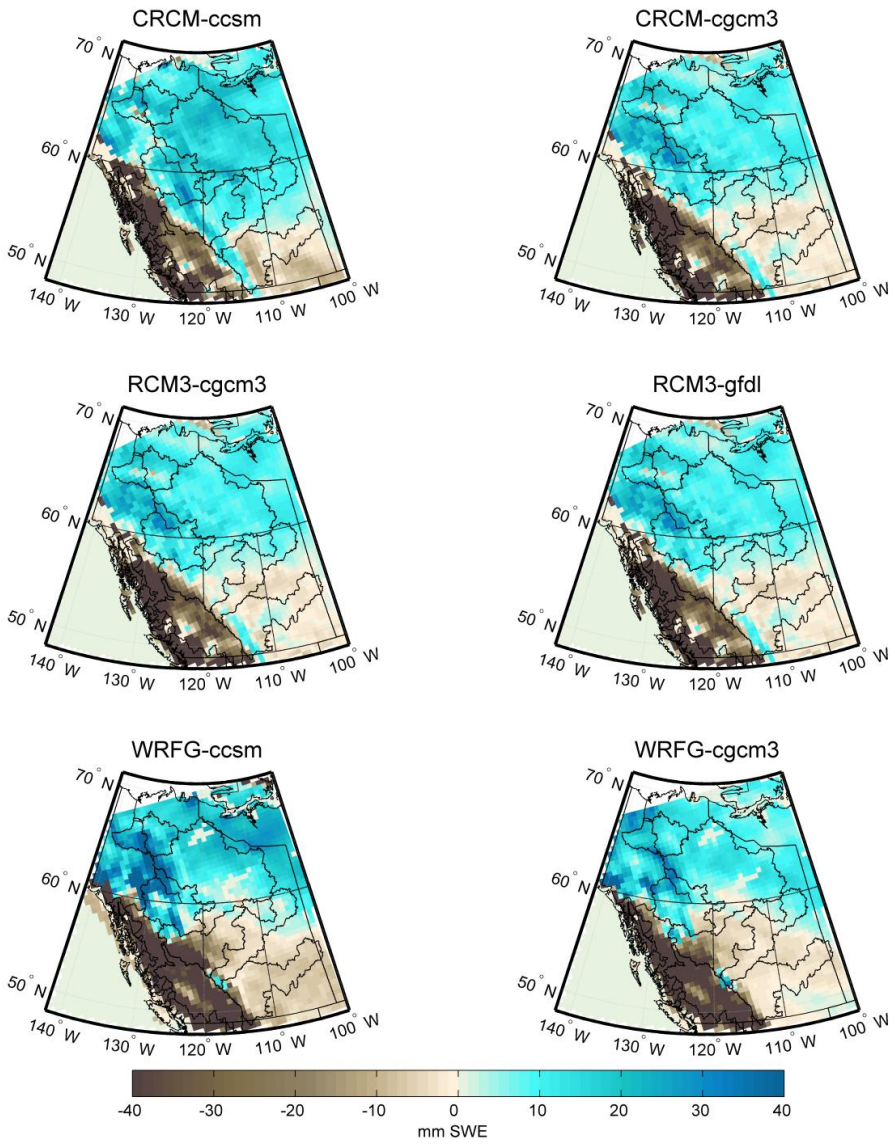

Figure B.114. Difference in SWE between 1971-2000 and 2041-2070 during January.

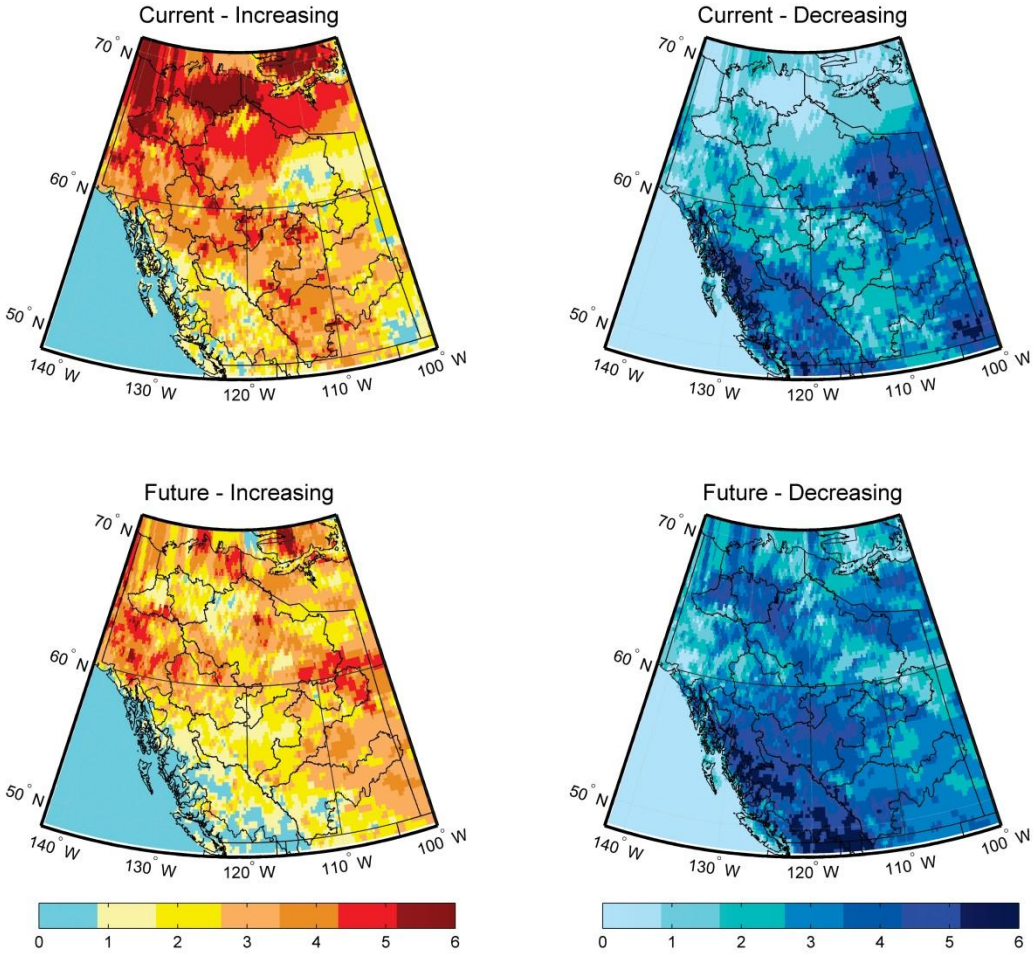

Figure B.115. Number of models showing increasing or decreasing rates of change in SWE during the current (1971-2000) and future (2041-2070) time periods during January.

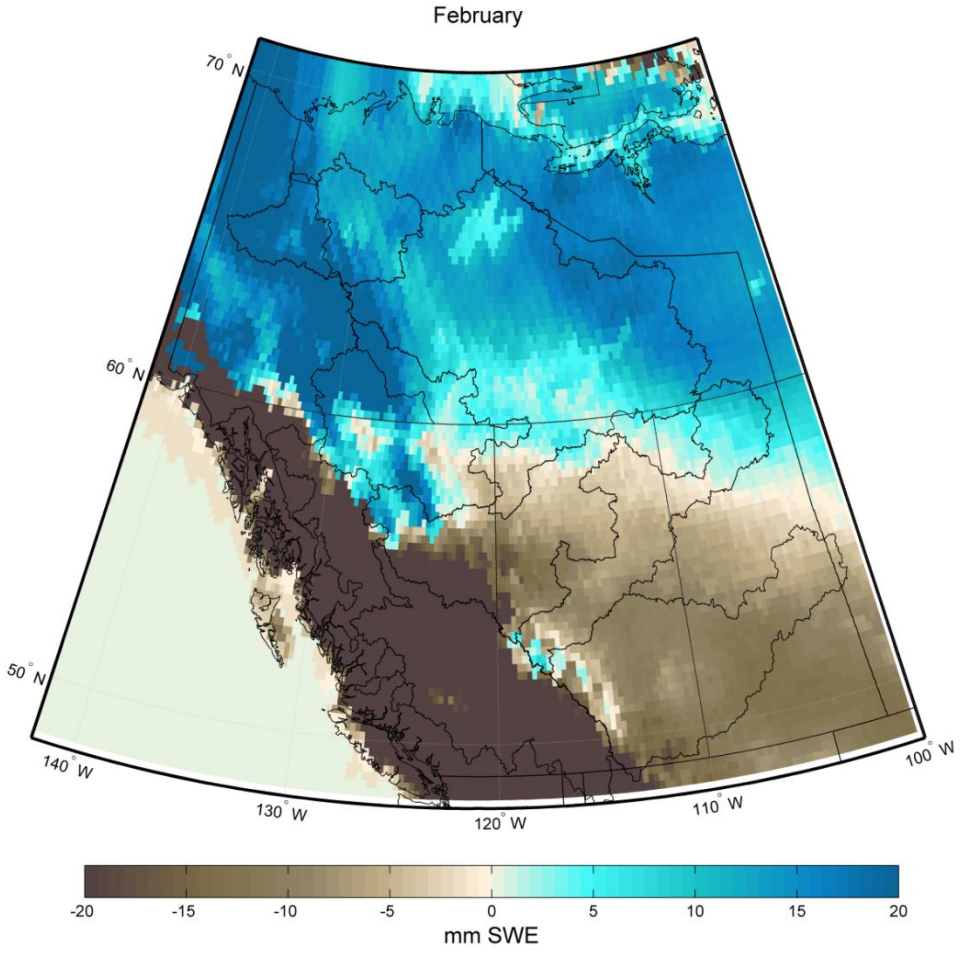

Figure B.116. Multimodel mean difference in monthly SWE between the current and future periods during February.

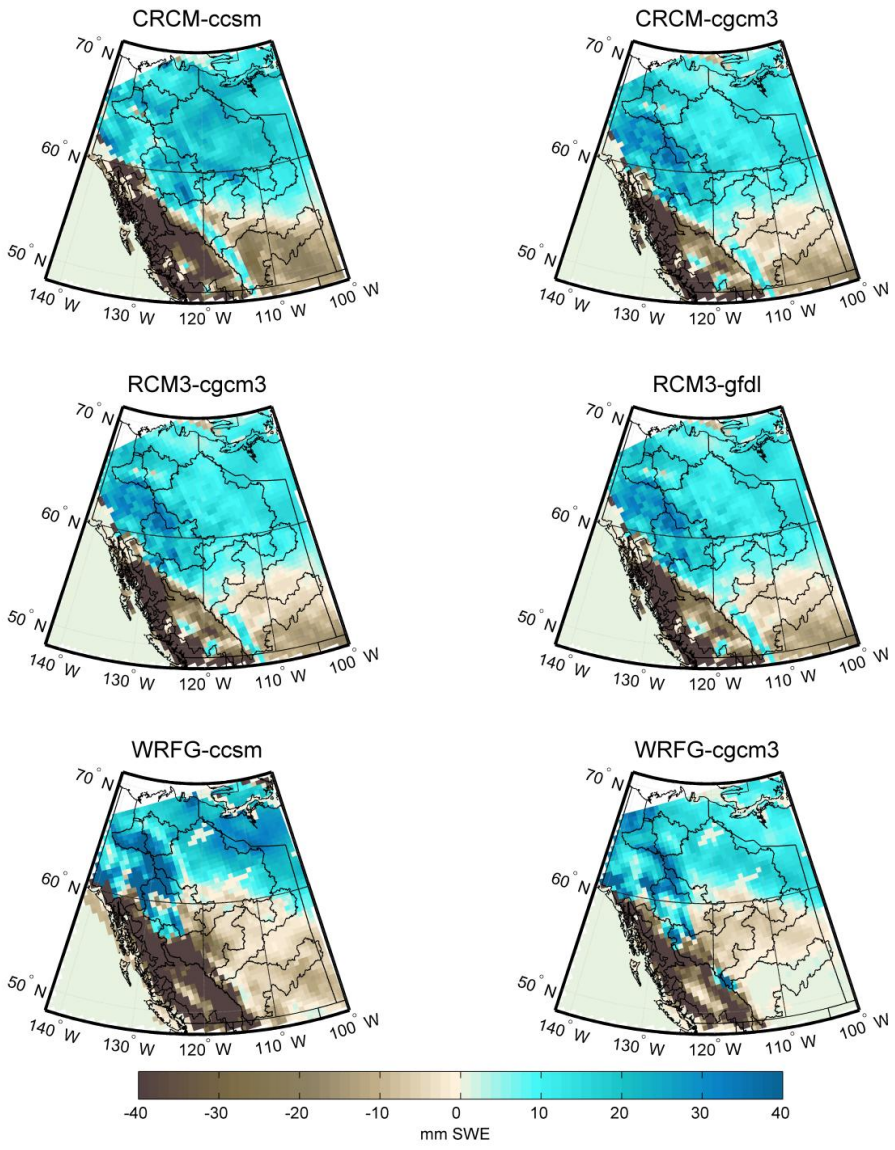

Figure B.117. Difference in SWE between 1971-2000 and 2041-2070 during February.

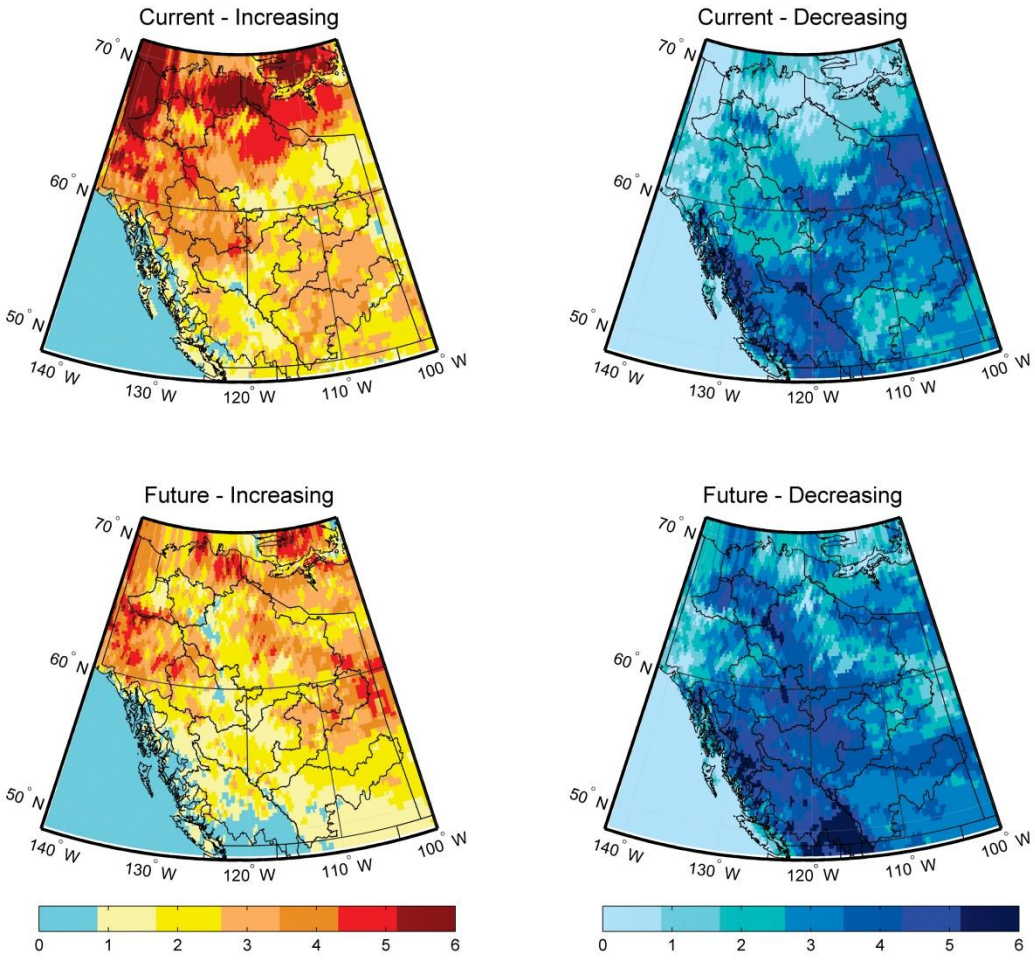

Figure B.118. Number of models showing increasing or decreasing rates of change in SWE during the current (1971-2000) and future (2041-2070) time periods during February.

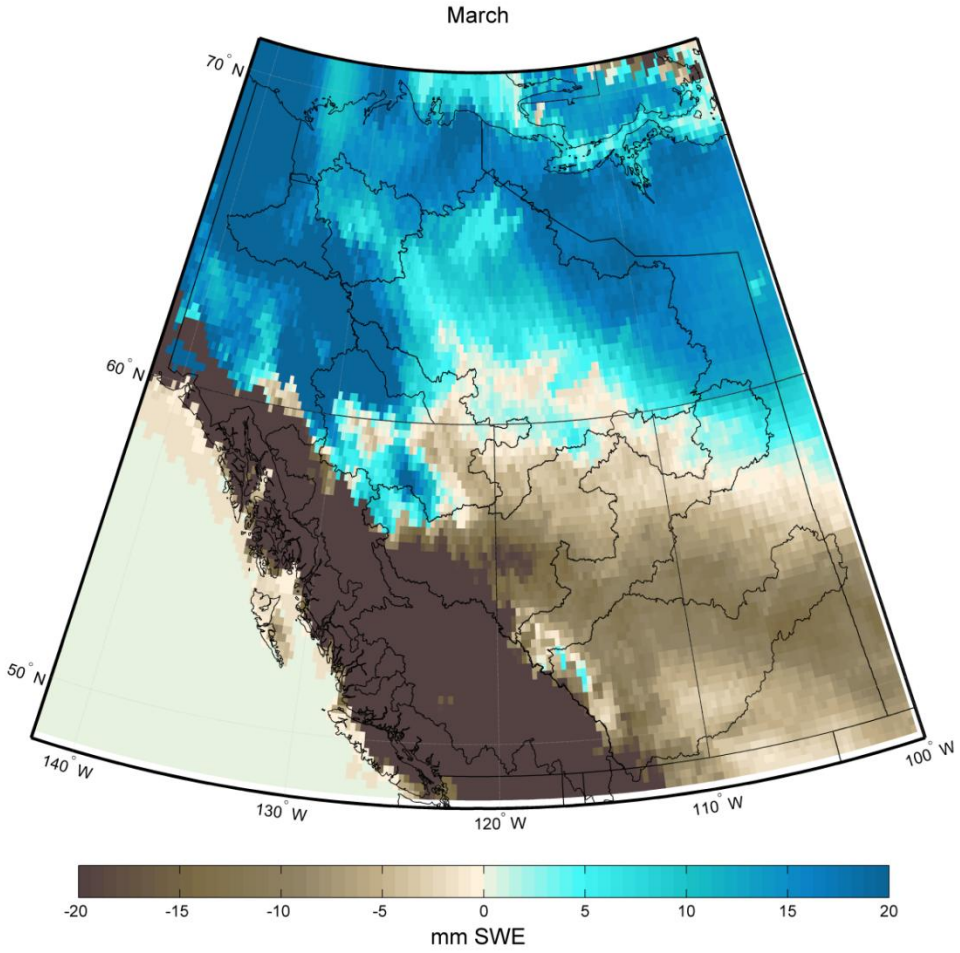

Figure B.119. Multimodel mean difference in monthly SWE between the current and future periods during March.

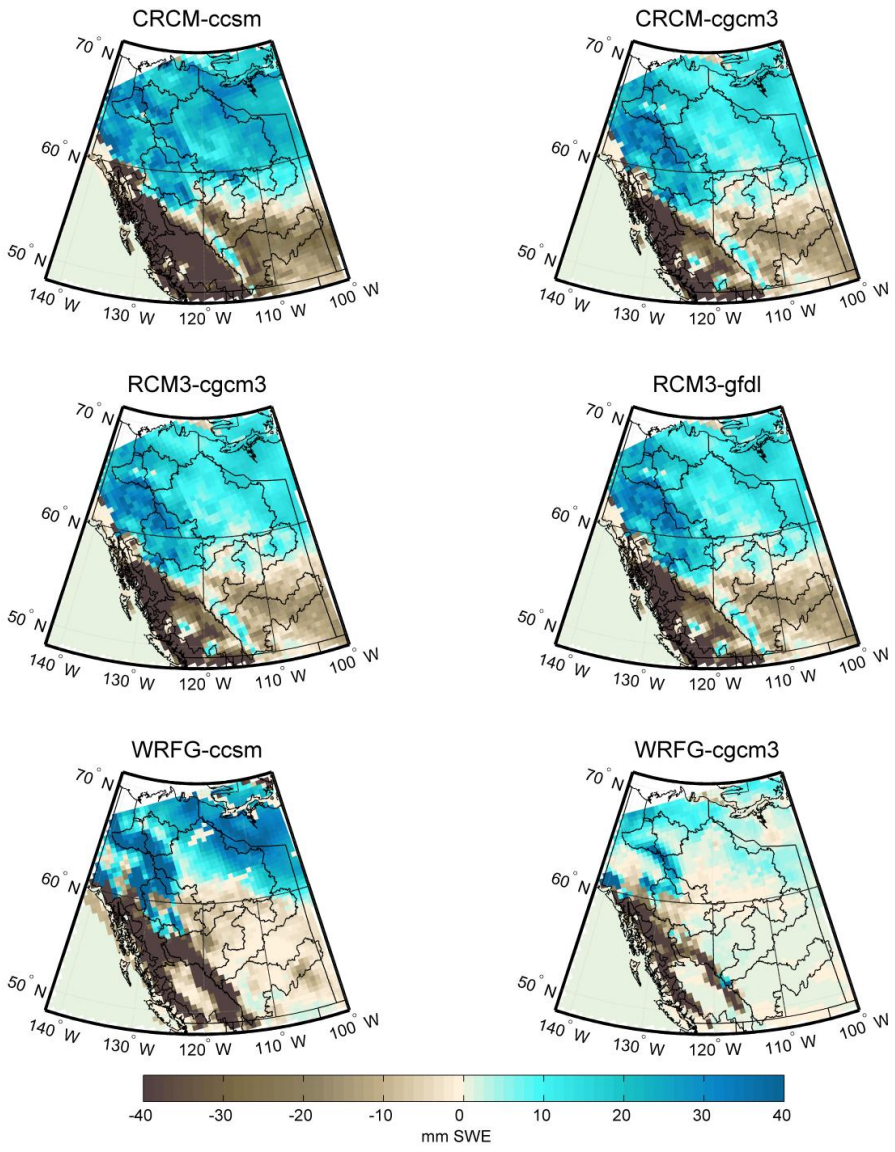

Figure B.120. Difference in SWE between 1971-2000 and 2041-2070 during March.

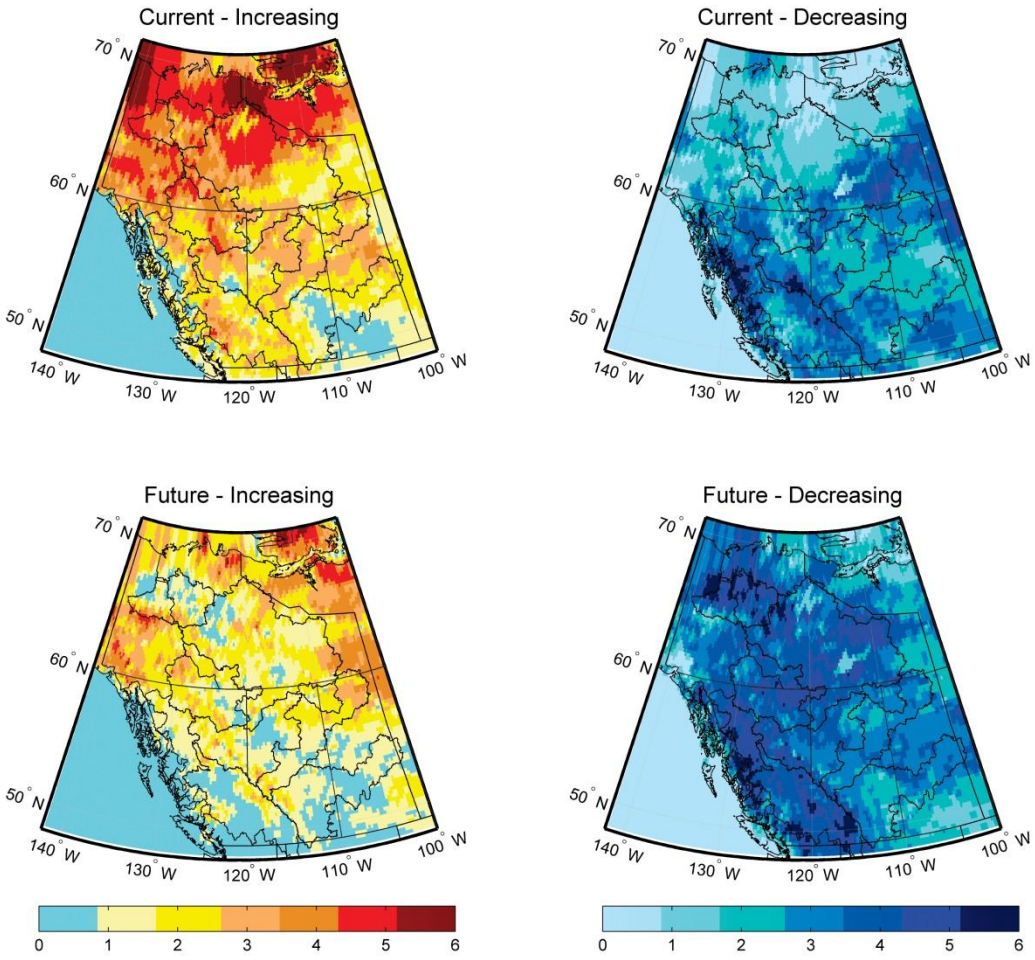

Figure B.121. Number of models showing increasing or decreasing rates of change in SWE during the current (1971-2000) and future (2041-2070) time periods during March.

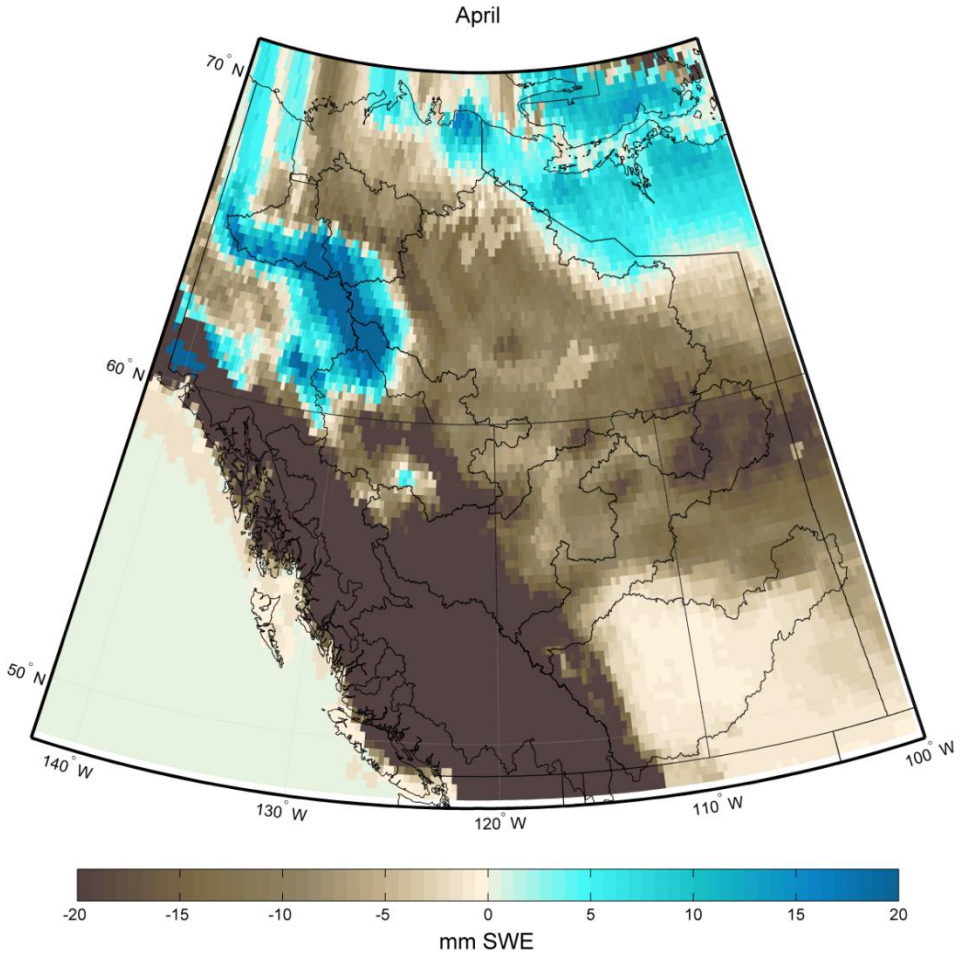

Figure B.122. Multimodel mean difference in monthly SWE between the current and future periods during April.

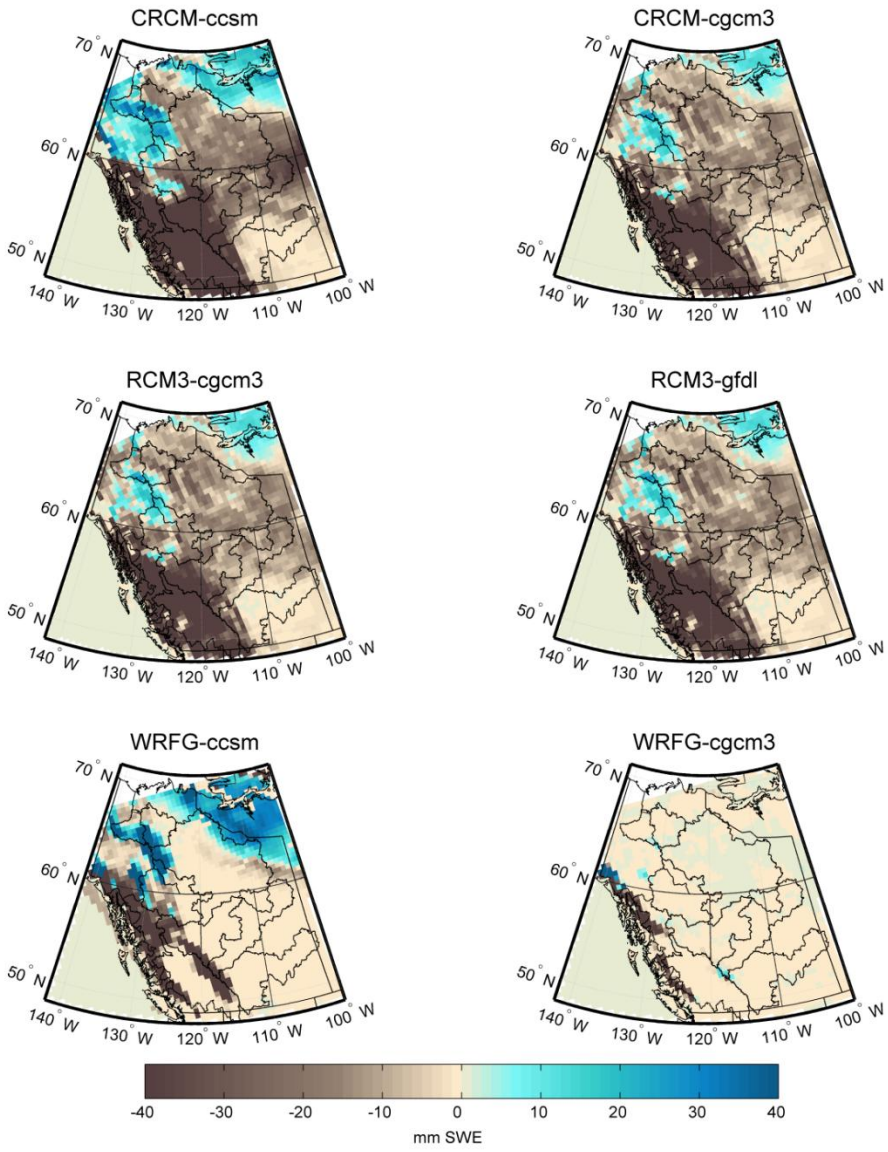

Figure B.123. Difference in SWE between 1971-2000 and 2041-2070 during April.

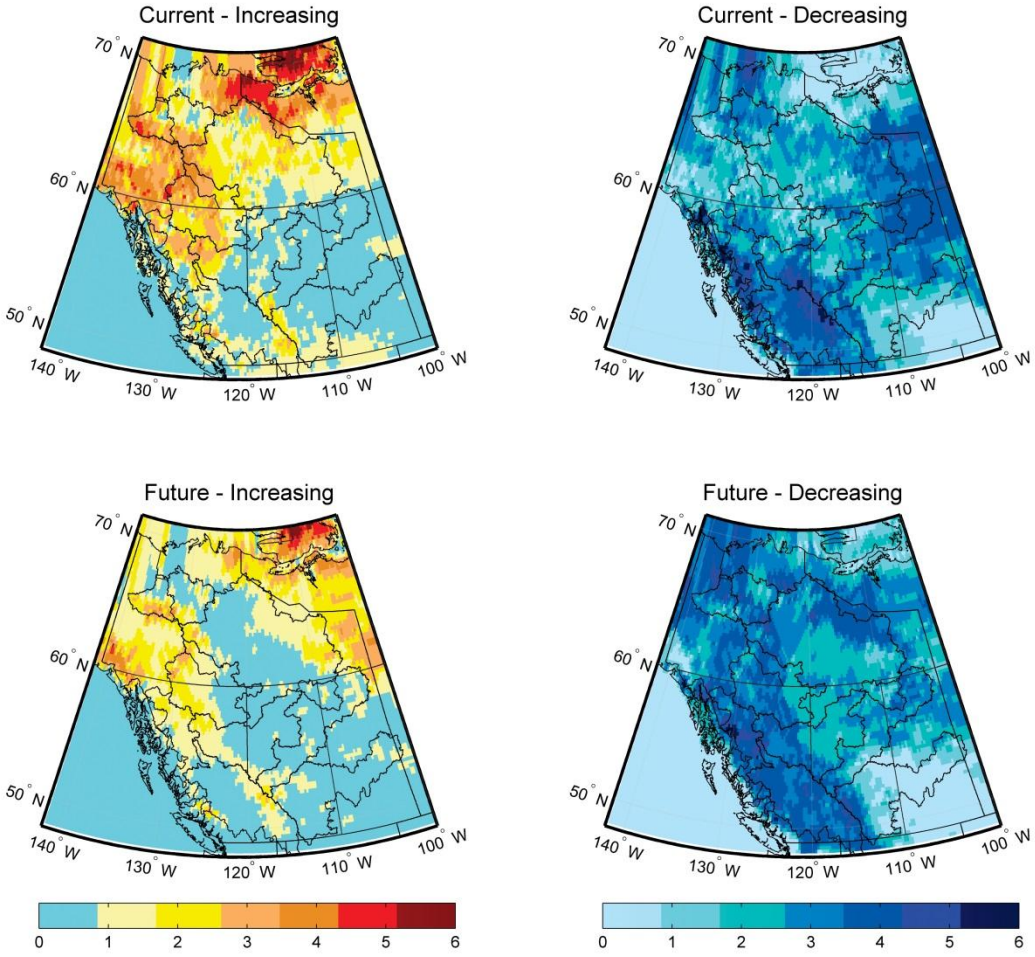

Figure B.124. Number of models showing increasing or decreasing rates of change in SWE during the current (1971-2000) and future (2041-2070) time periods during April.

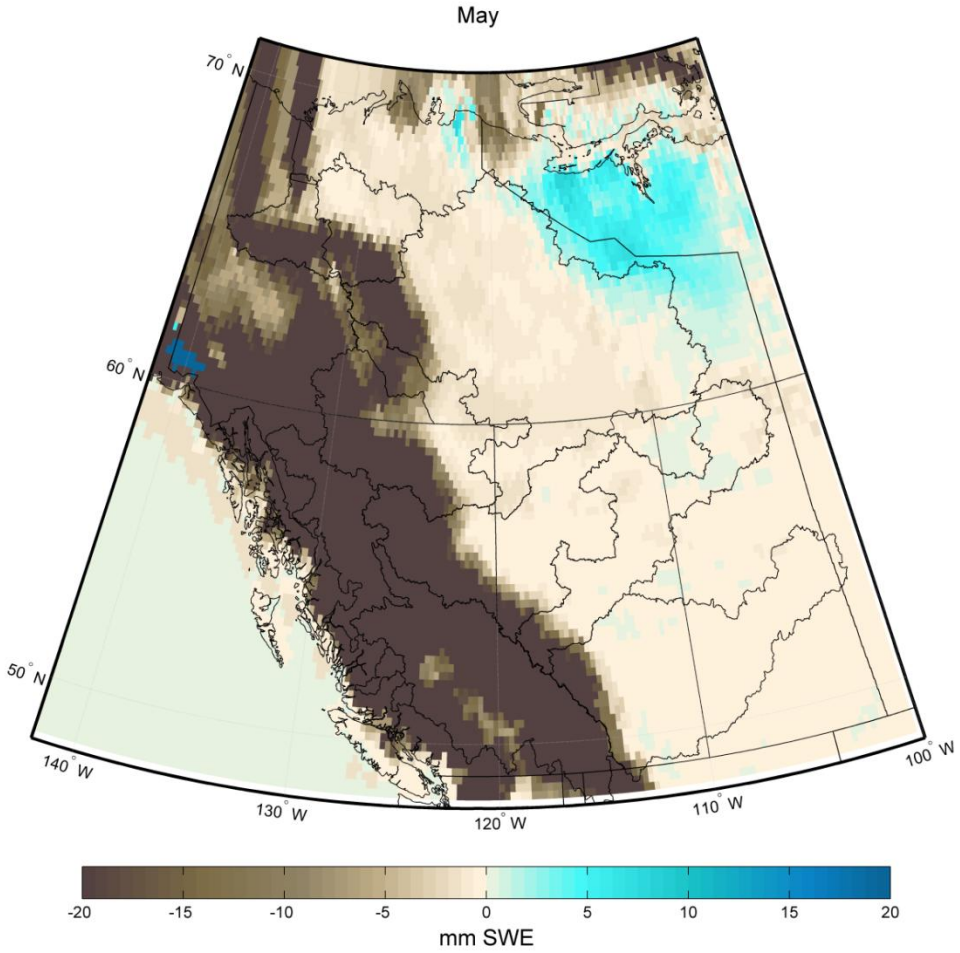

Figure B.125. Multimodel mean difference in monthly SWE between the current and future periods during May.

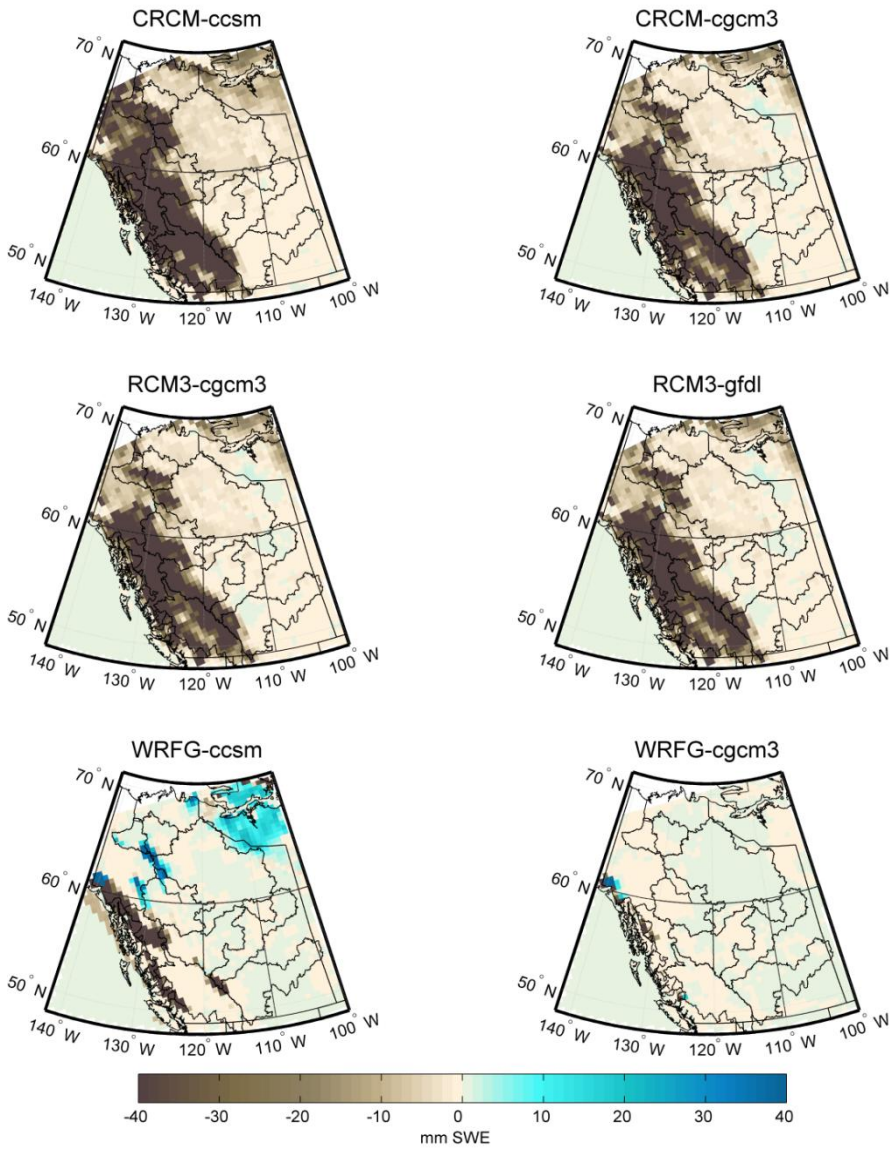

Figure B.126. Difference in SWE between 1971-2000 and 2041-2070 during May.

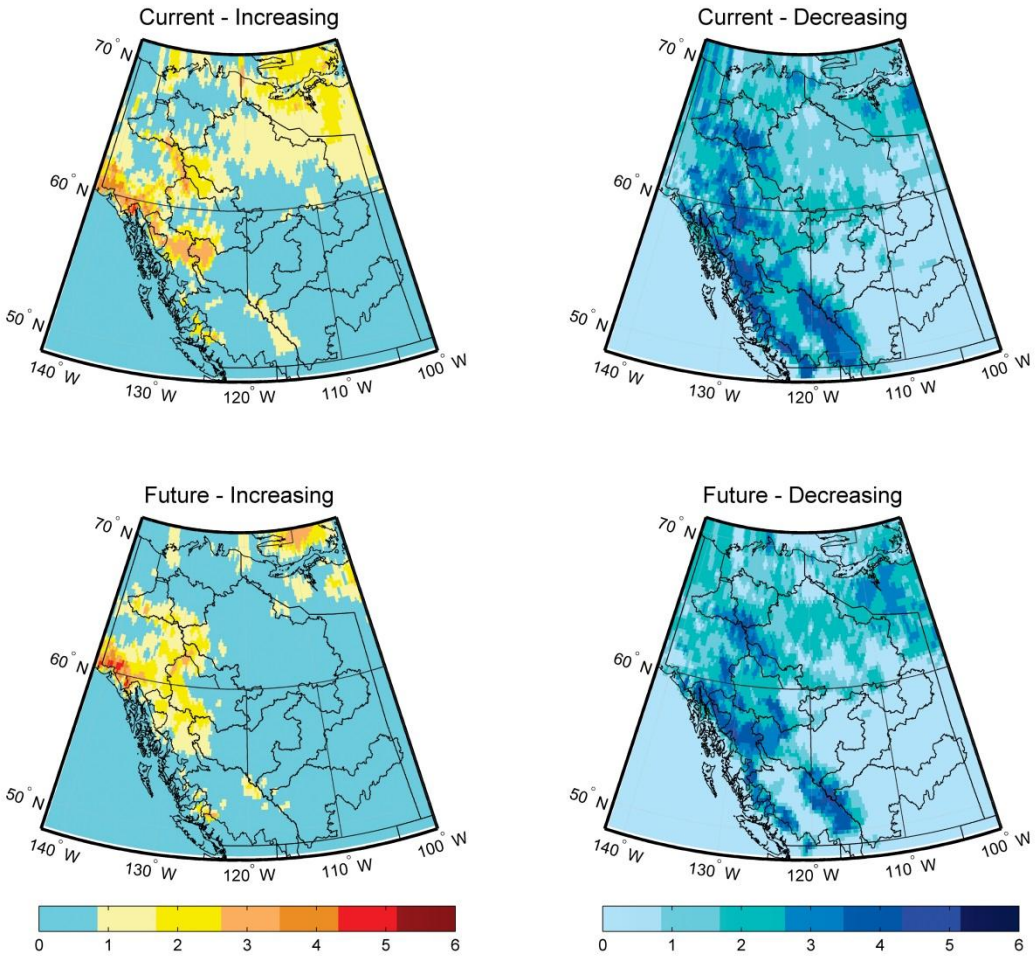

Figure B.127. Number of models showing increasing or decreasing rates of change in SWE during the current (1971-2000) and future (2041-2070) time periods during May.

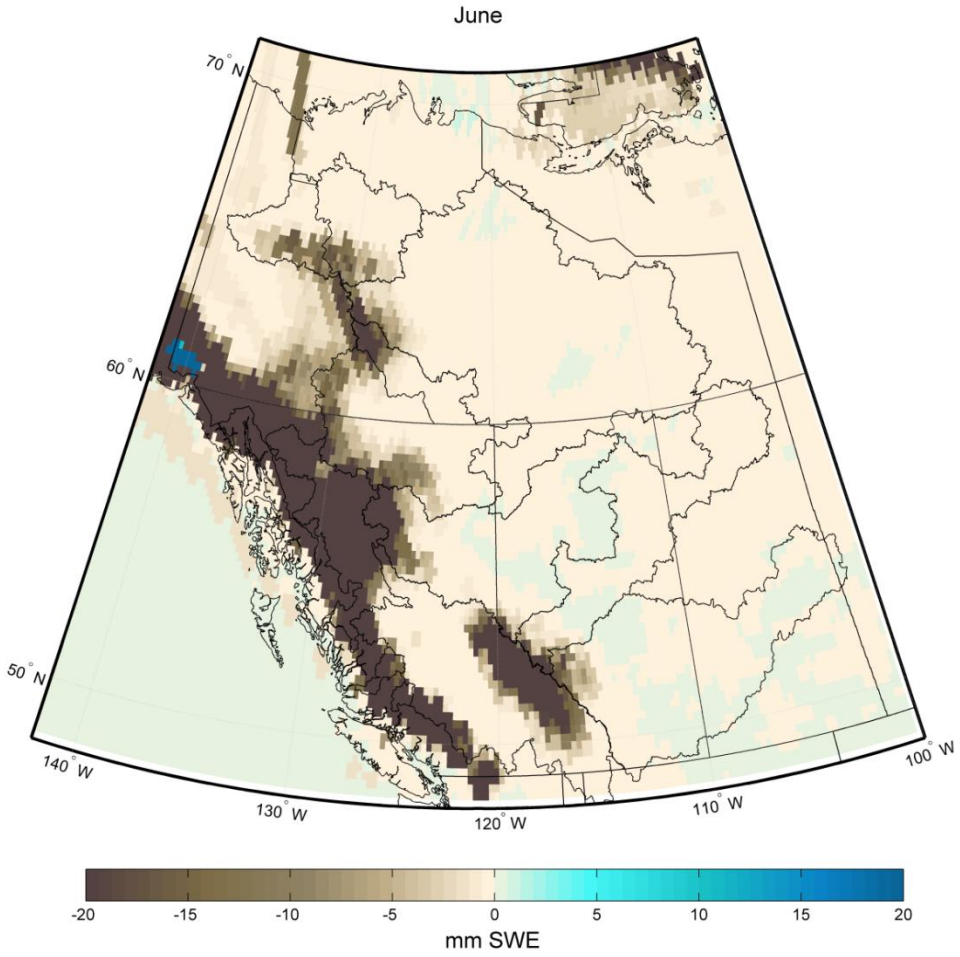

Figure B.128. Multimodel mean difference in monthly SWE between the current and future periods during June.

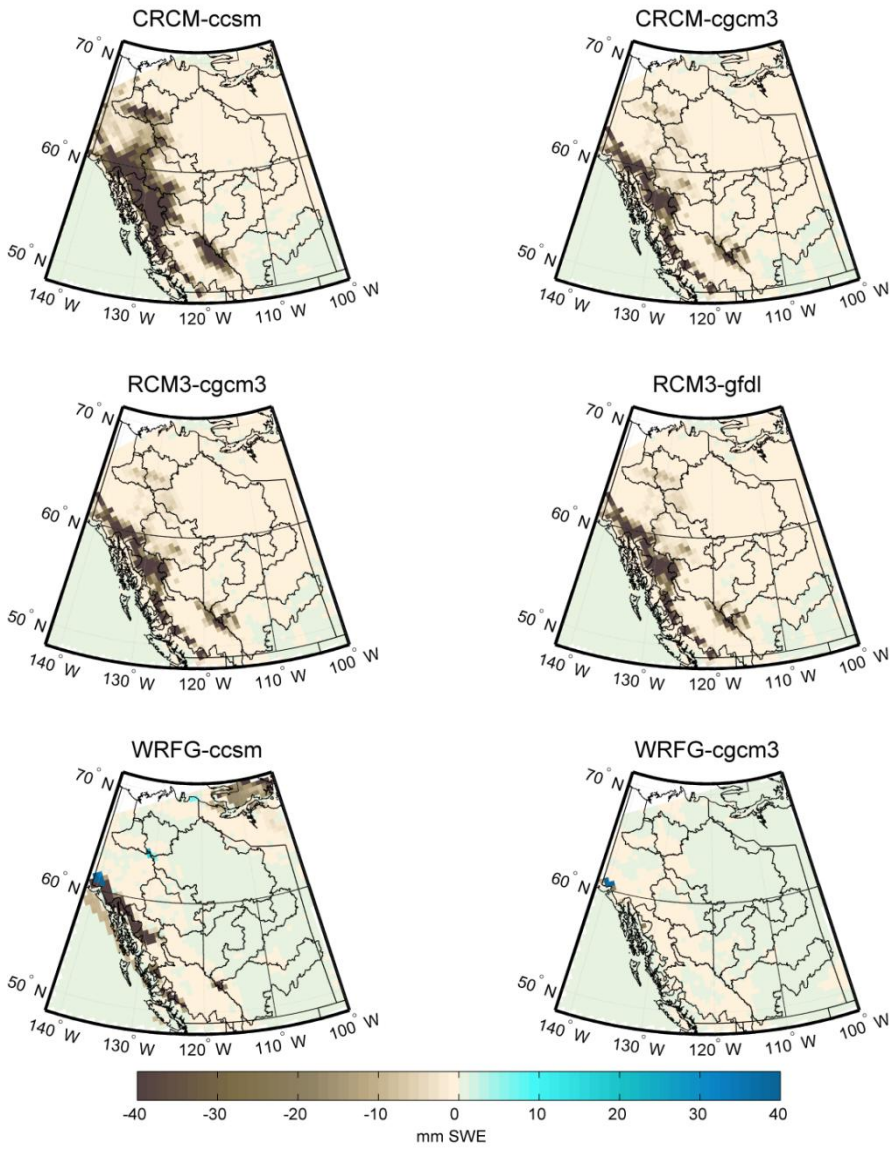

Figure B.129. Difference in SWE between 1971-2000 and 2041-2070 during June.

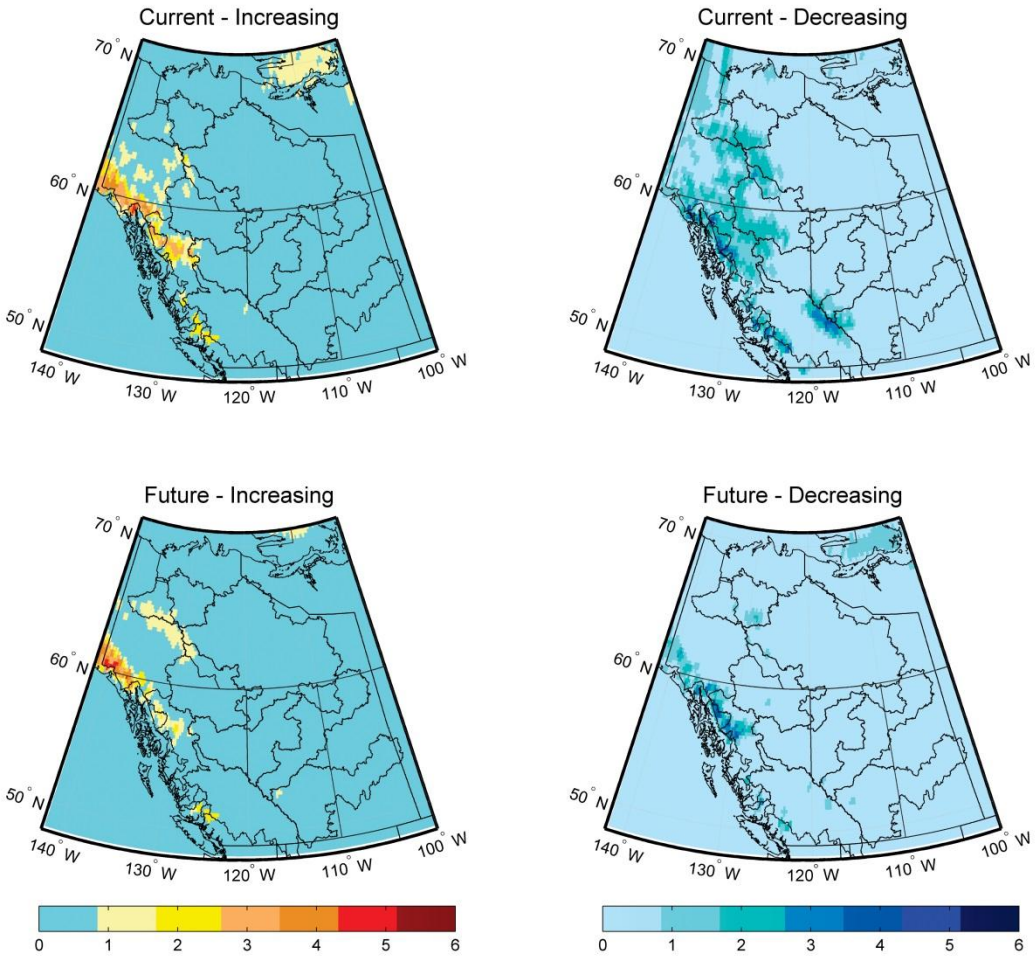

Figure B.130. Number of models showing increasing or decreasing rates of change in SWE during the current (1971-2000) and future (2041-2070) time periods during June.

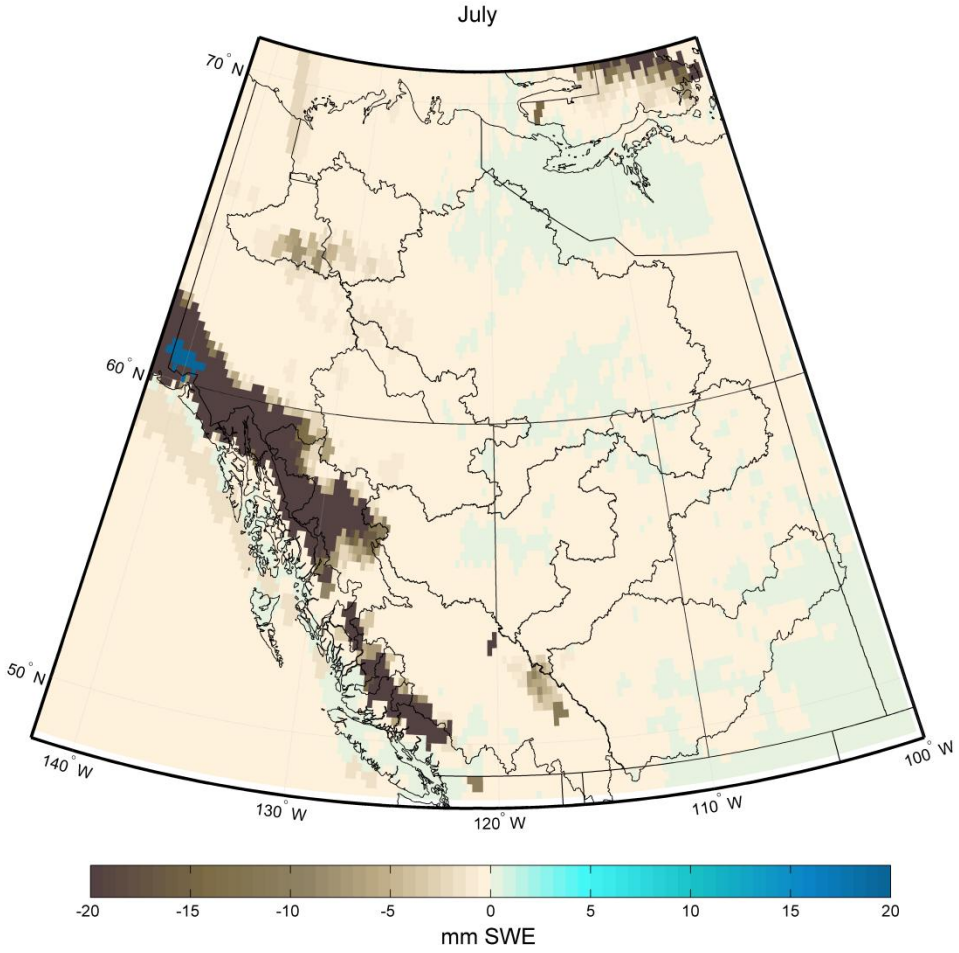

Figure B.131. Multimodel mean difference in monthly SWE between the current and future periods during July.

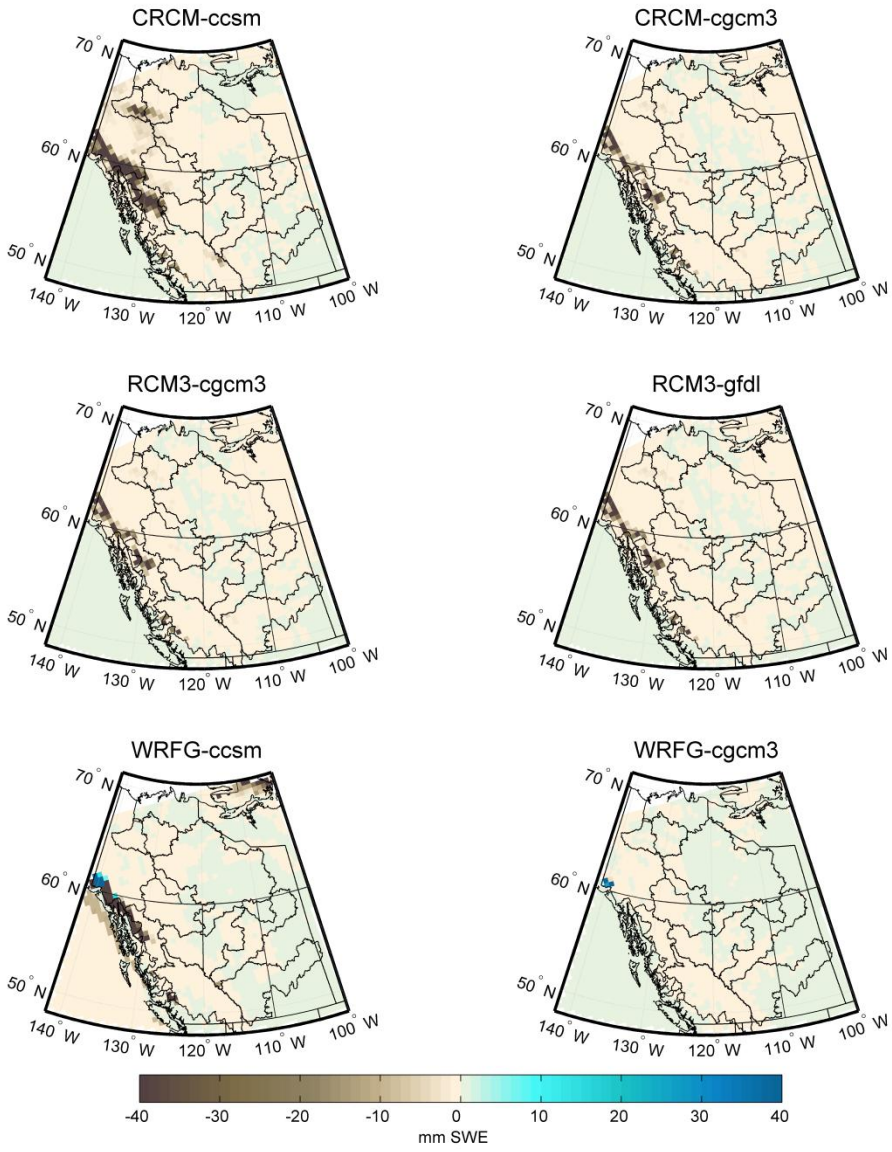

Figure B.132. Difference in SWE between 1971-2000 and 2041-2070 during July.

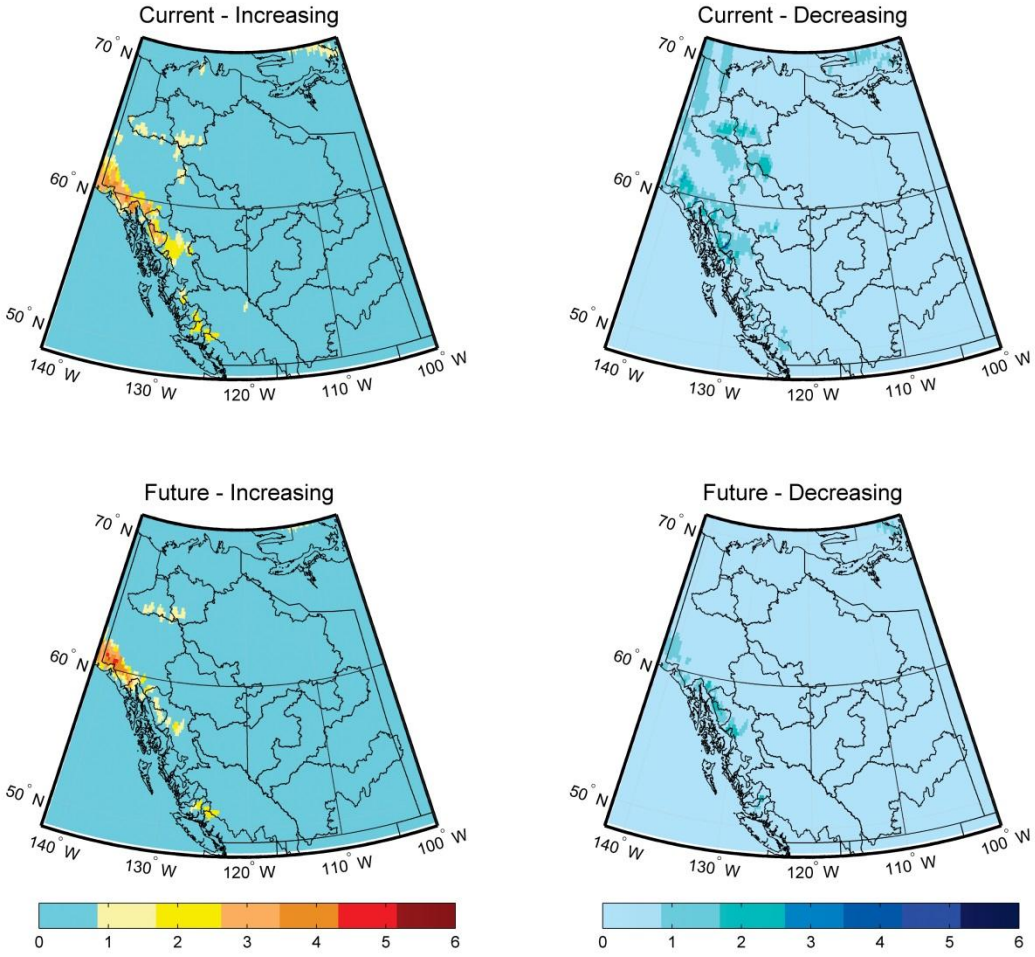

Figure B.133. Number of models showing increasing or decreasing rates of change in SWE during the current (1971-2000) and future (2041-2070) time periods during July.

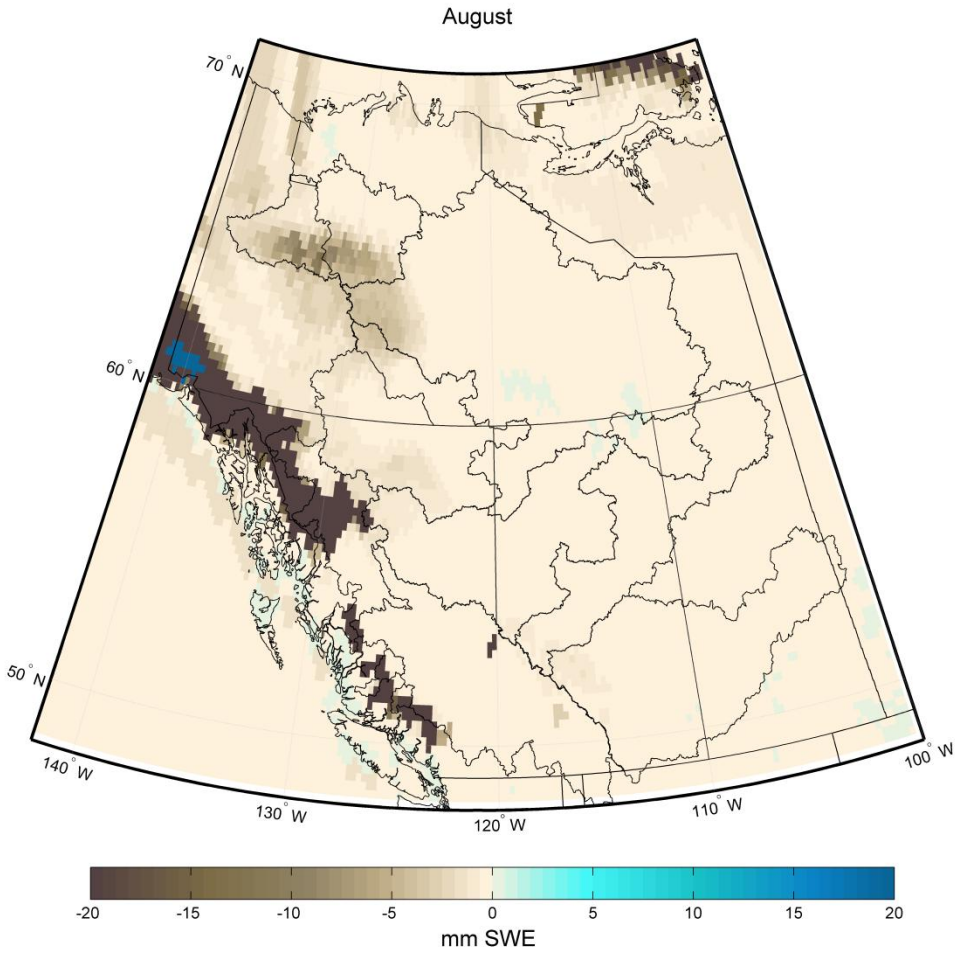

Figure B.134. Multimodel mean difference in monthly SWE between the current and future periods during August.

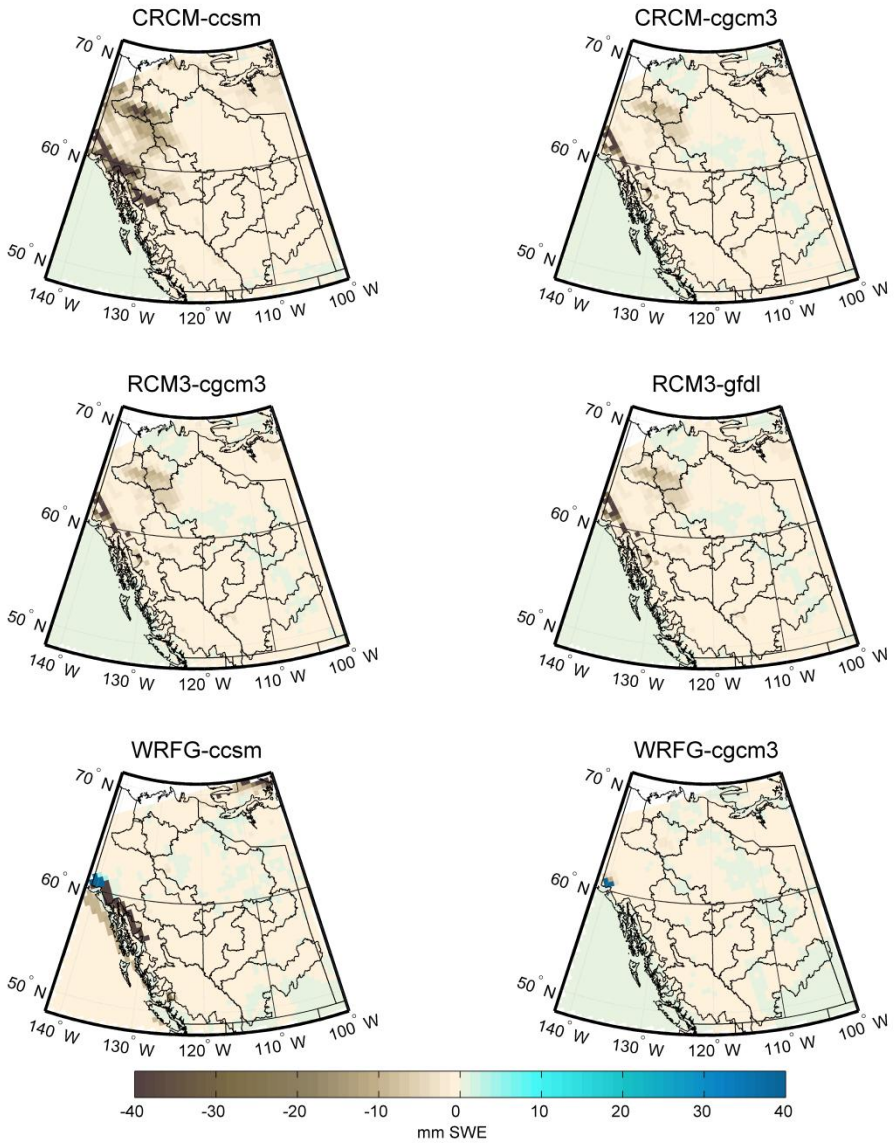

Figure B.135. Difference in SWE between 1971-2000 and 2041-2070 during August.

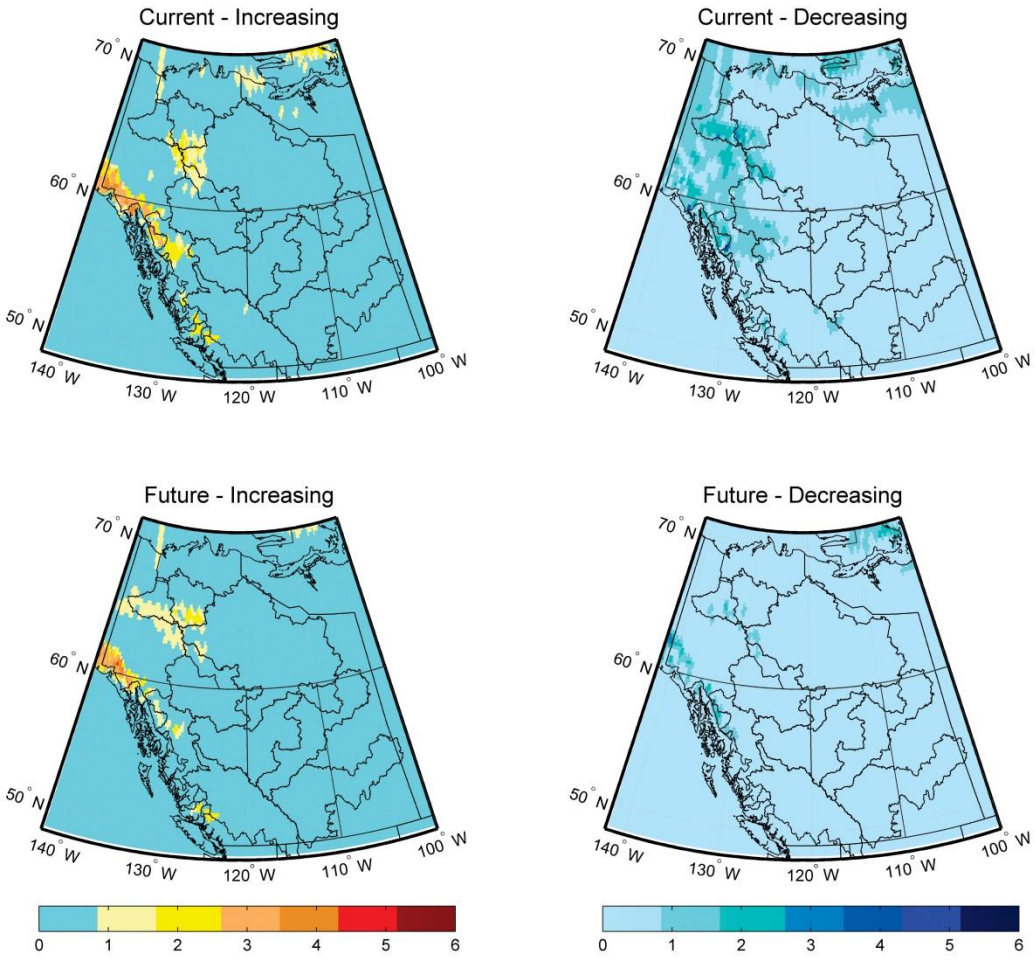

Figure B.136. Number of models showing increasing or decreasing rates of change in SWE during the current (1971-2000) and future (2041-2070) time periods during August.

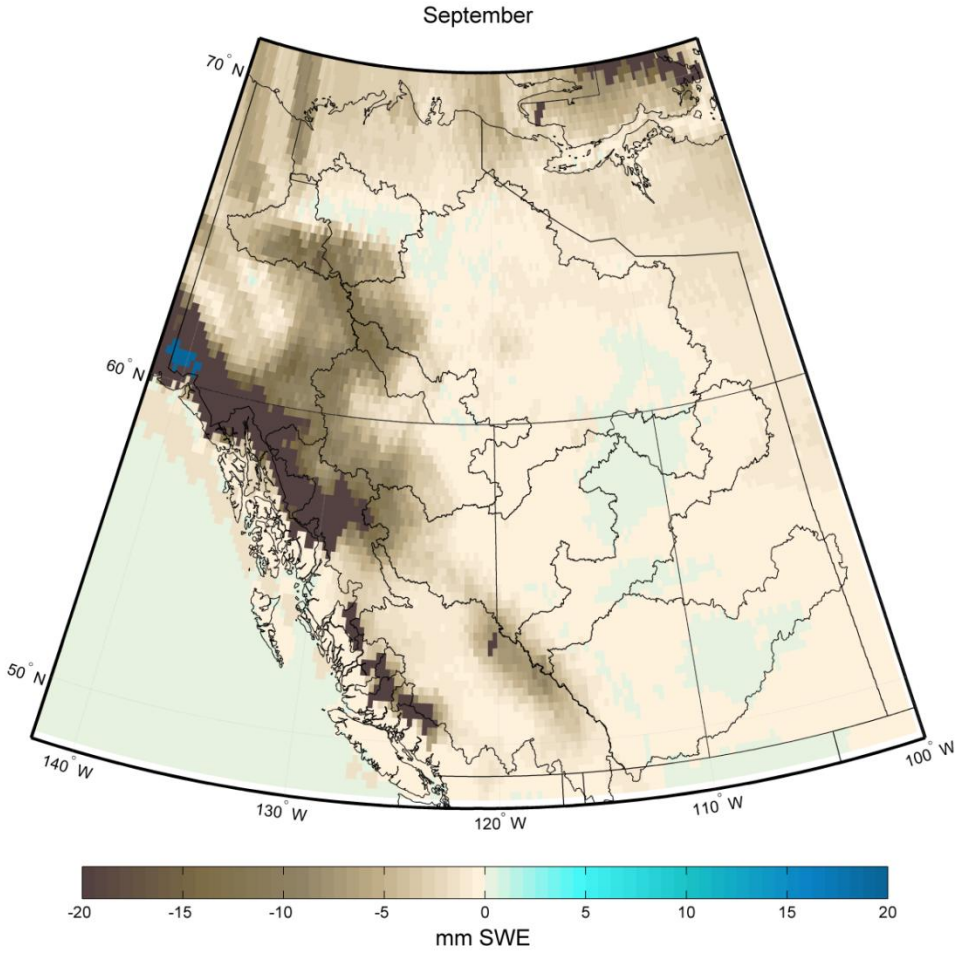

Figure B.137. Multimodel mean difference in monthly SWE between the current and future periods during September.

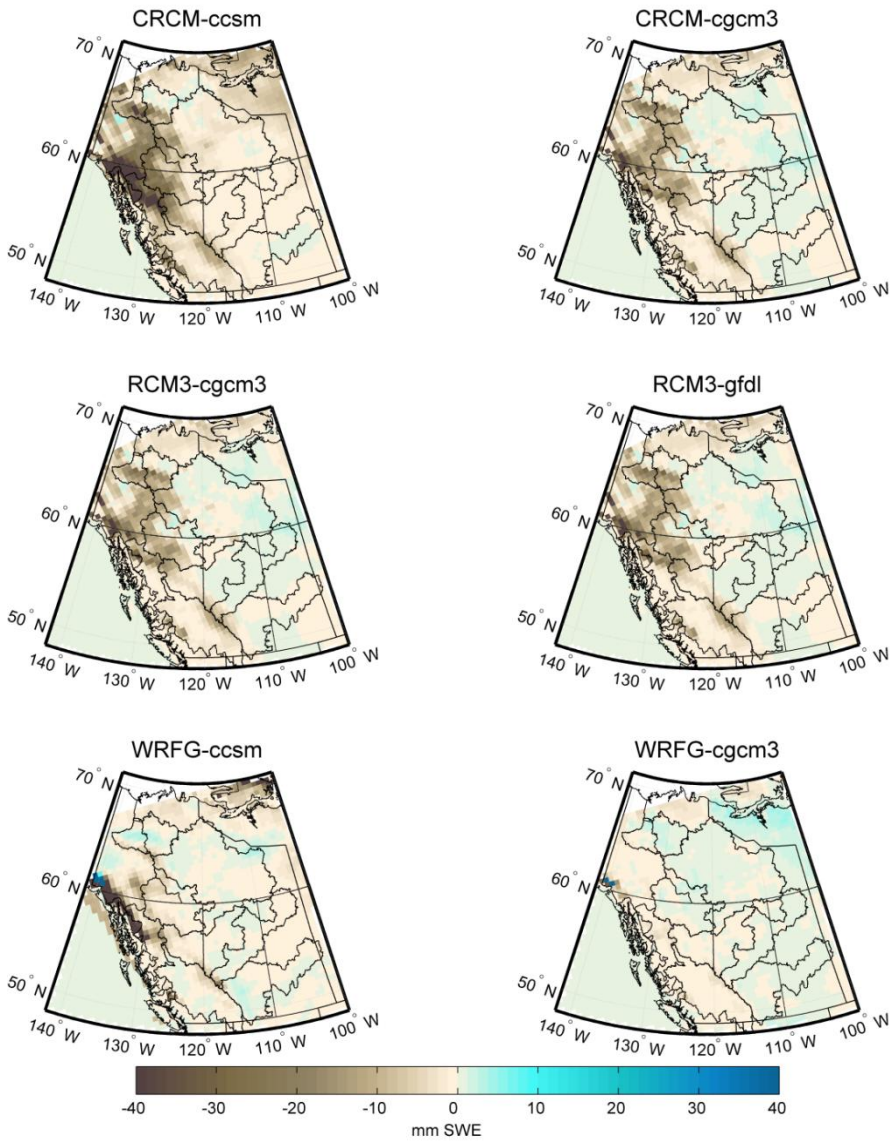

Figure B.138. Difference in SWE between 1971-2000 and 2041-2070 during September.

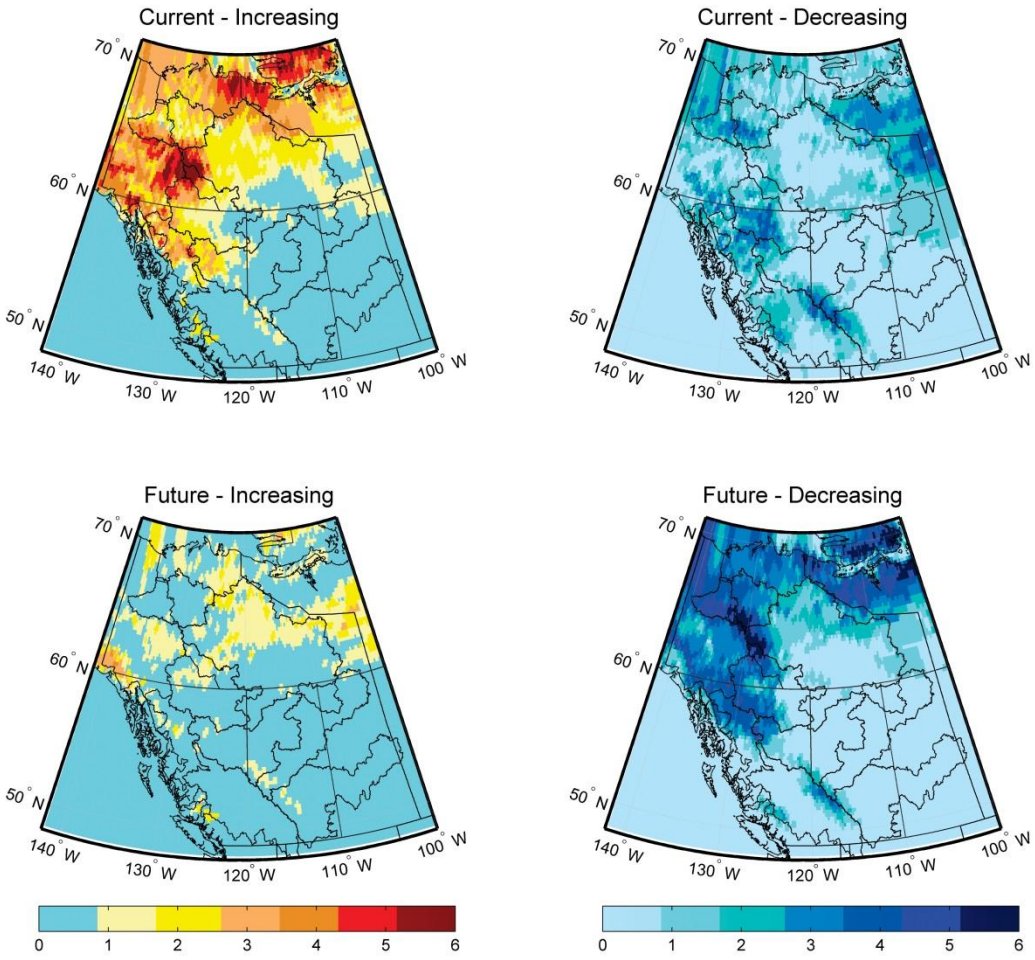

Figure B.139. Number of models showing increasing or decreasing rates of change in SWE during the current (1971-2000) and future (2041-2070) time periods during September.

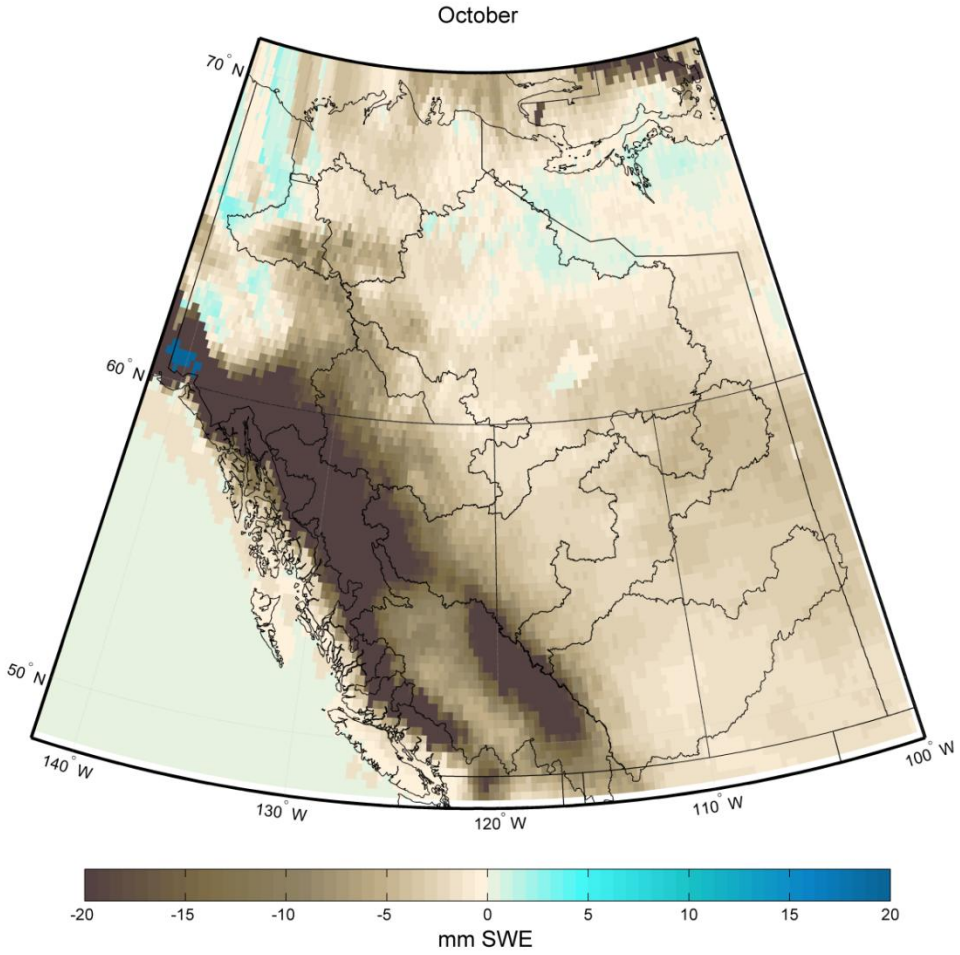

Figure B.140. Multimodel mean difference in monthly SWE between the current and future periods during October.

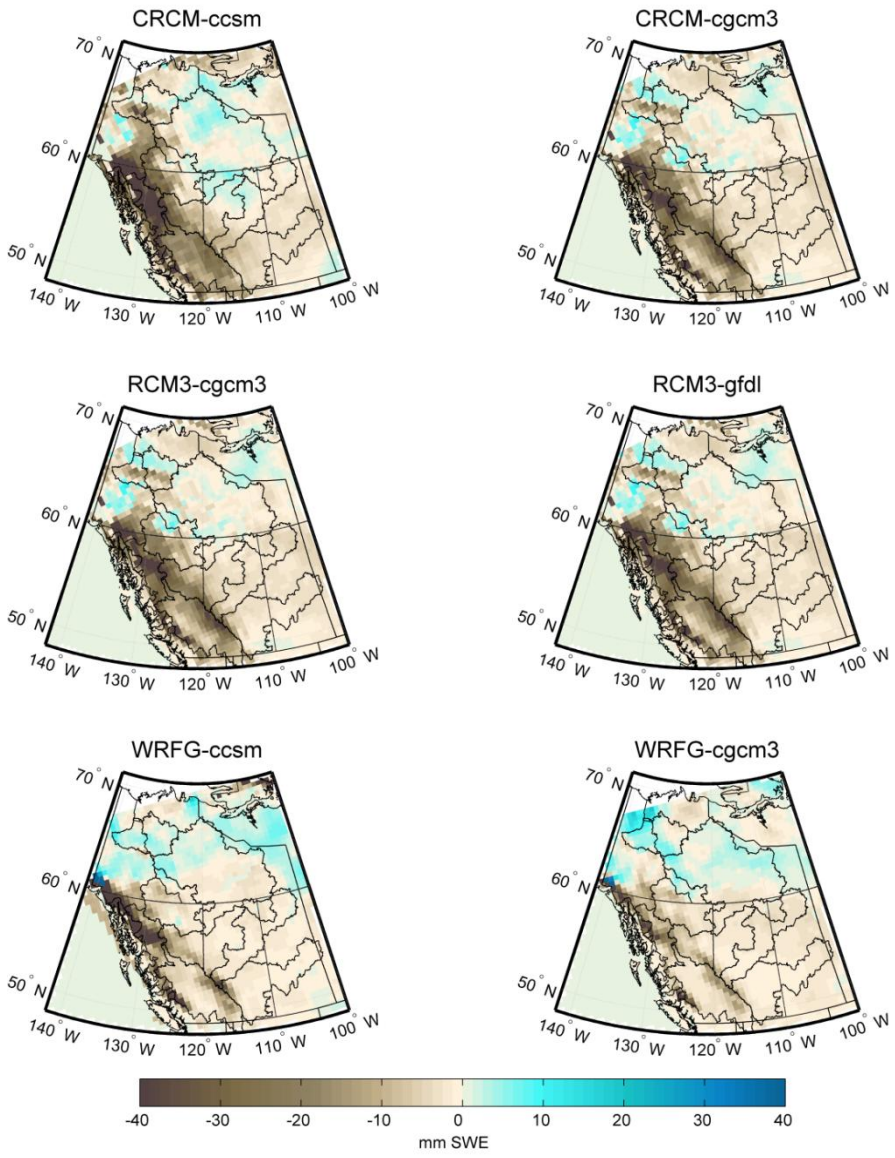

Figure B.141. Difference in SWE between 1971-2000 and 2041-2070 during October.

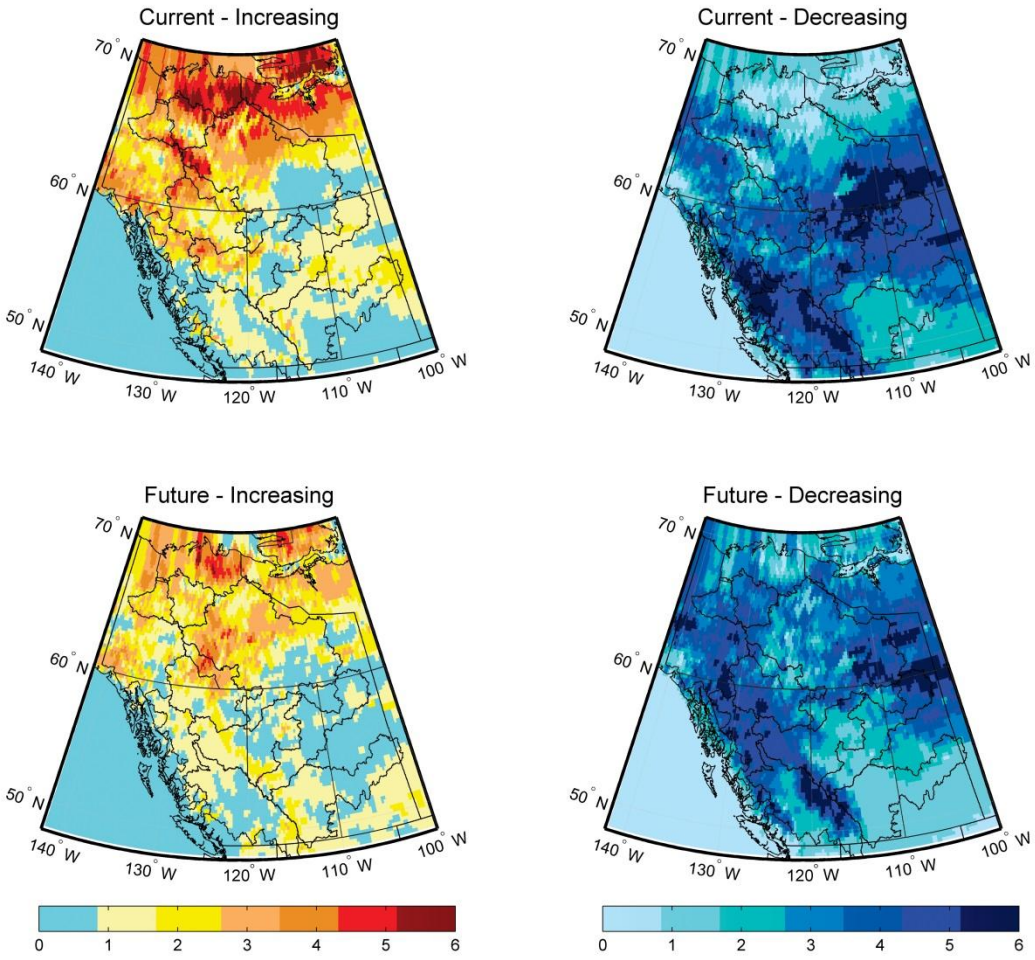

Figure B.142. Number of models showing increasing or decreasing rates of change in SWE during the current (1971-2000) and future (2041-2070) time periods during October.

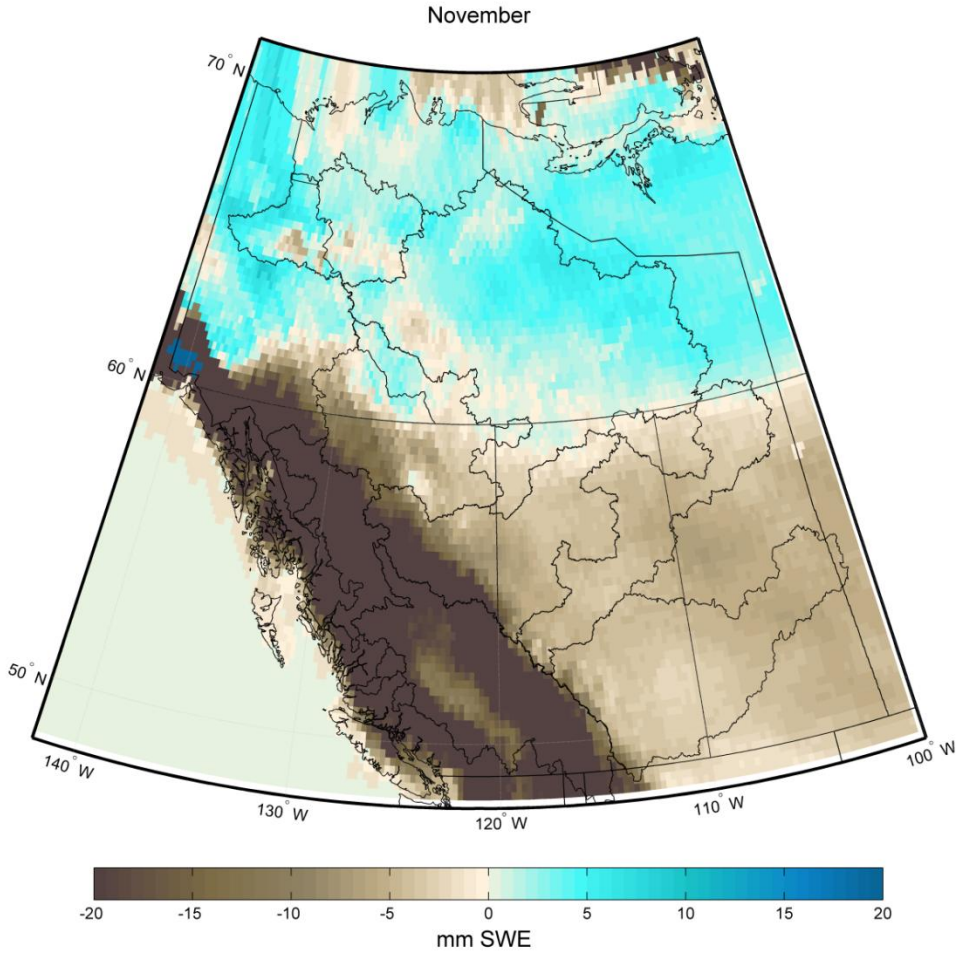

Figure B.143. Multimodel mean difference in monthly SWE between the current and future periods during November.

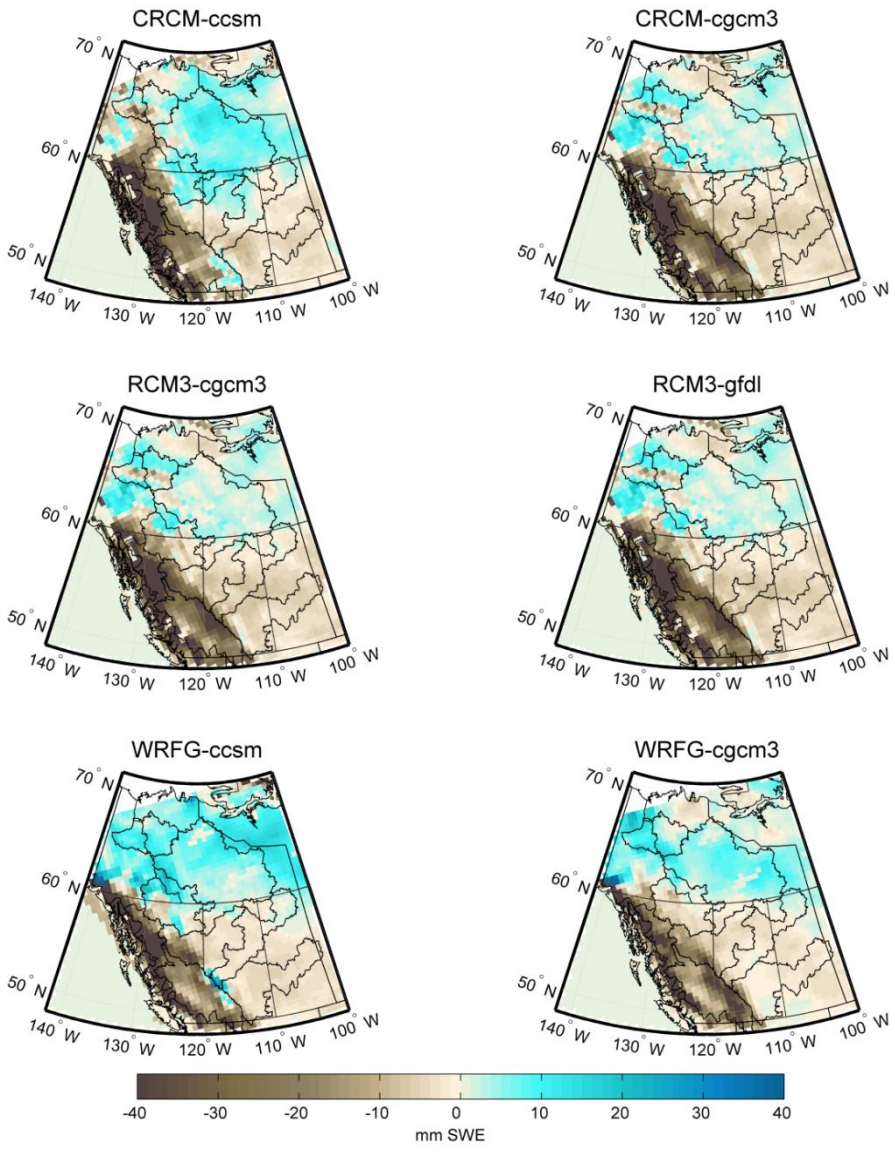

Figure B.144. Difference in SWE between 1971-2000 and 2041-2070 during November.

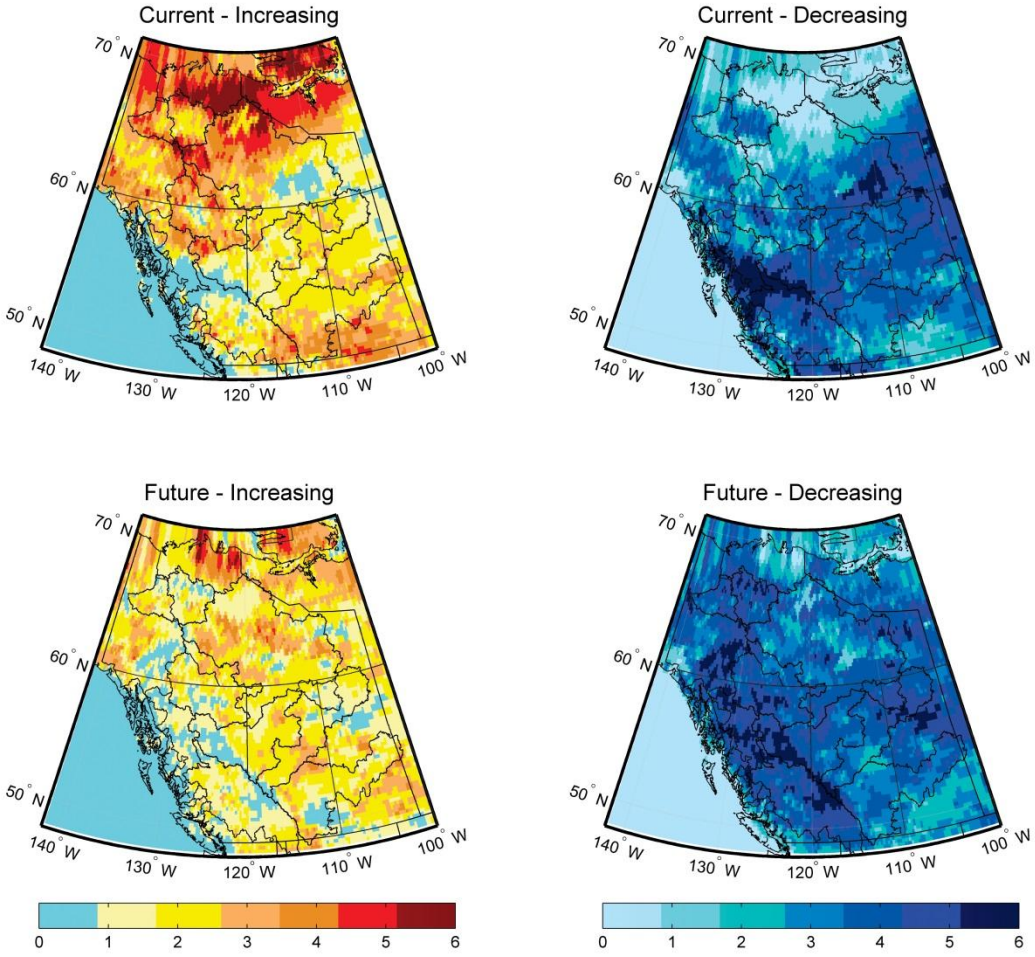

Figure B.145. Number of models showing increasing or decreasing rates of change in SWE during the current (1971-2000) and future (2041-2070) time periods during November.

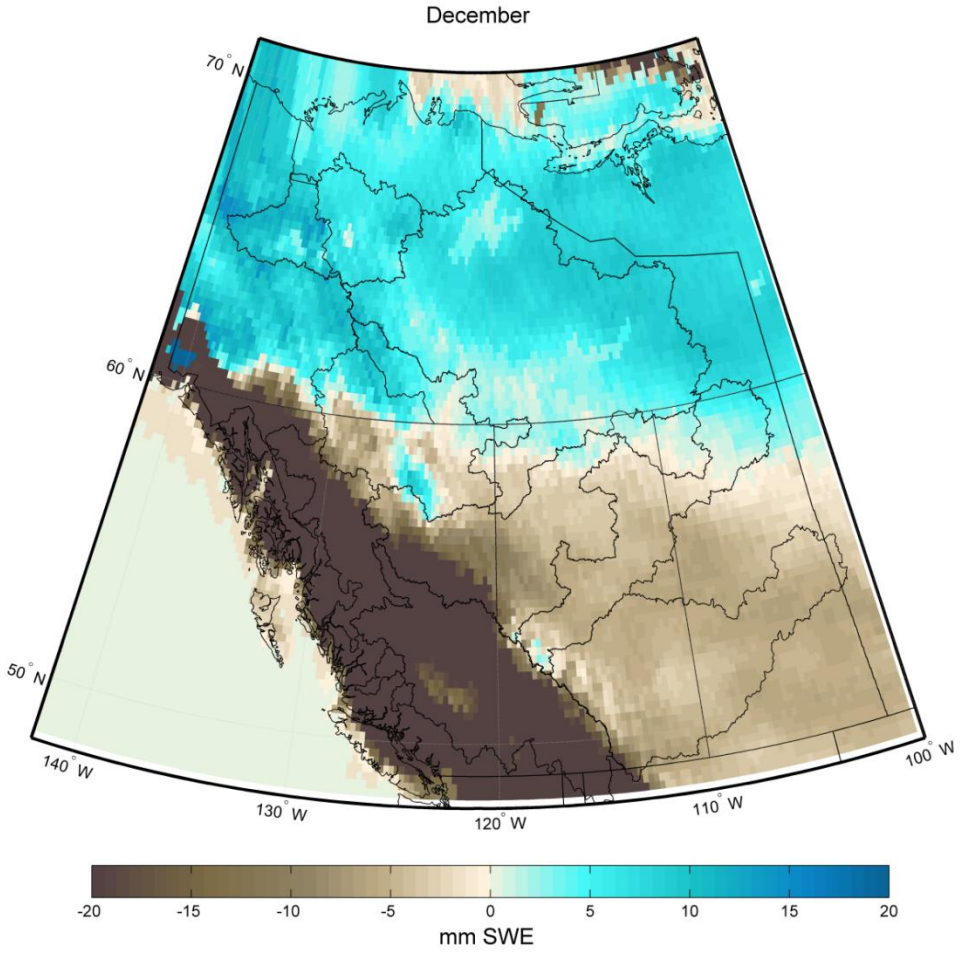

Figure B.146. Multimodel mean difference in monthly SWE between the current and future periods during December.

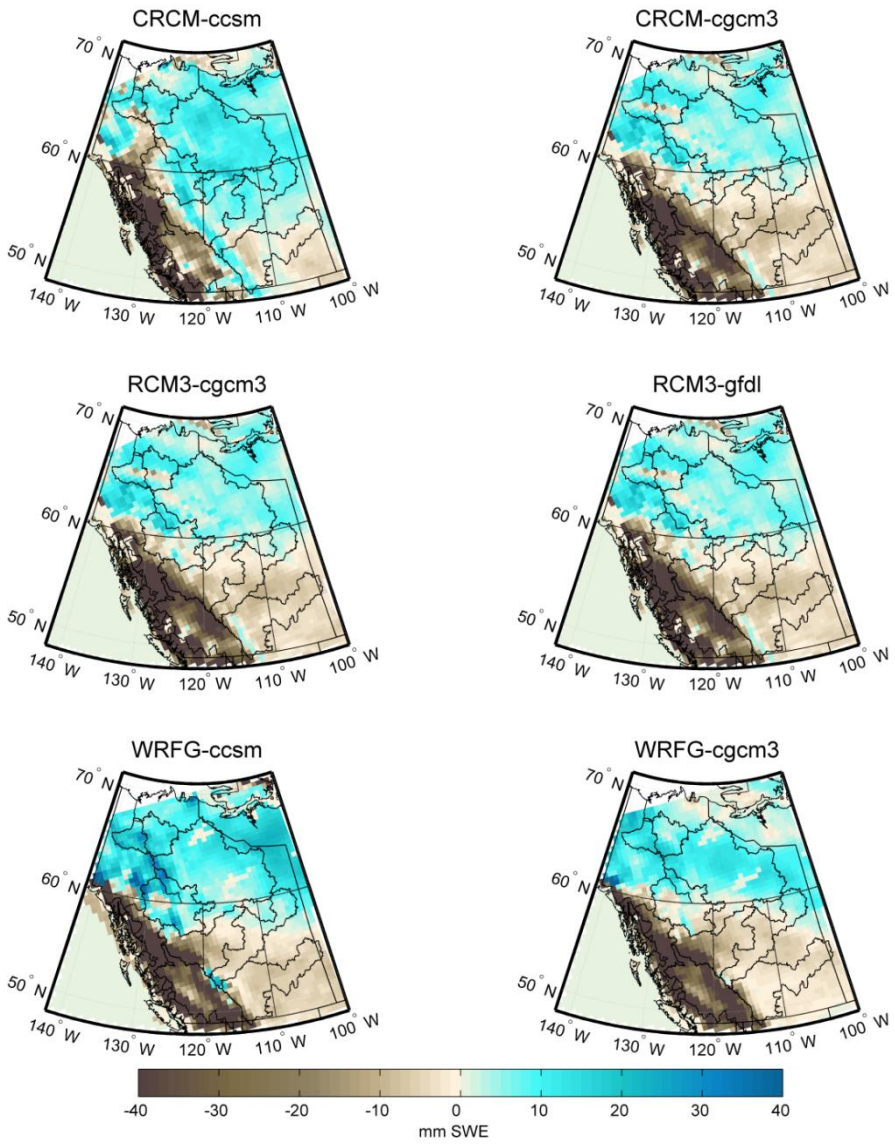

Figure B.147. Difference in SWE between 1971-2000 and 2041-2070 during December.

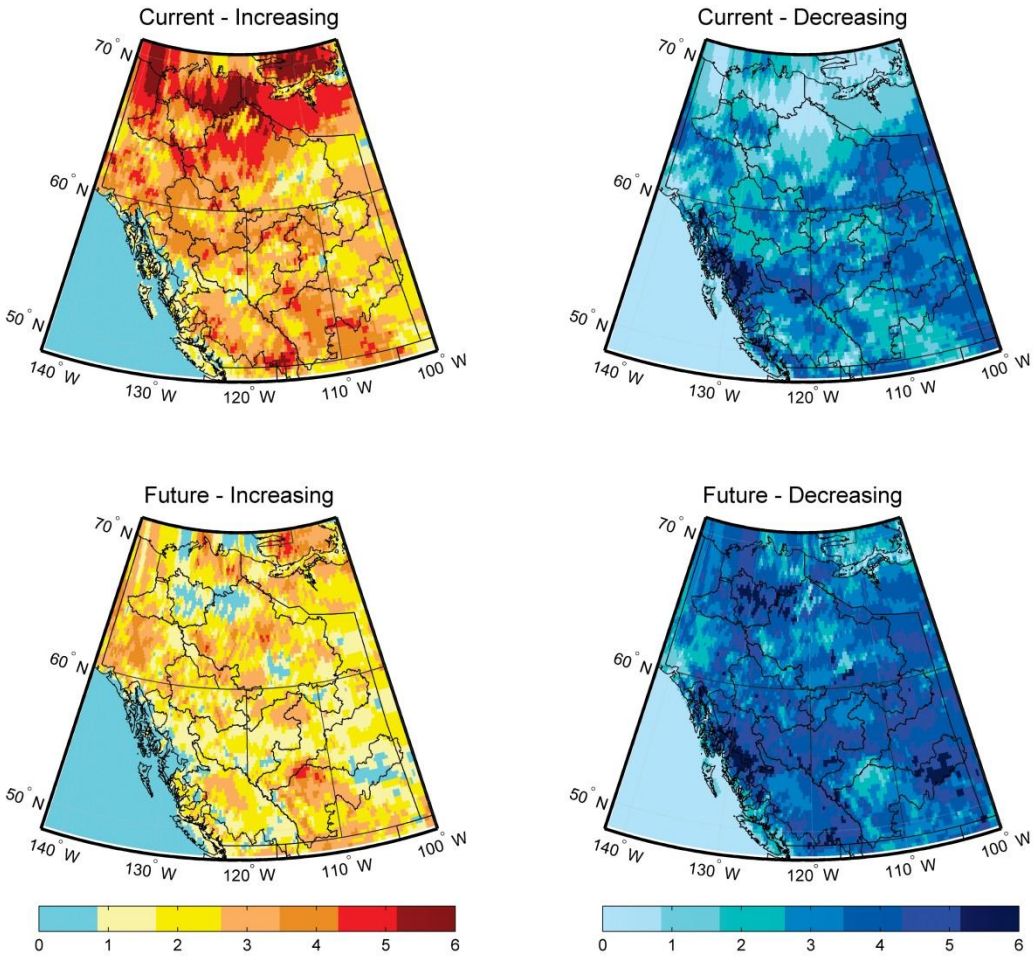

Figure B.148. Number of models showing increasing or decreasing rates of change in SWE during the current (1971-2000) and future (2041-2070) time periods during December.

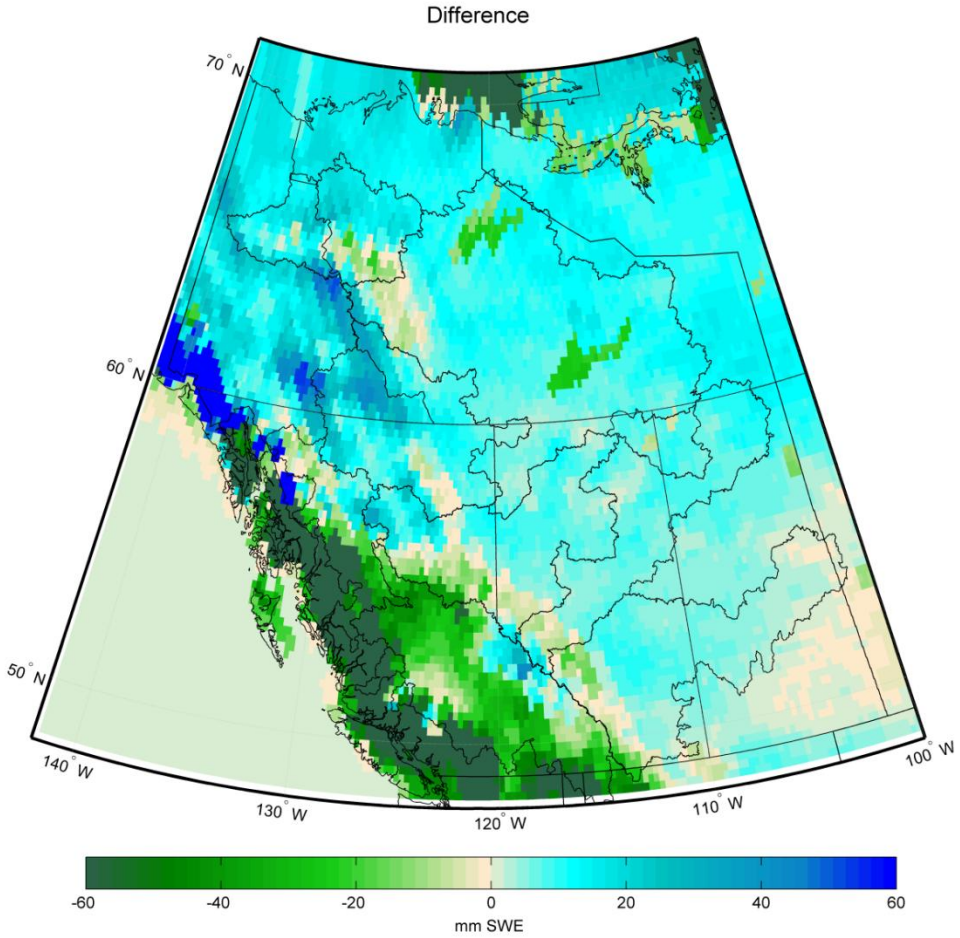

Figure B.149. Multimodel mean difference in annual snowmelt between the current and future periods.

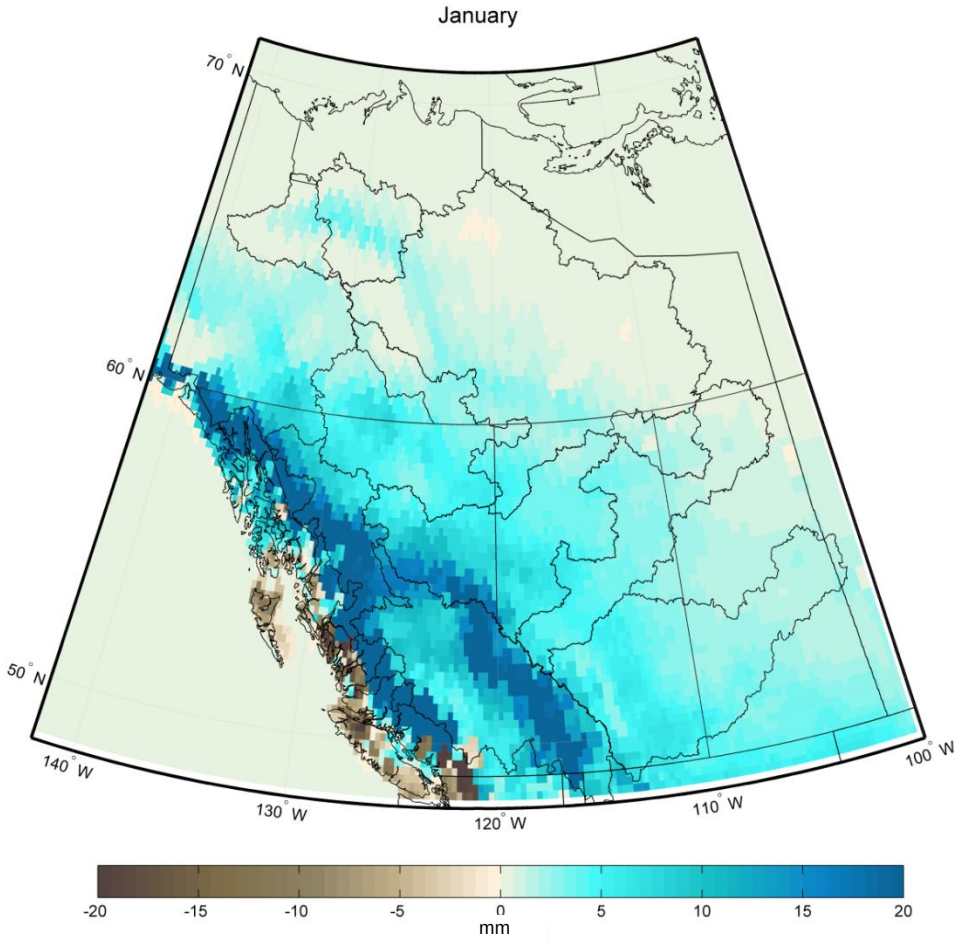

Figure B.150. Multimodel mean difference in monthly snowmelt between the current and future periods during January.

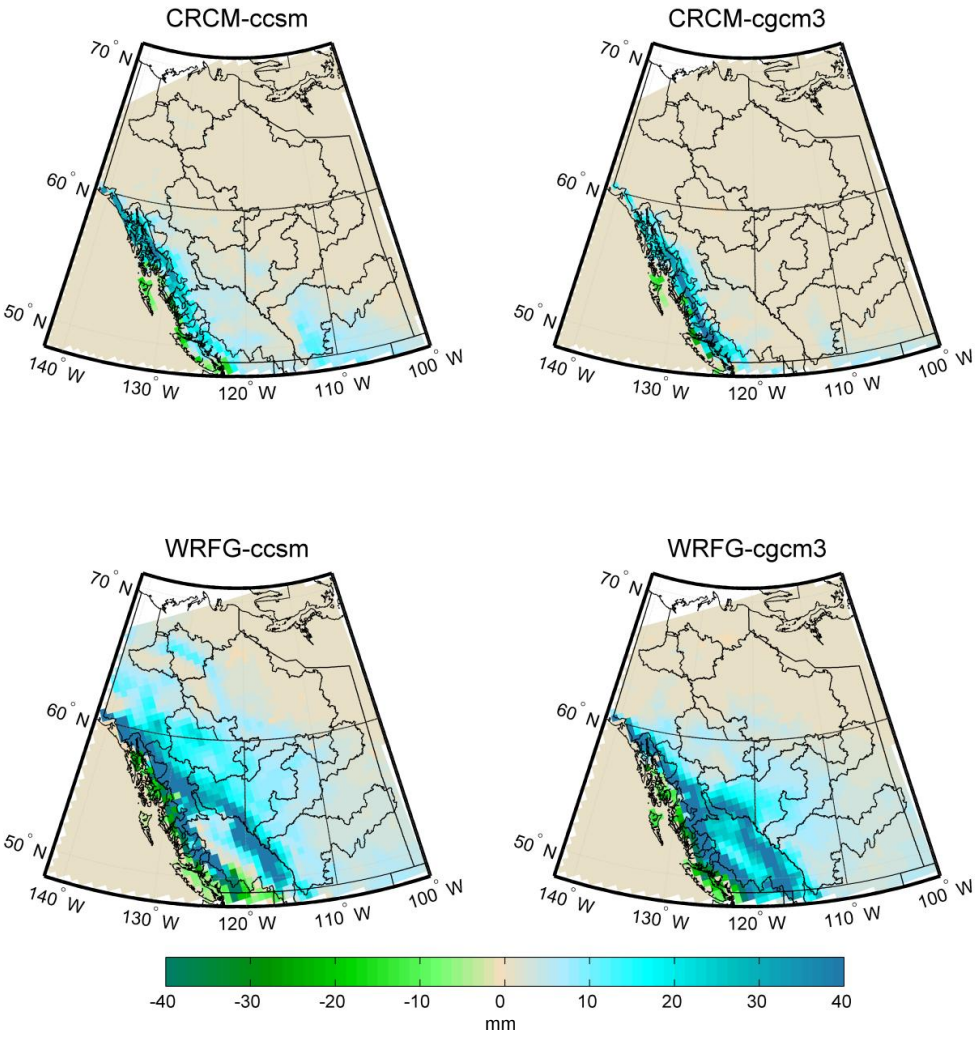

Figure B.151. Difference in snowmelt totals between 1971-2000 and 2041-2070 during January.

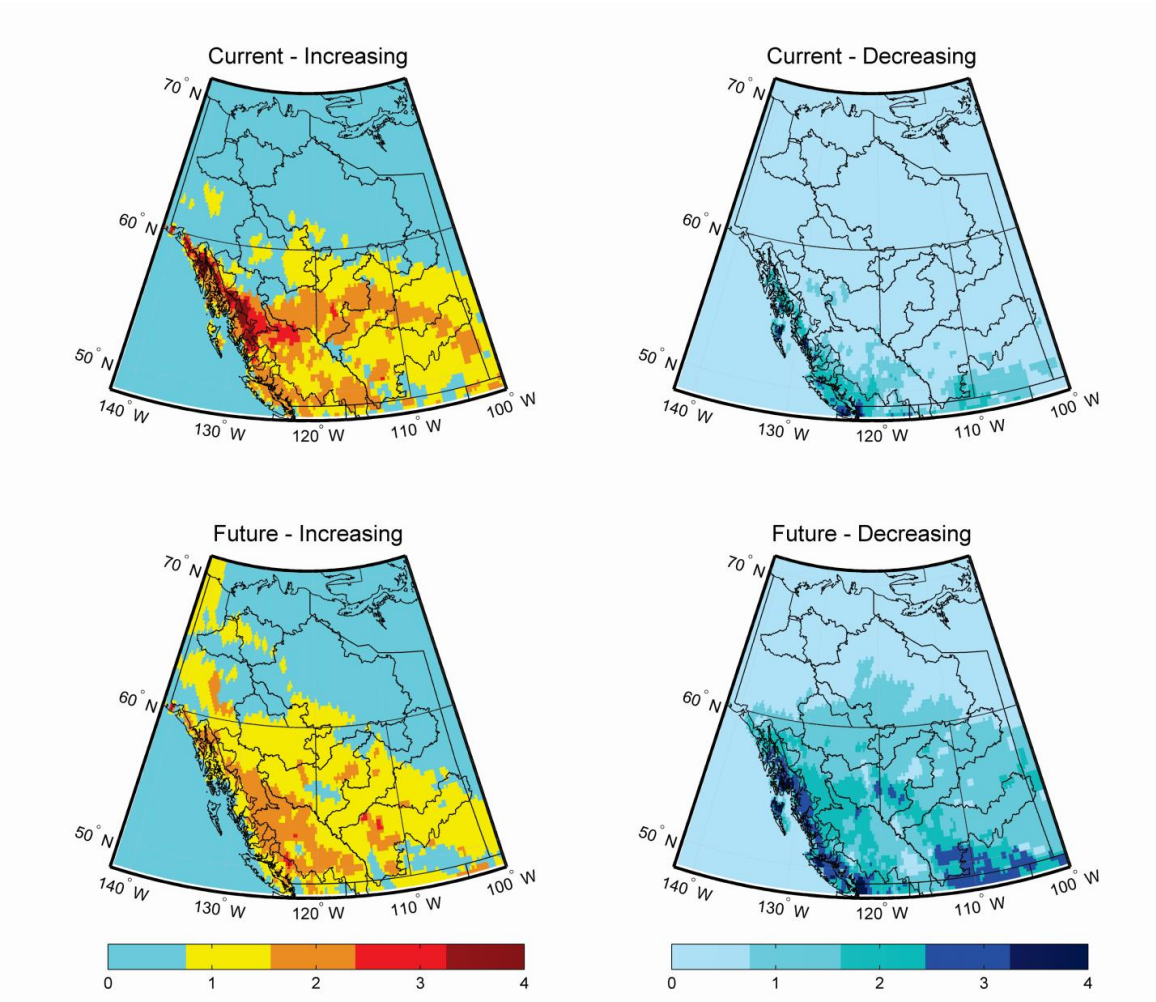

Figure B.152. Number of models showing increasing or decreasing rates of change in snowmelt during the current (1971-2000) and future (2041-2070) time periods during January.

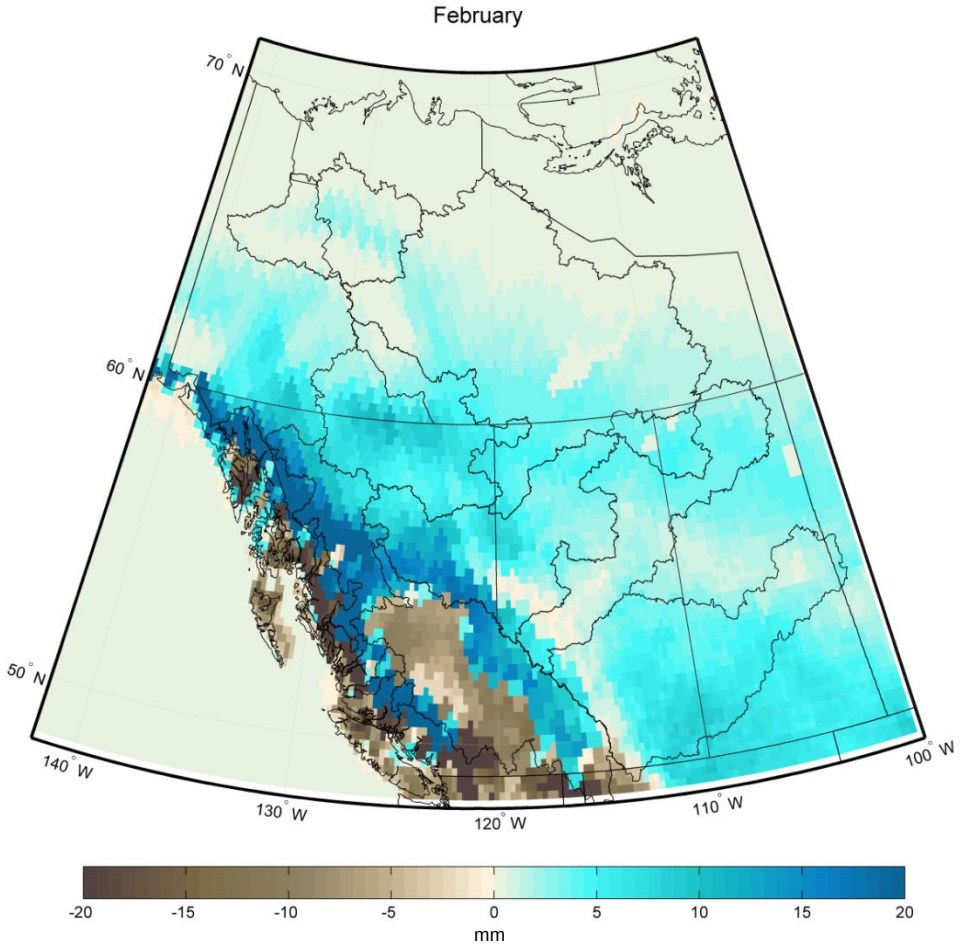

Figure B.153. Multimodel mean difference in monthly snowmelt between the current and future periods during February.

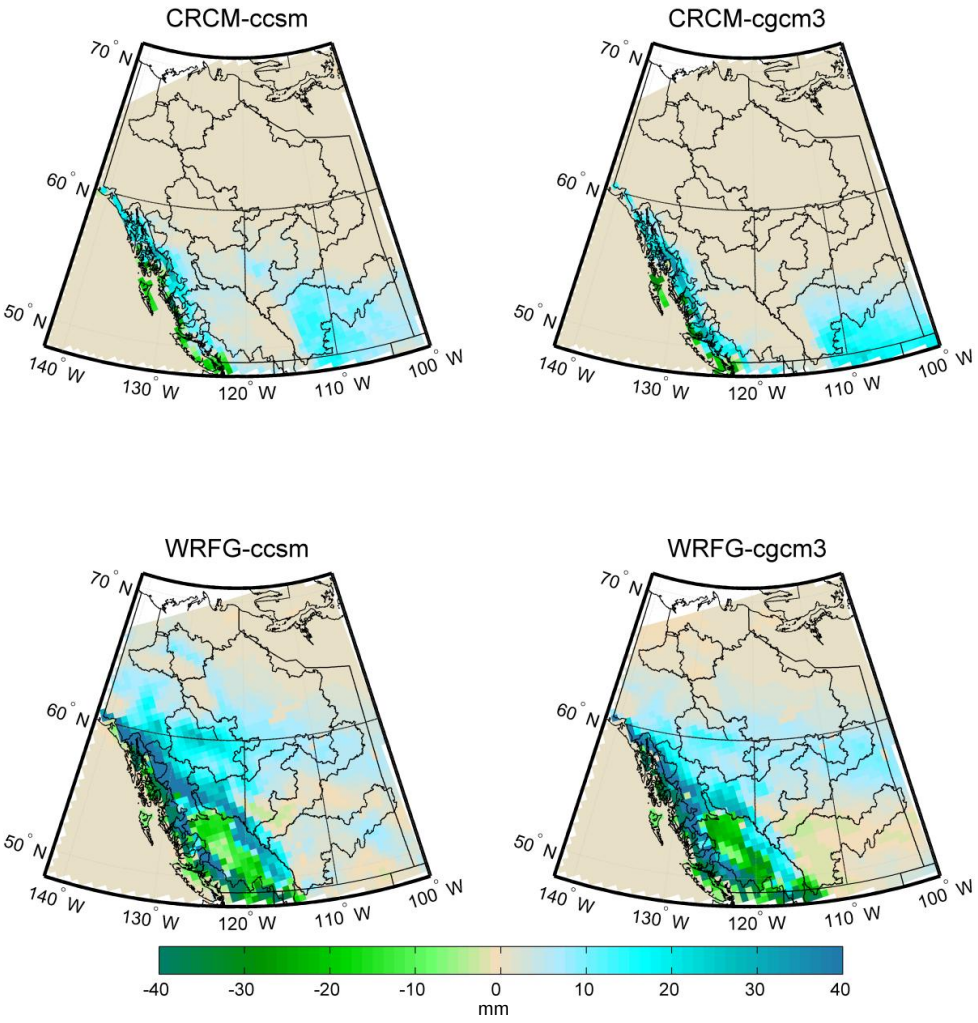

Figure B.154. Difference in snowmelt totals between 1971-2000 and 2041-2070 during February.

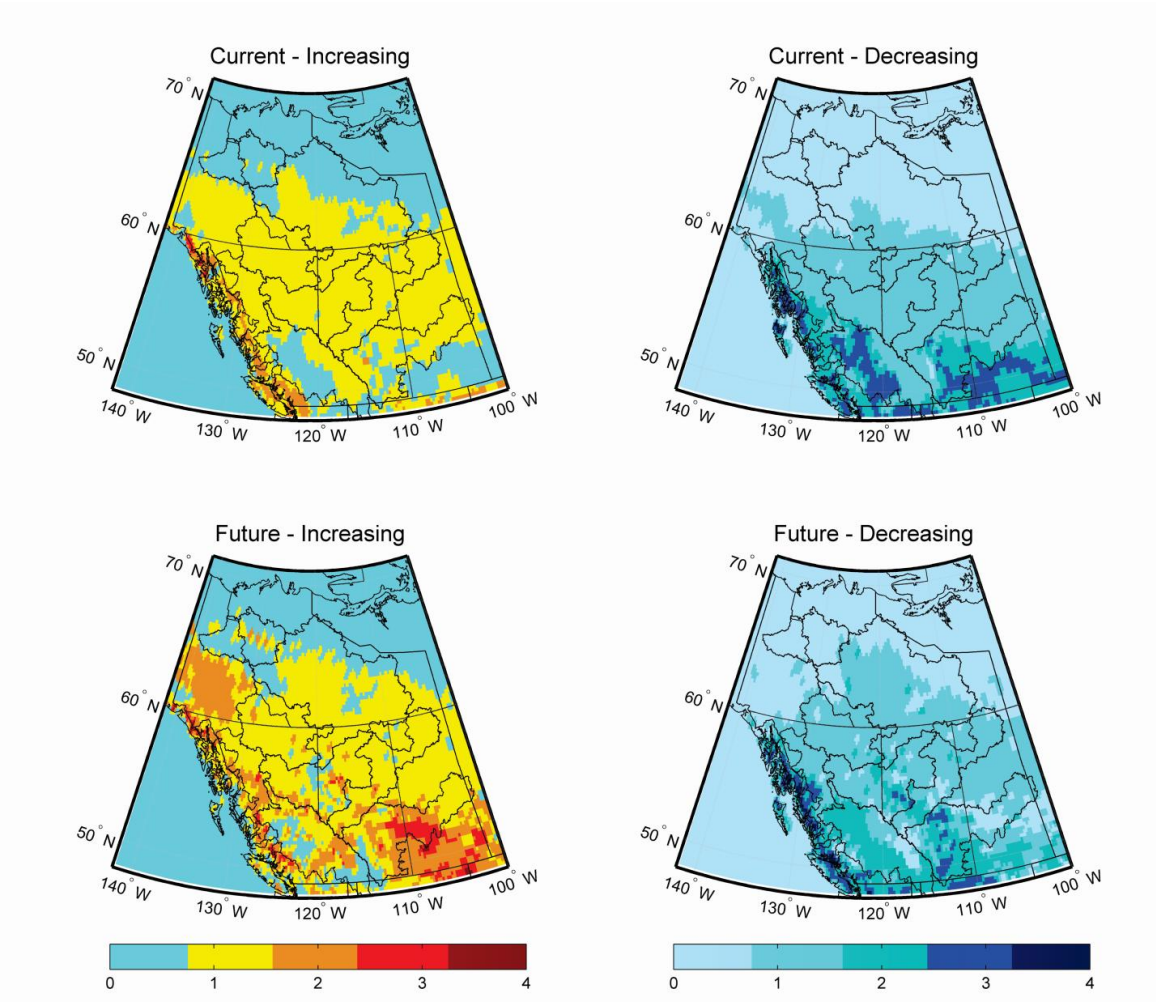

Figure B.155. Number of models showing increasing or decreasing rates of change in snowmelt during the current (1971-2000) and future (2041-2070) time periods during February.

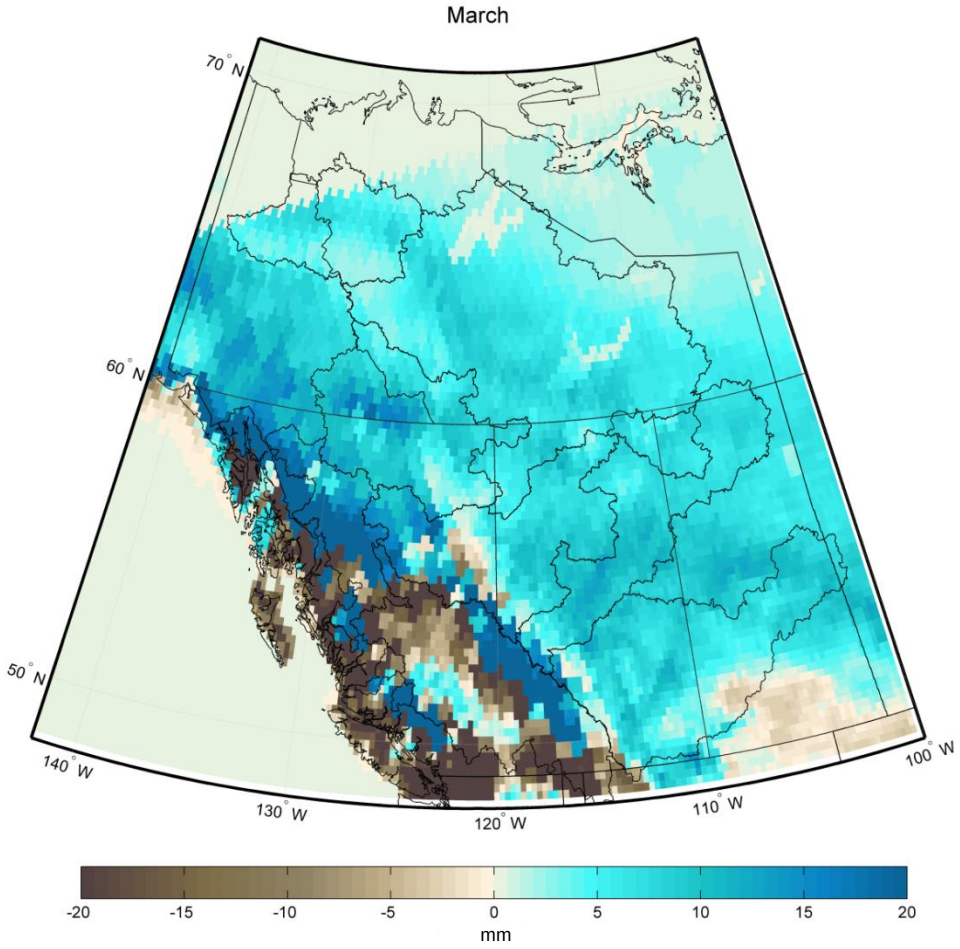

Figure B.156. Multimodel mean difference in monthly snowmelt between the current and future periods during March.

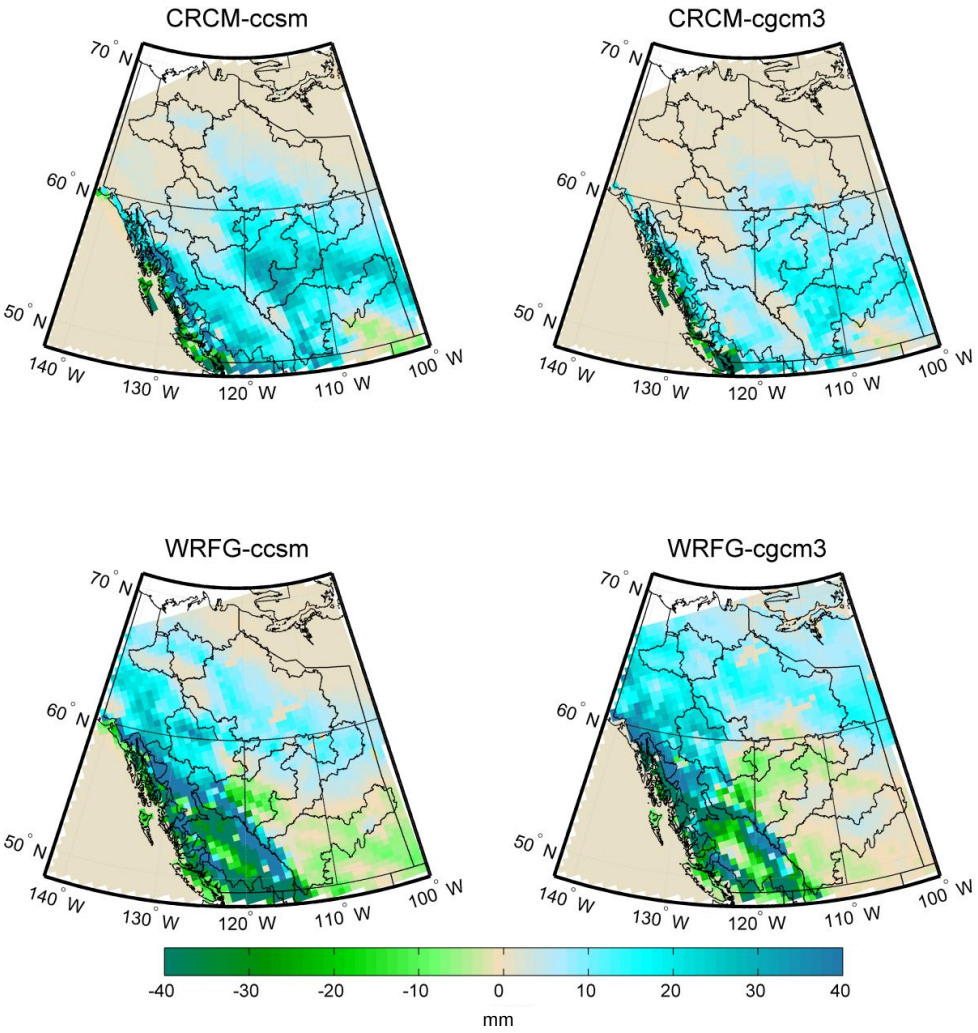

Figure B.157. Difference in snowmelt totals between 1971-2000 and 2041-2070 during March.

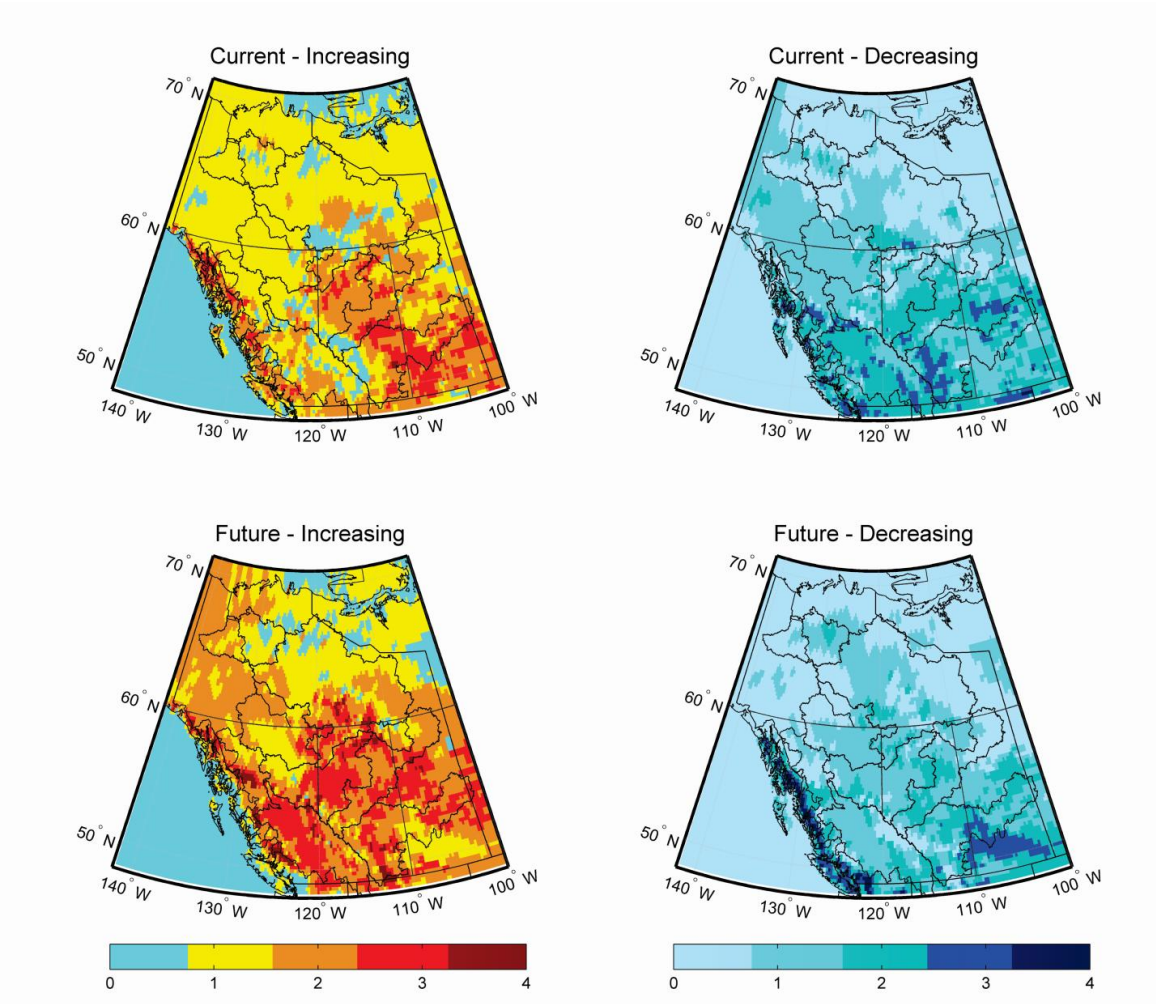

Figure B.158. Number of models showing increasing or decreasing rates of change in snowmelt during the current (1971-2000) and future (2041-2070) time periods during March.

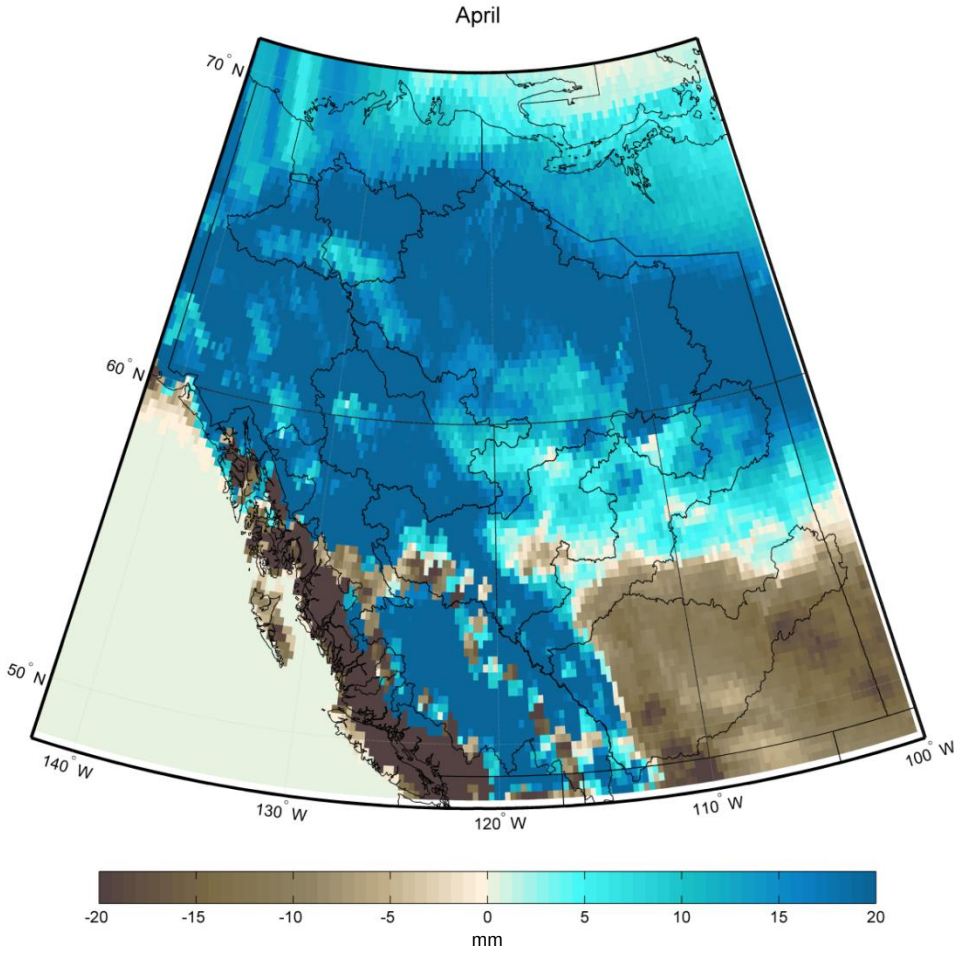

Figure B.159. Multimodel mean difference in monthly snowmelt between the current and future periods during April.

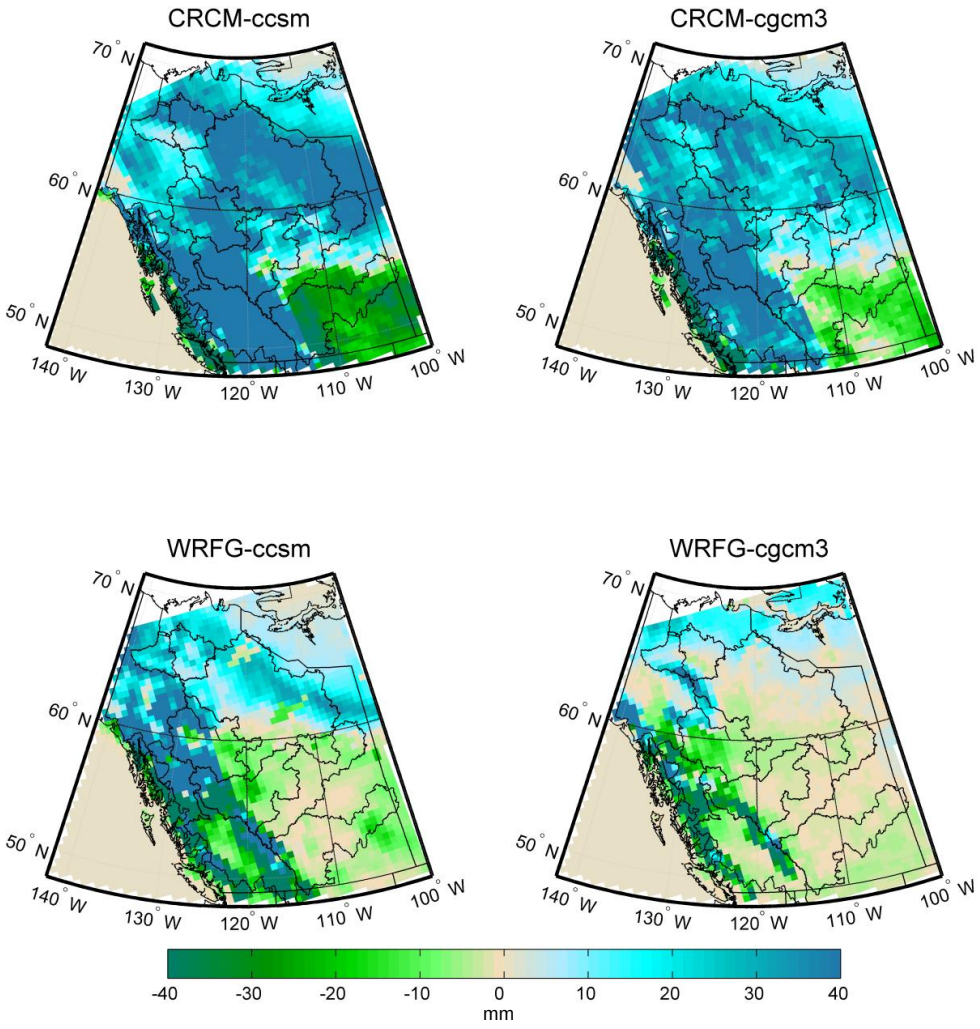

Figure B.160. Difference in snowmelt totals between 1971-2000 and 2041-2070 during April.

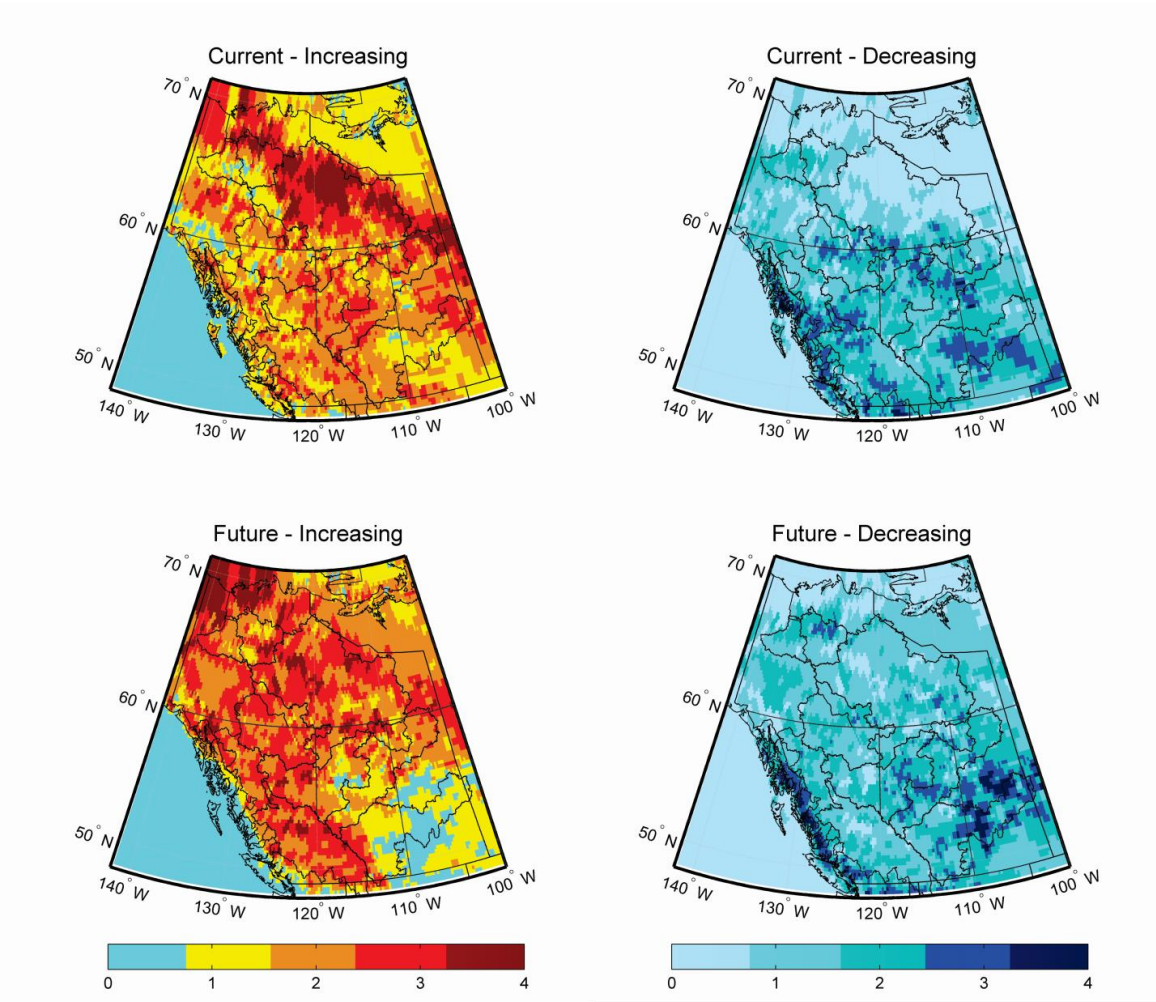

Figure B.161. Number of models showing increasing or decreasing rates of change in snowmelt during the current (1971-2000) and future (2041-2070) time periods during April.

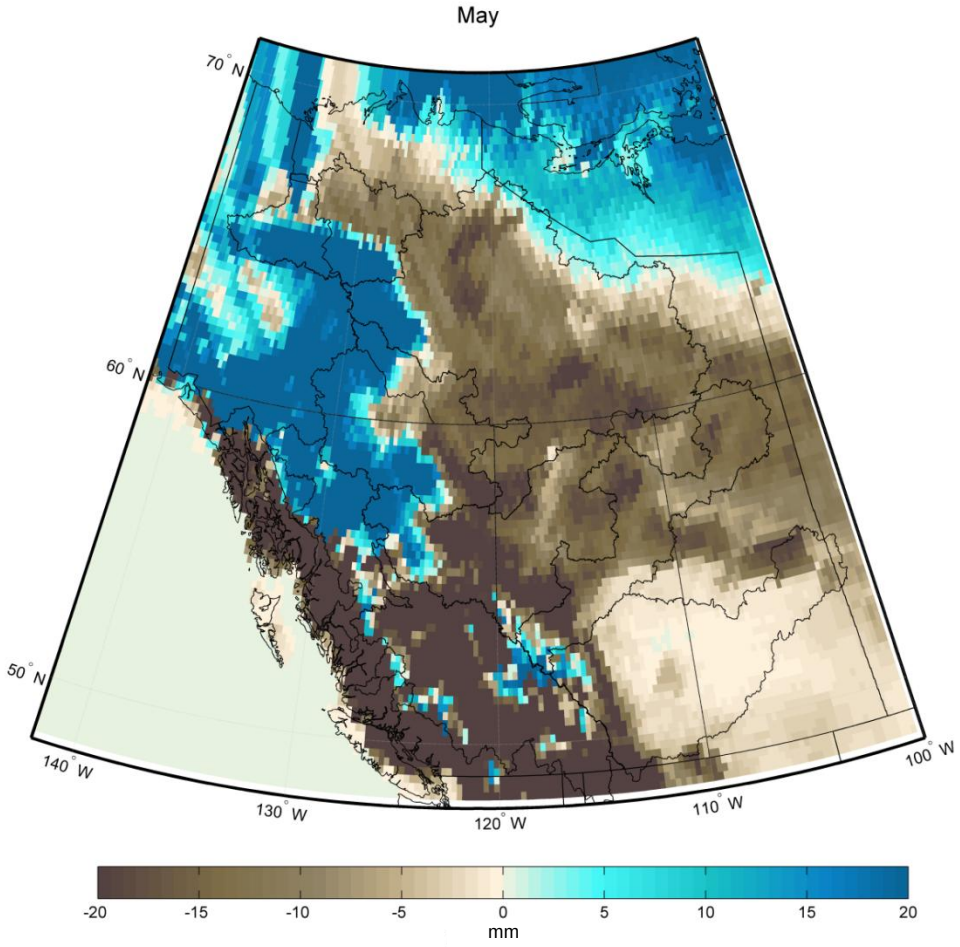

Figure B.162. Multimodel mean difference in monthly snowmelt between the current and future periods during May.

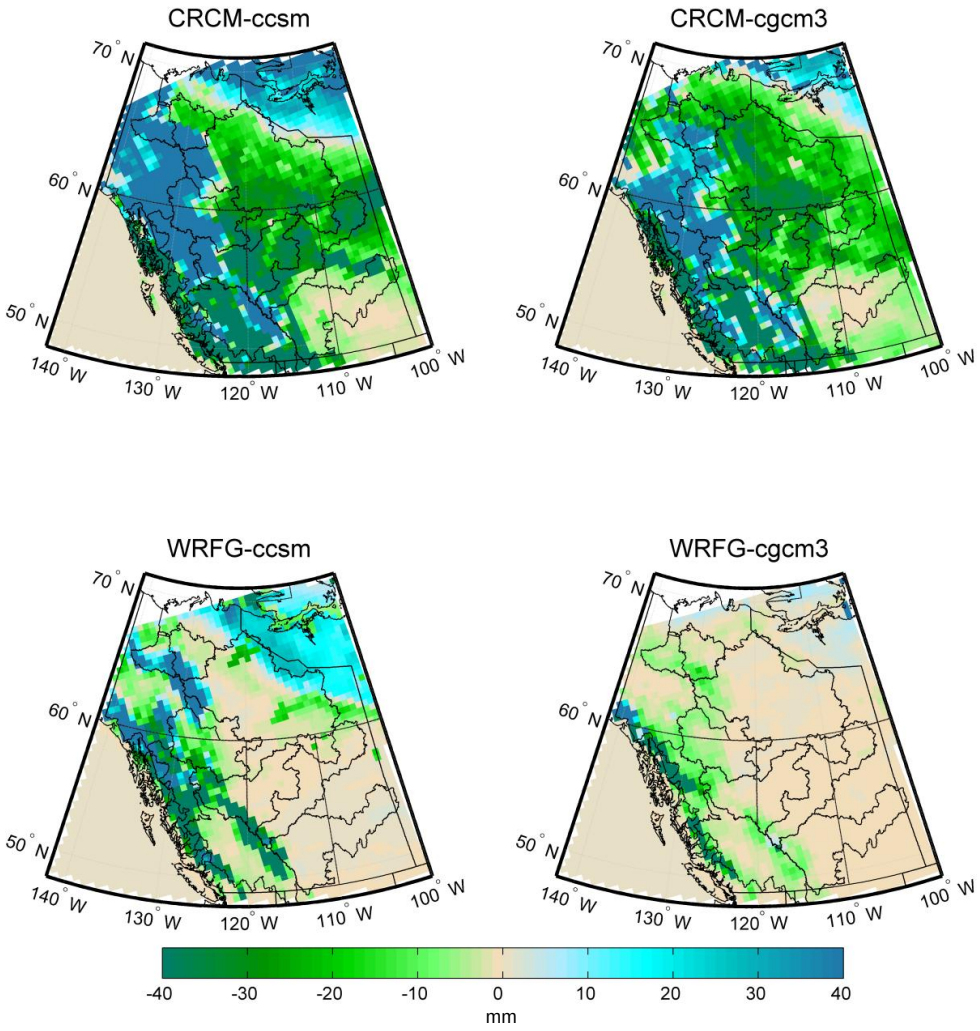

Figure B.163. Difference in snowmelt totals between 1971-2000 and 2041-2070 during May.

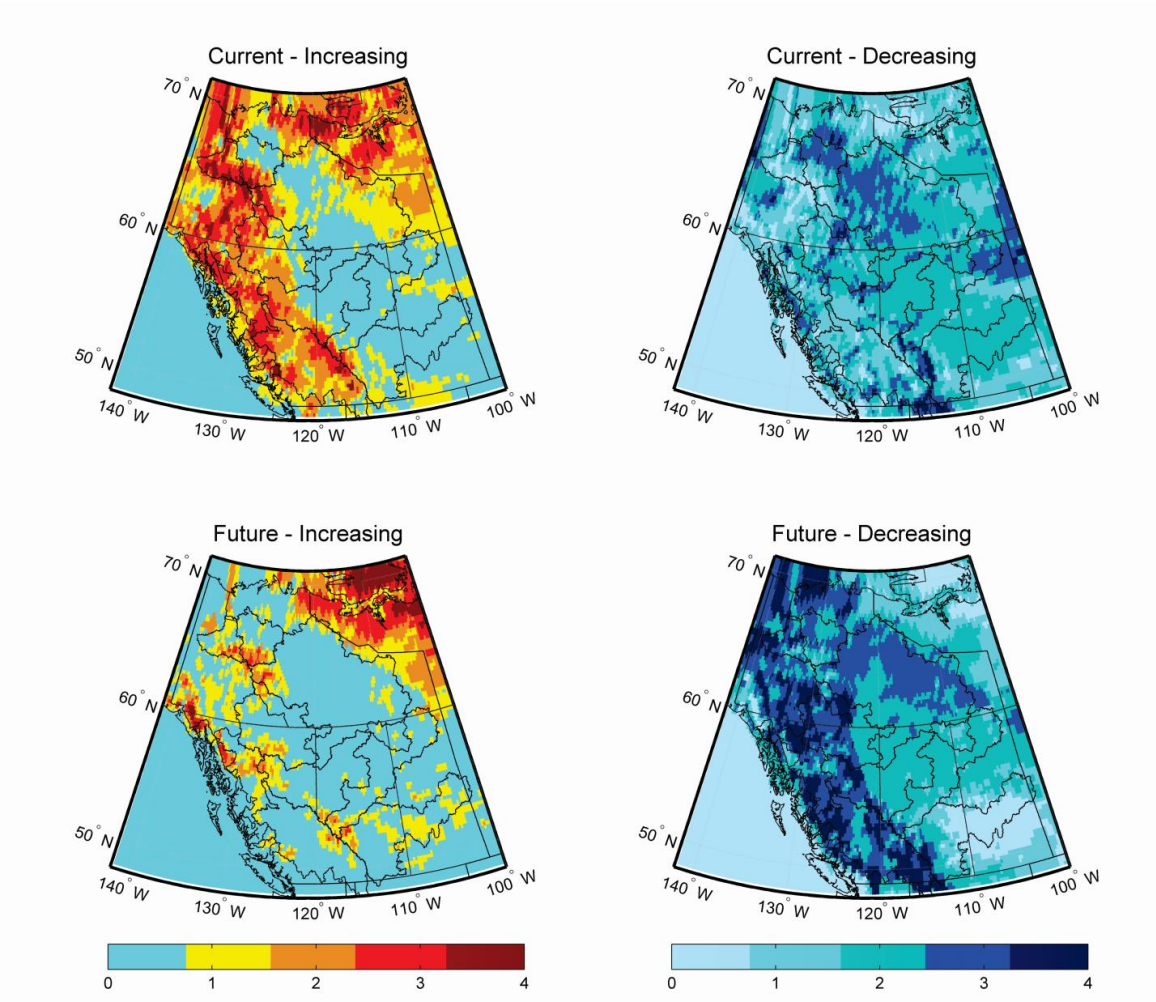

Figure B.164. Number of models showing increasing or decreasing rates of change in snowmelt during the current (1971-2000) and future (2041-2070) time periods during May.

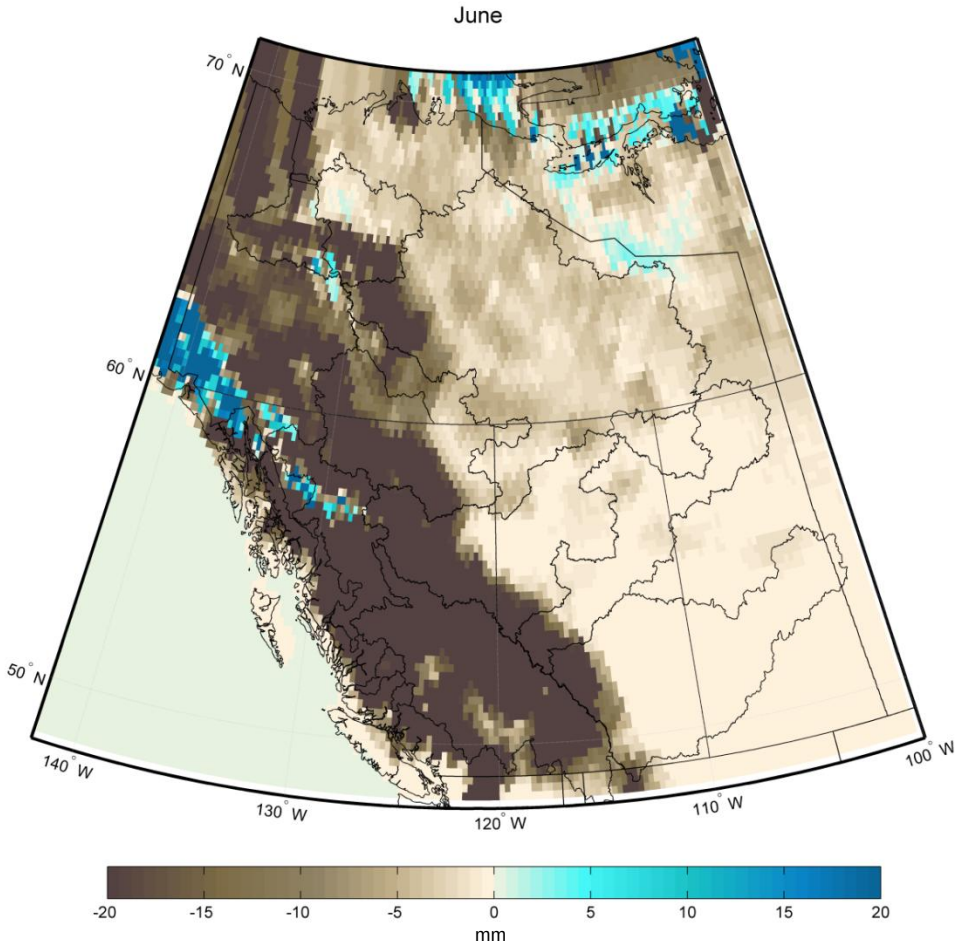

Figure B.165. Multimodel mean difference in monthly snowmelt between the current and future periods during June.

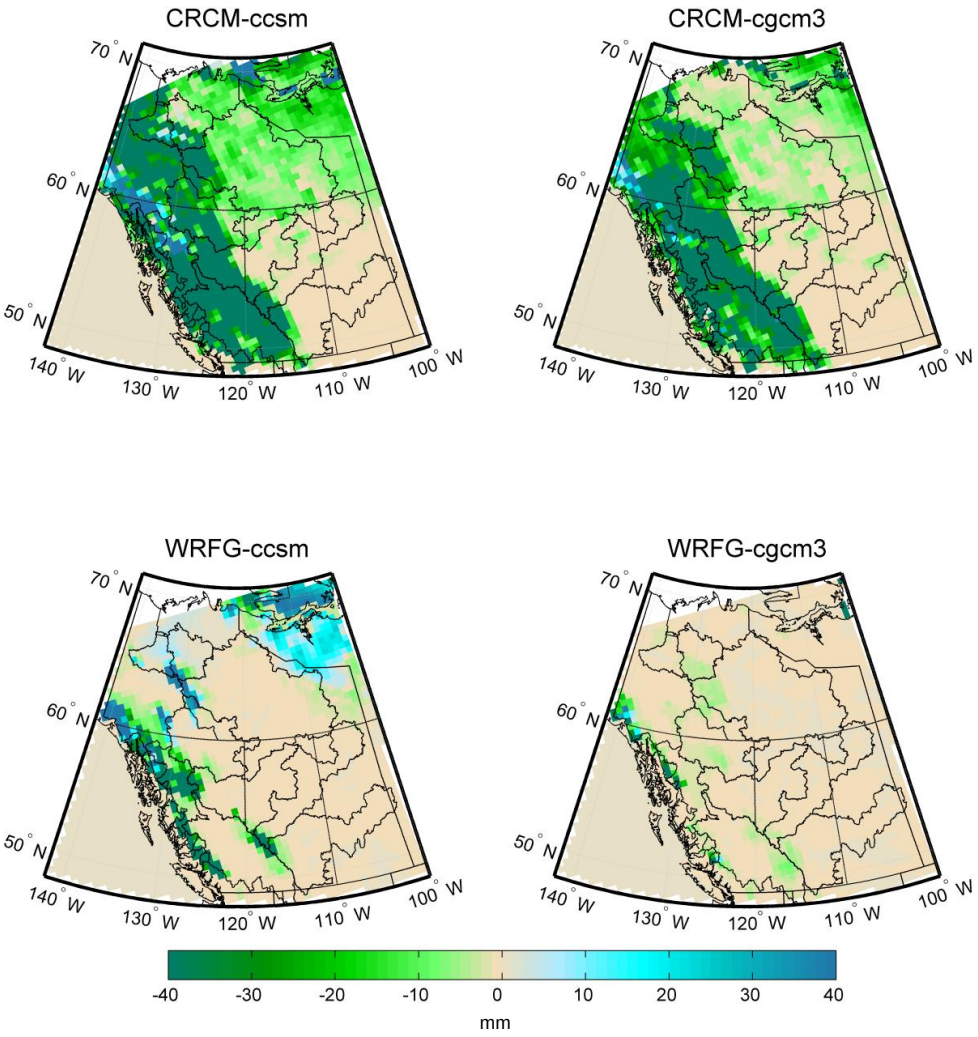

Figure B.166. Difference in snowmelt totals between 1971-2000 and 2041-2070 during June.

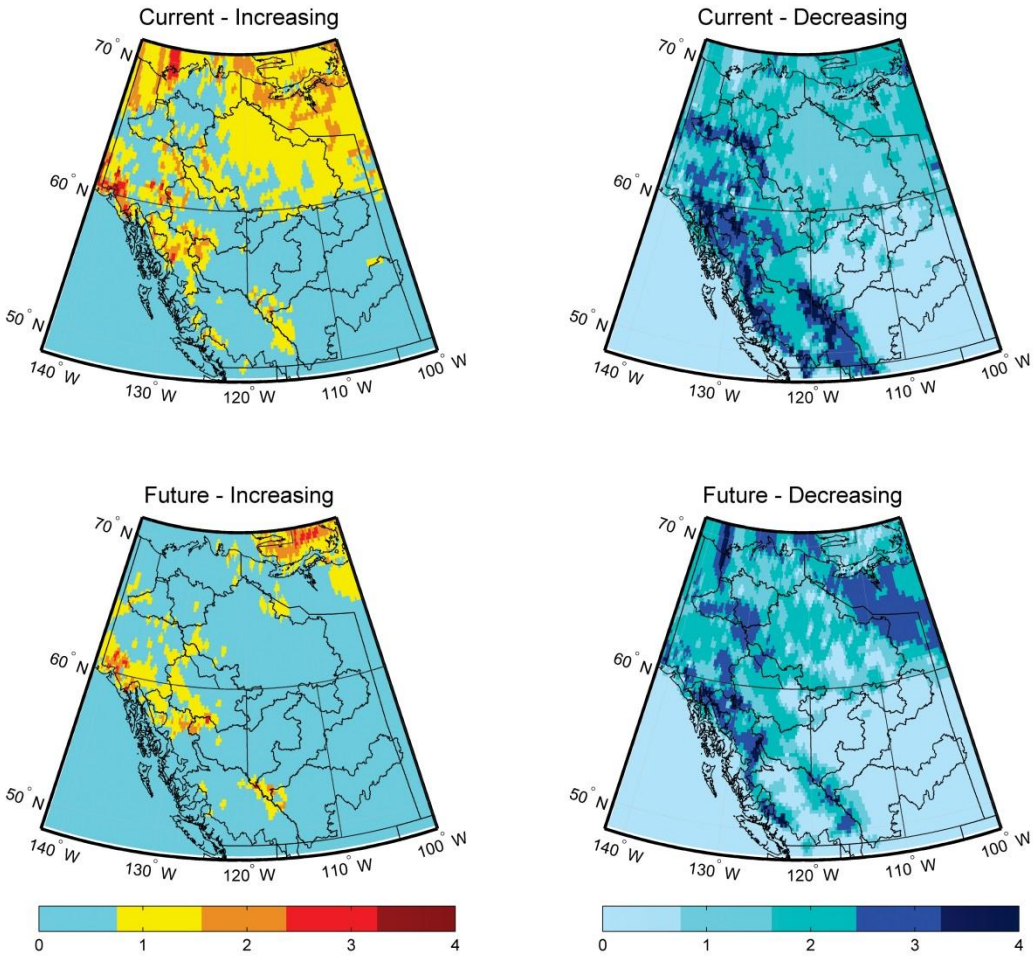

Figure B.167. Number of models showing increasing or decreasing rates of change in snowmelt during the current (1971-2000) and future (2041-2070) time periods during June.

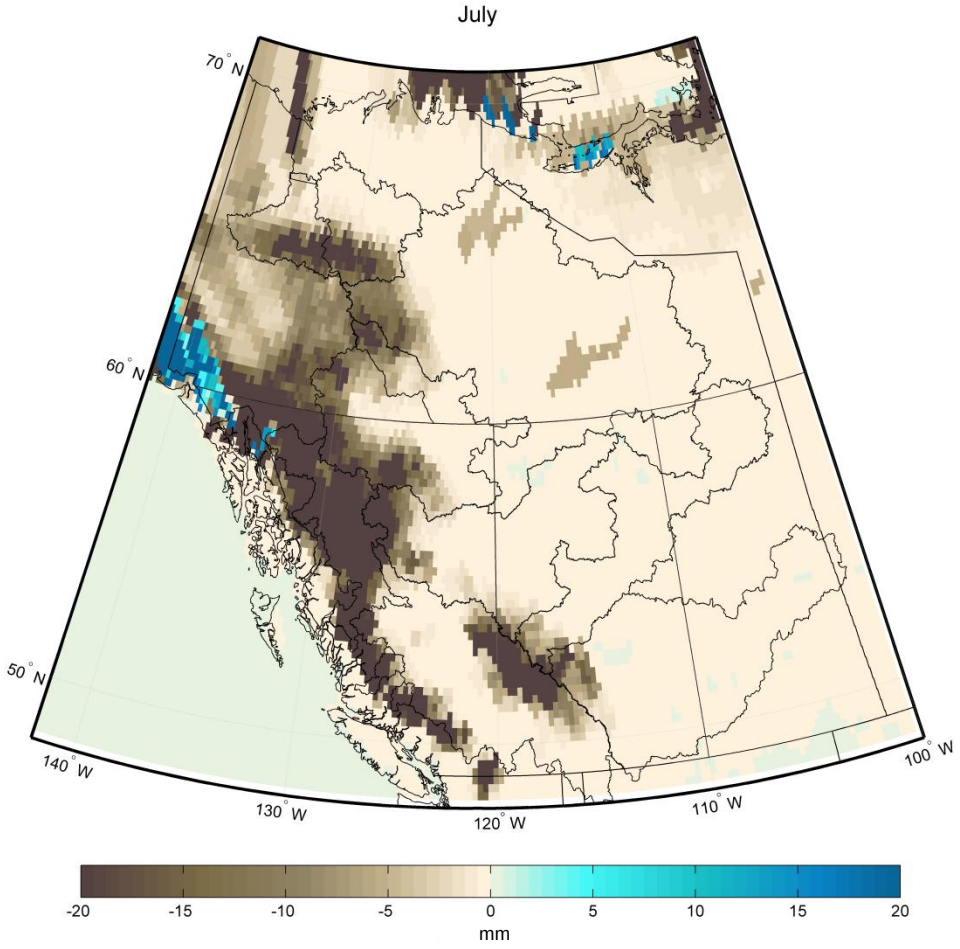

Figure B.168. Multimodel mean difference in monthly snowmelt between the current and future periods during July.

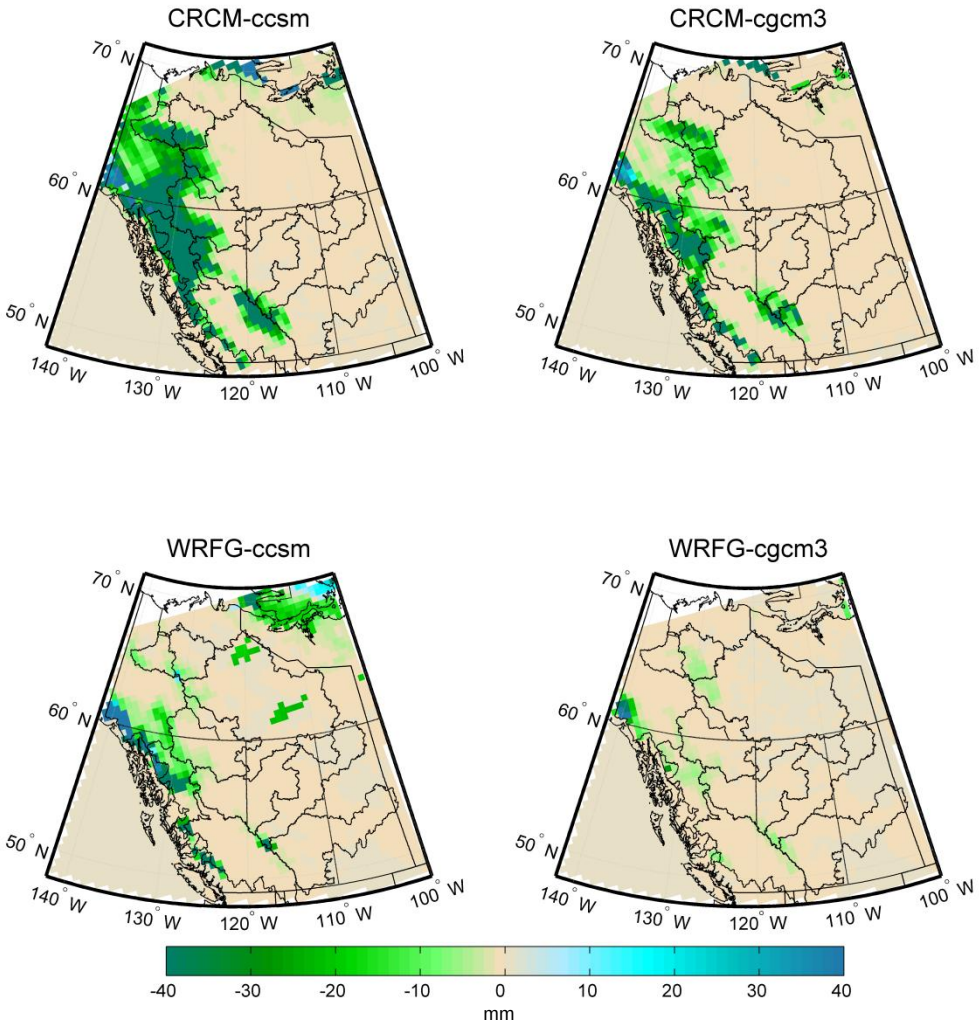

Figure B.169. Difference in snowmelt totals between 1971-2000 and 2041-2070 during July.

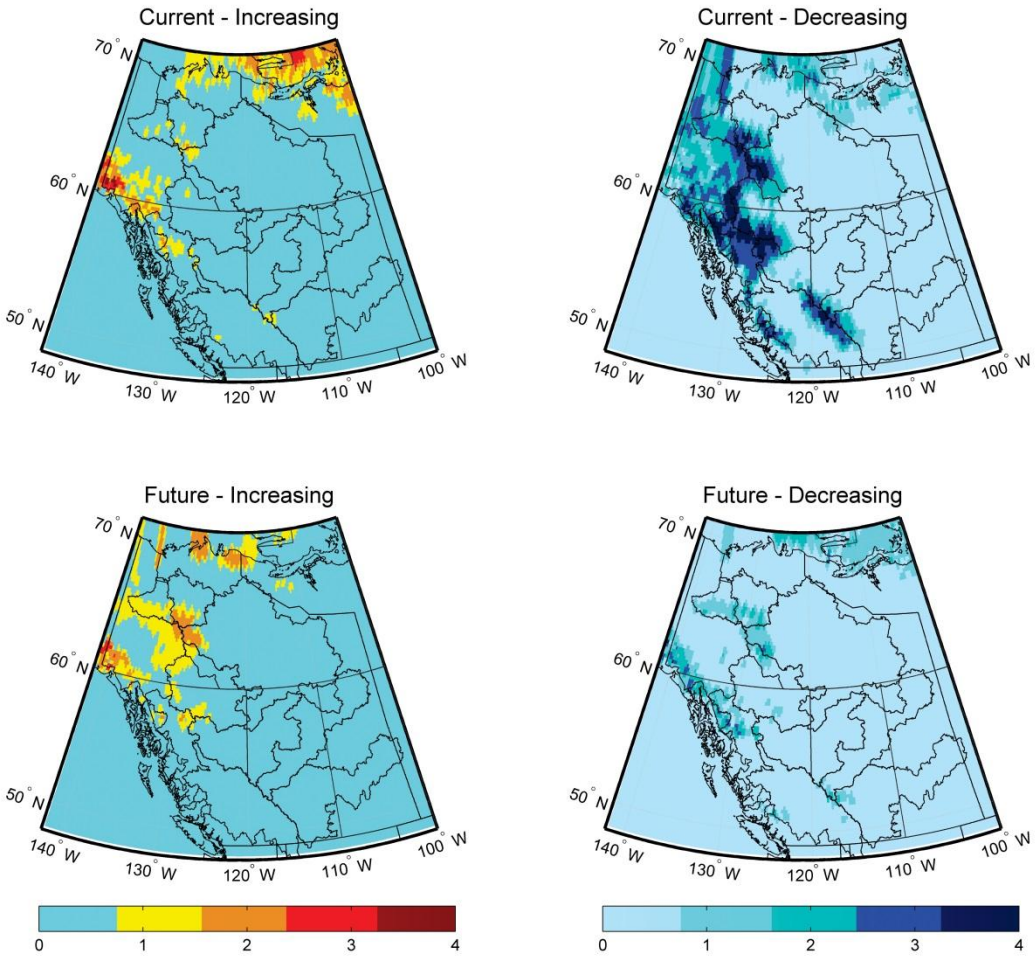

Figure B.170. Number of models showing increasing or decreasing rates of change in snowmelt during the current (1971-2000) and future (2041-2070) time periods during July.

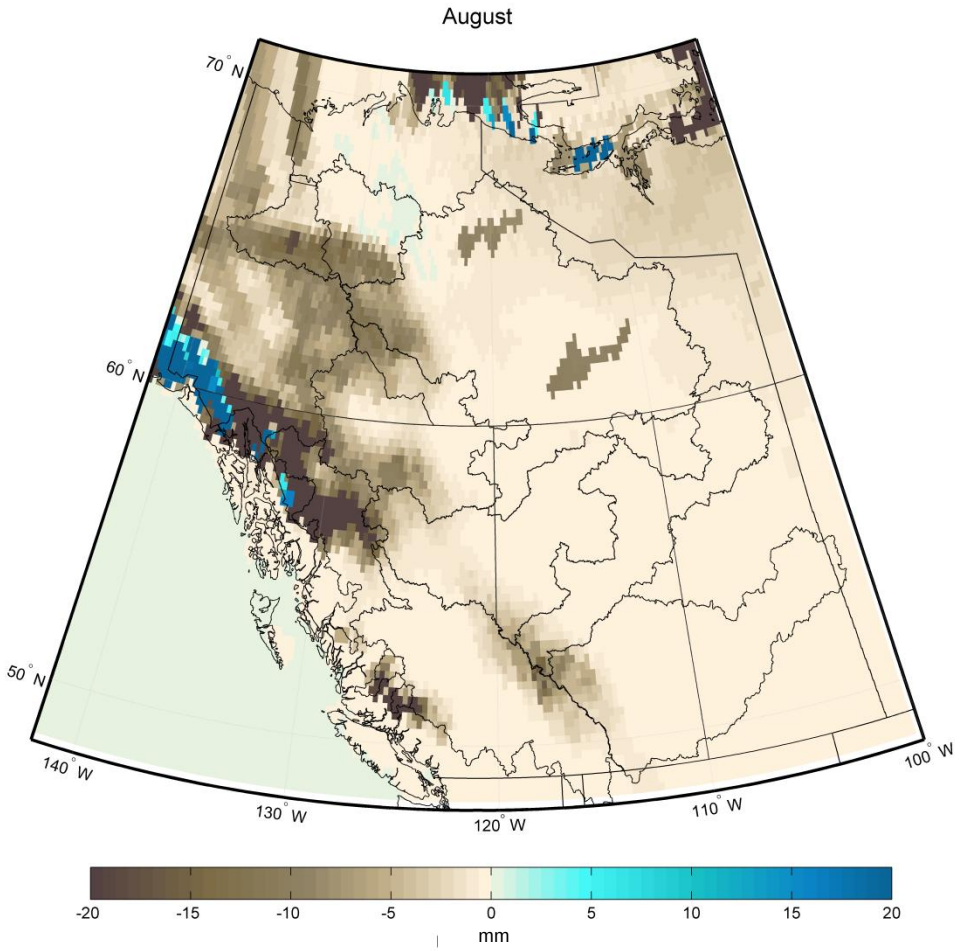

Figure B.171. Multimodel mean difference in monthly snowmelt between the current and future periods during August.

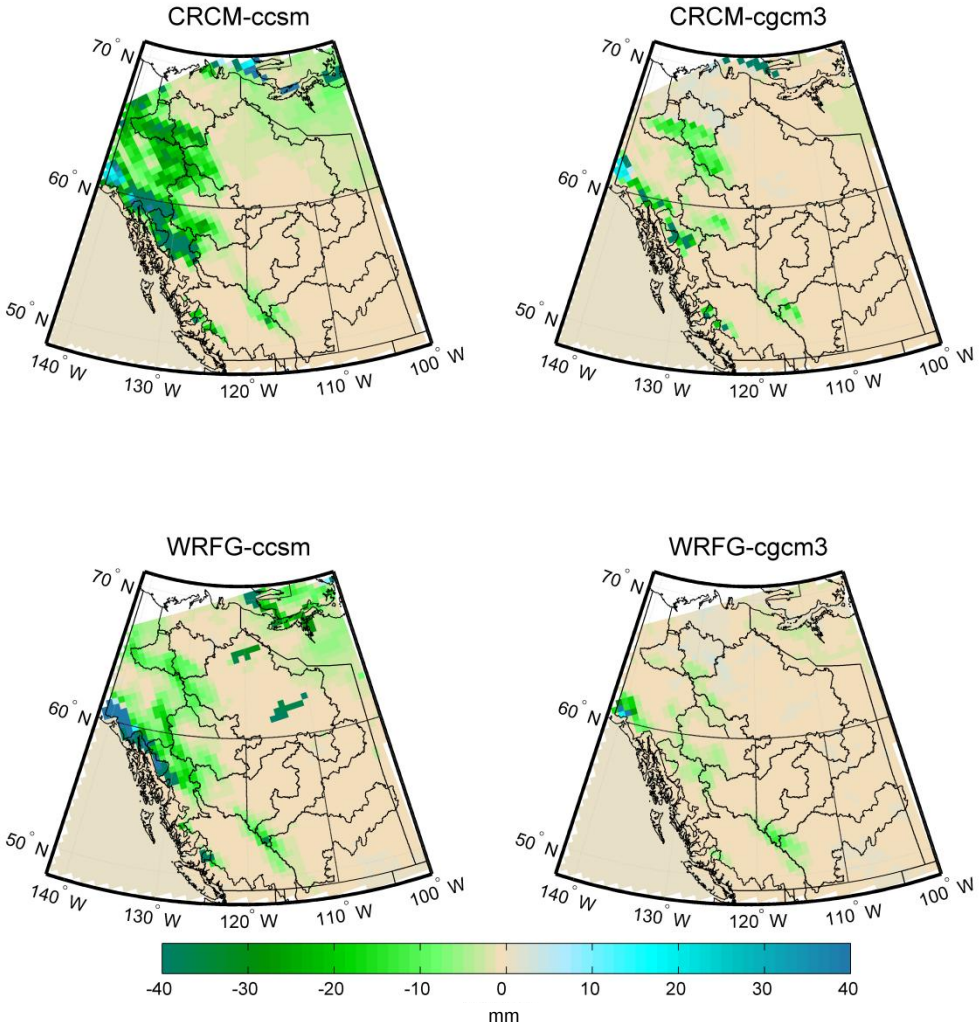

Figure B.172. Difference in snowmelt totals between 1971-2000 and 2041-2070 during August.

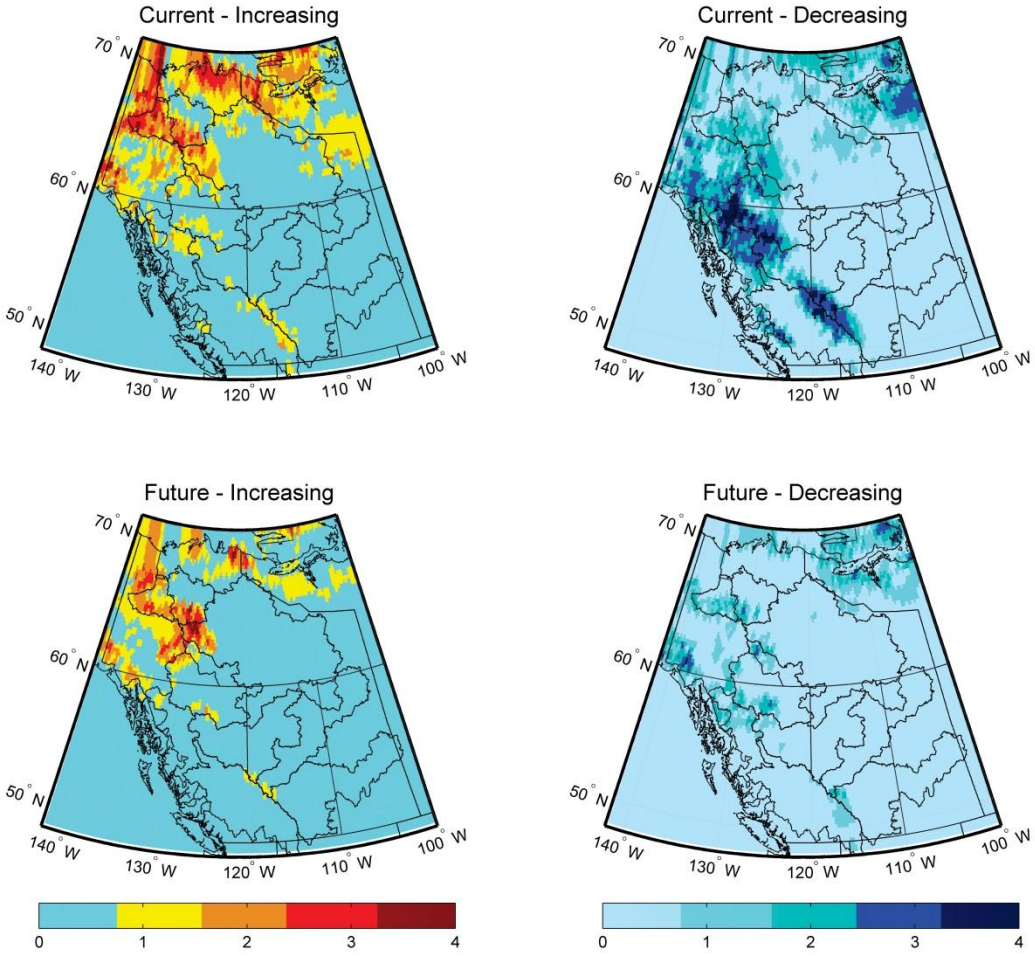

Figure B.173. Number of models showing increasing or decreasing rates of change in snowmelt during the current (1971-2000) and future (2041-2070) time periods during August.

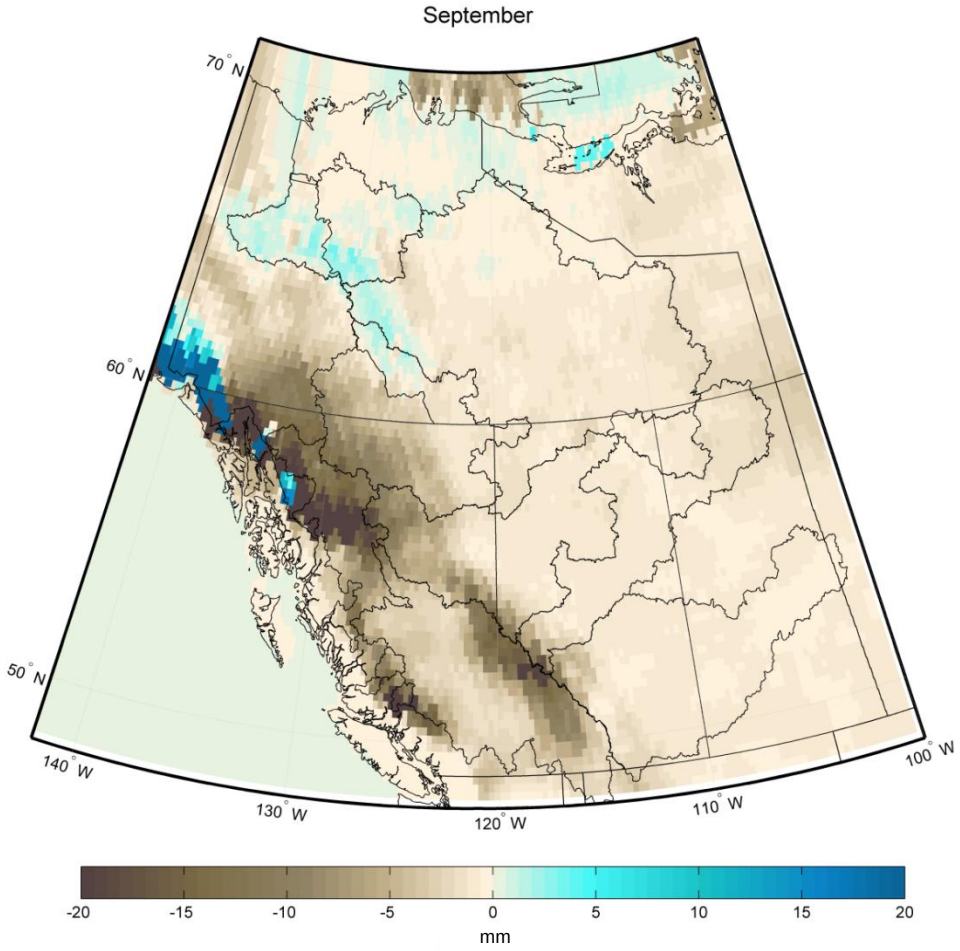

Figure B.174. Multimodel mean difference in monthly snowmelt between the current and future periods during September.

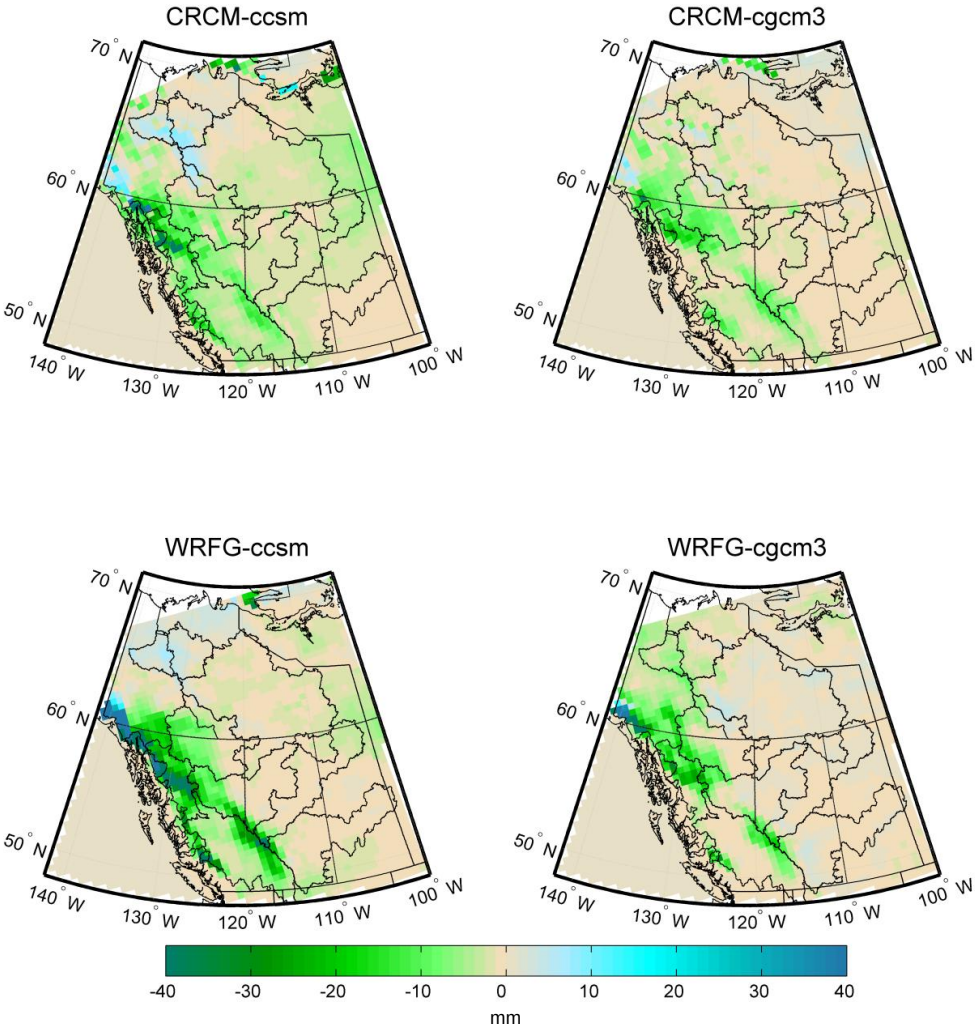

Figure B.175. Difference in snowmelt totals between 1971-2000 and 2041-2070 during September.

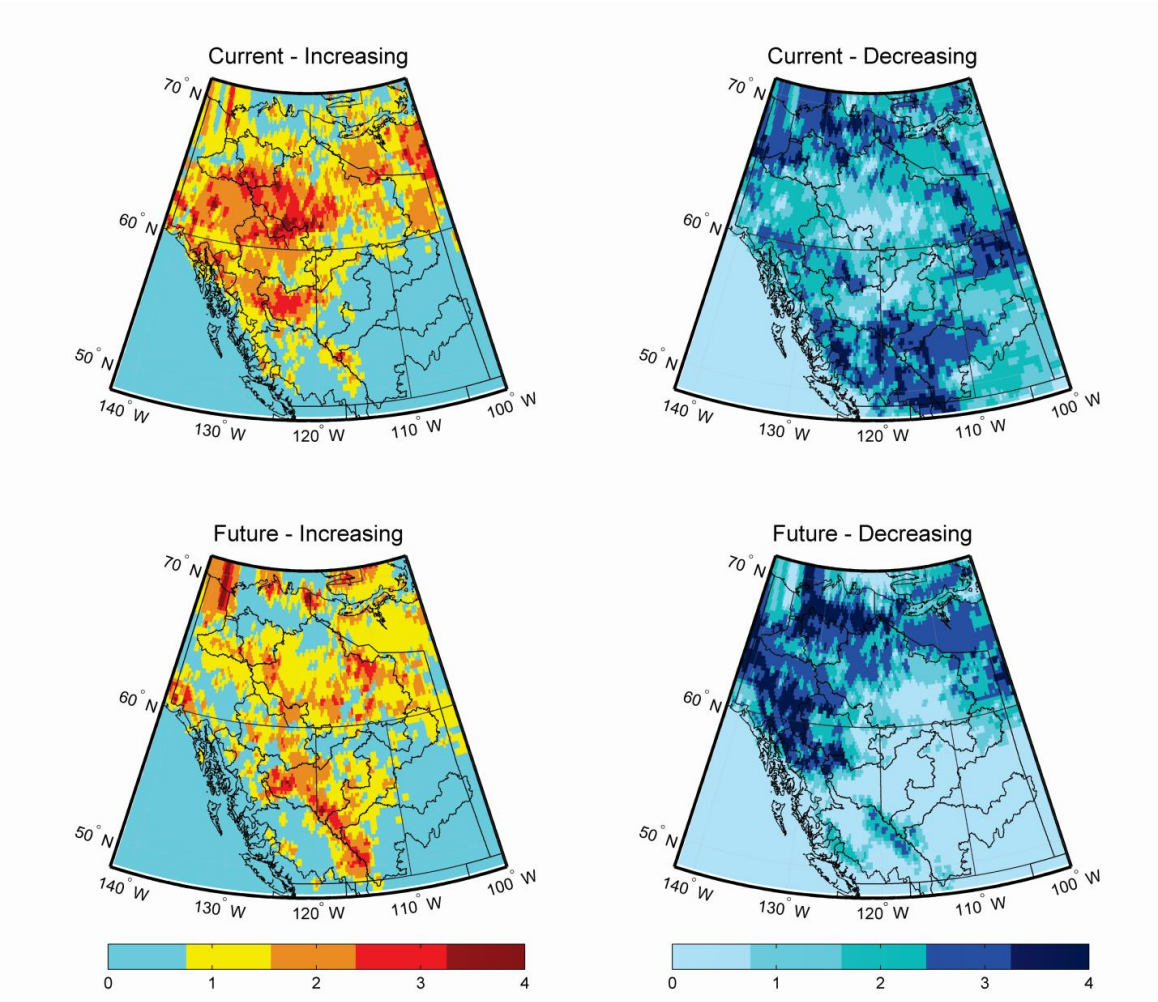

Figure B.176. Number of models showing increasing or decreasing rates of change in snowmelt during the current (1971-2000) and future (2041-2070) time periods during September.

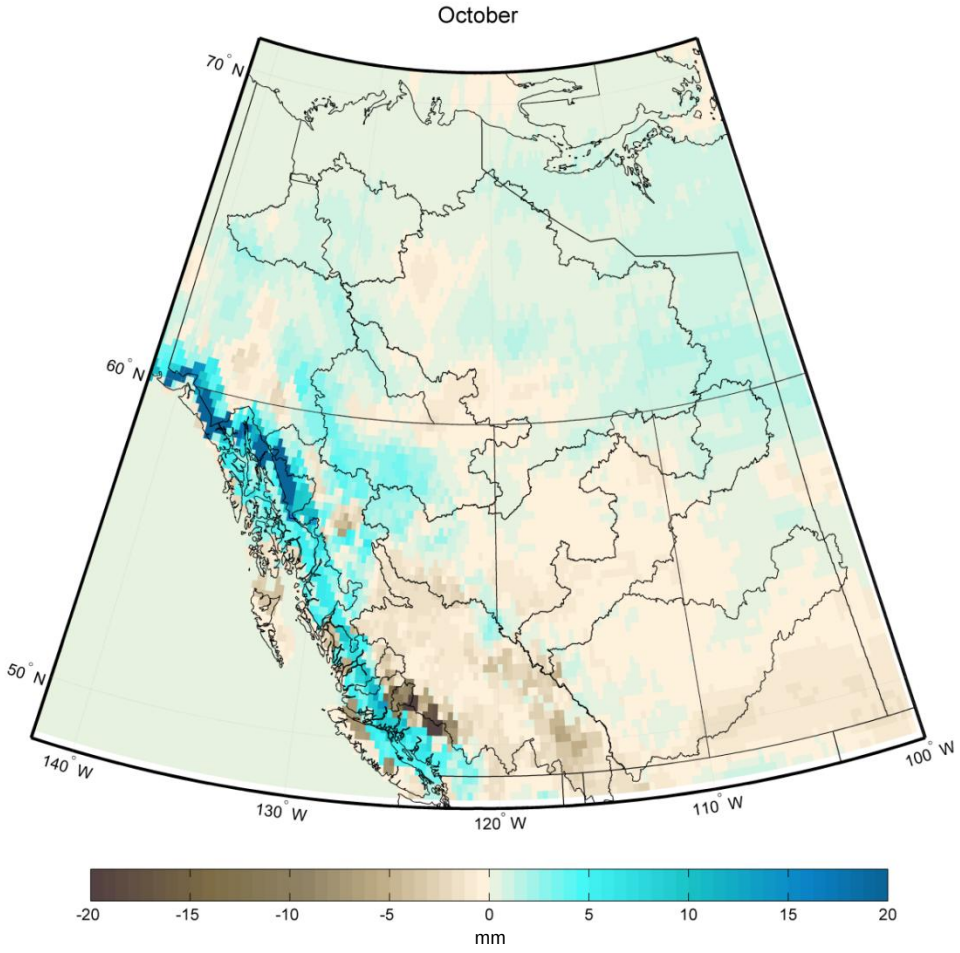

Figure B.177. Multimodel mean difference in monthly snowmelt between the current and future periods during October.

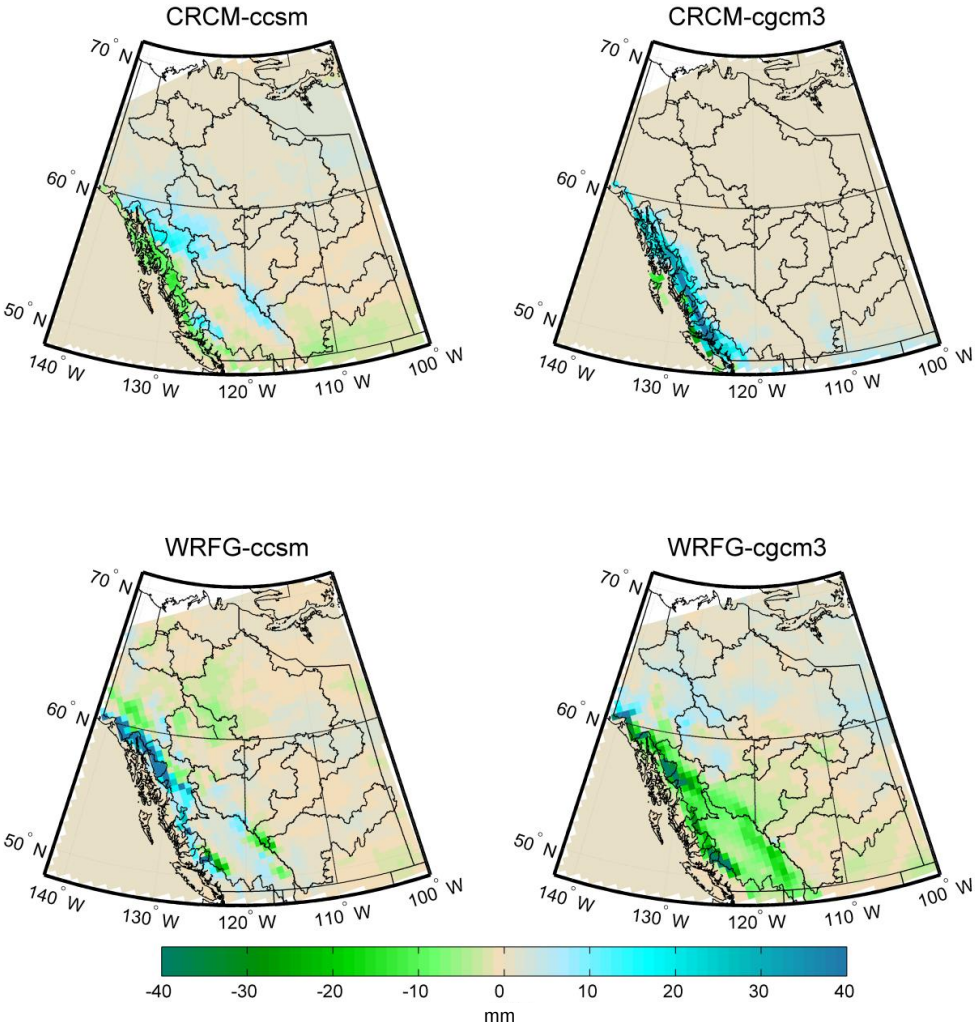

Figure B.178. Difference in snowmelt totals between 1971-2000 and 2041-2070 during October.

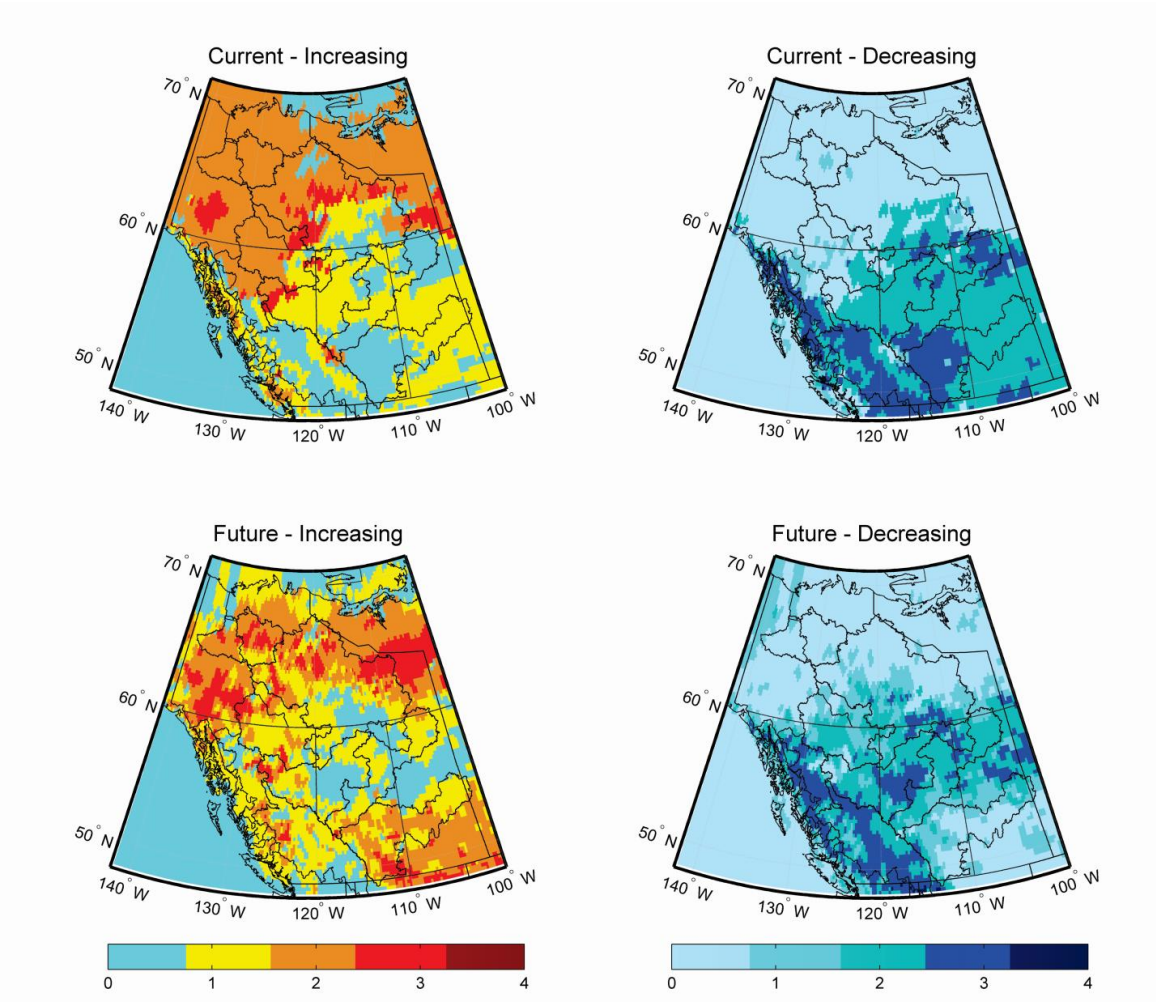

Figure B.179. Number of models showing increasing or decreasing rates of change in snowmelt during the current (1971-2000) and future (2041-2070) time periods during October.

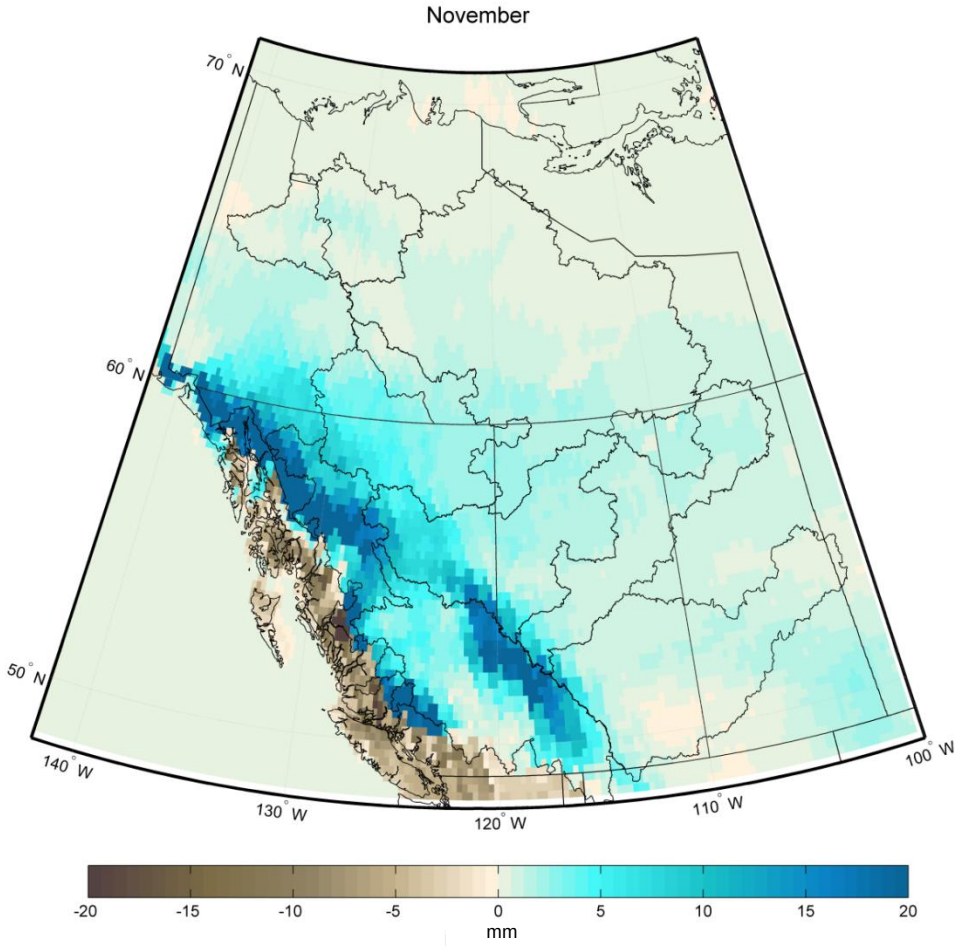

Figure B.180. Multimodel mean difference in monthly snowmelt between the current and future periods during November.

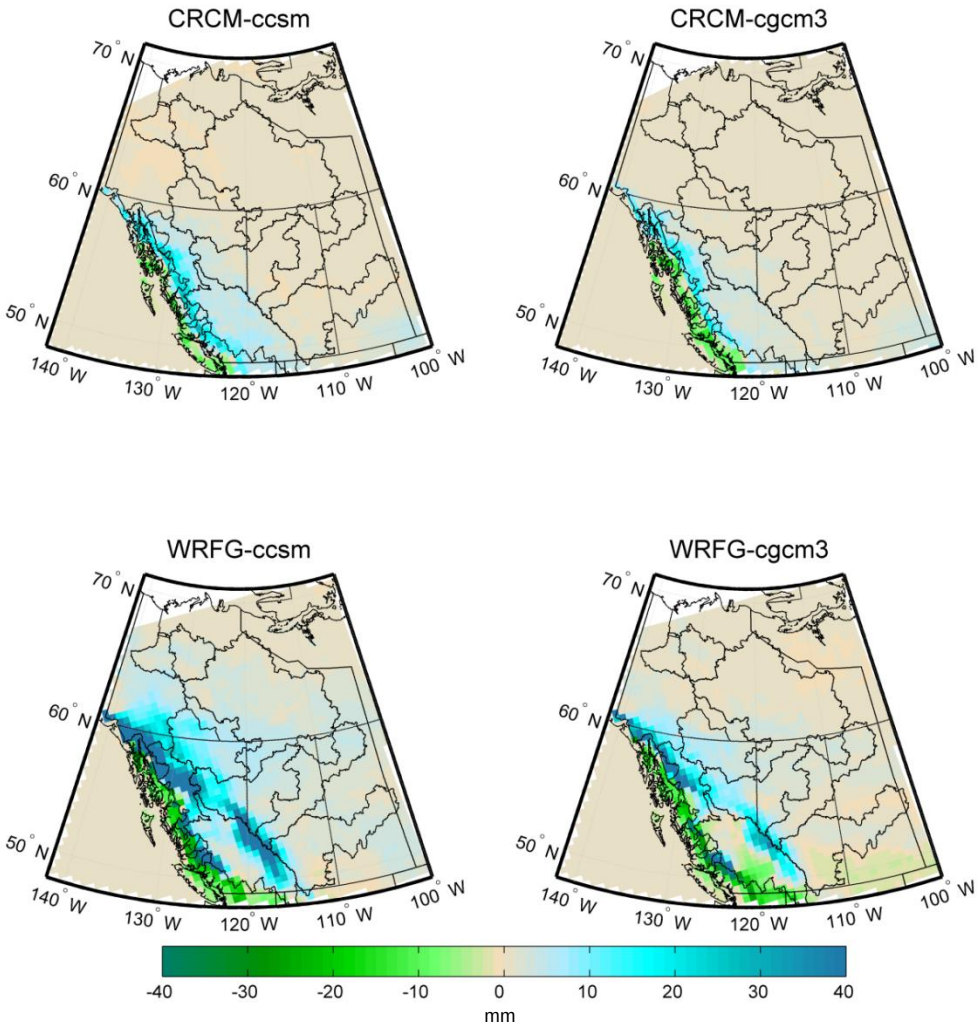

Figure B.181. Difference in snowmelt totals between 1971-2000 and 2041-2070 during November.

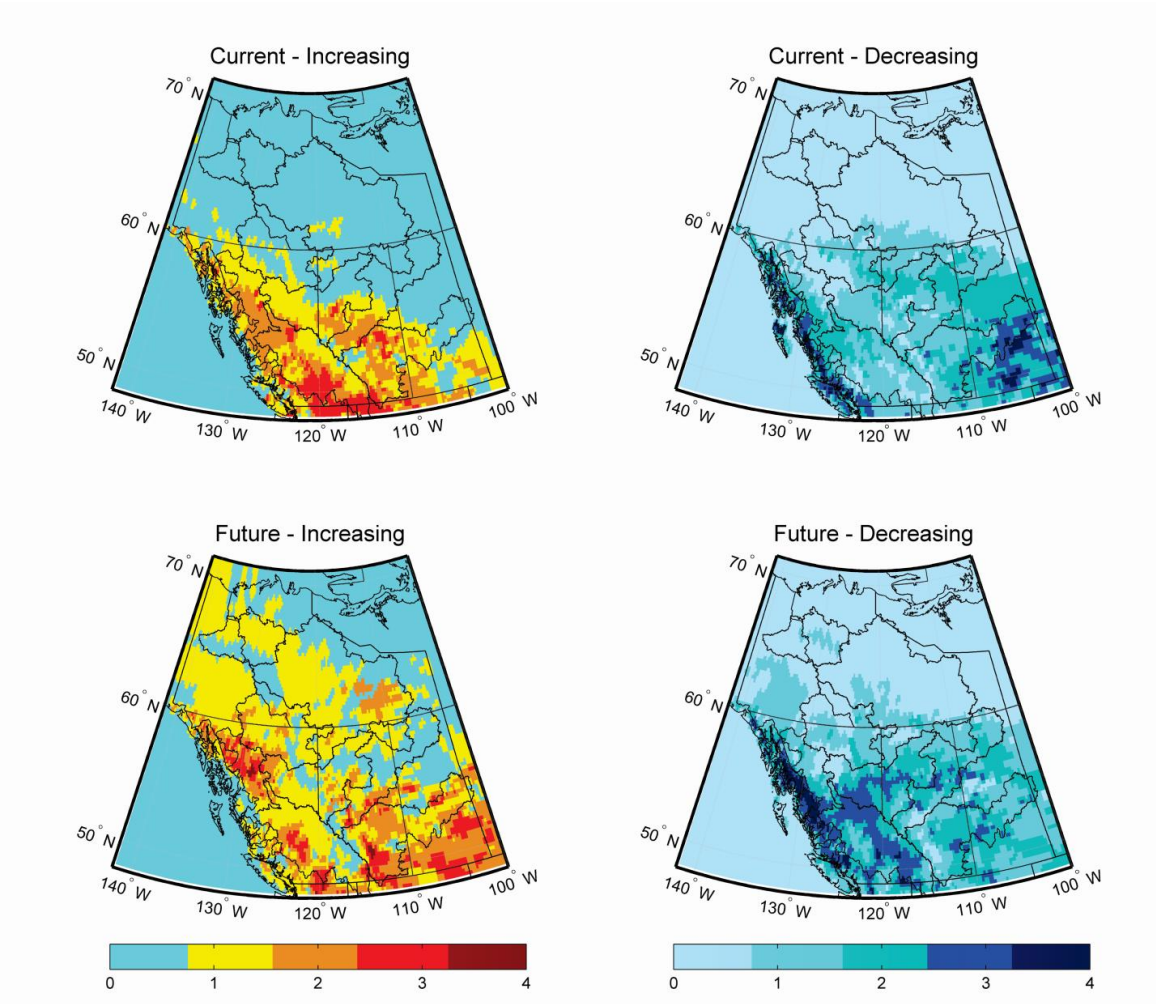

Figure B.182. Number of models showing increasing or decreasing rates of change in snowmelt during the current (1971-2000) and future (2041-2070) time periods during November.

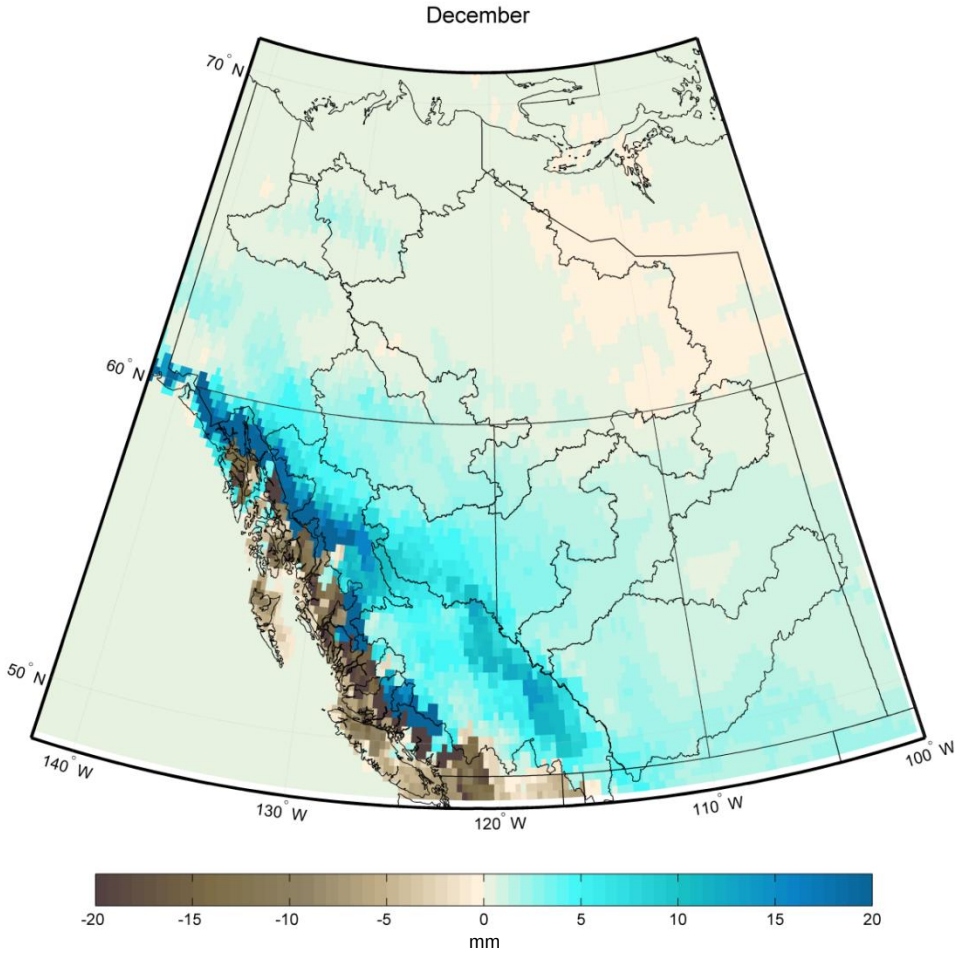

Figure B.183. Multimodel mean difference in monthly snowmelt between the current and future periods during December.

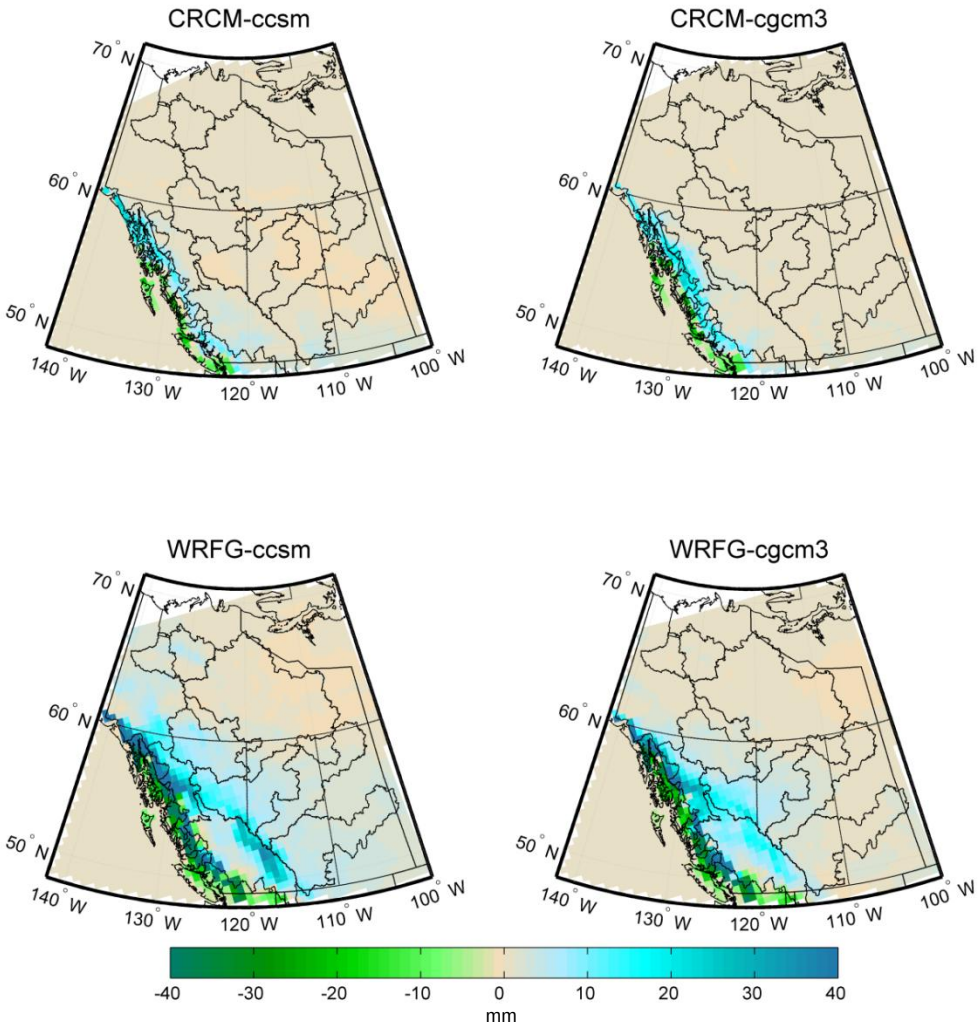

Figure B.184. Difference in snowmelt totals between 1971-2000 and 2041-2070 during December.

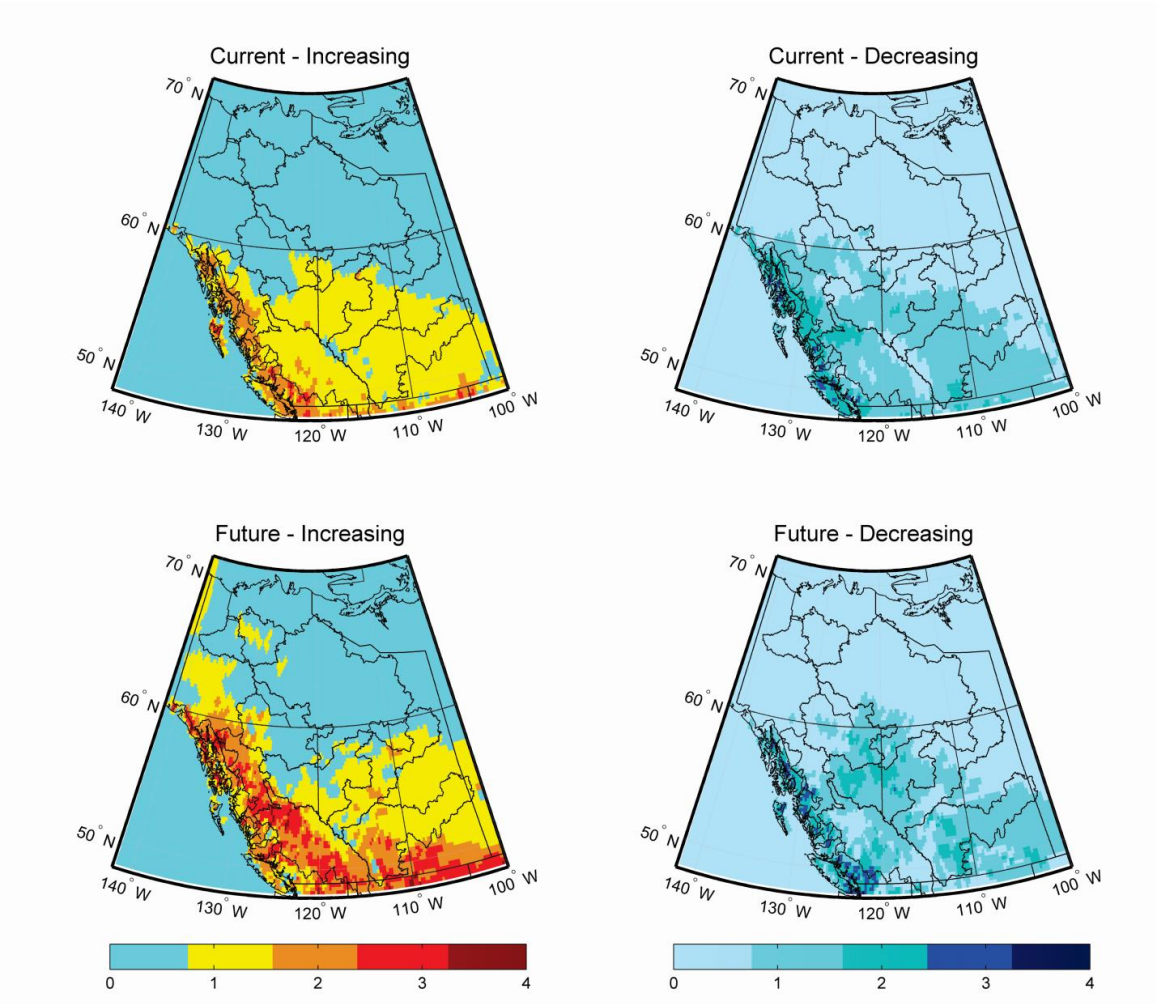

Figure B.185. Number of models showing increasing or decreasing rates of change in snowmelt during the current (1971-2000) and future (2041-2070) time periods during December.